MECHANISMS OF DRYING OF PARTICULATE SLURRIES

by

GURINDER SINGH BAINS

Doctor of Philosophy

THE UNIVERSITY OF ASTON IN BIRMINGHAM

May 1990

THE UNIVERSITY OF ASTON IN BIRMINGHAM

Mechanisms of Drying of Particulate Slurries

Gurinder Singh Bains

Doctor of Philosophy May 1990

SUMMARY

The literature on the evaporation of pure liquid drops and the drying of drops of solutions and slurries has been reviewed with particular reference to spray drying.

A 0.1-0.2 mm glass filament-thermocouple was constructed and used to study simultaneously, heat and mass transfer from a single suspended drop placed in a humidity and temperature controlled, 28 mm OD vertical wind tunnel. Heat conduction through the filament was minimised eg at 100°C, it accounted for only 9.3% of the total heat transferred to a drop.

Evaporation of single water drops was also studied in a 101 mm OD vertical wind tunnel. The Nusselt number was found to be a function of the Reynolds, Prandtl and Transfer number over an air temperature range of 17°C to 107°C. The proposed correlation is:

$$Nu = 2+(-12.96B+0.76)Re^{0.5}Pr^{0.33}$$

Experimental drying studies were carried out on single suspended 1 to 2.5 mm diameter drops of aqueous sodium sulphate decahydrate, sodium chloride, potassium sulphate, copper sulphate and sodium acetate solutions and slurries at temperatures of 20°C to 124°C. Dried crusts were examined by Scanning Electron Microscopy.

The drying history of any material depended upon the nature of the crust formed. Sodium acetate formed a non-rigid skin prior to the formation of a rigid crust.

A modified receding evaporation interface model was proposed for the drying of solutions and slurries. This covered both the constant rate period prior to crust formation and the subsequent falling rate period. The model was solved numerically for the variation in core temperature, drop weight and crust thickness. Good agreement was obtained between model predictions and experimental results for materials forming rigid crusts ie sodium sulphate decahydrate, sodium chloride, potassium sulphate and copper sulphate. However the drying histories of drops of 10-20% weight initial concentration sodium acetate were unpredictable since formation of a non-rigid skin deviated from the model assumption of a rigid outer surface. At higher initial concentrations (40% weight) where, a rigid crust was formed for sodium acetate, good agreement was obtained between experimental results and model predictions.

Single suspended drop studies are concluded to provide a valuable insight into the drying mechanisms of specific solutions and slurries.

KEY WORDS: Droplet Evaporation, Droplet Drying, Receding Evaporation Interface

DEDICATION

To My Mother, Brother And Sisters,

The Friends I Made As An Undergraduate and Postgraduate, And

Finally To The Memory Of My Father Missed By Us All But

Never Forgotten

ACKNOWLEDGEMENTS

The author wishes to express his gratitude to Dr C.J. Mumford for his interest and guidance throughout the course of this work and most particularly for the helpful comments and suggestions in the preparation of this thesis.

The author also wishes to express his gratitude to Professor G.V. Jeffreys for the conception of this project and the interest shown in the results.

The author wishes to thank Dr E.L. Smith for his help with the mathematical modelling.

The author wishes to thank the University of Aston in Birmingham for the award of a University Studentship.

The author would finally like to express his gratitude to Miss T. Smith for being so patient in typing this thesis.

CONTENTS

LIST OF FIGURES

LIST OF TABLES

LIST OF PLATES

LIST OF APPENDICES

CHAPTER ONE

INTRODUCTION

INTRODUCTION

Spray drying is now a common drying operation, finding applications in all our major industries ranging from production under the most stringent of conditions in food and pharmaceutical manufacture to the high tonnage outputs within such chemical fields as mineral ores and clays.

Spray drying is, by definition, the transformation of a feed in the form of a solution, slurry or paste into a dried particulate form by spraying the feed into a hot drying medium, usually air. The feed is atomised. This involves the break-up of the liquid bulk into a myriad of individual drops to form a spray. A large surface area is thereby created, and moisture is removed from the feed by a simultaneous heat and mass transfer process.

Spray drying consists of four process stages:

i) Atomisation of the feed into a spray.
ii) Spray-air contact (mixing and flow).
iii) Drying of spray (moisture/volatiles evaporation).
iv) Separation of dried product from the air.

Each stage is carried out according to the specific drier design and mode of operation and, together with the physical and chemical properties of the feed, defines the characteristics of the dried product.

Spray drying applications date back over 100 years. Intensive Research & Development, particularly over the last thirty years has resulted in it becoming a highly competitive means of drying a wide variety of materials when a particulate product is required. Masters (1) lists an extensive range of spray dried products in

applications in different industries;

i) Chemical industry eg, plastics, resins, ceramic materials, detergents and surface active agents, pesticides, dye stuffs and pigments.

ii) Food industry eg, milk products, egg products, food products, fruit and vegetable products.

iii) Biochemical industry eg, pharmaceutical products, yeast products.

iv) Industries utilising chemicals from timber eg, tanning, cellulose.

v) Offal and food industry eg, slaughterhouse products, fish products.

1.1 ADVANTAGES AND DISADVANTAGES OF SPRAY DRYING

Of the many industrial drier types available, few accept pumpable fluids as the feed material at the drier inlet and discharge a dry particulate at the outlet as shown in Table 1.1. Spray drying is unique in being able to produce powders with a relatively narrow particle size and moisture content irrespective of drier capacity and product heat sensitivity.

Feed Form		Suitable Drier
Solution	Pumpable, non-heat sensitive	Drum, Spray
	Pumpable, heat sensitive	Spray
Slurry	Pumpable, non-heat sensitive	Drum, Spray
	Pumpable, heat sensitive	Spray
Paste	Pumpable, non-heat sensitive	Drum, Spray
	Pumpable, heat sensitive	Spray
Semi-Wet Particulates	Dispersible in gas streams	Flash
	Fluidisable	Fluid Bed
	Non-fluidisable	Fluid Bed
	Non-fluidisable, non-sticky	Fluid Bed (back mix)
	Non-fluidisable, sticky	Rotary Spouted Bed
Fibrous	Dispersible in gas streams	Flash

Table 1.1 Suitability of Industrial Driers to Feed Material Forms

These characteristics are of such importance to many industrial operations that spray drying becomes the only rational choice to dry fluid feedstocks even though, being a convectional type drier, its thermal efficiency is lower than competing direct contact driers that also receive fluid feed materials. Advantages of spray drying include;

i) Ease of operation.

ii) Wide range of designs available to meet specific product specifications.

iii) Applicability to both heat-sensitive and heat-resistant materials.

iv) Wide range of feedstocks eg, solution, slurry, paste or melt form can be handled if pumpable.

v) Spray driers can be designed to any individual capacity requirements.

Spray drying is disadvantaged by high installation costs. Industrial units are physically larger per unit of powder output than other drier types. They are therefore more expensive to fabricate. Furthermore their large diameters or tall drying chambers require expensive buildings and/or supporting structures. Drying air exhausted from spray driers contains large amounts of low grade waste heat which is expensive to remove in heat exchange equipment since this must handle powder-laden air at saturated or near-saturated conditions which leads to the need for sophisticated heat exchanger design.

Although empirical scale-up procedures are used, the optimum design of spray driers requires a knowledge of the controlling

mechanisms within the heat and mass transfer process. This can only be obtained by fundamental research, covering at least the first three process stages identified earlier.

1.2 FUNDAMENTAL SPRAY DRYING RESEARCH

Because of the complexities and impracticability of investigating rate-controlling mechanisms for the distribution of drop sizes travelling through a spray drier, research has tended to be divided into:

a) Atomisation studies, which attempt to correlate drop-size distribution with feed characteristics, atomiser design, pressure (or rotational speed) and throughput.
b) Studies of gas flow patterns and residence times.
c) Single drop drying studies.
d) Mathematical models which attempt to bring together the data from a-c to simulate drier performance.

The present study was concerned with experimental and mathematical modelling aspects of single suspended drops of pure liquid (water) and of drops containing solids.

1.2.1 Single Drop Drying Studies

Single drop drying studies involve pure liquids, solutions, slurries or pastes as discrete drops, generally in temperature and humidity controlled wind tunnels. Drops may be suspended from filaments (2,3), filament-thermocouples (4), or rotating nozzles (5,7). Alternatively they may be suspended in free flight (6,7).

Single drop studies have been criticised as being unrealistic for several reasons (8,9). Suspended or free-flight drops are at

least an order of magnitude larger in diameter (1-5 mm) than sprayed droplets. Larger drops are necessary because (i) they are easier to handle and transfer, and their use avoids significant drying occurring during the initial transient period ie, when the drop is attaining the wet bulb temperature, (ii) a significant weight is required for an accurate determination if weight change is measured to follow the drying history, and (iii) the drops must be large enough to observe when visual recordings are used to follow the drying. In addition, filament suspended drops are not allowed to rotate freely whilst drying. Furthermore any suspension device provides a heat source and may act as a site for vapour bubble nucleation within the drop. Late in the drying process it may tend to deform the drop, if this is of a pure liquid.

Single drop studies are however relatively easy to observe and control. They have provided fundamental insight into the drying process notably through the works of Frossling (2), Ranz and Marshall (3) and Charlesworth and Marshall (10). Their experimental methods are still very much in use (11,12). These studies can also assist drying technology in a particular industrial application by,

i) Comparison of drying rate between products and different formulations.

ii) Assessment of particle morphology.

iii) Assessment of maximum gas temperature (eg avoiding fragmentation due to 'explosions', minimising flavour and/or aroma loss).

iv) Design and/or simulation. By insertion of data in complex models accounting for size distribution, trajectories, gas flow patterns (temperature and humidity profiles), residence time etc.

Although studies of the evaporation of pure liquids have been extensive, less work has been carried out on drops containing dissolved or suspended solids. This can be attributed, in part, to the complexities in analysing the heat and mass transfer processes after a solid crust has formed.

The presence of dissolved solids leads to a decrease in the vapour pressure of the liquid at the drop surface. The overall pressure driving force is thereby reduced, resulting in a reduction in the mass transfer rate. The surface temperature of the evaporating drop will consequently increase above the thermodynamic wet-bulb temperature. The drying characteristics are then related to the formation of a solid phase on the surface of the droplet. As the particle dries, the crust increases in thickness resulting in an increase in the resistance to heat and mass transfer. Subsequently drying is product-specific. Further complications may arise due to:

i) Variation in the mechanism of moisture movement during drying, with drop size, temperature etc.

ii) Inflation, distortion or shrinkage of the drop.

iii) Skin formation externally and internally. These may add to resistance to diffusion or favour a protrusions - ballooning mechanism leading to volatiles release.

iv) Crusts may crack, case harden, fracture completely giving shell fragments and fines.

v) Different constituents may migrate at formulation - dependent rates.

The process is therefore complex and difficult to model mathematically.

The drying of drops containing dissolved solids is shown in Figure 1.1. Initially a drying rate is established immediately the drop contacts the drying air as represented by period AB. The initial drying rate increases, or decreases, until the heat transfer across the drop-air interface reaches equilibrium. Period BC represents conditions of dynamic equilibrium. It is characterised by evaporation from a free liquid surface, termed the "constant rate" period. The drop surface is maintained saturated by adequate migration of moisture from within the drop to the surface. The point C is termed the "critical" point, at which moisture within the drop can no longer maintain surface saturation. The period CD therefore represents the "falling rate" period. This period can form more than one zone, if local areas of wetness remain on the drop surface. The period CD continues until no areas of wetness remain. The major resistance to mass transfer is now presented by the solid crust. Evaporation continues at a decreasing rate until the drop acquires a moisture content at equilibrium with the surrounding air.

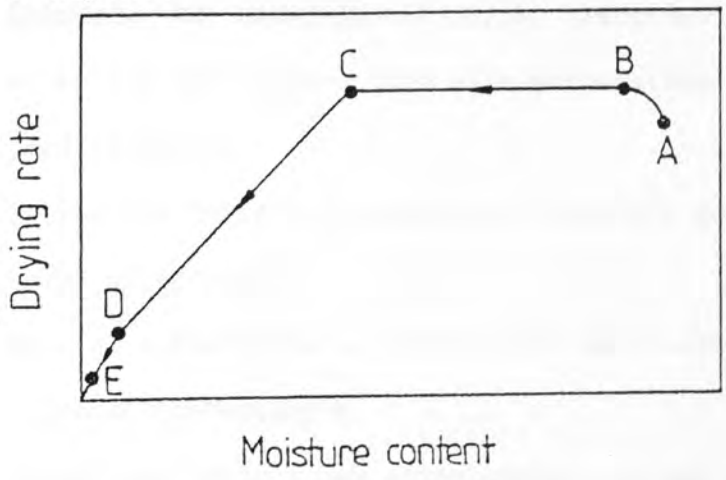

Figure 1.1 Drying of a Drop Containing Solids

The process described above represents an ideal case. In reality drying curves have no sharply defined points. Some of the

drying zones as shown may not even occur. A typical case is when the product is heat sensitive. The air temperatures are then maintained so low that the period AB can well extend until the critical point is reached. With solutions and slurries of high solids content, a crust may form immediately the drop contacts the hot air. The drying rate would then fall and no constant rate period would be observed.

As part of a series of investigations related to spray drying fundamentals, the present work was initiated to further the understanding of the mechanisms involved in the drying of drops containing solids which form rigid porous crusts, rigid non-porous crusts and skins. A glass filament-thermocouple which enabled simultaneous measurements of drop core temperatures and weights was used to study the drying histories of single droplets suspended on the tip of the filament placed inside a humidity and temperature controlled vertical wind tunnel.

The objectives of the work were,

i) Determine the experimental drying histories of the above materials and compare them with mathematical model predictions.

ii) Extend the receding evaporation interface model (4,112) to cover solutions.

iii) Develop a technique to improve the manufacture of the glass filament-thermocouple.

iv) Design and build a new experimental rig and test its validity using pure water drops.

CHAPTER TWO

LITERATURE REVIEW

2.0 MASS TRANSFER ACROSS A PHASE BOUNDARY

- 2.0.1 Two-film Theory
- 2.0.2 The Penetration Theory
- 2.0.3 Film Penetration Theory
- 2.0.4 Boundary Layer Theory

2.1 LITERATURE REVIEW FOR PURE LIQUID DROPS

2.2 EVAPORATION FROM PURE LIQUID DROPS

- 2.2.1 Experiments Under Natural Convection
- 2.2.2 Experiments Under Forced Convection
- 2.2.3 Mass Transfer
- 2.2.4 Heat Transfer
- 2.2.5 Evaporation from Single Droplets in High Temperature Surroundings

2.3 DROPS CONTAINING DISSOLVED AND SUSPENDED SOLIDS

2.4 MECHANISMS OF MOISTURE MOVEMENT THROUGH POROUS MEDIA

- 2.4.1 Diffusion Theory
- 2.4.2 Capillary Flow Theory
- 2.4.3 Evaporation Condensation Theory

2.5 LITERATURE REVIEW FOR DROPS CONTAINING SOLIDS

2.5.1 Single Drop Studies

2.5.2 Evaporation from Sprays of Drops

2.5.3 Sprays of Pure Liquids

2.5.4 Sprays of Drops Containing Dissolved and Suspended Solids

2.5.5 Temperature of Evaporating Drops

2.5.6 Measurements of Drop Temperatures

2.5.7 Heat Conducted by Suspension Devices

2.5.8 Drop Temperature Histories

2.5.9 Particle Morphology Studies

2.6 CONCLUSIONS

2.0 MASS TRANSFER ACROSS A PHASE BOUNDARY

When a concentration gradient exists within a fluid consisting of two or more components, there is a tendency for each constituent to flow in a direction to reduce the concentration gradients; this process is known as Mass Transfer.

Mass transfer can take place in either a gas phase or a liquid phase, or in both simultaneously. Evaporation from liquid drops involves the transfer of vapour from the drop surface to the bulk of the gas. The driving force for mass transfer is provided by the concentration gradient which exists across the interface.

A number of theories have been proposed to describe the mechanism of mass transfer across a phase boundary. Whitman (13) in 1923 suggested that the resistance to transfer in each phase could be regarded as residing in a thin film near the interface. The transfer across each film was regarded as a steady state process of molecular diffusion with the turbulence in the bulk fluid dying out at the interface. This is the Two-Film Theory. In 1935 Higbie's Penetration Theory (14) suggested that the transfer process was largely attributable to fresh material being brought by the eddies to the interface, where a process of unsteady state transfer took place for a fixed period at the freshly exposed surface. Dankwerts (15) suggested a modification to this theory with the material which was brought to the surface remaining there for a varying period of time. Subsequently Toor and Marchello (16) proposed a more general theory, the Film Penetration Theory, and have shown that each of the earlier theories is a particular limiting case of their own. More recently the Boundary Layer Theory has been used particularly for spherical drops.

The drying of drops containing solids is a special case, because of the solid crust that is formed. In comparison to pure liquid drops, this provides an additional, and often controlling, resistance to heat and mass transfer. The overall coefficients are therefore dependent on both the crust coefficient and the gas film coefficient. For mass transfer they are expressed as;

$$\frac{1}{K_o} = \frac{1}{Hk_g} + \frac{1}{k_c} \qquad 2.1$$

where H is Henry's constant

2.01 Two-Film Theory

Whitman's Two-Film Theory was the first serious attempt to represent conditions occurring when material is transferred from one fluid stream to another. Although it does not closely reproduce the conditions in most practical equipment, it enables expressions to be derived which can be applied to the experimental data which are generally available. For this reason it is extensively used.

The theory assumes that turbulence dies out at the interface and that a laminar layer exists in each of the two fluids. The basis of the theory is the assumption that the zones in which the resistance to transfer lies can be replaced by two hypothetical layers, one on each side of the interface, in which transfer is entirely by molecular diffusion. The concentration gradient is therefore linear in each of these layers and zero outside. Using Fick's law of diffusion (17), the model predicts that the overall mass transfer coefficient K_o, is directly proportional to the diffusivity D.

2.02 The Penetration Theory

In the Penetration Theory it is assumed that the eddies in the fluid bring an element of fluid to the interface where it is exposed to the second phase for a definite interval of time, after which the surface element is re-mixed with the element. Thus, fluid whose initial composition corresponds with that of the bulk fluid remote from the interface is suddenly exposed to the second phase. It was assumed that equilibrium is immediately attained by the surface layers and that a process of unsteady state molecular diffusion then occurs and that the element is remixed after a fixed interval of time. The model predicts that the mass transfer coefficient is proportional to $D^{0.5}$.

Danckwerts (15) modified the Penetration Theory by supposing that the surface is continuously being replaced by fresh fluid in a random fashion. Assuming the rate of production of fresh surface S, is independent of the age of the element, he showed that the average mass transfer coefficient is proportional to $(DS)^{0.5}$.

2.03 Film Penetration Theory

This theory incorporates some of the principles of both the Two-Film Theory and the Penetration Theory. The whole of the resistance to transfer is regarded as lying within a laminar film at the interface, as in the Two-Film Theory, but the mass transfer is regarded as an unsteady state process. It is assumed that fresh surface is formed at intervals from fluid which is brought from the bulk of the fluid to the interface by the action of the eddy currents. Mass transfer then takes place, as in the Penetration Theory with the exception that the resistance is confined to the finite film, and material which traverses this film is immediately completely mixed with the bulk of the fluid.

2.04 Boundary Layer Theory

The Boundary Layer Theory is the most common approach for predicting the heat and mass transfer coefficients for spherical drops. The equations of motion, continuity and energy can be solved approximately to obtain the velocity, concentration and temperature profiles in a thin boundary layer at the interface. Outside the respective boundary layers, flat profiles are assumed. Frossling (2) applied this theory to evaporation of spherical drops and showed that the mass transfer coefficient is proportional to $D^{0.67}$.

2.1 LITERATURE REVIEW FOR PURE LIQUID DROPS

The phenomena associated with evaporation from a single drop and the methods of predicting its rate are important in the analysis of engineering operations involving such processes as spray drying, cooling, absorption, desorption, humidification and combustion. An extensive amount of literature has been built up covering both experimental and theoretical research with pure liquid drops. However there is significantly less data available on the drying of drops containing solids.

The literature pertaining to the heat and mass transfer process as associated with pure liquid drops, drops containing dissolved and/or suspended solids, and sprays of drops has been reviewed, Each of these categories were subdivided according to the types of experiments carried out.

2.2 EVAPORATION FROM PURE LIQUID DROPS

The process of evaporation from pure liquid drops involves simultaneous heat and mass transfer. The basis of the theory related to evaporation from drops, motionless with respect to an infinite and uniform gaseous medium was laid down by Maxwell (18). For a perfectly spherical drop with a vapour concentration C_s at the surface, continuously saturated, it was shown that,

$$\frac{-dW}{dt} = 4\pi rD(C_s - C_\infty) \qquad 2.2$$

From equation 2.2, a gas phase mass transfer coefficient can be defined under stagnant conditions as,

$$k_g = \frac{-dW/dt}{4\pi r^2(C_s - C_\infty)} = \frac{D}{r} \qquad 2.3$$

The Sherwood number can therefore be expressed as,

$$Sh = \frac{2k_g r}{D} = 2 \qquad 2.4$$

Evaporation rates however, increase with an increase in relative velocity between the drop and air due to the additional evaporation caused by convection in the boundary-layer around the drop. Frossling (2) using boundary-layer theory, showed that to account for the contribution of forced convection to mass transfer, equation 2.4 should be multiplied by a wind factor ø ie.

$$Sh = 2(1 + \text{ø}\ Re^{0.5}Sc^{0.33}) \qquad 2.5$$

where ø = 0.276

The validity of this equation has been confirmed by numerous workers, the main difference being in the value of ø. The most widely used correlation was obtained by Ranz and Marshall (3) who evaluated ø as 0.3.

The majority of experiments on pure liquid drops have been carried out on drops suspended on the end of a filament or a capillary. A few experiments have also been conducted on drops in free flight.

The literature on liquid drops has therefore been divided into the following categories:

(i) Drops evaporating under natural convection.

(ii) Drops evaporating under forced convection.

(iii) Drops evaporating in free flight.

(iv) Drops evaporating under conditions of intense heat and mass transfer.

2.2.1 Experiments under Natural Convection

The very early experiments were conducted on drops placed on weighing pans. There was then a progression to using drops placed on the end of glass filaments or capillaries. However other methods have also been used eg techniques involving internally heated brass spheres coated with the material in question.

Sreznevskii (19) was the first to determine rates of evaporation into still air. Experiments were conducted using a convex liquid meniscus at the upper end of a 3 mm diameter tube and on drops of liquid placed on the flat top of vertical, cylindrical columns of 1.8 to 3.6 mm diameter such that the drop covered the top. Evaporation rates for hemispherical drops of water, carbon disulphide, chloroform, ether and benzene were determined by following the outline of drops through a horizontal microscope.

Morse (20) studied the evaporation into air of spheres of iodine placed on the pan of a micro-balance. He found that the rate of evaporation was proportional to the radii of the spheres. Subsequently Langmuir (21) used the results obtained by Morse and derived a modified version of Maxwell's equation to account for this proportionality.

In 1934 Whytlaw-Gray and Patterson (22) also used the

technique of placing drops on the pan of a quartz microbalance. Using 2-4 mm drops of water, aniline, p-creosol, quinoline and methyl salicate, they found that the surface of the drop decreased linearly with time, although the volume decreased by a factor of almost a hundred.

The technique of using a filament, or a capillary to suspend drops superseded the above techniques of placing drops on flat surfaces. These conditions would be expected to more closely resemble the conditions of evaporation of a free drop since the drop remains approximately spherical and virtually all the surface area is available for convective heat and mass transfer.

Topley et al (23) used 2 mm spheres of iodine fused to a quartz fibre. These spheres were placed in a cylindrical vessel of 4 cm diameter, whose walls and bottom were covered with a thin layer of KOH to absorb the iodine vapour. Their results provided the first quantitative support for Maxwell's equation.

Houghton (24) measured the rate of evaporation of water drops suspended from glass fibres using a horizontal microscope. Different sized fibres varying from 1.25-120 μm radii enabled drops of 50-100 μm radii to be studied. The fibres were coated with a thin layer of paraffin, firstly to reduce the distortion of the drop and secondly to prevent wetting of the fibre. No details were given regarding the dimensions of the experimental chamber. The drop temperature was not measured directly but was assumed to be equal to the wet-bulb temperature of the air.

Langstroth et al (25) studied the evaporation of drops of 1-2 mm in diameter in still air. The liquids chosen were graded according to volatility from toluene to aniline and included water. A glass fibre (100 μm diameter) or a copper constantan thermocouple was used to suspend the drops at the centre of a spherical glass

flask of 2 cm inner diameter. The drop diameter was measured by means of a microscope fitted with an ocular micrometer and viewed horizontally through a small plane window. Although radiation effects were accounted for, the heat flux through the glass fibre was ignored. The experimental results obtained agreed with calculations based on diffusion and heat transfer history.

Ranz and Marshall (3) used a thermo-element and a capillary to study the evaporation of a number of pure liquids including water, benzene and aniline. Drop diameters ranged from 0.6-1.1 mm and air temperatures up to 220° C. They correlated their results by;

$$Nu = 2 + 0.6Pr^{0.33}Gr^{0.25} \qquad 2.6$$

$$Sh = 2 + 0.6Sc^{0.33}Gr^{0.25} \qquad 2.7$$

Mathers et al (26) were the first to solve the simultaneous heat and mass transfer equations numerically for natural convection. Internally heated brass spheres (12.7 and 25.4 mm diameter) coated with naphthalene were used in their studies. They proposed that

$$Nu = 2 + 0.282\ (GrPr)^{0.37} \qquad 2.8$$

$$Sh = 2 + 0.282\ (GrSc)^{0.37} \qquad 2.9$$

For GrPr (or Sc) <100

And

$$Nu = 2 + 0.5\ (GrPr)^{0.25} \qquad 2.10$$

$$Sh = 2 + 0.5\ (GrSc)^{0.25} \qquad 2.11$$

For 100 <GrPr(or Sc) $<10^6$

Steinberger and Treybal (27) used benzoic acid spheres of different sizes (12.7, 19.1 and 25.4 mm) immersed in a Dewar flask full of water. The subsequent solution was titrated for its benzoic acid content. They divided their data using the condition that the

boundary layer became turbulent when $GrSc > 10^8$. The data was then correlated according to,

$$Sh = 2 + 0.569\ (GrSc)^{0.25} \qquad 2.12$$

for $(GrSc) < 10^8$

And

$$Sh = 2 + 0.0254\ (GrSc)^{0.33} \qquad 2.13$$

for $(GrSc) > 10^8$

However the accuracy of equation 2.13 is questionable since it was obtained from only three data points.

Frazier and Chang (28) pointed out that the numerous models developed for the vaporisation of pure liquids were based on a number of approximations and restrictions and had never been tested adequately at high temperatures. In particular, large changes in property values can occur through the vapour film surrounding the drop and a question therefore arises as to how to best average the properties for acceptable agreement with experimental results. They used integrated mean values of the physical and transport properties over the film length. A model proposed by Frossling in which,

Total vaporisation rate = rate in absence of convection + rate due to convection

was used to fit the experimental data of Hoffman and Gauvin (29) and Kobayashi (30). The rate due to convection was calculated from an experimental correlation. They found good agreement with the data.

Yuge (31) studied the heat transfer under natural convection conditions using internally heated carbon-chrome steel and brass spheres. The sphere was suspended from two sides by thermocouple wires. The data was correlated by the expression,

$$Nu = 2 + 0.392\ Gr^{0.25} \qquad 2.14$$

For $1<Gr<10^5$

A Millikans condenser has also been used by a number of investigators (115,116,117) to study the evaporation of free drops. The drop is introduced into the apparatus and the potential across the condenser continuously varied such that the electrostatic and gravitational fields are balanced and the drop remains stationary. Although drops as small as 1-6 microns could be studied, the results were found to be less accurate than methods for suspended drops.

2.2.2 Experiments Under Forced Convection

The results of most importance with regard to spray drying are those for the evaporation of drops moving relative to a medium under the influence of gravity and/or inertia. The experiments in this field can be classified according to either the mass transfer or heat transfer approach.

2.2.3 Mass Transfer

Majama (32) was amongst the first to measure the rates of evaporation into a moving air stream from pure organic liquids or drops of water of 0.2 mm diameter. A horizontal glass fibre of 5 microns diameter was used to suspend the drops. He found that the rate of change of the diameter squared was constant.

One of the pioneering works, that has served as a model for subsequent work in this field, was that of Frossling (2). Using a glass fibre or a thermocouple, extremely accurate measurements were made of the rates of evaporation of drops of water, aniline or nitrobenzene and spheres of naphthalene. Drops of 0.2-1.88 mm were used. They were suspended 20 cm above the exit of a vertical wind tunnel. The air velocity was varied from 0.2-7 m/s and the

evaporation rates were determined photographically. Equation 2.5 was derived. The results from the naphthalene spheres confirmed boundary layer theory that a drop undergoes a maximum evaporation rate at the forward face, reducing to a minimum just past the equator and increasing to a lower maximum on the trailing face which experiences velocities in the reverse direction.

Vryubov (33) used a 1 m long vertical tube to study the evaporation of free-falling water drops of 2 mm diameter. Heated air from 40-100° C was passed down the tube at 1 m/s, with the drops being collected on a weighing pan. The results were expressed as,

$$Sh = 0.52Re^{0.5} \qquad 2.15$$

For 100<Re<500

Kinzer and Gunn (34) carried out a theoretical and experimental study of the physical behaviour of freely falling water drops. The study was divided into three categories;

(i) Drops travelling within Stoke's law region, or slightly above (Re=0.7).

(ii) Those falling with sufficient speed (Re=7-2000) to ventilate adequately the transition layer of vapour and temperature.

(iii) Re>2000, where there is deformation from the normal spherical shape.

A Schlieren optical method of observing small variations in the index of refraction of transparent materials was adapted to permit measurements of small temperature differences between adjacent areas of water contained in an adjacent cell. This method was used to measure the drop temperature. For the range of drop sizes of 0.6-3 mm diameter, they obtained the same relationship as Frossling with a Ø value of 0.23 for 100<Re<1600.

Ranz and Marshall (3) derived the most widely quoted equations for heat and mass transfer ie,

$$Nu = 2 + 0.6Re^{0.5}Pr^{0.33} \qquad 2.16$$

$$Sh = 2 + 0.6Re^{0.5}Sc^{0.33} \qquad 2.17$$

The study was restricted to a Reynolds number range of 0 to 200, the range usually encountered in spray-drying operations. Drop diameters ranged from 0.6 mm to 1.1 mm and air temperatures up to 220° C. Results of studies on water, benzene and aniline confirmed the analogy between heat and mass transfer at low Reynolds number, and verified the simple expression for the Nusselt number at zero Reynolds number. A general correlation of existing data on spherical particles gave good agreement with equations 2.16 and 2.17, five times beyond the experimental range of Reynolds numbers. The above equations were a confirmation of Frossling's earlier results. They used a glass capillary burette to suspend drops of aniline, benzene and water. Liquid was supplied continuously through the burette to keep the drop size constant.

Using a similar method of keeping the drop diameter constant, Hsu et al (35) measured the rates of evaporation of heptane drops with a diameter of 1.8 mm at 37° C over a Reynolds number range of 70-300. The large size of the drops and low surface tension resulted in drop shapes which deviated significantly from the spherical form. On fine capillaries (0.1 mm) the drops were pear shaped and on wide capillaries (0.8 mm) truncated spheres. They expressed their results by

$$Sh = 2(1+0.272\ Re^{0.5}Sc^{0.33})\ (1 + 1.147(1-\mu_h))(1 - 0.0371(1-d_v/d_h)) \qquad 2.18$$

Where $\mu_h = 6V_l/Sd_h$

V_l = volume of the drop m^3

S = Surface area of the drop m^2

d_h = Maximum horizontal distance m

d_v = Height of the drop m

They found that the evaporation rate increased rapidly with deviations from a sphere; the oblate spheroids yielded higher evaporation rates than the pendant drops.

Maisel and Sherwood (36) carried out tests on wetted plane surfaces, cylinders, spheres and discs evaporating into turbulent gas steams (Re=2000-50,000). For spheres they found that;

$$J_d = 0.43Re^{-0.44} \qquad 2.19$$

where J_d = Chilton-Colburn factor.

Garner and Grafton (37) used a cine camera to measure the rates of dissolution of 12.7 mm diameter pressed benzoic acid spheres in a stream of water at room temperature. Their experimental results were correlated by;

$$Sh = 44 + 0.48Re^{0.5}Sc^{0.33} \qquad 2.20$$

for $20<Re<1000$

This result is significantly different in the constant term expressed by Frossling (2) and Ranz and Marshall (3). They explained that this was due to natural convection effects. However Garner and Suckling (39) used the same apparatus and technique in a later study but covered a larger range of sphere sizes. Using 9.5 mm to 12.7 mm adipic acid, and 9.5 mm to 19.1 mm benzoic acid, spheres they correlated their results together with the earlier work

above. Using the assumed limiting value of 2, they found that,

$$Sh = 2 + 0.95Re^{0.5}Sc^{0.33} \qquad 2.21$$

for $100<Re<700$

Garner and Hoffman (38) used a similar method, measuring the rate of dissolution of 9.5 mm benzoic acid spheres at 30° C over a range of Re numbers of 1-130. They found that the interaction between free and forced convection was complex. Free convection effects did not disappear entirely until Re = 250 for the 9.5 mm spheres and Re=750 for 19.1 mm spheres. They pointed out that Acrivos (40) had solved the Navier-Stokes equation and Fick's second law for transfer from a sphere. This was simplified by the normal assumptions of boundary layer theory. He predicted that the transition from forced to free convection and vice-versa was gradual, especially at high Prandtl numbers and that the two effects were non-additive.

Evnochides and Thodos (41) used celite spheres saturated with either water or nitrobenzene. Each sphere was supported horizontally and rotated just above the discharge end of a 20 cm round duct. The temperature of the sphere was measured by thermocouples inserted into it. The spheres were periodically weighed in order to determine the rate of evaporation.

Pasternak and Gauvin (42) used the same technique as above and obtained the correlation,

$$Sh = 0.692\ Re^{0.514}Sc^{0.33} \qquad 2.22$$

This expression was confirmed by the results from later experiments (43) on radioactive celite spheres saturated with acetone in free flight. The particle velocity was determined by a radioactive tracer technique.

Fuchs (44) suggested that internal circulation in a drop may enhance heat and mass transfer. This was verified by Bowman (45) whose theoretical analysis postulated that the external flow patterns were affected by internal circulation thereby decreasing the resistance to transfer in the external fluid. Ward et al (46) verified this hypothesis by their work on circulating spheres. Their results for four systems, water drops in cyclohexanol, and from, drops of cyclohexanol, isobutanol and o-toluidine into water confirmed that Sherwood numbers were in good agreement with theoretical predictions and the results showed a four to six fold enhancement of mass transfer over that of a non-circulating drop. This effect was shown to depend on the ratio of continuous to dispersed phase viscosity of the system. Thus for a system such as water drops in cyclohexanol (μ_c/μ_d = 25), the rates were as expected several times that of the solid spheres. However for cyclohexanol drops in water (μ_c/μ_d = 0.04) there was little enhancement due to circulation. Consequently, for liquid drops in air, where the ratio μ_c/μ_d will be very small, it is reasonable to assume that negligible enhancement in mass transfer will occur from internal circulation.

Garner et al (47) stated that circulation in liquid drops was not detected in their experiments. Using Bond and Newton's correlation they predicted that water drops greater than 5 mm should circulate when falling in gases. This correlation relates the ratio of the maximum hydrostatic head inside a drop to the surface tension forces tending to keep the drop spherical. No direct connection was found between drop shape or oscillation with the internal resistance to mass transfer.

In comparison to Garner and Hoffman (38), Steinberger and Treybal (27) proposed that natural and forced convection to spheres

was additive. Pei (48) in a review of this area of research stated that Steinberger and Treybal were the only authors to come to this conclusion. All other research has suggested that the transition from forced to natural convection, or vice-versa, was gradual and that the two convective terms were not additive. Steinberger and Treybal proposed that

$$Sh = Sh_0 + 0.347Re^{0.62}Sc^{0.31} \qquad 2.23$$

This equation gave good agreement at low Reynolds numbers but was less successful at higher values.

Jones and Smith (49) studied mass transfer from solid spheres (2.4 mm - 19.1 mm) of naphthalene, camphor and benzoic acid suspended in an air stream moving at high velocity through rotameter tubes. The particles were found to spin and have an erratic motion both axially and radially. Using ball bearings in the spheres to stop spinning allowed a comparison of the rates. However no differences were found in the rates. This was attributed to the fact that when the particle is spinning, one side is stationary relative to the gas while the other side meets the gas at twice its linear velocity. When a particle is not spinning, both sides meet an equal velocity. They found that plotting the results in a conventional way resulted in a wide scatter of the data. It was shown that this spread for the mass transfer coefficient at a constant particle Reynolds number was correlated by the Reynolds number of the gas; that is by taking into account the turbulence of the gas generated by the tube as well as that generated by the particles. Two correlations were proposed.

Laminar region : $Sh = 2 + 25\ (ReScRe_t^{0.5})^{0.33}$ 2.24

Turbulent region : $Sh = 2 + 0.055(ReScRe_t^{0.5})^{0.5}$ 2.25

Kinard et al (50) considered separately the forced convection in front of, and behind, the separation zone of the boundary layer. Noting that boundary layer theory cannot accurately predict mass transfer, since it neglects transfer from the rear surface of the sphere, they added an additional term to account for this transfer in the wake of the drop. Using data from Ranz and Marshall (3), Garner and Suckling (39), and Steinberger and Treybal (27) they proposed:

$$Sh = 2 + Sh_o + 0.45Re^{0.5}Sc^{0.33} + 0.00484ReSc^{0.33} \qquad 2.26$$

Audu (5) used a stainless steel rotating nozzle located inside a horizontal wind tunnel for suspension of drops of water. One drawback to this technique was that hemispherical drops were used which were of the same size (1-5 mm) as the nozzle. The flow patterns around the drop would therefore be disturbed by the presence of the nozzle and would not be consistent with those of a spherical drop. For ambient conditions the proposed correlation was;

$$Sh = 2 + 0.473Re^{0.5}Sc^{0.33} \qquad 2.27$$

Frazier (51) developed a model to fit the data of Houghton (24) and Duguid and Stampfer (52). They found that surface tension effects on vapour pressure were negligible for drops of the size of several hundred microns. They proposed that the evaporation rate could be expressed as

$$N_A = N_{Ao}\,[(1+f(GrPr)] \qquad 2.28$$

where $f(GrPr) = A(Gr,Pr)^{1/n}$

$A = 0.15$, $n=2$, $Gr < 4.22/Pr$

$A = 0.215$, $n=4$, $4.22/Pr < Gr < 10^5$

Good agreement was observed with Houghton's (24) results. However the model underpredicts Duguid and Stampfers' (52) results for relatively small drops (6-18 μm). Even allowing for the effects of forced convection (2%) and surface tension on the vapour pressure (0.02%) it did not give good agreement. The drops of 10 μm size lie in a transition zone between macroscopic and microscopic behaviour. Brownian motion can then lead to a continuous distortion of the heat and mass transfer film around the drop. The heat and mass transfer rates are then enhanced above that given by macroscopic continuum motions.

Miura et al (53) used a similar experimental arrangement to Garner and Kendrick (54) to study rates of heat and mass transfer from floating water drops in an ascending air stream. Drops were floated by an 'inverted' parabolic velocity profile, ie low velocity in the centre, surrounded by an annular region of high velocity. Using drops of 2.9-3.3 mm diameter, air temperatures of 53 or 75°C and 7.5-9 m/s air velocity they found that their data gave good agreement with Ranz and Marshall's results obtained from drops suspended on a fine capillary.

A recent study by Sandoval - Robles et al (55) was conducted for mass transfer from a sphere in perfect streamline conditions. A suspended brass sphere of 5,7,9 or 10mm diameter was rotated at a constant velocity around a circular channel filled with motionless electrolytic solution. This provided conditions of no turbulence and a flat velocity profile. Their results showed a significant dependence on the Reynolds number. Clearly the number of digits in the constants and exponents on Re are optimistic in view of the experimental technique.

$$Sh = 1.032Re^{0.385}Sc^{0.33} \qquad 2<Re<20 \qquad 2.29$$

$$Sh = 0.803Re^{0.475}Sc^{0.33} \qquad 20<Re<2000 \qquad 2.30$$

$$Sh = 0.3Re^{0.593}Sc^{0.33} \qquad 2000<Re<23000 \qquad 2.31$$

They also studied electrochemically (56) mass transfer around single spheres in a highly turbulent liquid. A 94 mm diameter, vertical column was used in which a brass sphere was suspended. Turbulence in the liquid flowing past the sphere was generated by causing it to flow through a polyethylene porous plate fixed at the bottom of the column. Mass transfer from the sphere was measured by using an electrochemical method. Their results were correlated by the expression;

$$Sh = 6.82Re^{0.559}f^{0.069} \qquad 2.32$$

where f = turbulence intensity

At low f values the data obtained was in good agreement with the previously published correlation for laminar conditions.

2.2.4 Heat Transfer

In a spray drier the effects of heat transfer by convection and radiation are important. Many of the experimental studies however have used drops suspended from filaments, capillaries or nozzles. The suspension device therefore acts as a heat conductor into the drop. This extra heat source should be taken into account when working out heat and mass transfer rates. However some investigators have neglected this term. In the present study it was shown that, over the temperature range as shown in Table 6.1, this term accounted for 10-15% of the total heat transferred to the drop. Neglecting it can therefore introduce errors.

Kramers (57) used steel spheres of 7.1, 7.9 and 12.6 mm diameter, suspended vertically by a pair of fine thermocouple leads in a vertical stream of air, water and oil. The spheres were heated by high frequency induction and maintained at a constant, uniform temperature. The experimental results were correlated by;

$$Nu = 2 + 1.3Pr^{0.15} + 0.66Re^{0.5}Pr^{0.37} \qquad 2.33$$

For,

$0.4 < Re < 2000$ and $0.7 < Pr < 400$

The second term on the right hand side of equation 2.33 was necessary to bring together the data for the different fluid streams. However, as pointed out by Rowe (59), the Prandtl term may be a result of disturbance by the high frequency field used for heating the sphere. It is also likely that temperature gradients at the surface of the spheres affected the physical properties of the liquids.

Tsubouchi and Sato (58) used an original technique to measure steady state heat transfer. They suspended thermistor spheres of 0.3 to 2 mm diameter in a wind tunnel. A current was supplied to the sphere and measurements of the voltage, current and resistance gave the amount of heat dissipated and the temperature. Their results, which should only be applied for Pr=0.71 at which the data were obtained, were correlated by

$$Nu = Nu_o + 0.29\ (Re^{0.5} + 1.41Gr^{0.25}) \qquad 2.34$$

which includes the effects of natural convection on forced convection at low Reynolds numbers.

A thorough investigation by Yuge (31) was carried out on metal spheres suspended in a wind tunnel. He compared the effects of cross, counter and parallel flow. Spheres less than 6 mm in

diameter were preheated in an electric furnace outside the wind tunnel before being introduced into the air stream. The larger spheres used (6-60 mm) were heated internally. The results were presented as

$$Nu = 2 + 0.493\ Re^{0.5} \qquad 2.35$$

for

$10 < Re < 1.8 \times 10^3$

and

$$Nu = 2 + 0.3Re^{0.5664} \qquad 2.36$$

for

$1.8 \times 10^3 < Re < 1.5 \times 10^5$

An index of four decimal places can only be justified if the experimental technique is very accurate so that the constants and exponents probably require rounding-up

Rowe et al (59) presented a review of heat and mass transfer to and from spheres in the range $10<Re<10^4$. Additional results were presented in which heat transfer was measured in air and water using internally heated copper spheres of 12.7 mm and 38.1 mm diameter. Mass transfer was also studied for the sublimation of naphthalene spheres in air and the dissolution of benzoic acid spheres in water. The results were presented as,

$$\text{For air} \quad Nu \text{ (or } Sh) = 2 + 0.69Re^{0.5}Pr^{0.33} (\text{or } Sc^{0.33}) \qquad 2.37$$

$$\text{For water } Nu \text{ (or } Sh) = 2 + 0.79Re^{0.5}Pr^{0.33} \text{ (or } Sc^{0.33}) \qquad 2.38$$

The higher coefficient of 0.79 for water could be due to uncertainties in predicting the diffusion coefficient in water.

2.2.5 Evaporation for Single Droplets in High-Temperature Surroundings

When a pure liquid drop evaporates there is a balance between the heat lost by the drop as a result of vaporisation and the heat transferred to the drop from the surroundings as a result of convection or radiation. In high temperature surroundings the sensible heat required to heat the vapour from the drop surface temperature to the gas temperature becomes significantly larger. There is therefore a reduction in the actual amount of heat reaching the drop surface. Ranz (60) in his study on the evaporation of a drop of liquid in high temperature surroundings showed that the heat reaching the surface of an evaporating drop may be as little as 25% of the total heat transferred, the rest being absorbed by the cold vapour in its radial flow from the drop. This therefore has to be taken into account in the heat balance. The same is also true for drops of solutions and slurries.

Marshall (61) studied droplet evaporation at air temperatures greater than 150° C. A differential equation was developed to describe the differential heat balance over a spherical shell through which heat is passing inwards towards the drop, whilst mass is passing outwards. This equation was solved to give the temperature T as a function of distance x through the gas film surrounding the drop.

$$\frac{T-T_s}{T_g-T_s} = \frac{\exp(-E/x)-\exp(-E/r_1)}{\exp(-E/r_2)-\exp(-E/r_1)} \qquad 2.39$$

Where $E = mCp/4\pi k_v$

r_1 = radius of the evaporating drop

r_2 = outer radius of the gas film

one obvious simplification was to ignore the variation in the thermal conductivity and heat capacity of the gas film caused by temperature and concentration gradients. However the effects of this would be small. The above equation was differentiated at the drop surface to yield an expression for the Nusselt number Nu.

$$Nu = \frac{2(E/r_1)}{\exp(E(\frac{1}{r_1} - \frac{1}{r_2})) - 1} \qquad 2.40$$

In the case of burning drops Godsave (62) showed that the value of the Nusselt number when evaporation occurred was $\frac{1}{4}$ the value for heat transfer to a non-volatile sphere. Thus, when simultaneous evaporation occurs the value of Nu can fall below the theoretical minimum value of 2 which means that the effective heat transfer calculated from equation 2.16 is too high when evaporation rates are high.

Hoffman and Gauvin (29) measured the rates of evaporation of stationary drops of water, methanol, cumene, pentane and benzene placed on the tip of a thin glass fibre in the centre of a electrically heated 229 mm diameter stainless steel sphere with a 9.5 mm wall. The gaseous environment consisted of the superheated vapour of the liquid under investigation and the wall and gas temperatures were in all cases the same. Drop diameters ranged from 0.4 mm to 1.4 mm and temperatures from 100° C to 500° C. The sphere had viewing ports on the sides and the evaporation rates were recorded photographically. The evaporation rate of stationary drops in high temperature surroundings did not appear to be governed by the rate of heat transfer by natural convection since there was no dependency of the Nusselt number on the Grashof number. The experimental data however was successfully correlated in terms of

Spalding's Transfer number B (63). The resulting correlation was

$$Nu = 3.2 \frac{B^{0.97}}{B'} Pr^{0.33} \qquad 2.41$$

Where

$$B = \frac{Cp\,\Delta T}{L_v} \quad \text{(Radiation not included)} \qquad 2.42$$

$$B' = Cp\,\Delta T / \frac{(L_v - Q_{rad})}{N_A} \quad \text{(Radiation included)} \qquad 2.43$$

However the equation is only valid when the gas and containing walls are at the same temperature.

Pei and Gauvin (64) used the same experimental technique as Hoffman and Gauvin (29). Porous celite spheres (6.35 mm - 12.7 mm diameter) were used to measure the rate of evaporation of water, benzene and methanol at temperatures between 204° C and 537° C. They found that the heat transfer was dependent on the parameter Gr/Re^2 and proposed the correlation

$$Nu = \frac{3.32}{B} (Re^{0.5} Pr^{0.33}) (Gr/Re^2)^{0.007} \qquad 2.44$$

However an exponent of 0.007 suggests that the results could have been correlated omitting this ratio.

The above experimental apparatus was modified by Pei et al (48) to provide a stream of superheated steam at 150° C to 750° C with a Reynolds number range of 5.5 to 510. The effects of natural and forced convection were demonstrated as non-additive and the transition from one to the other was gradual. It was concluded that natural convection was negligible when $(Gr/Re^2) < 0.2$ and forced convection was negligible when $(Gr/Re^2) > 10$. However a heat transfer equation was not proposed to account for this dependency.

Downing (65) studied the rates of evaporation of pure liquid drops evaporating in streams of high temperature air. 1 mm diameter drops of water, acetone, benzene or n-hexane were placed in an air stream at 27° C to 340° C with a Re range of 24 to 325. The resulting correlation was expressed as

$$Nu = MN (Ln (1 + B')/B') (2 + 0.6Re^{0.5}Pr^{0.33}) \quad 2.45$$

$$Sh = M (2 + 0.6Re^{0.5}Sc^{0.33}) \quad 2.46$$

Where

$$M = 1 - 0.4 (1-T_s/T_g) \quad 2.47$$

$$N = 1 - 0.4 (1 - ln (1 + B')/B') \quad 2.48$$

The average physical and transport properties were calculated at an average film temperature T_f, defined as

$$(T_f-T_s) = 0.6 (T_g-T_s) \quad 2.49$$

and therefore should only be used in this context.

Frazier and Hellier (66) studied the evaporation of Freon 113 drops in a high temperature air stream photographically. A stream of 440 μm diameter drops was passed through an air stream at 669° C. They concluded that the mass transfer was four times higher than that predicted by Ranz and Marshall's correlation (3).

However Crosby and Stewart (67) recalculated the results using the interfacial energy balance

$$N_A\lambda + Q_C + Q_R = 0 \quad 2.50$$

Where

Q_C = conductive heat flux into the gas phase

Q_R = net radiant flux from the drop

This holds for vaporisation from an isothermal drop. They found that the deviation was much smaller (33%) which is in good agreement, in view of the uncertainties in the measurement and in estimates of the physical properties of this system.

Toei et al (68) used a correlation ratio which was similar to the equivalent correction for the temperature in the vapour film used by Downing (65) to correlate their experimental results on the evaporation of water drops into superheated stream. Their data was correlated as;

$$Sh = \frac{(P_{bm})^{0.2}}{P}(2 + 0.65Re^{0.5}Sc^{0.33}) \qquad 2.51$$

where P_{bm} is the average partial pressure in the boundary layer.

Lee and Ryley (69) used a 50 μm diameter glass fiber to suspend drops of 230-1130 μm in a horizontal brass section. They studied the evaporation of water drops in superheated steam for Re numbers of 64-250 and steam pressures of 14.7-29 psia. The evaporation rates were measured using a microscope. The correlation found was similar to that of Ranz and Marshall (3).

$$Nu = 2 + 0.74Re^{0.5}Pr^{0.33} \qquad 2.52$$

Matlosz (70) studied experimentally and theoretically the evaporation of drops into a stagnant environment at high temperatures and pressure. Experimental drop temperature-time and radius-time histories were obtained for n-hexane drops evaporating in a nitrogen or argon environment. Drops of 720-910 μm or 1420-1780 μm were used at 286° C with gas pressures ranging from 6.8-102 atmospheres. They found that the effects of the non-ideal behaviour of the gas phase was important for the theoretical

predictions of drop temperature and radius versus time, especially at high pressures. At low pressures (6.2 atm) the effective molecular diffusion coefficient was in good agreement with the calculated molecular diffusion coefficient. However at 102 atmospheres the effective molecular diffusion coefficient was six times greater than the calculated molecular diffusion coefficient, suggesting that molecular mass transport may not be the controlling mechanism for the evaporation process.

Trommelen and Crosby (71) evaporated drops of water into air and superheated steam. Drops of 1.56 mm diameter were used in air streams of 1.5 to 2.1 m/s with the drying medium temperature ranging from 150° C to 250° C. The experimental procedure followed that of Charlesworth and Marshall (10), suspending a drop at the junction of a chromel-constantan thermocouple which was itself fixed to the end of a fine horizontal glass fibre. This technique enabled the simultaneous measurement of drop weight and temperature. Evaporation was found to take place more slowly in superheated steam than in air, but the difference decreased at higher temperatures. Their results confirmed the findings of Toei et al (68) and, like Lee and Ryley (69), confirmed that the accepted correlation for the heat transfer coefficient applicable for evaporation of small drops of pure liquid in air is also valid for evaporation in a superheated vapour. Their analysis took into account the heat transferred by radiation and conduction along the thermocouple wires. However by using the cross-sectional area of the wires rather than the area of the bead, they underestimated the surface area by a factor of four.

Audu (5) used a horizontal wind tunnel in which drops were suspended on the tip of a rotating nozzle to determine rates of evaporation. A temperature correction factor was proposed to account for the results at temperatures in the range of 26.5° C to 118.5° C.

$$Sh = 2 + 0.44 ((T_g - T_d)/T_{amb})^{-0.008} Re^{0.5} Sc^{0.33} \qquad 2.53$$

However an index of -0.008 is too small to have any significant effect.

Kadota and Hiroyasu (72) carried out a theoretical study on the evaporation of single drops in high temperature and pressure gaseous environments. A theoretical model which included the effects of natural convection, non-ideal behaviour and effects of high mass transfer rates on temperature and concentration profiles and boundary layer thickness was derived. Results from an earlier study (73) on the evaporation of drops of ethanol, n-heptane, benzene and water drops were found to be in good agreement with the model. Interestingly they found that radiative heat flow from the walls and conductive heat flow through the quartz thread shortened the lifetime of the drop by 15%.

Yuen and Chen (74) measured heat transfer rates of porous spheres saturated with water or ethanol in a vertical hot air tunnel. The experiments were limited to Reynolds numbers of 200-2000, air temperatures of 150-960° C and a velocity of 2.1 to 11.4 m/s. They correlated their data by,

$$Nu_f (1 + B) = 2 + 0.6 Re_m^{0.5} Pr_f^{0.33} \qquad 2.54$$

Where

$$Re_m = p_A V_A d_p / \mu_f \qquad 2.55$$

The experimental data therefore showed that at higher air temperatures, evaporation reduces heat transfer rates directly by a factor of (1 + B). However the study was limited to drops with a maximum B of 0.5.

Renkizbulut and Yuen (75) recently used the same experimental technique as above to measure heat transfer to single drops of water, methanol or heptane. Covering a larger Reynolds number range of 25 to 2000 and a Transfer number of 0.07 to 2.79, they correlated their results by,

$$Nu_f\ (1 + B_f)^{0.7} = 2 + 0.57\ Re_m^{0.5} Pr_f^{0.33} \qquad 2.56$$

However these techniques are subject to question because of total vapour pressure depression at micro-undulations and surface tension effects.

2.3 DROPS CONTAINING DISSOLVED AND SUSPENDED SOLIDS

Although work on the evaporation of pure liquid drops has been extensive, less work has been carried out on drops containing dissolved or suspended solids. This is the condition which exists within a spray drier and the lack of information is probably due to the complexities in analysing the heat and mass transfer processes after a crust has formed. Whereas, in the consideration of heat and mass transfer from a drop of pure liquid, conditions within the drop may be assumed to be uniform, they cannot be if there is a non-volatile material present.

The presence of dissolved solids and, to a lesser extent suspended solids, leads to a decrease in the vapour pressure of the liquid at the drop surface. The overall pressure driving force is thereby reduced, resulting in a reduction in the mass transfer rate. The surface temperature of the evaporating drop will consequently

increase above the thermodynamic wet-bulb temperature. The drying characteristics are then related to the formation of a solid phase on the surface of the drop. As the particle dries, the crust increases in thickness resulting in an increase in the resistance to heat and mass transfer. The nature of crusts encountered in spray drying also vary considerably. Crusts with low porosities, high porosities, or ones experiencing blow holes and fractures of the surface are often evident from electron microphotographs of industrially dried drops and single drops dried in laboratory equipment. The process is further complicated with some solutions when a film or membrane is formed prior to crust formation, thereby reducing the evaporation rate further.

It is often observed (76) that these materials undergo considerable deformation of the drop structure. Work on coffee drops has shown that the drop undergoes considerable inflation and deflation with protrusions becoming evident on the surface. The process can therefore be highly complex and very difficult to model mathematically.

Generally experimentation on drops containing solids has shown that evaporation proceeds at a constant rate (77,78). In this period drying proceeds by diffusion of the vapour from the saturated surface through a gas-film around the drop into the environment. The surface is kept saturated as long as moisture movement from within the material is sufficiently rapid to maintain a completely wet surface. When the drop's moisture content falls below a critical value termed the 'Critical Moisture Content', a solid crust commences from a preferential site, usually the point of maximum mass transfer, and spreads around the drop. As the crust thickens, its resistance to mass transfer becomes rate controlling and the

evaporation rates falls. This period is termed the 'Falling Rate Period'. This period is usually divided into two zones; the zone of unsaturated surface drying and the zone where internal moisture movement controls. In the first zone, the entire evaporating surface can no longer be maintained saturated by moisture movement from within the drop. Wet patches exist on the surface and the drying rate decreases from the unsaturated portion and hence the rate for the total surface decreases.

As drying proceeds, the point is reached where all the exterior surface is unsaturated. The plane of evaporation recedes into the solid, and the drying process enters the second falling-rate period. The drying rate is now governed by the rate of internal moisture movement with the influence of external variables diminishing. This period usually predominates in determining the overall drying period.

2.4 MECHANISMS OF MOISTURE MOVEMENT THROUGH POROUS MEDIA

The manner in which moisture moves through a solid and hence out into the air during the drying process is termed the "mechanism" of drying. This mechanism is of considerable practical interest in industrial drying since it determines the particular variables which are likely to govern the rate of drying and the quality of the product.

There are three generally accepted theories which have been proposed for the migration of moisture in porous media, the Diffusion Theory, Capillary Flow Theory, and the Evaporation Condensation Theory. Moisture may also be distributed or moved in a solid during drying by the action of gravity, by external pressure and by convection. The force of gravity tends to pull water to the bottom of the solid. This distribution is effective where the

interstices are large and interconnecting. Gravity acts only vertically, whereas diffusion acts in the direction of decreasing concentration, and capillarity in the direction of decreasing capillary diameter. Temperature differences within a solid effect a change in the rate of flow of a liquid by diffusion, capillarity, or gravity; they may also cause movement by convection.

2.4.1 Diffusion Theory

Diffusion has been proposed as the major mechanism of moisture movement by a number of workers (77,79). Based on this theory Sherwood (78) regarded the drying process as taking place in two different ways.

(i) Diffusion of the liquid from the interior to the solid surface, followed by evaporation of the liquid at the surface and diffusion of the vapour into the surrounding air; or

(ii) Evaporation of the liquid at a point beneath the surface of the solid, followed by diffusion of the water vapour through the pores to the surface and into the ambient air.

The limitations of this theory lie in the difficulties encountered in solving the diffusion equations for the case of variable diffusivities and when shrinkage occurs.

2.4.2 Capillary Flow Theory

The concept of a capillary potential rather than a concentration potential was laid down by Buckingham (80). Capillarity refers to the flow of a liquid through the interstices, and over the surface, of a solid due to molecular attraction between the liquid and the solid.

The outer surface of a porous solid has pore entrances of various sizes. As liquid is evaporated from the surface during the

constant rate period, a liquid meniscus is formed across each entrance and capillary forces are set up by interfacial tension between the liquid and solid. These forces draw liquid from the interior to the outer surface. At the critical moisture content, some of the menisci begin to retreat into the pores. The wetted outer surface gradually decreases and, although the drying rate per unit area of wetted outer surface remains constant, drying rate based on total outer surface decreases. This stage of unsaturated surface drying of porous materials is the first falling rate period. During this stage, gas begins to enter the pores, but the internal liquid phase is continuous; the liquid is said to be in the funicular state. If the pores are small and not of uniform size, the retreat of the liquid phase is not uniform. Small pores produce stronger capillary forces than larger pores, thus small pores draw liquid out of large pores. As more liquid is removed, the outer surface dries completely and a point is reached where there is not enough internal liquid left to maintain a continuous phase linking all interior pores. Residual liquid retreats to isolated pockets in the smallest pores, and gas enters far enough into the material so that gas forms the continuous phase. The liquid then obtains the 'pendular state'. This point is the second critical moisture content in porous materials because there is a second break in the drying rate profile. All heat for vaporisation must now pass by conduction through the material to the liquid pockets, the temperature rises, and the residual liquid vaporises and diffuses in the gas phase to the surface.

2.4.3 Evaporation-Condensation Theory

When a temperature gradient exists in a solid, there may be vapour pressure gradients set up which result in evaporation of the

liquid and its subsequent condensation on a colder surface. For example, when a wet solid is heated at its bottom surface and dry air is circulated over the top, vaporisation may occur at the bottom where the temperature is highest, and the vapour diffusing upward may be repeatedly condensed and vaporised before finally escaping as vapour into the air.

Gurr et al (81) and others (82,83) have proved this assumption valid for systems subjected to a temperature gradient. Harmathy (84) developed a model based on this theory to successfully predict the drying rates of clay bricks.

2.5 LITERATURE REVIEW FOR DROPS CONTAINING SOLIDS

The drying of drops containing dissolved solids is of great importance for the design of spray driers. Fundamental information has been obtained from single drop drying studies concerning the heat and mass transfer processes occurring during drying. More recently there has been a growing interest in particle morphology and the factors which affect this. The particle morphology affects the packing density of the final product. It also affects drying rates and may also influence rehydration characteristics and volatiles loss. Hence it may characterise product quality.

In comparison to pure liquid drops, there is a scarcity of data for drying of drops containing solids. Of these studies, the earliest work focused on drops drying whilst suspended on the end of a filament or a thermocouple. This technique was originally developed by Ranz and Marshall (3) and modified by Charlesworth and Marshall (10). It has subsequently been used by a number of investigators (11,12). Variations on this theme include drops drying in free flight and more recently (8) being held in an ultrasonic wave field.

2.5.1 Single Drop Studies

Ranz and Marshall (3) studied the evaporation of solutions of ammonium nitrate and sodium chloride, a non-soluble, suspended green dye and reconstituted dried whole milk. Drops were suspended on the tip of a glass filament or a thermocouple. Evaporation rates and drop temperatures were therefore measured in separate experiments. A simplifying assumption was made that during the constant rate period the drop surface was saturated regardless of the average concentration of the drop. Experiments with solutions of ammonium nitrate confirmed this although using calcium chloride solutions of four different initial concentrations, this hypothesis was later tested and challenged by Charlesworth and Marshall (10). Experiments with the inert dye proved that the vapour pressure lowering effects were negligible for suspended solids. Ranz and Marshall pointed out the difficulties in trying to model the drying of drops containing solids with complications due to heats of solution and crystallisation, and changes in density and shrinkage during drying.

Charlesworth and Marshall (10) carried out a comprehensive study on the drying of sixteen different systems. A balance was used which enabled the weight of a drop to be measured at intervals throughout the course of the drying. The main element of this balance was a glass filament 43 cm in length tapered from a diameter of 425 μm at its fixed end to 210 μm at its free end. The large end was fixed to the vertically travelling micrometer stage of a cathetometer. Welded at right angles to the free end was a 3.2 cm suspension filament. This consisted of a vertical glass filament 340 μm in diameter with a 200 μm knob upon which the drops were placed. The weight of the drop was measured by measuring the

vertical distance through which it was necessary to raise the fixed end of the weighing filament so that the free end was restored to its zero position. The experimental technique used had the disadvantage that the air flow to the drop had to be stopped for about ten seconds to enable weighing of the drop. They stated that this interruption in the flow did not noticeably affect the results. As with Ranz and Marshall's work, separate temperature and weight experiments were performed.

An equation was proposed for predicting the time of complete formation of a solid crust with the following simplifying assumptions,

(i) The droplet was at its wet-bulb temperature.

(ii) The initial evaporation rate was equal to the rate of evaporation of a pure water drop of the same size as calculated from the mass transfer correlation of Ranz and Marshall.

However both these assumptions are invalid when the dissolved solid causes an appreciable lowering of the vapour pressure from that of a pure water drop under the same conditions. Miura et al (85) found that the equation proposed by Charlesworth and Marshall (10) was reasonably accurate giving values 8% to 11% greater than calculated values.

Charlesworth and Marshall from their observations, presented a generalised description of the drying of a drop as shown in Figure 2.1. Up to the point of crust formation, the characteristics were similar irrespective of the solute concentration and drying conditions. After crust formation however, the behaviour of the drop was entirely controlled by the nature of the crust and whether

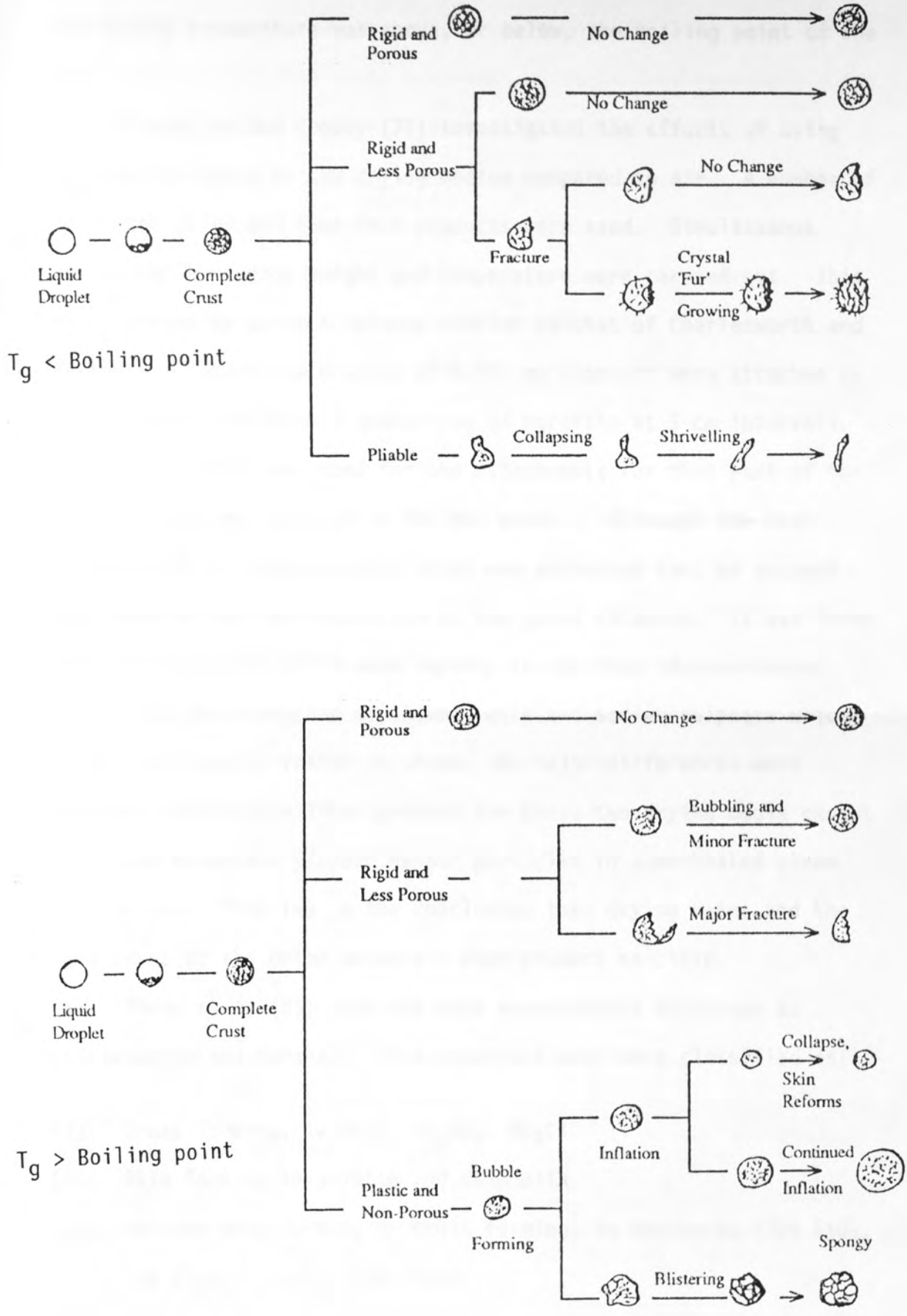

Figure 2.1 Drying Characteristics of Single Droplets (10)

the drying temperature was above, or below, the boiling point of the drop.

Trommelen and Crosby (71) investigated the effects of using superheated steam as the drying medium compared to air. A number of inorganic salts and four food products were used. Simultaneous measurements of drop weight and temperature were carried out. This was achieved by using a balance similar to that of Charlesworth and Marshall. Thermocouple wires of 0.051 mm diameter were attached to the filament with minute quantities of paraffin at 3 cm intervals. A silicone cement was used for the attachments for that part of the balance which was exposed to the hot gases,. Although the heat conducted by the thermocouple leads was accounted for, no account was taken of the heat conducted by the glass filament. It was found that all materials dried more rapidly in air than in superheated steam with the exception of skimmed milk and sodium sulphate which dried considerably faster in steam. No major differences were observed between the final product for these two drying media except that some materials yielded denser particles in superheated steam than in air. This led to the conclusion that drying rates and the structures of the dried materials were product specific.

Miura et al (85) used the same experimental technique as Charlesworth and Marshall. The materials used were classified as;

(i) Crust forming, ie NaCl, Na_2SO_4, NH_4Cl

(ii) Skin forming ie gelatin and skim milk

(iii) Neither skin-forming or crust forming, ie Bentonite (70% SiO_2, 15% Al_2O_3 + Fe_2O_3, CaO, MgO).

At an air temperature of 150° C they observed that an aqueous sodium sulphate drop dried at an initial constant rate until the

crust formed, then a falling rate proceeded. After the crust was completely formed, the inner temperature of the drop rose, until the crust was broken by a 'sort of boiling' and water appeared on the surface. This was followed by another constant rate period. When this boiling phenomena came to an end, the water in the drop was almost totally evaporated and the drying rate accordingly decreased until the end of drying. At a lower air temperature of 99° C, nearly the same phenomena as above was observed, but crust bursting by boiling did not occur. Skimmed milk drops clearly showed the transition from constant rate to a falling rate if the initial moisture content was high. However this distinction between the rates was not so clear at low initial moisture contents. At high air temperatures (>100° C) the drop was observed to inflate after skin formation. This was not observed at low air temperatures (<100° C). With Bentonite, the drying rate was identical to that of pure water drops for all temperatures and initial moisture contents. They proposed a model to predict skin thicknesses based on a material balance on the solids within a drop,

$$Y-1 = \frac{1-X^3}{3AX^2-3A^2X+A^3} \qquad 2.57$$

Where

X	=	r_d/r_{do}	=	dimensionless diameter
Y	=	C/C_o	=	dimensionless concentration
A	=	a/r_{do}	=	dimensionless thickness
a	=	thickness of skin		mm
r_d	=	radius of the drop		mm
r_{do}	=	initial drop radius		mm
C	=	concentration of solute		g solute/ml
C_o	=	initial concentration of solute		g solute/ml

However the model was derived on the basis of a similar density for the crust and core which is a gross over-simplification. No precise

measurements of skin thickness were obtained.

Audu and Jeffreys (86) studied the drying of sodium sulphate and detergent drops in a horizontal wind tunnel. They proposed a crust mass transfer coefficient k_c, expressed as;

$$k_c = \frac{DE^{1.5}}{\beta} \qquad 2.58$$

Where D = molecular diffusivity. m^2/s
E = crust porosity
β = crust thickness m

The concept of a crust coefficient is based on the fact that once a crust forms, the heat and mass transfer paths are different and the Colburn (87) analogy no longer applies. They found experimentally that the crust resistance accounted for as much as 64.2% of the total resistance for sodium sulphate drops and 97.5% for detergent drops. The disadvantage of this experimental technique is that the stainless steel nozzles used for suspending the drops were of the same size as the drop (2mm). There would therefore be a substantial amount of heat being conducted into the drop via the suspension device. This was not taken into account. The rates of evaporation were also determined by using a hygrometer to measure changes in air humidity before and after the drop and were therefore dependent on instrument accuracy. No drop temperatures were measured. A crust thickness model was proposed based on a mass balance of moisture in the surrounding air. However this model predicted values as much as 20% higher than experimental results.

The above apparatus was used by Ali (7) with a slight modification to the nozzles used. Again no account was made for conduction along the nozzle, or radiation from the surrounding chamber. Ali et al (88) found that for solutions of sodium sulphate decahydrate and various organic dyes the crust thickness growth rate increased with an increase in air mass flowrate, air temperature and the initial moisture content. The crust structure when examined under a Scanning Electron Microscope (SEM) showed a variation. Some crusts were crystalline porous, rough non-crystalline, or very smooth and less porous. Hence the drying rate after crust formation was, and in all practical drying will always be, specific to the product under consideration.

Duffie and Marshall (89) spray-dried a number of materials including inorganic salts, a water dispersible organic dyestuff, a dispersing agent, whole milk, gelatin, coffee extract and corn syrup. They studied the effects of drying air temperature, liquid feed temperature and feed concentration on the bulk densities of the products. From the observations of the dried product characteristics they were able to postulate four factors which contributed to the formation of hollow particles;

1) Hollow particles may result from the rapid formation of a vapour-impervious film on the drop surface causing 'puffing' when the vaporising moisture within cannot readily escape.
2) Internal voids may be created when the rate of evaporation exceeds the rate of diffusion of solids back into the drop.
3) If a rigid porous shell is formed initially, capillary suction draws liquid and solids to the surface thereby creating sub-atmospheric pressures and internal voids. The particle may eventually collapse.

4) Entrained gases in the feed can result in the formation of hollow particles.

Materials were classified according to their particle structure, ie film forming or crystalline materials, but it was observed that the mechanism of hollow particle formation may be different with each classification.

Basing their work on the experimental results of Van der Lijn (90), who introduced a concentration and temperature dependent diffusion coefficient, Wijlhuizen et al (91) proposed a 'solid sphere' and 'hollow sphere' model for an evaporating drop of skimmed milk. The 'hollow sphere' model assumed an initial gas bubble of known size in a drop and a uniform concentration profile. Using the necessary boundary conditions, the diffusion equations were solved to predict moisture concentrations and drop temperatures during drying. The model does not however allow for the formation of a crust which limits its usefulness, particularly in the falling-rate period which is of primary concern in a spray drier.

Haertling (92) proposed a model to predict the drying rates of porous hygroscopic materials such as clay brick and burned clay. The model assumes that mass transfer in the clay occurs by a simultaneous process of vapour diffusion and liquid moisture movement by capillary suction. The model however, over-estimates the drying rates of low porosity clay brick and burned clay by about 21%, particularly at high temperatures. This suggests that liquid moisture migration by capillary suction is less significant in low porosity materials.

A momentum heat transfer model was developed by Esubiyi (93). This was based on an assumed vapour velocity through the pores of a solid crust described by the Kozeny equation (94) with the crust

coefficient k_c, expressed as

$$k_c = \frac{E^3 p_c}{5(1-E)^2 \mu S_b^2 \beta} \qquad 2.59$$

The validity of this model was confirmed by using five different sources of Portland cement.

Sano and Keey (11) developed a model to describe the drying of single drops containing colloidal material to produce solid hollow spheres. The mechanism for the formation of hollow spheres was based on the assumption that once the equilibrium vapour pressure of the moisture inside the drop exceeds the pressure of the ambient air, the particle inflates instantaneously and ruptures. After inflation, two limiting ways of deformation were proposed;

(i) The maximum radius remains constant, but the void radius increases due to moisture loss; or

(ii) The void radius does not change, but the outer radius shrinks.

Using an experimental technique similar to Charlesworth and Marshall (10) they found that for the drying of drops of skimmed milk at 100° C to 150° C, the second proposal gave the best approximation to the experimental results. Theoretical computations, however, required an experimentally determined inflation ratio, which was the ratio of the maximum radius after inflation to the initial radius. Although their results were computed with an inflation ratio of 0.88, they found that a ratio of 1.1 was required to fit the data of Trommelen and Crosby (71), for the same material and temperature.

Sano and Yamamoto (95) used the basis of the above model to predict the drying rates of drops of polyacrylonitrile in dimethyl

formamide assuming a receding interface and a constant concentration distribution. A modified diffusion coefficient, derived empirically, had to be used to fit the data.

Cheong (4) recently developed a model based on a receding interface to describe the drying of drops in the falling rate period. A unique thermocouple was developed which overcame the drawbacks of Charlesworth and Marshalls' (10) technique. Single slurry drops of sodium sulphate decahydrate of 1-1.5 mm diameter were dried over a temperature range of 20-78° C. An interesting observation was made of the drop core temperature at 33° C. There was a drop in the core temperature due to the enantiomorphic changes occurring with the decahydrate at 33° C (96). When this was taken into account the model gave good agreement with the experimental results. It is interesting to note that Ali (7) also studied the drying of drops of sodium sulphate decahydrate at similar temperatures. However in his study a thermocouple was inserted into the drop to measure the temperature, which failed to detect the change in the drop temperature at 33° C. This highlights the advantage of the thermocouple/glass filament developed by Cheong (4).

More recently Nescic (97) used the technique of Charleworth and Marshall (10) to study the drying of drops containing solids. A mathematical model, based on a number of simplifying assumptions, was derived to describe the whole drying process including the heating up period, equilibrium evaporation, growth of crystal formation and boiling. Experimental results and mathematical predictions were in good agreement for a number of materials including colloidal silica, sodium sulphate and skimmed milk.

2.5.2 Evaporation from Sprays of Drops

The foregoing developments for the rates of evaporation and the drying times of drops apply only to the case of a drop or drops of a uniform initial diameter. However, under actual conditions of spray drying, an atomiser produces a spectrum or distribution of drop sizes, and consequently the drops will evaporate or lose moisture at varying rates depending upon their initial diameters. Further, the smallest drops will lose their moisture first and so will be subject to overheating and possible degradation by prolonged exposure to high temperatures. Conversely excessively large drops will require an inordinately longer time than the average and will, therefore, constitute the controlling time in the drying process.

The problem of estimating the total evaporation time for a spectrum of drops is complicated, among other things, by the fact that information is required on the drop-size distribution created by the atomiser. Although the same basic theories apply to both sprays and single drops, any analysis of spray evaporation must consider.

(i) The relative velocity between the air and drops (if significant).

(ii) The particle trajectories.

(iii) The droplet population density.

(iv) Spray representation by a mean diameter and/or drop size distribution.

(v) Droplet or particle agglomeration eg, near the atomiser.

2.5.3 Sprays of Pure Liquids

Probert (98) made a mathematical analysis of the variation of the size distribution in a fuel spray which was assumed to follow the Rosin-Rammler distribution function (99), Assuming no relative

velocity and a simple expression for the heat transfer coefficient, equations were derived for the variation of the mass median diameter with time under various conditions of spray uniformity and also for the relation between the percentage of spray unevaporated with time. From the calculations it was concluded that a spray with a narrow size distribution and small mass median diameter would evaporate completely in a shorter time than would a spray with a wide size range and a larger mass median diameter.

Considerations of spray evaporation in which a relative velocity occurred were made by Fledderman and Hanson (100) who assumed a Nukiyama - Tanasawa distribution function (101). However no usable results were developed.

A comprehensive stepwise method for the evaluation of spray evaporation was proposed by Marshall (61). The size distribution was divided into small size groups, which enable the change in the average drop diameter in each selected group to be calculated over short time intervals. Although the method was only presented for pure liquid drops at zero relative velocity, the results are useful in illustrating the nature of changes likely to take place in a drier. For example it predicted that in the majority of spray drying operations 90% of the evaporation will be completed during the first 1.5 seconds, and that during this period the air temperature will fall to within 17°C of the outlet temperature.

Dloughy and Gauvin (102) conducted an investigation on evaporation rates in spray drying, by progressively following the evaporation of a spray of water drops down a purpose-built co-current spray drier. They considered the drying chamber to consist of three distinct zones; the nozzle zone, in which drops decelerate from their initial release velocity to their terminal settling velocity,

the evaporation zone, where the mechanism of evaporation is the same as that from a free liquid surface (ie the constant rate period) and finally the drying zone in which moisture diffusion through the crust becomes the controlling factor (ie the falling rate period). In order to calculate the rates of heat and mass transfer in the evaporation zone, samples of air and water drops were taken at a succession of points down the tower and instantaneous heat and mass transfer coefficients were calculated from energy and material balances. They concluded that the presence of the drops as a spray had no influence on the rate of evaporation. Furthermore, for the range of drop sizes considered in the study (11.5-38.5 μm), the heat and mass transfer coefficients were the same as for single stationary drops evaporating in still air (ie Nu=Sh=2.0). This was attributed to equal eddy diffusivities of the drops and the surrounding air, resulting in a negligible relative velocity. Although the evidence presented appears to be conclusive, it is doubtful whether it can be extended to include the much larger drops that may be present in industrial driers.

The conclusions drawn by Dloughy and Gauvin (102) were in fact contradicted by Bose and Pei (103) in a later study. Both of these studies were similar in nature but a larger range of drop size (40-125 μm) was considered in the latter investigation. Repeating the procedure of Dloughy and Gauvin, Bose and Pei found that their experimentally determined values of heat and mass transfer coefficients could not be adequately correlated by Nu=Sh=2.0. They therefore proceeded to evaluate droplet relative velocities and compared their experimental coefficient values with the Ranz and Marshall correlation (3). A much better agreement was obtained, suggesting that the effect of relative velocity existing between the

drop and the surrounding air is not negligible. They concluded that for industrial applications, where the drop diameters have a wider distribution, relative velocities between the air and the drop must be taken into consideration in the calculation of heat and mass transfer effects.

Manning and Gauvin (104) developed a useful measuring technique in their study of the heat and mass transfer characteristics of water sprays in concurrent and crosscurrent air flows. Spray evaporation was measured by a colourimetric method using a red dye and the drop size distribution was determined using an immersion cell containing varsol. However there was considerable scatter amongst the experimental data. This may have arisen, in part, due to the uncertainty in predicting relative velocities and drop sizes in the vicinity of the atomising nozzle.

Dickinson and Marshall (105) conducted a computational study on the rates of evaporation of sprays with non-uniform drop size distributions. They considered the cases of negligible and appreciable relative velocities with respect to the evaporation rates. In order to simplify the modelling, certain assumptions were made. These included an ideal air flow (ie no backmixing) and, more importantly that the spray comprised drops of pure liquid (implying that the drop temperatures remained constant at the wet-bulb temperature). Nevertheless, the study did highlight several significant phenomena. For sprays moving at negligible relative velocity the investigation showed that

(i) The drying air temperature falls as the spray evaporates, resulting in a decrease in evaporation rate.

(ii) Sprays with less uniform drop size distributions evaporate more rapidly at first than more homogeneous sprays with the same mean diameter. This is because the smaller drops present, evaporate at higher rates. However the less uniform sprays take much longer to effect complete drying because of the larger drops that are present.

(iii) No mean diameter can adequately characterise a spray with respect to evaporation; two sprays with the same mean diameter but with different drop size distributions will almost certainly take different lengths of time to evaporate. Hence the drop size distribution must be taken into account.

(iv) The size distribution of drops changes during evaporation: for non-uniform sprays the mean diameter first increases initially and then decreases until completion of evaporation.

For sprays moving with significant relative velocity the study highlighted additional features:

(i) To achieve a given degree of evaporation the spray must travel a far greater distance. This is because the residence time of such sprays in a given length of tower is less than for drops travelling at their terminal velocities.

(ii) The effect of relative velocity is more significant at higher initial velocities and at higher drying temperatures.

(iii) For high initial velocities, the relative error in neglecting drop velocity is greatest for small drops. This is because such drops evaporate extremely rapidly and a large proportion of the evaporation occurs during droplet deceleration.

Miura et al (53) studied the evaporation rates from a water drop surrounded by glass beads. The effects of drop to drop interaction were measured and the effects of diameter and distances between the surface of the drop and the glass bead were investigated. The experiment was set up in three ways as shown in Figure 2.2. The water drop and glass beads were set up in series, parallel and in a zig-zag pattern. They proposed that

SERIES

$$b/d_g < 2 \quad \frac{Nu}{Nu_o} \text{ or } \frac{Sh}{Sh_o} = 0.71\,(b/d_g)^{0.25}(d_p/d_g)^{0.67} + 0.07 \qquad 2.60$$

$$b/d_g > 2 \quad \frac{Nu}{Nu_o} \text{ or } \frac{Sh}{Sh_o} = 0.42\,(b/d_g)^{0.125} + 0.41 \qquad 2.61$$

PARALLEL

$$b/d_g = 1 \quad \text{ie, no effect of the beads} \qquad 2.62$$

ZIG-ZAG

$$d_p/B < 2 \quad \frac{Nu}{Nu_o} \text{ or } \frac{Sh}{Sh_o} = 1 \qquad 2.63$$

$$d_p/B > 4 \quad " \text{ or } " = 0.57 \qquad 2.64$$

2.5.4 Sprays of Drops Containing Dissolved and Suspended Solids

The presence of solids leads to a lowering of the vapour pressure. The extent of the lowering, and the resistances to moisture transfer, will vary throughout the size distribution. As evaporation proceeds, the concentration of solids in the smaller drops increases much faster than in the larger drops, resulting in a wide variation in the concentration driving force. The appearance of the solid phase on the surface of the drop is also varied for different drops. The analysis is therefore highly complex and investigations in this field are limited.

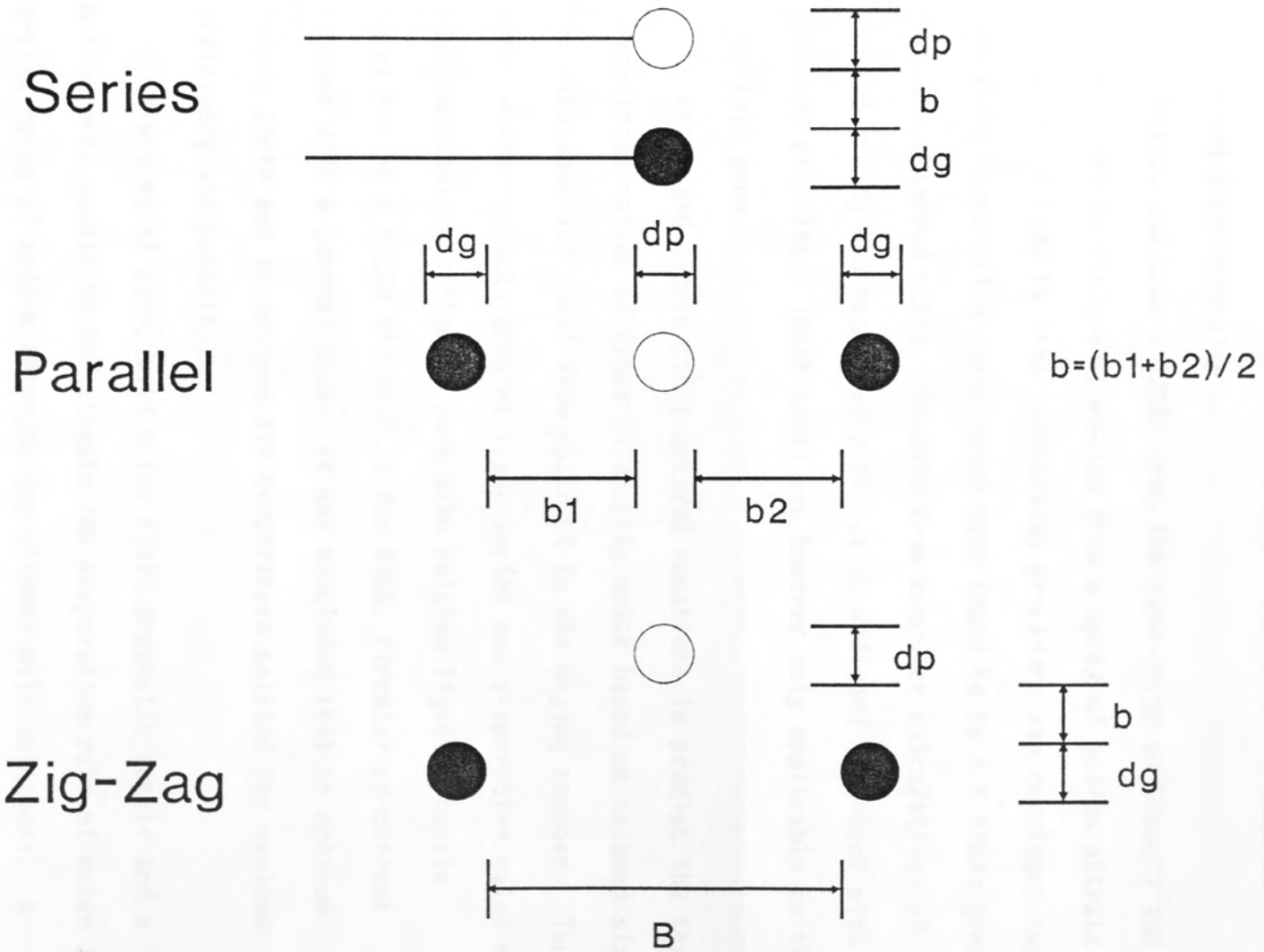

Figure 2.2 Drop to Drop Interaction Studies (53).

Dloughy and Gauvin (102), using techniques similar to Manning and Gauvin (104), investigated the evaporation of sprays of calcium lignosulphonate solution in a cocurrent drier. Accurate prediction of the drying rate curve was achieved employing the stepwise method of calculation proposed by Marshall (61). However, their method requires a knowledge of drop size distribution which must be determined experimentally.

Baltas and Gauvin (106) used the same drier as Dloughy and Gauvin (102) to study evaporation from a spray of sodium nitrate solution. A step by step prediction procedure was developed to calculate evaporation rates which were found to be 3.5 times greater than the observed rates. Results from computer calculations of local humidity and mass flow profiles showed good agreement with observed profiles. Their model was however only applicable to the free fall zone.

Katta and Gauvin (107) derived equations to predict the three-dimensional motion of drops in a spray drier based on assumed size distributions and ideal flow patterns in the drying chamber. The model which predicts droplet trajectories and evaporation rates was experimentally verified by work with calcium lignosulphonate solutions in a 1.22m diameter, 1.83m high, circular co-current chamber with a conical base. It was concluded that an optimum nozzle depth and an optimum air temperature existed for maximum efficiency and capacity.

Miura et al (108) used a two fluid pneumatic nozzle and a hollow cone nozzle to investigate the evaporation rate of water and drying rates of sodium chloride and skimmed milk solutions. A Nukiyama-Tanasawa distribution was assumed in their analysis and the results more accurately correlated by equations 2.60 and 2.61 for

evaporation in a spray cloud, than by Ranz and Marshalls correlation for single drops (3).

2.5.5 Temperature of Evaporating Drops

The surface temperature of a drop is required to define the temperature driving force so that rates of evaporation or evaporation times can be estimated. For pure liquid drops when dynamic equilibrium is established between the rates of heat and mass transfer, a simple heat balance yields

$$Q_{In} = -N_A L_v \qquad 2.65$$

On substitution of the various quantities, the above equation can be rearranged to give the surface temperature of the drop T_s as;

$$\frac{T_g - T_s}{P_s - P_g} = \frac{k_g A_m L_v}{h_g A_h} \qquad 2.66$$

where A_h and A_m are the respective areas for heat and mass transfer. If these are taken to be equal, the familiar expression for the surface temperature or the wet-bulb temperature is derived;

$$\frac{T_g - T_s}{P_s - P_g} = \frac{k_g L_v}{h_g} \qquad 2.67$$

The effect of dissolved solids is to lower the vapour pressure of the solution below that of pure water. The temperature of the drop will therefore be higher than that predicted from the wet-bulb temperature for water at its normal vapour pressure. This vapour pressure lowering effect is dependent on the nature of the dissolved solids. When a drop contains insoluble solids, there are negligible vapour pressure lowering effects and the surface temperature will

initially approximate that for a pure liquid drop. However in both cases, the solid crust formed presents an additional resistance to mass transfer with a rise in the sensible heat content of the core and the core temperature rising above the saturated wet-bulb temperature.

The effects of crystallisation of the dissolved or suspended solids can also be important in estimating the surface temperature when the heat of crystallisation is large. For example the heat of crystallisation for solutions of ammonium nitrate is 20% of the latent heat of vaporisation (109).

2.5.6 Measurements of Drop Temperatures

As shown in section 2.5.5. it is important to measure the temperature of evaporating drops. The earliest work on single drop studies, notably that of Ranz and Marshall (3) and Charlesworth and Marshall (10) measured the heat and mass transfer histories separately of evaporating drops. Thermo-elements of manganin - constantan wire of 0.5 mil to 2 mil were embedded into the drop. This technique of measuring the drop temperature was adopted by other investigators (11,12).

Trommelen and Crosby (71) were the first investigators to carry out a simultaneous measurement of drop weight and drop temperature. They used a glass filament to suspend the drop and attached a chromel-constantan thermocouple to this filament to measure the drop temperature.

In a development to the above methods, Cheong (4) combined the glass filament and thermocouple wires to create a unique filament/thermocouple to measure the heat and mass transfer rates simultaneously. A 50 μm nickel wire was inserted into a hollow glass filament of ~0.2 mm outer diameter. The whole filament was

coated with copper by a vacuum technique and, by leaving a small amount of copper wire at the tip of the filament, a junction was created upon which the droops could be suspended. However by using 0.5 mm length junctions for 1-1.5 mm drops a substantial portion of the drops cross section was covered and an average drop temperature rather than the core temperature was measured.

Equipment which has been used for studying drops in free flight (6) suffers from the disadvantage that no measurements of drop temperatures can be made. This seriously affects their usefulness.

2.5.7 Heat Conducted by Suspension Devices

The suspension devices used for single drop studies provide a natural path for conduction of heat into the core of a drop. In order to avoid errors this extra heat term has to be accounted for.

Fuchs (44) found that for typical experimental conditions of drop diameters of 1 mm and wire diameters of 25 μm, the ratio of heat flux through the wire to that through the gaseous medium may have values as high as 0.8 for copper constantan and 0.04 for quartz and glass fibres. Clearly therefore when measuring drop temperatures by inserting thermocouples into the drop, a significant proportion of heat may be conducted into the drop. Cheong (4) stated that at an air temperature of 79°C and a drop diameter of 0.5 mm, heat conducted by the filament and radiation from the surroundings accounted for 24.7% of the total heat transferred to the drop. However the magnitude of the individual terms was not given.

A number of investigators took no account of this extra heat term. In particular the nozzles used by Audu (5) and Ali (7) for their studies were made of stainless steel and were of the same

order of size as the drop. 33% of the area of the hemisphere was therefore in contact with the nozzle and a significant proportion of heat would be expected to have been conducted into the drop.

2.5.8 Drop Temperature Histories

Ranz and Marshall (3) and Charlesworth and Marshall (10) used the same experimental technique of embedding a thermoelement junction into a suspended drop to measure the drop temperature. Their technique could not be used to measure simultaneous heat and mass transfer effects. Ranz and Marshall followed the temperature histories of drops of sodium chloride and ammonium nitrate. They found that these drops evaporated with a surface temperature corresponding to that of the saturated solution even though the initial concentration was less than saturation. This is probably due to the fact that there is a lowering of the vapour pressure when solutions of these materials are used. However this lowering of the vapour pressure is only slightly affected by the concentration of the solution. Although sensible heat transferred from the feed solution was accounted for, no allowance was made for conduction along the thermocouple leads.

Trommelen and Crosby (71) measured the temperature histories of clay slurries, inorganic salts and food products. They found that, unlike clay slurries and inorganic salts, the food products exhibited no constant temperature period. The temperature histories were also interrupted by fracture, inflation and collapse which varied from one drop to another as shown in Figure 2.3.

Miura et al (85) suspended drops of inorganic salts, skimmed milk and bentonite from a quartz filament of 0.3 mm diameter and measured the drop temperature by inserting a 40 μm manganin-constantan thermocouple into the centre of a drop. For sodium

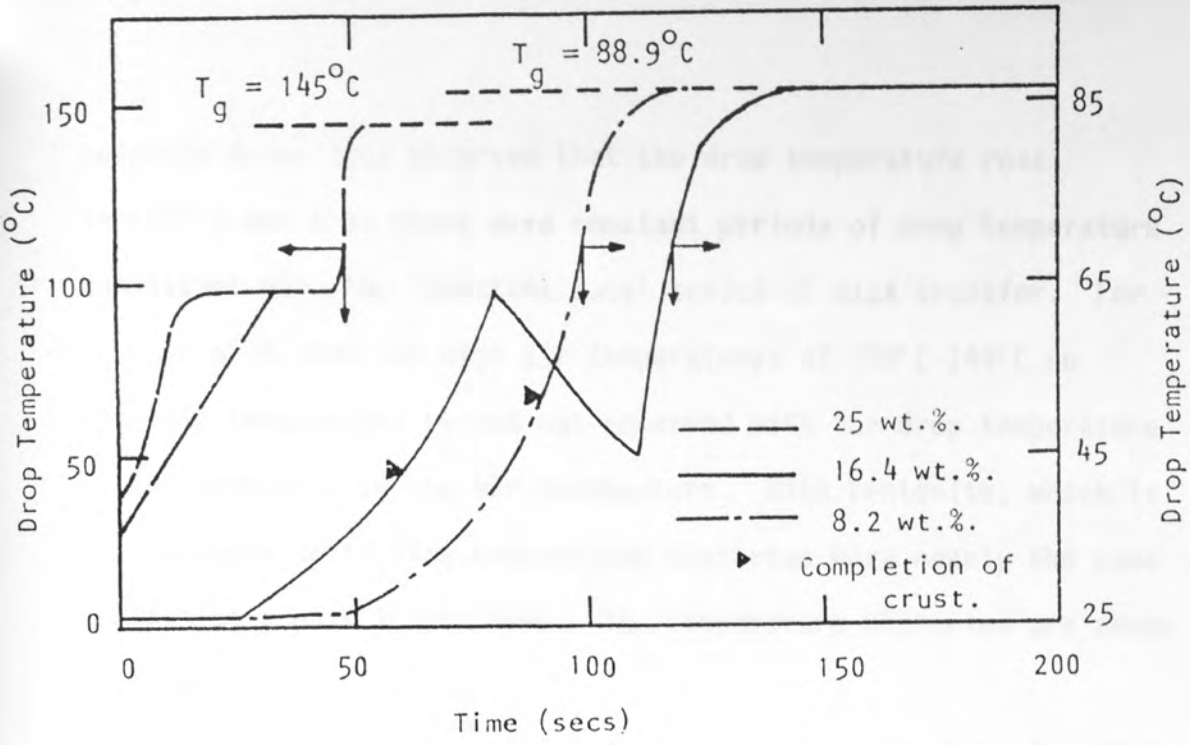

Figure 2.3 Drop Temperature Histories for Aqueous Sodium Sulphate (71) Decahydrate

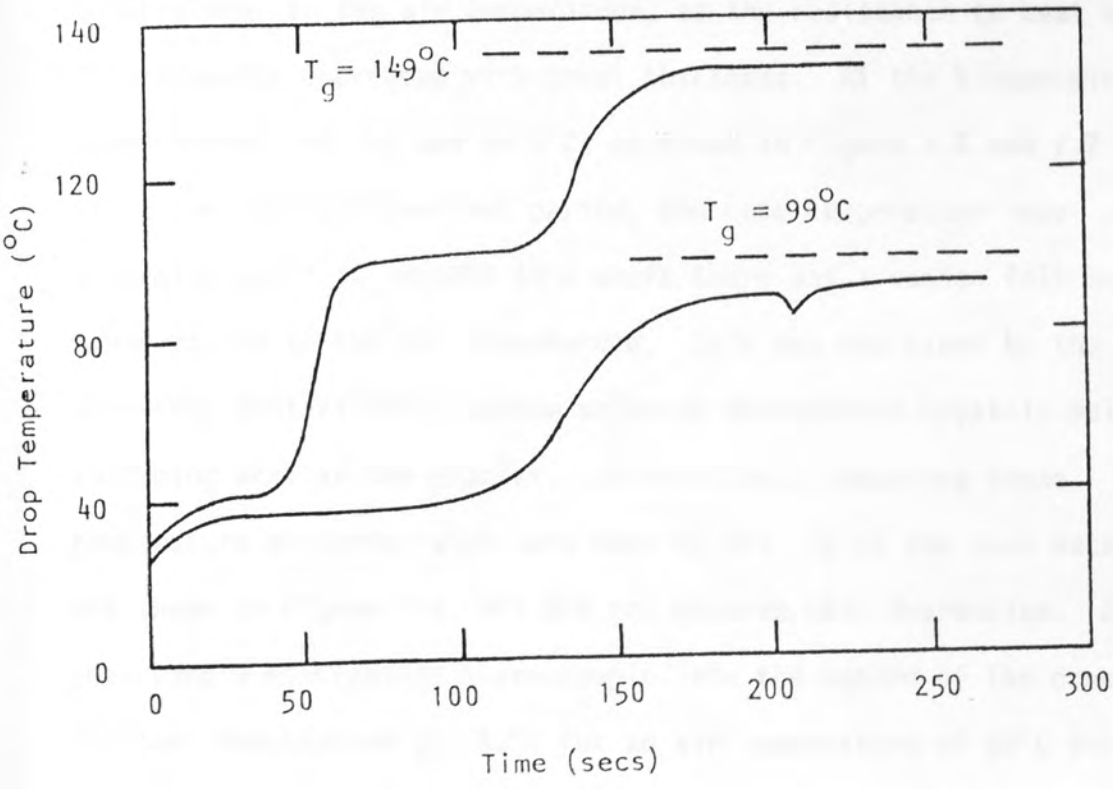

Figure 2.4 Drop Temperature Histories for Aqueous Sodium Sulphate (85) Decahydrate

sulphate drops they observed that the drop temperature rose initially and that there were constant periods of drop temperature consistent with the 'constant rate' period of mass transfer. For skimmed milk drops at high air temperatures of 100°C-144°C no wet-bulb temperature period was observed with the drop temperature rising gradually to the air temperature. With bentonite, which is an insoluble solid, the temperature histories were nearly the same as that of a pure liquid drop. The temperature histories are shown in Figure 2.4.

Cheong (4) working with sodium sulphate decahydrate found some very interesting drop temperature histories at air temperatures of 20°C-78°C. At low air temperatures (20°C) as shown in Figure 2.5 the core temperature curve showed an initial transient period before equilibrium was established and the core temperature reduced to the wet-bulb temperature. There was then a steady rise in the core temperature, to the air temperature, as the resistance to heat and mass transfer increased with crust thickness. At the higher air temperatures (40.7°C and 59.3°C) as shown in Figure 2.6 and 2.7 after the initial transient period, the core temperature rose gradually until it reached 33°C where there was a sudden fall before again rising to the air temperature. This was explained by the knowledge that at 33°C, sodium sulphate dechaydrate crystals melt absorbing heat in the process. Interestingly comparing these temperature histories with work done by Ali (7) on the same material and shown in Figure 2.8, Ali did not observe this depression. By inserting a Ni-Cr/Ni-Al thermocouple into the centre of the drop a constant temperature at ~33°C for an air temperature of 60°C was observed. This highlights the sensitivity of the thermocouple/ balance developed by Cheong (4).

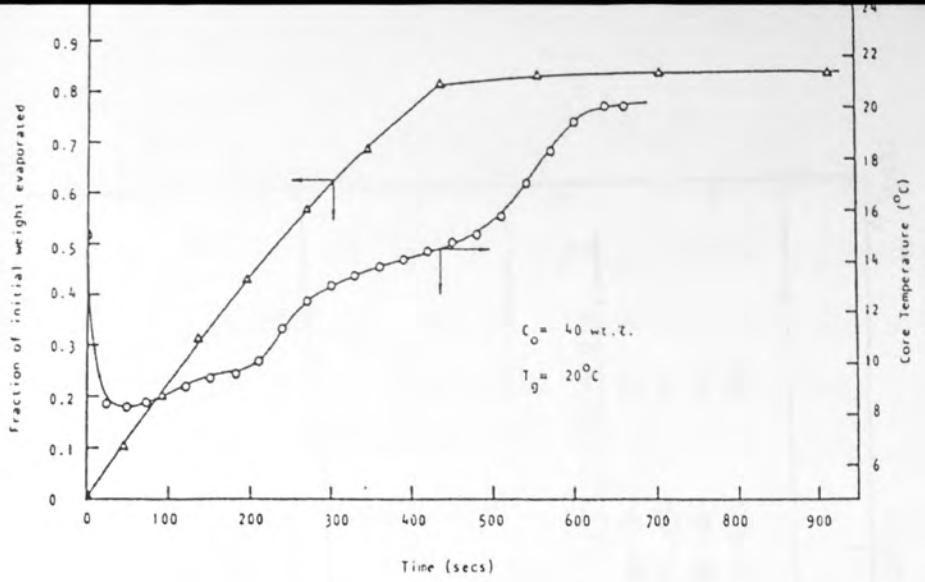

Figure 2.5 Drop Drying Histories for Aqueous Sodium Sulphate (4) Decahydrate

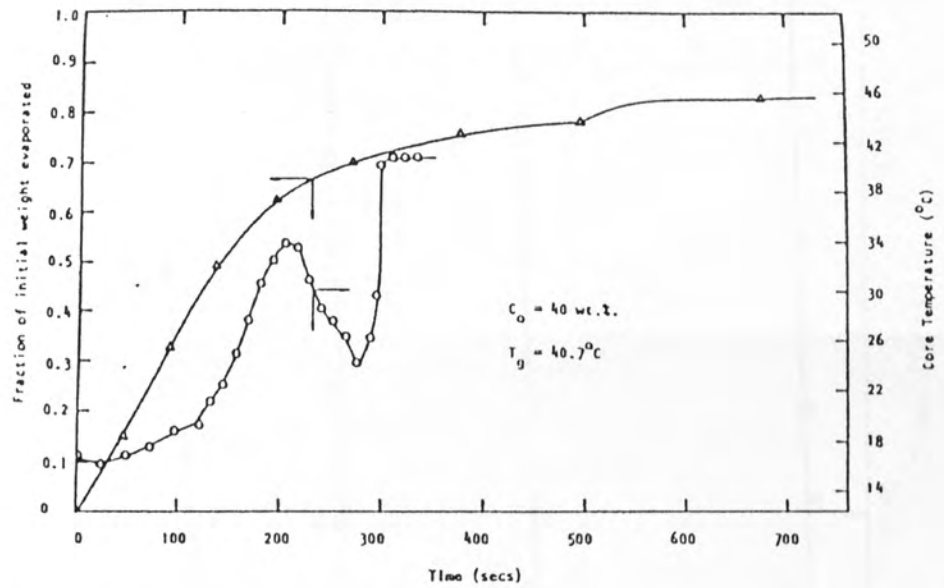

Figure 2.6 Drop Drying Histories for Aqueous Sodium Sulphate (4) Decahydrate

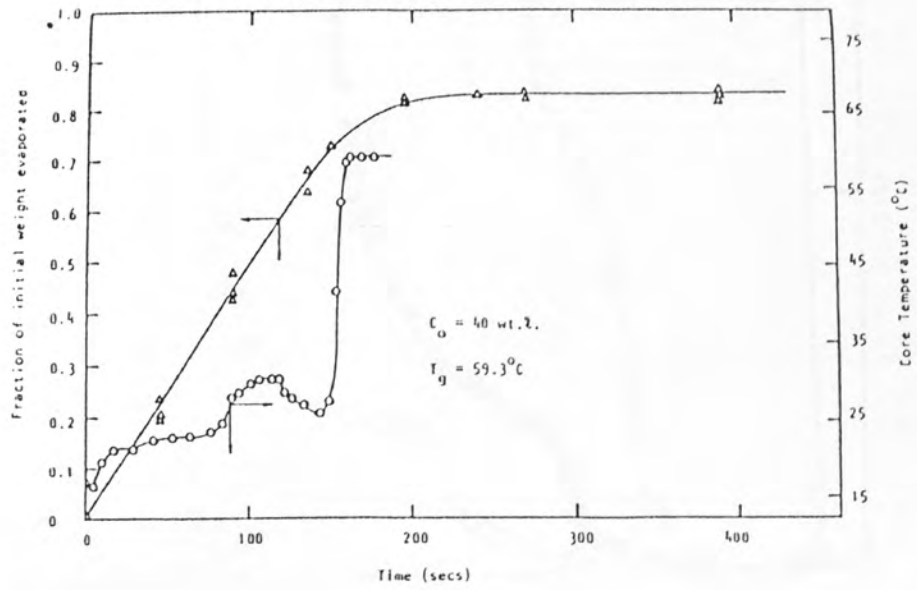

Figure 2.7 Drop Drying Histories for Aqueous Sodium Sulphate (4) Decahydrate

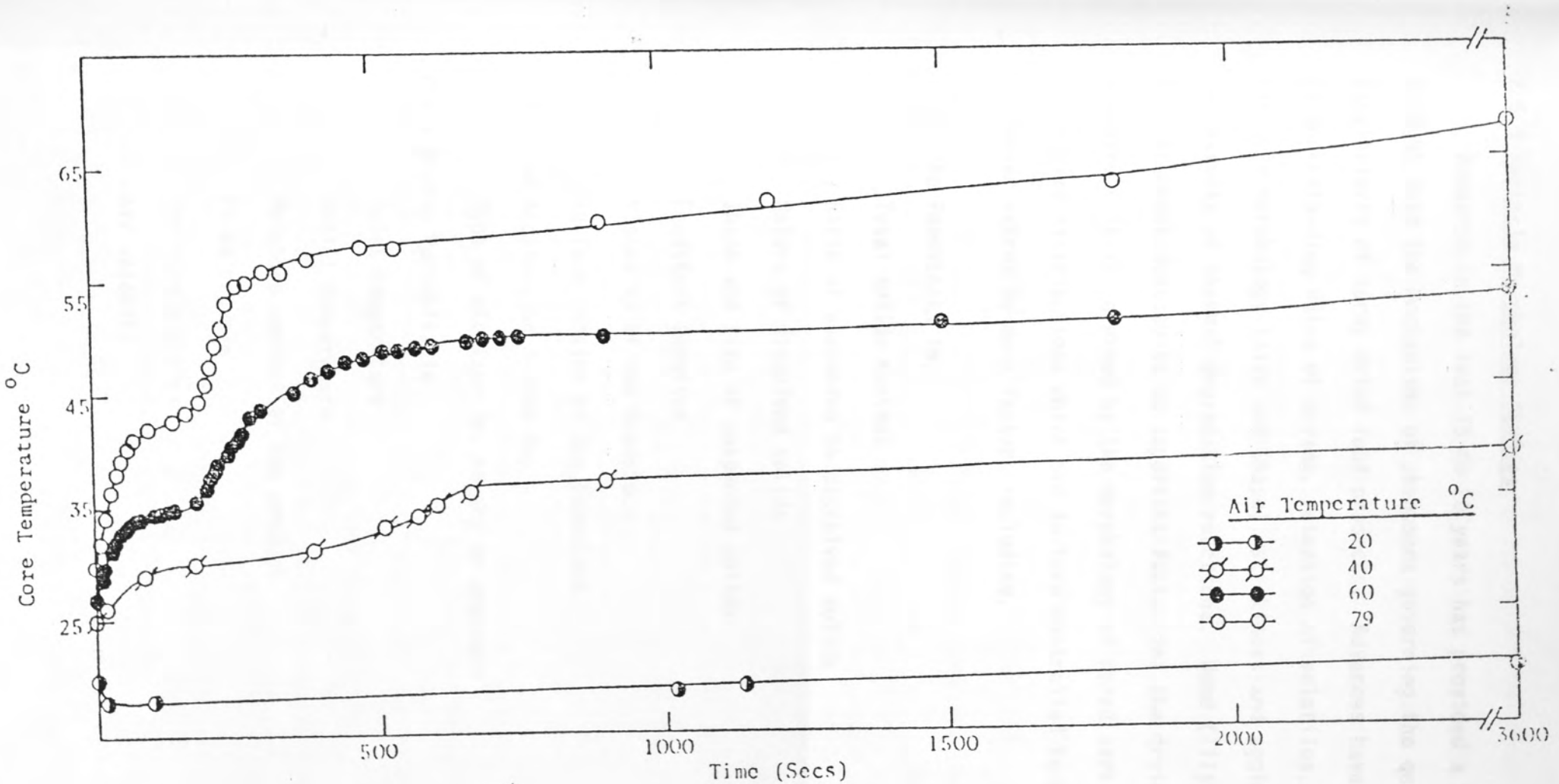

Figure 2.8 Drop Temperature Histories for Aqueous Sodium Sulphate (7) Decahydrate

2.5.9 Particle Morphology Studies

Research in the last 15 to 20 years has provided a fundamental insight into the mechanisms of phenomena governing the quality particularly of spray dried food products. Advances have been made in understanding rates of drying, retention of volatiles, changes in particle morphology (size and shape), stickiness and agglomeration and extents of thermal degradation reactions. Wood (111) states that the bulk density is an important factor for the drying industry. It is governed by the morphology of dried particles and their size distributions which are in turn controlled to a greater or lesser extent by many factors including,

(i) The Feedstocks ie,

- Total solids content
- Ratio of suspended to dissolved solids
- Nature of dissolved solids
- Shape and size of suspended solids
- Feedstock aeration
- Viscosity of the feedstock
- Surface tension of the feedstock

(ii) The Atomisation System ie,

- Type of atomiser ie, rotary or pressure

(iii) Drying Variables ie,

- Inlet temperature
- Outlet temperature
- Moisture content of the product
- Fines recycle
- Air flow patterns
- Air velocity

Several different experimental approaches have been used to study particle morphologies. The simplest is to collect the final dried product and examine it using an optical or scanning electron microscope. Charlesworth and Marshall (10) and subsequently Crosby et al (118) used glass filaments to suspend drops. Toei et al (8) used an ultrasonic field to suspend a drop. Both these techniques yielded valuable information but required relatively large drops and the monitoring of changes over time scales of at least a few minutes. A modified approach uses an ultrasonic field to hold a drop in place in an up-flowing, warm-air stream (120). In this way, times for the appearance of solid crystals on the surfaces of drops of aqueous solutions of inorganic substances have been measured and interpreted through mass-transfer models (120). Greenwald et al (121) considered the mechanisms by which internal voids form and particles inflate during spray drying. It was postulated that a bubble of air is formed inside the drop. This can come from mechanical entrainment of bubbles during atomisation (122), or can come from bubble formation through absorption of dissolved air or gas. Following formation this bubble grows by vaporisation of water to reach the equilibrium partial pressure of water, which increases as the drop temperature increases. As the mole fraction of air in the bubble consequently decreases, the bubble, and hence the drop grow in size. By this mechanism, the morphology can be strongly affected by the initial nucleation step for air bubbles.

Alexander (123) considered the mechanisms which cause folds and shrivelling ridges to be present or absent on particle surfaces. It was postulated that folds, once formed by uneven shrinkage forces, will tend to flow under a surface-tension driving force.

The flow is resisted by the viscosity of the concentrate. A dimensionless group G in which the viscosity was the most sensitive variable was used to describe the mechanism,

$$G = \frac{\sigma_t}{\mu_{dr} n d_p} \left| \frac{dr}{dt} \right| \qquad 2.68$$

Where σ_t = surface tension
μ_{dr} = viscosity
d_p = drop diameter

$\left| \frac{dr}{dt} \right|$ = absolute rate of change of particle radius due to drying.

Thus the tendency to develop folds or not is related to a critical value of the viscosity of the concentrate at the time when folding can occur.

Figure 2.9 illustrates the role of particle morphology in spray drying. In recent years. much has been learnt about the relationships between certain operating variables such as air temperature, drop size and feed concentration, and the resulting morphological properties of the product. There is still a need, however, to link these same variables with the development of morphological changes in the drying drops. Wood (111) discusses the effects of various factors on the bulk density as found in industrial spray drying applications. These include;

(i) Nature of Feed

- Feeds of dissolved materials, particularly those of an organic nature (eg dyes, surfactants) lead to the formation of smooth-walled hollow spheres. The bulk density depends on the crust thickness in relation to sphere size and the crust porosity.

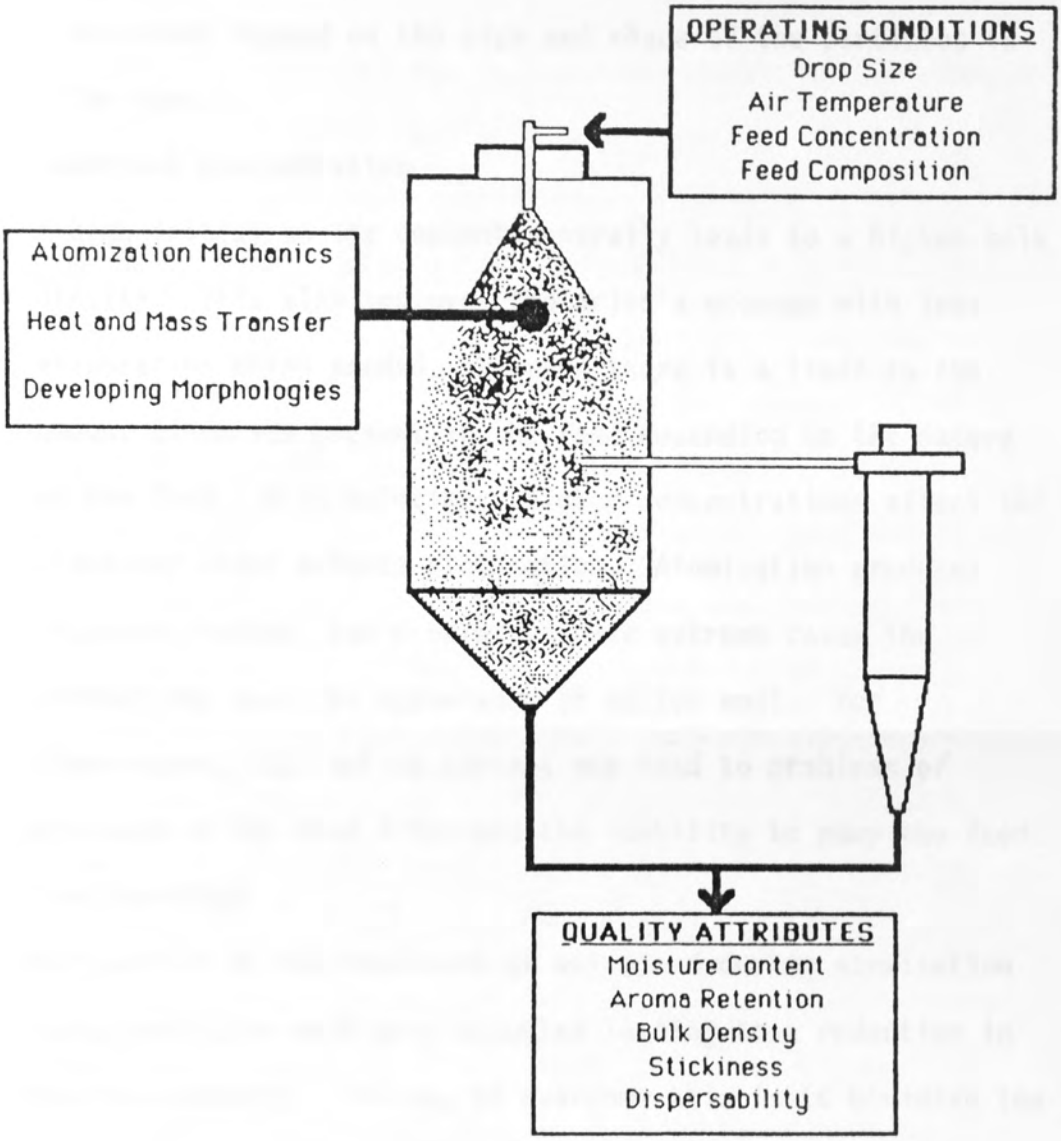

Figure 2.9 The Role of Particle Morphology in Spray Drying

- Feeds made up of solutions with no dispersed solids form thin-walled spheres with a low bulk density.

- Feeds made of dispersions results in products whose structure depend on the size and shape of the particles in the feed.

(ii) Feedstock Concentration

A high initial solids content generally leads to a higher bulk density. This also improves the drier's economy with less evaporation being needed. However there is a limit to the amount of solids present in the feed depending on the nature of the feed. With solutions, higher concentrations affect the viscosity which affects atomisation. Atomisation produces ligaments rather than droplets and in extreme cases the product may have the appearance of cotton wool. For dispersions, high solids content may lead to problems of blockage of the feed lines and the inability to pump the feed.

(iii) Feed Aeration

Air bubbles in the feedstock or entrained during atomisation forms particles with many vacuoles leading to a reduction in the bulk density. The way to overcome this is to minimise the amount of aeration through the drying process. This can include steps such as using a slow feed tank agitator and blanketing the nozzle with steam.

2.6 CONCLUSIONS

A considerable amount of work has been carried out on the evaporation of pure liquid drops. Most of the work presented supports the correlations of Ranz and Marshall (3). However there is less agreement under conditions of intense heat and mass transfer.

In comparison to pure liquid drops, less work has been carried out on the drying of drops containing solids. Of the studies carried out, the most widely used technique was to suspend a single drop on the tip of a glass filament to measure the weight history. The drop temperature history was measured separately by inserting a thermocouple into the centre of the drop. Trommelen and Crosby (71) combined the above technique by attaching a thermocouple to the outside of a filament. Simultaneous measurements of drop weight and temperature were carried out. Cheong (4) took the above technique one step further by combining the filament and thermocouple into a single unit with a 50 μm copper wire running through a hollow filament. By vacuum coating the surface of the filament and leaving a junction at the tip, a filament-thermocouple was developed for simultaneous measurements of the drops weight and temperature history. However very little experimental data was given using this technique.

The present study was therefore initiated to study a range of single drops of materials containing dissolved and/or suspended solids using the filament-thermocouple and to model the different drying characteristics of single drops.

CHAPTER THREE

MATHEMATICAL MODELS

3.0 INTRODUCTION

Only limited mathematical models are available to describe the drying process experienced by drops containing solids. Charlesworth and Marshall (10) presented one of the first models. Equation 3.1 was derived to predict the time of appearance of crystals on the surface of a drop containing dissolved solids. The major assumptions of this model were:

(i) Moisture transfer in the drop is by diffusion only.

(ii) The concentration gradients in the drop are spherically symmetrical.

(iii) The drop is at its wet bulb temperature.

(iv) The initial evaporation rate is equal to that of a pure-water drop of the same size, calculated from the mass transfer correlation of Ranz and Marshall (3).

$$t_c = \frac{(r_o^2 D)\ln(C_{sat}/C_{so})}{y^2 + 2B\ln(C_{sat}/C_{so})} \qquad 3.1$$

Where y is the positive root of

$$\tanh y = y/(1+B) \qquad 3.2$$

And B is defined as an evaporation constant

$$B = (dr^2/dt)(1/8D) \qquad 3.3$$

However this model was not applicable to the falling rate period once a crust had formed on the surface of the drop, which is the period of most significance in practice. Miura et al (85) tested the resulting equation and found that the calculated times for a number of salt solutions were less than the actual times. The discrepancy could be attributed to the assumption by Charlesworth

and Marshall that molecular diffusion was the sole mechanism of transfer in a droplet whereas circulation of liquid near the surface and convective transfer of liquid within the droplet, are also possible.

Furuta et al (120) developed two models to predict the time of crystal formation on the surface of a drop, a Diffusion Model and a Perfect Mixing Model.

1) Diffusion Model (DM)

This model was based on the following simplifying assumptions:

(i) No internal circulation takes place inside the droplet, and the solvent (water) and solute (salt) are induced to move concomitantly in the radial direction only by molecular diffusion.

(ii) There are no temperature gradients inside the droplet, and the heat of crystallisation can be neglected.

(iii) Volumetric additivity holds between solute and solvent, that is:

$$1/\rho_{sol} = 1/\rho_s + 1/\rho_w \qquad 3.4$$

Equations 3.5 and 3.6 describe the change in concentration of water and drop temperature with time. These were solved by an implicit finite difference method. The time of crystal formation was determined when the surface concentration of the salt reached the saturation level for the temperature.

$$\frac{\partial x_w}{\partial t} = \frac{1}{r^2}\frac{\partial}{\partial r}\left(r^2 D \frac{\partial x_w}{\partial r}\right) - \frac{2D}{x_w + C}\left(\frac{\partial x_w}{\partial r}\right)^2 \qquad 3.5$$

$$\frac{dT_d}{dt} = \frac{h_g(T_g - T_d) + r^2 L_v \rho_w dr/dt)}{(r/3)(\rho_w Cp_w + \rho_s Cp_s)} \qquad 3.6$$

(The symbols are all defined in the Nomenclature).

2) Perfect Mixing Model (PMM)

This model was based on the assumption that the fluid was perfectly mixed within the drop, ie there are no internal concentration or temperature distributions. Simultaneous ordinary differential equations 3.7 and 3.8 were derived for the change in the radius of the drop and its temperature. These were solved using a Runge-Kutta method.

$$dr/dt = -k_g(C_s-C_g)/p_w \qquad 3.7$$

$$\frac{dT_d}{dt} = \frac{3(h_g(T_d-T_g) - k_g(C_R-C_g)L_v)}{R(p_wCp_w+(C_{so}Cp_s+C_{wo}Cp_w-C_wCp_w)(r_o/r)^3)} \qquad 3.8$$

Results for a number of salts are shown in Figures 3.1, 3.2, 3.3 and 3.4. These demonstrate that both the DM and PMM models provided good agreement with the experimental results. This is somewhat surprising since, according to the assumptions made in the models, the PMM would tend to over estimate the time for formation of crystals and the DM to underestimate it.

Nescic (97) derived a model to describe the whole drying process. This included:

(i) Initial heating and evaporation.
(ii) Constant rate period
(iii) Falling rate period
(iv) Boiling period, and,
(v) Porous particle drying

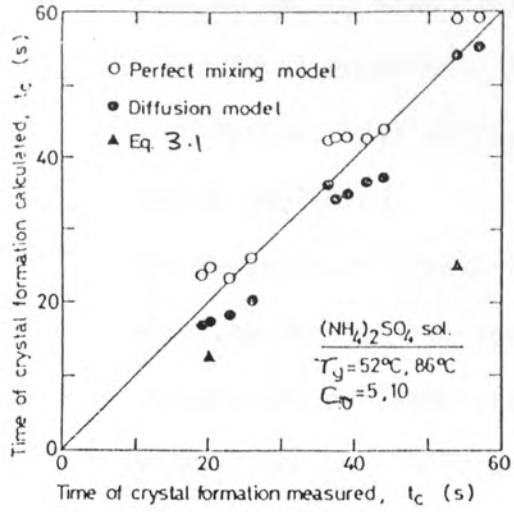

Figure 3.1 A Comparison of the Perfect Mixing and Diffusion Model Predictions for $(NH_4)_2$ SO_4 (128)

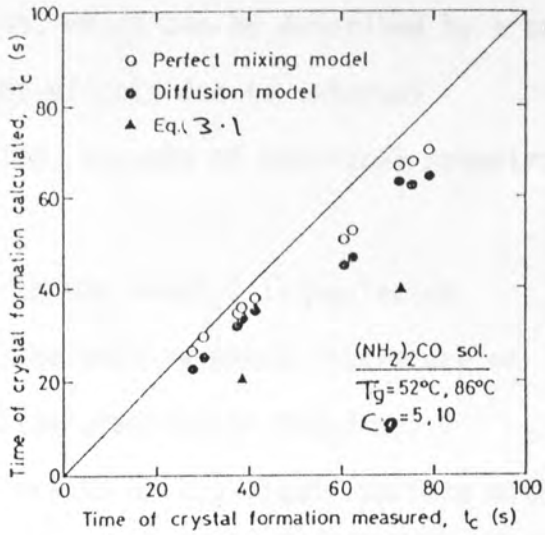

Figure 3.2 A Comparison of the Perfect Mixing and Diffusion Model Predictions for $(NH_4)_2$ CO (128)

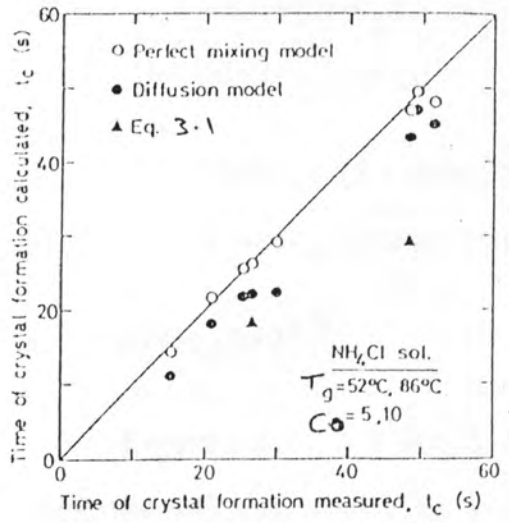

Figure 3.3 A Comparison of the Perfect Mixing and Diffusion Model Predictions for NH_4Cl (128)

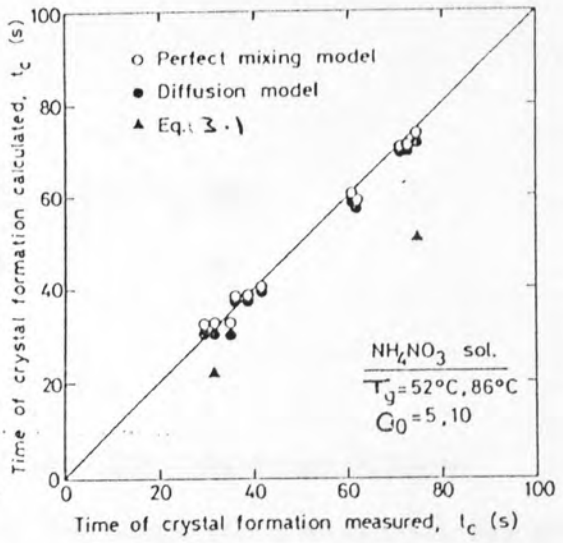

Figure 3.4 A Comparison of the Perfect Mixing and Diffusion Model Predictions for NH_4NO_3 (128)

The major assumptions of this model were:

(i) An unstationary concentration gradient is established in the droplet during evaporation, which can be described by a one dimensional equation. Any effects due to internal circulation, heat diffusion, absence of spherical symmetry can be neglected.

(ii) The temperature gradient in the droplet is neglected.

(iii) When the droplet reaches the boiling point, there are no temperature or concentration gradients in the drop.

(iv) An equilibrium condition exists on the liquid surface with the vapour partial pressure in equilibrium with the liquid phase concentration on the surface and dependent on the liquid surface.

Equations 3.9, 3.10, 3.11 describe the change in droplet mass, temperature and size with time.

$$\frac{dW}{dt} = \frac{2\pi RDSh(C_R - C_g)}{1+(ShD\beta/(2D(R-\beta)))} \qquad 3.9$$

$$\frac{dT_d}{dt} = \frac{(1/WCp_d)\ (2\pi RNuk_A(T_g - T_R) + L_v \frac{dW}{dt})}{(1+Nuk_A(\beta/(R-\beta)/2/k_{cr}))} \qquad 3.10$$

$$R = (3W/4/p_d/\pi)^{1/3} \qquad 3.11$$

Figures 3.5, 3.6 and 3.7 show the comparison between experimental and predicted mass and temperature histories for drops containing suspended solids (colloidal silical), dissolved solids (sodium sulphate) and a skin forming material (skimmed milk). These apparently demonstrate good agreement between experimental data and model predictions for both initial skin forming and non-skin forming materials.

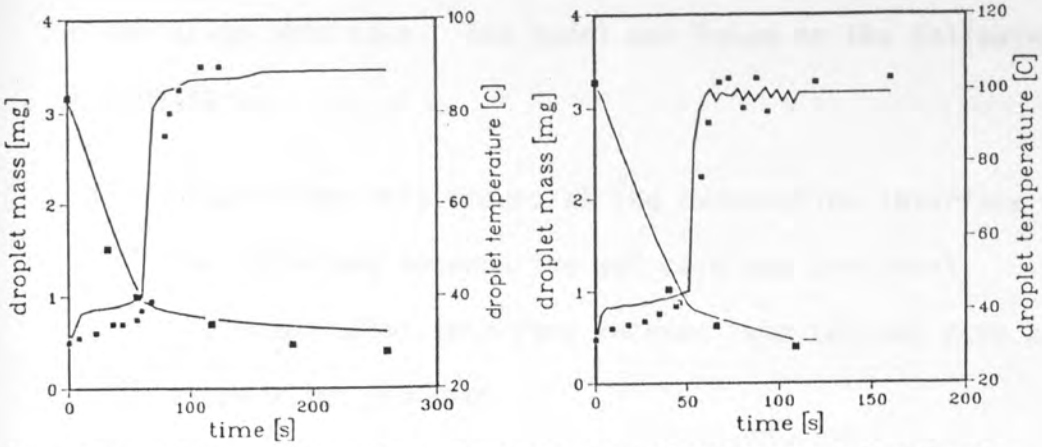

Figure 3.5 A Comparison of Experimental and Model Predictions for Aqueous Sodium Sulphate Drops (97)

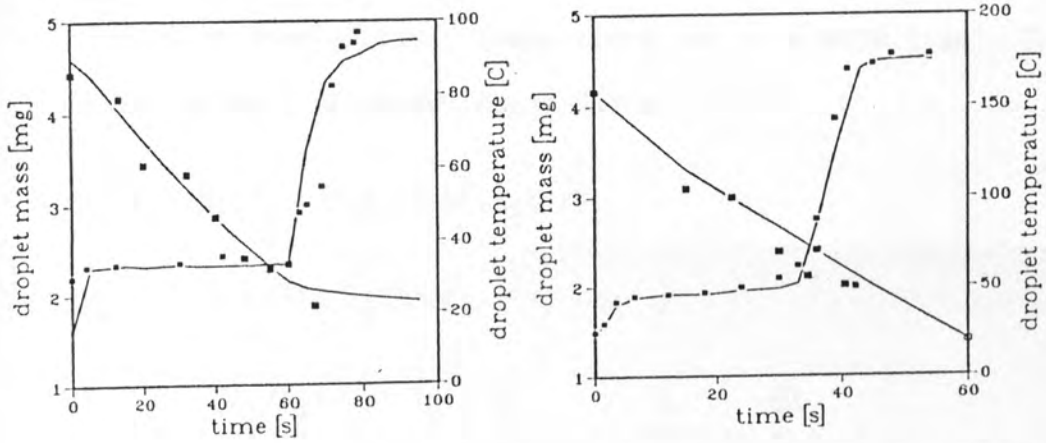

Figure 3.6 A Comparison of Experimental and Model Predictions for Colloidal Silica Drops (97)

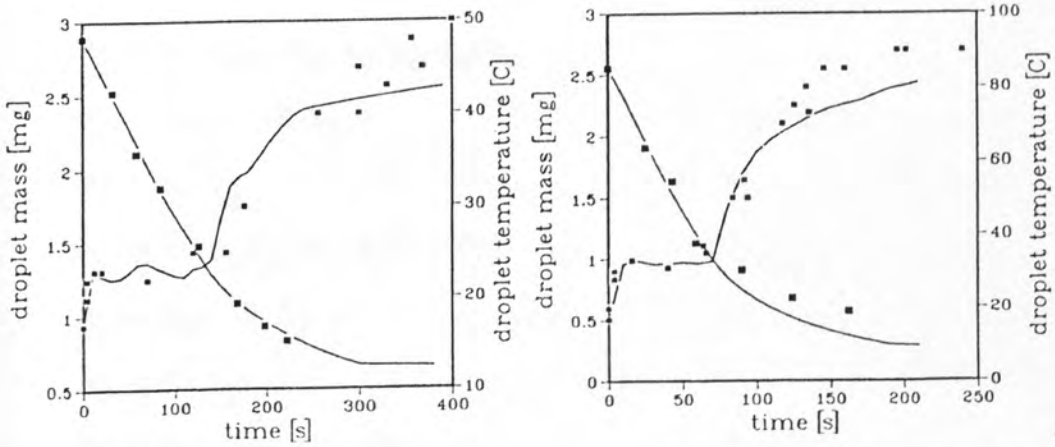

Figure 3.7 A Comparison of Experimental and Model Predictions for Skimmed Milk Drops (97)

Cheong et al (112) derived a model based on the receding evaporation interface. The model was based on the following major assumptions.

(i) Evaporation only occurs at the evaporation interface which is the interface between the wet core and dry crust.

(ii) The evaporation interface recedes into the wet core as evaporation proceeds.

(iii) The crust once formed does not shrink or inflate.

(iv) The core temperature is uniform throughout the core.

Equations 3.12, 3.13 and 3.14 were developed to describe changes in droplet mass, temperature and size with time. These were solved using a 4th order Runge-Kutta.

$$dX/dt = B_1(P_g - P_c)/(B_2X^2+B_3X)/T_c \qquad 3.12$$

$$dW/dt = -4\pi X^2 p_c x_w dX/dt \qquad 3.13$$

$$\frac{dT_c}{dt} = \frac{(A_1/A_4)}{(A_2X^2+A_3X)} \frac{T_g - T_c}{X} + \frac{1}{A_4 X} \frac{dX}{dt} \qquad 3.14$$

Where,

$$B_1 = R^2 D_{eff} M_w k_g/p_c/x_w/R_c \qquad 3.15$$

$$B_2 = D_{eff} - R k_g \qquad 3.16$$

$$B_3 = R^2 k_g \qquad 3.17$$

$$A_1 = R^2 h_g k_{cr}/p_c/X/(L_v-Cc) \qquad 3.18$$

$$A_2 = k_{cr} - R h_g \qquad 3.19$$

$$A_3 = R^2 h_g \qquad 3.20$$

$$A_4 = Cp_c/3/x_w/(L_v-Cc) \qquad 3.21$$

Experiments were carried out with single droplets of sodium sulphate decahydrate. This presents difficulties in testing the model because above 33° C it forms hydrates with incongruent melting points (96). However it was an ideal material for testing the sensitivity of the thermocouple. No predicted weight histories were given but typical temperature histories are shown in Figures 3.8 and 3.9. Although good agreement was obtained at low temperatures the unusual behaviour of the sodium sulphate decahydrate above 33° C complicated matters. The model has the disadvantage that it only applies to solutions concentrated to saturation or above. It also predicts a final solid particle or one with a relatively thick crust which is contrary to common experience with many spray-dried products (111). Van der Lijn (90) noted that spray dried particles are usually hollow, and modelled shrinking droplets with a trapped, central air bubble. The bubble was assumed to maintain thermal and vapour-liquid equilibrium with the internal liquid surface of the drop. The drop was assumed to be plastic, a situation which does not always prevail in practice and the bubble pressure was equated to atmospheric pressure. However this model does not account for a viscous response in the drop, which would hinder bubble growth and could lead to rupture.

Sano and Keey (11) also modelled expansion in a shrinking, drying drop. As opposed to Van der Lijn's model, they assumed the drop to shrink uniformly without void formation until the boiling point of the solution was reached. The degree of expansion was measured experimentally and entered as a parameter. A single expansion was assumed. The two cases examined after expansion were (i) a fixed inner surface with a shrinking outer surface and (ii) a

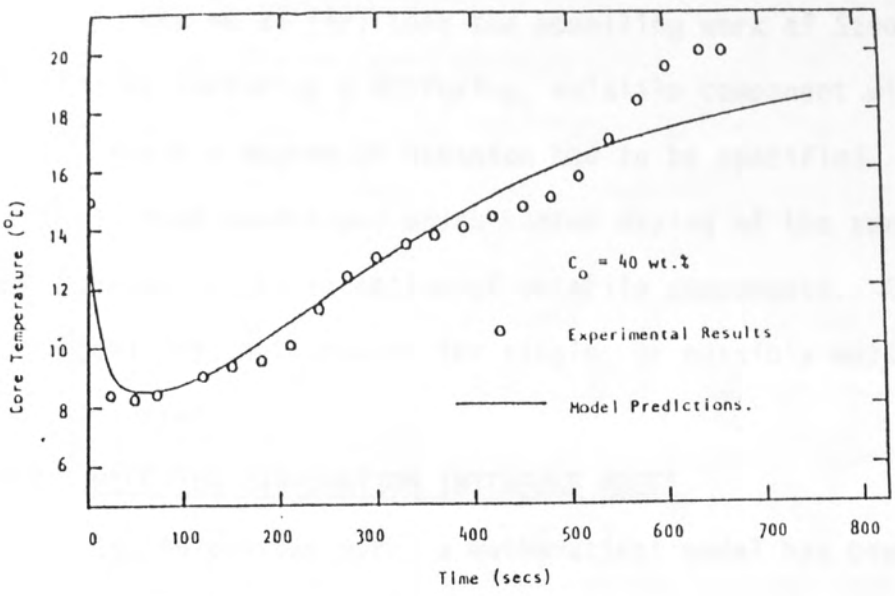

Figure 3.8 Comparison of Experimental Core Temperatures with Model Predictions (T_g=20° C) (112)

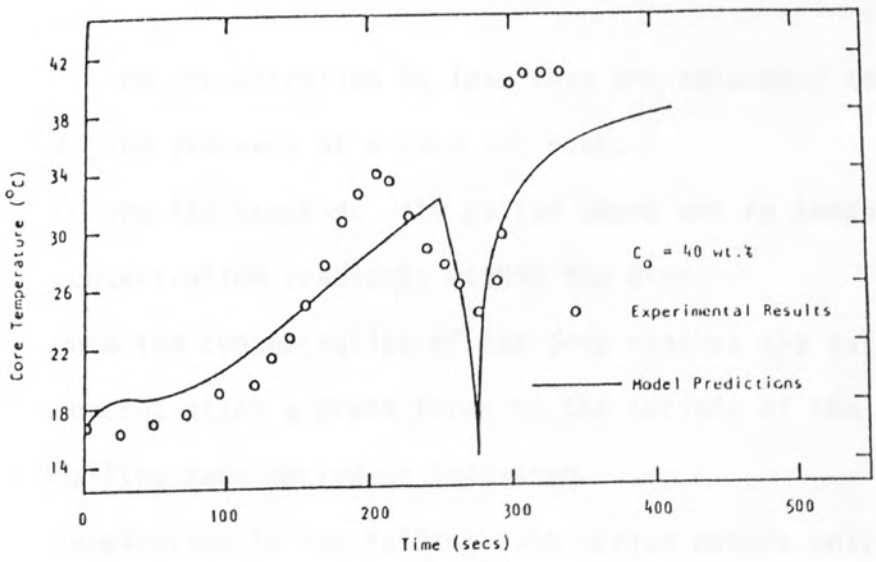

Figure 3.9 Comparison of Experimental Core Temperatures with Model Predictions (T_g=40.7° C) (112)

fixed outer surface with a shrinking inner surface. The model does not account for actual expansion and rupture and may lead to discrepancies when rupture is a dominant mass-transfer path.

Furuta et al (12) took the modelling work of Sano and Keey further by including a diffusing, volatile component within the drop. Again a degree of expanion had to be specified. The model predicts that conditions which hasten drying of the surface lead to an increase in the retention of volatile components. Again however the model does not account for single, or possibly multiple rupture of the surface.

3.1 RECEDING EVAPORATION INTERFACE MODEL

In the present work, a mathematical model has been developed to describe the drying of a drop based on a receding evaporation interface. The drying process is considered in two parts, a constant rate period during which the concentration of solute in the drop is less than saturation and a falling rate period after a crust has formed on the surface of the drop. The model is based on the following assumptions.

1. If the concentration is less than the saturated concentration drying proceeds at a constant rate.
2. During the constant rate period there are no temperature and concentration gradients within the drop.
3. Once the concentration of the drop reaches the saturated concentration a crust forms on the surface of the drop and a falling rate period is initiated.
4. Evaporation in the falling rate period occurs only at the evaporation interface, which is the interface between the wet core and dry crust.

5. The evaporation interface recedes into the wet core as evaporation proceeds.
6. Once formed the crust does not shrink or inflate and no fractures or blowholes occur.
7. The core temperature is uniform throughout the core.
8. Heat is transferred from the drying air to the crust solely by convection.
9. Heat is transferred through the crust by conduction.
10. Moisture is transferred from the evaporation interface by vapour diffusion through the pores, represented by an effective diffusivity.
11. The concentration of the core remains constant during the falling rate period.
12. The energy and vapour storage within the crust are negligible, implying that the crust is relatively thin.

3.1.1 Mass Balance Over the Drop

Change in weight of the drop = Rate of vapour diffusing from the drop.

$$-dW/dt = -k_g 4\pi X^2 (C_s - C_g) \qquad 3.22$$

Now for a spherical drop

$$W = 4\pi X^3 p_d/3 \qquad 3.23$$

Therefore,

$$dX/dt = -k_g (C_s - C_g)/p_d \qquad 3.24$$

3.1.2 Heat Balance Over the Drop

Heat in = Heat out + Accumulation 3.25

Heat in = Heat convected to the drop surface - Heat lost in heating the diffusing vapour to the air temperature. 3.26

$$\text{Heat in} = h_g 4\pi X^2 (T_g - T_d) - k_g 4\pi X^2 Cp_w (C_s - C_g)(T_g - T_d) \quad 3.27$$

Heat out = Heat lost by vaporisation + sensible heat loss

$$= k_g 4\pi X^2 (C_s - C_g) L_v + k_g 4\pi X^2 Cp_w (C_s - C_g) T_d \quad 3.28$$

$$\text{Accumulation} = 4/3\,\pi X^3 \rho_d Cp_d \, dT_d/dt \quad 3.29$$

Rearranging,

$$dT_d/dt = 3(h_g(T_g - T_d) - k_g(C_s - C_g)(L_v + Cp_w T_g))/\rho_d/Cp_d/X \quad 3.30$$

Equations 3.24 and 3.30 were solved simultaneously using a 4th order Runge Kutta.

When the concentration in the drop reaches a saturated concentration a solid crust is deposited on the surface of the drop and the heat and mass balances change.

Consider a drop after the solid crust has formed. Let the outer radius of the crust be r = R and the evaporation interface be r = X as shown in Figure 3.10.

3.1.3 Heat Balance at the Interface (On the Core)

$$Q_{In} = Q_{Out} + \text{Accumulation} \quad 3.31$$

Where,

$$Q_{In} = \text{Rate of heat flowing into the interface.} \quad 3.32$$

$$Q_{Out} = \text{Rate of heat flowing out of the interface.} \quad 3.33$$

$$A = \text{Accumulation of heat within the core.} \quad 3.34$$

3.1.4 Heat In

Heat flows into the core by conduction through the crust. The rate of heat flow Q is given by:

$$Q_{In} = k_{cr} 4\pi X^2 \left. -\frac{\partial T}{\partial r} \right|_{x,\epsilon} \quad 3.35$$

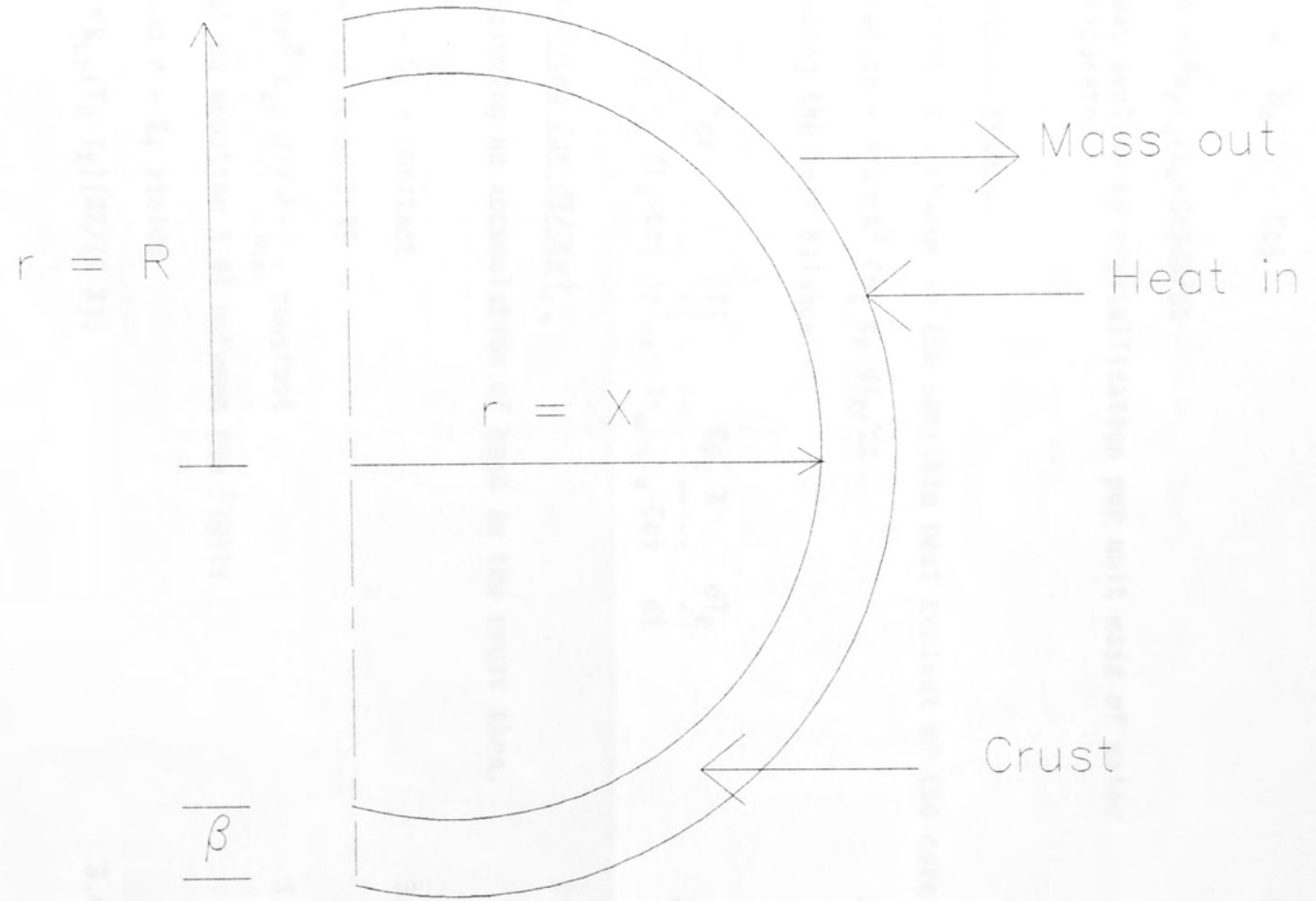

Figure 3.10 A Drops Cross-Section

3.1.5 Heat Out

Heat is lost from the core due to the latent heat of vaporisation carried away by the diffusing water vapour.

$$Q_{Out} = -N_A(L_v - Cc) \qquad 3.36$$

$$= -4\pi X^2 p_c x_w (L_v - Cc) dX/dt \qquad 3.37$$

Cc = Heat evolved by crystallisation per unit mass of water evaporated.

3.1.6 Accumulation

There is a change in the sensible heat content of the core.

$$\text{Accumulation} = 4/3\,\pi X^3\, Cp_c\, p_c\, dT_c/dt \qquad 3.38$$

Rearranging the heat balance.

$$\frac{-dX}{dt} = \frac{k_{cr}}{p_c\, x_w\, (L_v - Cc)} \left.\frac{\partial T}{\partial r}\right|_{x,t} - \frac{Cp_c\, X}{3x_w\, (L_v - Cc)} \frac{dT_c}{dt} \qquad 3.39$$

3.1.7 Solving for $\partial T/\partial r\big|_{x,t}$

Assuming no accumulation of heat in the crust then,

$$Q_R = Q_r = Q_X = \text{constant} \qquad 3.40$$

Now from equation 3.35

$$Q_r = 4\pi r^2 k_{cr} \left.\partial T/\partial r\right|_{r,t} = \text{constant} \qquad 3.41$$

Integrating equation 3.41 between the limits

r = R and r = X, yields

$$Q_r = 4\pi k_{cr}(T_R - T_X)(RX/(R-X)) \qquad 3.42$$

Since,

$$Q_X = 4\pi k_{cr} X^2 \left.\partial T/\partial r\right|_{x,t} \qquad 3.43$$

And $Q_r = Q_X$

$$\left.\partial T/\partial r\right|_{x,t} = (T_R - T_X)\, R/X/(R-X) \qquad 3.44$$

Furthermore assuming the temperature of the interface corresponds to the core temperature then

$$T_X = T_C \qquad 3.45$$

And

$$\partial T/\partial r\Big|_{=x,\epsilon} (T_R-T_C)\ R/X/(R-X) \qquad 3.46$$

3.1.8 Solving for T_R

Considering the gas film around the drop, the heat transfer from the gas to the drop can be expressed as,

$$Q_{gas} = h_g\ 4\pi R^2(T_g-T_R) \qquad 3.47$$

Now some of this heat will be consumed in heating the diffusing vapour to the gas temperature.

$$\text{Therefore } Q_R = Q_{gas} - Q_{\text{heat vapour}} \qquad 3.48$$

$$= (h_g-k_g Cp_w(C_R-C_g))4\pi R^2(T_g-T_R) \qquad 3.49$$

Equating equations 3.42 and 3.49

$$(T_R-T_c)X/R/(R-X) = (h_g-k_g Cp_w(C_R-C_g))(T_g-T_R)/k_{cr} \qquad 3.50$$

$$\text{let } a_o = R(R-X)(h_g-k_g Cp_w(C_R-C_g))/k_{cr}/X \qquad 3.51$$

Then

$$T_R = a_o T_g/(1+a_o) + T_c/(1+a_o) \qquad 3.52$$

Equating equations 3.46 and 3.52

$$\partial T/\partial r\Big|_{=x,\epsilon} (a_o/(1+a_o))(T_g-T_c)R/X/(R-X) \qquad 3.53$$

And substituting equations 3.53 and 3.51 into equation 3.39 the energy balance becomes,

$$-dX/dt=(a_1/(a_2X^2+a_3X))(T_g-T_c)-a_4X\ dT_c/dt \qquad 3.54$$

Where,

$$a_1 = R^2k_{cr}(h_g-k_g Cp_w(C_R-C_g))/p_c/x_w/(L_v-Cc) \qquad 3.55$$

$$a_2 = k_{cr}-R(h_g-k_g Cp_w(C_R-C_g)) \qquad 3.56$$

$$a_3 = R^2(h_g-k_g Cp_w(C_R-C_g)) \qquad 3.57$$

$$a_4 = Cp_c/3/x_w/(L_v-Cc) \qquad 3.58$$

3.1.9 Mass Balance at the Evaporation Interface

From Fick's law of diffusion,

$$N_{Ax} = -D_{eff}\ A\ \partial C/\partial r\Big|_{x,\epsilon} \qquad 3.59$$

Now the output from the core can also be expressed as the change in water content of the core,

$$= -4\pi X^2 p_c x_w \, dX/dt \qquad 3.60$$

On the assumption that there is no accumulation of mass in the crust, ie

$$N_{Ax} = \text{constant} \qquad 3.61$$

Then

$$N_{Ar} = -D_{eff} 4\pi r^2 \partial C/\partial r \Big|_{r,t} = \text{constant} \qquad 3.62$$

Integrating equation 3.62 between the limits r = X and r = R, yields.

$$N_{Ar} = -D_{eff} 4\pi RX(C_R - C_X)/(R-X) \qquad 3.63$$

3.1.9.1 Solving for C_R

Consider the gas film around the droplet.

The rate of mass transfer from the drop is

$$N_{AR} = -k_g 4\pi R^2 (C_R - C_g) \qquad 3.64$$

Equating equation 3.63 and 3.64 and rearranging,

$$C_R = C_g b_o/(1+b_o) + C_X/(1+b_o) \qquad 3.65$$

Where

$$b_o = k_g R(R-X)/D_{eff}/X \qquad 3.66$$

Equating equations 3.59 and 3.63

$$\frac{\partial C}{\partial r}\Big|_{x,t} = R\,(C_R - C_X)/X/(R-X) \qquad 3.67$$

Substituting for C_R from equation 3.65

$$\partial C/\partial r \Big|_{x,t} = R(C_g - C_X) b_o/(1+b_o)/X/(R-X) \qquad 3.68$$

Hence

$$N_{Ax} = -D_{eff} 4\pi X^2 R(C_g - C_X) b_o/(1+b_o)/X/(R-X) \qquad 3.69$$

Equating with equation 3.60

$$dX/dt = Rb_o D_{eff}(C_g - C_X)/X/(R-X)/(1+b_o)/p_c/x_w \qquad 3.70$$

But

$$C = M_w P/R_c/T \qquad 3.71$$

Hence

$$dX/dt = Rb_o D_{eff} M_w (P_g/T_g - P_c/T_c)/X/(R-X)/(1+b_o)/R_c/p_c/x_w \quad 3.72$$

Substituting for b_o from equation 3.66 and letting

$$b_1 = R^2 D_{eff} M_w k_g/R_c/p_c/x_w \quad 3.73$$

$$b_2 = D_{eff} - Rk_g \quad 3.74$$

$$b_3 = R^2 k_g \quad 3.75$$

$$dX/dt = b_1 (P_g/T_g - P_c/T_c)/(b_2 X^2 + b_3 X) \quad 3.76$$

From equation 3.54

$$dT_c/dt = a_1 (T_g - T_c)/a_4/(a_2 X^2 + a_3 X)/X + 1/a_4/X \; dX/dt \quad 3.77$$

And the rate of mass transfer can be expressed as

$$dW/dt = -4\pi X^2 p_c x_w dX/dt \quad 3.78$$

Equations 3.76, 3.77 and 3.78 were solved simultaneously using a 4th order Runge-Kutta method to give the crust thickness, core temperature and weight of the drop as a function of time.

A computer program (File name : GSB5.FOR) was written in Fortran 77 to solve the differential equations above using a IBM PC model PS2/50. A listing of the program is included in Appendix C.2.

3.2 PURE LIQUID DROPS

Some deviations will occur from the above model solely due to experimental methods. Thus a drop suspended on the tip of a filament, placed inside a wind tunnel, receives heat by convection, conduction along the filament, and radiation from the gas.

Fuchs (44) states that for typical experimental conditions of a drop diameter of 1 mm and wire diameters of 25 μm, the ratio of heat flux through the wire to that through the gaseous medium may have values of 0.8 for copper-constantan, and 0.04 for quartz glass filaments. This additional heat flux therefore has to be taken into account. Indeed it has been shown (112) that for an air temperature

of 79°C and a drop diameter of 0.5 mm this extra heat accounted for 24.7% of the total heat transferred. This draws into question correlations proposed by investigators (5,7) who ignored this heat term. The stainless steel nozzles used by Audu (5) and Ali (7) were similar in size to the hemispherical drops suspended on them. Indeed 33% of the total heat transfer area of the drop was in contact with the nozzle. A substantial amount of heat would therefore have been expected to have been conducted along the nozzle. However no allowance was made for this.

A mathematical model has therefore been derived to allow for the extra heat flux received by mechanically supported drops in a wind tunnel

3.2.1 Experimental Nusselt Number

Dimensional analysis has shown that for forced convection (94) the Nusselt number is a function of the Reynolds and Prandtl number ie,

$$Nu = f(Re, Pr) \qquad 3.79$$

This relationship has been expressed as

$$Nu = 2 + \emptyset Re^{0.5} Pr^{0.33} \qquad 3.80$$

The value of $\emptyset$ has been quoted as 0.69 (59), 0.625 (68), and 0.6 (3).

The experimental value of the Nusselt number can be determined based on the following assumptions.

(i) Heat is transferred to the drop by convection, Q_{conv}, through the filament, Q_{fil}, and by radiation, Q_{rad}.

(ii) The drop is spherical with a constant density.

(iii) The drop's surface temperature is equal to the wet bulb temperature.

(iv) The temperature driving force remains constant.

(v) The thermal conductivity is evaluated at the mean temperature of the air and the drop.

A simple heat balance on the drop can be expressed as,

$$-N_A L_v = Q_{In} = Q_{conv} + Q_{fil} + Q_{rad} \qquad 3.81$$

For a spherical drop,

$$N_A = (-\pi p_d d_p/4) d(d_p 2)/dt \qquad 3.82$$

$$Q_{conv} = h_g A \triangle T \qquad 3.83$$

Substituting 3.82 and 3.83 into 3.81 and rearranging.

$$Nu = (-p_d L_v/4/k_A/\triangle T)\ d(d_p^2)/dt - ((Q_{rad}+Q_{fil})/k_A/d_p/\pi/\triangle T) \qquad 3.84$$

$$\text{Where } Nu = h_g d_p/k_A \qquad 3.85$$

3.2.2 Heat Transferred to a Drop by Radiation

Assuming

(i) The geometry factor F_A, is unity since the drop for all purposes is surrounded by the drying chamber.

(ii) The emissivity e, is that of the drop since it is so much smaller than the drying chamber.

$$Q_{rad} = \sigma A F_A e (T_g^4 - T_d^4) \qquad 3.86$$

Where σ = Stefan-Boltzmann constant.

3.2.3 Heat Transferred to a Drop Through the Filament

For a drop suspended on a filament, heat is transferred from the filament to the drop. It is also transferred from the hot drying air to the filament. The following assumptions were therefore made in deriving an expression for Q_{fil}.

(i) Heat is transferred to the filament from the surroundings by radiation and convection.

(ii) The temperature around the filament is constant and equal to the air temperature.

(iii) The filament construction is assumed to be of a 50 μm constantan wire surrounded by glass, with a coating of copper on the surface. There are no radial temperature gradients.

(iv) The physical properties of the filament and the heat transfer coefficient on the surface of the filament are constant.

(v) The filament length is very much larger than its diameter ie, it is of an infinite length.

(vi) The geometry factor is assumed to be unity.

Consider an element of size ΔZ of the filament as shown in Figure 3.11

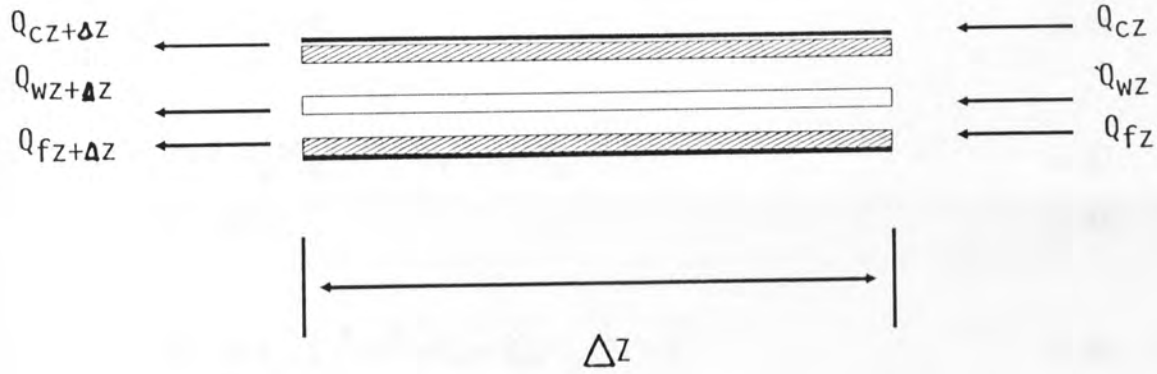

Figure 3.11 Element of the Filament

A heat balance on the element can be expressed as,

$$Q_{conv}+Q_{rad}+Q_{cz}+Q_{wz}+Q_{fz} = Q_{cz+\Delta z}+Q_{wz+\Delta z}+Q_{fz+\Delta z} \quad 3.87$$

Where

$$Q_{conv} = h_f (\pi d_f \Delta Z) (T_g-T) \quad 3.88$$

$$Q_{rad} = \sigma(\pi d_f \Delta Z)e_g(T_g^4-T^4) \quad 3.89$$

$$Q_{cz} = -k_{co}A_c dT/dZ \quad 3.90$$

$$Q_{wz} = -k_w A_w dT/dZ \quad 3.91$$

$$Q_{fz} = -k_f A_f dT/dZ \quad 3.92$$

k_{co}, k_w, k_f are the thermal conductivities of the copper,

constantan wire and glass and A_c, A_w, A_f are the respective heat transfer areas.

Substituting equations 3.88 to 3.92 into 3.87, rearranging and dividing by ΔZ.

$$(Q_{cz+\Delta z}-Q_{cz}+Q_{wz+\Delta z}-Q_{wz}+Q_{fz+\Delta z}-Q_{fz})/\Delta Z$$
$$=\sigma\pi d_f e_g(T_g^4-T^4)+h_f\pi d_f(T_g-T) \qquad 3.93$$

In the limit as ΔZ approaches zero,

$$dQ_c/dZ+dQ_w/dZ+dQ_f/dZ= \sigma\pi d_f e_g(T_g^4-T^4)+h_f\pi d_f(T_g-T) \qquad 3.94$$

From Fouriers law,

$$Q = -kAdT/dZ \qquad 3.95$$

Substituting 3.95 into 3.94 and letting

$$K = -k_{co}A_c-k_wA_w-k_fA_f \qquad 3.96$$

Gives

$$d^2T/dZ^2=(\sigma\pi d_f e_g(T_g^4-T^4)+h_f\pi d_f(T_g-T))/K \qquad 3.97$$

Letting $P = dT/dZ$ 3.98

Then

$$PdP/dT = (\sigma\pi d_f e_g(T_g^4-T^4)+h_f\pi d_f(T_g-T))/K \qquad 3.99$$

Integrating equation 3.99 and using the boundary conditions that, at $Z = \infty$, $T = T_g$, $dT/dZ = 0$ therefore $P^2/2 = 0$

And substituting for P

$$(dT/dZ)^2 =\pi d_f/K(2\sigma e_g T_g^4(T-T_g)+0.4\sigma e_g(T_g^5-T^5)-h_f(T-T_g)^2) \qquad 3.991$$

Taking square roots

$$dT/dZ\Big|_{z=o} = \pm (\pi d_f/K(2\sigma e_g T_g^4(T-T_g)+0.4\sigma e_g(T_g^5-T^5)-h_f(T-T_g)^2))^{0.5} \qquad 3.992$$

The rate of heat transfer to the drop via the filament can therefore be expressed as,

$$Q_{fil} = Q_c+Q_f+Q_w \qquad 3.993$$

Where the individual heat terms can be calculated from,

COPPER

$$Q_c = -k_{co}A_c \, dT/dZ \qquad 3.994$$

GLASS

$$Q_f = -k_f A_f \, dT/dZ \qquad 3.995$$

WIRE

$$Q_w = -k_w A_w \, dT/dZ \qquad 3.996$$

The areas used are the surface areas actually in contact with the drop.

The experimental Nusselt number can therefore be calculated from equation 3.84. This requires values for Q_{rad} and Q_{fil} which can be calculated from equations 3.86 and 3.993. The rate of change of the diameter squared is calculated experimentally.

A computer program (EXPT1.FOR) written in Fortran 77 for an IBM PC model PS2/50 was used to calculate the experimental Nusselt number. This program also corrected for the buoyancy effects of upward flowing air. A listing of the program is given in Appendix C.1.

CHAPTER FOUR

EXPERIMENTAL APPARATUS

EXPERIMENTAL APPARATUS

4.0 INTRODUCTION

Most spray processes are performed to achieve heat and mass transfer effects. Spray drying is a specific example in which moisture is evaporated from a solution, or slurry, by forced convective heat transfer from a gas stream; it is unusual in that a phase change is also involved to produce essentially dry, particulate product. Because of the complexity, time-consuming pilot scale experimentation is normally required covering a wide range of variables (eg, feed condition, feed concentration, atomisation process, gas temperature and flow characteristics) before a process or a process modification can be introduced to production.

The basic aim of single droplet work is to develop methods of predicting the drying rate of drops and to obtain fundamental information on the phenomena occurring during the drying process. This could eventually be inserted into complete drier models to simulate the full-scale drying process (110).

In a spray drier the particle size distribution features as one of the most important dried product specifications. Ideally a homogeneous product would be required, ie one of monosized particles each of similar moisture content. However at present, this is not feasible, although by the careful selection of atomising and operating variables the size range can be narrowed, albeit with some broken shells and sphere fragments often being present (111). Within a spray drier the typical sizes range from 10 to 1000 μm. These sizes are considerably smaller than can be used within the present laboratory equipment. However single droplet studies have been carried out on drops ranging from 1-5 mm in diameter. Drops of

1 -2.5 mm were used in the present study.

A variety of techniques have been used for suspending and studying single drops during drying. Early experiments using glass filaments were carried out by Frossling (2), Trommlen and Crosby (71), and Charlesworth and Marshall (10). A number of investigators (11,12) have also used the techniques which they devised. All of these experiments involved suspending drops on the tips of very fine glass filaments (0.1 mm OD) or very fine thermocouples. The disadvantage of this technique is that separate heat and mass transfer experiments have to be carried out. The advantage of using glass filaments are that they can be fabricated to very small diameters and therefore much smaller, more spherical, drops can be studied. Cheong et al (112) provided a natural extension to the Charlesworth and Marshall (10) technique. A novel filament-thermocouple was developed which incorporated provision for the simultaneous measurement of drop weight (by deflection) and drop temperature. Nickel and copper were used as the conducting materials for the design of the thermocouple. A more conventional choice of materials for the thermocouple has been used in the present study. A combination of copper and constantan or type T thermocouple was developed (126). A comparison of the outputs from the two types of thermocouples shows that there was a larger EMF change per degree change in temperature for the type T thermocouple compared with the copper-nickel thermocouple. This is illustrated in Figure 4.1. The present filament type T thermocouple also compared favourably with a standard type T thermocouple as shown in Table 4.1.

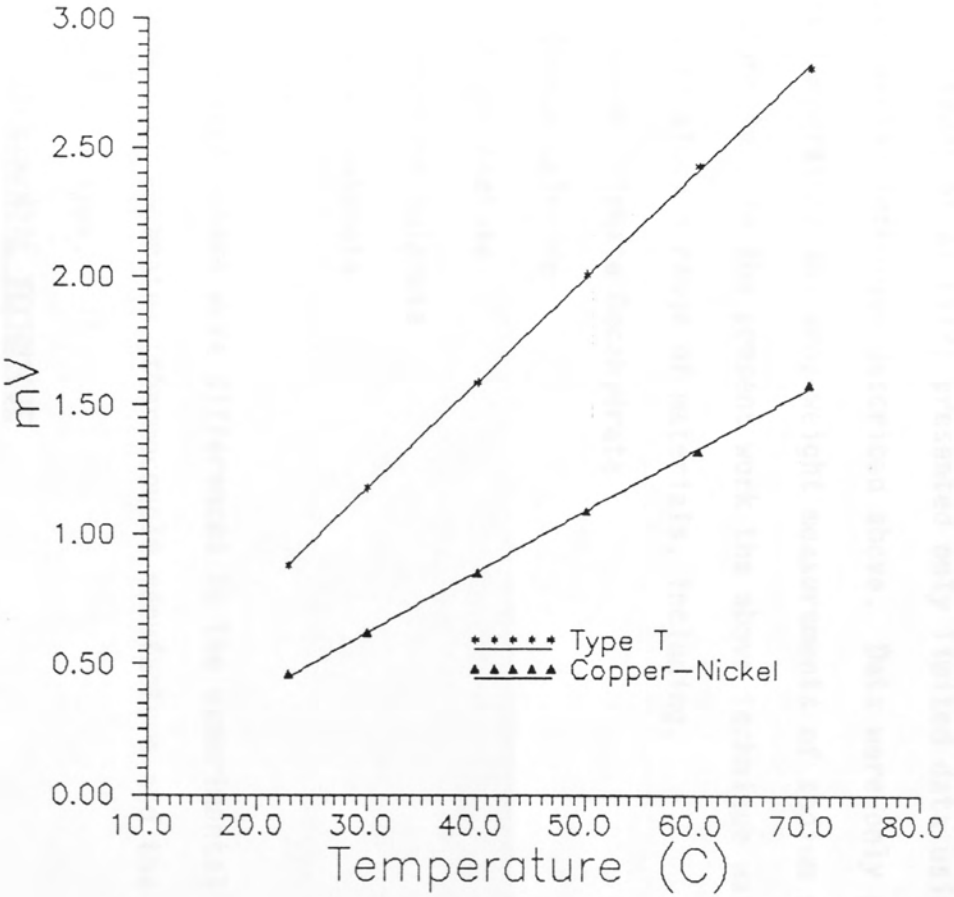

Figure 4.1 A Comparison of the Outputs of the Filament–Thermocouples

Temperature (°C)	Thin Film type T (mV)	Standard type T (mV)
30	1.18	1.20
40	1.59	1.61
50	2.01	2.04
60	2.43	2.47
70	2.81	2.91

Table 4.1 A Comparison of the Outputs of the Filament-Thermocouple Versus the Standard Type T Thermocouple

Cheong et al (112) presented only limited data using the experimental technique described above. Data were only provided for core temperature and drop weight measurements of sodium sulphate decahydrate. In the present work the above technique was used as a basis to study a range of materials, including,

1) Sodium Sulphate Decahydrate
2) Sodium Chloride
3) Sodium Acetate
4) Potassium Sulphate
5) Copper Sulphate
6) Water

However there were differences in the experimental technique, experimental apparatus, thermocouple manufacture and the thermocouple type.

4.1 EXPERIMENTAL TECHNIQUE

The experimental technique facilitated simultaneous measurement of the drop temperature and drop weight. This involved suspending a drop on the tip of the thermocouple/balance. The thermocouple tip was designed so that the junction at the tip would be located at the centre of the drop. In Cheong's design (4) a 0.5 mm long junction was used but for the drop size range in this study (1 -2.5 mm diameter) this would have represented a

substantial proportion of the drop's cross-section. Therefore the temperature measured would not necessarily have been the drop's core temperature. The size of the junction was therefore reduced to 0.1 mm. A full description of the manufacture of the thermocouples is given in Section 4.3.

The drop weight was measured by continuously noting the deflection of the thermocouple/balance. Cheong used a protractor located at the rear of the thermocouple and measured the angular deflection visually. In the present study a cathetometer located on a sliding vertical frame was used (Plate 4.1). The frame was marked with a vertical vernier scale and the eyepiece of the cathetometer had crosshairs etched on it. These were used to focus-in on a specific part of the thermocouple. To measure the drop weight a small mark (Plate 4.2) was placed on the side of the thermocouple approximately 60 mm from the tip. The crosshairs were then focused continuously onto this mark and the cathetometer moved vertically, as required, to follow this mark. The initial drop weight, the drop weight inside the tower and the final drop weight outside the tower were measured. The sphericity of the drop could be measured by measuring its vertical and horizontal diameters using the cathetometer.

4.2 EXPERIMENTAL APPARATUS

The experimental apparatus consisted of a vertical wind tunnel through which hot air was passed at a constant humidity and temperature. Two separate experimental rigs were used. The first one based on Cheong's design (4) and incorporating a 28 mm OD vertical wind tunnel was used for experiments on different solutions and slurries. The equipment was modified slightly to allow provision for direct measurement of the air humidity by means of a

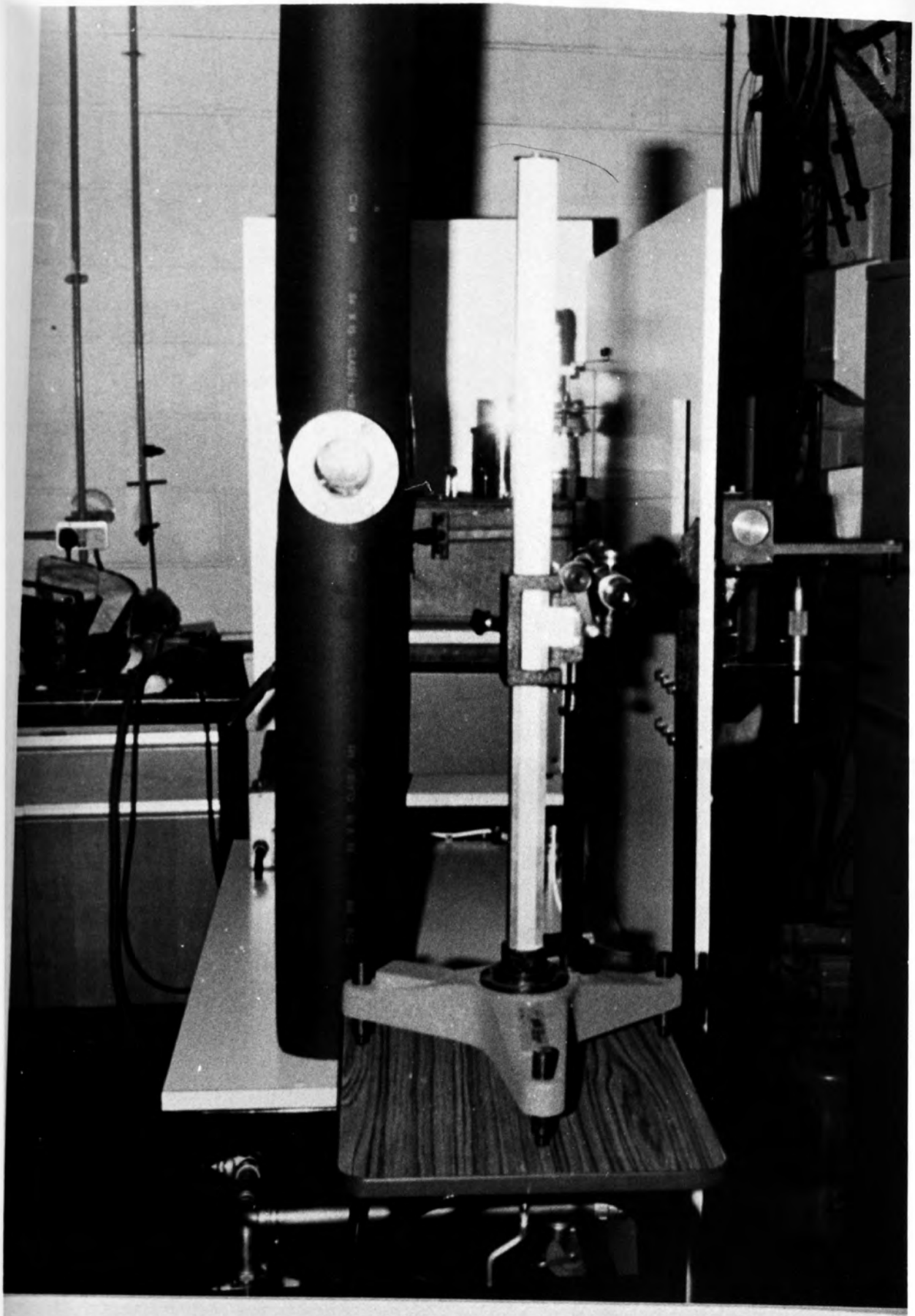

Plate 4.1 The Vertical Cathetometer.

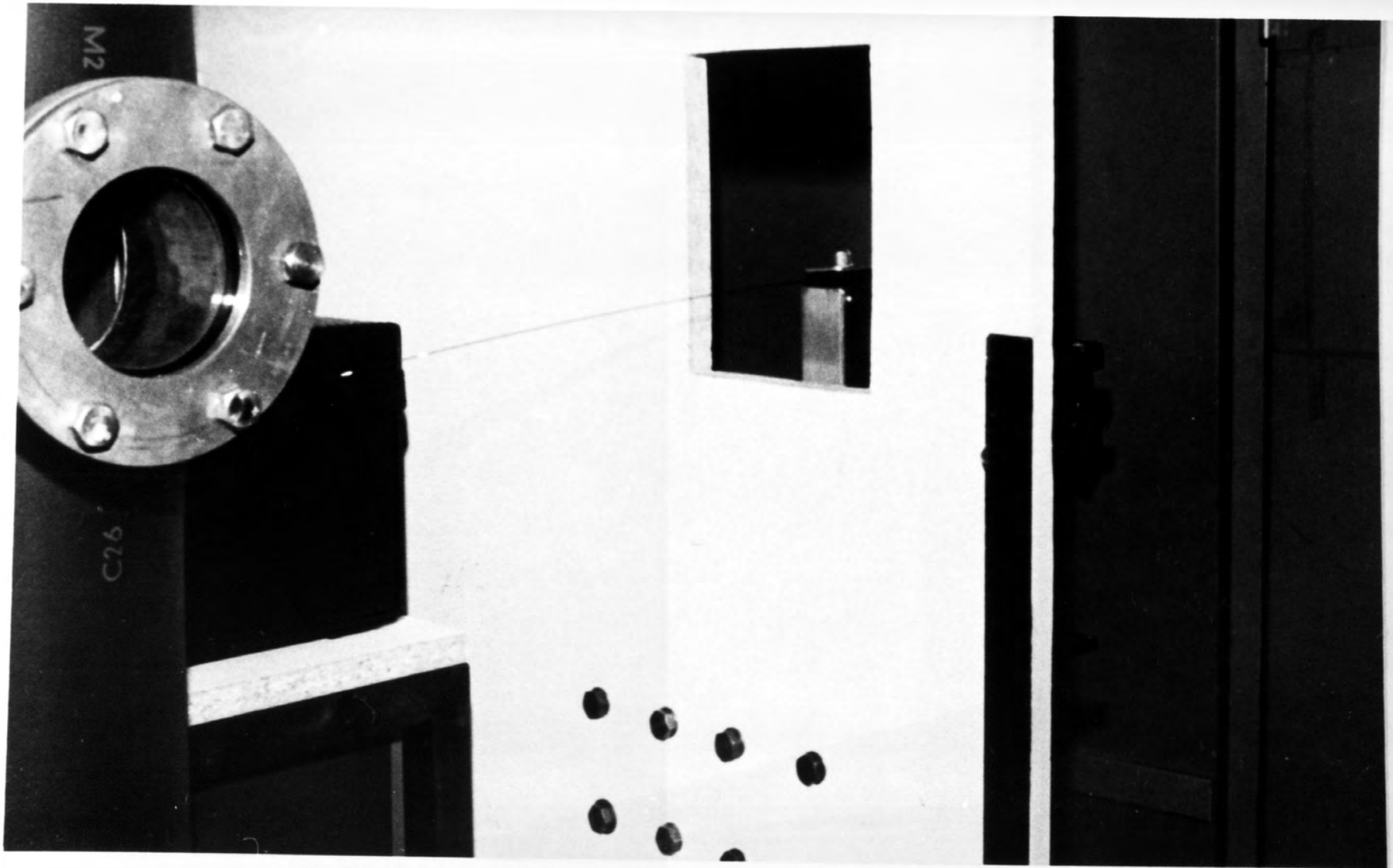

Plate 4.2 The Glass Filament Thermocouple/Balance.

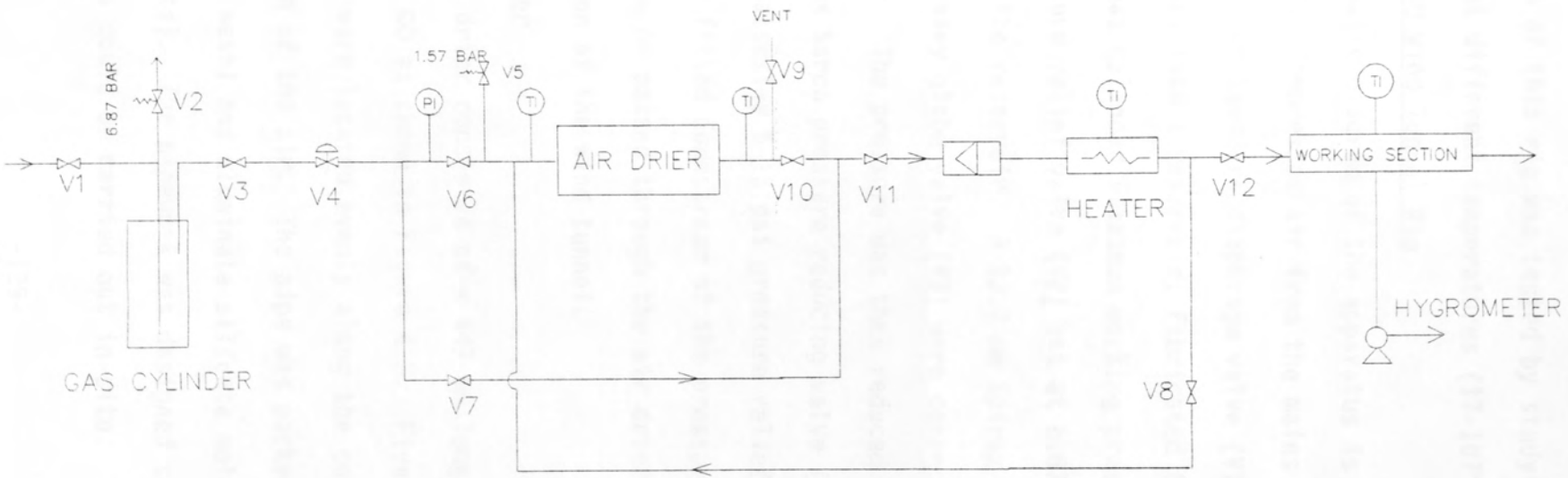

Figure 4.2 Schematic Diagram of the 28 mm Wind Tunnel

hygrometer. A second experimental rig was designed and constructed. This was based on the same principles as the first rig but incorporated a 101 mm OD wind tunnel. The advantage of this was that the influence of any wall effects on the drop were minimised. The operation of this rig was tested by studying the evaporation of water drops at different temperatures (17-107° C).

4.2.1 28 mm OD Wind Tunnel Rig

A schematic diagram of the apparatus is shown in Figure 4.2 and Plate 4.3. Compressed air from the mains at 6.53 bar was piped through a 12.7 mm Saunders diaphragm valve (V1) and a 12.7 mm Spirax Sarco strainer, into a reservoir, fabricated from a standard pressurised gas cylinder (maximum working pressure 21.7 bar). A 12.7 mm pressure relief valve (V2) set at 6.87 bar was connected to the inlet of the reservoir. A 12.7 mm Spirax Sarco strainer and a 12.7 mm Hatersley globe valve (V3) were connected on the outlet of the reservoir. The pressure was then reduced to 1.43 bar through a 12.7 mm Spirax Sarco pressure reducing valve (V4). A pressure gauge and a 15 mm Hatersley 5-15 psi pressure relief valve (V5) set at 1.57 bar were fitted downstream of the pressure reducing valve. The air could then be passed through the air drier and heater to the working section of the wind tunnel.

4.2.2 Air Drier

The air drier consisted of a 447 mm long QVF horizontal glass pipe of 87 mm OD as shown in Figure 4.3. Five 'three-quarter' baffle plates were located evenly along the column to aid redistribution of the air. The pipe was packed with self-indicating silica gel (6 mesh) and aluminate silicate molecular sieve (Type 4A, 1.59 mm pellets). The pipework was designed so that regeneration of the desiccants could be carried out in-situ. This operation was

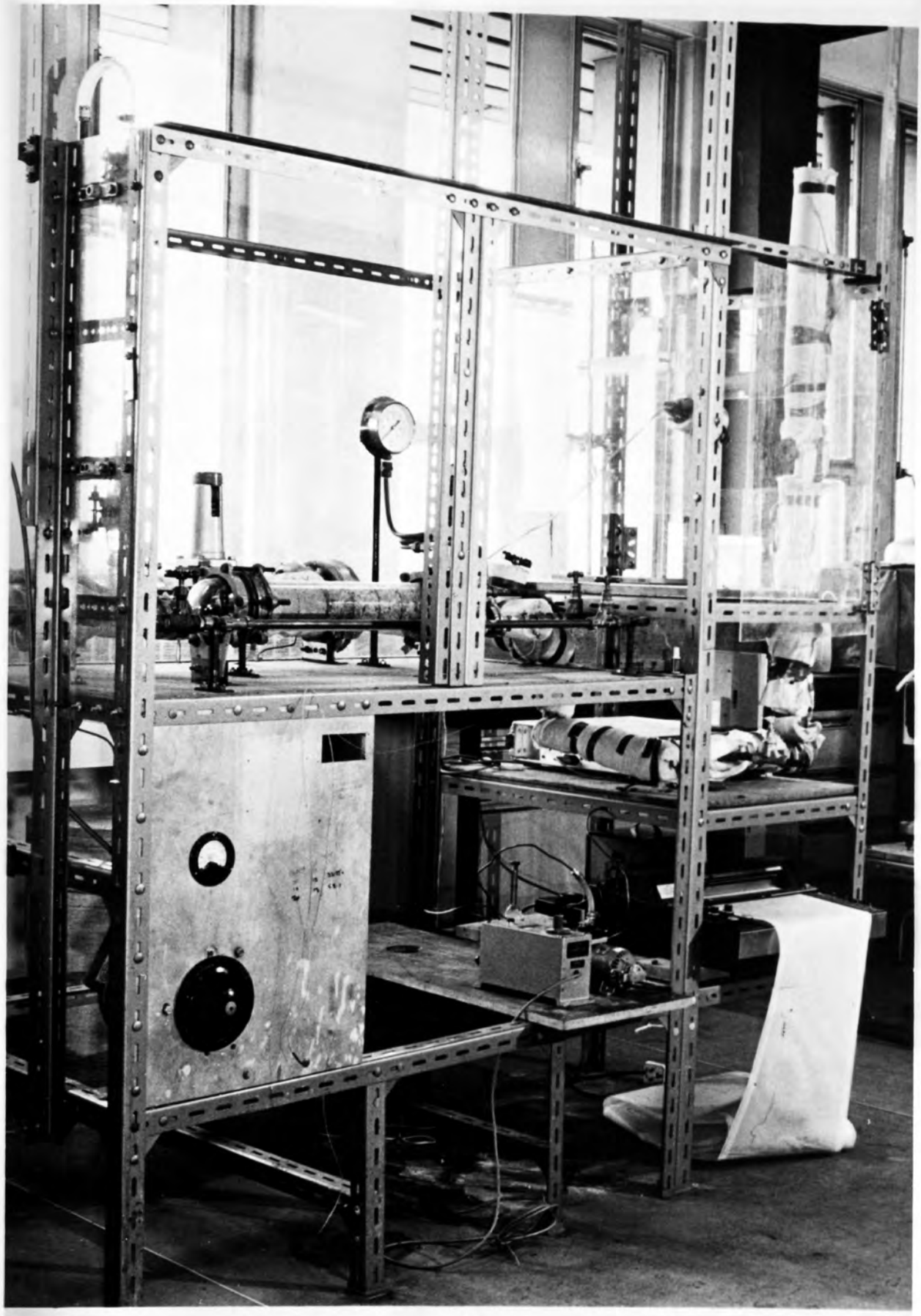

Plate 4.3 Photograph of the 28 mm Wind Tunnel

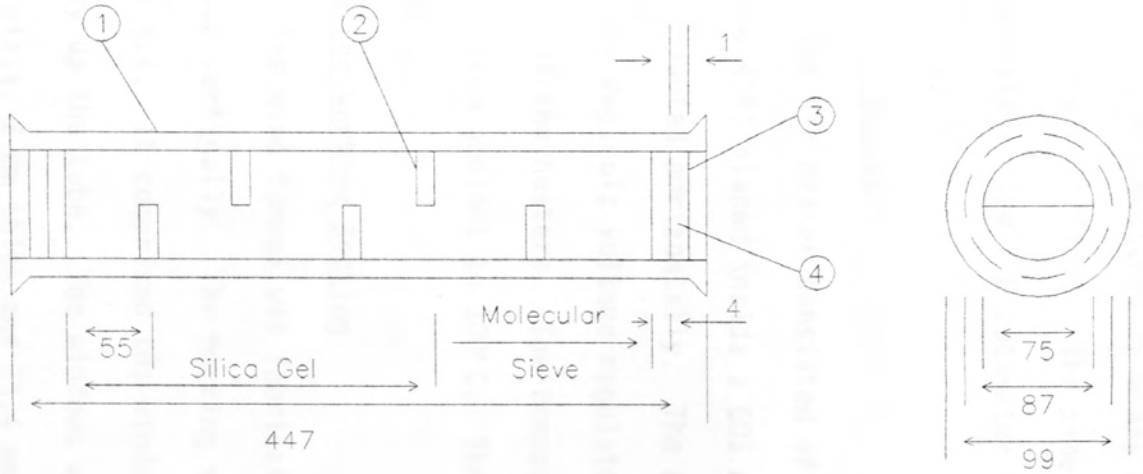

All Dimensions in mm's

Item no	Description	Material
1	QVF pipe section	Glass
2	Baffle plates	Copper
3	Wire mesh	Stainless steel
4	Knit mesh	Stainless steel

Figure 4.3 Air drier

performed by opening valve V7, closing V6 and V10, opening V9 and V8 and finally closing V12 in that order.

The humidity inside the wind tunnel was regularly measured by means of a hygrometer (Section 5.1.3). Regenerated desiccant was always used for any set of runs to ensure that the humidity inside the wind tunnel remained constant.

4.2.3 Rotameter

The air flowrate was controlled with a 12.7 mm Crane needle valve (V6) and measured by means of a 14 F G.E.C. Elliot rotameter with a Duralumin float. The pipe fittings were also designed to accommodate a size 7 F rotameter for better accuracy at low air velocities.

4.2.4 Air Heater

The air heater consisted of two 1KW electric bar heaters (Figure 4.4) placed inside a 605 mm long standard 80 mm OD copper tube, mounted horizontally. The air temperature was controlled with a Rotary Regavolt voltage regulator connected to the electrical supply of the heaters. The temperature of the heater could be varied from ambient to 300° C. The air was then passed to the wind tunnel.

4.2.5 The Working Section

The wind tunnel was fabricated from 28 mm OD copper tube, mounted vertically. The working section is shown in Figure 4.5 and Plate 4.4. It comprised two windows located opposite each other midway up the tube. The windows were flanged to take an optically flat glass, 2 mm thick and 25.4 mm diameter, through which the suspended drop could be photographed, with the required back lighting. Drops were photographed using a Chinon 35 mm camera with a telephoto extension lens. An access slit 80 mm long was provided

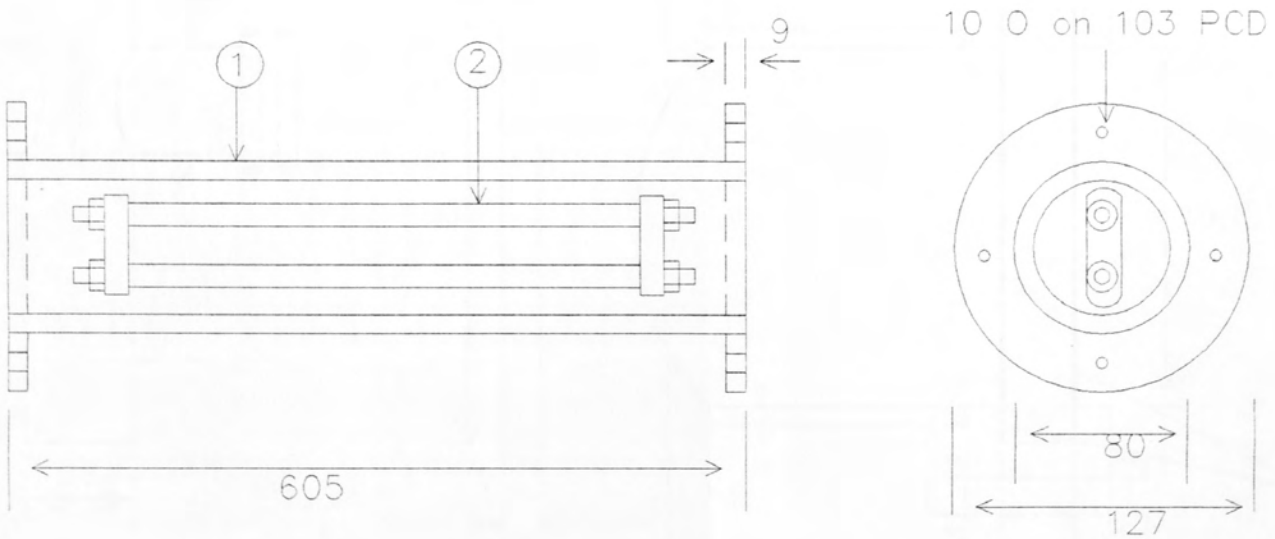

All Dimensions in mm's

Item no	Description	Material
1	Heater pipe	Copper
2	Heater elements	Tungsten

Figure 4.4 Air heater

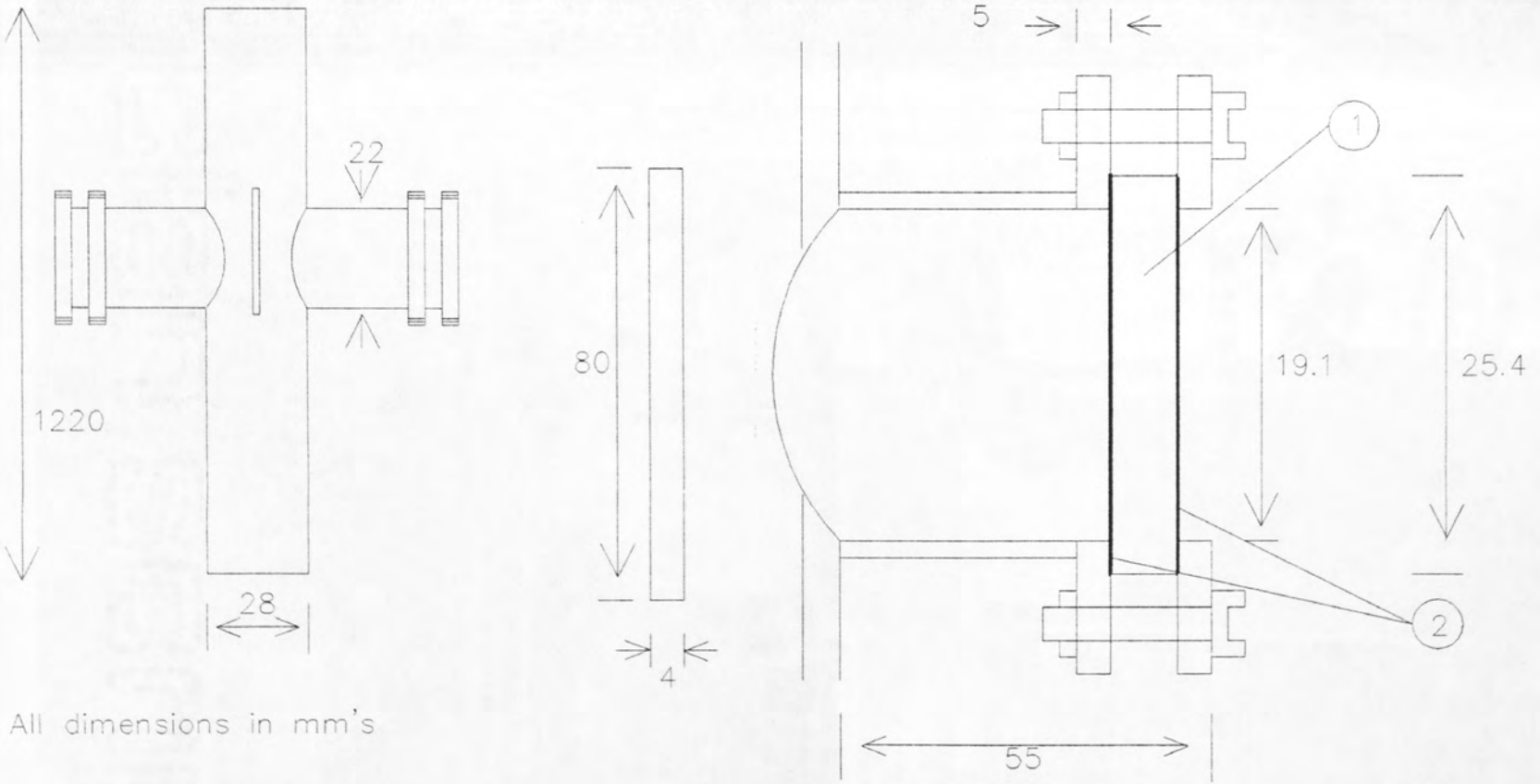

All dimensions in mm's

Item no	Description	Material
1	2 mm thick Optically flat	Glass
2	1 mm gaskets	Asbestos fibre

Figure 4.5 Working Section of the 28 mm Wind Tunnel

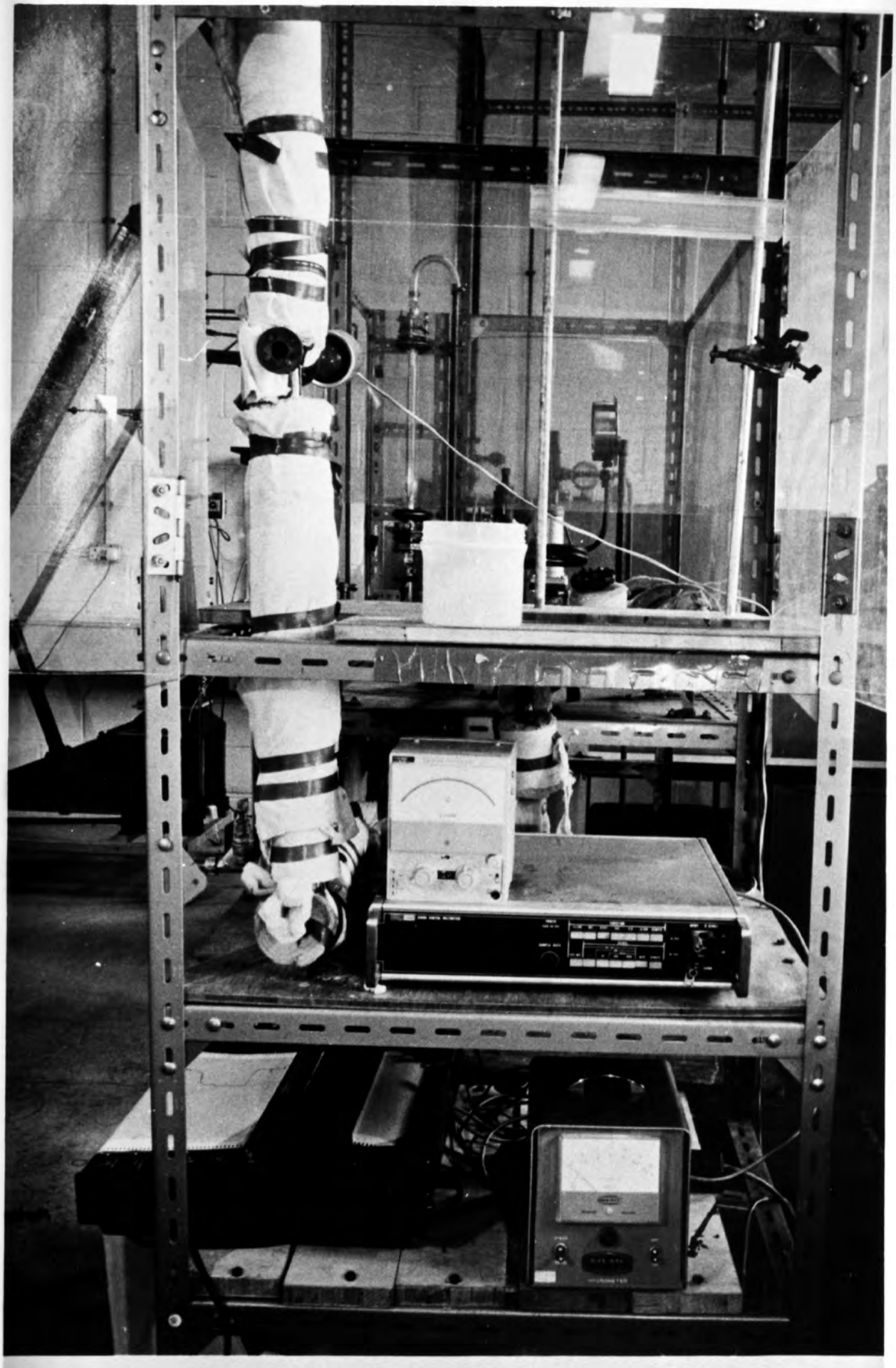

Plate 4.4 Working Section of a 28mm Wind Tunnel.

at the side of the working section at right angles to the window. The filament with a suspended drop on its tip was then inserted through this slit. The inlet to the wind tunnel was coupled to the rest of the pipework by a 28 mm copper right-angled elbow. The inside of this elbow was packed with steel wool between two layers of 5 mm thick Knitmesh (0.15 mm wire diameter, 4 stitches per cm), held together by two pieces of 30 mesh, 32 gauge wire mesh. Three layers of fine stainless steel wire mesh (100 mesh, 41 gauge) spaced one millimetre apart were placed about 6 pipe diameters upstream from the point of drop suspension. All this ensured that a flat velocity profile would be presented to the suspended drop. A typical velocity profile across the section where the drop was suspended was measured using a hot-wire anemometer and is shown in Figure 4.6.

4.3 THERMOCOUPLE MANUFACTURE

Cheong (4) originally developed a technique for manufacturing a glass filament-thermocouple. A hollow filament was drawn from a piece of 100 mm long soda-lime glass tube of 12.7 mm OD, 11.1 mm ID. After one end of the tube had been sealed, the centre section was heated gently and 'blown' from the open end to give a thin walled 'bulb'. The expanded section was again heated gently until the bulb just began to flow. The two ends were then rapidly stretched apart, giving a hollow filament of between 0.18-0.2 mm OD.

A length of about 250 mm was then broken off. A 50 μm nickel wire was next threaded through this capillary. This involved passing the wire through the filament carefully by hand. The technique had the drawback of being very slow. Considering the filaments were very fragile and easily broken, a more efficient and quicker method of manufacture was developed. This unique technique

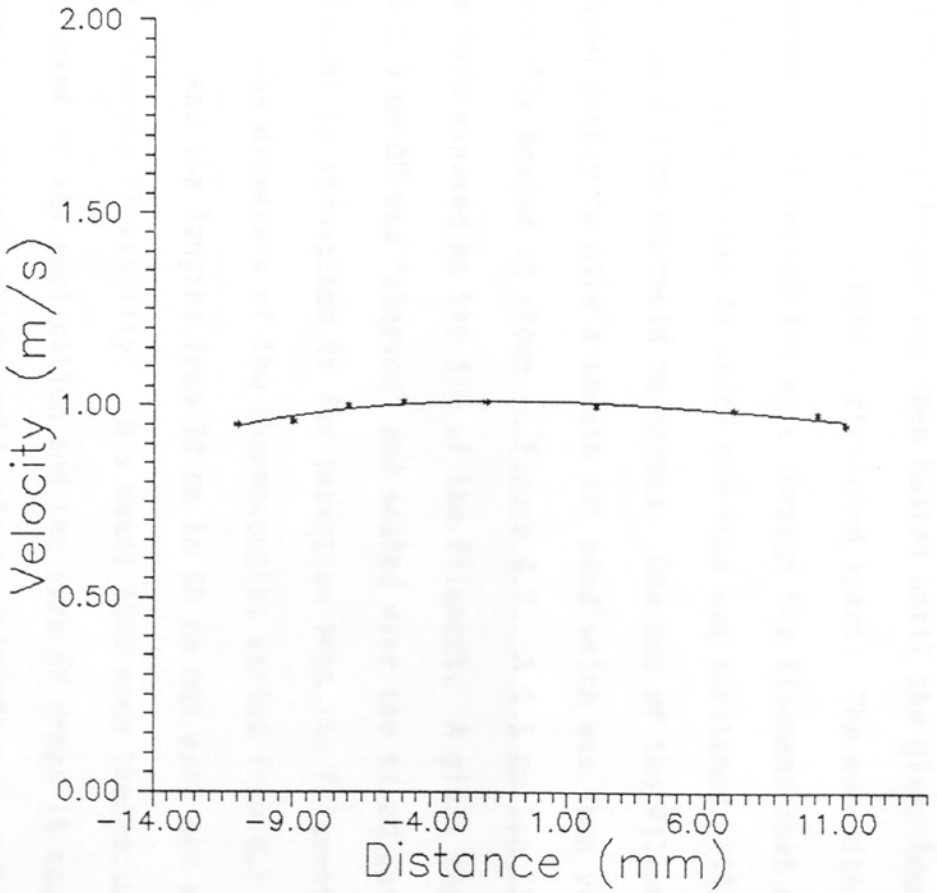

Figure 4.6 Velocity Profile across the Working Section.

overcomes the shortcomings of Cheong's (4) method. 100 mm of a 12.7 mm OD soda lime glass tube was used. The free end of a roll of 50 μm constantan wire was placed in the glass tube. The roll of wire was placed on a vertical stand so that it could rotate easily. One end of the glass tube along with the free end of the wire in it was then heated until it became red hot. This end was then squeezed with a pair of tweezers and allowed to cool so that the wire was firmly encased inside it. A section of the glass tube located 2-3 mm from this end was then heated until the glass began to flow. The tube was then rapidly stretched apart. The end with the wire encased in it pulled the wire through the filament that was formed. By varying the rate at which the tube was stretched, filaments as fine as 0.1 mm OD could be formed. One end of the filament was next heated gently to give a smooth 45° bend which was then very carefully sealed as shown in Figure 4.7. A 0.1 mm length of wire was left exposed at the tip of the filament. A glass capillary of 0.4-0.5 mm OD was 'sleeved' and sealed over the fixed end of the filament to strengthen it for insertion into the filament holder.

The diameters of the thermocouples varied from 0.1 mm to 0.5 mm and the lengths from 30 cm to 50 cm but each was unique in its size and flexibility. This meant that each thermocouple was different in its application and the size of drops it could suspend. These were factors which could only be determined by trial and error.

The filaments were coated with copper by a vacuum chamber (Plate 4.5) at a pressure of 10^{-4} to 10^{-5} mmHg to produce a coating of 50-100 Å thick. A number of filaments could therefore be coated at any one time. To obtain a durable and adhesive coating, the filaments were initially cleaned with a detergent (Decon 90). After

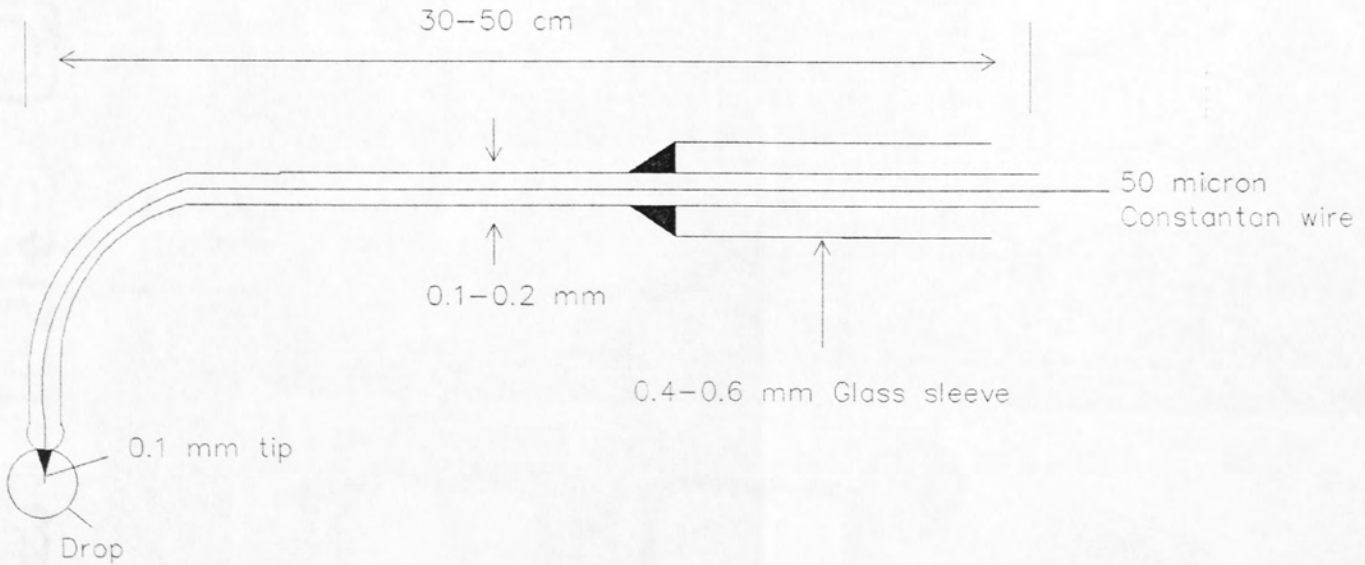

Figure 4.7 Filament – Thermocouple

Plate 4.5 Vacuum Chamber for Coating the Filaments.

rinsing with distilled water, final cleaning was achieved with iso-propanol.

4.3.1 Thermocouple Holder

The thermocouple holder is shown in Figure 4.8. The fixed end of the thermocouple was placed between the two rubber supports which were mounted on a perspex block. This block was in turn attached to a larger horizontal perspex frame along which it could be moved freely. This facilitated movement of the filament in and out of the working section. The frame was mounted on two retort stands which allowed easy movement horizontally and vertically. The filament could therefore be placed in any desired position for insertion into the working section.

The cold junction of the thermocouple was set up as shown in Figure 4.9. A 50 μm copper wire was attached to the fixed end of the filament and a junction created by connecting this wire to a 50 μm constantan wire. This junction was then placed inside a Dewar flask, full of melting ice. The flask was in turn placed into a bath of melting ice.

The voltage from the thermocouple was measured using a Fluke type 8300A digital voltmeter. This had a resolution of 0.001 mv. This output from the voltmeter was connected to a JJ instruments type 652S chart recorder.

4.4 101 MM OD WIND TUNNEL RIG

A schematic diagram of the apparatus is shown in Figure 4.10 and Plate 4.6. A larger diameter tunnel enables a relatively small drop to reside in the centre of a larger tower where the flow patterns around the drop are the most uniform and therefore less likely to be disturbed by the walls of the tower. The drop was also more easily visible and hence accessible for photography. The setup

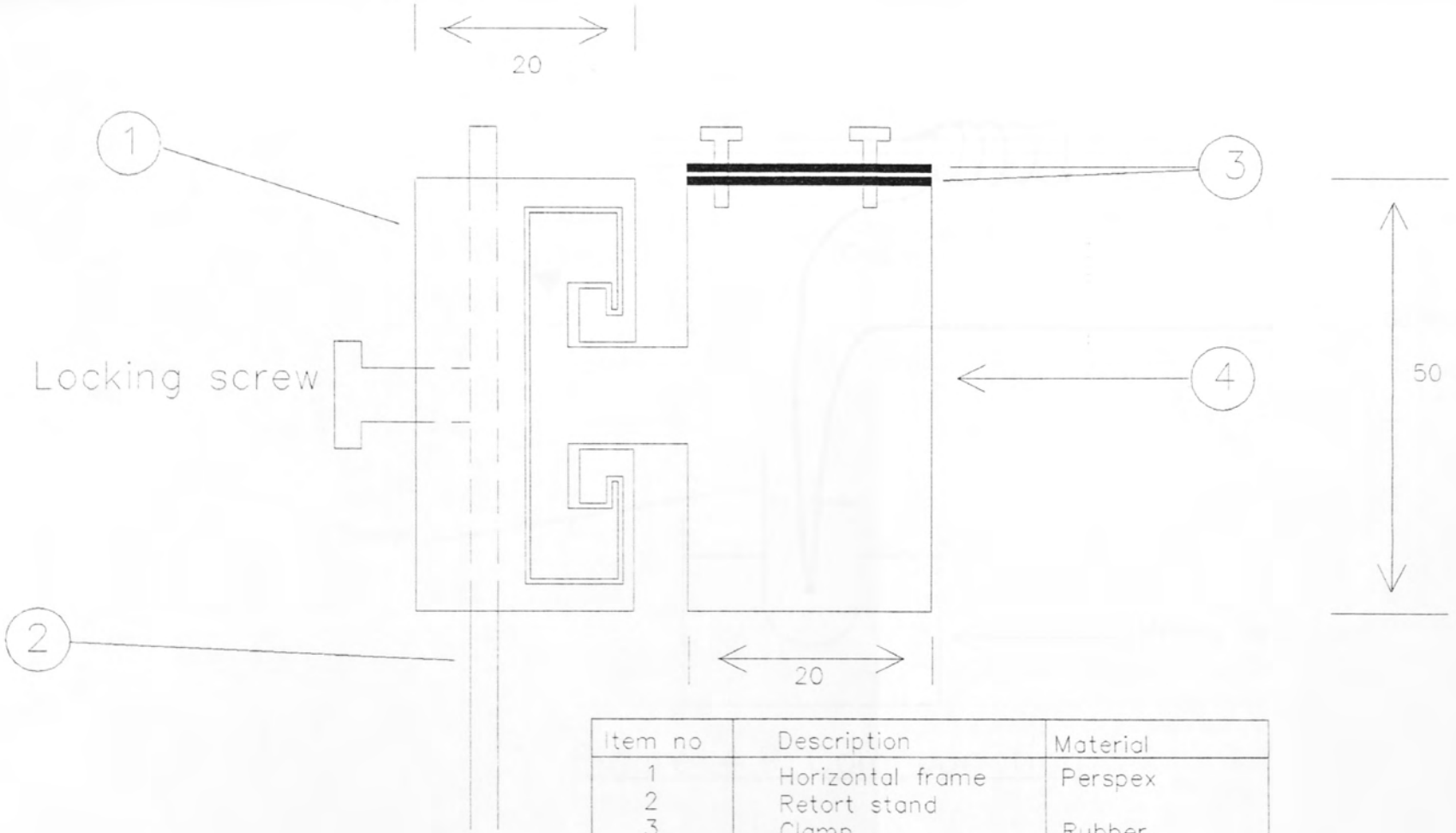

Item no	Description	Material
1	Horizontal frame	Perspex
2	Retort stand	
3	Clamp	Rubber
4	Thermocouple holder	Perspex

Figure 4.8 Thermocouple Holder

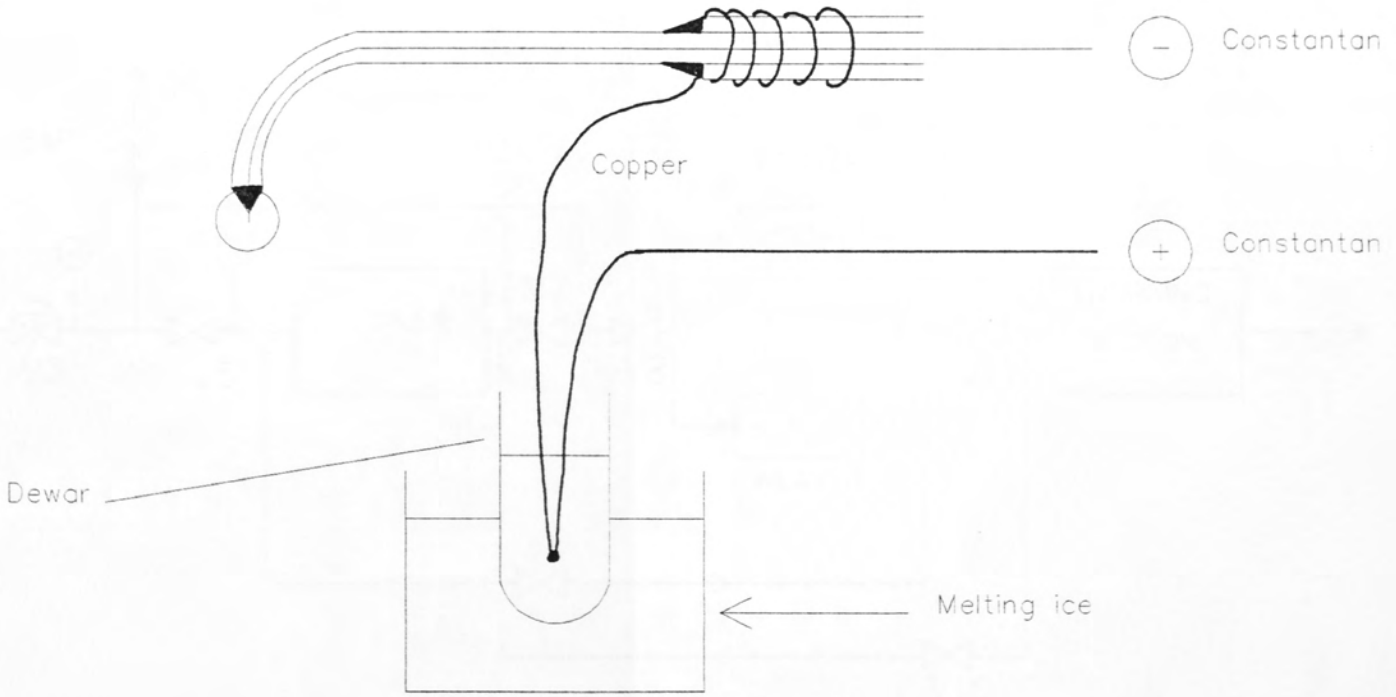

Figure 4.9 Cold Junction

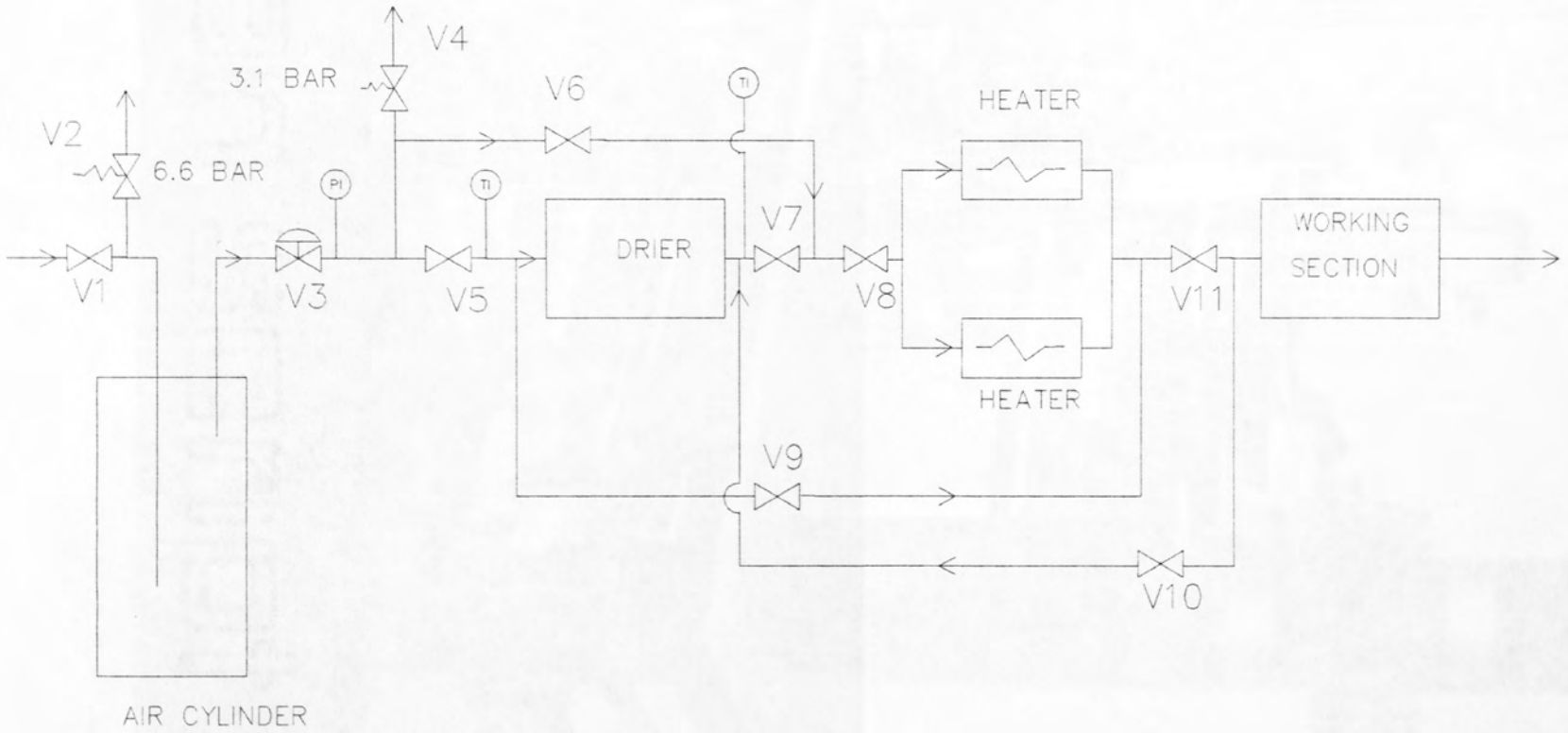

Figure 4.10 Schematic Diagram of the 101 mm Wind Tunnel

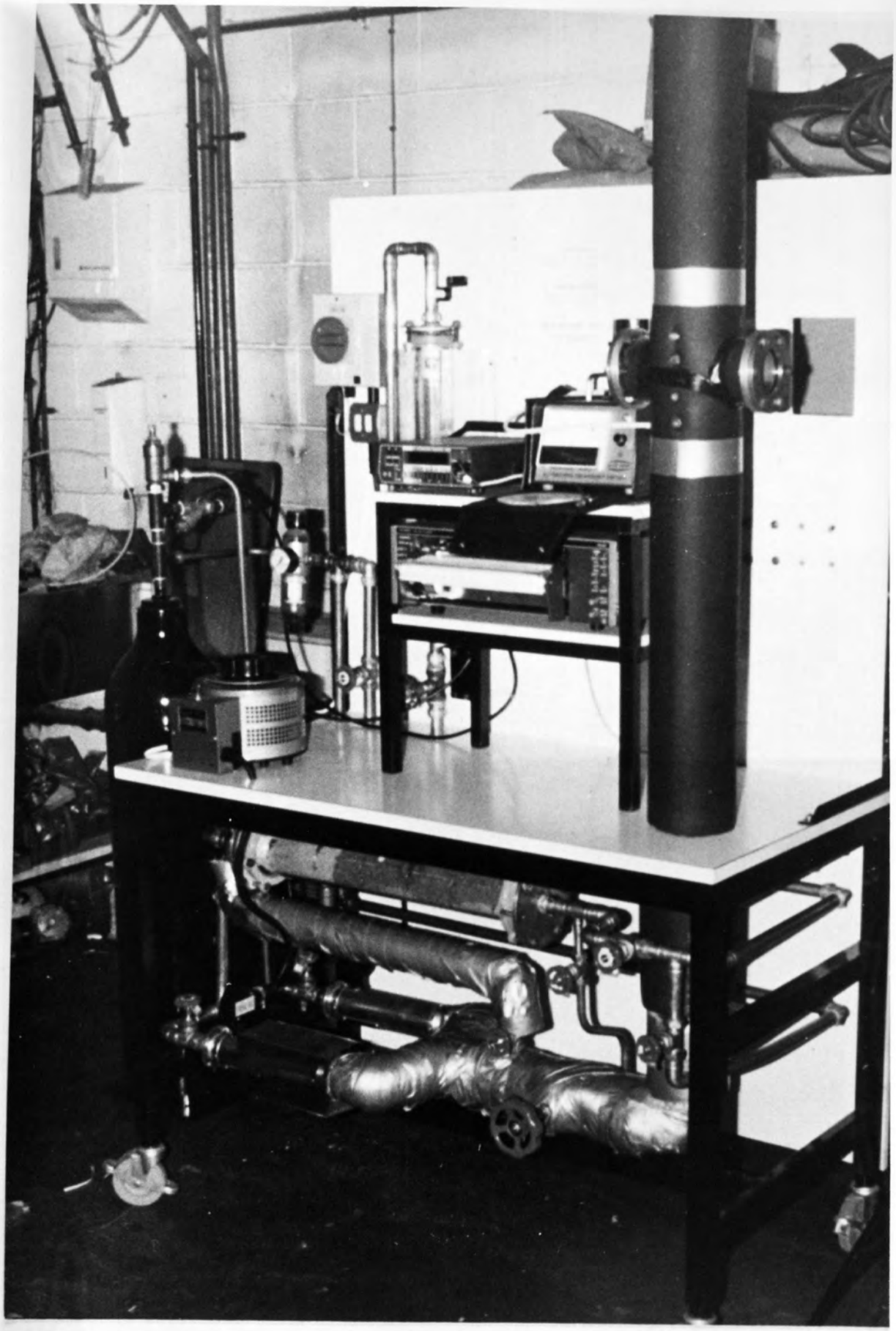

Plate 4.6 Photograph of the 101 mm Wind Tunnel

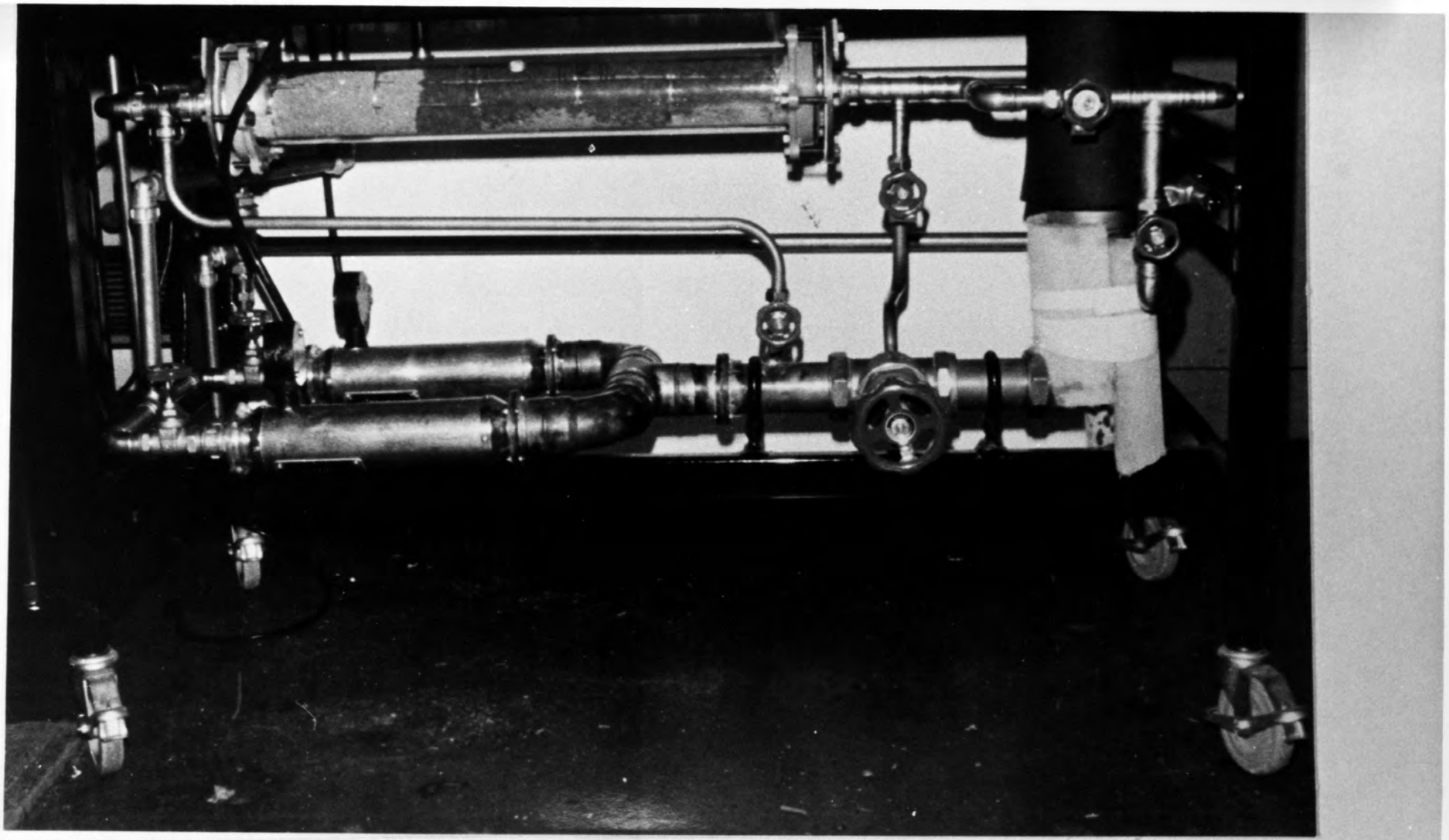

Plate 4.7 The Air Drier and Heater for the 101mm Wind Tunnel.

of this apparatus was similar to the one for the 28 mm OD vertical wind tunnel with the main differences being:

a) Compressed air supply

The air supply to the receiving gas cylinder was set at 5.4 bar. The pressure relief valve on the air receiver was set as 6.6 bar. The regulating valve V1 was set to give a delivery pressure of 2.7 bar with a pressure relief valve on the piping set at 3.1 bar.

b) Air heater

The air heater consisted of two 2KW bar heaters connected in parallel (Plate 4.7). This enabled one, or both, heaters to be used depending on the air temperature required. The heaters were connected to a Regavolt variable transformer.

CHAPTER FIVE

EXPERIMENTAL PROCEDURE

EXPERIMENTAL PROCEDURE

5.0 INTRODUCTION

The experimental procedure consisted of simultaneously measuring the drop temperature and weight histories. This was done by measuring the mV output and deflection of the thermocouple as they varied with time. In addition the air temperature, velocity and humidity were also measured. The calibration of the instruments for this and of the thermocouples is discussed in the next Sections.

5.1 INSTRUMENT CALIBRATIONS

5.1.1 Air Flowrate

A 14 F G.E.C. rotameter with a Duralumin float was used to measure the air flowrate through the 28 mm wind tunnel. For the 101 mm wind tunnel a 47 F G.E.C. rotameter with a ceramic float was used. A Parkinson wet gas meter was used to calibrate the flowrate of dry gas at ambient temperature. Local air velocities at ambient temperature were also measured in the tower using a hot wire anemometer. Air velocities at different temperatures could then be calculated by using the appropriate air density.

5.1.2 Air Temperature

The air temperature was measured at various points along the apparatus. The temperature at the entrance to the air drier, the heater wall temperature and the temperature within the working section were each measured using standard type K Ni-Cr/Ni-Al thermocouples. A Comark digital thermometer (type 3301) and a twenty-way manual selector unit (type 1694) was used to measure the outputs from the thermocouples for the drier and heater.

In the 28 mm wind tunnel a type K thermocouple was inserted through the side opening which was then sealed. The temperature

profile within the tunnel could then be measured by varying the position of the thermocouple inside the wind tunnel. Similarly a 5 mm side port was used in the 101 mm wind tunnel for insertion of a thermocouple into the working section. A Comark digital thermometer (type 1608) with a resolution of 0.1°C was used to measure the output from the thermocouple.

5.1.3 Air Humidity

The air humidity was measured using a Shaw hygrometer. This consisted of a moisture meter reading dew points from -20°C to -80°C, a moisture sensing element, a constant temperature unit and a sampling pump.

The constant temperature unit maintained a constant temperature in the air flowing to the sensing element. It also prevented condensation from the air onto the sensing element, by maintaining the gas at a temperature well above its dew point. A constant flow of air through the unit was supplied from the working section by the sampling pump. The inlet to the sampling pump was connected to the working section so that the humidity of the air passing the drop would be measured.

5.1.4 Drop Weight

The weight of an evaporating drop was measured by measuring the change in deflection of the glass filament upon which the drop was suspended. A small mark 60 mm from the tip was made on the side of the filament. The deflection of this mark was then observed using a cathetometer with a vertical vernier scale. The deflection of the filament was calibrated using different lengths of cotton thread as standard weights. The threads were attached to the tip of the filament using a touch of vaseline.

A typical calibration curve for drop weight against deflection is shown in Figure 5.1. This exhibits a linear relationship between drop weight and deflection. A linear regression was used to analyse the results. A typical relationship between drop weight and deflection was,

$$\text{Weight} = -0.055 + 0.081 \text{ Deflection} \qquad 5.1$$

The measured deflections during a run then had to be corrected for the drag force caused by the upward flowing air. The total drag force F_t, is made up of the drag force on the drop, F_d, and on the length of the filament inside the tower F_f. It can be expressed as;

$$F_t = F_d + F_f \qquad 5.2$$

For the drop

$$F_d = \frac{C_d A_d p_A V_A^2}{2} \qquad 5.3$$

And for the filament

$$F_f = \frac{C_f A_f p_A V_A^2}{2} \qquad 5.4$$

For the typical following experimental conditions of,

V_A = 1 m/s	T_A = 20 C
d_p = 2.5 E- 3m	μ_A = 1.8 E-5 kg/m/s
d_f = 1.7 E- 4m	p_A = 1.205 kg/m^3

Then for the filament,

$$Re_f = \frac{1.7E\text{-}4*1*1.205}{1.8E\text{-}5}$$

$$= 11.4$$

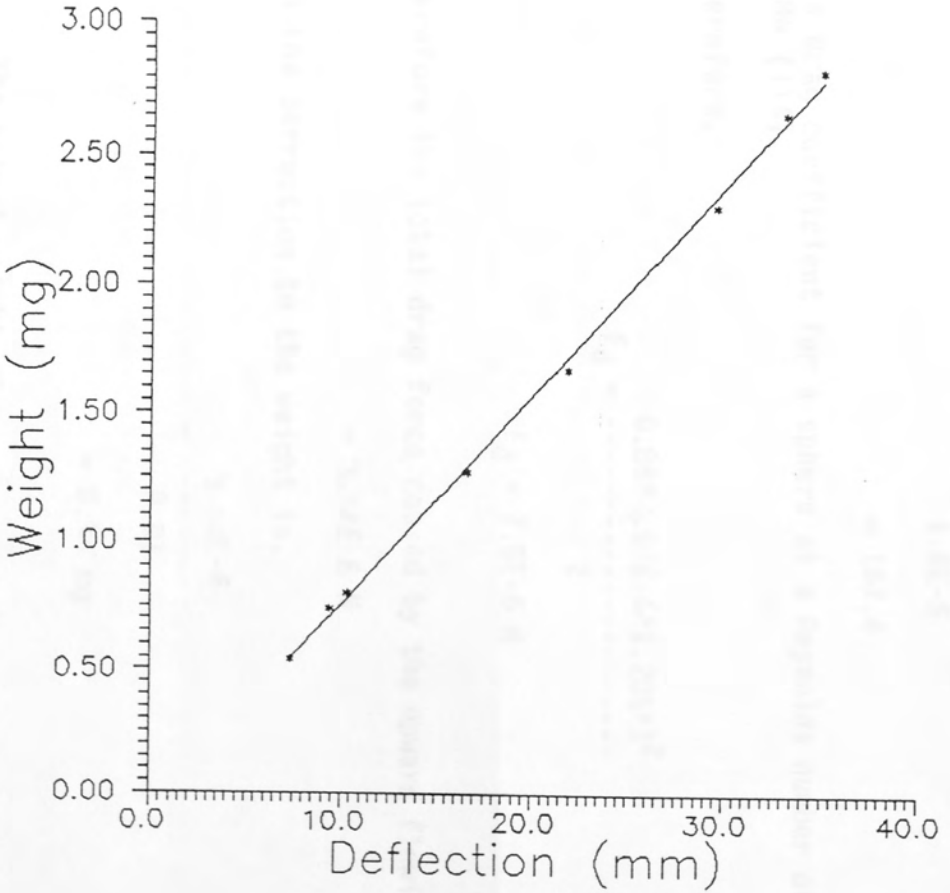

Figure 5.1 Calibration Graph of the Drop Weight

The drag coefficient for a horizontal cylinder at a Reynolds number of 11.4 is 0.8 (113).

Therefore

$$F_f = \frac{0.8 * 2.04E\text{-}6 * 1.205 * 1^2}{2}$$

$$= 9.83\ E\text{-}7\ N$$

Similarly for the drop

$$Re = \frac{2.5E\text{-}3 * 1 * 1.205}{1.8E\text{-}5}$$

$$= 167.4$$

The drag coefficient for a sphere at a Reynolds number of 167.4 is 0.86 (114).

Therefore,

$$F_d = \frac{0.86 * 4.91E\text{-}6 * 1.205 * 1^2}{2}$$

$$F_d = 2.5E\text{-}6\ N$$

Therefore the total drag force caused by the upward flowing air is,

$$= 3.48E\text{-}6\ N$$

and the correction to the weight is,

$$= \frac{3.48E\text{-}6}{9.81}$$

$$= 0.35\ mg$$

The actual weight of a suspended drop was therefore the measured weight (from the deflection) plus the correction due to the buoyancy forces.

5.1.5 Drop Temperature

The drop temperature was measured using the glass filament thermocouple. The voltage output was measured using a Fluke digital voltmeter (type 8300A) with a resolution of 0.001 mV and recorded

using a JJ instruments chart recorder. Dry air at a velocity of 2 ms^{-1} was used as the uniform temperature source for calibration. The thin film thermocouple was calibrated against a standard type K thermocouple.

Figures 5.2 and 5.3 show typical calibration graphs for different thermocouples. These demonstrate that the relationship can be represented approximately by a straight line and therefore a linear regression analysis was used. A typical relationship between the voltage output and temperature was,

$$T_d = 2.09 + 21.437\ mV \qquad 5.5$$

Figures 5.2 and 5.3 show that the thermocouples can be manufactured to give close approximations in their outputs. This confirms the reproducibility of the manufacturing process for the thermocouples.

5.2 EXPERIMENTS

Experiments were chosen to cover a representative range of different materials.

Firstly materials were selected which were known to form rigid porous and non-porous crusts, ie ones to which the receding evaporation interface model could be expected to apply. These materials were known to cover a range of different properties (85). In particular sodium sulphate decahydrate was chosen so that results could be compared directly with those of Cheong (4).

A series of experiments on water over a range of temperatures (17-107° C) were also carried out to test the 101 mm OD experimental rig and to standardise the experimental method.

Sodium acetate was also studied because it was a material known to form an external skin instead of, or prior to, forming a crust.

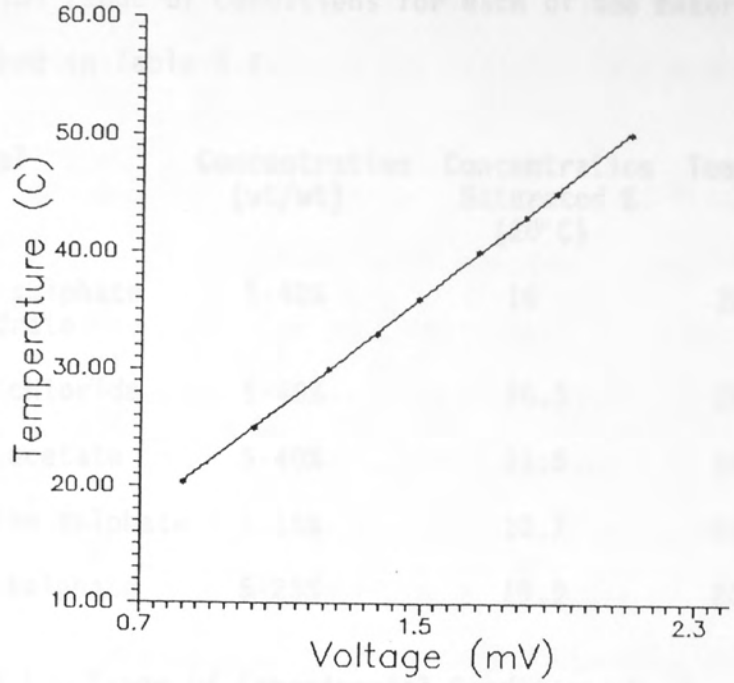

Figure 5.2 Calibration Graph of the Drop Temperature

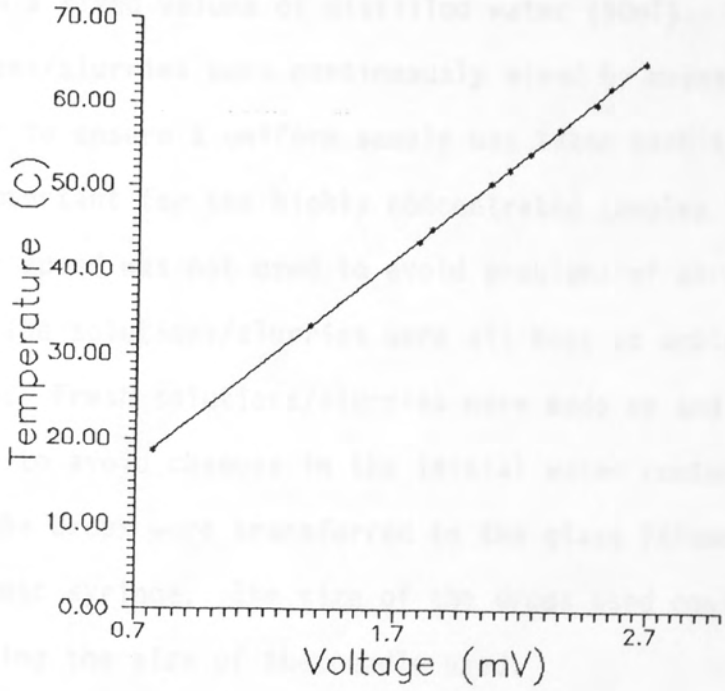

Figure 5.3 Calibration Graph of the Drop Temperature

The range of conditions for each of the materials used are described in Table 5.1.

Material	Concentration (wt/wt)	Concentration Saturated % (20°C)	Temperature (°C)	Air Vel (m/s)
Sodium sulphate decahydrate	5-40%	16	20-83	0.6-1
Sodium chloride	5-40%	26.5	20-124	0.5-1
Sodium acetate	5-40%	31.5	56-105	1
Potassium sulphate	5-15%	10.7	20-91	0.8-1.4
Copper sulphate	5-25%	19.9	20-110	1

Table 5.1 Range Of Experimental Conditions Used

5.3 DROPS OF AQUEOUS SOLUTIONS AND SLURRIES

Solutions and slurries of the different materials were made up by dissolving and/or mixing the desired amount of Analar quality salt in a fixed volume of distilled water (50ml). The solutions/slurries were continuously mixed by means of a magnetic stirrer to ensure a uniform sample was taken each time. This was most important for the highly concentrated samples. Too high a stirrer speed was not used to avoid problems of aeration of the feed. The solutions/slurries were all kept at ambient temperature (~20°C). Fresh solutions/slurries were made up and used within 30 minutes to avoid changes in the initial water content.

The drops were transferred to the glass filament by means of a hypodermic syringe. The size of the drops used could then be varied by varying the size of the needle used.

At the beginning of a run the initial deflection of the filament with a drop suspended on it was measured. This gave the initial drop weight. During the run the filament deflection was

measured continuously as described in Section 5.1.4. The millivolt output from the thermocouple was measured continuously as described in Section 5.1.5.

At the end of a run the deflection of the filament whilst supporting the final dried sample outside the wind tunnel was measured. This corresponded to the final dried weight of the drop and could be compared to the final drop weight inside the wind tunnel corrected for buoyancy effects, heat conducted by the filament and any radiated heat to the drop. Typical results are shown in Table 5.2. demonstrating good agreement between the two weights.

Wherever possible the final dried particle attached to the filament was gently removed. However due to the fragile nature of the filament this was not always possible. The tip of the filament was then washed with distilled water to remove any fine particles from it before being used again.

The nature of the crust structure of selected drops was observed using a Scanning Electron Microscope. The final dried sample was placed in a vacuum chamber and a thin film of gold-palladium deposited onto the particle by a spluttering technique. The coated sample could then be introduced into the specimen chamber of the S.E.M. Selected areas were photographed with a 35 mm camera attached to the S.E.M.

Experimental Reference	Final Weight (mg)	Final Weight Predicted (mg)
D46	0.95	1.17
58	0.25	0.24
64	1.18	1.07
76	0.46	0.44
86	0.36	0.37
93	0.15	0.17
120	0.22	0.23
144	0.90	0.95
152	6.79	6.93

Table 5.2 Predicted and Actual Final Weights

CHAPTER SIX

EXPERIMENTAL RESULTS

EXPERIMENTAL RESULTS

6.0 INTRODUCTION

Single drops of aqueous sodium sulphate decahydrate, sodium chloride, potassium sulphate, copper sulphate and sodium acetate of different concentrations were dried under various conditions as shown in Table 5.1.

Simultaneous drop weight and drop core temperature measurements were made, as described in sections 5.1.4 and 5.1.5. The measured weight was corrected for the buoyancy effects of the upward flowing air and radiation, convection and conduction effects. A full listing of these terms is given in Appendix B7 and typical heat transfer flows over a range of air temperatures (18-100°C) in Table 6.1. These results were obtained from a computer program EXPT1.FOR which was used to analyse the experimental data. A description and listing of the program is given in Appendix C.1. The results of the drying rates and core temperatures are tabulated in Appendix B.

Experiments on water drops are presented in terms of Nusselt numbers. The instantaneous value of $d(dp^2)/dt$ at each drop size was used to calculate the experimental Nusselt number for each drop size during a run by equation 3.992.

Reference	Air Temperature °C	% Heat Flow		
		Convection	Radiation	Filament
D61	18.4	89.3	2.8	7.9
D71	36.4	88.7	3.9	7.4
D78	68.4	88.0	4.2	7.8
D90	91.0	85.4	5.8	8.8
D101	100.0	85.3	5.4	9.3

Table 6.1 A Comparison of the Relative Contributions of the Different Heat Flows

6.1 DROPS OF AQUEOUS SODIUM SULPHATE DECAHYDRATE

The experimental results for drops containing solids are presented in two ways. Various investigators (10,85,112) have presented the drop weight histories in terms of fraction of initial weight evaporated (change in drop weight) versus time. Hence results have been presented in this way here to smooth-out any slight variations in the initial weight of the drop and to assist comparison with published results. The effects of experimental variables, eg air temperature, air velocity and initial drop concentration can be easily interpreted from these plots. However this method of presentation does not represent a drying rate as such. This is represented by the gradient of the curves. Therefore simultaneous drying rate and core temperature histories have also been used. The various drying periods, eg the constant rate and the falling rate, and the relationship between the rates and the core temperature are more easily obtained from these plots.

6.1.1 Effect of Initial Concentration

Figure 6.1 illustrates the effect of the initial concentration on the drying rates, for drops of the same initial size. Increasing the initial drop concentration reduces the drying rate obtained. At the higher concentrations a crust begins to form immediately the drop contacts the hot air stream. The crust formed represents a major resistance to mass transfer. Audu (5) states that 65% of the total resistance is represented by the crust for sodium sulphate drops.

Interestingly as shown in Figure 6.1 the initial drying rates were similar at the lower concentrations of 5% and 15% weight. However once a crust forms there is a sharp difference in the curves with a decrease in the drying rate at the higher concentration.

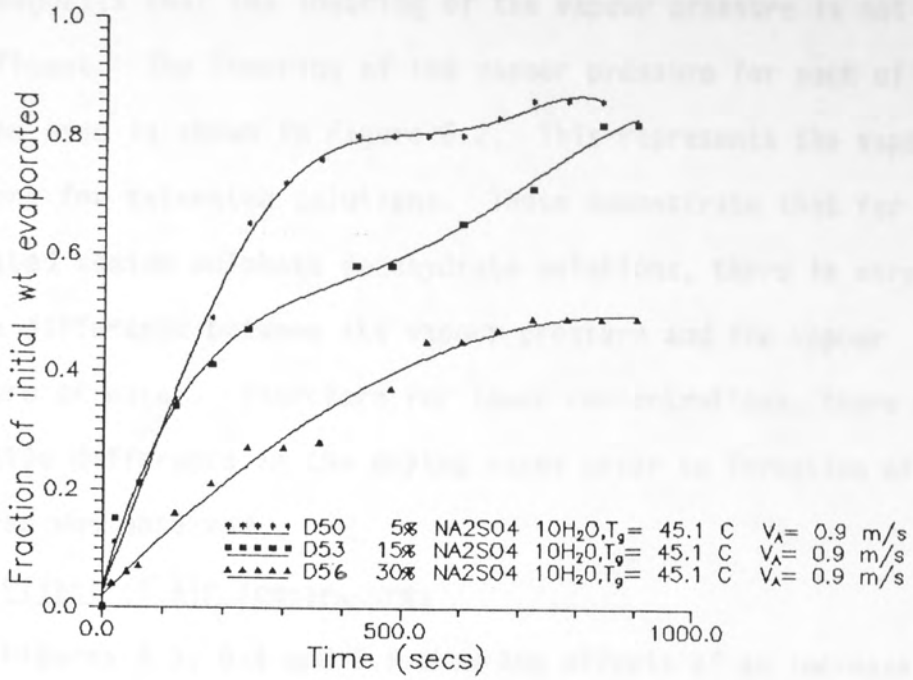

Figure 6.1 Drying of Drops of Aqueous Sodium Sulphate Decahydrate at Varying Initial Concentrations.

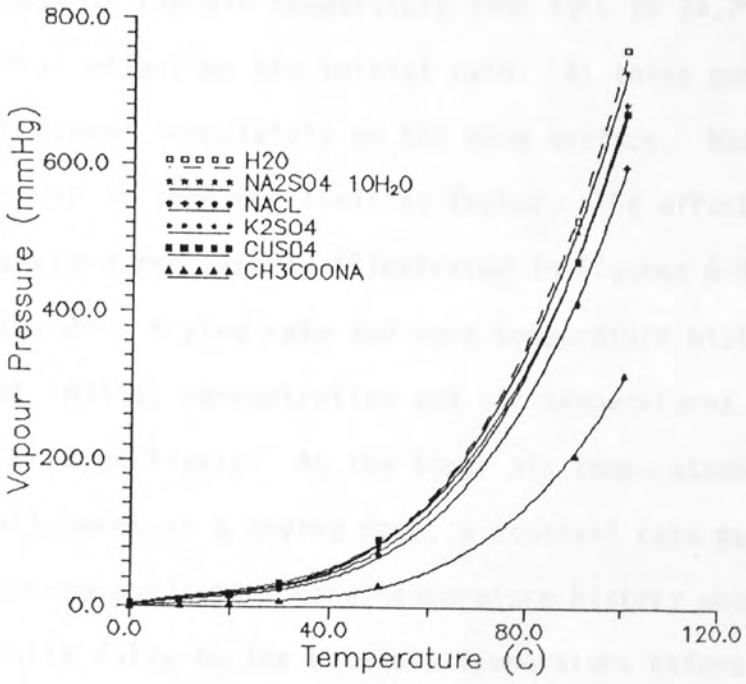

Figure 6.2 The Effect of Solute Nature on the Vapour Pressure of the Saturated Solution (128).

This suggests that the lowering of the vapour pressure is not significant. The lowering of the vapour pressure for each of the solutes used is shown in Figure 6.2. This represents the vapour pressure for saturated solutions. These demonstrate that for saturated sodium sulphate decahydrate solutions, there is very little difference between its vapour pressure and the vapour pressure of water. Therefore for lower concentrations, there would be little difference in the drying rates prior to formation of the crust as was observed.

6.1.2 Effect of Air Temperatures

Figures 6.3, 6.4 and 6.5 show the effects of an increase in the air temperature for 5% (45-68°C), 15% (45-74°C) and 40% (31-54.7°C) by weight initial concentrations. As expected an increase in the air temperature increased the drying rate in all cases. However at the higher concentrations (40% weight) an increase in the air temperature from 43°C to 54.7°C had only a marginal effect on the initial rate. At these concentrations a crust formed immediately on the drop surface. Mass transfer through the crust is then the limiting factor. The effects of the air temperature are clearly illustrated in Figures 6.6 and 6.7 which are simultaneous drying rate and core temperature histories for 40% weight initial concentration and air temperatures of 20.4°C and 54.7°C respectively. At the lower air temperature of 20.4°C, after establishment of a drying rate, a constant rate period was observed. This corresponds to a core temperature history where the temperature initially falls to the wet-bulb temperature before rising steadily to the air temperature. From a simple heat balance on the core,

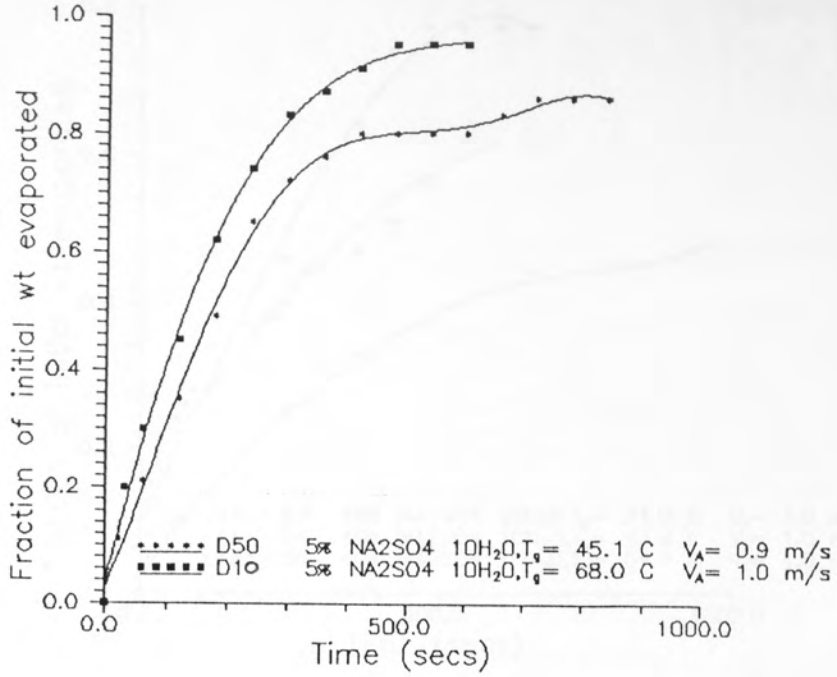

Figure 6.3 Drying of Drops of Aqueous Sodium Sulphate Decahydrate (5 % wt/wt) at Varying Air Temperatures.

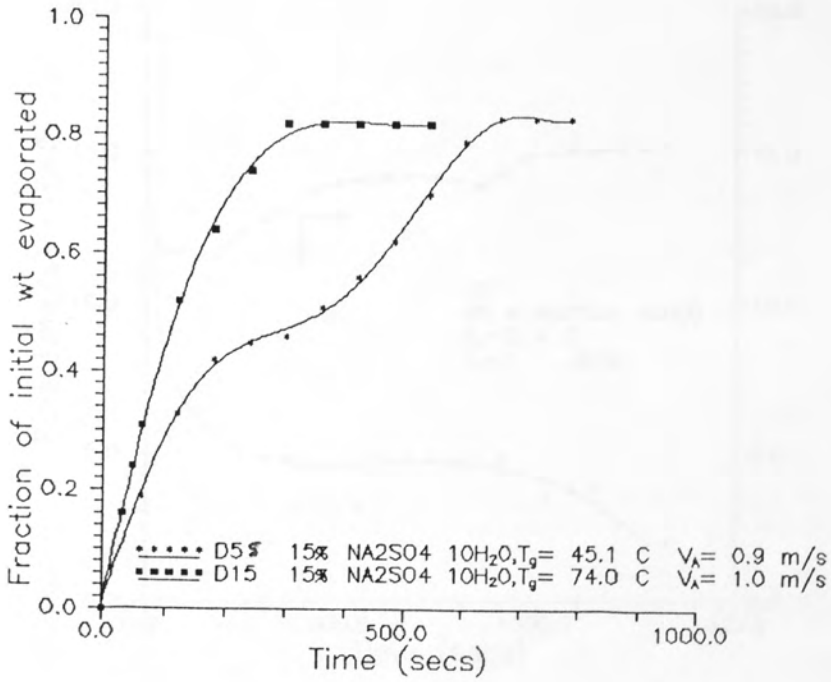

Figure 6.4 Drying of Drops of Aqueous Sodium Sulphate Decahydrate (15 % wt/wt) at Varying Air Temperatures.

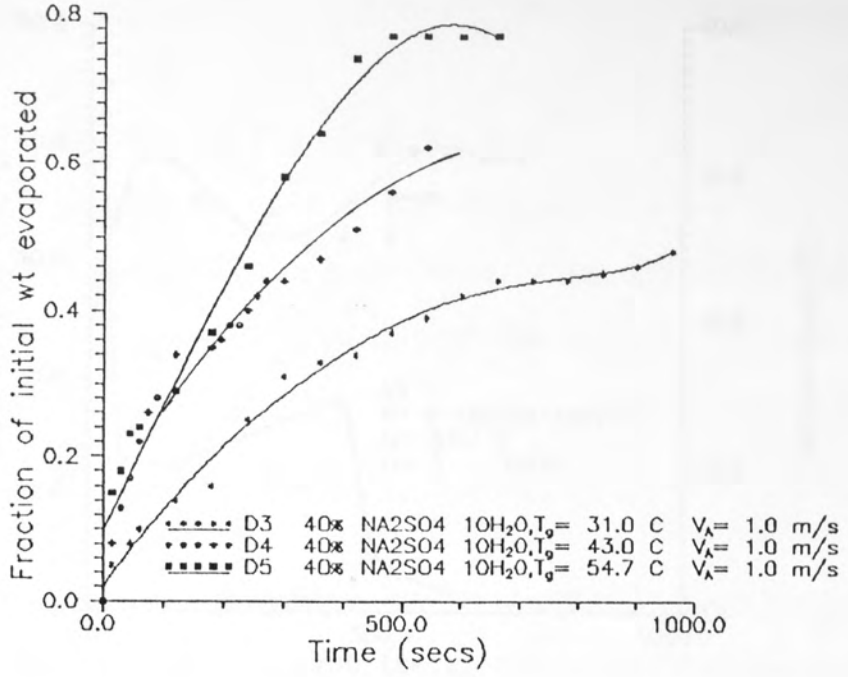

Figure 6.5 Drying of Drops of Aqueous Sodium Sulphate Decahydrate (40 % wt/wt) at Varying Air Temperatures.

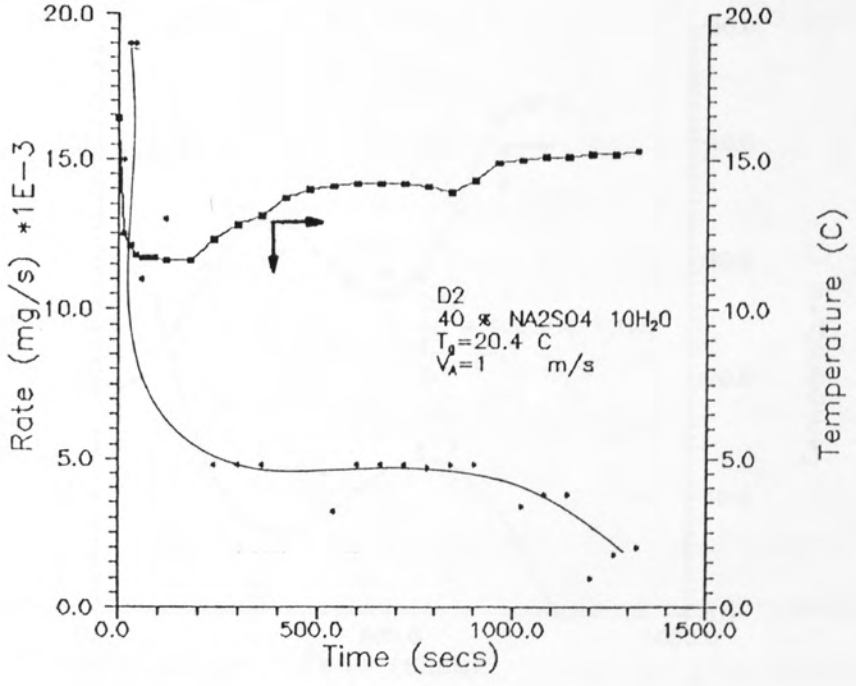

Figure 6.6 Simultaneous Core Temperature and Rate Histories for Aqueous Sodium Sulphate Decahydrate (40 % wt/wt) at T_g=20.4 C

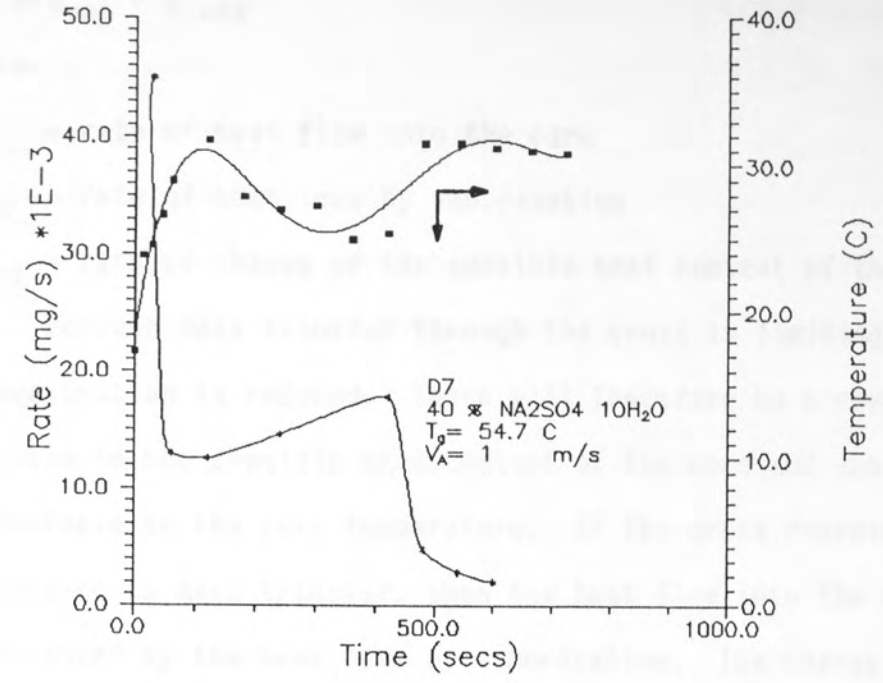

Figure 6.7 Simultaneous Core Temperature and Rate Histories for Aqueous Sodium Sulphate Decahydrate (40 % wt/wt) at T_g=54.7 C

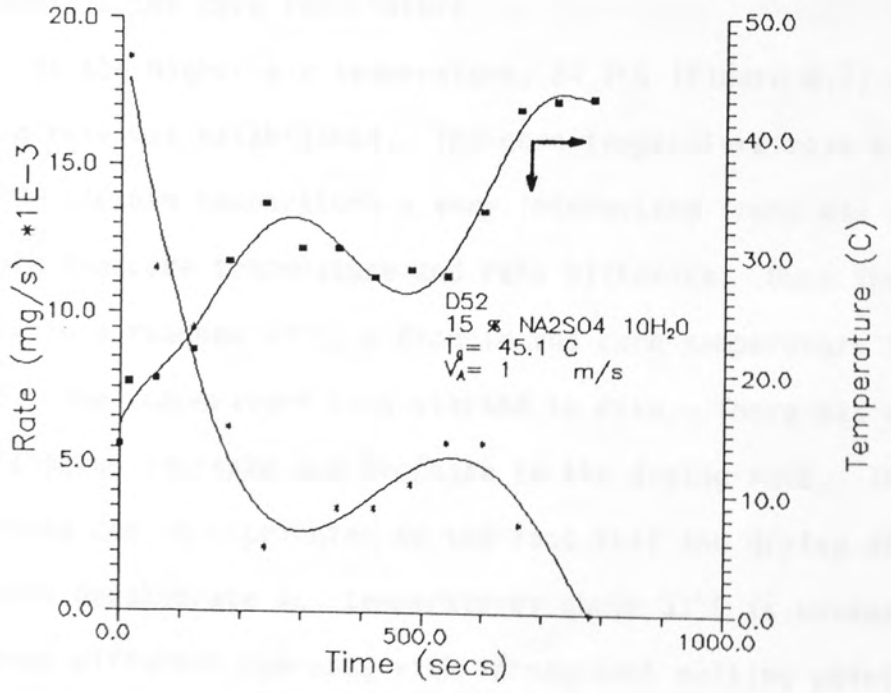

Figure 6.8 Simultaneous Core Temperature and Rate Histories for Aqueous Sodium Sulphate Decahydrate (15 % wt/wt) at T_g=45.1 C

$$Q_{In} = Q_{vap} + Q_{sens} \quad 6.1$$

Where,

Q_{In} = rate of heat flow into the core

Q_{vap} = rate of heat loss by vaporisation

Q_{sens} = rate of change of the sensible heat content of the core

Because mass transfer through the crust is limiting, the rate of evaporation is reduced. There will therefore be a corresponding increase in the sensible heat content of the core and subsequently an increase in the core temperature. If the crust represented no resistance to mass transfer, then the heat flow into the core would be balanced by the heat loss by vaporisation. The change in the sensible heat content of the core would be negligible and the core temperature would remain constant at the wet-bulb temperature. Conversely if heat transfer through the crust were limiting, there would be a decrease in the sensible heat content of the core and a decrease in the core temperature.

At the higher air temperature, 54.7°C (Figure 6.7) a higher drying rate was established. The core temperature rose steadily to 33°C. At this temperature a very interesting trend was observed in both the core temperature and rate histories. Once the temperature reached 33°C, a drop in the core temperature to 25°C was noted. The temperature then started to rise. There was a simultaneous increase and decrease in the drying rate. This phenomena can be attributed to the fact that the drying of sodium sulphate decahydrate at temperatures above 33°C is unusual in that it forms different hydrates with incongruent melting points (96) absorbing heat in the process.

Below the transition temperature of 32.6°C, the monoclinic decahydrate crystals are in equilibrium with the liquid phase. At

the transition point, the rhombic crystals of anhydrous sulphate commence to separate and exist in equilibrium with the decahydrate and the saturated solution. From the transition going up to about 125°C, the solubility of the anhydrous sulphate decreases with increasing temperature. The enantiomorphic change occurs at 33°C releasing 0.51kg water/kg of decahydrate. The water released subsequently diluted the core's concentration below saturation. This then leads to a larger vapour pressure driving force leading to an increase in the mass transfer rates. This behaviour is clearly demonstrated in Figures 6.7 and 6.8. These particular results highlight the advantage of using the filament/balance for studying simultaneous heat and mass transfer rates.

At higher air temperatures this sharp decrease in the core temperature at 33°C was not observed. For a drop initially of 15% weight concentration at 74°C, the core temperature increased rapidly to 33°C as shown in Figure 6.9. The temperature then rose steadily to the air temperature. It is probable that the higher air temperatures and subsequent higher heat transfer rates would tend to very rapidly re-establish the equilibrium at 33°C. From Figures 6.6 to 6.9 it is clear that only at a low air temperature (20.35°C) was a constant rate period established. At higher air temperatures after commencement of drying, a falling rate was initiated. This is indicative of a final crust of low porosity. Electron micrographs in Plates 6.1, 6.2 and 6.3 show the inner and outer structure of a drop of 40% weight concentration sodium sulphate decahydrate dried at an air temperature of 31°C and 1m/s air velocity. The structure of both the inside and outside crust is of a very fine nature with no evidence of fractures or blow holes as are often observed with spray-dried materials.

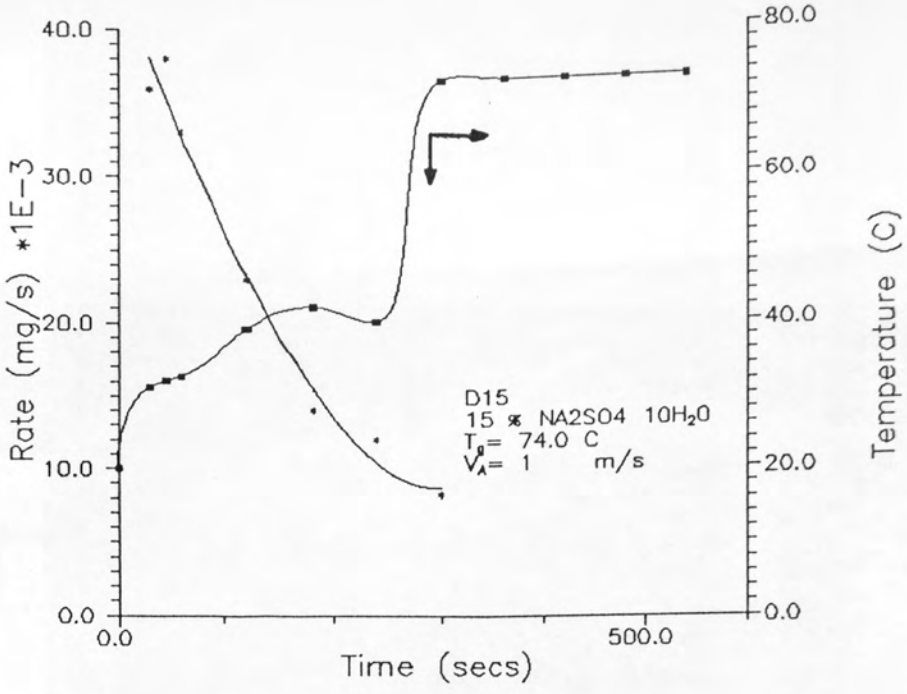

Figure 6.9 Simultaneous Core Temperature and Rate Histories for Aqueous Sodium Sulphate Decahydrate (15 % wt/wt) at T_g=74.0 C

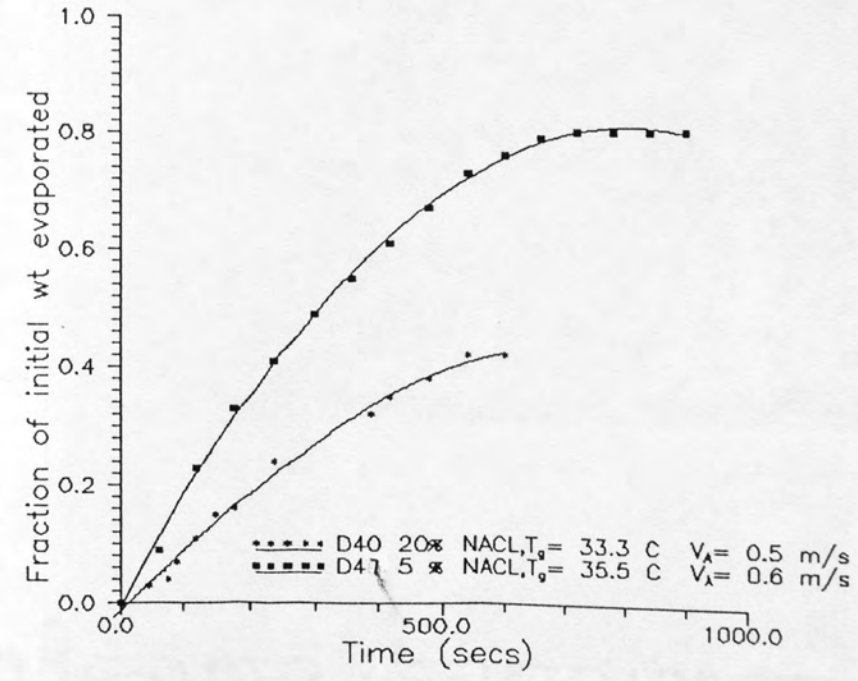

Figure 6.10 Drying of Drops of Aqueous Sodium Chloride at Varying Initial Concentrations.

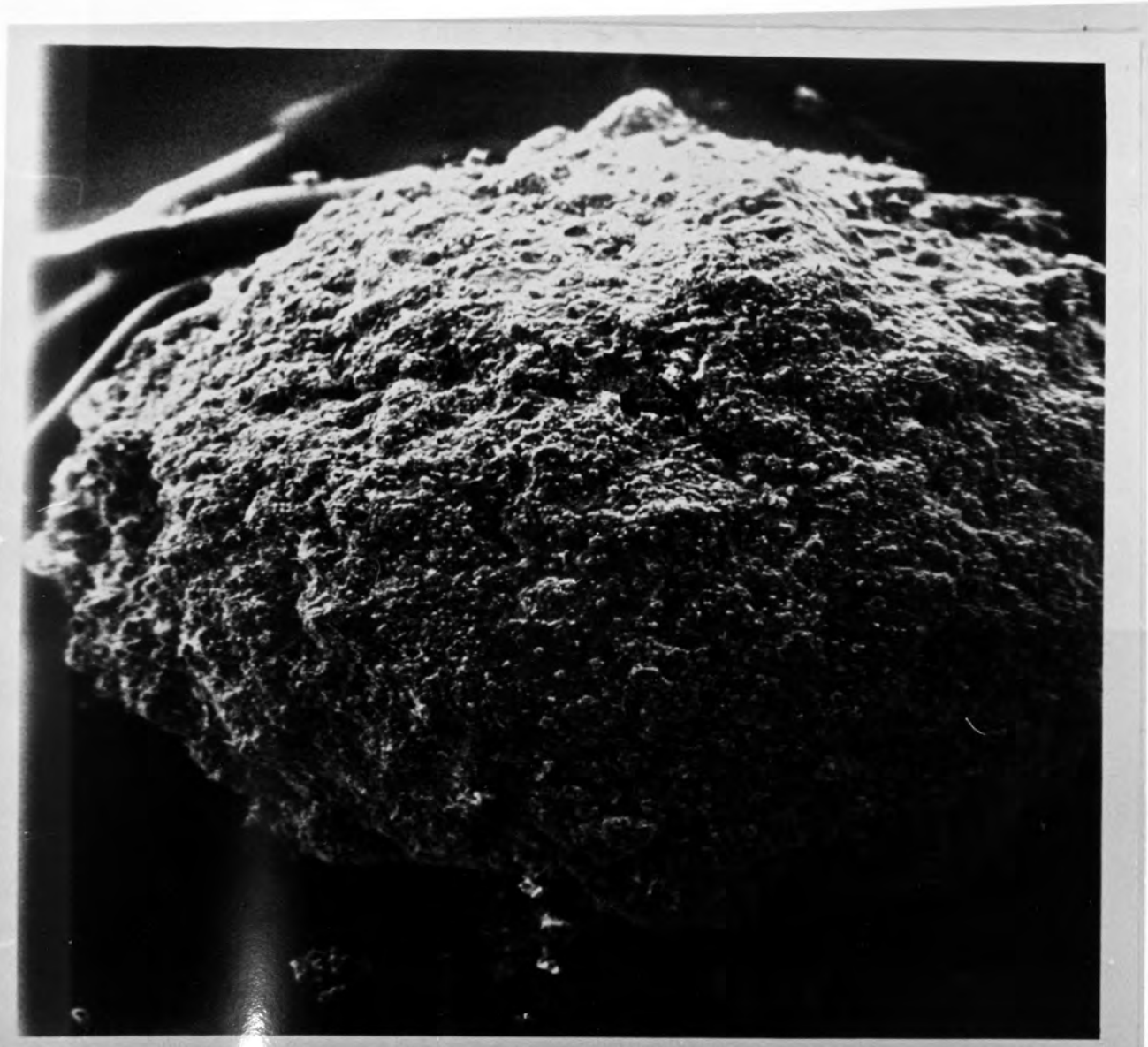

Plate 6.1 Outer Crust Surface of a 40% Weight Sodium Sulphate Dechaydrate Drop (31°C, 1m/s).

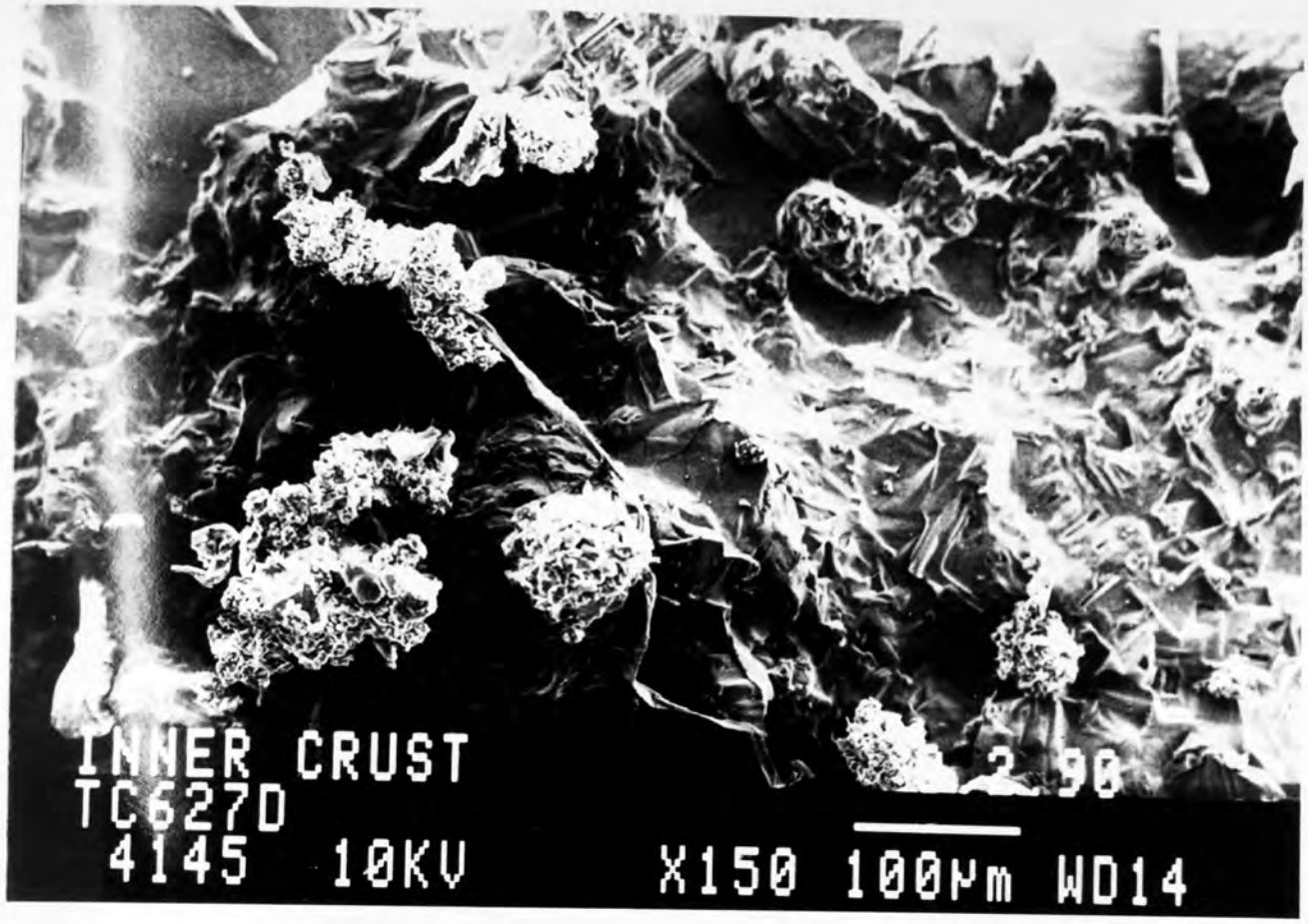

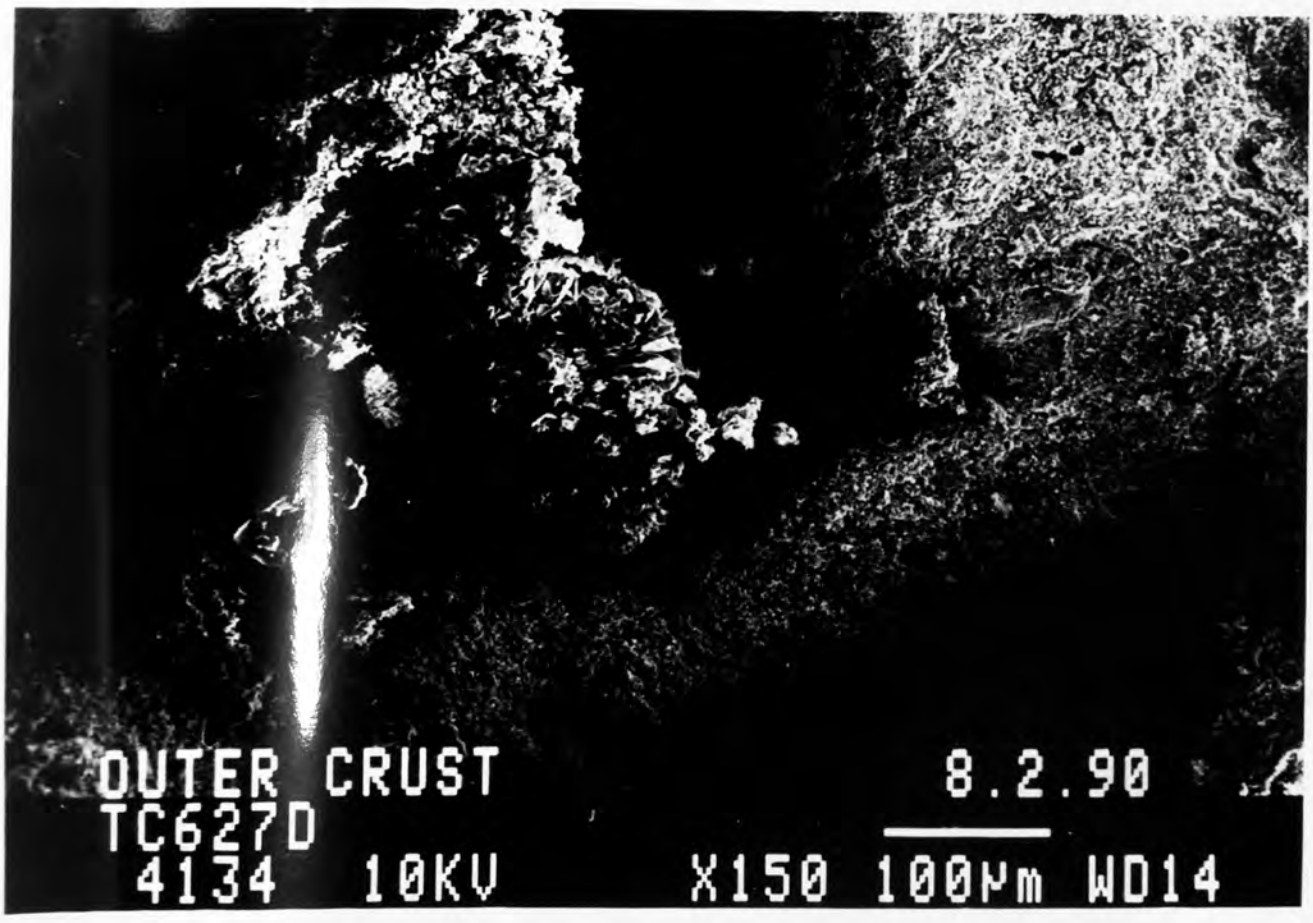

Plate 6.2 Inner and Outer Crust Surface of a 40% Weight Sodium Sulphate Decahydrate Drop (31°C, 1m/s).

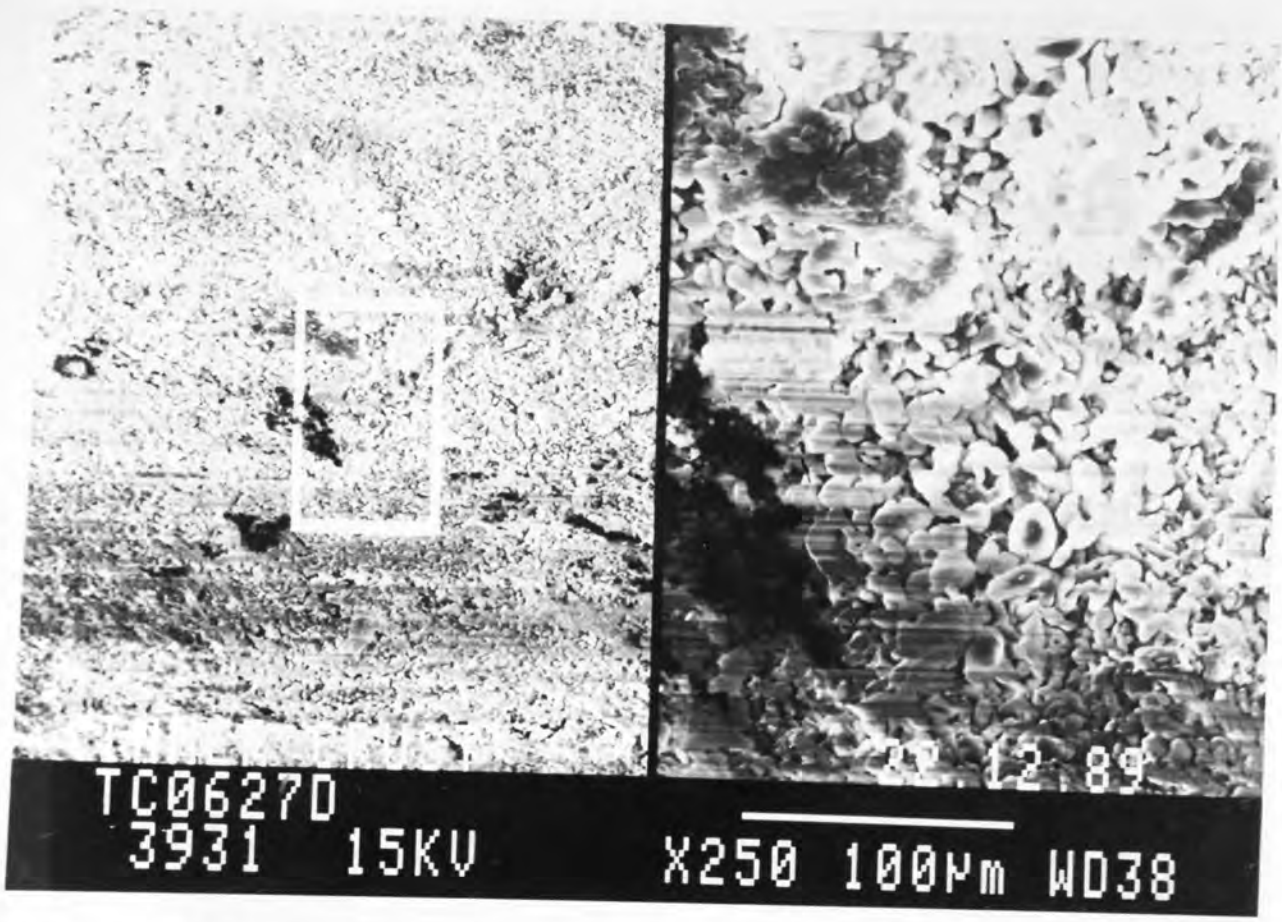

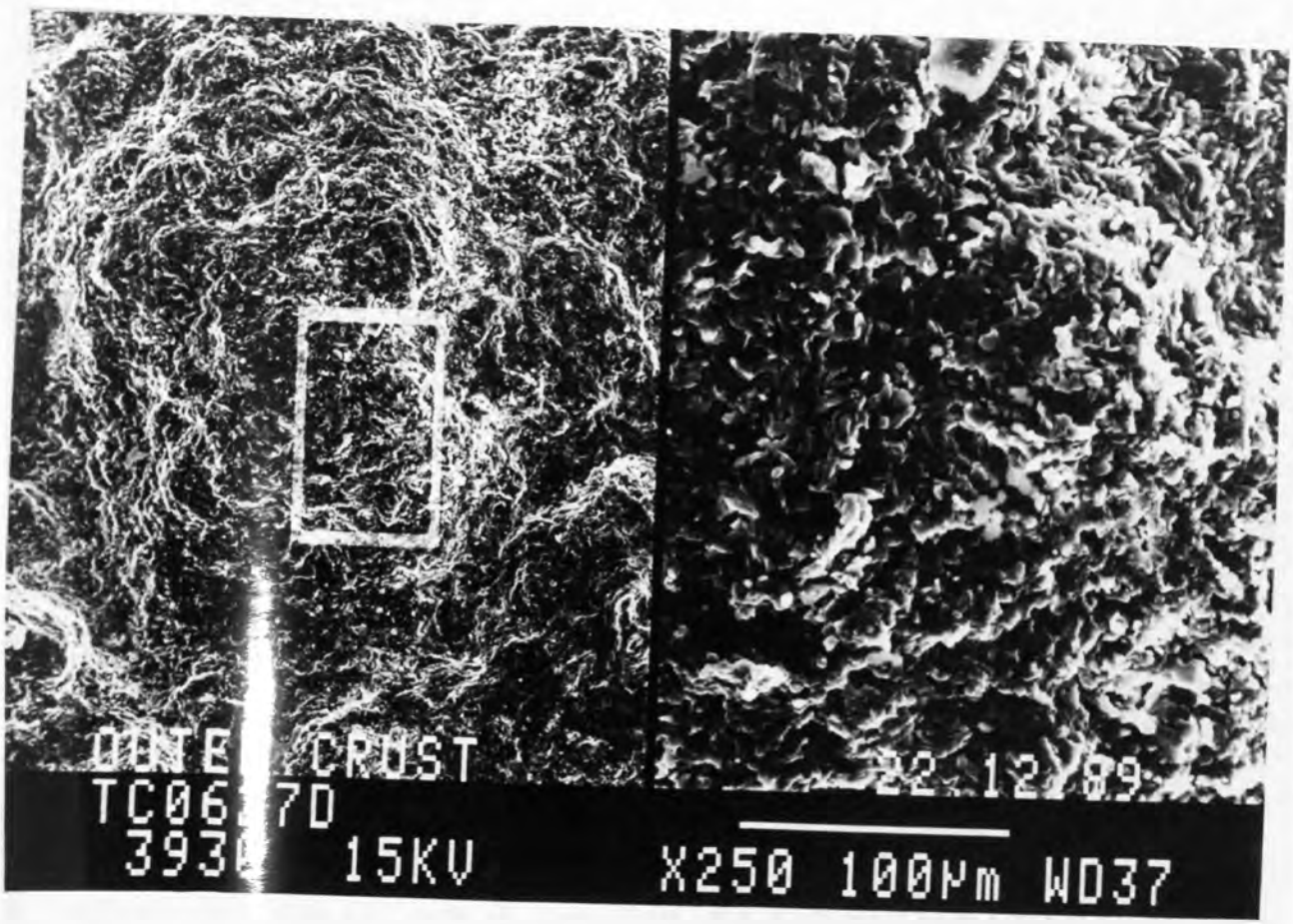

Plate 6.3 Inner and Outer Crust Surface of a 40% Weight Sodium Sulphate Decahydrate Drop (31°C, 1m/s).

6.2 DROPS OF AQUEOUS SODIUM CHLORIDE

6.2.1 Effect of Initial Concentration

Commencement from a higher initial solids content of 20% weight compared to 5% weight leads to a decrease in the drying rate as shown in Figure 6.10. This confirms the fact that the lowering of the vapour pressure for sodium chloride is significant, as has already been shown in Figure 6.2.

6.2.2 Effect of Air Temperature and Air Velocity

Figures 6.11 and 6.12 show the effect of air temperature upon the drying rate at 20% weight and 40% weight initial concentrations respectively. From the gradients of the curves, it can be established that the drying rate increases threefold for the 20% weight and is doubled for the 40% weight drops when the air temperature in increased from 30° C to 49° C and 54° C to 66° C. The crust does not therefore represent a significant resistance to heat transfer. From Figures 6.13 and 6.14 doubling the air velocity from 0.5m/s to 1m/s led to a similar two to three times increase in the drying rate.

The gas phase resistance to mass transfer therefore represents a significant proportion of the total resistance. This is an indication that the crust is of a very open, porous network as was observed. A thick, non-porous crust would have represented a major resistance to mass transfer and the effect of air velocity would not have been so significant.

The electron micrographs in Plates 6.4, 6.5 and 6.6 of the crust structure highlight the porous nature of the crust. These plates represent the crust for a 40% weight initial concentration sodium chloride drop drying at different air temperatures of 54° C, 63° C and 112.5° C.

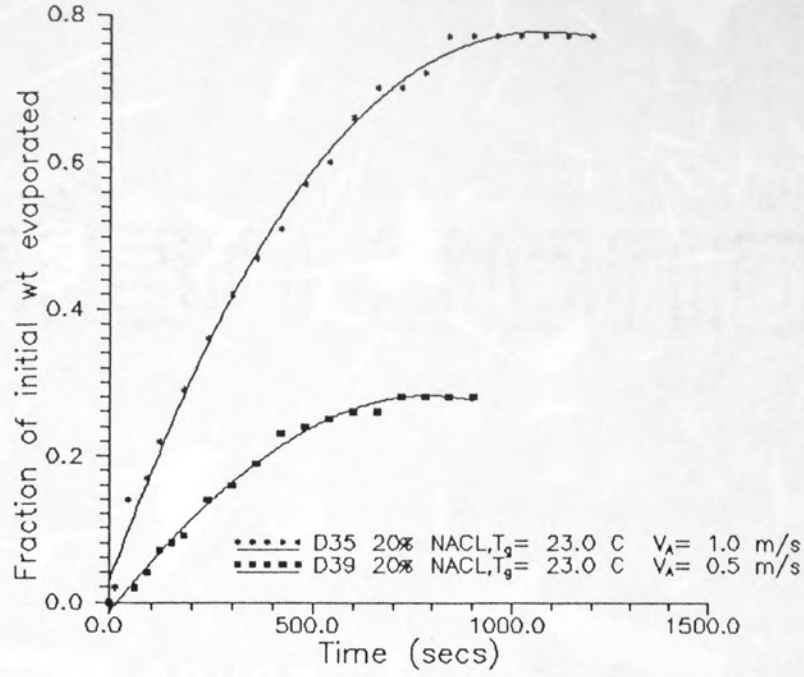

Figure 6.13 Drying of Drops of Aqueous Sodium Chloride (20 % wt/wt) at Varying Air Velocities.

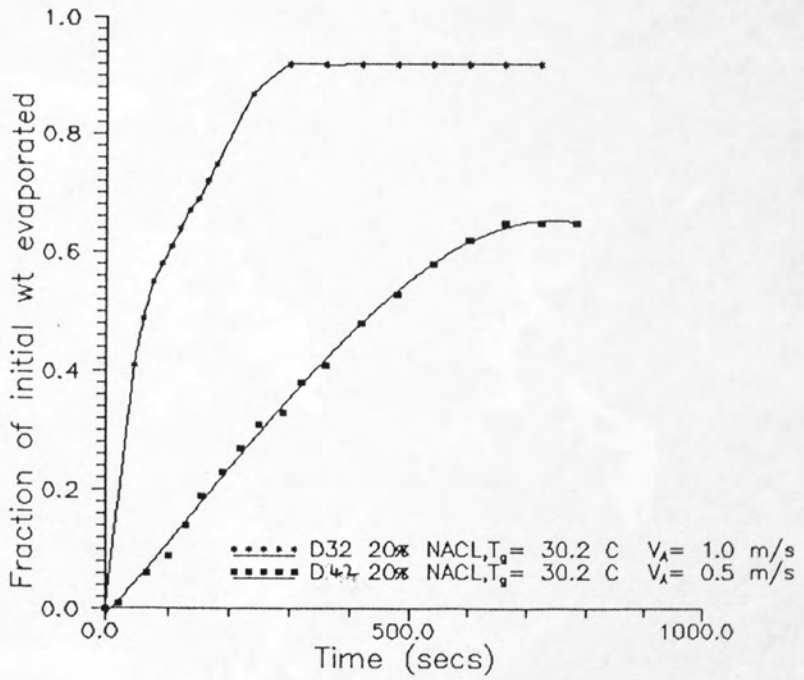

Figure 6.14 Drying of Drops of Aqueous Sodium Chloride (20 % wt/wt) at Varying Air Velocities.

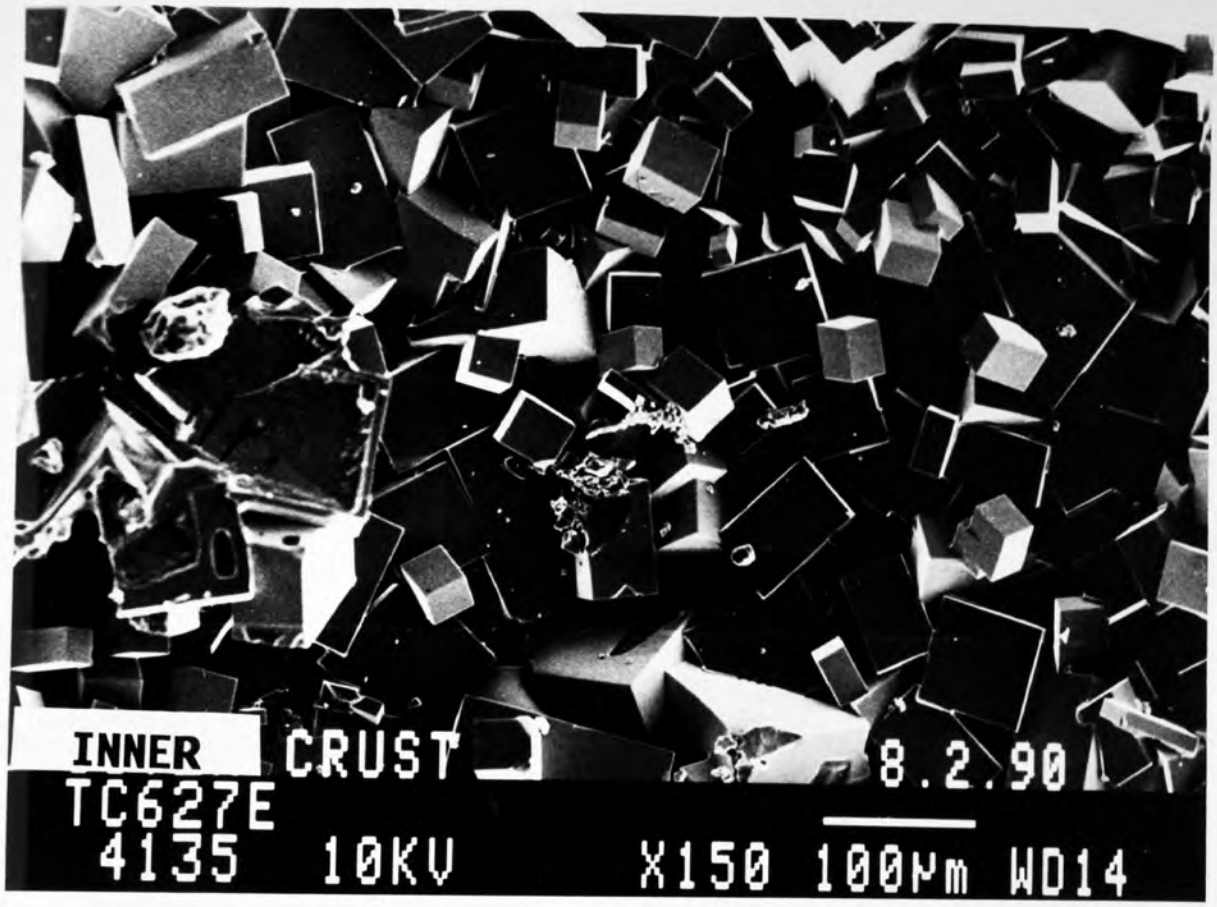

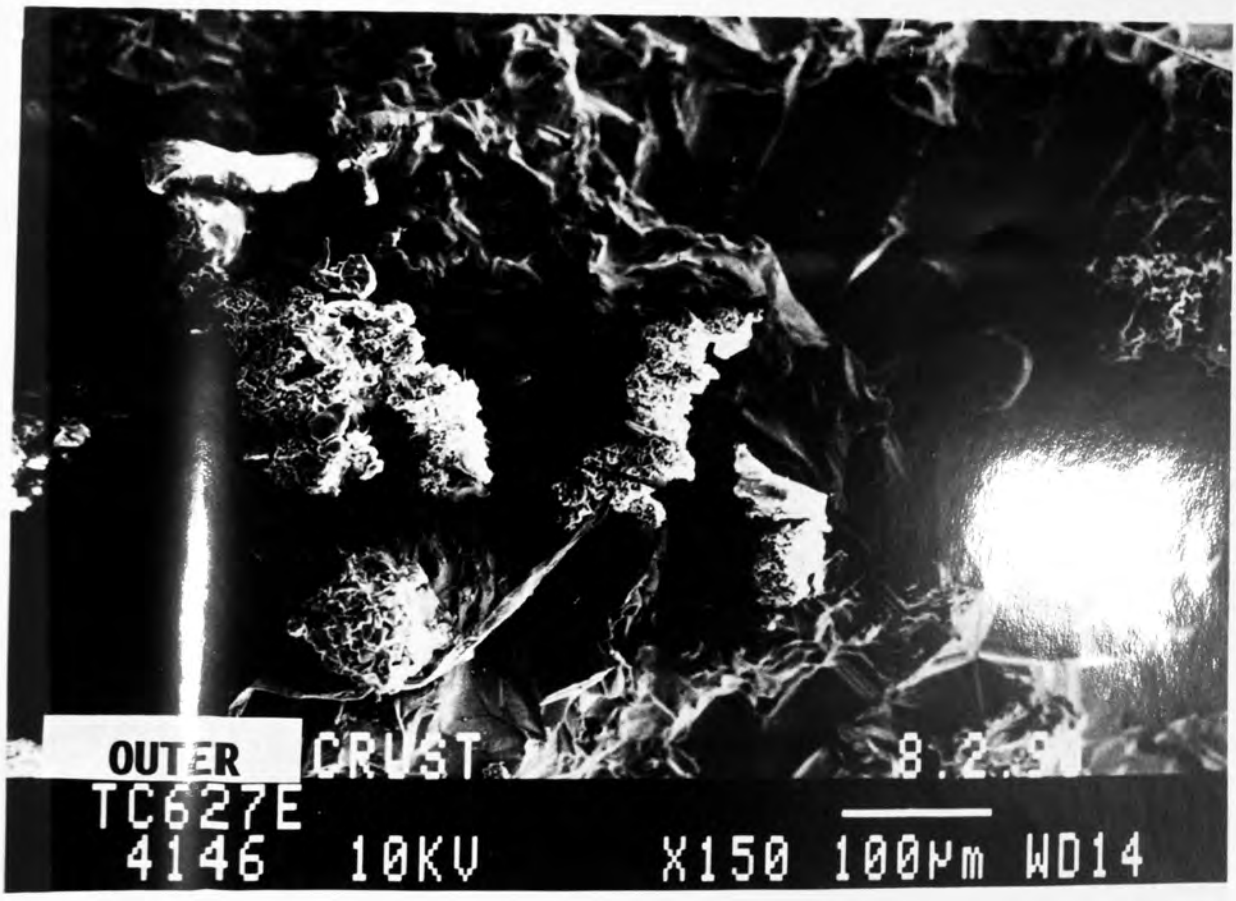

Plate 6.4 Inner and Outer Crust Surface of a 40% Weight Sodium Chloride Drop (54°C, 1m/s).

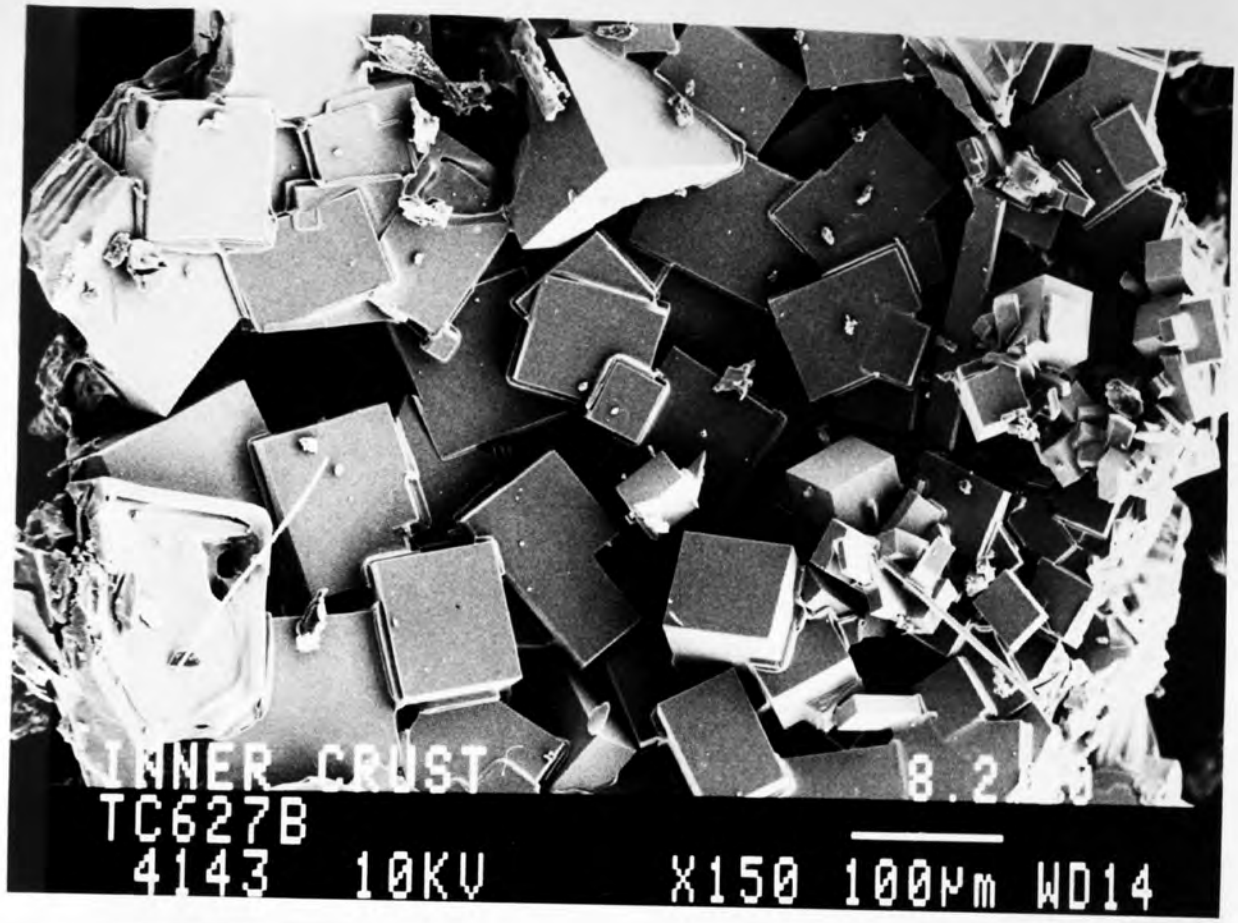

Plate 6.5 Inner and Outer Crust Surface of a 40% Weight Sodium Chloride Drop (63.5°C, 1m/s).

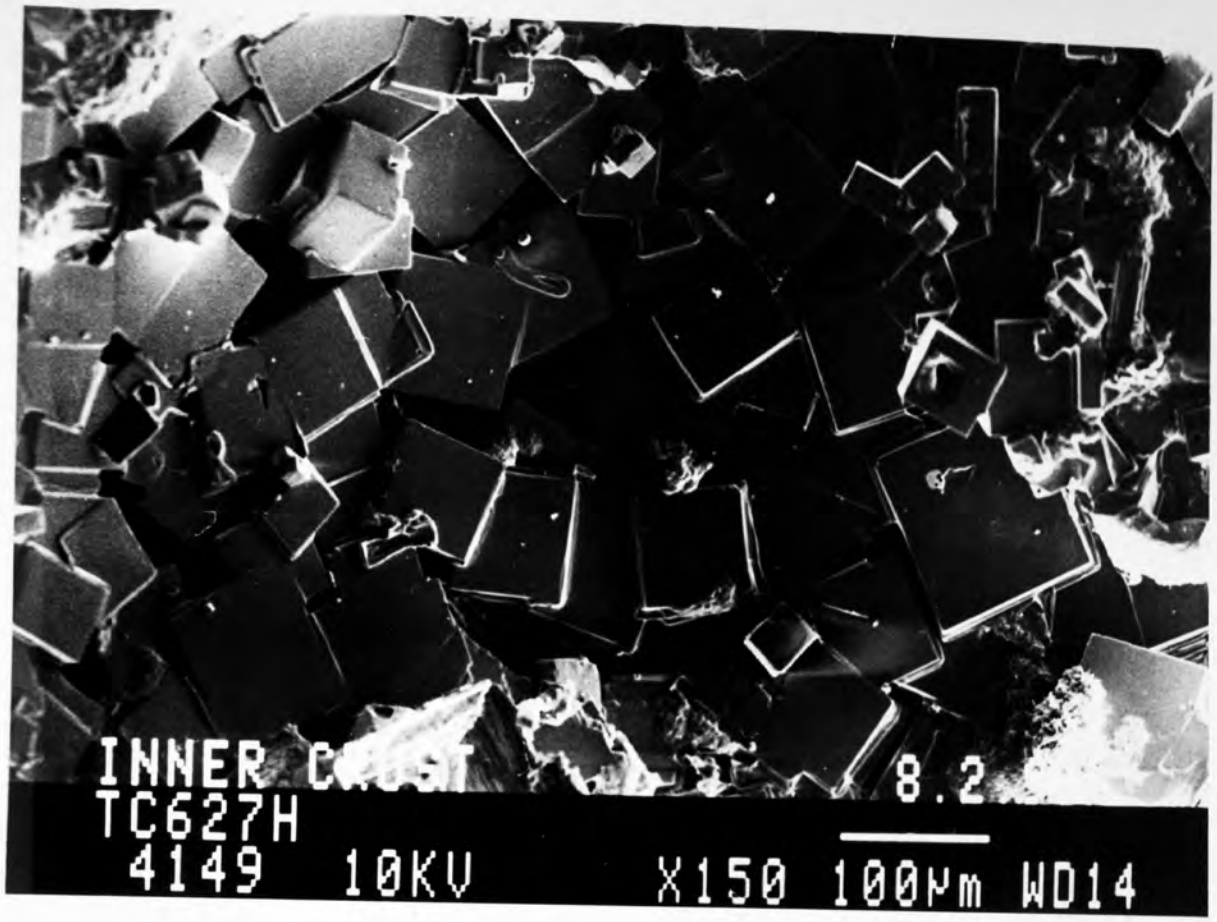

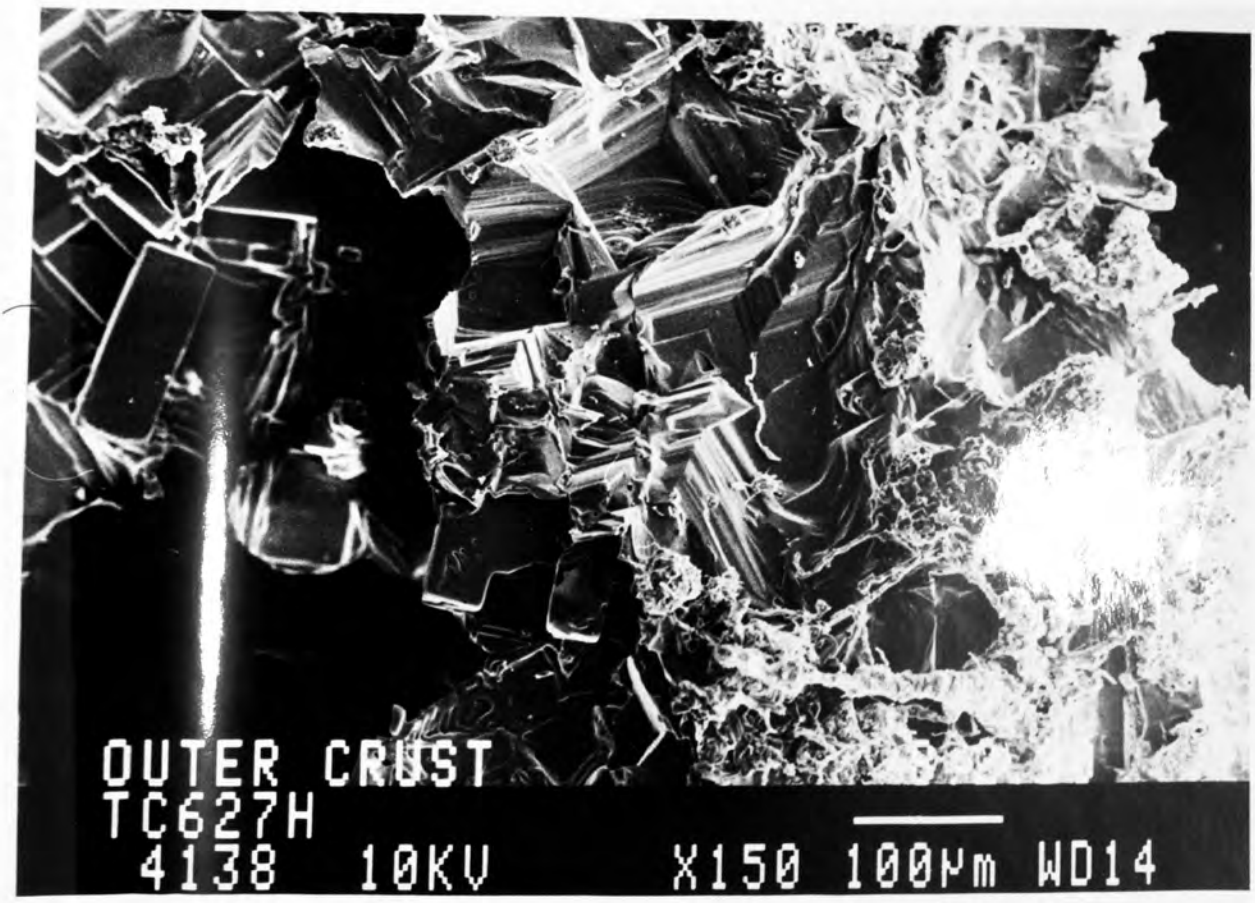

Plate 6.6 Inner and Outer Crust Surface of a 40% Weight Sodium Chloride Drop (112.5°C, 1m/s).

Significantly the micrographs of the inner crust, all taken at the same magnification show that there is little difference in the inner crust structure as a result of increasing air temperature. The crust is very crystalline with large gaps of 100μm between the crystals. However there is a definite difference in the outer crust structure with a change from a rather smooth surface at the lower air temperature to a progressively crystalline and rougher outer surface. The crystalline nature of the crust is very well illustrated in these micrographs.

Simultaneous drying rate and core temperatures are shown in Figures 6.15 and 6.16. From Figure 6.15, at 5% weight initial solution concentration, a constant rate period followed after establishment of a drying rate. This is reflected in the core temperature measurements. The drop temperature rose to the wet-bulb temperature and remained at this temperature for the duration of the constant rate period before gradually rising to the air temperature as the drying rate proceeded to fall. A similar pattern was observed, as shown in Figure 6.16, for a 20% weight concentration drop.

6.3 DROPS OF AQUEOUS POTASSIUM SULPHATE

6.3.1 Effect of Initial Concentration

The initial concentration had little effect on the initial drying rate as shown in Figures 6.17 and 6.18. However the rates diverge once a crust had formed on the surface of the drop. This indicates that the concentration of solids has little effect on the lowering of the vapour pressure of the solution.

6.3.2 Effect of Air Temperature and Air Velocity

An increase in air temperature increased the drying rate as shown in Figure 6.19. However, Figure 6.20 shows that an increase in the air velocity had only a slight effect on the drying rate.

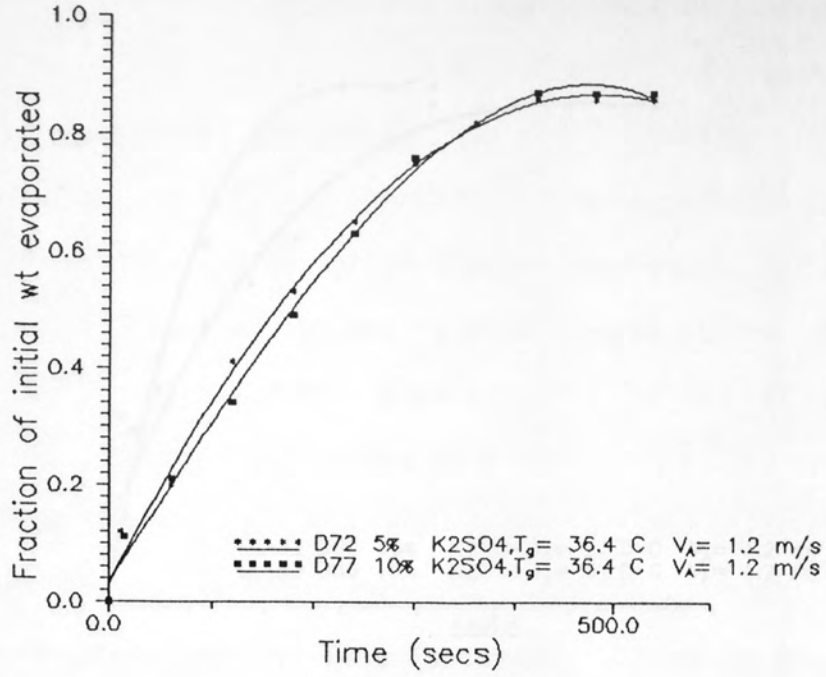

Figure 6.17 Drying of Drops of Aqueous Potassium Sulphate at Varying Initial Concentrations.

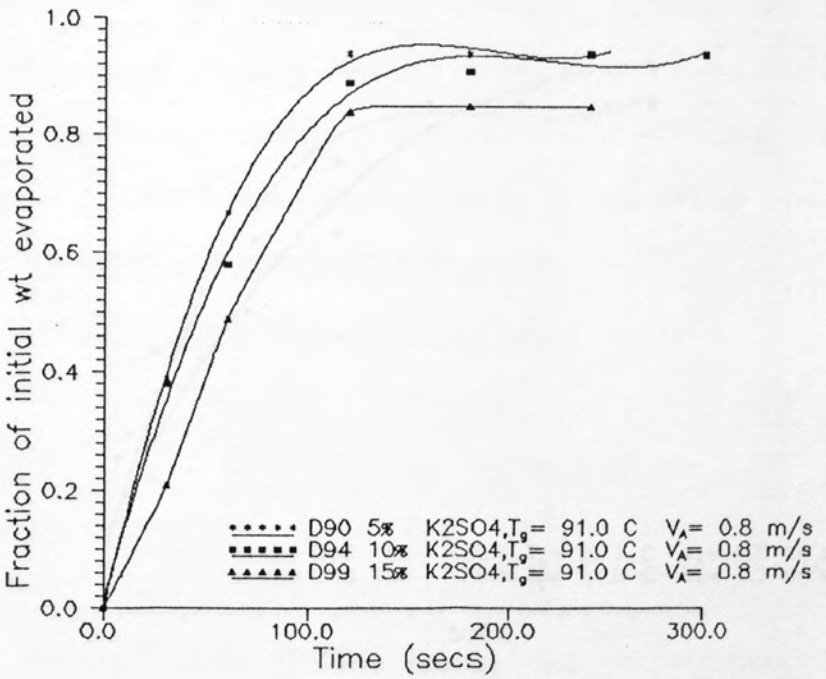

Figure 6.18 Drying of Drops of Aqueous Potassium Sulphate at Varying Initial Concentrations.

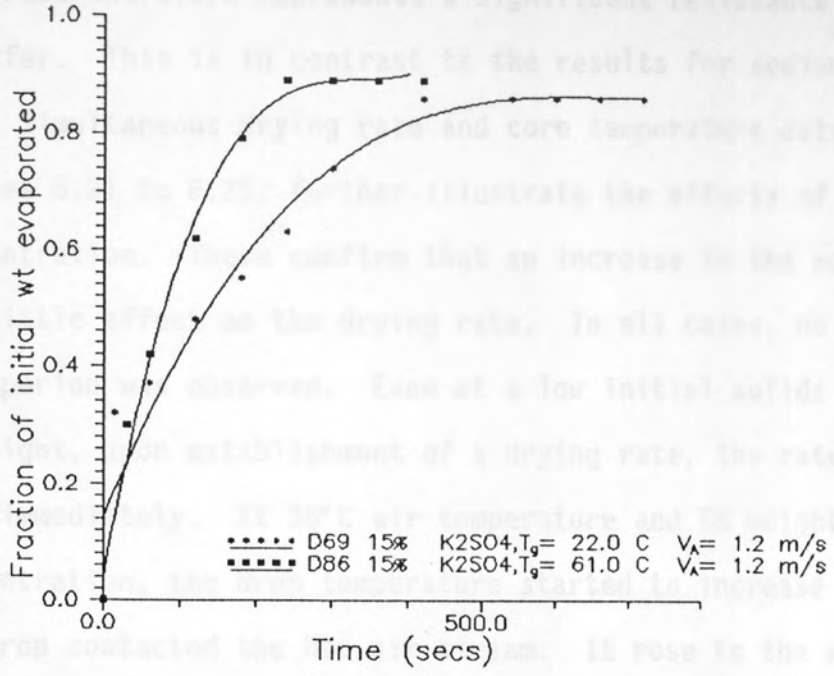

Figure 6.19 Drying of Drops of Aqueous Potassium Sulphate (15 % wt/wt) at Varying Air Temperatures.

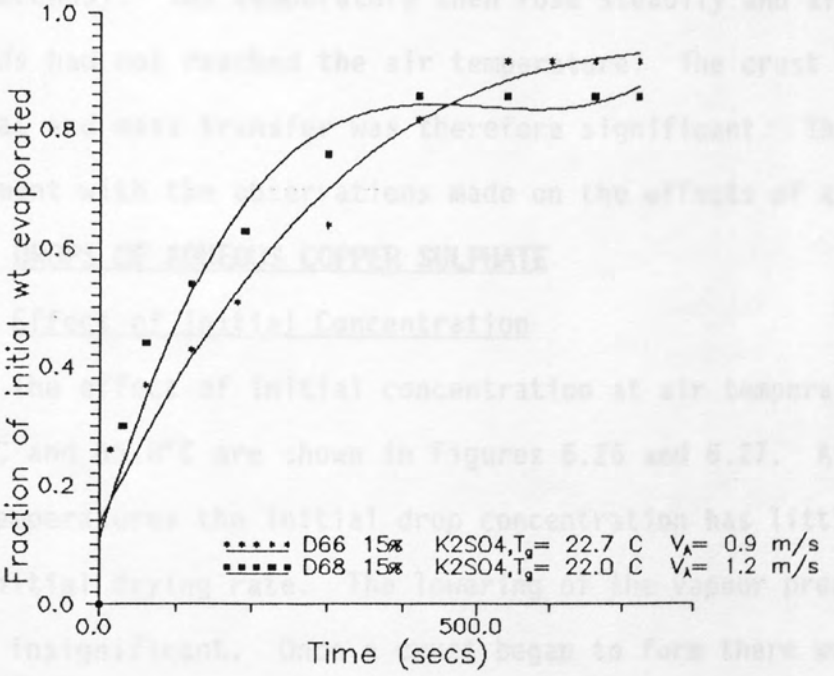

Figure 6.20 Drying of Drops of Aqueous Potassium Sulphate (15 % wt/wt) at Varying Air Velocities.

The crust therefore represents a significant resistance to mass transfer. This is in contrast to the results for sodium chloride.

Simultaneous drying rate and core temperature data shown in Figures 6.21 to 6.25, further illustrate the effects of initial concentration. These confirm that an increase in the solids content had little effect on the drying rate. In all cases, no constant rate period was observed. Even at a low initial solids content of 5% weight, upon establishment of a drying rate, the rate began to fall immediately. At 36° C air temperature and 5% weight concentration, the drop temperature started to increase immediately the drop contacted the hot air stream. It rose to the wet-bulb temperature and stayed there for 130 seconds before rising steadily as the crust formed on the surface of the drop. After 480 seconds, the drop had reached the air temperature. For the 10% weight concentration drop, the wet-bulb temperature period was very short (50 seconds). The temperature then rose steadily and after 660 seconds had not reached the air temperature. The crust resistance to heat and mass transfer was therefore significant. This is in agreement with the observations made on the effects of air velocity.

6.4 DROPS OF AQUEOUS COPPER SULPHATE

6.4.1 Effect of Initial Concentration

The effect of initial concentration at air temperatures of 20.9° C and 65.8° C are shown in Figures 6.26 and 6.27. At the low air temperatures the initial drop concentration has little effect on the initial drying rate. The lowering of the vapour pressure was again insignificant. Once a crust began to form there was a reduction in the drying rates.

6.4.2 Effect of Air Temperature

The effect of air temperature on drops initially of 5%, 10%

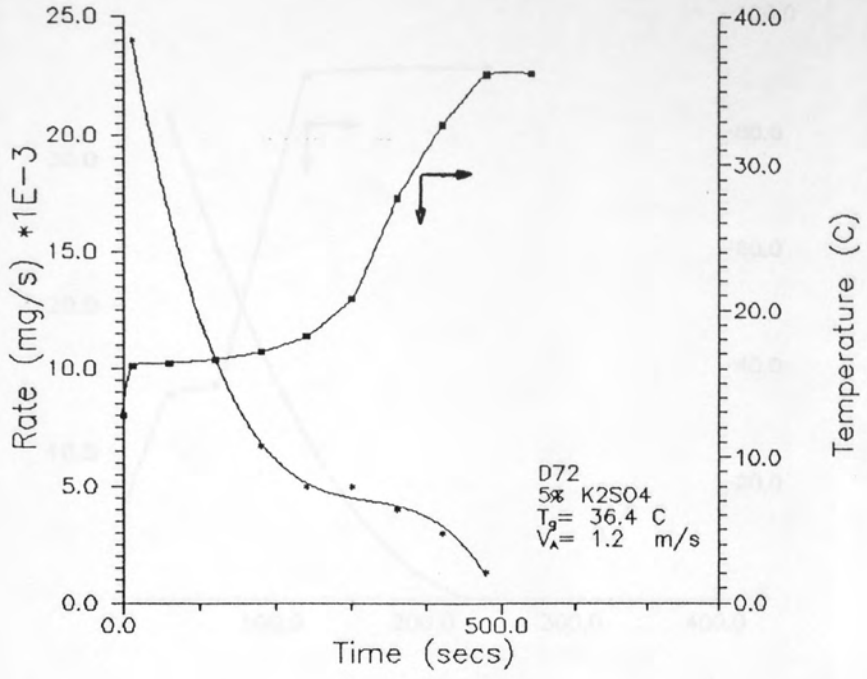

Figure 6.21 Simultaneous Core Temperature and Rate Histories for Aqueous Potassium Sulphate (5 % wt/wt) at T_g=36.4 C

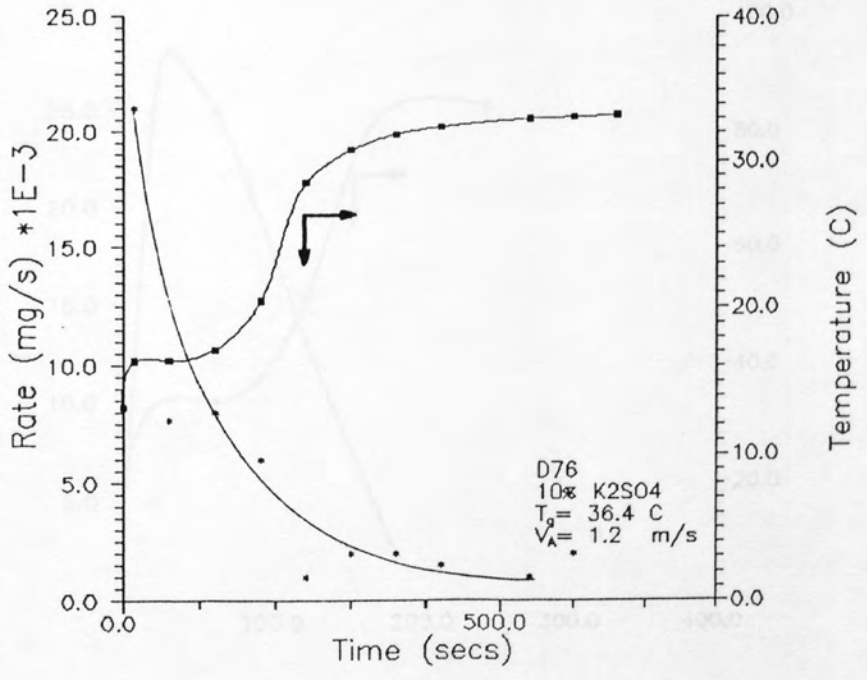

Figure 6.22 Simultaneous Core Temperature and Rate Histories for Aqueous Potassium Sulphate (10 % wt/wt) at T_g= 36.4 C

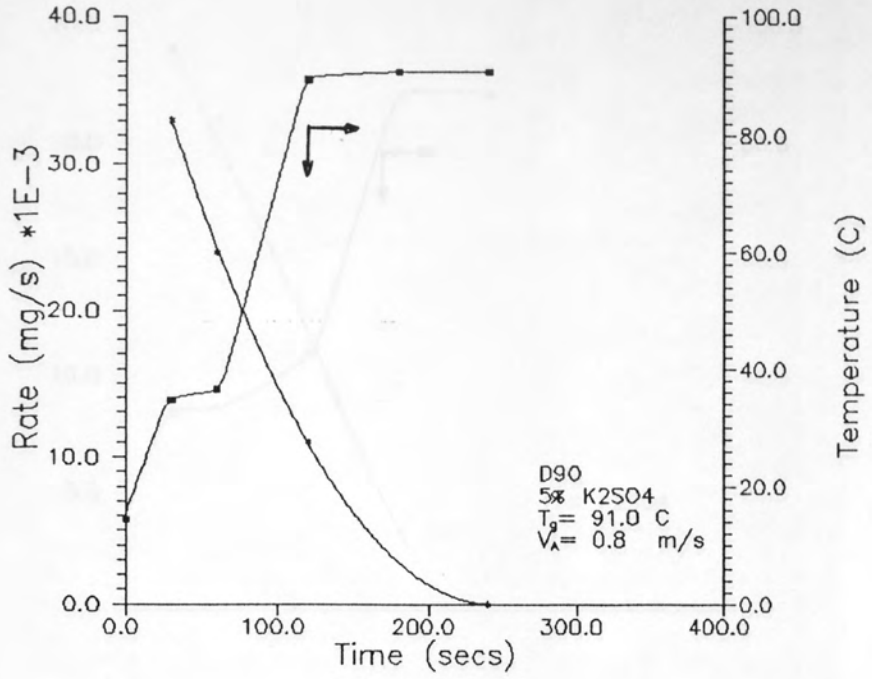

Figure 6.23 Simultaneous Core Temperature and Rate Histories for Aqueous Potassium Sulphate (5 % wt/wt) at T_g= 91.0 C

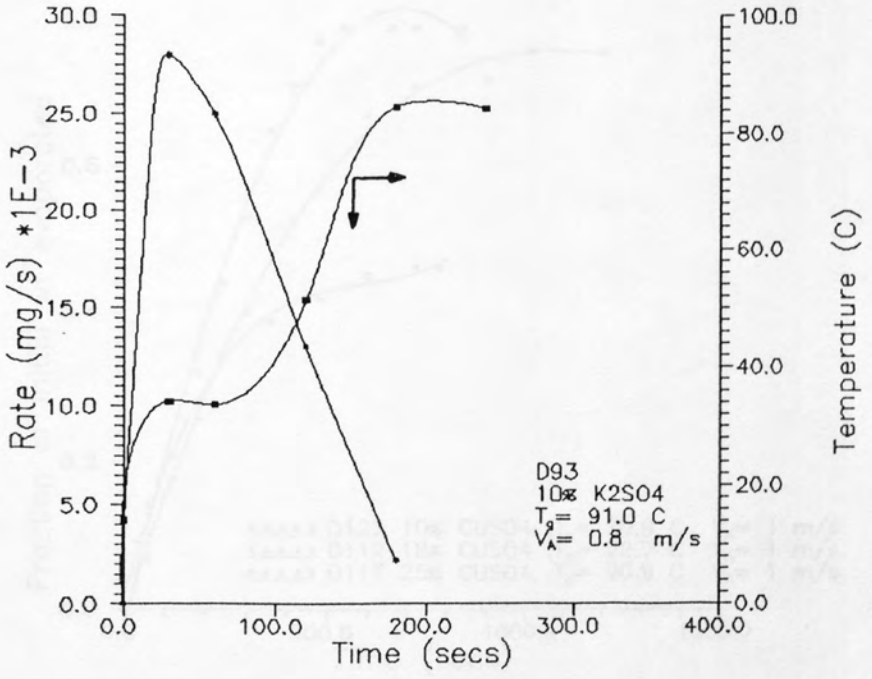

Figure 6.24 Simultaneous Core Temperature and Rate Histories for Aqueous Potassium Sulphate (10 % wt/wt) at T_g= 91.0 C

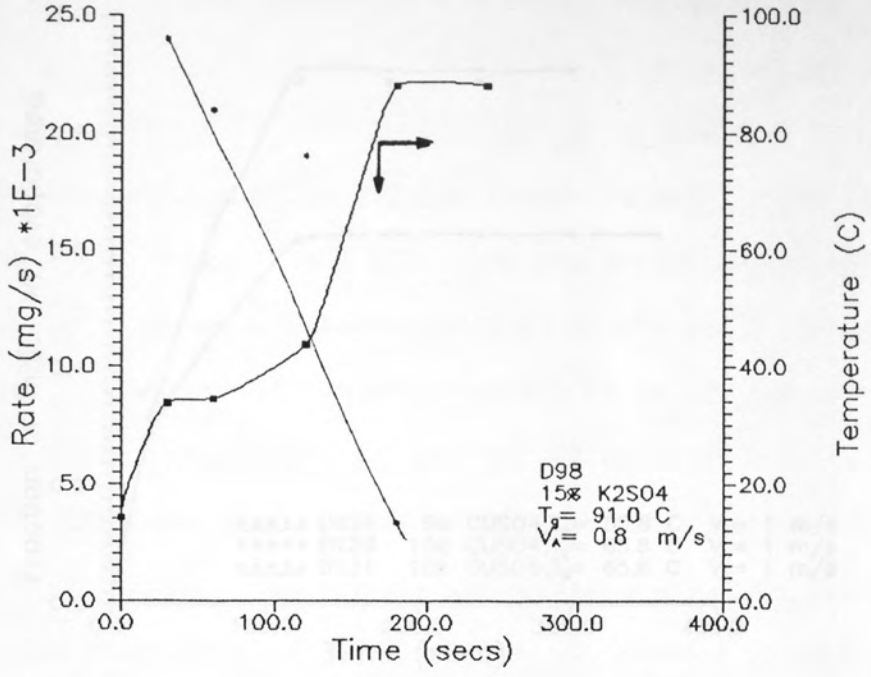

Figure 6.25 Simultaneous Core Temperature and Rate Histories for Aqueous Potassium Sulphate (15 % wt/wt) at T_g= 91.0 C

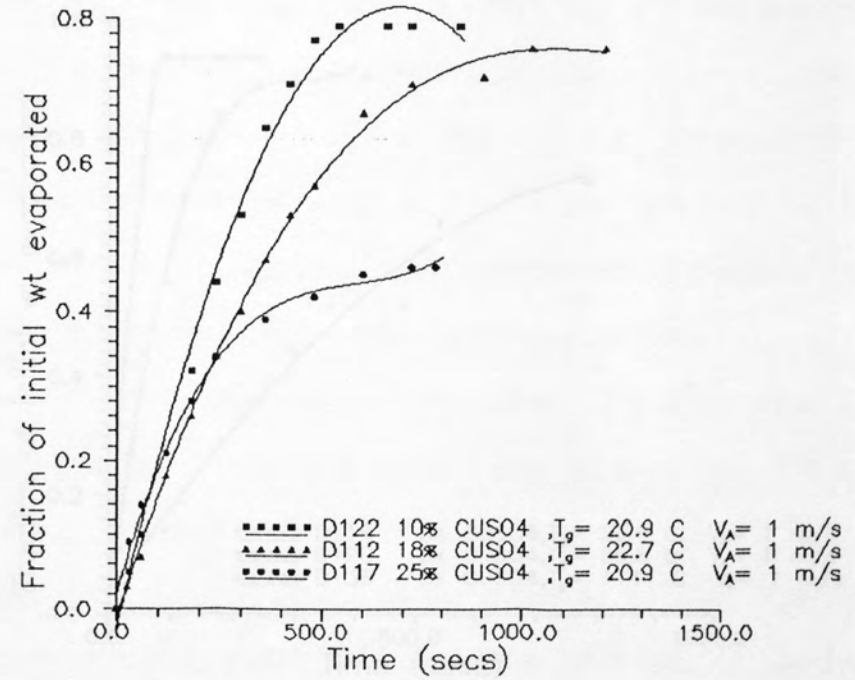

Figure 6.26 Drying of Drops of Aqueous Copper Sulphate at Varying Initial Concentrations.

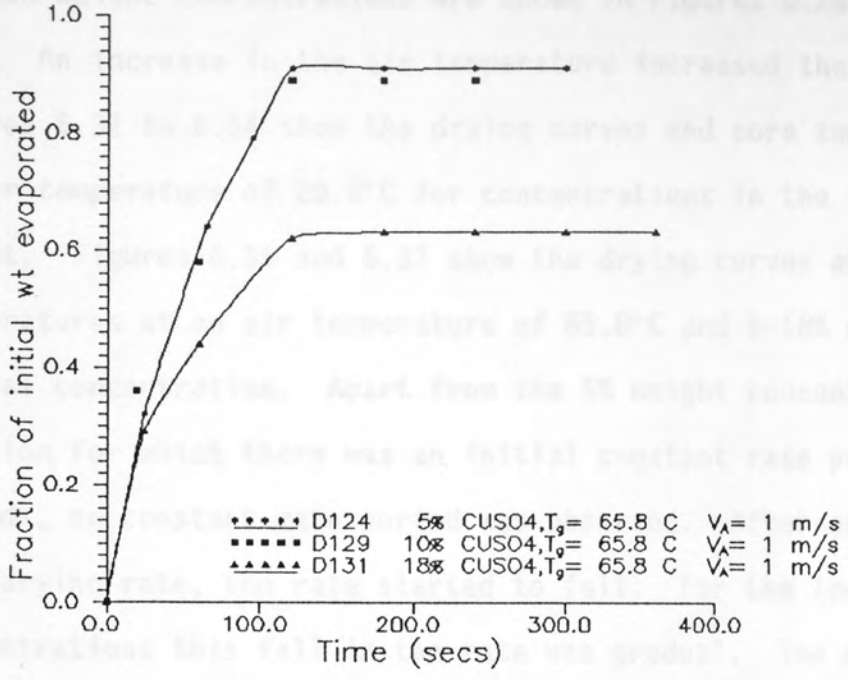

Figure 6.27 Drying of Drops of Aqueous Copper Sulphate at Varying Initial Concentrations.

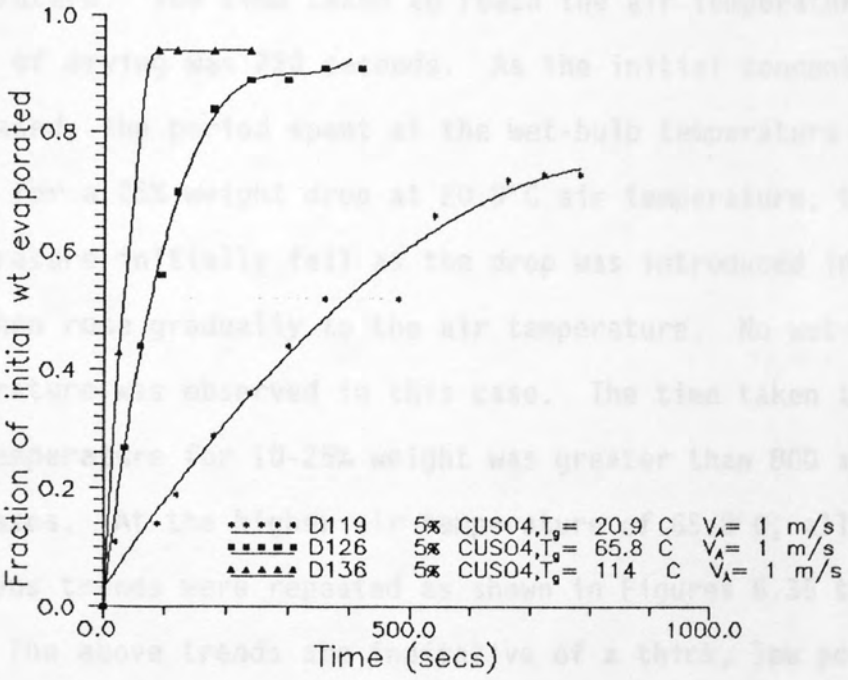

Figure 6.28 Drying of Drops of Aqueous Copper Sulphate (5 % wt/wt) at Varying Air Temperatures.

and 18% weight concentrations are shown in Figures 6.28, 6.29 and 6.30. An increase in the air temperature increased the drying rate. Figures 6.31 to 6.34 show the drying curves and core temperatures at an air temperature of 20.9°C for concentrations in the range 5-25% weight. Figures 6.35 and 6.37 show the drying curves and core temperatures at an air temperature of 65.8°C and 5-18% weight initial concentration. Apart from the 5% weight concentration solution for which there was an initial constant rate period of 100 seconds, no constant rate period was observed. After establishment of a drying rate, the rate started to fall. For the lower concentrations this fall in the rate was gradual. The drop core temperature histories are quite interesting. At 20.9°C air temperature and 5% weight initial concentration, the drop temperature fell to the wet-bulb temperature; it then remained at this temperature for 400 seconds before rising slowly to the air temperature. The time taken to reach the air temperature from the start of drying was 720 seconds. As the initial concentration was increased, the period spent at the wet-bulb temperature decreased until for a 25% weight drop at 20.9°C air temperature, the drop temperature initially fell as the drop was introduced into the tower and then rose gradually to the air temperature. No wet-bulb temperature was observed in this case. The time taken to reach the air temperature for 10-25% weight was greater than 800 seconds in all cases. At the higher air temperature of 65.8°C, all of the previous trends were repeated as shown in Figures 6.35 to 6.37.

The above trends are indicative of a thick, low porosity crust. Electron micrographs, Plates 6.7 to 6.12 show the inner and outer crust structures for copper sulphate drops.

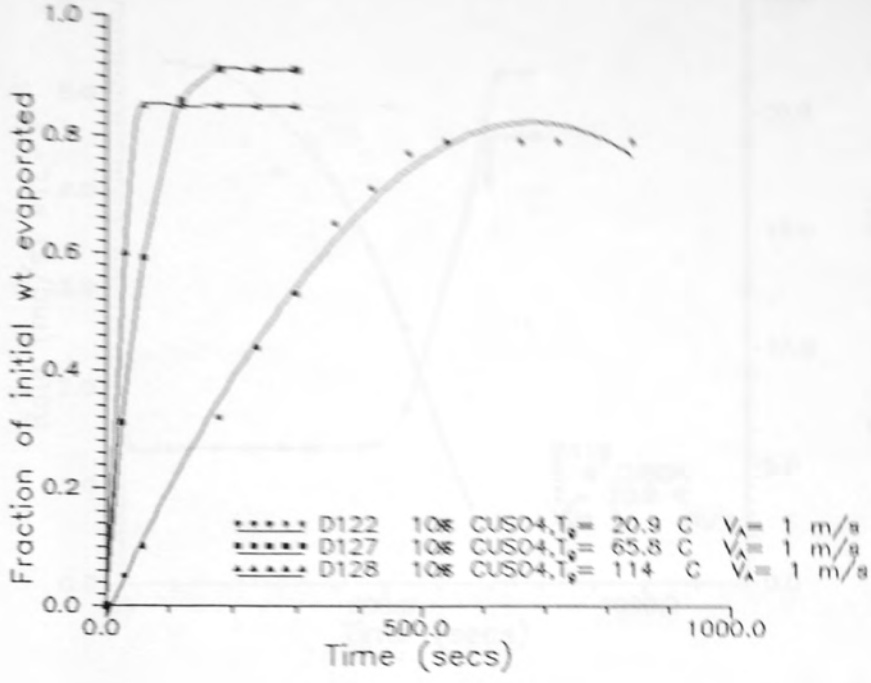

Figure 6.29 Drying of Drops of Aqueous Copper Sulphate (10 % wt/wt) at Varying Air Temperatures.

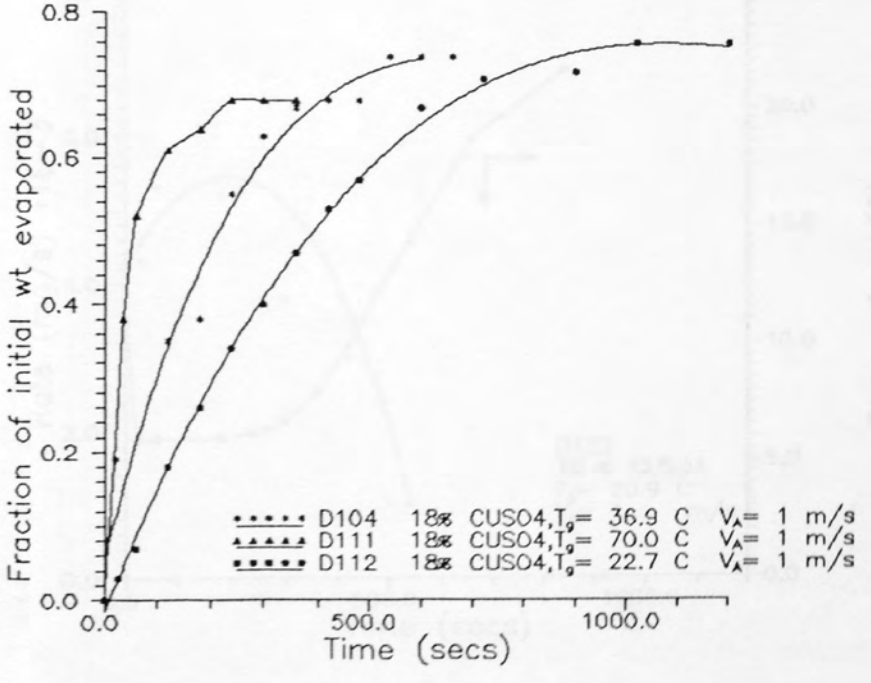

Figure 6.30 Drying of Drops of Aqueous Copper Sulphate (18 % wt/wt) at Varying Air Temperatures.

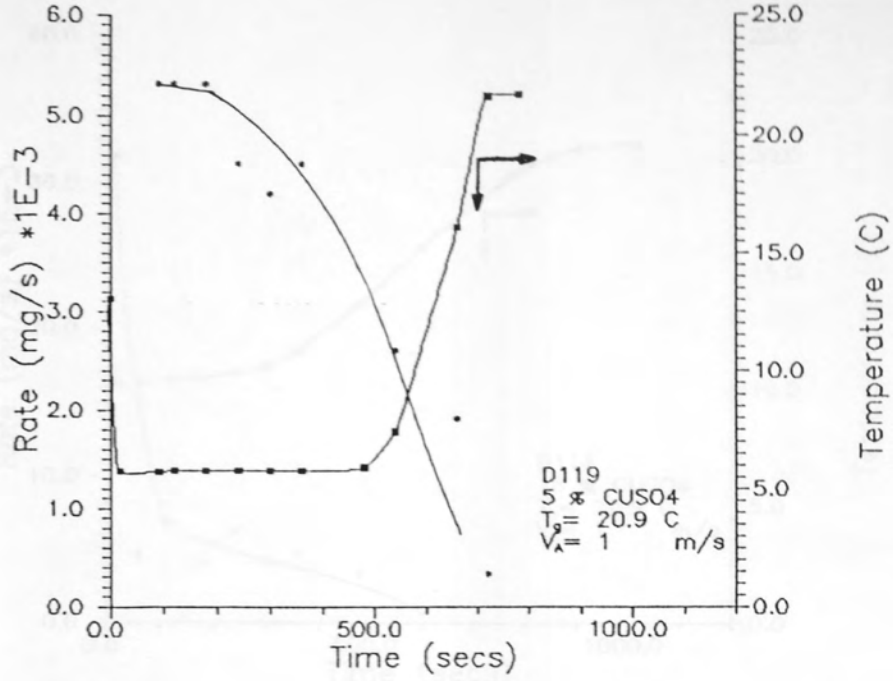

Figure 6.31 Simultaneous Core Temperature and Rate Histories for Aqueous Copper Sulphate (5 % wt/wt) at T_g= 20.9 C

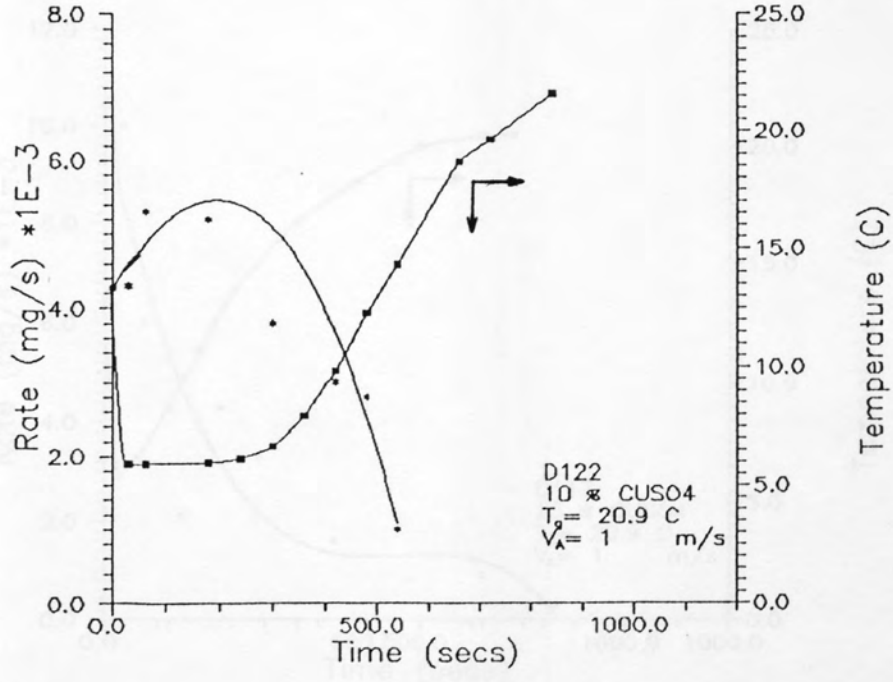

Figure 6.32 Simultaneous Core Temperature and Rate Histories for Aqueous Copper Sulphate (10 % wt/wt) at T_g= 20.9 C

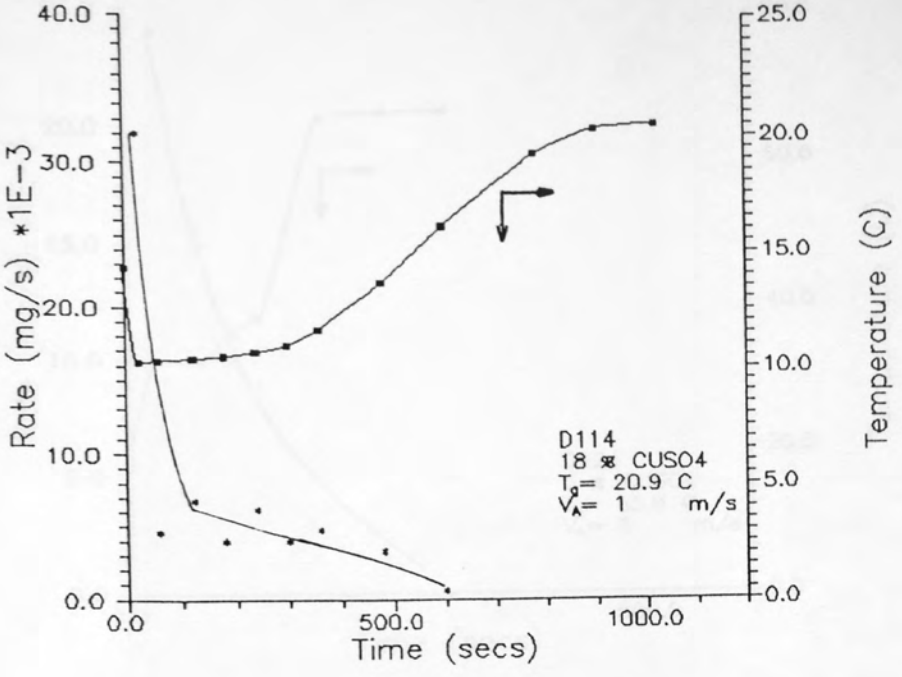

Figure 6.33 Simultaneous Core Temperature and Rate Histories for Aqueous Copper Sulphate (18 % wt/wt) at T_g= 20.9 C

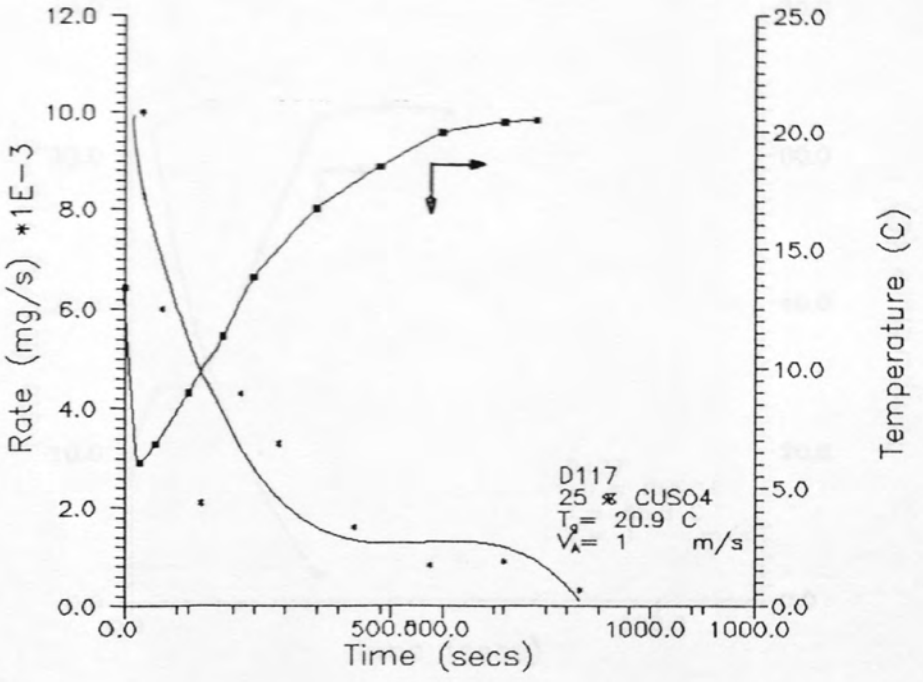

Figure 6.34 Simultaneous Core Temperature and Rate Histories for Aqueous Copper Sulphate (25 % wt/wt) at T_g= 20.9 C

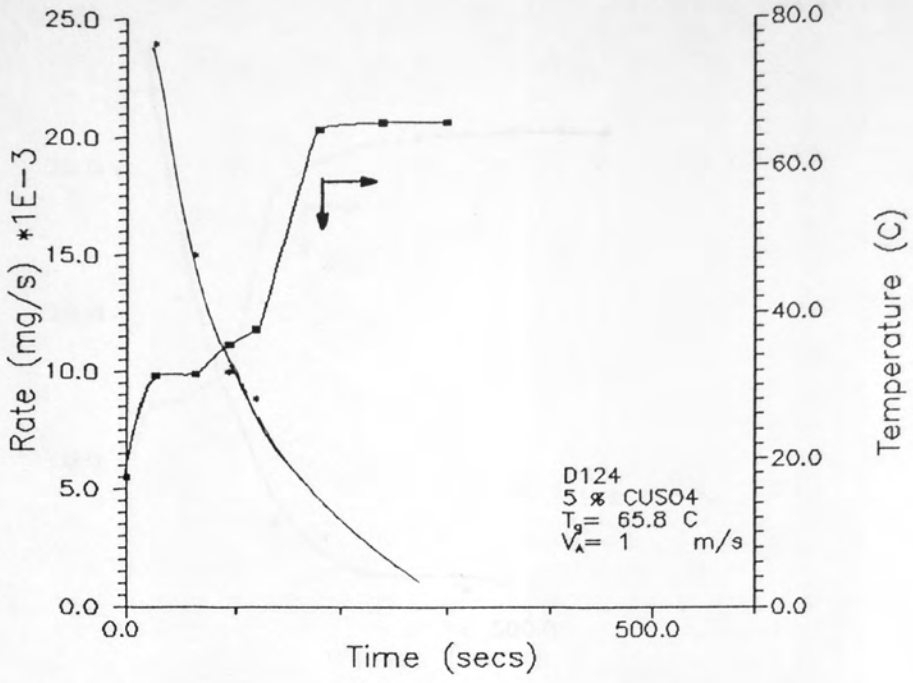

Figure 6.35 Simultaneous Core Temperature and Rate Histories for Aqueous Copper Sulphate (5 % wt/wt) at T_g= 65.8 C

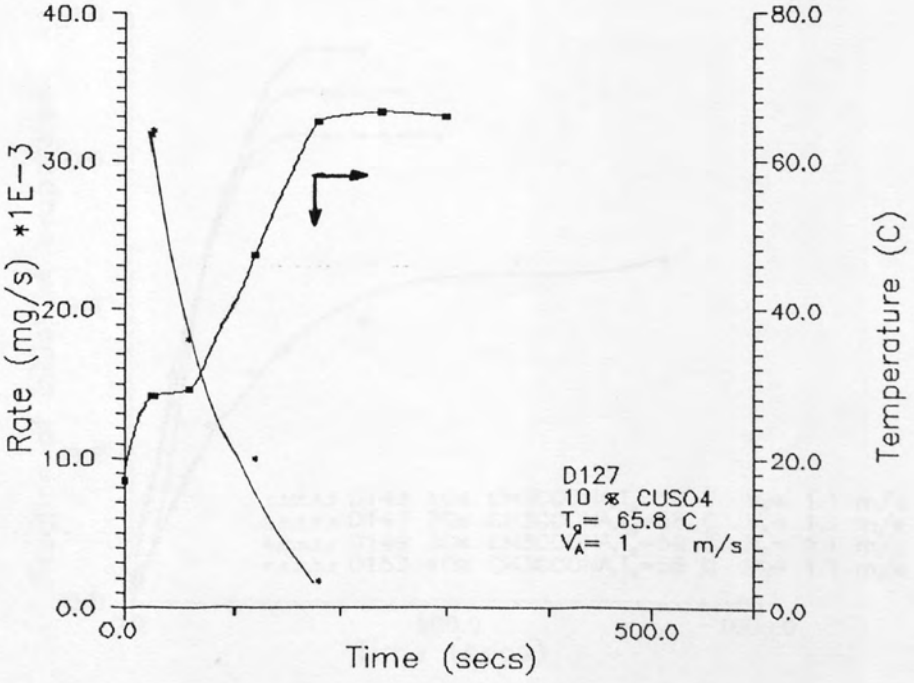

Figure 6.36 Simultaneous Core Temperature and Rate Histories for Aqueous Copper Sulphate (10 % wt/wt) at T_g= 65.8 C

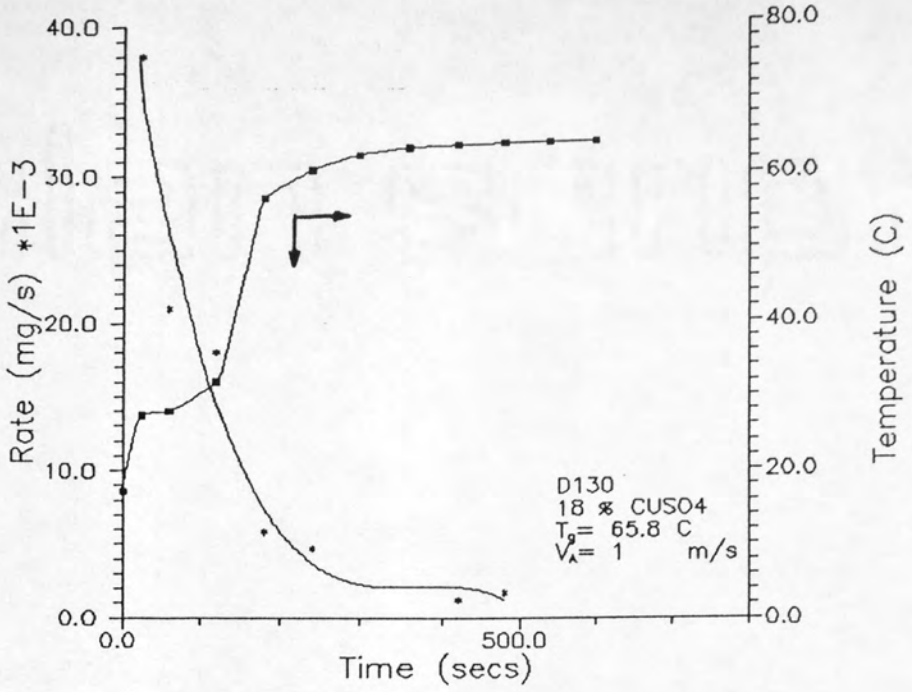

Figure 6.37 Simultaneous Core Temperature and Rate Histories for Aqueous Copper Sulphate (18 % wt/wt) at T_g= 65.8 C

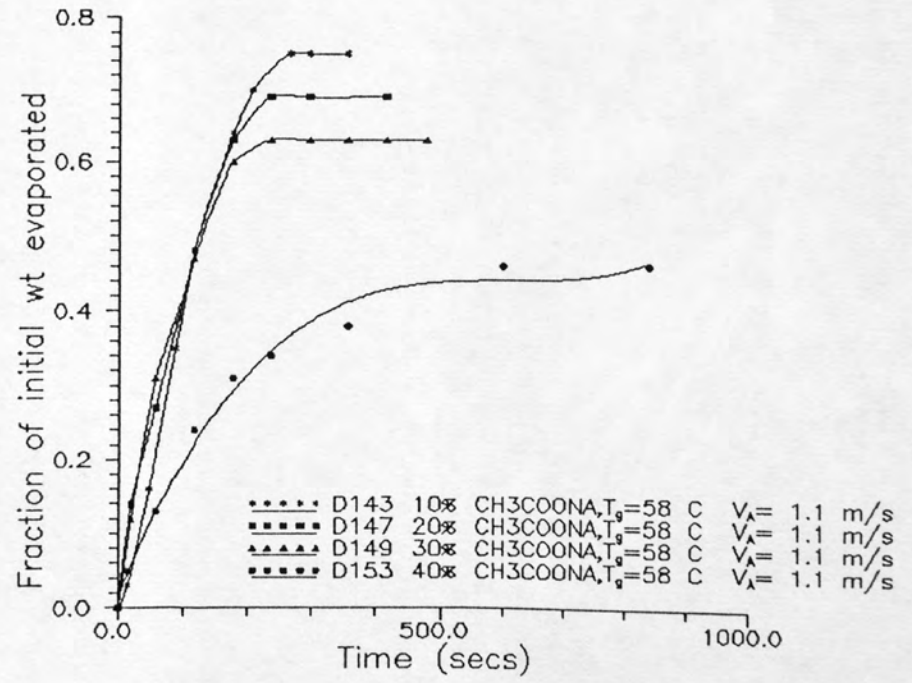

Figure 6.38 Drying of Drops of Aqueous Sodium Acetate at Varying Initial Concentrations.

Plate 6.7 Inner and Outer Crust Surface of a 5% Weight Copper Sulphate Drop (65.8°C, 1m/s).

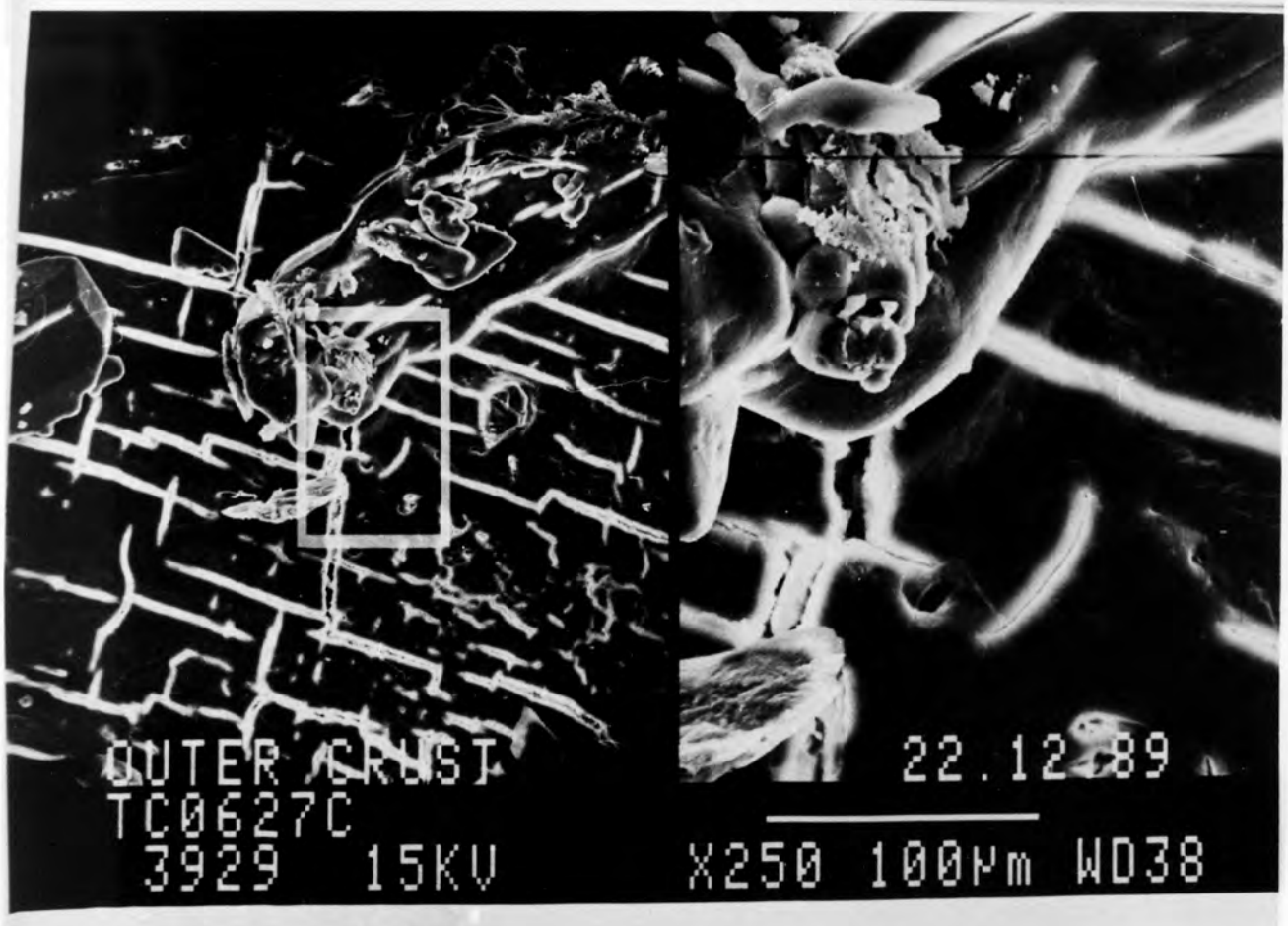

Plate 6.8 Inner and Outer Crust Surface of a 5% Weight Copper Sulphate Drop (65.8°C, 1m/s).

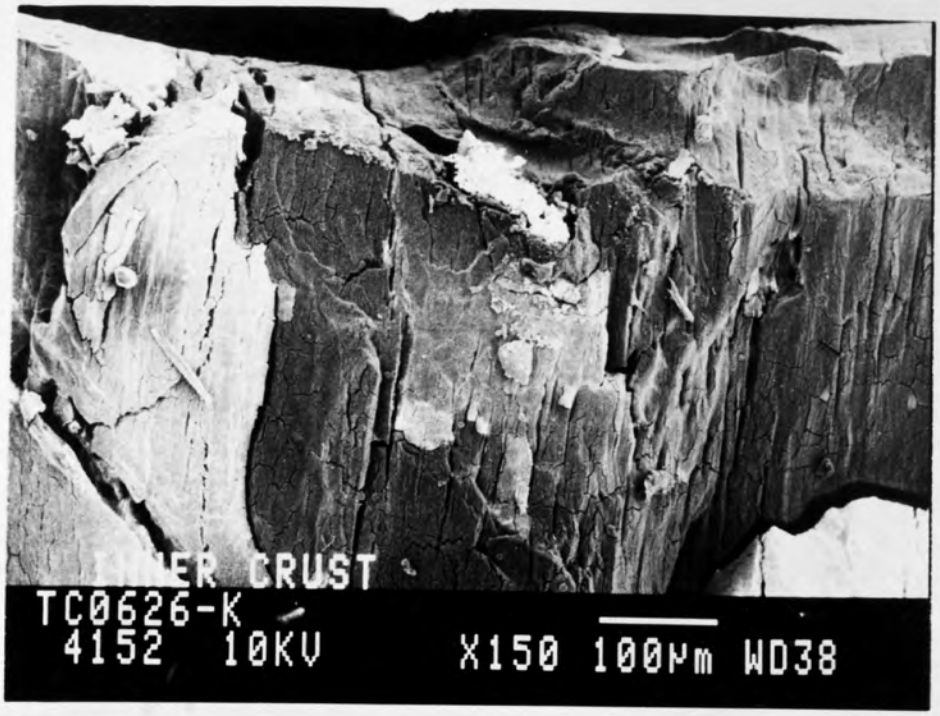

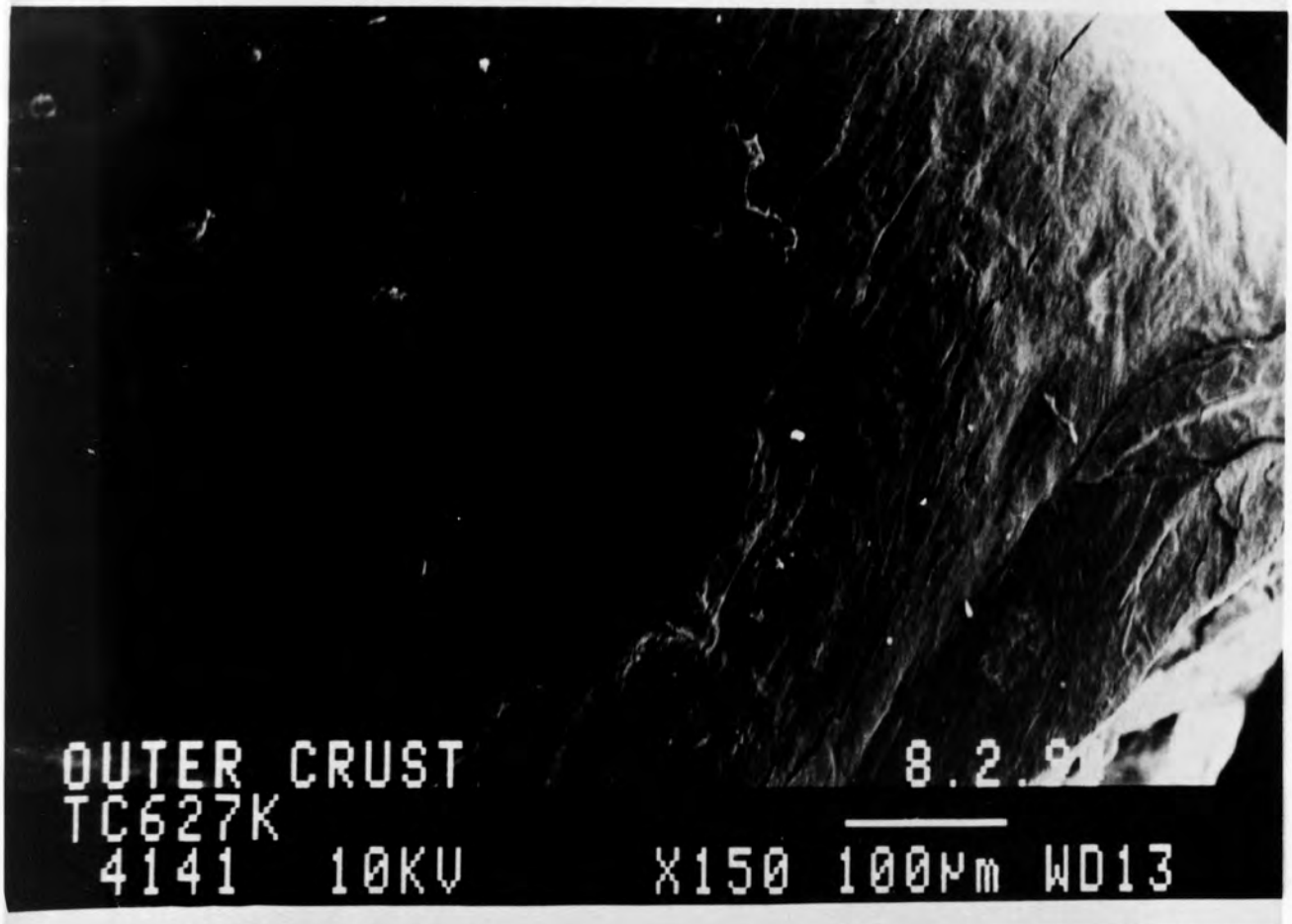

Plate 6.9 Inner and Outer Crust Surface of a 18% Weight Copper Sulphate Drop (20.9°C, 1m/s).

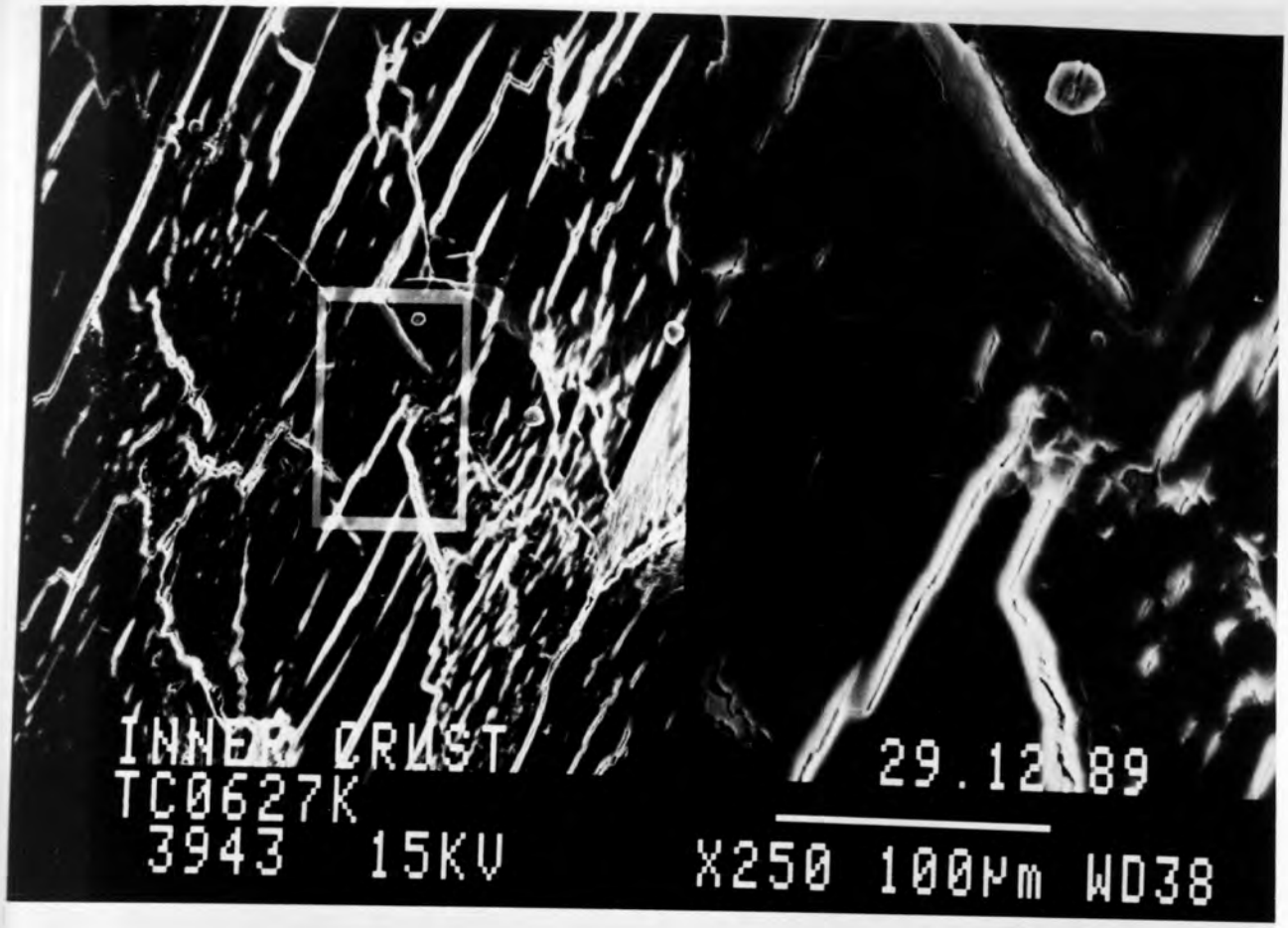

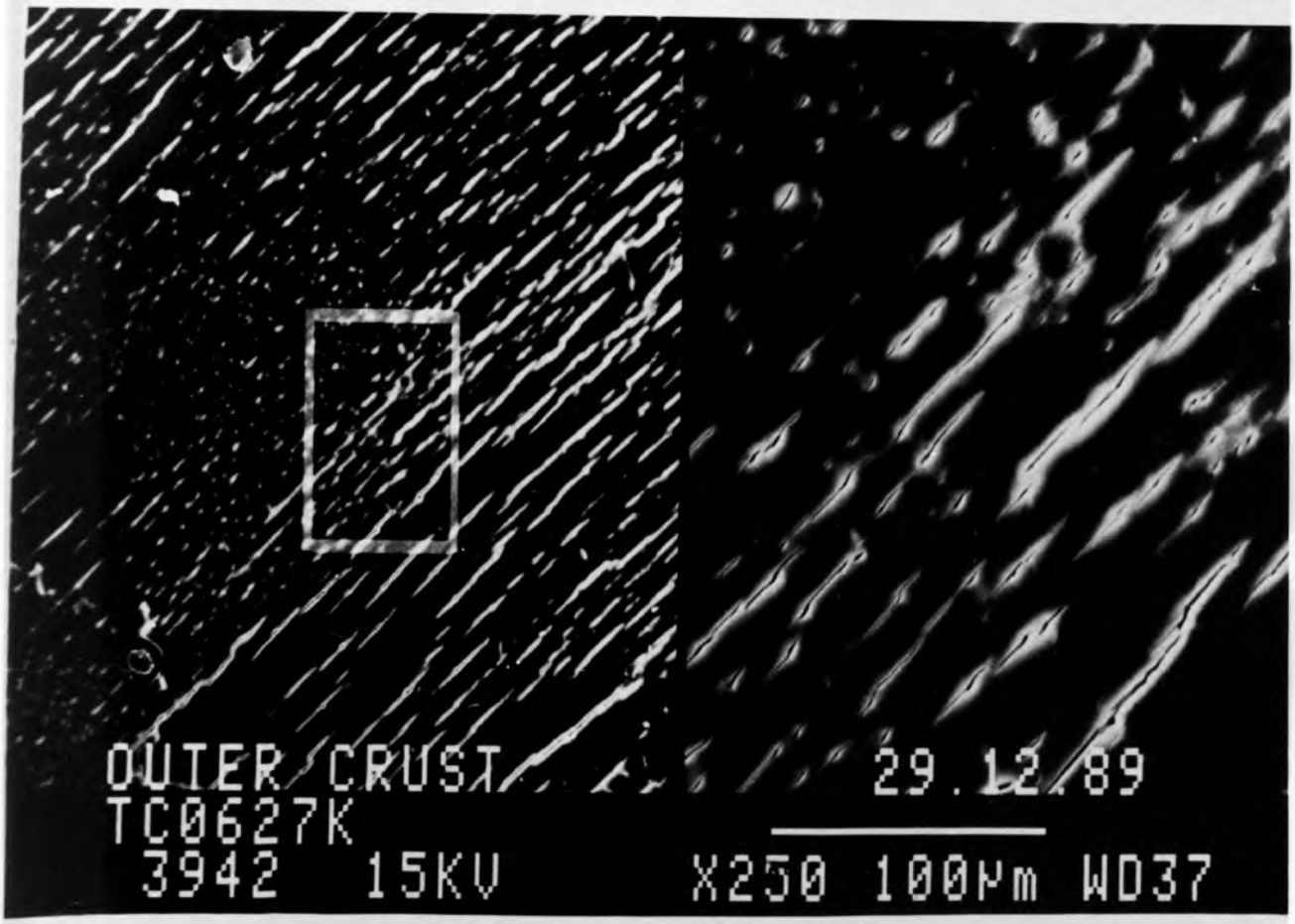

Plate 6.10 Inner and Outer Crust Surface of a 18% Weight Copper Sulphate Drop (20.9°C, 1m/s).

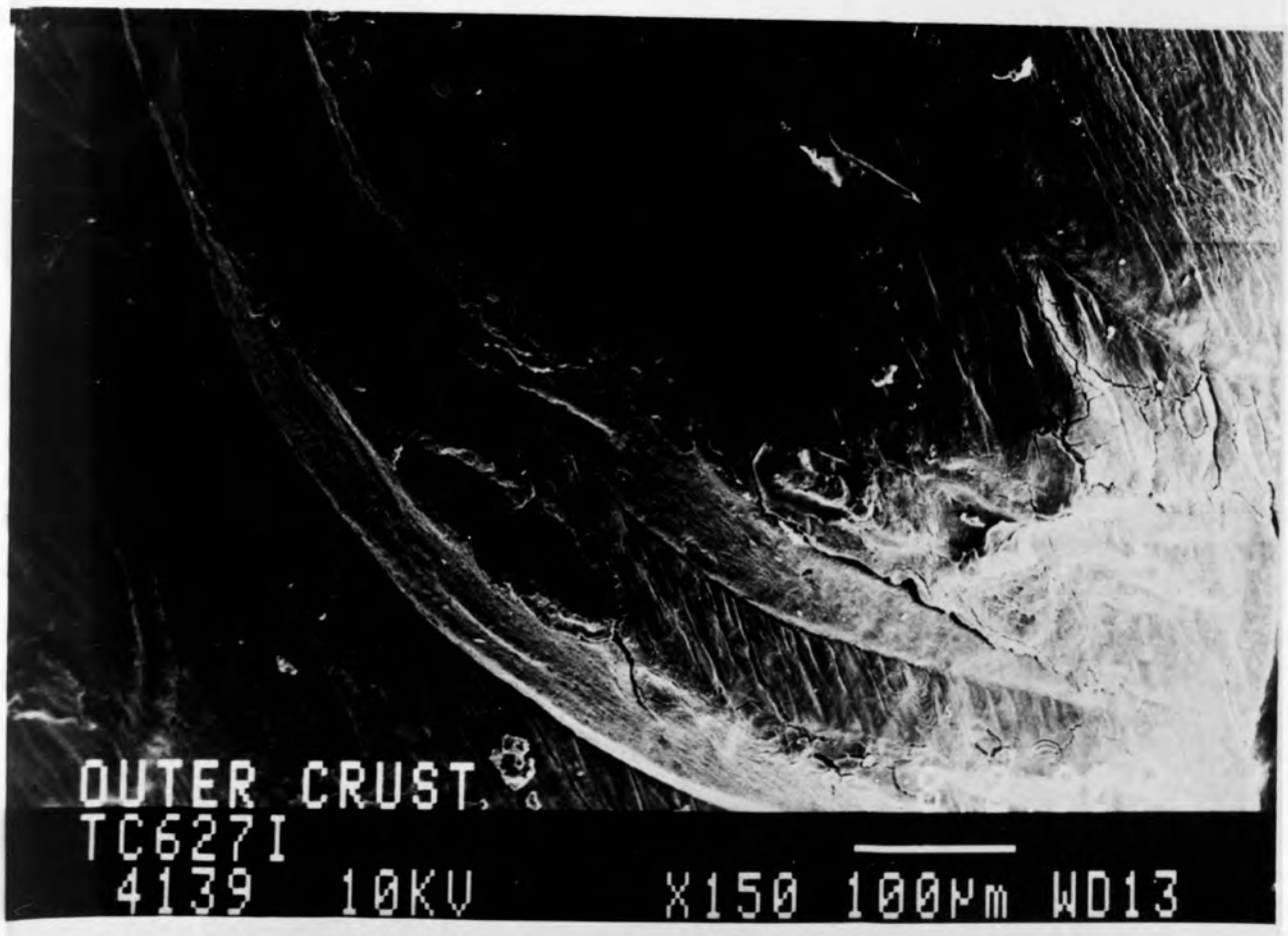

Plate 6.11 Inner and Outer Crust Surface of a 25% Weight Copper Sulphate Drop (22.7°C, 1m/s).

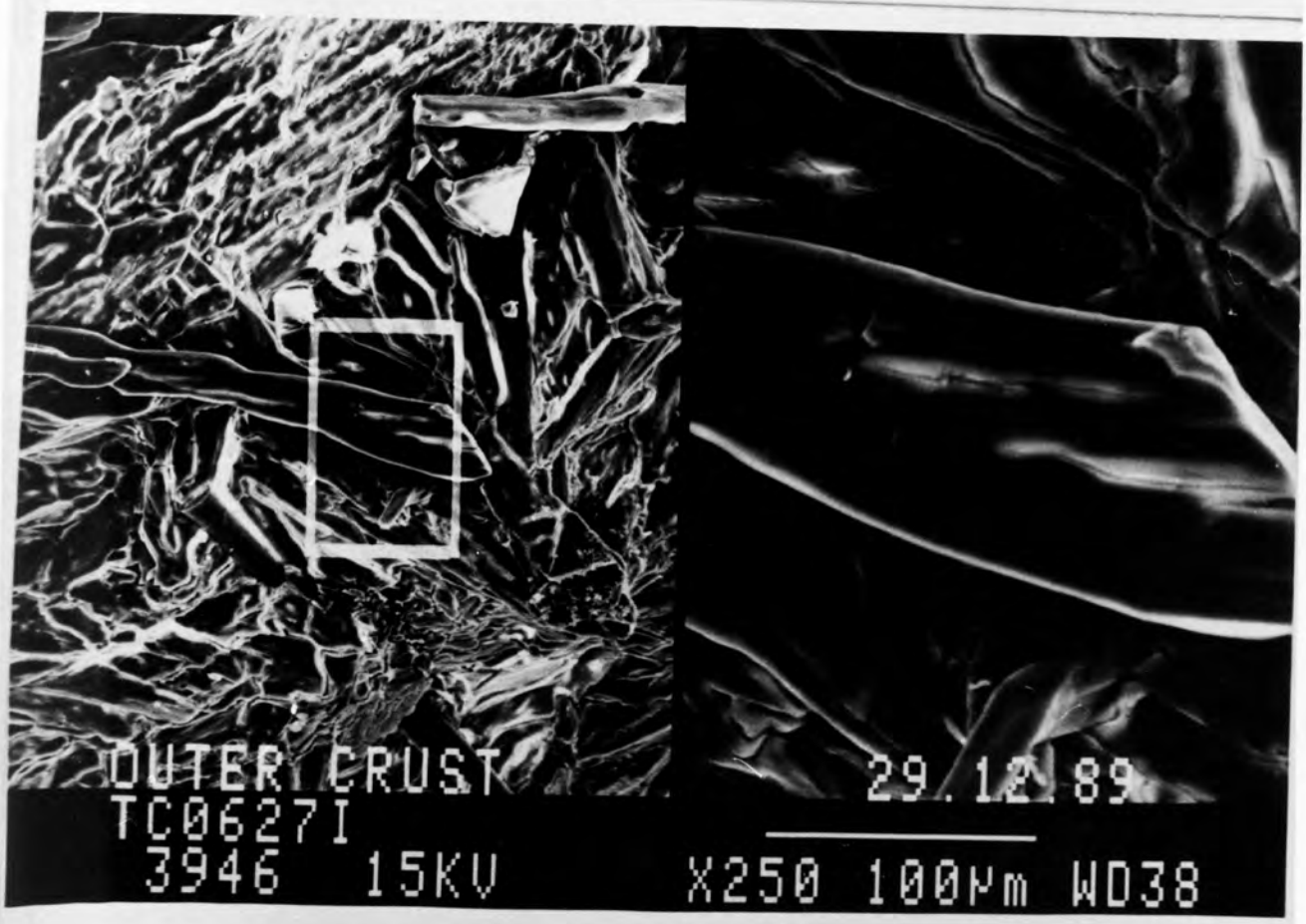

Plate 6.12 Inner and Outer Crust Surface of a 25% Weight Copper Sulphate Drop (22.7°C, 1m/s).

The crust was very smooth with numerous fractures; no differences were apparent in the inner and outer crusts. Plate 6.11 shows a blow-hole in the outer crust surface.

6.5 DROPS OF AQUEOUS SODIUM ACETATE

6.5.1 Effect of Initial Concentration

Figure 6.38 shows the effect of differences in the initial concentration within the range 10-40% weight at 58°C air temperature. Little effect on the drying rates was observed over the range from 10-30% weight solids. However at 40% weight concentration the drying rate was significantly altered. Figures 6.39 to 6.42 illustrate this more clearly for an air temperature of 58°C. For 10% weight the drying rate was 6-36mg/s, for 20% weight, 8-48mg/s, for 30% weight, 4-37mg/s and for 40% weight, 3-27mg/s.

6.5.2 Effects of Air Temperature

An increase in the air temperature increased the rate of drying as shown in Figure 6.43. The core temperature history was similar to those observed for potassium sulphate and copper sulphate. At the low concentration (10% weight) and 58°C air temperature, the drop temperature rose to the wet-bulb temperature; it remained at the wet-bulb temperature for 100 seconds before rising to the air temperature in 340 seconds. At the higher concentration (40% weight) the wet-bulb temperature period was not observed as shown in Figure 6.42. It took 840 seconds to reach the air temperature in this case. This trend was also observed at higher air temperatures of 104°C for a 10% weight concentration drop as shown in Figure 6.44. Plate 6.13 shows the crust structure for a 30% weight concentration drop dried at 88.5°C and 1m/s air velocity.

As observed experimentally sodium acetate forms a skin prior to a crust. Protrusions and splitting of the skin were observed during the course of drying.

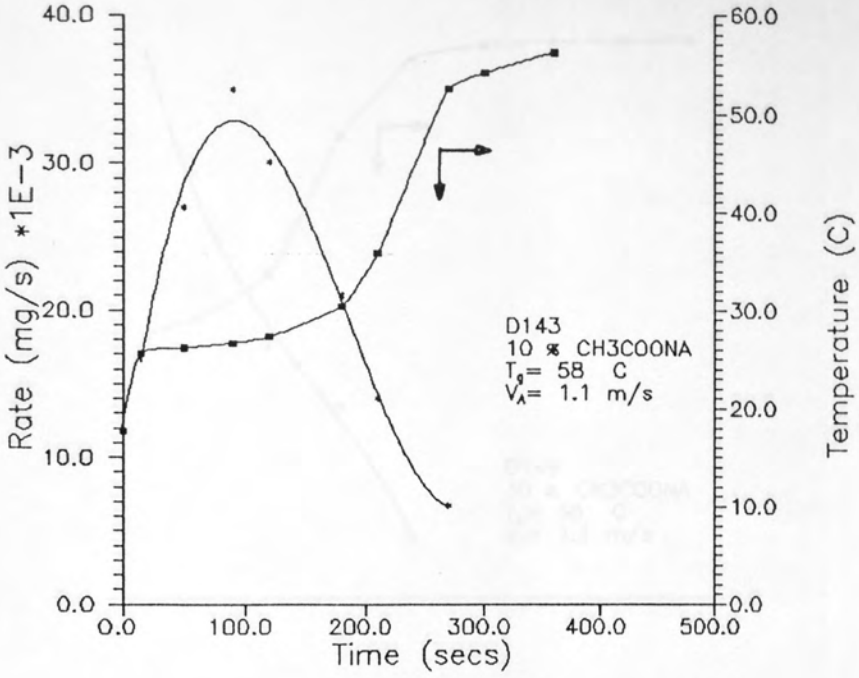

Figure 6.39 Simultaneous Core Temperature and Rate Histories for Aqueous Sodium Acetate (10 % wt/wt) at T_g= 58.0 C

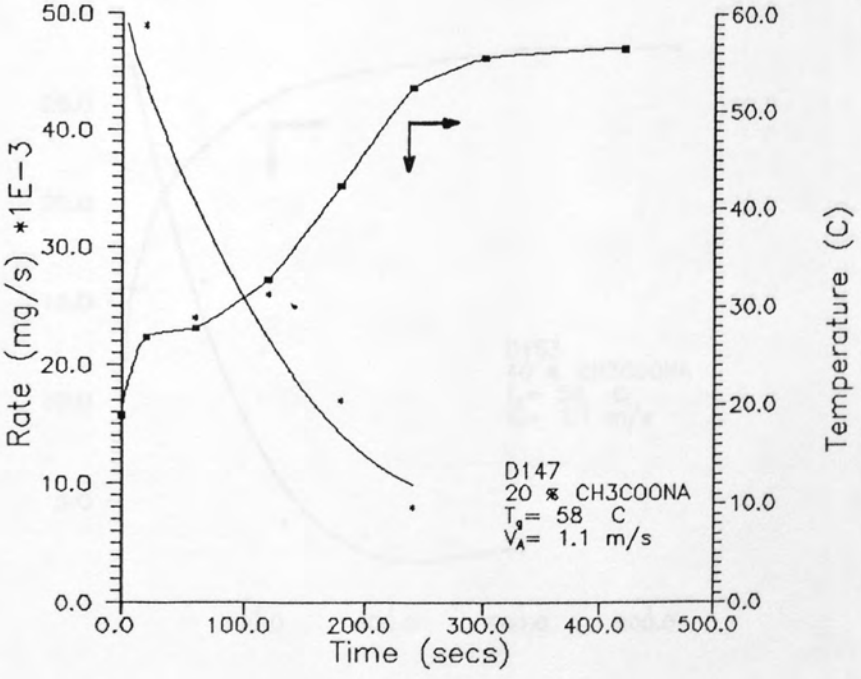

Figure 6.40 Simultaneous Core Temperature and Rate Histories for Aqueous Sodium Acetate (20 % wt/wt) at T_g= 58.0 C

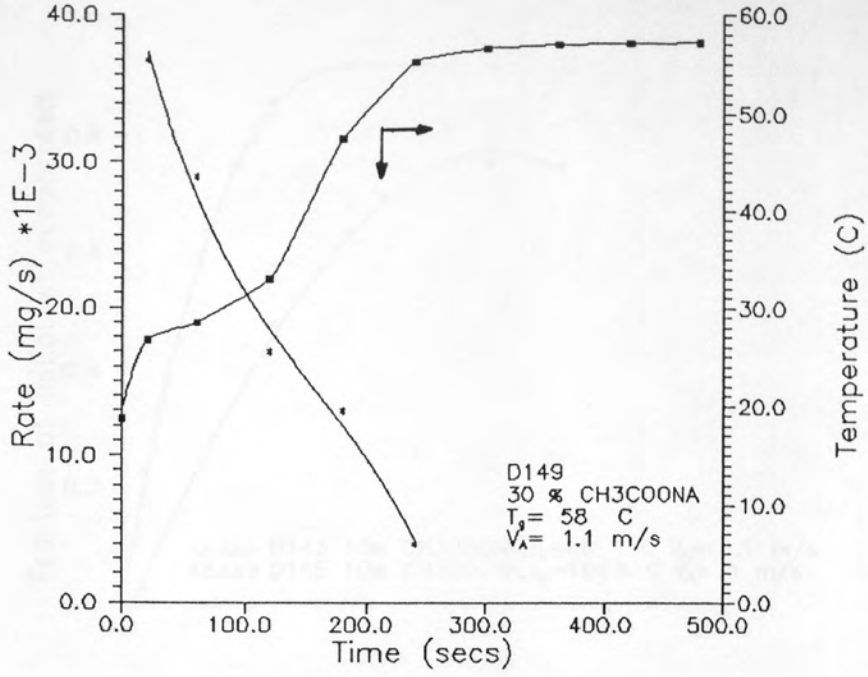

Figure 6.41 Simultaneous Core Temperature and Rate Histories for Aqueous Sodium Acetate (30 % wt/wt) at T_g= 58.0 C

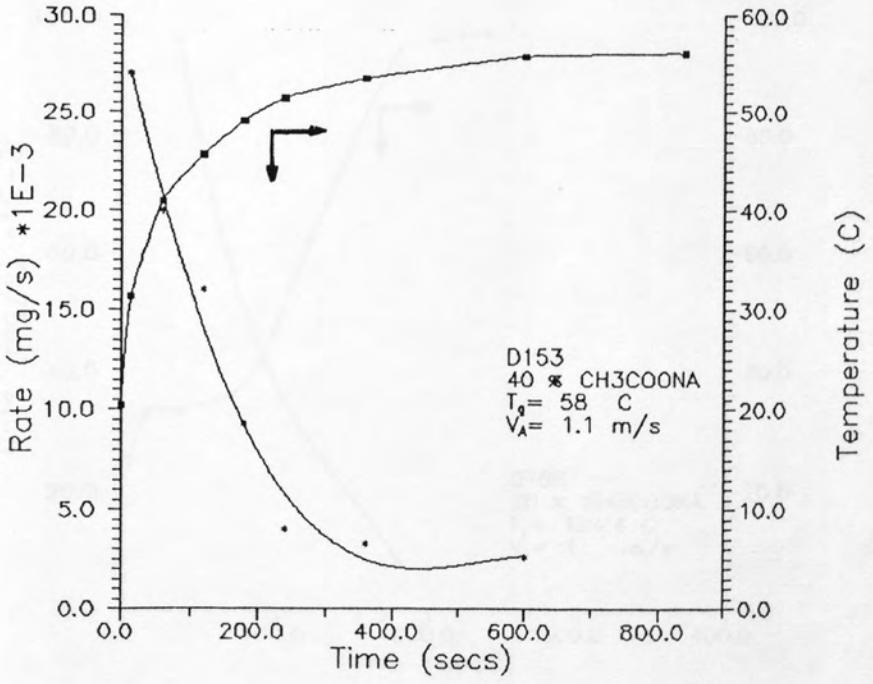

Figure 6.42 Simultaneous Core Temperature and Rate Histories for Aqueous Sodium Acetate (40 % wt/wt) at T_g= 58.0 C

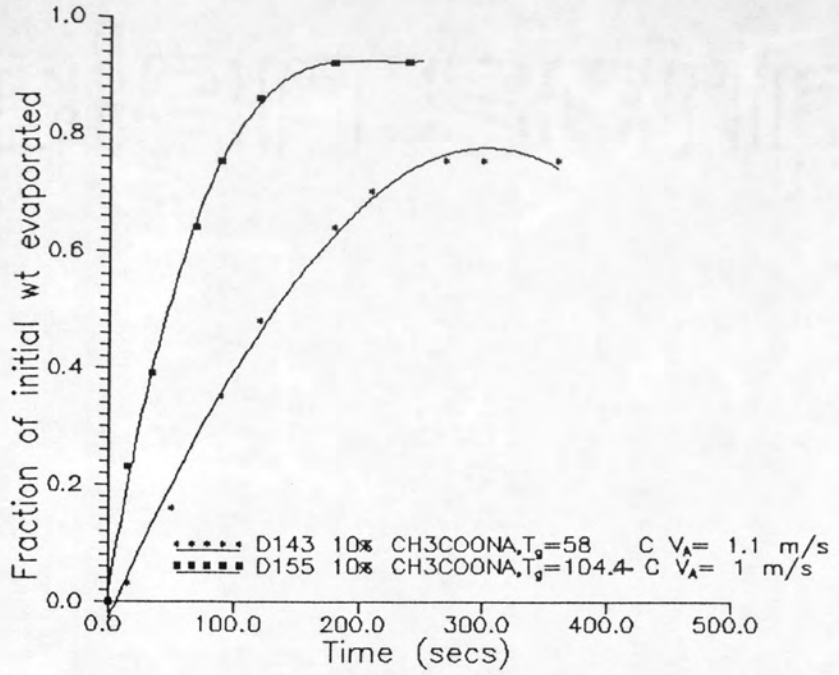

Figure 6.43 Drying of Drops of Aqueous Sodium Acetate (10 % wt/wt) at Varying Air Temperatures.

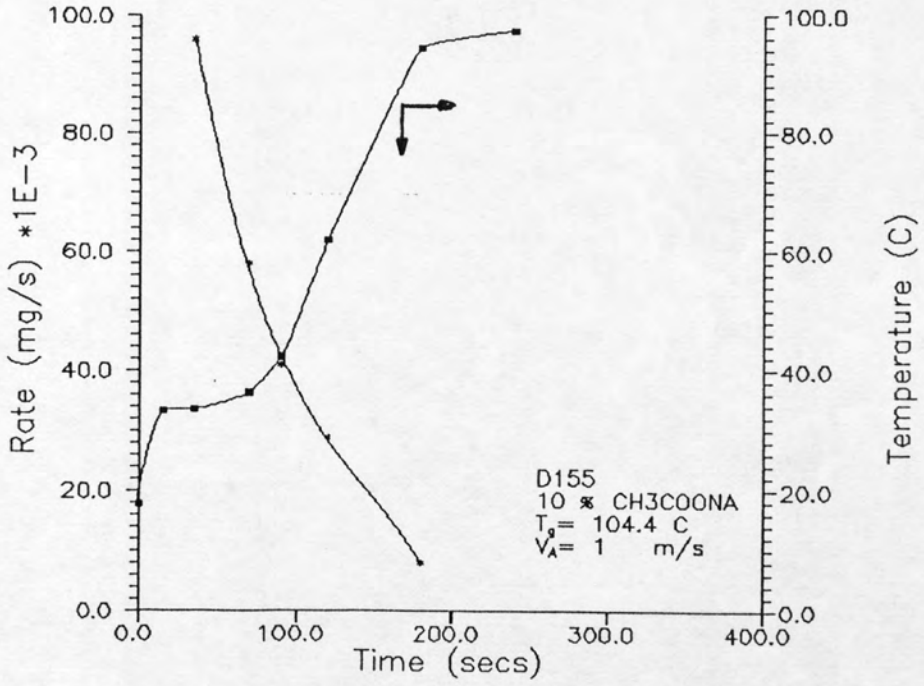

Figure 6.44 Simultaneous Core Temperature and Rate Histories for Aqueous Sodium Acetate (10 % wt/wt) at T_g= 104.4 C

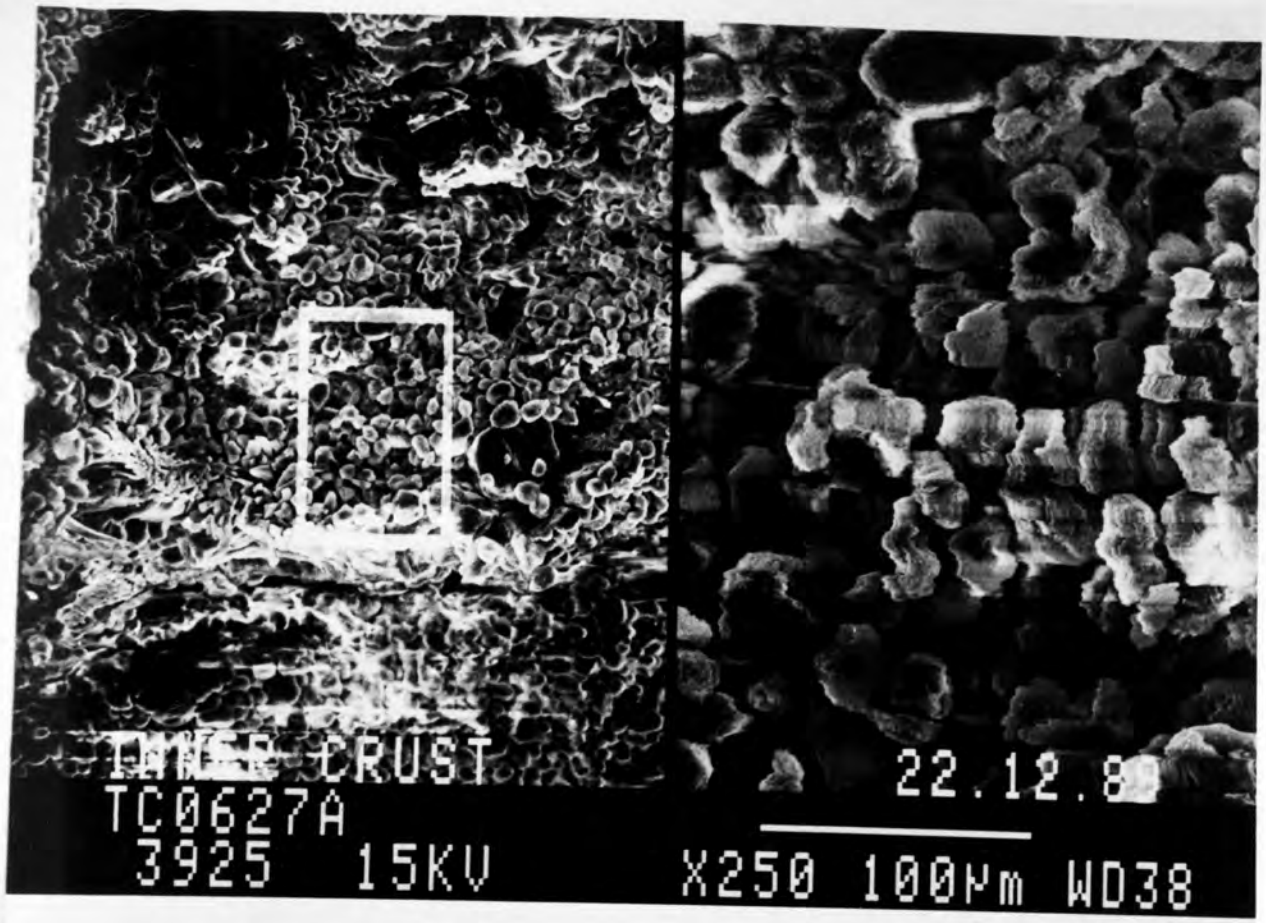

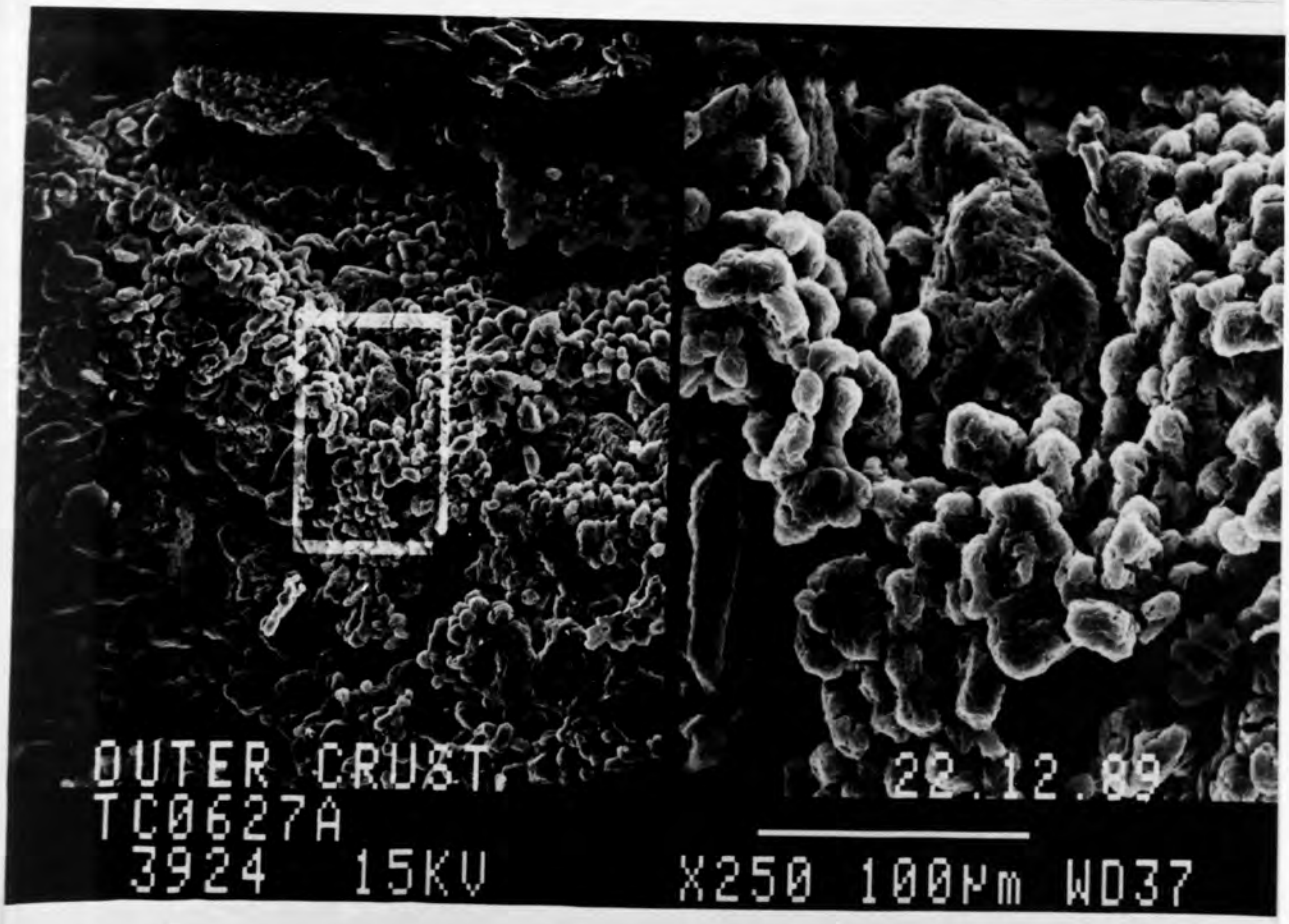

Plate 6.13 Inner and Outer Crust Surface of a 30% Weight Sodium Acetate Drop (88.5°C, 1m/s).

6.6 WATER DROPS

The experimental results for water drops were correlated as Nusselt numbers as described in section 3.2.1. The Nusselt numbers were calculated from equation 3.84. This has been corrected for heat transfer by radiation and conduction along the filament as described in sections 3.2.2 and 3.2.3.. The results were correlated by a least-squares technique according to equation 3.80. The results are shown in Figures 6.45 to 6.48 and Appendix B.6. The value of ø for each temperature is shown in Table 6.2. The results show that the data cannot be fitted by a single value of ø; ø appears to be a function of temperature. This has been observed by a number of investigators (4,5,7).

Hoffman and Gauvin (29) have shown that the relatively cold vapours leaving the drop can seriously reduce the heat transfer rate at the drop surface. A similar analysis has also been presented by a number of different investigators (60,61,65). Hoffman and Gauvin (29) state that the effect of evaporation rate on heat transfer to drops is dependent on the the magnitude of Spalding's Transfer Number $B = Cp\,\Delta T/Lv$.

The Transfer Number has been used to correlate the effects of temperature on ø (65,4,5,7). Typical correlations were,

$$Nu = 2 + 0.19\,(1/B)^{0.24}Re^{0.5}Pr^{0.33} \qquad 6.2$$

$$Nu = 2 + 0.228\,(1/B)^{0.2}Re^{0.5}Pr^{0.33} \qquad 6.3$$

ø was therefore plotted against B as shown in Figure 6.49. This demonstrates a linear relationship between ø and B which is represented by,

$$ø = -12.96B + 0.76 \qquad 6.4$$

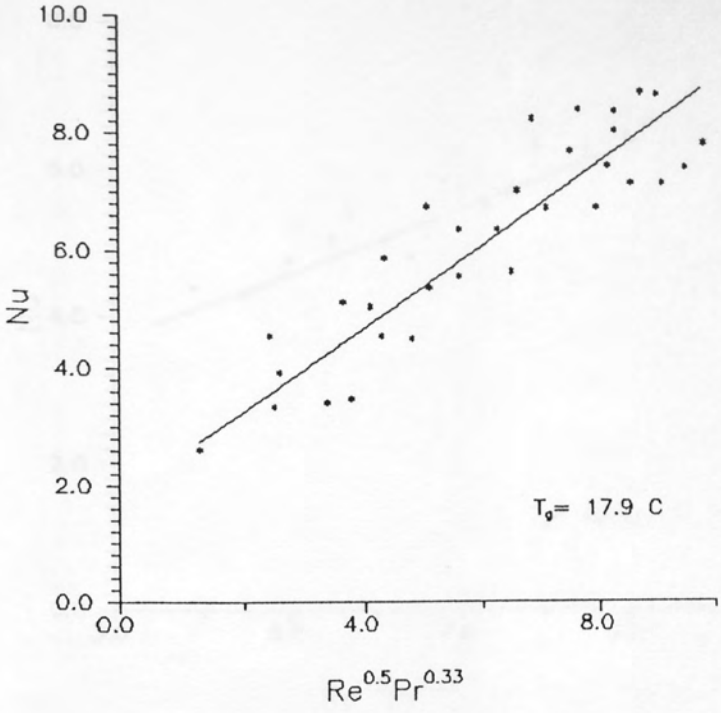

Figure 6.45 Plot of Nu vs $Re^{0.5}Pr^{0.33}$ at T_g= 17.9 C

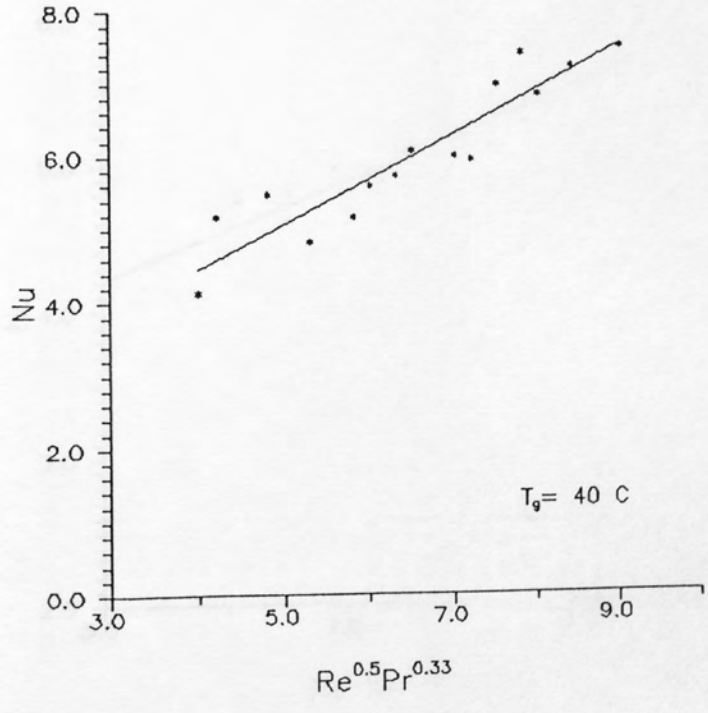

Figure 6.46 Plot of Nu vs $Re^{0.5}Pr^{0.33}$ at T_g=40 C

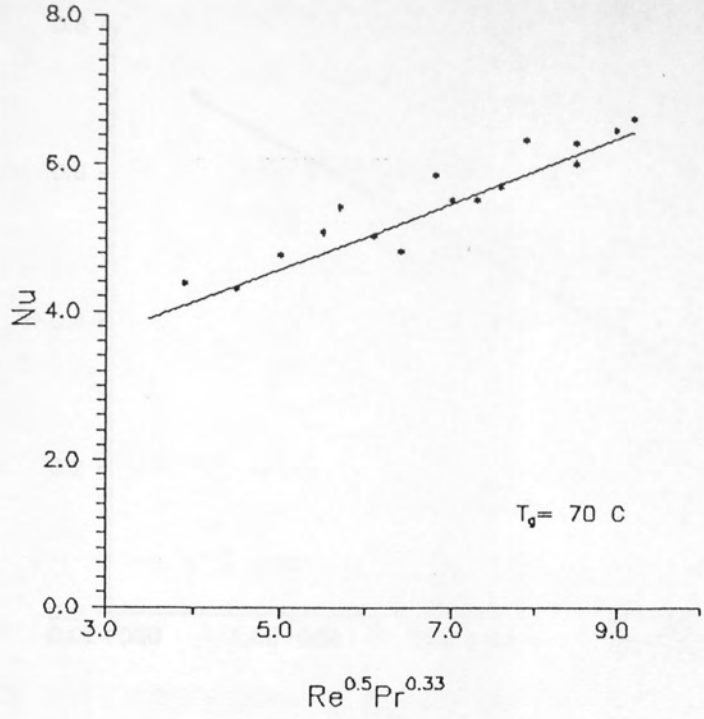

Figure 6.47 Plot of Nu vs $Re^{0.5}Pr^{0.33}$ at T_g= 70 C

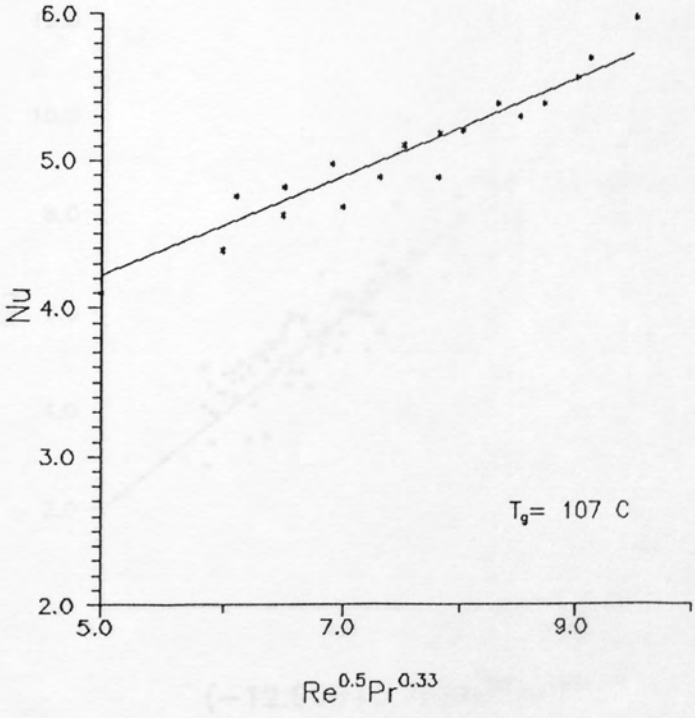

Figure 6.48 Plot of Nu vs $Re^{0.5}Pr^{0.33}$ at T_g= 107 C

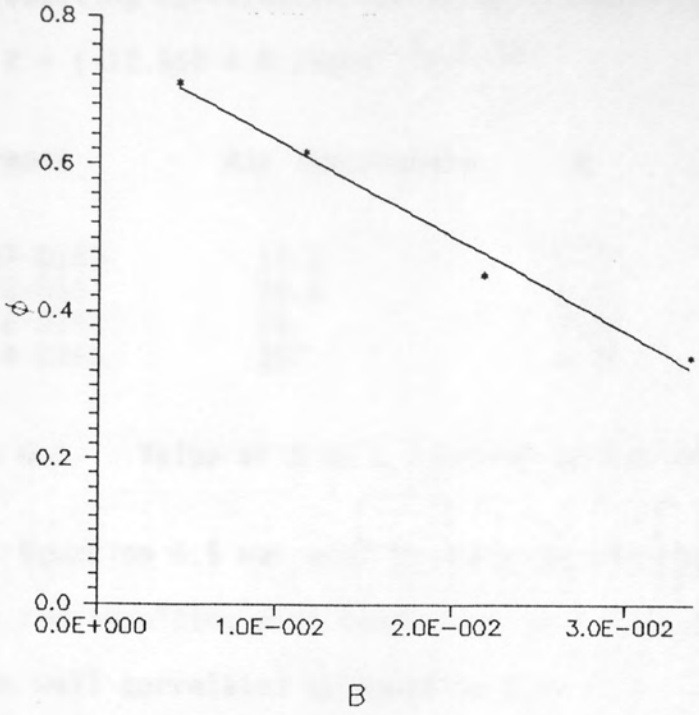

Figure 6.49 Plot of B vs θ

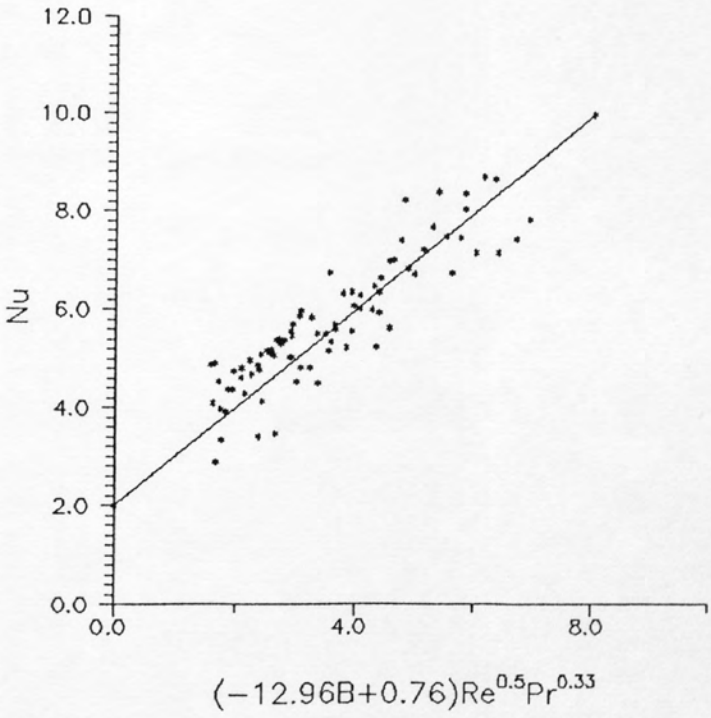

Figure 6.50 Plot of Nu vs $(-12.96B+0.76)Re^{0.5}Pr^{0.33}$

The resulting correlation for Nusselt number is

$$Nu = 2 + (-12.96B + 0.76)Re^{0.5}Pr^{0.33} \qquad 6.5$$

Reference	Air Temperature	ø	Correlation Coefficient
D157-D159	17.3	0.71	0.94
D160-D161	38.8	0.62	0.97
D162-D163	74	0.45	0.97
D164-D165	107	0.34	0.98

Table 6.2 Value of ø as a Function of Air Temperature

Equation 6.5 was used to correlate the data. Figure 6.50 shows the resulting plot confirming that the experimental results can be well correlated by equation 6.5.

CHAPTER SEVEN

MATHEMATICAL MODEL PREDICTIONS

MATHEMATICAL MODEL PREDICTIONS

7.0 INTRODUCTION

The receding evaporation interface model derived in section 3.1 was used to describe the drying of single solution/slurry drops of aqueous sodium sulphate decahydrate, sodium chloride, potassium sulphate, copper sulphate and sodium acetate. The gas film heat and mass transfer coefficients were calculated according to the correlations of Ranz and Marshall (3).

Simultaneous ordinary differential equations 3.76, 3.77 and 3.78 describing the variation in core temperature, crust thickness and drop weight were solved using a Runge-Kutta fourth-order integration. A computer program, file name GSB5.FOR, was written in Fortran 77 for an IBM PC model PS2/50. A full listing and flowsheet of the program is given in Appendix C.2.

The program requires;

(i) Initial drop weight

(ii) Initial drop temperature

(iii) Initial drop concentration

(iv) Air velocity

(v) Air humidity

(vi) Drop porosity

The determination of (i) to (v) is described in Chapter 5. The nature of the filament did not facilitate recovery of intact final dried crusts and hence experimental crust porosities could not be determined. For modelling purposes, an empirical correlation derived by Cheong et al (112) expressing the crust porosity as a function of a dimensionless crust thickness was used. This is expressed as

$$Ev_f = 1 - 2.4\beta/R \qquad 7.1$$

Here the porosity varies from an initial value of 1 to a final fixed value. The crust porosity was also modelled as a single fixed value E_f.

7.1 SODIUM SULPHATE DECAHYDRATE

The effect of using a variable porosity predicted by Equation 7.1 and fixed porosities are shown in Figures 7.1 and 7.2 for a 40% wt drop at an air temperature of 20.4° C and 1 m/s air velocity. Little difference in the predicted results was found using a fixed porosity of 0.9 and a variable porosity decreasing to a final fixed value of 0.9. Assuming a fixed porosity of 0.5 the model predicted higher initial temperatures and lower rates than with a variable porosity of 0.5. The best agreement between experimental and model results was obtained using a porosity of 0.9.

For air temperatures above 33° C, the model was modified to include an additional heat absorption term to account for the unusual behaviour of the decahydrate crystals. Thus

$$\Delta H = \frac{4}{3} \pi R^3 P_c \; L_f (1 - x_\omega)$$

and $$\Delta T = \frac{\Delta H}{W C_{pc}}$$

Where ΔH = Heat of absorption
L_f = Heat of solution of the decahydrate
ΔT = Fall in the drop temperature

The above process at 33° C also results in 0.51 kg water/kg decahydrate being released into the core. For a drop of 40% wt concentration and a weight of 10.49 mg, as shown in Figure 7.4, this represents 2.1 mg of water. The fraction of initial weight evaporated then has a final value of 0.8. From Figure 7.4, a porosity of 0.9 gives good agreement for the weight history of the

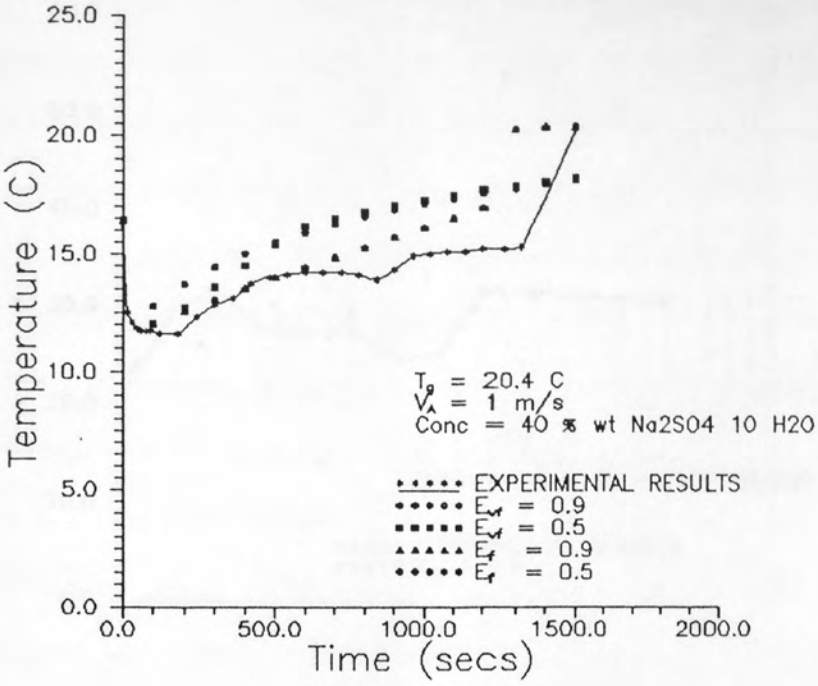

Figure 7.1 A Comparision of Model Predictions and Experimental Results for the Core Temperature History of Aqueous Sodium Sulphate Decahydrate (40 % wt/wt, T_g = 20.4 C)

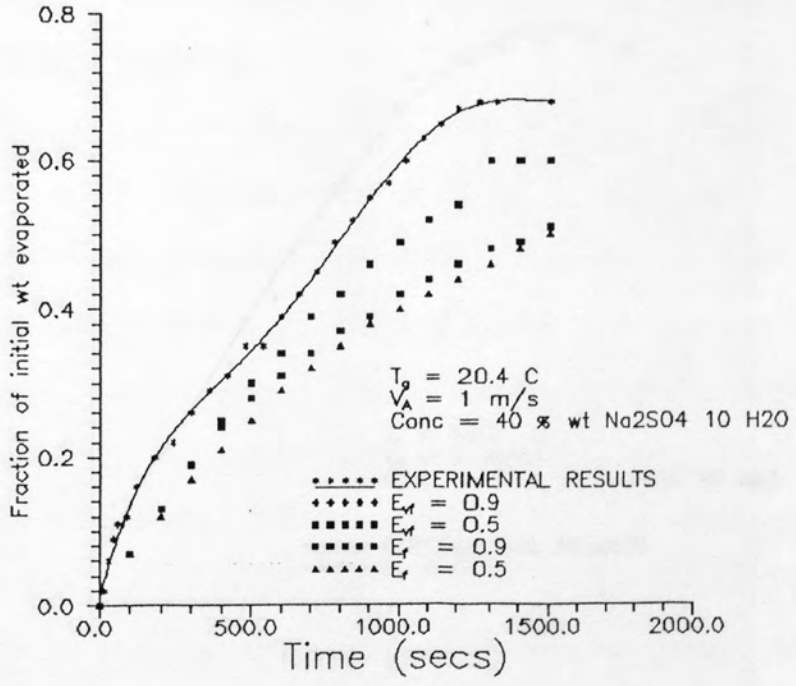

Figure 7.2 A Comparision of Model Predictions and Experimental Results for the Weight History of Aqueous Sodium Sulphate Decahydrate (40 % wt/wt, T_g = 20.4 C)

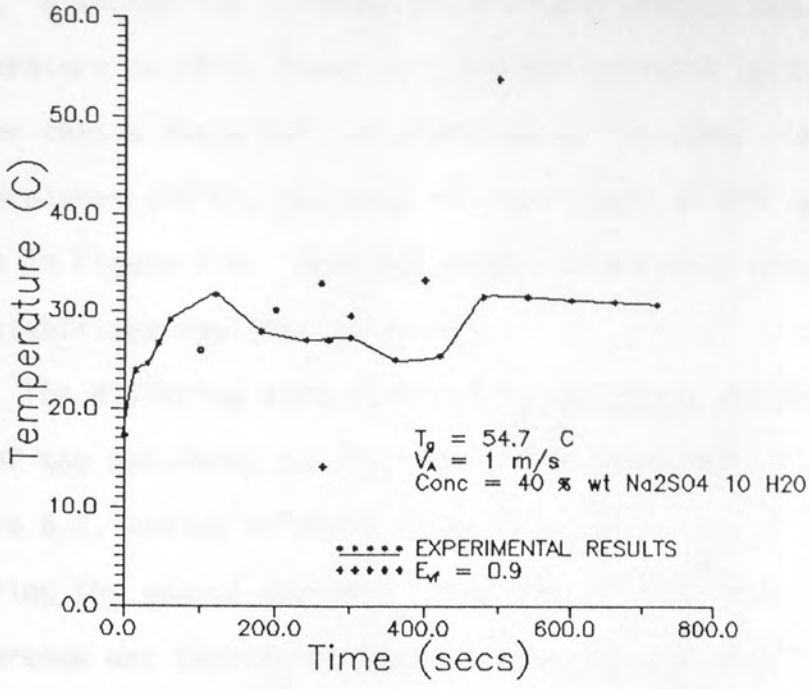

Figure 7.3 A Comparision of Model Predictions and Experimental Results for the Core Temperature History of Aqueous Sodium Sulphate Decahydrate (40 % wt/wt, T_g = 54.7 C)

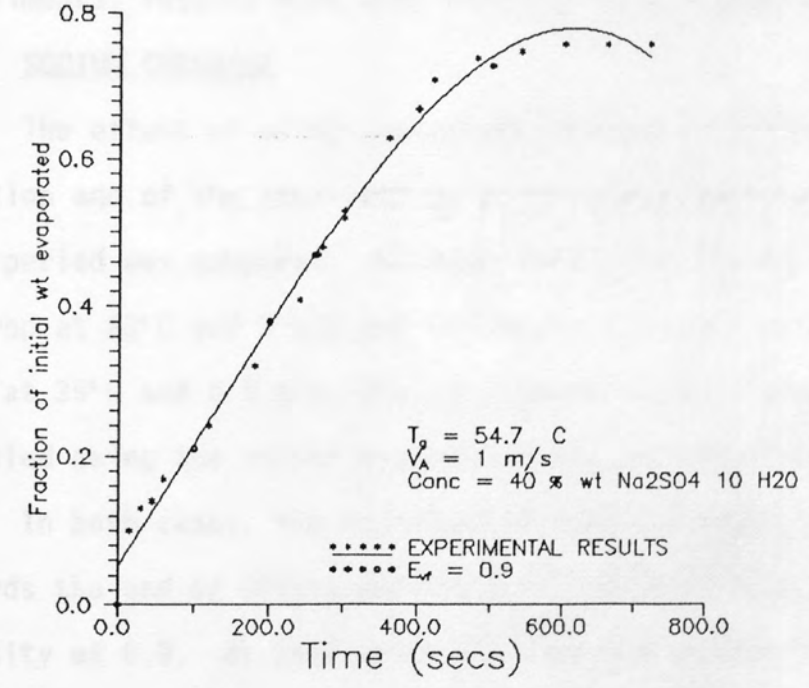

Figure 7.4 A Comparision of Model Predictions and Experimental Results for the Weight History of Aqueous Sodium Sulphate Decahydrate (40 % wt/wt, T_g = 54.7 C)

drop. Although the filament-thermocouple detects the drop in temperature at 33°C, there is a gradual decrease in the temperature rather than a sharp fall as predicted by the model. At higher air temperatures (74°C), the drop in temperature at 33°C was lower as shown in Figure 7.5. Here the higher temperature driving force re-establishes equilibrium quickly.

The differing effects of using the vapour pressure of water and of the saturated solution were also modelled. As shown in Figure 6.2, sodium sulphate decahydrate has only a slight effect on lowering the vapour pressure below that of pure water. Little difference was therefore noted in the predicted results as shown in Figures 7.5 and 7.6.

Taking into account the process occurring at 33°C, good agreement was obtained between experimental results and model predictions for air temperatures above and below 33°C. The experimental results were best modelled using a porosity of 0.9.

7.2 SODIUM CHLORIDE

The effect of using the vapour pressure of water, of the solution and of the saturated solution in the model for the constant rate period was compared. As shown in Figures 7.7 and 7.8 for a 20% wt drop at 23°C and 1 m/s and in Figures 7.9 and 7.10 for a 20% wt drop at 35°C and 0.5 m/s, the experimental results were best modelled using the vapour pressure of the solution and a porosity of 0.9. In both cases, the experimental rates of evaporation decreased towards the end of drying and could no longer be modelled by a porosity of 0.9. At this point the crust resistance to mass transfer has increased as a result of an increase in its thickness.

7.3 POTASSIUM SULPHATE

The effect of using a range of variable and fixed porosities from 0.2-0.9 in the model are shown in Figures 7.11 to 7.14 for a

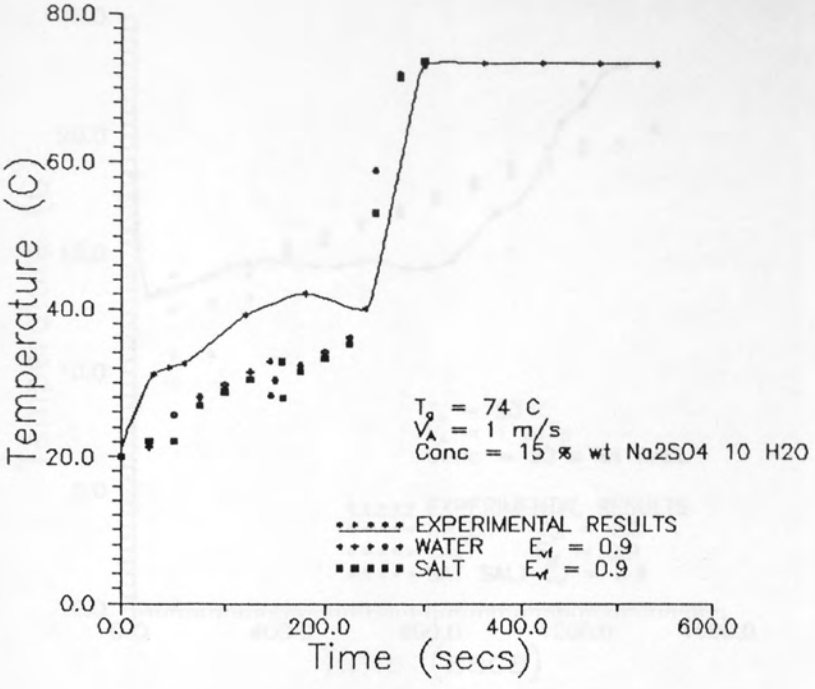

Figure 7.5 A Comparision of Model Predictions and Experimental Results for the Core Temperature History of Aqueous Sodium Sulphate Decahydrate (15 % wt/wt, T_g = 74.0 C)

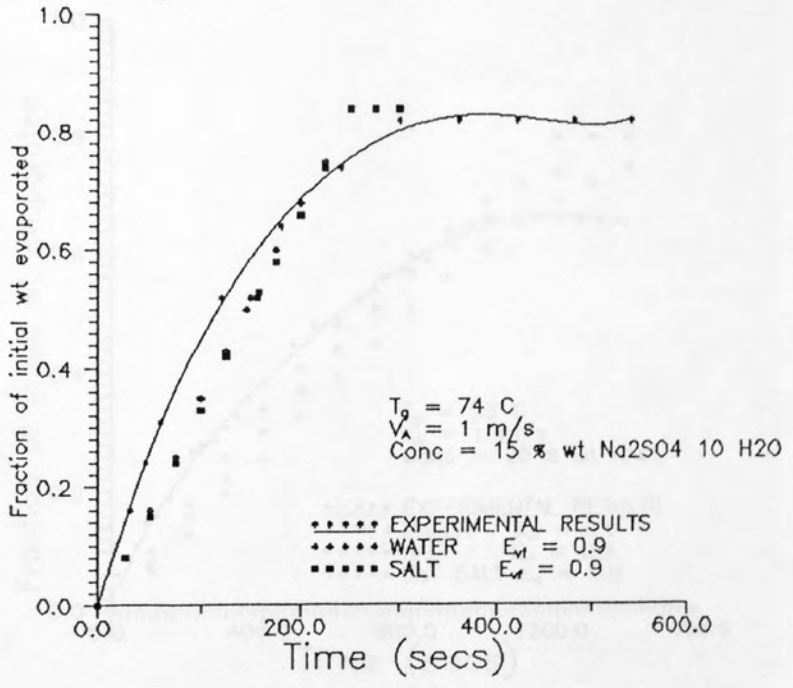

Figure 7.6 A Comparision of Model Predictions and Experimental Results for the Weight History of Aqueous Sodium Sulphate Decahydrate (15 % wt/wt, T_g = 74.0 C)

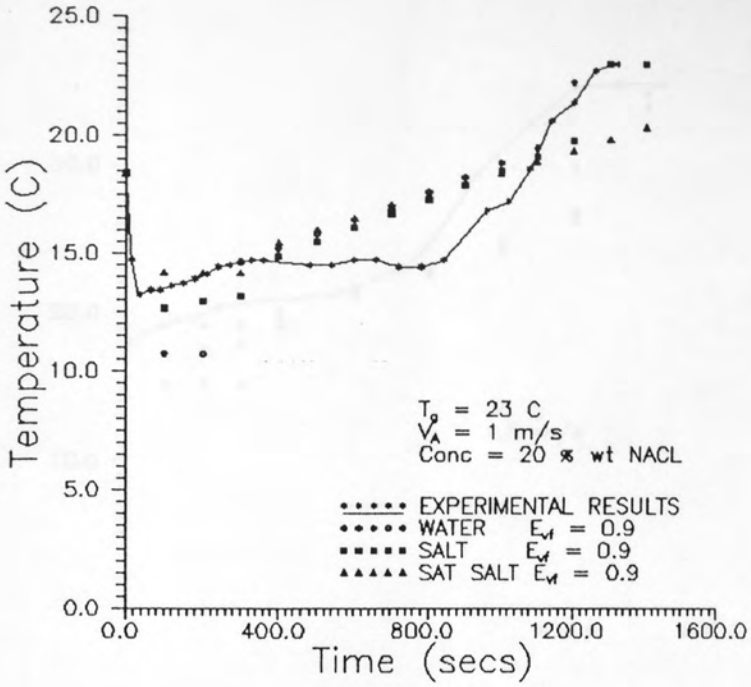

Figure 7.7 A Comparision of Model Predictions and Experimental Results for the Core Temperature History of Aqueous Sodium Chloride (20 % wt/wt, T_g = 23.0 C)

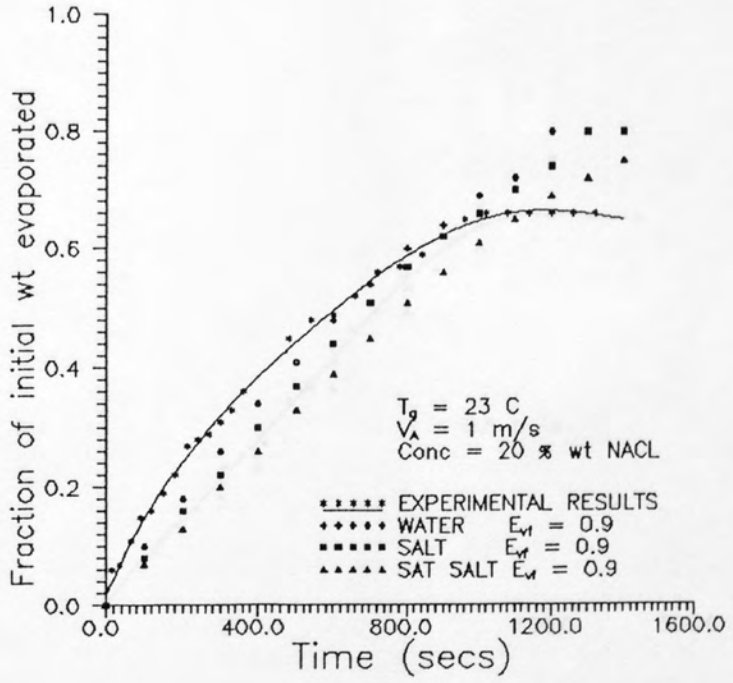

Figure 7.8 A Comparision of Model Predictions and Experimental Results for the Weight History of Aqueous Sodium Chloride (20 % wt/wt, T_g = 23.0 C)

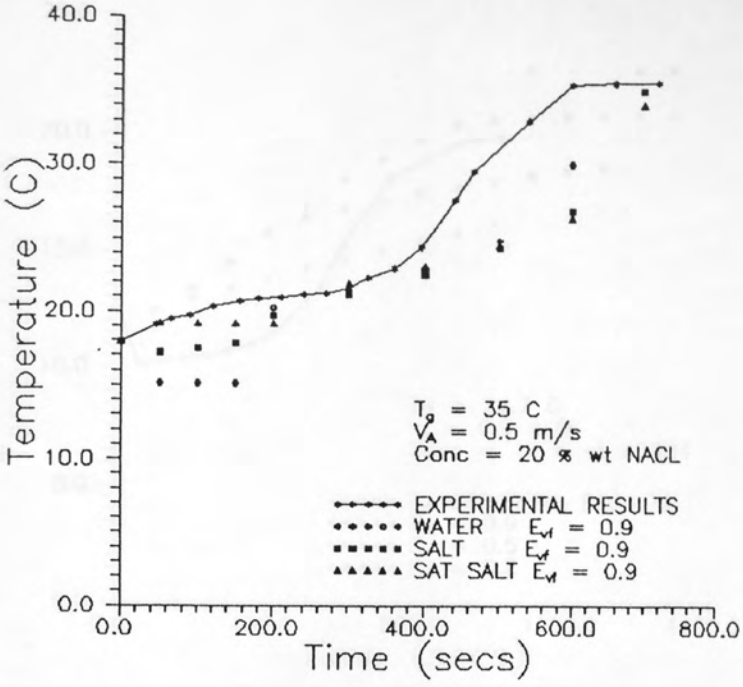

Figure 7.9 A Comparision of Model Predictions and Experimental Results for the Core Temperature History of Aqueous Sodium Chloride (20 % wt/wt,T_g = 35.0 C)

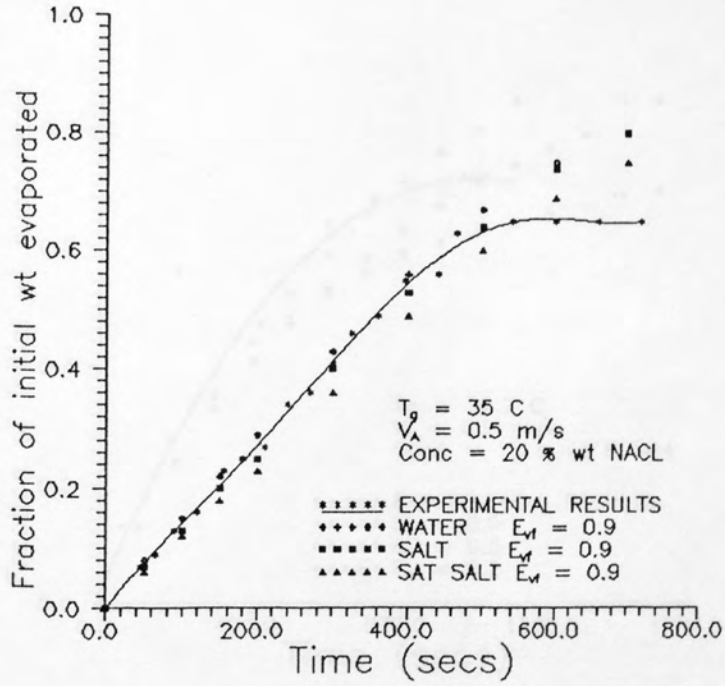

Figure 7.10 A Comparision of Model Predictions and Experimental Results for the Weight History of Aqueous Sodium Chloride (20 % wt/wt,T_g = 35.0 C)

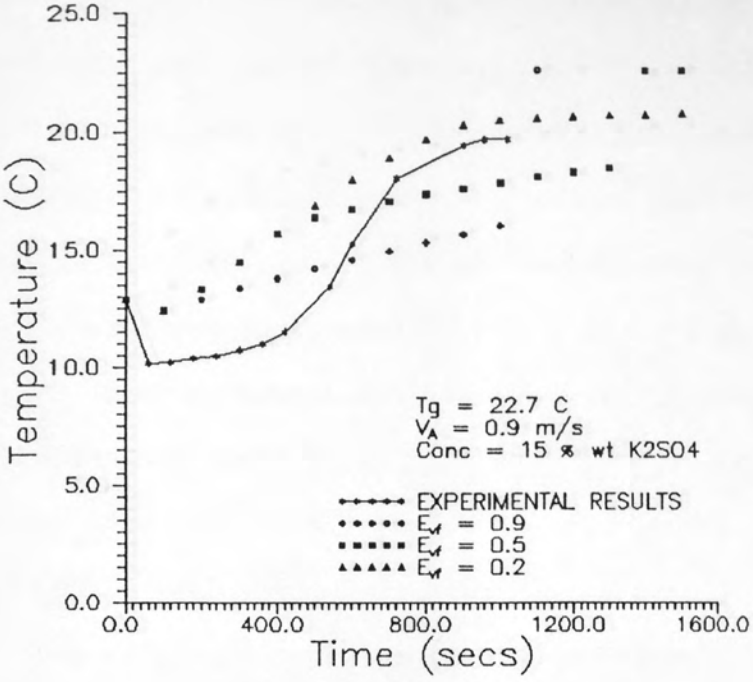

Figure 7.11 A Comparision of Model Predictions and Experimental Results for the Core Temperature History of Aqueous Potassium Sulphate (15 % wt/wt, T_g = 22.7 C)

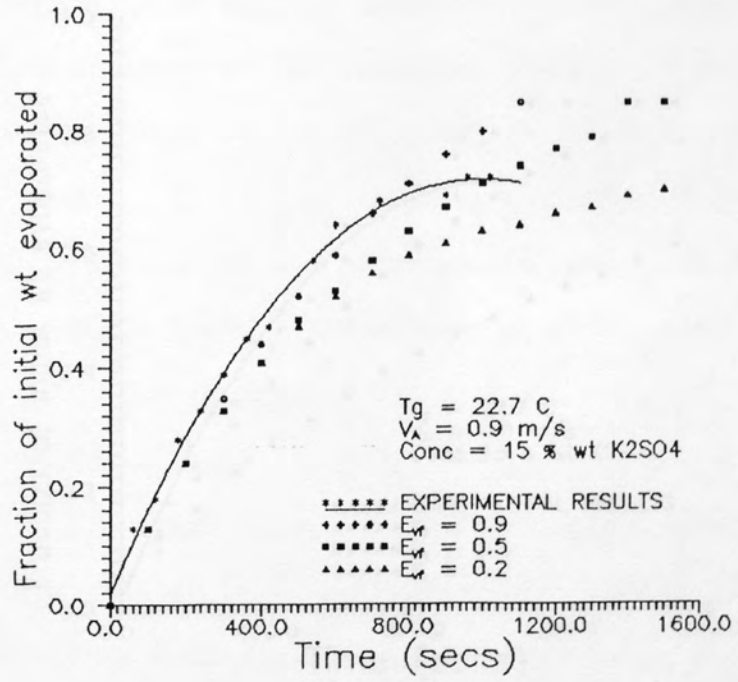

Figure 7.12 A Comparision of Model Predictions and Experimental Results for the Weight History of Aqueous Potassium Sulphate (15 % wt/wt, T_g = 22.7 C)

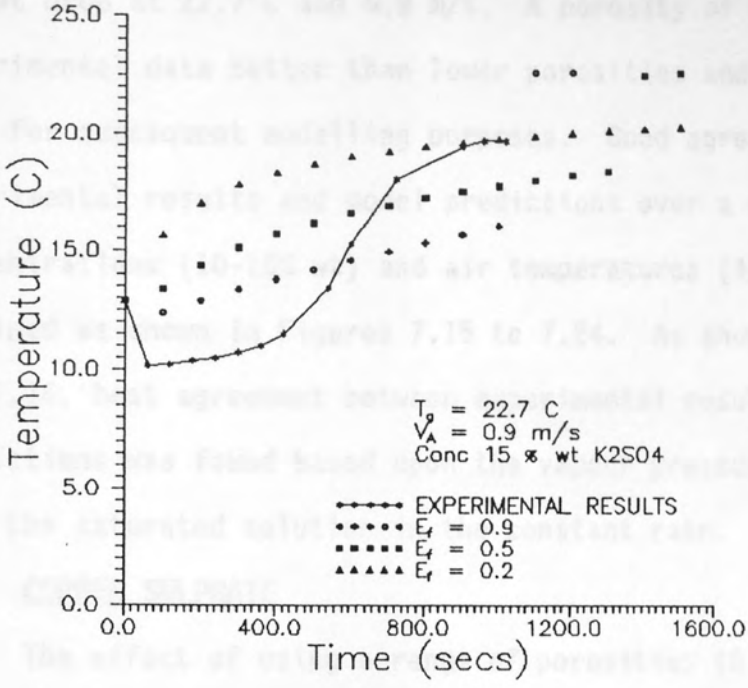

Figure 7.13 A Comparision of Model Predictions and Experimental Results for the Core Temperature History of Aqueous Potassium Sulphate (15 % wt/wt, T_g = 22.7 C)

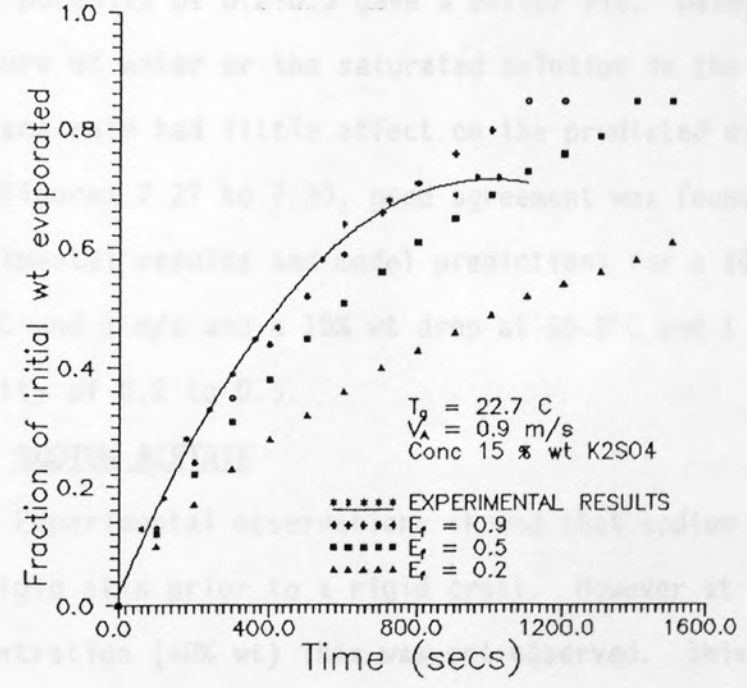

Figure 7.14 A Comparision of Model Predictions and Experimental Results for the Weight History of Aqueous Potassium Sulphate (15 % wt/wt, T_g = 22.7 C)

15% wt drop at 22.7°C and 0.9 m/s. A porosity of 0.9 fitted the experimental data better than lower porosities and was therefore used for subsequent modelling purposes. Good agreement between experimental results and model predictions over a range of concentrations (10-15% wt) and air temperatures (46-91°C) was hence obtained as shown in Figures 7.15 to 7.24. As shown in Figures 7.15 and 7.16, best agreement between experimental results and model predictions was found based upon the vapour pressure of water rather than the saturated solution in the constant rate.

7.4 COPPER SULPHATE

The effect of using a range of porosities (0.2-0.9) and the vapour pressure of water or the saturated solution for modelling the constant rate are shown in Figures 7.25 and 7.26. Initially a porosity of 0.9 fits the experimental data. However as the crust increases in thickness, its resistance to mass transfer grows and a lower porosity of 0.2-0.5 gave a better fit. Using the vapour pressure of water or the saturated solution in the model for the constant rate had little effect on the predicted drying histories. From Figures 7.27 to 7.30, good agreement was found between experimental results and model predictions for a 10% wt drop at 20.9°C and 1 m/s and a 18% wt drop at 65.8°C and 1 m/s using a porosity of 0.2 to 0.5.

7.5 SODIUM ACETATE

Experimental observations showed that sodium acetate formed a non-rigid skin prior to a rigid crust. However at high concentration (40% wt) this was not observed. This non-rigid skin obviously represents a deviation from the model assumption of a rigid outer surface. As shown in Figures 7.31 to 7.38 for a 10% wt drop at 58°C and 1 m/s, a 20% wt drop at 58°C and 1.1 m/s and a 10% wt drop at 104.4°C and 1 m/s, the model predictions deviated

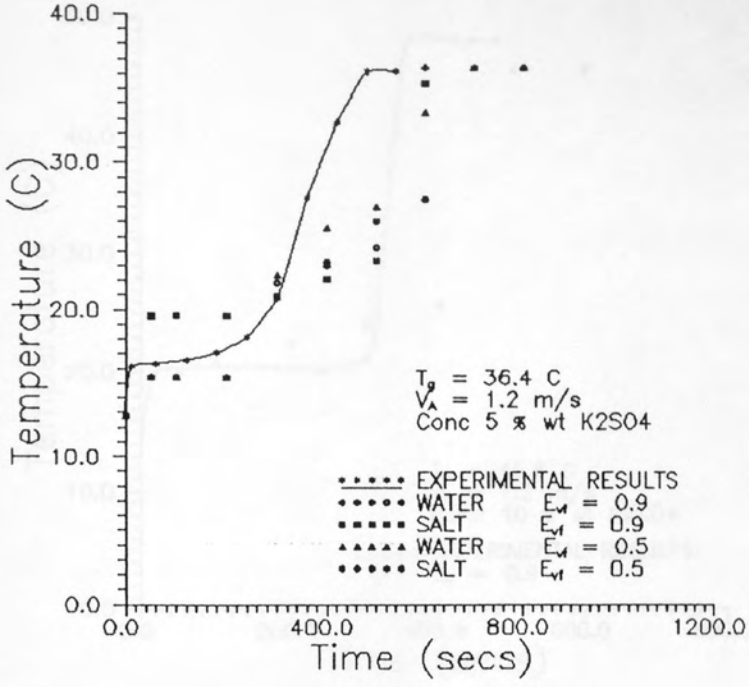

Figure 7.15 A Comparision of Model Predictions and Experimental Results for the Core Temperature History of Aqueous Potassium Sulphate (5 % wt/wt,T_g = 36.4 C)

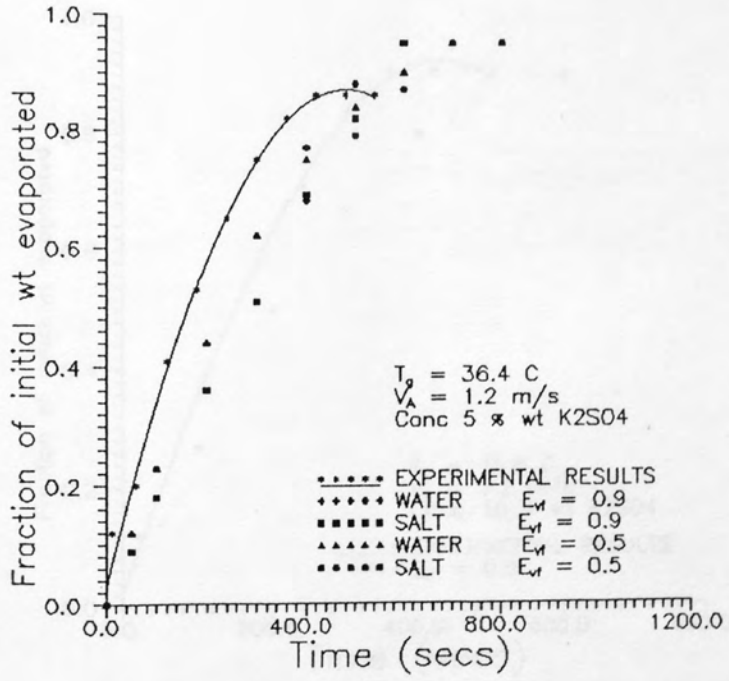

Figure 7.16 A Comparision of Model Predictions and Experimental Results for the Weight History of Aqueous Potassium Sulphate (5 % wt/wt,T_g = 36.4 C)

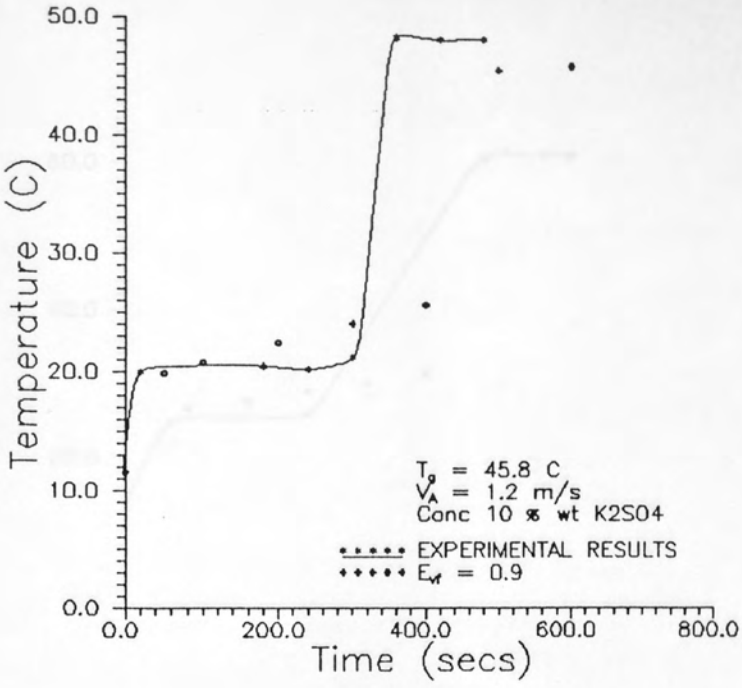

Figure 7.17 A Comparision of Model Predictions and Experimental Results for the Core Temperature History of Aqueous Potassium Sulphate (10 % wt/wt, T_g = 45.8 C)

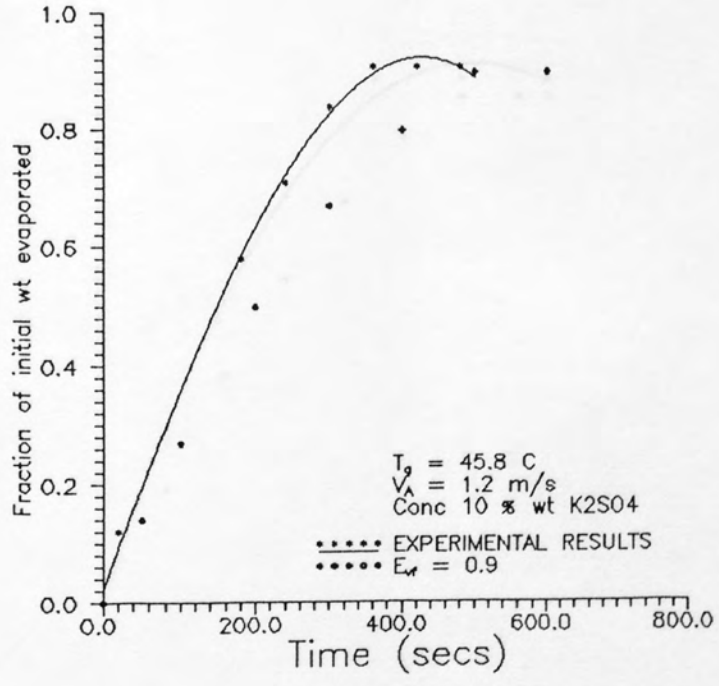

Figure 7.18 A Comparision of Model Predictions and Experimental Results for the Weight History of Aqueous Potassium Sulphate (10 % wt/wt, T_g = 45.8 C)

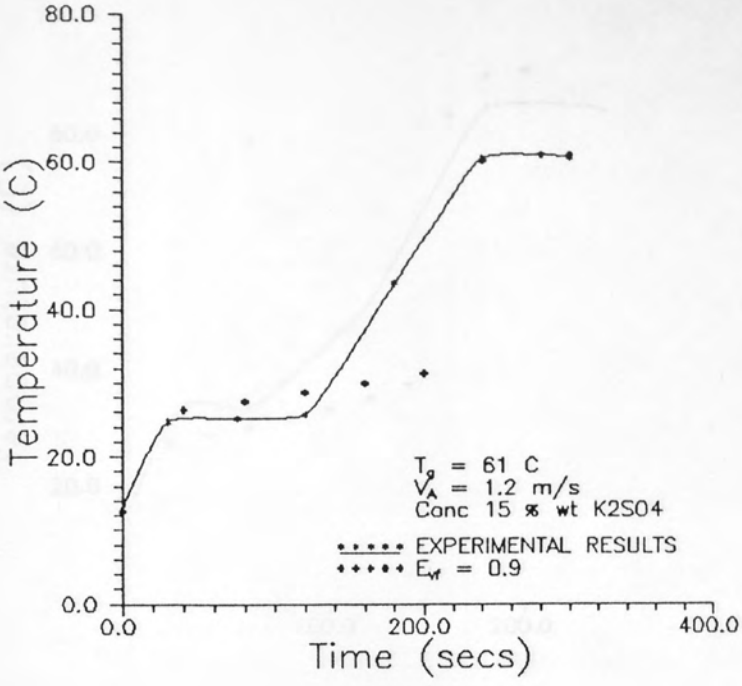

Figure 7.19 A Comparision of Model Predictions and Experimental Results for the Core Temperature History of Aqueous Potassium Sulphate (15 % wt/wt, T_g = 61.0 C)

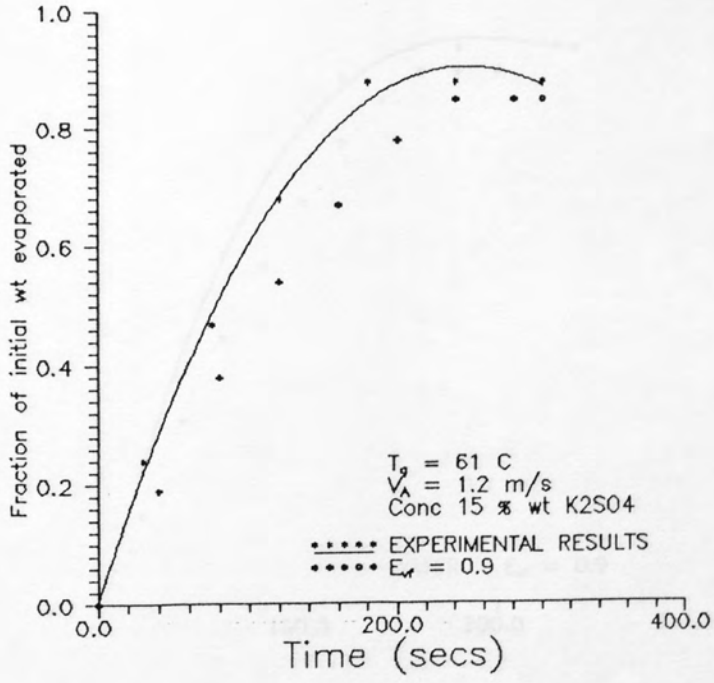

Figure 7.20 A Comparision of Model Predictions and Experimental Results for the Weight History of Aqueous Potassium Sulphate (15 % wt/wt, T_g = 61.0 C)

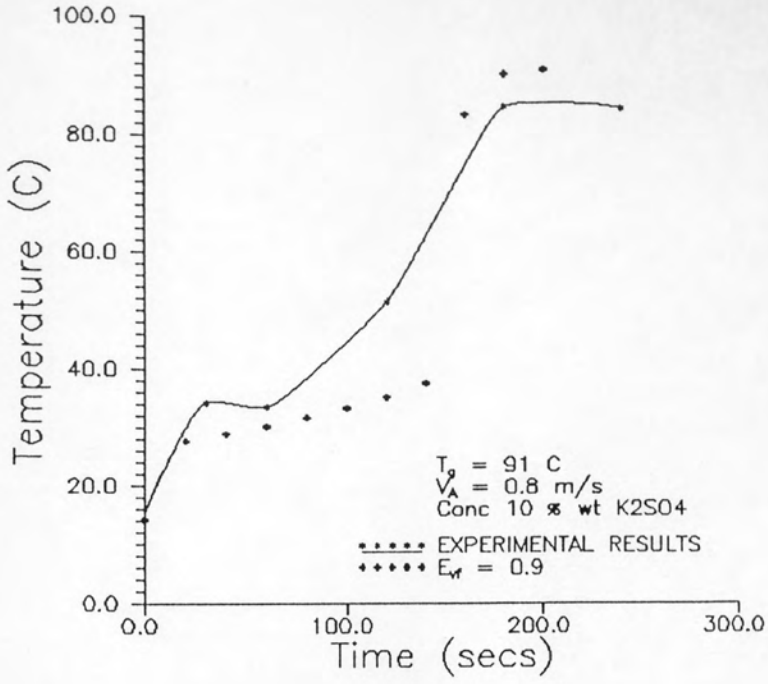

Figure 7.21 A Comparision of Model Predictions and Experimental Results for the Core Temperature History of Aqueous Potassium Sulphate (10 % wt/wt, T_g = 91.0 C)

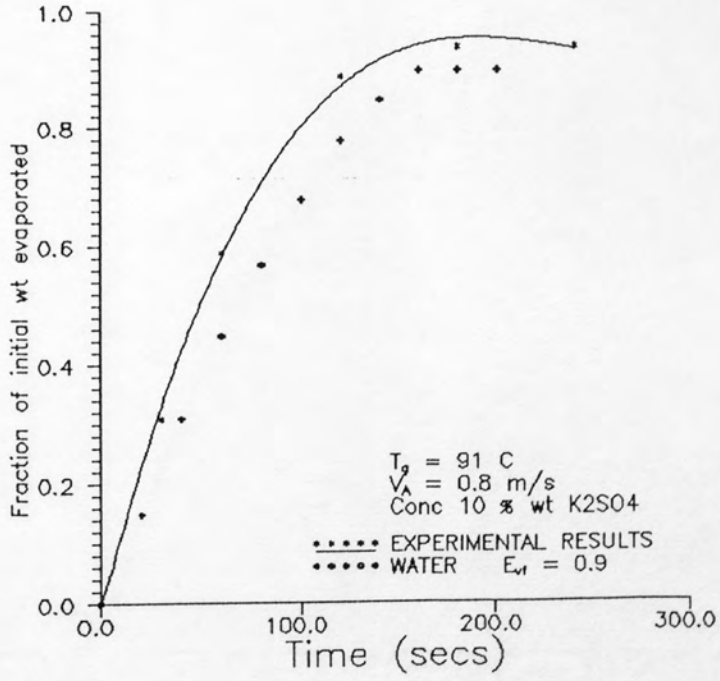

Figure 7.22 A Comparision of Model Predictions and Experimental Results for the Weight History of Aqueous Potassium Sulphate (10 % wt/wt, T_g = 91.0 C)

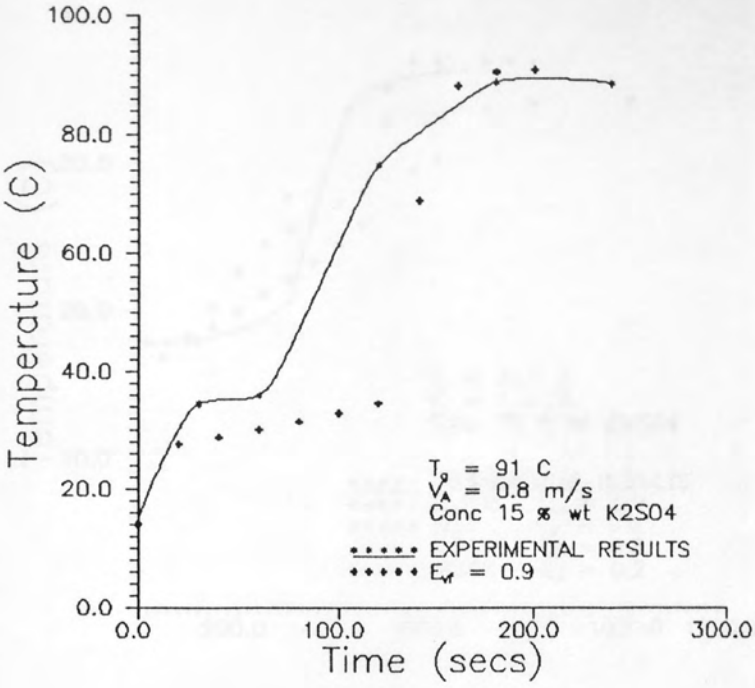

Figure 7.23 A Comparision of Model Predictions and Experimental Results for the Core Temperature History of Aqueous Potassium Sulphate (15 % wt/wt, T_g = 91.0 C)

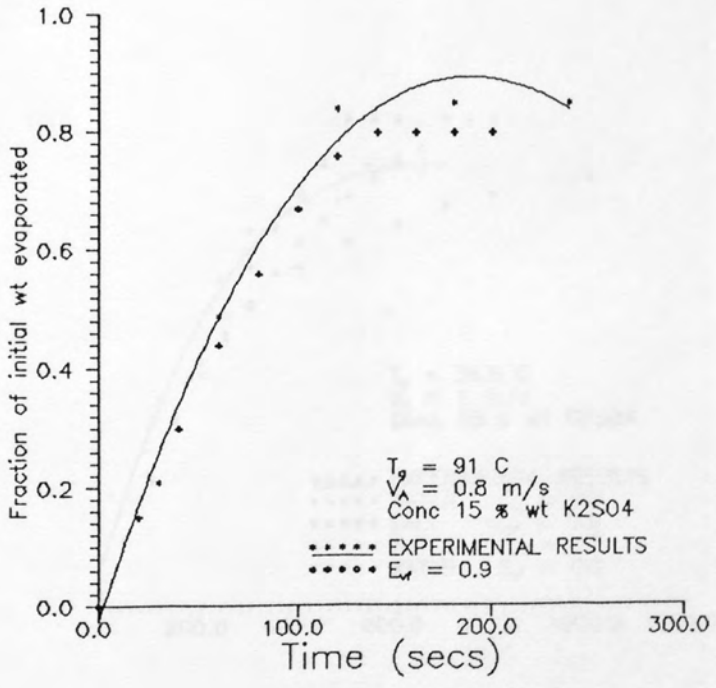

Figure 7.24 A Comparision of Model Predictions and Experimental Results for the Weight History of Aqueous Potassium Sulphate (15 % wt/wt, T_g = 91.0 C)

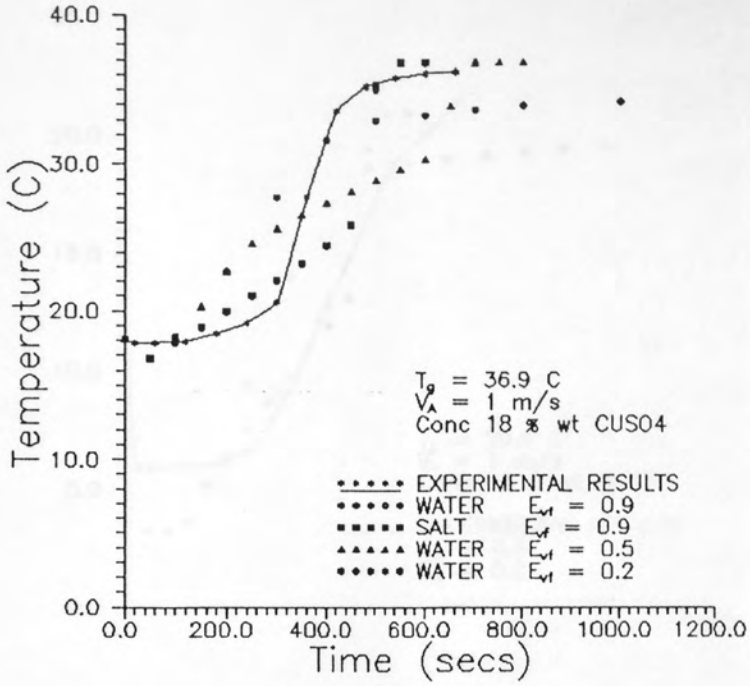

Figure 7.25 A Comparision of Model Predictions and Experimental Results for the Core Temperature History of Aqueous Copper Sulphate (18 % wt/wt, T_g = 36.9 C)

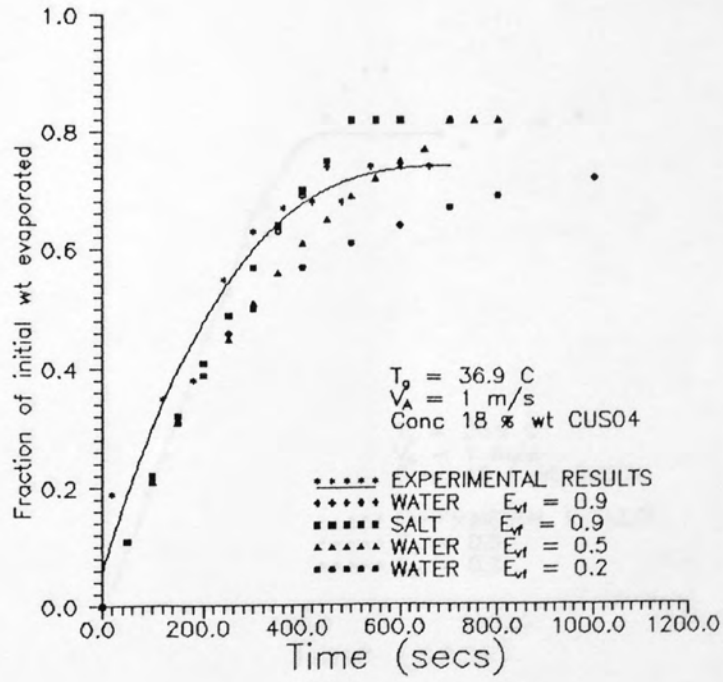

Figure 7.26 A Comparision of Model Predictions and Experimental Results for the Weight History of Aqueous Copper Sulphate (18 % wt/wt, T_g = 36.9 C)

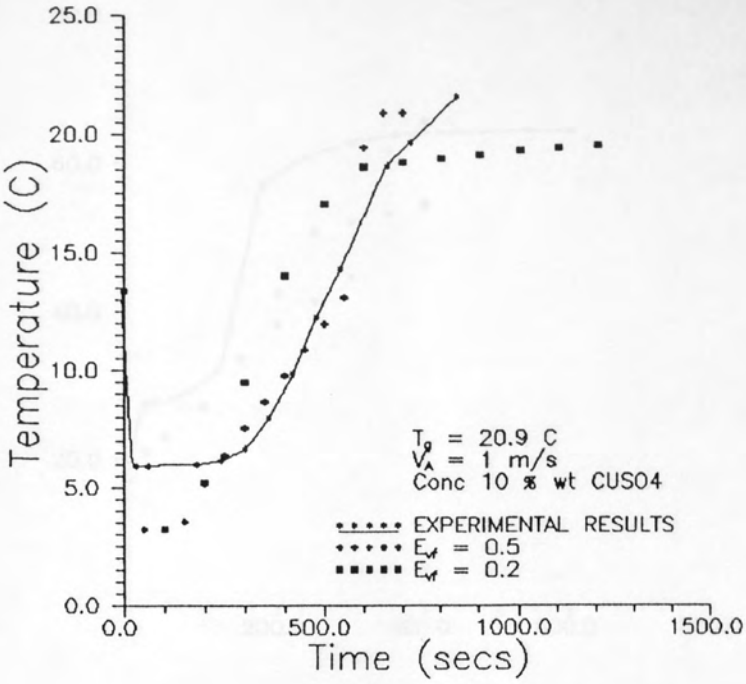

Figure 7.27 A Comparision of Model Predictions and Experimental Results for the Core Temperature History of Aqueous Copper Sulphate (10 % wt/wt, T_g = 20.9 C)

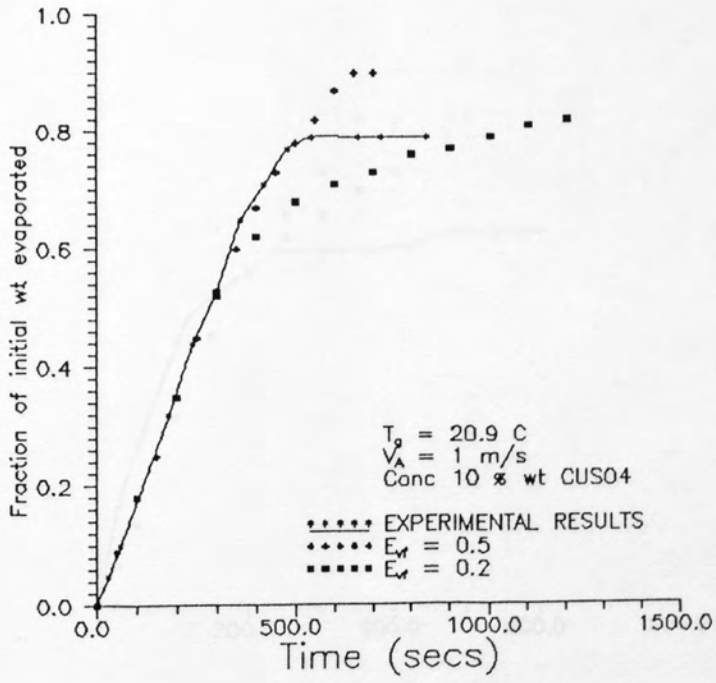

Figure 7.28 A Comparision of Model Predictions and Experimental Results for the Weight History of Aqueous Copper Sulphate (10 % wt/wt, T_g = 20.9 C)

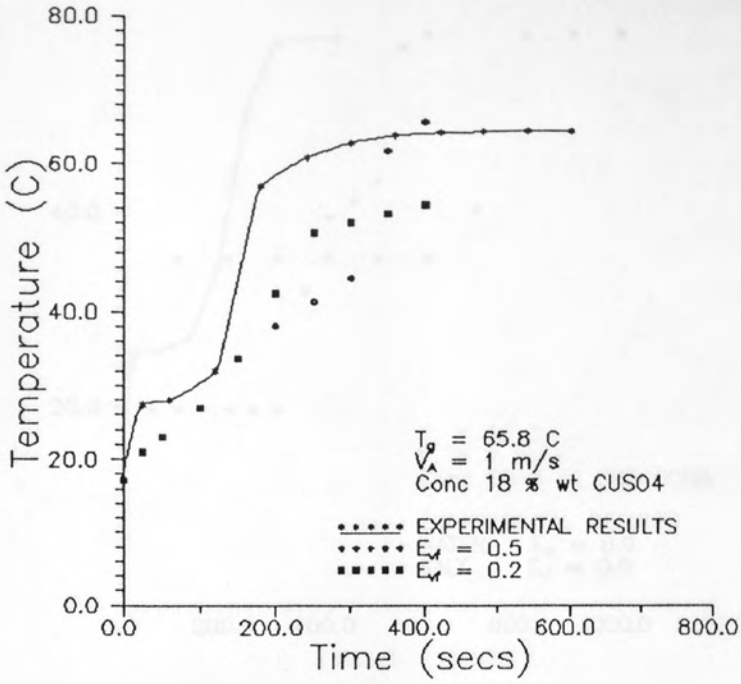

Figure 7.29 A Comparision of Model Predictions and Experimental Results for the Core Temperature History of Aqueous Copper Sulphate (18 % wt/wt, T_g = 65.8 C)

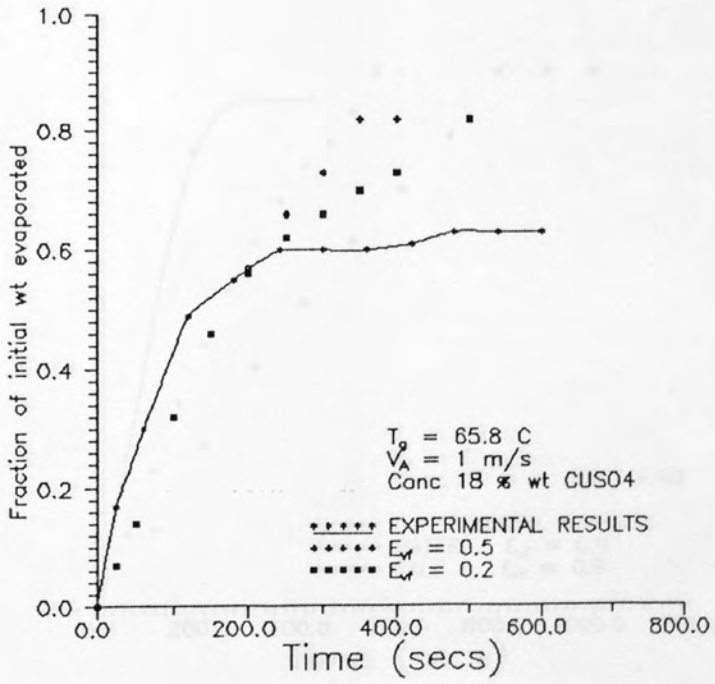

Figure 7.30 A Comparision of Model Predictions and Experimental Results for the Weight History of Aqueous Copper Sulphate (18 % wt/wt, T_g = 65.8 C)

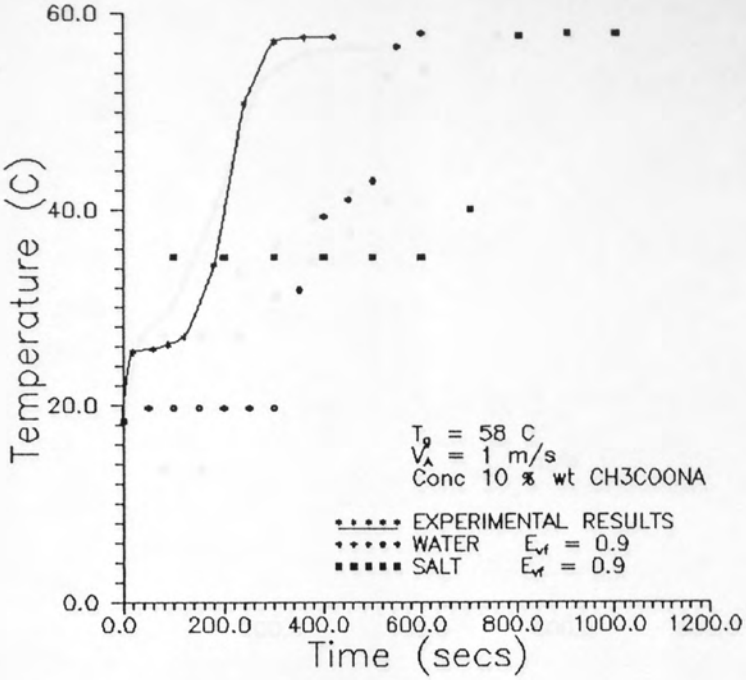

Figure 7.31 A Comparision of Model Predictions and Experimental Results for the Core Temperature History of Aqueous Sodium Acetate (10 % wt/wt, T_g = 58.0 C)

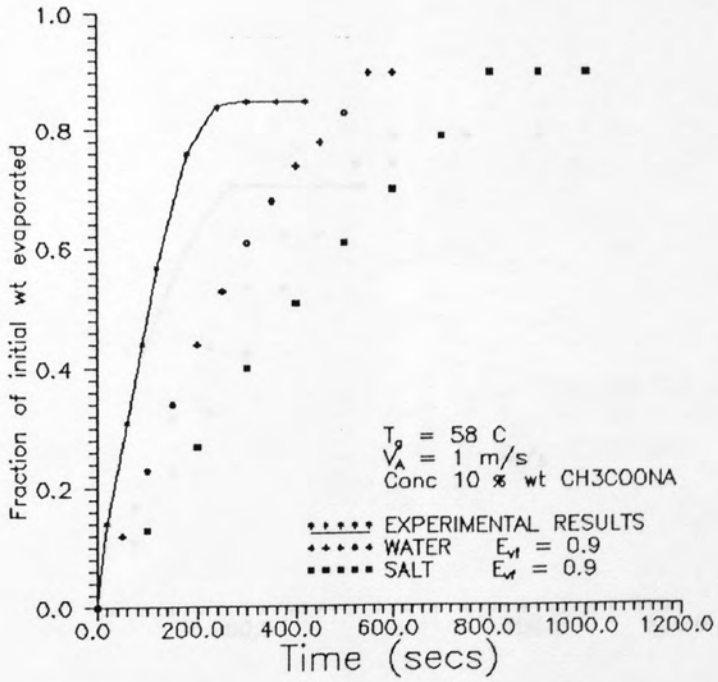

Figure 7.32 A Comparision of Model Predictions and Experimental Results for the Weight History of Aqueous Sodium Acetate (10 % wt/wt, T_g = 58.0 C)

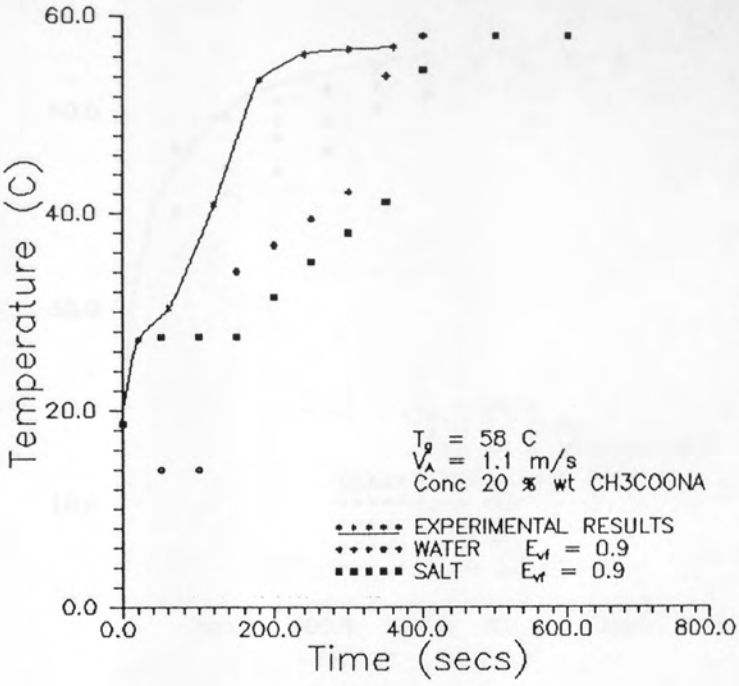

Figure 7.33 A Comparision of Model Predictions and Experimental Results for the Core Temperature History of Aqueous Sodium Acetate (20 % wt/wt, T_g = 58.0 C)

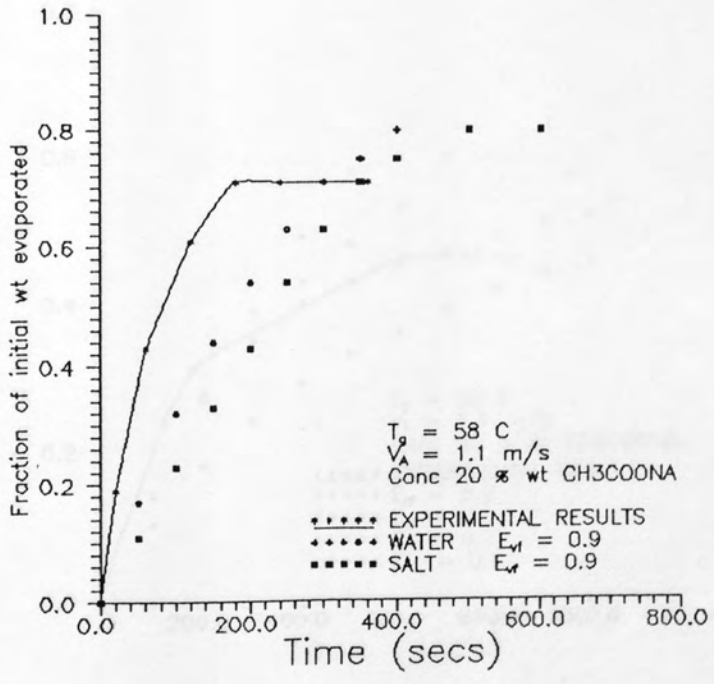

Figure 7.34 A Comparision of Model Predictions and Experimental Results for the Weight History of Aqueous Sodium Acetate (20 % wt/wt, T_g = 58.0 C)

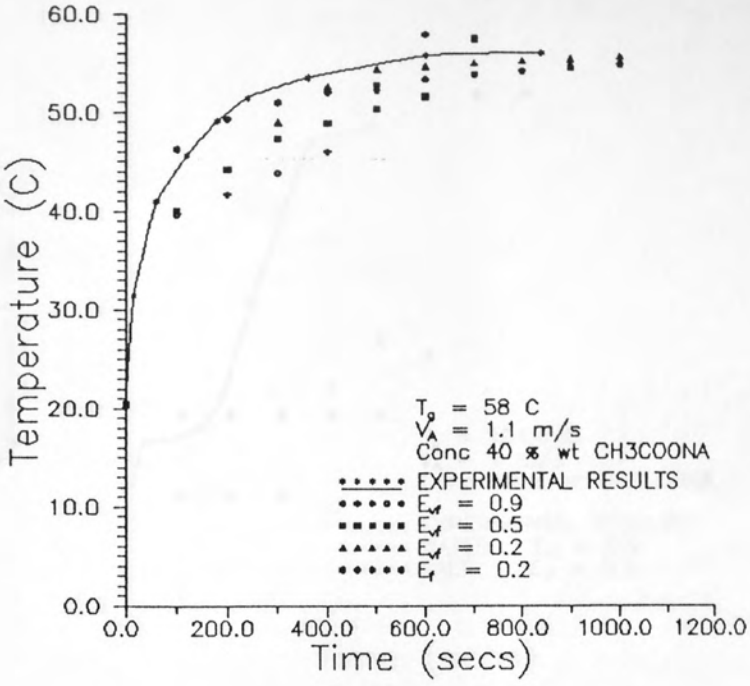

Figure 7.35 A Comparision of Model Predictions and Experimental Results for the Core Temperature History of Aqueous Sodium Acetate (40 % wt/wt, T_g = 58.0 C)

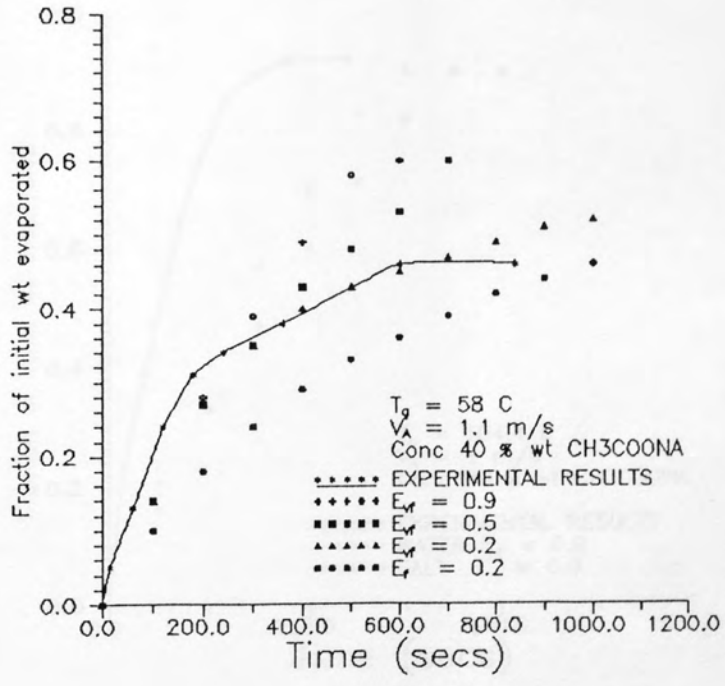

Figure 7.36 A Comparision of Model Predictions and Experimental Results for the Weight History of Aqueous Sodium Acetate (40 % wt/wt, T_g = 58.0 C)

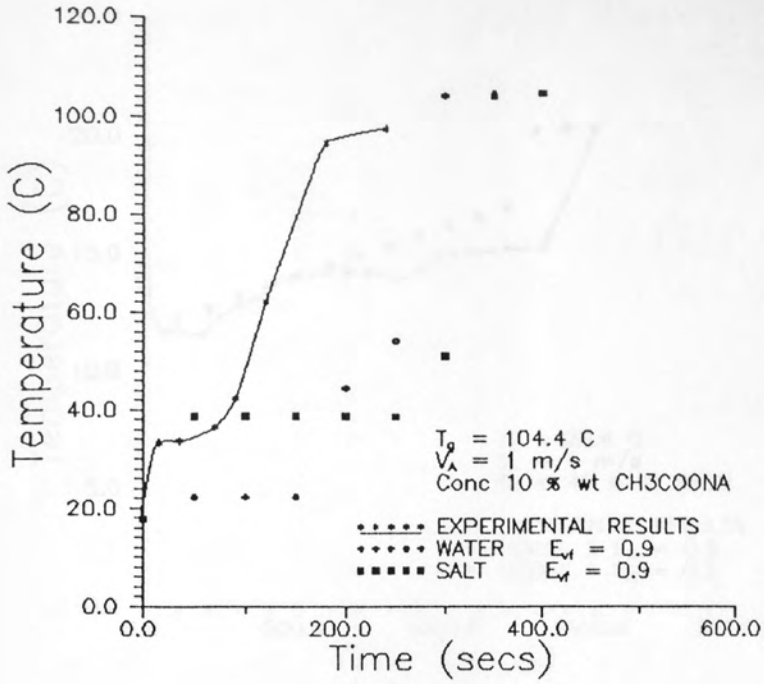

Figure 7.37 A Comparision of Model Predictions and Experimental Results for the Core Temperature History of Aqueous Sodium Acetate (10 % wt/wt, T_g = 104.4 C)

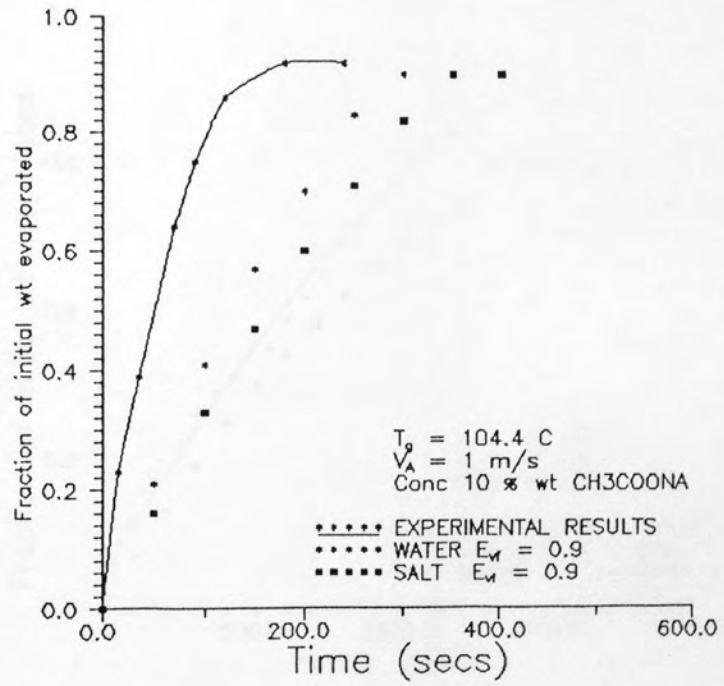

Figure 7.38 A Comparision of Model Predictions and Experimental Results for the Weight History of Aqueous Sodium Acetate (10 % wt/wt, T_g = 104.4 C)

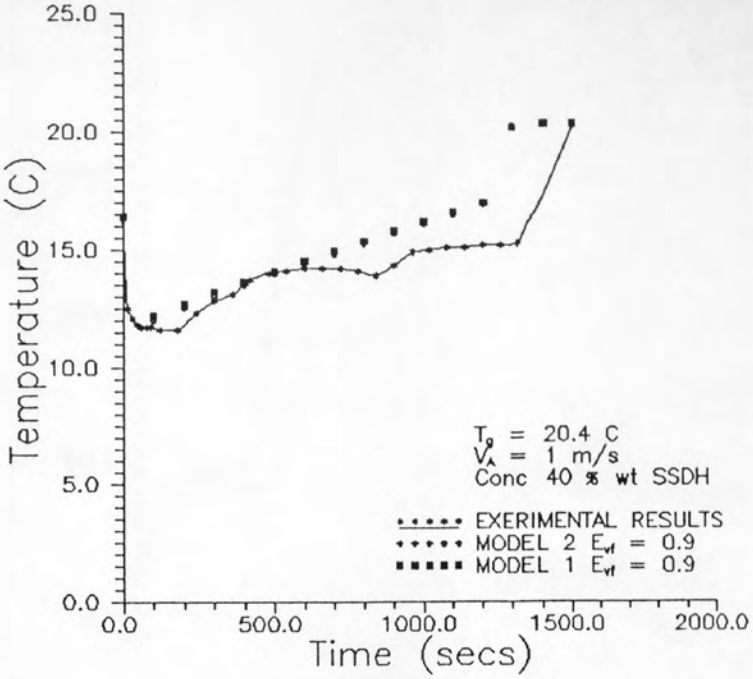

Figure 7.39 A Comparision of the Predicted Core Temperature Histories from Model 1 and Model 2 for Aqueous Sodium Sulphate Decahydrate (40 % wt/wt,T_g=20.4 C)

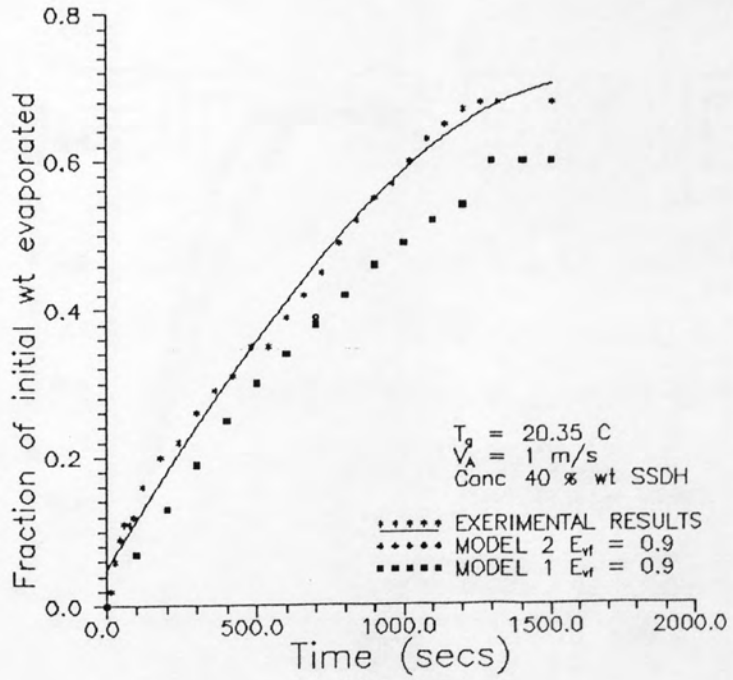

Figure 7.40 A Comparision of the Predicted Weight Histories from Model 1 and Model 2 for Aqueous Sodium Sulphate Decahydrate (40 % wt/wt,T_g=20.4 C)

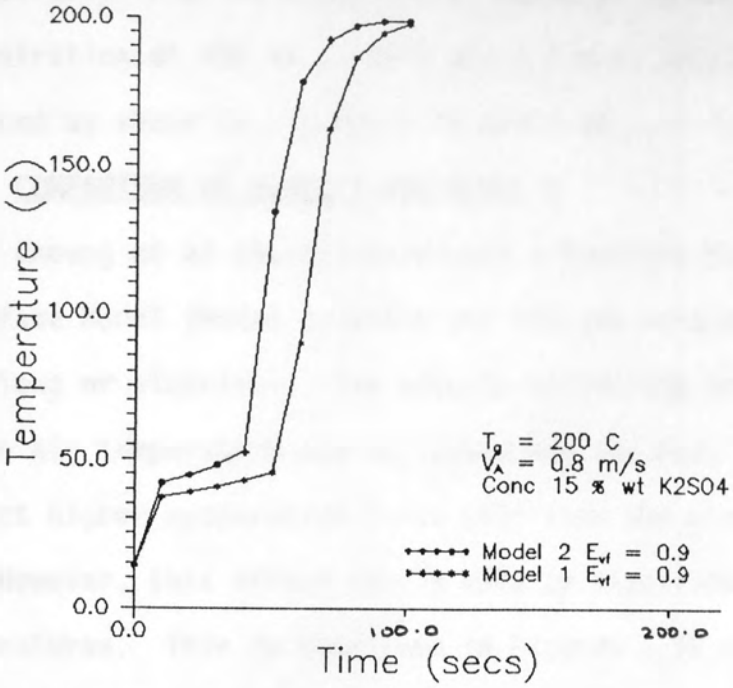

Figure 7.41 A Comparision of the Predicted Core Temperature Histories from Model 1 and Model 2 for Aqueous Potassium Sulphate (15 % wt/wt,T_g=200 C)

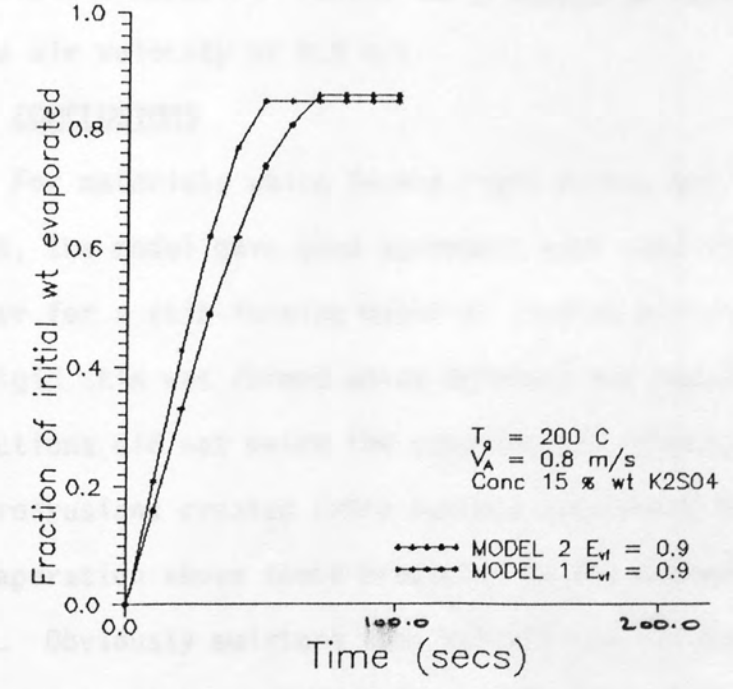

Figure 7.42 A Comparision of the Predicted Weight Histories from Model 1 and Model 2 for Aqueous Potassium Sulphate (15 % wt/wt,T_g=200 C)

considerably from the experimental results. However at the higher concentration of 40% wt at 58° C and 1.1 m/s, very good agreement was obtained as shown in Figures 7.35 and 7.36.

7.6 COMPARISON OF MODEL 1 AND MODEL 2

Cheong et al (4,112) developed a Receding Evaporation Interface Model (Model 1) which was limited to drops of saturated solutions or slurries . The effects of heating the diffusing vapour to the air temperature was neglected and the model would therefore predict higher evaporation rates (61) than the present model (Model 2). However, this effect should only be significant at high air temperatures. This is confirmed in Figures 7.39 and 7.40 for a sodium sulphate decahydrate drop of 40% weight concentration at 20.35° C and 1 m/s. There is little difference between the results predicted by Models 1 and 2. However at high air temperatures the difference is more marked as shown in Figures 7.41 and 7.42 which represents theoretical curves for a potassium sulphate drop at 200° C and an air velocity of 0.8 m/s.

7.7 CONCLUSIONS

For materials which formed rigid porous and low porosity crusts, the model gave good agreement with experimental results. However for a skin-forming material (sodium acetate) where a non-rigid skin was formed which deformed and ruptured the model predictions did not match the experimental results. In this case, the protrusions created extra surface area which enhances the rates of evaporation above those predicted by the assumption of a rigid crust. Obviously moisture loss was also assisted by splitting since there was an additional route for diffusion. However at the higher concentrations, the model accurately predicted the experimental results with the skin representing a similar resistance to diffusion as a rigid crust.

In comparison to Model 1, the present model covers both the constant rate period and the falling rate period. The effects of heating the diffusing vapour to the air temperature have been accounted for, although this only has a significant effect at high air temperatures. The model has been shown to be applicable to materials which form rigid crusts but cannot predict the drying behaviour of skin-forming materials under conditions where there is a deviation from the assumption of a rigid outer surface.

CHAPTER EIGHT

DISCUSSION

DISCUSSION

8.0 EXPERIMENTAL TECHNIQUES

Studies on the evaporation of single droplets of pure liquids, and the drying of single droplets of solutions and slurries, have been carried out in order to gain a fundamental insight into the heat and mass transfer effects occurring inside a spray drier. The main differences in the techniques have been in the types of devices used for suspending single droplets. Carefully designed wind tunnels were used to supply air at a constant humidity and temperature to the suspended drop. Other novel techniques have included drops suspended in free-flight and in an ultrasonic field.

8.1 SUSPENSION DEVICES

Capillaries and nozzles have been used to study the evaporation of pure liquid drops. Rates of evaporation were determined by measuring the rate of supply of liquid to keep a constant drop diameter. Filaments have also been used, with the rate of evaporation being measured by the change in drop diameter. Techniques involving the continuous feeding of liquid cannot be used with a drop containing solids once a rigid crust forms on the surface of the drop. The technique of suspending the drop on the end of a filament was the most common for these studies. Drop weights were measured by measuring the deflection of the filaments. However the majority of drop temperature studies were made by inserting thermocouples into the centre of drops or suspending drops on thermocouples. This involved the use of separate heat and mass transfer studies. This is not ideal because, by its very nature, the drying of drops is a simultaneous heat and mass transfer process.

Trommelen and Crosby (71) used a glass filament and attached a thermocouple to its surface to measure simultaneously the drop's temperature and weight history. Cheong (4) developed this technique to design a glass filament-thermocouple as a single unit. A 50 μm nickel wire was inserted into a 0.2 mm glass filament of 25 cm length. One end of the filament was heated gently to give a 45° bend and a 0.5 mm length of nickel wire left exposed at this end. The end was sealed and the whole filament coated with a layer of copper by a vacuum deposition technique. A junction was thereby created upon which a single drop could be suspended. The junction extended into the drop and measured the drops inner temperature. However for drops of 1-1.5 mm in diameter the junction would be immersed in 33-50% of the drops cross-section and would not necessarily measure the drops core temperature but rather an average drop temperature. In the present study a 0.1 mm junction was used. From the temperature histories shown in Chapter 6, it is clear that the core temperature of the drop has been measured. If an average temperature had been measured, or the junction had been exposed to the air, the temperatures measured would have risen rapidly to the air temperature.

Cheong (4) constructed the filament-thermocouple by inserting a 50 μm nickel wire into a 0.2 mm filament by hand. This technique was also initially copied in this work. However a considerable amount of time was required to construct one filament. A novel technique was therefore developed. As described in section 4.3, a 50 μm constantan wire was drawn through a filament at the same time as the filament was made. This was done by encasing the wire in one end of a 2 cm, 12.7 mm soda-lime glass tube. The tube was then heated until the glass began to 'flow' and then rapidly stretched

apart drawing the wire through the filament. By varying the rate at which the tube was stretched, filaments of a desired diameter and length could be made. This ease of manufacture was required since, because of their fragile nature, filaments could be easily broken. Even taking extreme care when placing drops on the tip of the filament, moving the filament in and out of the wind tunnel and removing the final dried crust from the tip did not always prevent breakage.

Cheong (4) used copper-nickel as the material for the thermocouple. In the present study, a copper-constantan or type T thermocouple was designed. A comparison of the mV outputs of the two types of filament-thermocouple, (Figure 4.1) shows that the type T thermocouple is more sensitive to changes in drop temperature having a larger mV output per °C than the copper-nickel thermocouple. The type T filament-thermocouple also compared favourably with the output of a standard type T thermocouple as shown in Table 4.1. The method of manufacture enabled thermocouples to be manufactured to give good reproducibility in their outputs as shown in Figures 5.2 and 5.3.

Cheong (4) used a protractor located at the rear of the filament-thermocouple to visually observe the deflection of the filament. In the present study a cathetometer was used to focus in on a mark located 6 cm from the point of drop suspension. During the course of drying, the position of this mark was monitored continuously using an eye piece and its position noted relative to a vertical scale on the sliding frame of the cathetometer. Unlike the mV outputs, the deflection of each thermocouple was a unique feature which varied from thermocouple to thermocouple. Each thermocouple was different in its application and the size of drops it could

suspend. In practise for drops of 1-2.5 mm in diameter, filament-thermocouples of 0.1-0.2 mm OD were used. However very fine (<0.1 mm) or larger (up to 0.5 mm) thermocouples were made. The advantages of very fine filaments are that drops smaller than 1 mm could be used. The heat conduction through the filament is minimised and the filament would be more sensitive to changes in drop weight. In the present study, very fine filaments were found to fluctuate occasionally when placed in the wind tunnel and therefore could not be relied upon to give an accurate weight reading. However the filaments designed could provide an alternative to the nozzles used in the experimental apparatus of Audu (5) and Ali (7) in which relatively large (>2 mm) stainless steel nozzles were used to suspend hemispherical drops in a horizontal wind-tunnel. The major disadvantage of this technique was that the nozzle precluded direct measurements of drop weight or temperature and, due to its material of construction, conducted more heat into the drop than the glass filament-thermocouple.

Each filament-thermocouple was calibrated individually by attaching threads of different weights to the tip. Figure 5.1 shows a calibration graph of a filament-thermocouple. From this a linear relationship between weight and deflection was found. This was repeated for all the filament-thermocouples used in this study. A full list of the calibrations are given in the computer program EXPT1.FOR in Appendix C.1.

Since the suspension device was located inside a vertical wind tunnel, there was a displacement in its position as a result of the buoyancy effects of the upward flowing air. This can be related to the drag force exerted on the drop and filament located in the

tunnel. Section 5.1.4 describes the calculation of these forces. In addition any suspension device used would be expected to act as a heat source into the very core of the drop. It is therefore erroneous to neglect this heat transfer term. In addition, the drop also receives heat by radiation which has to be taken into account. Ideally heat conduction via the suspension device should be minimised by using materials of low thermal conductivity and minimising the surface area of the device in contact with the drop. The filaments used in this study, were in contact with only a small proportion of the drops area. For a 2 mm, drop where the filament extended into the core of the drop, it was in contact with 6% of the drops surface area. This compares favourably with the nozzles used by Audu (5) and Ali (7), where a 2 mm nozzle would be in contact with 33% of a hemispherical drop's surface area. Equation 3.84 was derived to take into account the heat conducted by the filament and by radiation in addition to the heat convected to the drop. Appendix B7 lists the magnitude of these terms. As shown in Table 6.1, over a temperature range of 18-100°C, the heat conducted by the filament was 7.4-9.3%, by radiation 2.8-5.8% and by convection 85.3-89.3%. Clearly the heat conducted and radiated has to be taken into account; for example at air temperatures (>100°C), it would represent a significant proportion of the total heat transferred.

A check on the corrections to the drop weight caused by the buoyancy effects of the air stream, heat conducted by the filament, and radiation to the drop was made by;

i) Measuring the deflection of the filament whilst inside the wind tunnel with the final crust suspended on the tip.

ii) Taking account of the buoyancy effects and the additional heat transfer effects to give a predicted weight.

iii) Taking the filament + dried crust outside the wind tunnel and measuring the deflection. This gave the actual final weight.

A comparison could therefore be made between the final predicted weight and the final weight measured. As shown in Table 5.2, good agreement between the two weights was obtained.

The advantages of the glass filament-thermocouple are,

i) Flexibility in size

ii) Reliability of manufacture

iii) Minimal heat conduction

iv) Simultaneous drop weight and temperature measurements.

The major disadvantage is that a drop drying on the tip of the filament encases the tip as it dries. Complete crusts are not therefore recoverable and a study of the particle morphology cannot be made.

8.2 THE WIND TUNNEL

The purpose of a wind tunnel is to supply air at a constant humidity and temperature to the working section, where the suspended drop resides. Different types of wind tunnel have been used previously, ie horizontal wind tunnels (5,7), vertical wind tunnels (10,4) and tunnels specially designed to keep a drop suspended in free flight (6).

In a horizontal wind tunnel, the suspended drop would be displaced slightly in the direction of the air flow. In addition, the suspension device used would disturb the flow patterns around the drop.

In a vertical wind tunnel, the suspension device resides in the wake of the drop where it is least likely to disturb the flow.

The air flow patterns around the drop are also more likely to represent the flow patterns around a drop in free flight.

By careful design, with the use of specially shaped wire gauzes, an air velocity profile can be created which consists of a region of high velocity at the sides of a vertical wind tunnel, with a lower velocity in the middle. A single drop can then be suspended in free flight ie, with no attached devices. This eliminates problems associated with a suspended drop and heat conduction into the drop via the suspension device. However, at present, these techniques do not give a direct measurement of the drop weight or temperature which limits their usefulness. Some researchers have tested novel techniques, such as use of an ultrasonic field (8). Although they allow free rotation these introduce droplet circulation and oscillation leading to different heat and mass transfer coefficients.

A vertical wind tunnel was therefore used in this study. An experimental rig was also designed and built incorporating a 101 mm diameter tower. Experiments with pure water drops confirmed the design's validity.

As stated previously, the purpose of a wind tunnel is to supply air at a constant humidity and temperature and under conditions where the velocity profile across the tower is constant. To achieve this, a drier packed with desiccant was placed prior to the wind tunnel. The humidity in the tower was measured in two ways, by means of a hygrometer as described in section 5.1.3 and by measurement of the wet and dry bulb temperatures. The wet-bulb temperature was measured by covering the junction of a type K thermocouple with a thin paper tissue saturated with distilled water and inserting it into the working section of the wind tunnel. Prior

to experiments, the desiccant was regenerated by passing hot air at 200° C over it.

The humidity in the tower was measured regularly and at ambient temperature was found to be 0.29 g water vapour/kg dry air with this value not deviating by more than 1%. Garner (125) states that in a good wind-tunnel turbulence is regular and uniform in its characteristics, and consists of a uniformly distributed eddying motion, with eddies of very small amplitude in which the components in different directions have the same average magnitude and in which there is no correlation between the components in different directions. This was achieved here by packing the pipework prior to the wind tunnel with wire mesh and steel wool, to ensure an even velocity profile across the working section. A flat velocity profile measured at ambient temperature is shown in Figure 4.6.

8.3 DROPS OF AQUEOUS SOLUTIONS AND SLURRIES

Drop core temperature and weight histories were measured using the filament-thermocouple. The weight history was represented in two ways; as a fraction of initial weight evaporated (This was used to be consistent with previous investigators (4,10) and also to smooth out any slight variations in the drops initial weight) and, as drying rate curves. These enabled different drying periods such as the "constant-rate" and the "falling-rate" to be determined.

8.3.1 Sodium Sulphate Decahydrate

At low air temperatures (20.4° C) and for high concentrations (40% w/w), as shown in Figure 6.6, an initial constant rate period was observed. Although upon contact with the air stream, a crust began to form on the surface of the drop, evaporation was from a free liquid surface with moisture migration from within the drop maintaining a moisture saturated surface. As the crust thickened, its resistance to mass transfer grew and a saturated surface could

no longer be maintained. The evaporation front receded and the drying rate fell. This was also reflected in the core temperature history, ie the drop temperature initially fell to the wet-bulb temperature before rising slowly to the air temperature. At the higher air temperatures (Figures 6.7 and 6.8), a very interesting phenomena was observed in both the temperature and rate histories. After establishment of a drying rate, the rate for a 15% weight concentration and 40% weight concentration drop proceeded to fall. This was accompanied by a rise in the core temperature. When the temperature reached 33° C, there was a sharp decrease and subsequent increase in the core temperature. This was accompanied by a simultaneous increase in the drying rate, before the rate proceeded to fall again. This behaviour was due to the fact that above 33° C, the decahydrate is unusual in that it forms different hydrates with incongruent melting points (96). Below the transition temperature of 32.4° C, the monoclinic decahydrate crystals are in equilibrium with the liquid phase. At the transition temperature, the rhombic crystal of anhydrous sulphate commence to separate. The enantiomorphic changes occurring at 33° C, release 0.51 kg water per kg decahydrate into the core. This extra water dilutes the core's concentration leading to a larger mass transfer driving force and a subsequent increase in the mass transfer rates. If no extra water were released, the fraction of initial weight evaporated curves for a drop of 40% weight concentration would have a final value of 0.6. However from Figure 6.5, for a drop of 40% weight concentration at 54.7° C air temperature, the final value was 0.78. At higher air temperatures (74° C), the above phenomena was not observed, as shown in Figure 6.9. Here the higher temperature driving forces re-establish equilibrium quickly and a large decrease in the core temperature was not measured.

The above results on sodium sulphate decahydrate demonstrate the sensitivity of the filament-thermocouple. Ali (7) studied the history of a sodium sulphate decahydrate drop, suspended on a nozzle by inserting a thermocouple into the drop. As shown in Figure 2.8 no decrease in the core temperature was observed at 33°C.

8.3.2 Drops of Aqueous Sodium Chloride, Potassium Sulphate, Copper Sulphate and Sodium Acetate

A suspended drop of sodium chloride was found to dry at a constant rate prior to the falling rate period. From Figures 6.15 and 6.16, the drop core temperature also stayed at the wet-bulb temperature before rising to the air temperature. This behaviour was confirmed by electron micrographs of the final dried crust. As is evident from Plates 6.4 to 6.6, the final dried crust consisted of an open crystalline structure. The gas phase resistance was found to be significant with a variation in the air velocity having a marked effect on the drying history as shown in Figures 6.13 and 6.14.

No significant constant rate period was observed with potassium sulphate drops. For drops of 5-15% initial weight concentration, upon establishment of a drying rate, the rate proceeded to fall. In comparison to sodium chloride, the air velocity did not have a significant effect on the drying rate (Figure 6.20). This was also noted with copper sulphate. For this material, the micrographs of the final dried crust highlighted a smooth inner and outer surface with numerous fine fractures. This was in comparison to the rougher, more porous nature of the crusts of the other materials. If the formation of these fractures had been a dominant mass transfer effect, a sudden increase in the drying rate would have been noted. However this was not found.

Even at relatively low air temperatures (20.9°C) these fractures occurred. This suggests that they were not due to the effect of any internal pressure but arose from the nature of the material itself. Fractures and blowholes are often found with spray dried materials which have been subjected to high air temperatures (220-300°C). Therefore an interesting study would be to observe the particle morphologies of different materials as a function of air temperature.

Results with sodium acetate confirmed the formation of a skin prior to a crust. At the low concentrations (10-20% wt), the skin was found to be non-rigid, resulting in protrusions on the surface and a splitting of the skin. However at the high concentrations (40% wt) a rigid crust was formed. For this material skin formation appears to be a function of the initial concentration.

8.3.3 Effects of Solute Concentration on the Vapour Pressure

The relative lowering of the vapour pressure of a saturated solution to that of pure water, is shown in Figure 6.2 for each of the materials studied. Only sodium chloride and sodium acetate have a significant effect, and would therefore be expected to affect the drying history. The effects of a lowering of the vapour pressure is to reduce the partial pressure driving force for mass transfer resulting in a higher wet-bulb temperature than predicted for pure water, and lower drying rates.

The above effects are shown in Figures 6.1, 6.17, and 6.26. For materials which do not lower the vapour pressure, the rates were similar, prior to crust formation.

For sodium chloride, there was a significant difference in the initial drying rates as shown in Figure 6.10. This was also observed in the core temperature history. From Appendix B.2,

(Experiments D40 and D47), for a 5% wt drop, the wet-bulb temperature was 16.3° C and for a 20% wt drop 20° C. For sodium acetate no significant differences were found in the initial drying rates for 10-30% wt drops as shown in Figure 6.48.

8.4 MATHEMATICAL MODEL PREDICTIONS VERSUS EXPERIMENTAL RESULTS

A mathematical model based on a receding evaporation interface was used to model the drying histories of the materials studied. The model predictions were compared with experimental results. As described in section 7.0, the model requires the following inputs,

i) Initial drop weight
ii) Initial drop temperature
iii) Air velocity
iv) Air temperature
v) Air humidity
vi) Drop porosity

Except for the porosity, all of the above were determined experimentally. Audu and Jeffreys (86) have shown that the porosity of a drop is related to the crust mass transfer coefficient by

$$k_c \alpha E^{1.5} \qquad 8.1$$

A high porosity is representative of a crust with a low resistance to mass transfer. Audu and Jeffreys (86) related the porosity to the specific surface area of the pores in the drop by a modified Kozeny equation 8.2.

$$E \alpha \left(\frac{S_b^2 \beta}{\Delta P}\right)^{0.33} \qquad 8.2$$

Where S_b = specific surface area of the pores
β = crust thickness
ΔP = pressure drop across the crust.

However the pressure drop across the crust is required. The apparatus used to measure this (7) requires a whole hemi-spherical crust. The nature of the filament-thermocouple, with the final crust encasing the tip, did not facilitate recovery of intact crusts. No experimental crust porosities were therefore measured. This is an obvious disadvantage of the technique. For a study of particle morphology, a different type of suspension device such as a modified version of Audu's nozzles (5) is required.

An empirical correlation derived by Cheong et al (112,4) was used for modelling purposes. This relates the crust porosity to a dimensionless crust thickness by;

$$E = 1 - 2.4 \frac{\beta}{R} \qquad 8.3$$

In addition to a variable porosity predicted by equation 8.3, fixed porosities were also used. A variable porosity predicts lower initial core temperatures and subsequently higher evaporation rates than a fixed porosity.

For sodium sulphate decahydrate, the drop in temperature at 33° C was modelled as;

$$\Delta T = \frac{\Delta H}{W C p_d} \qquad 8.4$$

Where ΔT = Drop in temperature
ΔH = Mass decahydrate x L_f
L_f = Latent heat of fusion
W = Mass of the drop
Cp_d = Specific heat capacity of the drop

An assumed crust porosity of 0.9 fitted the experimental results best. Use of the vapour pressure of the saturated solution in the

constant rate period calculation instead of the vapour pressure of water, had little effect on the predicted results. Allowing for the changes occurring at 33° C, the model gave good agreement with experimental results for air temperatures >33° C and <33° C.

For sodium chloride, an assumed crust porosity of 0.9 fitted the experimental results best. However the model over predicts the core temperature due to the nature of the crust. The crust was very porous, so that the temperature was maintained at the wet-bulb beyond the point at which a crust had formed on the drop surface.

For potassium sulphate, the experimental results in the constant rate were best modelled using the vapour pressure of water. Once a crust had formed, an assumed porosity of 0.9 gave good agreement with experimental results.

For copper sulphate, assumed porosities in the range 0.2-0.5 gave good agreement with experimental results. The predicted core temperature history fitted well with experimental results. However the actual drying rates decreased rapidly towards the end of drying. This suggests that the final dried crust is of a low porosity which was confirmed by the electron micrographs (Plates 6.7-6.12). It is interesting to note that the model gave good agreement with experimental results for copper sulphate, for which the final dried crust consisted of a number of fine fractures. This suggests that their formation was not the dominant mass transfer effect.

For sodium acetate, the model did not match the experimental results at low concentrations (10-20% wt). At these concentrations a deviation from the assumption of a rigid crust by the formation of a non-rigid skin was noted. Generation of a surface area, greater than that of a sphere, by the formation of protrusions on the surface of the drop leads to higher heat and mass transfer rates

than predicted by the model. However at the higher concentrations (40% wt), the material behaved like a rigid material and the model predictions fitted the experimental results well.

The model has been shown to be applicable to materials which form rigid crusts. In its present state, it cannot predict the drying histories of materials which form skins, nor predict the formation of fractures or blowholes in the drops surface. However if the formation of these is not the dominant mass transfer effect, as shown by the results for copper sulphate, the model would be expected to give good agreement with experimental results.

8.5 WATER DROPLET EXPERIMENTS

The evaporation of pure liquids has been studied extensively. The majority of research has confirmed the correlations proposed by Ranz and Marshall (3).

$$Nu = 2 + \emptyset Re^{0.5} Pr^{0.33} \qquad 8.5$$

$$Sh = 2 + \emptyset Re^{0.5} Sc^{0.33} \qquad 8.6$$

Where $\emptyset$ = 0.6, with the only variation being in the value of $\emptyset$.

A 101 mm wind tunnel was designed and tested using pure water drops. At ambient temperature, the value of $\emptyset$ was 0.71, which is in good agreement with published data, 0.69, Rowe et al (59), 0.63, Miura et al (85). This agreement confirmed the reliability of the present design of wind tunnel and drop suspension technique.

Over the range of air temperatures studied (17-107°C), $\emptyset$ was found to vary with temperature. This has been observed by a number of investigators (4,6,7,65). It has been accounted for by the fact that some of the heat transferred from the drying medium is taken up by the outward diffusing vapour. Spalding (63) has shown that this

effect can be accounted for by the dimensionless transfer number B. The transfer number also approximates for inaccuracies in assuming constant film properties since it includes the temperature driving force and heat capacity. This has been used by a number of investigators to account for the effects of temperature on ø:

$$Nu = \frac{MN}{B} \ln (1 + B) [2 + 0.6\ Re^{0.5} Pr^{0.33}] \qquad 8.7$$

$$Nu = 2 + 0.19\ (1/B)^{0.24} Re^{0.5} Pr^{0.33} \qquad 8.8$$

$$Nu = 2 + 0.23\ (1/B)^{0.2} Re^{0.5} Pr^{0.33} \qquad 8.9$$

ø was therefore plotted against B as shown in Figure 6.49. A linear relationship was obtained (Equation 6.4) and taking this into account the resulting correlation was,

$$Nu = 2 + (-12.96B + 0.76) Re^{0.5} Pr^{0.33} \qquad 8.10$$

8.6 APPLICABILITY OF SINGLE DROPLET DRYING STUDIES

Spray drying is a complex process involving the atomisation of a liquid feed, its breakdown into a spray of drops, spray-air contacting patterns and then droplet drying. Each of these has been studied as a separate area of research and the results of the individual studies brought together in mathematical models which describe the whole drying process. Single drop drying has provided a valuable tool for the investigation of the heat and mass transfer effects. It is however disadvantaged by the fact that the drops studied are at least an order of magnitude larger (1-5 mm) than sprayed droplets (10-1000 μm). However relatively large drops have to be studied in order to determine accurate drying histories and also to allow for visual observations of the drying process. A review of the literature has highlighted the lack of published data

relating to the drying of drops containing solids. The majority of studies have concentrated on the less complex case of evaporation of pure liquid drops. Single droplet drying studies, however, represent the only method of determining the heat and mass transfer effects that may occur in a spray drier. The inherent assumption is therefore that studies on larger sized drops can be directly related to the heat and mass transfer processes occurring in a spray drier. This can only be justified if the rate controlling factors are the same. For the constant-rate period, where diffusion through the gas-film around the drop represents the resistance to mass transfer, studies have shown that the correlations derived by Ranz and Marshall are applicable to small drops (53). However once a crust forms, it represents an additional, and major, resistance to the heat and mass transfer process. The nature of this crust depends on the material used and has been shown to be a function of the drying conditions (ie, concentration, air temperature, air velocity). If conditions for single drop studies and those encountered in a spray drier are identical, the applicability of single drop studies is related to the assumption that following crust formation the particle morphology is independent of the particle size. Particle morphology studies have been very limited (127). No studies have been encountered which directly compare the morphologies of particles found in spray driers and those produced in laboratory equipment. A need therefore exists for this to be investigated. In conjunction with heat and mass transfer studies of single suspended drops, this would provide valuable information on the drying process and directly relate it to industrial spray driers.

However single drop work has provided valuable information on the drying process. The correlations proposed by Ranz and Marshall (3) have been verified by many workers over the past 35 years. Another important advantage of this method has been the ability to observe the behaviour of the drop as it dries and record it photographically. This advantage, in itself, is often worth more than the quantitative data obtained. By such observations of the drying of drops of whole milk and coffee (127), it was at once apparent why it is feasible to spray dry coffee from large drops but not feasible to dry large drops of milk. The latter develops a viscous and impermeable skin which greatly retards the evaporation rate. Conversely coffee, although it formed a skin exhibited a highly fluid and mobile condition during evaporation which appeared not to hinder the drying rate. In the present study, work on coffee drops (76) using the experimental apparatus of Audu (5) and visually studying the nature of the drop formed, confirmed the above hypothesis. In addition it was observed that a critical air temperature (138-154°C) existed where a film of low porosity was formed which impeded vapour diffusion out of the drop. At higher air temperatures (220°C) the drop underwent severe deformation during drying. This work provided valuable information for an industrial spray drier.

The receding evaporation interface model is only applicable to materials which form rigid crusts. Materials which form rigid skins can also be modelled. The model was also applicable to a material which formed fractures on the surface, as long as their formation was not the rate determining step. However the model was not applicable to materials forming non-rigid skins.

In industrial spray driers, unusual structures such as mushroom caps and spheres within spheres have been found. The model cannot be used to predict such phenomena. Indeed no model has been developed in the literature which can predict these structures. In addition materials which form cracks or blowholes as a result of an internal build-up of pressure with a sudden release of vapour cannot be described by the existing model.

Interestingly the receding evaporation interface model has been used as part of an overall model (110) to predict the performance of an industrial spray drier for skimmed milk drops. As noted previously skimmed milk forms an impervious rigid skin which can be modelled by the receding evaporation interface model. Good agreement was obtained between predicted and experimental humidity and temperature profiles and the moisture content of the final product.

CHAPTER NINE

CONCLUSIONS AND RECOMMENDATIONS

CONCLUSIONS AND RECOMMENDATIONS

9.1 CONCLUSIONS

1) A novel technique has been developed for the manufacture of a copper-constantan glass filament-thermocouple suspension device. Thermocouples of a desired size (0.1-0.2 mm diameter) and length (30-55 cm) could be made to support drops of 1-2.5 mm diameter. The tip of the thermocouple was designed to extend into the centre of a single suspended drop and measure the core temperature.

The amount of heat conducted through the filament was minimised by using glass and accounted for 9.3% of the total heat transferred to a drop at an air temperature of 100° C.

2) Simultaneous heat and mass transfer studies have been carried out on solutions/slurries of a number of materials. Air temperatures of 20° C to 124° C, 0.5-1.4 m/s air velocities and initial solution concentrations between 5% weight to 40% weight were used. The nature of the final dried crust was determined using a Scanning Electron Microscope.

For single drops of sodium sulphate decahydrate solution, the filament-thermocouple successfully detected the drop in core temperature and increase in drying rate as a result of the enantiomorphic changes occurring at 33° C. This is in contrast to previous studies (5,7) which have failed to detect the above phenomena.

The drying history of a material was dependent on the nature of the crust formed. Solutions of porous materials such as sodium sulphate decahydrate and sodium chloride dried at an initial constant rate. The rate then fell as the crust formed, grew in thickness, and its resistance to mass transfer increased.

For solutions of low-porosity materials such as copper sulphate, at the higher concentrations, no constant rate period was observed. After establishment of a drying rate, the rate proceeded to fall.

For a skin-forming material, sodium acetate solution, no constant rate period was observed for 10-40% wt initial concentrations. At the low concentrations, 10-20% wt, a non-rigid skin formed on the drop surface. At the higher concentrations a rigid skin/crust was formed.

3) A mathematical model has been developed for the drying of drops, covering both the constant and falling rate periods. The model was based on the assumption of a receding evaporation interface, and a rigid outer crust. Good agreement between experimental and model predictions for core temperature and drop weight histories was obtained for materials forming rigid porous and rigid non-porous crusts. The model could not predict the drying histories of drops forming skins.

4) An experimental rig incorporating a vertical wind tunnel was designed and commissioned using pure water drops. In line with a number of investigators (4,6,7,65), Ø the 'wind-factor' was found to be a function of temperature. Spaldings dimensionless transfer number B, was used to correlate the results. This took into account the heat transferred to the diffusing vapour by the hot air stream. The proposed correlation, equation 6.5 agreed with previously published correlations.

It is concluded that studies of single suspended drops can provide a valuable insight into the drying mechanisms for specific solutions or slurries, as a function of initial concentration and gas temperature, in spray driers. The ability to relate maximum

drop temperature (134) and the dried particle morphology to drying conditions is advantageous for materials subject to thermal degradation (135) or where a particular surface characteristic is desired in the particulate products (eg dyestuffs, detergents). Such studies also enable variations in bulk density and the effects of aeration to be investigated, and controls proposed. Hence, in addition to their fundamental value, they can save on the expense and time involved in pilot-scale drying trials.

9.2 RECOMMENDATIONS FOR FUTURE WORK

1) A comparison of the particle morphology of final crusts of single suspended drops and those dried under similar conditions in an industrial spray drier.

2) The effects of parameters such as air temperature, air velocity and initial concentration on the morphology of different crust forming and skin forming materials should be studied. A suspension device allowing recovery of an intact, final dried crust should be used. Experiments should be carried out in conjunction with experiments on drops dried using the filament-thermocouple so that the drying histories can be obtained.

3) The mathematical model should be extended to cover skin-forming materials and compared with experiments on such materials ie, coffee, skimmed milk.

4) Very fine thermocouples (<0.1 mm) should be used to study the drying history of drops smaller than 1 mm, to determine whether there are any size-related phenomena not detectable in the present study or those by Cheong (4), Audu (5) or Ali (7).

NOMENCLATURE

A	----	Surface area	m^2
A_c	----	Surface area of copper in contact with the drop	m^2
A_d	----	Projected surface area of the filament (Eq'n 5.3)	m^2
A_f	----	Surface area of the filament in contact with the drop (Eq'n 3.87)	m^2
A_m	----	Surface area for mass transfer	m^2
A_h	----	Surface area for heat transfer	m^2
A_w	----	Surface area of wire in contact with the drop	m^2
b	----	Distance between glass bead surface and water droplet surface	
B	----	Distance between two glass beads' surfaces in zig-zag type (Eq'n 2.64)	m
C	----	$p_w/(p_s-p_w)$	m
Cc	----	Heat of crystallisation per kg of water evaporated	J/kg
C_d	----	Drag coefficient on the drop	
C_f	----	Drag coefficient on the filament	
C_g	----	Concentration in the gas stream	kg/m^3
Cp	----	Heat capacity of air	J/kg/K
Cp_c	----	Heat capacity of the core	J/kg/K
Cp_d	----	Heat capacity of the drop	J/kg/K
Cp_s	----	Heat capacity of the salt	J/kg/K
Cp_w	----	Heat capacity of water	J/kg/K
C_R	----	Concentration at the point r=R	kg/m^3

C_s	----	Concentration at the drop's surface	kg/m^3
C_{sat}	----	Salt concentration at crystal formation	kg/m^3
C_{so}	----	Original salt concentration	kg/m^3
C_{wo}	----	Original water concentration	kg/m^3
C_X	----	Concentration at the point r=X	kg/m^3
C_∞	----	Concentration at an infinite distance	kg/m
D	----	Molecular diffusivity	m^2/s
D_{eff}	----	Effective diffusivity	m^2/s
d_f	----	Diameter of the filament	m
d_g	----	Diameter of the glass bead	m
d_p	----	Diameter of the particle	m
e	----	Emissivity of the drop	
e_g	----	Emissivity of the glass filament	
E	----	Porosity	
E_f	----	Fixed crust porosity	
E_{vf}	----	Variable crust porosity	
f	----	Tubulence factor	
F_A	----	Geometry factor	
F_d	----	Drag force on the drop	N
F_f	----	Drag force on the filament	N
F_t	----	Total drag force	N
g	----	Acceleration due to gravity	m^2/s
h_f	----	Heat transfer coefficient for the filament	$W/m^2/K$
h_g	----	Gas film heat transfer coefficient	$W/m^2/K$

H	----	Henry's constant	
k_A	----	Thermal conductivity of air	$W/m^2/K$
k_c	----	Crust mass transfer coefficient	m/s
k_{co}	----	Thermal conductivity of copper	W/m/K
k_{cr}	----	Thermal conductivity of the crust	W/m/K
k_f	----	Thermal conductivity of the glass filament	W/m/K
k_g	----	Gas film mass transfer coefficient	m/s
k_v	----	Thermal conductivity at film conditions	W/m/K
K_o	----	Overall mass transfer coefficient	m/s
k_w	----	Thermal conductivity of the constantan wire	W/m/K
L_f	----	Heat of solution	J/kg
L_v	----	Latent heat of vaporisation	J/kg
m	----	Mass flow rate	kg/s
M_w	----	Molecular weight of water	
N_A	----	Rate of evaporation	kg/s
N_{Ao}	----	Rate of evaporation in a stagnant medium	kg/s
N_{Ar}	----	Rate of evaporation at the point r	kg/s
N_{AR}	----	Rate of evaporation at the point r=R	kg/s
N_{AX}	----	Rate of evaporation at the point r=X	kg/s_3
p_A	----	Density of air	kg/m^3
p_c	----	Density of the crust	kg/m^3
p_d	----	Density of the drop	kg/m_3
p_s	----	Density of the salt	kg/m_3

ρ_{sol}	----	Density of the solution	kg/m^3
ρ_w	----	Density of water	kg/m^3
P	----	Gas pressure	atmos
ΔP	----	Pressure drop across the crust	mm Hg
P_c	----	Vapour pressure at the interface	atmos
P_g	----	Partial pressure of water vapour in the air	atmos
P_s	----	Vapour pressure at the drop's surface	atmos
q	----	Rate of heat transfer	W
Q_{co}	----	Heat conducted by the copper	W
Q_c	----	Conductive heat flux into the gas phase	W
Q_{conv}	----	Heat convected to the drop	W
Q_f	----	Heat conducted through the glass filament	W
Q_{fil}	----	Total heat conducted by the suspension device	W
Q_{gas}	----	Heat convected from the gas	W
$Q_{heat\ vapor}$	----	Heat consumed in heating diffusing vapour to the gas stream temperature	W
Q_{In}	----	Total heat transferred to the drop	W
Q_{Out}	----	Total heat transferred from the drop	W
Q_r	----	Heat transfer at the point r	W
Q_R	----	Heat transfer at the point r=R	W
Q_{rad}	----	Total heat radiated to the drop	W
Q_{sens}	----	Rate of change of sensible heat content of the core	W
Q_{vap}	----	Rate of heat lost by vaporisation	W

Q_W	----	Heat conducted by the constantan wire	W
Q_X	----	Heat transfer at the point r=X	W
r	----	Radius of the drop	m
r_1	----	Radius of an evaporating drop	m
r2	----	Outer radius of the gas film	m
r_o	----	Initial radius of the gas film	m
R	----	Outer radius of the crust	m
R_c	----	Universal gas constant	atm m^3/kgmole/K
S	----	Rate of production of fresh surface	s^{-1}
S_b	----	Specific surface area of the pores	m^{-1}
Solu	----	Solubility	
t	----	Time	s
T	----	Temperature	K
T_{amb}	----	Ambient temperature	K
T_c	----	Temperature of the core	K
T_d	----	Temperature of the drop	K
ΔT	----	Temperature driving force	K
T_g	----	Temperature of the gas stream	K
T_R	----	Temperature at the point r=R	K
T_s	----	Temperature at the surface of the drop	K
T_X	----	Temperature at the point r=X	K
t_c	----	Time to crust formation	s
V_A	----	Velocity of air	m/s
W	----	Weight of the drop	kg
X	----	Radius of the core	m
x_w	----	Mass fraction of water	
ΔZ	----	Size of element in equation 3.87	m

Dimensionless Groups

B	----	Transfer number	$Cp\,\Delta T/L_v$
B_f	----	Transfer number at film conditions	
Gr	----	Grashof number	$d_p^3 p_A^2 g\beta'\Delta T/\mu_A^2$
Nu	----	Nusselt number	$h_g d_p/k_A$
Nu_f	----	Nusselt number at film conditions	
Nu_o	----	Nusselt number under stagnant conditions	
Pr	----	Prandtl number	$Cp\mu_A/k_A$
Pr_f	----	Prandtl number at film conditions	
Re	----	Reynold's number	$d_p V_A p_A/\mu_A$
Re_f	----	Reynold's number for the glass filament	
Re_t	----	Reynold's number for the gas stream	
Sc	----	Schmidt number	$\mu_A D/p_A$
Sh	----	Sherwood number	$k_g d_p/D$
Sh_o	----	Sherwood number under stagnant conditions	

Greek Symbols

β	----	Crust thickness	m
β'	----	Coefficient of expansion	
ø	----	Wind factor in Frossling's equation	
σ_ϵ	----	Surface tension	
σ	----	Stefan Boltzmann constant	
μ_A	----	Viscosity of air	kg/m/s
μ_c	----	Viscosity of the continuous phase	kg/m/s
μ_d	----	Viscosity of the dispersed phase	kg/m/s
μ_{dr}	----	Viscosity of the drop	kg/m/s
μ_f	----	Viscosity at film conditions	kg/m/s

REFERENCES

1. Masters, K.,
"Spray Drying Handbook",
3rd ed., George Godwin Limited., London (1985).

2. Frossling, N.,
"On the Evaporation of Falling Drops",
Gerlands. Beitrage. Zur. Geophysic. Aere Harwell Translation.,
August 1963, 52, 170 (1978).

3. Ranz, W.E., Marshall, W.R.,
"Evaporation from Drops",
Chem. Eng. Prog., 48, 3, 141 (1952).

4. Cheong, H.W.,
"The Drying of Small Drops of Particulate Slurries",
PhD Thesis., Aston University (1983).

5. Audu,T.O.K.,
"Studies of the Drying of Particulate Slurries",
PhD Thesis., Aston University (1973).

6. Akbar, S.,
"The Drying of Drops in Free-Flight",
PhD Thesis., Aston University (1989).

7. Ali, H.H.,
"The Mechanisms of Drying of Single Droplets",
PhD Thesis., Aston University (1985).

8. Toei, R., Furuta, T.,
"Drying of a Droplet in a Non-supported State",
A.I.Ch.E. Symp. Series., 78, 218, 111 (1982).

9. Greenwald, G.C.,
"Particle Morphology in the Spray Drying of Foods",
PhD Thesis., University of California, Berkeley (1980).

10. Charlesworth, D., Marshall, W.R.,
"Evaporation from Drops Containing Dissolved Solids",
A.I.Ch.E. Journal., 6, 9 (1960).

11. Sano, Y., Keey, R.B.,
"The Drying of a Spherical Particle Containing Colloidal
Material into a Hollow Sphere",
Chem. Eng. Sci., 37, 6, 881 (1982).

12. Furuta, T., Okazaki, M., Toei, R.,
"Flavour Retention on Drying of a Single Droplet under Various
Drying Conditions",
Drying '85, Int'l. Drying. Symp., Kyoto, Japan (1985).

13. Whitman, W.G.,
Chem. Met. Eng., 29, 147, (1923).

14. Higbie, R.,
"The Rate of Absorption of a Pure Gas into a Still Liquid during Short Periods of Exposure",
Trans. Am. Inst. Chem. Eng., 31, 365 (1935).

15. Danckwerts, P.V.,
"Significance of Liquid Film Coefficients in Gas Absorption",
Ind. Eng. Chem., 43, 1460 (1951).

16. Toor, H.L., Marchello, J.M.,
"Film Penetration Model for Mass and Heat Transfer",
A.I.Ch.E. Journal., 4, 97, (1958).

17. Fick, A.,
Ann. Phys., 94, 59 (1855).

18. Maxwell, J.C.,
"Diffusion",
Collected Scientific Papers Cambridge., 11, 625 (1890).

19. Sreznevskii, V,.
Zh. R. Ph. Kh. O., 14, 420, 483 (1882).

20. Morse, H.W.,
"Evaporation from the Surface of a Solid Sphere",
Proc. Am. Acad. Sci., 45, 363 (1910).

21. Langmuir, I.,
"The Evaporation of Small Spheres",
Physics Review., 12, 368 (1918).

22. Whytlaw-Gray, R., Patterson, H.,
Smoke (Dym)., 149 (1934).

23. Topley, B., Whytlaw-Gray, R.,
"On the Rate of Evaporation of Small Spheres",
Phil. Mag., 4, 873 (1927).

24. Houghton, H.G.,
"A Study of the Evaporation of Small Water Drops",
Physics., 4, 419 (1933).

25. Langstroth, G.O., Diehl, C.H., Winhold, E.J.,
"The Evaporation of Droplets in Still Air ",
Can. J. Res., 28A, 580 (1950).

26. Mathers, W.G., Madden, A.J., Piret, E.L.,
"Simultaneous Heat and Mass Transfer in Free Convection ",
Ind. Eng. Chem., 49, 16, 961 (1957).

27. Steinberger, R.L., Treybal, R.E.,
"Mass Transfer from a Solid Soluble Sphere to a Flowing Liquid Stream",
A.I.Ch.E. Jurnal, 6, 227 (1960).

28. Frazier, G.C., Chang, H.W.,
"Droplet Vaporisation in Moderately High Temperature Stationary Media",
Can. I. Chem. Eng., 55, 736 (1977).

29. Hoffman, T.W., Gauvin, W.H.,
"Evaporation of Staionary Droplets in High Temperature Surroundings",
Can. J. Chem. Eng., 129 (1960).

30. Kobayashi, K.,
Trans. J. S. M. E., 20, 826 (1954).

31. Yuge, T.,
"Experiments on Heat Transfer from Spheres Including Combined Natural and Forced Convection",
Trans. A. S. M. E., 82, Series C, 214 (1960).

32. Majama, T,.
Bull. Inst. Phys. Chem. Res (Tokoyo)., 9, 339 (1930).

33. Vyrubov, D.N.,
"Droplet Thermal Emission and Evaporation",
Trans. J. Techn. Physics (USSR)., 9, 21, 1923 (1939).

34. Kinzer, G.D., Gunn, R.,
"The Evaporation, Temperature and Thermal Relaxation-Time of Freely Falling Water Drops",
J. Meteor., 81, 71 (1951).

35. Hsu, N.T., Sato, K., Sage, B.H.,
"Material Transfer in Turbulent Gas Streams",
Ind. Eng. Chem., 46, 870 (1954).

36. Maisel, D.S., Sherwood, T.K.,
"Evaporation of Liquids into Turbulent Gas Streams",
Chem. Eng. Prog., 46, 3, 131 (1950).

37. Garner, F.H., Grafton, R.W.,
"Mass Transfer in Fluid Flow from a Solid Sphere",
Proc. R. Soc., A224, 64 (1954).

38. Garner, F.H., Hoffman, J.M.,
"The Evaporation from Free to Forced Convection in Mass Transfer from Solid Spheres",
A.I.Ch.E. Journal., 6, 4, 581 (1960).

39. Garner, F.H., Suckling, R.D.,
"Mass Transfer from a Soluble Solid Sphere",
A.I.Ch.E. Journal., 4, 1, 114 (1958).

40. Acrivos, A.,
"Combined Laminar Free and Forced Convection Heat Transfer in External Flows",
A.I.Ch.E. Journal., 4, 285 (1958).

41. Evnochides, S., Thodos, G.,
"Simultaneous Mass and Heat Transfer in the Flow of Gases Past Single Spheres",
A.I.Ch.E. Journal., 7, 78 (1961).

42. Pasternak, I.S., Gauvin. W.H.,
"Turbulent Heat and Mass Transfer from Stationary Particles",
Can. J. Chem. Eng., 38, 35 (1960).

43. Pasternak, I.S., Gauvin, W.H.,
"Turbulent Convective Heat and Mass Transfer from Accelerating Particles",
A.I.Ch.E. Journal., 7, 254 (1961).

44. Fuchs, N.A.,
"Evaporation and Droplet Growth in Gaseous Media",
Pergammon Press., London (1959).

45. Bowman, C.W., Ward, D.M., Johnson, A.I., Trass, O.,
"Mass Transfer from Fluid and Solid Spheres at Low Reynolds Numbers",
Can. J. Chem. Eng., 39, 9 (1961).

46. Ward, D.M., Trass, O., Johnson , A.I.,
"Mass Transfer from Fluid and Solid Spheres at Low Reynolds Numbers - Part II",
Can. J. Chem. Eng., 40, 164 (1962).

47. Garner, F.H., Lane, J.J.,
"Mass Transfer to Drops of Liquid Suspended in a Gas Stream",
Trans. Inst. Chem. Engrs., 37, 162 (1959).

48. Pei, D.C.T., Narasimhan, C., Gauvin, W.H.,
"Evaporation from Drops and Particles in High Temperature Surroundings",
Proc. Symp. Interaction between Fluids and Particles,
Inst. Chem. Engrs (London)., 243 (1962).

49. Jones, S.J.R., Smith, W.,
"Mass Transfer from Solids Freely Suspended in an Air Stream",
Proc. Symp. Interaction between Fluids and Particles,
Inst. Chem. Engrs (London., 190 (1962).

50. Kinard, G.E., Manning, F.S., Manning, W.P.,
"A New Correlation for Mass Transfer from Single Spheres",
Brit. Chem. Eng., 8, 326 (1963).

51. Frazier, G.C.,
"Water Droplet Vapourisation in Humid Atmospheres",
Can. J. Chem. Engr., 55, 678 (1977).

52. Duguid, H.A., Stampfer, J.F. Jr.,
J. Atmos. Sci., 28, 1238 (1971).

53. Miura, K., Miura, T., Ohtani, S.,
"Heat and Mass Transfer to and from Droplets",
A.I.Ch.E. Symp. Ser., 73, 95 (1977).

54. Garner, F.H., Kendrick, P.,
"Mass Transfer to Drops of Liquid Suspended in a Gas Stream",
Trans. Inst. Chem. Engrs., 137, 155 (1959).

55. Sandoval-Robles, J.G., Riba, J.P., Conderc, J.P.,
"Mass Transfer around a Sphere",
Trans. Inst. Chem. Engrs., 58, 132 (1980).

56. Sandoval-Robles, J.G., Pelmas, H., Conderc. J.P.,
"Influence of Turbulence on Mass Transfer between a Liquid and a Solid Sphere",
A.I.Ch.E. Journal., 27, 819 (1981).

57. Kramers, H.,
Physica's. Frav., 12, 61 (1946).

58. Tsubouchi, T., Sato, S.,
"Heat Transfer between Single Particles and Fluids in Relative Forced Convection",
Chem. Eng. Prog. Symp. Ser., 56, 269, 285 (1960).

59. Rowe, P.N., Claxton, K.T., Lewis, J.B.,
"Heat and Mass Transfer from a Single Sphere in an Extensive Flowing Fluid",
Trans. Inst. Chem. Engrs., 43, T14-T31 (1965).

60. Ranz, W.E.,
"On the Evaporation of a Drop of Volatile Liquid in High-Temperature Surroundings",
Trans. A.S.M.E., 78, 909 (1956).

61. Marshall, W.R. Jr.,
"Heat and Mass Transfer in Spray Drying",
Trans. A.S.M.E., 77, 1377 (1955).

62. Godsave, G.A.E.,
Nat. Gas. Turb. Establish (England), Report, R66 (1950).

63. Spalding, D.B.,
4th Int. Symp. On Combustion., 847, Williams and Williams, Baltimore, Maryland (1953).

64. Pei, D.C.T., Gauvin, W.H.,
"Natural Convection Evaporation from Spherical Particles in High-Temperature Surroundings",
A.I.Ch.E. Journal., 9, 3, 375 (1963).

65. Downing, G.C.,
"The Evaporation of Drops of Pure Liquids at Elevated Temperatures: Rates of Evaporation and Wet-Bulb Temperatures",
A.I.Ch.E. Journal., 12, 4, 760 (1966).

66. Frazier, G.C. Jr., Hellier, W.W. Jr.,
"Vapourisation of Liquid Droplets in High Temperature Air Streams",
Ind. Eng. CHem. Fundam., 8, 807 (1969).

67. Crosby, E.J., Stewart, W.E.,
"Vapourisation of Droplets in High-Temperature Gas Streams",
Ind. Eng. Che. Fundam., 9, 3, 515 (1970).

68. Toei, R., Okazaki, M., Kubota, K., Ohaski, K., Mizata, K.,
Chem-Eng (Japan)., 30, 43 (1966).

69. Lee, K., Ryley, D.J.,
"The Evaporation of Water Droplets in Superheated Steam",
J. Heat. Transfer., 445 (1968).

70. Matlosz, R.L., Leipziger, S., Torda, T.P.,
"Investigation of Liquid Drop Evaporation in a High Temperature and High Pressure Environment",
Int. J. Heat and Mass Transfer., 15, 831 (1972).

71. Trommelen, A.M., Crosby, E.J.,
"Evaporation and Drying of Drops in Superheated Vapours",
A.I.Ch.E. Journal., 16, 5, 857 (1970).

72. Kadota, T., Hiroyasu, H.,
"Evaporation of a Single Droplet at Elevated Pressures and Temperatures",
Bull. J.S.M.E., 19, 138, 1515 (1976).

73. Hiroyasu, H.,
Trans. J.S.M.E., 40, 3147, (1974).

74. Yuen, M.C., Chen, L.W.,
"Heat Transfer Measurments of Evaporating Liquid Droplets",
Int. J. Heat and Mass Transfer., 21, 537-542 (1978).

75. Renkizbulut, M., Yuen, M.C.,
"Experimental Study of Droplet Evaporation in a High-Temperature Air Stream",
J. Heat. Transfer., 105, 384 (1983).

76. Bains, G.S.
Unpublished Work., Aston University (1986).

77. Sherwood, T.K.,
"The Air Drying of Solids",
Trans. Am. Inst. Chem. Engrs., 32, 150 (1936).

78. Sherwood, T.K.,
The Drying of Solids-II",
Ind. Eng. Chem., 13, 427 (1921).

80. Buckingham, E.,
U.S. Dept. Agr. Bur. Solids. Bull., 38 (1907).

81. Gurr, C.G., Marshall, T.J., Hutton, J.T.,
"Movement of Water in Soil due to a Temperature Gradient",
Soil Sci., 74, 5, 335 (1952).

82. Hutcheon, W.L.,
Highw. Res. Bd. Spec, Rep., 40, 113 (1958).

83. Kuzmak, J.M., Sereda, P.J.,
"The Mechanism by which Water Moves Through a Porous Material Subjected to a Temperatures Gradient",
Soil Sci., 84, 419 (1957).

84. Harmathy, T.Z.,
"Simultaneous Moisture and Heat Transfer in Porous Systems with Particular Reference to Drying",
Ind. Eng. Chem. Fund., 8, 92 (1969).

85. Miura, K., Atarashiya, K., Ouchi. I., Ohtani, S.,
"Experimental Study of Drying Characteristics of Single Drops Containing Solids",
Kagaku Kogaku, 35, 643 (1971) - Translation -
Heat. Transfer. Jap. Res., 1, 11 (1972).

86. Audu, T.O.K., Jeffreys, G.V.
"The Drying of Drops of Particulate Slurries",
Trans. Inst. Chem. Eng., 53, 165 (1975).

87. Chilton, T.H., Colburn, A.P.,
"Mass Transfer (Absorption) Coefficients",
Ind. Eng. Chem., 26, 1183 (1934).

88. Ali, H.H., Mumford, C.J., Jeffreys, G.V., Bains, G.S.,
"A Study of Evaporation from, and Drying of Single Droplets",
6th International Drying Symposium., IDS '88, Versailles, France (1988).

89. Duffie, J.A., Marshall, W.R. Jr.,
"Factors Influencing the Properties of Spray-Dried Materials",
Chem. Eng. Prog., 49, 417 (1953).

90. Van der Lijn, J.,
"Simulation of Heat and Mass Transfer in Spray Drying",
PhD Thesis., Agricultural Uinversity, Wageninsen, Netherlands (1976).

91. Wijlhuizen, A.E., Kerkhof, R.J.A.M., Bruin, S.,
"Theoretical Study of the Inactivation of Phosphatase during Spray Drying of Skim-Milk",
Chem. Eng. Sci., 34, 651 (1979).

92. Haertling, M.,
"Prediction of Drying Rates,
Drying 80., Vol 1, Hemisphere Publ. Corp., Ny (1980).

93. Esubiyi, A.O.,
"Drying of Portland Cement Raw Material Slurries",
PhD Thesis., Aston University (1980).

94. Coulson, J.M., Richardson, J.F.,
"Chemical Engineering"
Volume 2., Pergammon Press., Oxford (1968).

95. Sano, Y., Yamamoto, S.,
Proc. Third. Int. Drying. Symp., 1, 535 (1982).

96. Glasstone, S.,
"Text Book of Physical Chemistry",
1st ed., Macmillan Ltd., London (1940).

97. Nescic, S.,
"The Evaporation of Single Droplets - Experiments and Modelling",
6th International Drying Symposium., IDS' 88,
Versailles, France (1988).

98. Probert, R.P,
"The Influence of Spray Particle Size and Distribution in the Combustion of Oil Droplets",
Phil. Mag., 37, 94 (1964).

99. Rosin, P., Rammler, E.,
J. Inst. Fuel., 7, 29 (1933).

100. Fledderman, R.G., Hanson, A.R.,
Univ. Michigan Res. Dept., Cm 667 (1951).

101. Nukiyama, S., Tanasawa, Y.,
Trans. Soc. Mech. Eng (Japan)., 4, 86 (1937).

102. Dloughy. J., Gauvin, W.H.,
"Heat and Mass Transfer in Spray Drying",
A.I.Ch.E. Journal., 6, 1, 29 (1960).

103. Bose, A.K., Pei, D.C.T.,
"Evaporation Rates in Spray Drying",
Can. J. Chem. Eng., 259 91964).

104. Manning, W.P., Gauvin, W.H.,
"Heat and Mass Transfer to Decelerating Finely Atomised Sprays",
A.I.Ch.E. Journal., 6, 184 (1960).

105. Dickinson, D.R., Marshall, W.R. Jr.,
"The Rates of Evaporation of Sprays",
A.I.Ch.E. Journal., 14, 4, 541 (1968).

106. Baltas, L., Gauvin, W.H.,
"Performance Predictions for a Co-Current Spray Dryer",
A.I.Ch.E. Journal., 15, 5, 764 (1969).

107. Katta, S., Gauvin, W.H.,
"Some Fundamental Aspects of Spray Drying",
A.I.Ch.E. Journal., 21, 1, 143 (1975).

108. Miura, T., Ohtani, S., Maeda, S.,
"Drying 80",
Vol 1., Hemisphere Publ. Corp., N.Y. (1980).

109. Williams, G.C., Schmitt, R.O.,
"Humidity Measurements in Prescence of Water Soluble Salts",
Ind. Eng. Chem., 38, 967 (1940).

110. Sharma, S.,
Work to be published., Aston University (1990).

111. Wood, W.M.L.,
"Effect of Drying Parameters on Quality of Spray-Dried Products",
Talk given to Solids Drying Subject Group of Inst. Chem. Engrs., 7, Jan (1986).

112. Cheong, H.W., Jeffreys, G.V., Mumford, C.J.,
"A Receding Evaporation Interface Model for the Drying of Slurry Droplets",
A.I.Ch.E. Journal., 32, 81, 1334 (1986).

113. Blevins, R.D.,
"Applied Fluid Dynamics Handbook",
Van Rostrand Reinhold Co Inc., USA (1984).

114. Perry, R.H., Chilton, C.H.,
"Perry's Chemical Engineers Handbook",
5th Ed., McGraw-Hill Ltd., N.Y. (1973).

115. Woodland, D.J., Mack, E.,
"The Effect of Curvature of Surface on Surface Energy. Rate of Evaporation of Liquid Droplets. Thickness of Saturated Vapour Films",
J. Amer. Chem. Soc., 55, 3149 (1933).

116. Nestle, R.,
Physics., 77, 174 (1932).

117. Gudris, N., Kulikova, L.,
Z. Physik., 25, 121 (1924).

118. Abdul-Rahman, Y.A.K., Crosby, E.J., Bradley, R.L. Jr.,
J. Dairy. Sci., 54, 111 (1971).

119. Crosby, E.J., Weyl, R.W.,
"Foam Spray Drying: General Principles",
A.I.Ch.E. Symp. Ser., 73, 163, 82 (1977).

120. Furuta, T., Okazaki, M., Toei, R., Crosby, E.J.,
"Formation of Crystals on the Surface of Non-Supported Droplets in Drying",
Drying 82., 157-164, Hemisphere Publ., N.Y. (1983).

121. Greenwald, C.G., Judson King, C.,
"The Mechanism of Particle Expansion in Spray Drying of Foods",
A.I.Ch.E. Symp. Ser., 78, 218, 101 (1982).

122. Verhey, J.G.P.,
Netherlands Milk and Dairy J., 25, 246 (1971).

123. Alexander, K.,
"Factors Governing Surface Morphology in the Spray Drying of Food Materials",
PhD Thesis., Univ. California, Berkely (1983).

124. Gerald, C.F.,
"Applied Numerical Analysis",
3rd ed., Addison and Wesley Publ Corp., London (1984).

125. Garner, F.H., Lane, J.J.,
"Mass Transfer to Drops of Liquid Suspended in a Gas Stream",
Trans. Inst. Chem. Engrs., 37, 162 (1959).

126. Bains, G.S., Mumford, C.J., Jeffreys, G.V.,
"Mechanisms of Drying of Particulate Slurries",
Inst. Chem. Engrs. Research Meeting., Nottingham University (1987).

127. Judson King, C.,
"Control of Food-Quality Factors in Spray Drying",
4th Int. Drying. Symp., Kyoto, Japan, July 9-12 (1984).

128. International Critical Tables.,
Vol 3, 1st ed., McGraw-Hill Ltd., N.Y. (1933).

129. Kirk-Othmer Encyclopaedia of Chemical Technology.,
Vol 21, 248, 3rd ed., John Wiley and Sons., N.Y. (1983).

130. Rychley, R.,
"Heat of Crystallisation of some Substances in Aqueous Solutions",
Kristal. and. Technik., 10, 16, K91-K93 (1975).

131. International Critical Tables.,
Vol 4, 1st ed., McGraw-Hill Ltd., N.Y. (1933).

132. International Critical Tables.,
Vol 5, 1st ed., McGraw-Hill Ltd., N.Y. (1933).

133. Coulson. J.M., Richardson, J.F., Sinnot, R.K.,
"Chemical Engineering",
Vol 6, 1st ed., Pergamon Press, England (1983).

134. Walton, D.,
Unpublished Work., Aston University (1990).

135. Sayed, A.,
Unpublished Work., Aston University (1990).

APPENDIX A

PHYSICAL PROPERTIES

A.1 SODIUM SULPHATE DECAHYDRATE

A.2 SODIUM CHLORIDE

A.3 POTASSIUM SULPHATE

A.4 COPPER SULPHATE

A.5 SODIUM ACETATE

A.6 WATER

A.7 AIR

A.8 GLASS FILAMENT

A.1 SODIUM SULPHATE DECAHYDRATE

Core Density (129)	$1000x1464/(1000x(1-x_w)+1464x_w)$	kg/m^3
Heat of Crystallisation per kg Water Evaporated (130)	152	J/kg
Heat of Solution (130)	253	J/kg
Solubility (132)	$T_c<306.15$ K $Solu=0.292x10^{(0.0337(T_c-273.15))}$ $T_c>306.15$ K $Solu=3.7125x10^{(-0.001(T_c-237.15))}$	
Specific Heat Capacity of the Core (133)	3300	J/kg/k
Thermal Conductivity of the Crust	0.6	W/m/k
Vapour Pressure of the Saturated Solution (129)	$(\exp(-5104/T_c+20.207))/760$	atmos

A.2 SODIUM CHLORIDE

Core Density (129)	Subroutine Dens	
Heat of Crystallisation per kg Water Evaporated (131)	25.8	J/kg
Specific Heat Capacity of the Core (133)	$3880.061+0.6059T_c$	J/kg/k
Solubility (132)	$Solu=0.3548+2.474E-5(T_c-273.15)$ $+1E-6(T_c-273.15)^2$ $+2.65E-8(T_c273.15)^3$	
Thermal Conductivity of the Crust	$11.2142-0.0157T_c$	W/m/k
Vapour Pressure of the Solution (129)	Subroutine Press	
Vapour Pressure of the Saturated Solution (129)	$(\exp(20.387-5210.47/T_c))/760$	atmos

A.3 POTASSIUM SULPHATE

Core Density (129)	Subroutine Dens 1	
Heat of Crystallistion per kg of Water Evaporated (131)	116.95	J/kg
Specific Heat Capacity of the Core (133)	$4870-327.5xC1+33.75xC1^2-1.25C1^3$ where $C1=(1-x_w)x100$	J/kg/k
Solubility (132)	$Solu=0.4199+0.0114(T_c-237.15)$ $-1.807E-5(T_c-273.15)^2$	
Thermal Conductivity of the Crust	0.104	W/m/k
Vapour Pressure of the Solution (129)	Subroutine Press 1	
Vapour Pressure of the Saturated Solution (129)	$(\exp(20.515-5185.226/T_c))/760$	atmos

A4 COPPER SULPHATE

Core Density (129)	Subroutine Dens 2	
Heat of Crystallisation per kg of water evaporated (131)	116	J/kg
Specific Heat Capacity of the Core (133)	$4184.22-48.1576C1+0.400408C1^2$ $-1.47E-3C1^3$	J/kg/k
Solubility (132)	$Solu=0.865+3.09E-2(T_c-237.15)$ $-6.96E-5(T_c-273.15)^2$ $+1.48E-5(T_c-237.15)^3$ $-7.21E-8(T_c-273.15)^4$	
Thermal Conductivity of the Crust	0.4	W/m/k
Vapour Pressure of the Saturated Solution (129)	$(\exp(19.4297-4281.1/T_c))/760$	atmos

A.5 SODIUM ACETATE

Core Density (129)	Subroutine Dens 3	
Heat of Crystallisation per kg of Water Evaporated (131)	170	J/kg
Specific Heat Capacity of the Core (133)	$4188.47-36.2015C1+6.29E-1C1^2$ $-8.51E-3C1^3$	J/kg/k
Solubility (132)	$Solu=4.584+1.88E-2(T_c-273.15)$ $+1.6E-3(T_c-273.15)^2$	

Thermal Conductivity of the crust	0.42	
Vapour Pressure of the Saturated Solution (129)	$(\exp(20.767-5600/T_c))/760$	atmos

A.6 WATER

Latent Heat of Vapourisation	$L_V=2326(1075.95-1.025(T_d-273.15))$	J/kg
Diffusivity of Vapour in Air	$D=0.22\ [(T_g+T_d)/2/273.15]^{1.75}$x1E-4	m^2/s
Emissivity of the Drop	e = 0.955	
Partial Pressure (134)	exp (18.3036-3816.44/ $(T_c-46.13))/760$	atmos

A.7 AIR

Density	$P_A=1.2929(273.15/T_g)$	kg/m^3
Thermal Conductivity	$k_A=(4.296E-5((T_g-273.15)+(T_d-273.15))/2+0.014)x1.731$	W/m/k
Viscosity	$\mu_A=4.568E-8((T_g-273.15)+(T_d-273.15)/2)+1.72E-5$	kg/m/s
Specific Heat Capacity	$C_p=0.355T_g+922.203$	J/kg/k

A.8 GLASS FILAMENT

Thermal Conductivity	k_f = 0.6404	W/m/k
Emissivity of the Filament	e_f = 0.94	
Heat Transfer Coefficient of the Filament	$h_f=C_f Re_f^m P_r^{0.33} k/d_f$	$W/m^2/k$

Where C_f = 0.989, m=0.33 for Re_f <4

C_f = 0.911, m=0.385 for 4 <Re_f <40

C_f = 0.683, m=0.466 for Re_f >40

APPENDIX B

EXPERIMENTAL RESULTS

B.1 SODIUM SULPHATE DECAHYDRATE

B.2 SODIUM CHLORIDE

B.3 POTASSIUM SULPHATE

B.4 COPPER SULPHATE

B.5 SODIUM ACETATE

B.6 WATER

B.7 A COMPARISON OF THE DIFFERENT HEAT TRANSFER TERMS

APPENDIX B1 SODIUM SULPHATE DECAHYDRATE

EXPERIMENTAL RESULTS

EXPERIMENTAL REFERENCE		D2
SODIUM SUL DECAHYDRATE		40.0 WT %
AIR TEMP----------(C)	=	20.4
AIR VELOCITY----(M/S)	=	1.00
DROP REYNOLDS NUMBER	=	161.41
FILAMENT REYNOLDS NUMBER	=	13.36

TIME	MV	TEMP(C)	WT (MG)	WT CORRECTED (MG)	FRACTION EVAPORATED
.0	.45	16.41	8.76	8.76	.00
15.0	.28	12.47	8.18	8.54	.02
45.0	.25	11.82	7.60	7.96	.09
60.0	.24	11.71	7.43	7.79	.11
240.0	.27	12.27	6.44	6.81	.22
300.0	.29	12.76	6.16	6.52	.26
360.0	.31	13.12	5.87	6.23	.29
600.0	.35	14.19	5.00	5.36	.39
720.0	.35	14.19	4.42	4.78	.45
780.0	.35	14.08	4.13	4.50	.49
1020.0	.39	15.04	3.15	3.51	.60
1080.0	.40	15.11	2.92	3.28	.63
1260.0	.40	15.20	2.51	2.88	.67
1320.0	.40	15.27	2.40	2.76	.68

EXPERIMENTAL RESULTS

EXPERIMENTAL REFERENCE		D3
SODIUM SUL DECAHYDRATE		40.0 WT %
AIR TEMP----------(C)	=	31.00
AIR VELOCITY----(M/S)	=	1.00
DROP REYNOLDS NUMBER	=	157.46
FILAMENT REYNOLDS NUMBER	=	12.46

TIME	MV	TEMP(C)	WT (MG)	WT CORRECTED (MG)	FRACTION EVAPORATED
.0	.42	15.76	10.03	10.03	.00
15.0	.44	16.21	9.16	9.54	.05
45.0	.46	16.63	8.87	9.25	.08
60.0	.47	16.90	8.70	9.08	.10
120.0	.54	18.38	8.29	8.67	.14
180.0	.65	20.79	8.01	8.38	.16
300.0	.94	27.35	6.56	6.94	.31
360.0	1.01	28.85	6.39	6.76	.33
420.0	1.06	29.99	6.27	6.65	.34
540.0	1.11	31.02	5.69	6.07	.39
660.0	1.11	31.20	5.29	5.67	.44
780.0	1.15	32.11	5.29	5.67	.44
840.0	1.17	32.38	5.17	5.55	.45
960.0	1.17	32.40	4.83	5.20	.48

EXPERIMENTAL RESULTS
==========

EXPERIMENTAL REFERENCE		D4
SODIUM SUL DECAHYDRATE		40.0 WT %
AIR TEMP----------(C)	=	43.00
AIR VELOCITY----(M/S)	=	1.00
DROP REYNOLDS NUMBER	=	127.65
FILAMENT REYNOLDS NUMBER	=	11.70

TIME	MV	TEMP(C)	WT (MG)	WT CORRECTED (MG)	FRACTION EVAPORATED
.0	.47	16.68	6.44	6.44	.00
15.0	.59	19.47	5.58	5.90	.08
45.0	.63	20.41	5.00	5.32	.17
60.0	.64	20.70	4.71	5.03	.22
75.0	.66	21.02	4.42	4.74	.26
90.0	.70	21.93	4.30	4.63	.28
180.0	1.16	32.22	3.84	4.17	.35
195.0	1.19	32.96	3.78	4.11	.36
210.0	1.21	33.41	3.67	3.99	.38
225.0	1.23	33.88	3.67	3.99	.38
240.0	1.27	34.64	3.55	3.88	.40
255.0	1.35	36.54	3.44	3.76	.42
270.0	1.43	38.17	3.26	3.59	.44
300.0	1.47	39.20	3.26	3.59	.44
360.0	1.48	39.45	3.09	3.41	.47
480.0	1.50	39.90	2.51	2.84	.56
540.0	1.49	39.65	2.11	2.43	.62

EXPERIMENTAL RESULTS
==========

EXPERIMENTAL REFERENCE		D5
SODIUM SUL DECAHYDRATE		40.0 WT %
AIR TEMP----------(C)	=	54.70
AIR VELOCITY----(M/S)	=	1.00
DROP REYNOLDS NUMBER	=	141.86
FILAMENT REYNOLDS NUMBER	=	10.96

TIME	MV	TEMP(C)	WT (MG)	WT CORRECTED (MG)	FRACTION EVAPORATED
.0	.68	21.49	10.78	10.78	.00
15.0	.60	19.70	8.76	9.13	.15
30.0	.82	24.73	8.47	8.85	.18
45.0	.99	28.44	7.89	8.27	.23
60.0	1.05	29.79	7.77	8.15	.24
120.0	1.41	37.77	7.31	7.69	.29
240.0	1.41	37.73	5.46	5.84	.46
300.0	1.24	33.99	4.13	4.51	.58
360.0	1.16	32.29	3.55	3.93	.64
420.0	1.59	41.75	2.40	2.78	.74
480.0	2.00	51.02	2.11	2.49	.77
540.0	2.09	53.12	2.11	2.49	.77
660.0	2.10	53.27	2.11	2.49	.77

EXPERIMENTAL RESULTS
==========

EXPERIMENTAL REFERENCE		D7
SODIUM SUL DECAHYDRATE		40.0 WT %
AIR TEMP----------(C)	=	54.70
AIR VELOCITY----(M/S)	=	1.00
DROP REYNOLDS NUMBER	=	144.32
FILAMENT REYNOLDS NUMBER	=	11.25

TIME	MV	TEMP(C)	WT (MG)	WT CORRECTED (MG)	FRACTION EVAPORATED
.0	.49	17.30	10.49	10.49	.00
30.0	.82	24.55	8.76	9.13	.13
60.0	1.01	28.96	8.35	8.73	.17
120.0	1.14	31.69	7.60	7.98	.24
240.0	.93	26.97	5.87	6.24	.41
420.0	.86	25.42	2.69	3.06	.71
480.0	1.49	39.70	2.40	2.77	.74
540.0	1.55	41.46	2.22	2.60	.75
600.0	2.04	52.24	2.11	2.48	.76
660.0	2.10	53.30	2.11	2.48	.76
720.0	2.15	53.40	2.11	2.48	.76

EXPERIMENTAL RESULTS
==========

EXPERIMENTAL REFERENCE		D11
SODIUM SUL DECAHYDRATE		5.0 WT %
AIR TEMP----------(C)	=	68.00
AIR VELOCITY----(M/S)	=	1.00
DROP REYNOLDS NUMBER	=	76.36
FILAMENT REYNOLDS NUMBER	=	10.20

TIME	MV	TEMP(C)	WT (MG)	WT CORRECTED (MG)	FRACTION EVAPORATED
.0	.50	17.46	8.51	8.51	.00
30.0	1.01	28.78	6.43	6.77	.20
60.0	1.01	28.85	5.60	5.92	.30
120.0	1.03	29.34	4.36	4.66	.45
180.0	1.16	32.29	2.97	3.25	.62
240.0	1.54	40.68	1.93	2.18	.74
300.0	2.13	53.83	1.24	1.47	.83
360.0	2.42	60.50	.90	1.13	.87
420.0	2.29	57.57	.55	.78	.91
480.0	2.74	67.55	.21	.43	.95
540.0	2.73	67.39	.21	.43	.95
600.0	2.73	67.30	.21	.43	.95

EXPERIMENTAL RESULTS
==========

EXPERIMENTAL REFERENCE		D15
SODIUM SUL DECAHYDRATE		15.0 WT %
AIR TEMP----------(C)	=	74.00
AIR VELOCITY----(M/S)	=	1.00
DROP REYNOLDS NUMBER	=	96.86
FILAMENT REYNOLDS NUMBER	=	9.89

TIME	MV	TEMP(C)	WT (MG)	WT CORRECTED (MG)	FRACTION EVAPORATED
.0	.61	19.97	6.78	6.78	.00
30.0	1.12	31.28	5.39	5.71	.16
45.0	1.15	32.09	4.84	5.14	.24
60.0	1.18	32.67	4.36	4.65	.31
120.0	1.47	39.16	2.97	3.26	.52
180.0	1.60	42.16	2.14	2.43	.64
240.0	1.51	40.12	1.45	1.74	.74
300.0	2.99	73.14	.97	1.25	.82
360.0	3.00	73.38	.97	1.25	.82
420.0	3.00	73.38	.97	1.25	.82
480.0	3.00	73.38	.97	1.25	.82
540.0	3.00	73.30	.97	1.25	.82

EXPERIMENTAL RESULTS
==========

EXPERIMENTAL REFERENCE		D50
SODIUM SUL DECAHYDRATE		5.0 WT %
AIR TEMP----------(C)	=	45.10
AIR VELOCITY----(M/S)	=	0.90
DROP REYNOLDS NUMBER	=	52.89
FILAMENT REYNOLDS NUMBER	=	10.51

TIME	MV	TEMP(C)	WT (MG)	WT CORRECTED (MG)	FRACTION EVAPORATED
.0	.51	12.68	3.88	3.88	.00
20.0	.76	18.74	3.20	3.44	.11
60.0	.76	18.81	2.83	3.06	.21
120.0	.77	19.06	2.31	2.53	.35
180.0	.79	19.40	1.79	1.99	.49
240.0	.84	20.66	1.16	1.36	.65
300.0	1.01	24.82	.87	1.07	.72
360.0	1.40	34.38	.77	.95	.76
420.0	1.29	31.56	.61	.77	.80
480.0	1.39	34.04	.61	.76	.80
540.0	1.43	34.97	.61	.76	.80
600.0	1.72	41.95	.61	.76	.80
660.0	1.31	32.12	.51	.66	.83
720.0	1.32	32.32	.38	.53	.86
780.0	1.38	33.75	.38	.53	.86
840.0	1.37	33.63	.38	.53	.86

EXPERIMENTAL RESULTS
==========

EXPERIMENTAL REFERENCE D52
SODIUM SUL DECAHYDRATE 15.0 WT %
AIR TEMP----------(C) = 45.10
AIR VELOCITY----(M/S) = 0.90
DROP REYNOLDS NUMBER = 78.41
FILAMENT REYNOLDS NUMBER = 10.40

TIME	MV	TEMP(C)	WT (MG)	WT CORRECTED (MG)	FRACTION EVAPORATED
.0	.57	14.00	4.14	4.14	.00
15.0	.78	19.16	3.62	3.86	.07
60.0	.79	19.52	3.10	3.34	.19
120.0	.89	21.88	2.52	2.77	.33
180.0	1.20	29.40	2.15	2.40	.42
240.0	1.40	34.31	2.05	2.27	.45
300.0	1.24	30.49	2.05	2.25	.46
360.0	1.25	30.52	1.84	2.04	.51
420.0	1.14	27.99	1.63	1.83	.56
480.0	1.17	28.74	1.37	1.57	.62
540.0	1.15	28.23	1.03	1.23	.70
600.0	1.38	33.68	.69	.89	.79
660.0	1.73	42.27	.51	.71	.83
720.0	1.76	43.00	.51	.71	.83
780.0	1.76	43.17	.51	.71	.83

EXPERIMENTAL RESULTS
==========

EXPERIMENTAL REFERENCE D53
SODIUM SUL DECAHYDRATE 15.0 WT %
AIR TEMP----------(C) = 45.10
AIR VELOCITY----(M/S) = 0.90
DROP REYNOLDS NUMBER = 96.40
FILAMENT REYNOLDS NUMBER = 10.43

TIME	MV	TEMP(C)	WT (MG)	WT CORRECTED (MG)	FRACTION EVAPORATED
.0	.54	13.27	3.54	3.54	.00
20.0	.80	19.67	2.78	3.01	.15
60.0	.81	20.03	2.57	2.81	.21
120.0	1.00	24.58	2.10	2.34	.34
180.0	1.00	24.53	1.84	2.08	.41
240.0	.85	20.91	1.63	1.87	.47
420.0	.92	22.63	1.27	1.50	.58
480.0	.92	22.68	1.27	1.50	.58
600.0	1.15	28.23	1.00	1.24	.65
720.0	1.41	34.55	.79	1.03	.71
840.0	1.63	39.88	.40	.64	.82
900.0	1.69	41.39	.40	.64	.82

EXPERIMENTAL RESULTS

EXPERIMENTAL REFERENCE		D57
SODIUM SUL DECAHYDRATE		30.0 WT %
AIR TEMP----------(C)	=	49.7
AIR VELOCITY----(M/S)	=	0.90
DROP REYNOLDS NUMBER	=	127.81
FILAMENT REYNOLDS NUMBER	=	10.12

TIME	MV	TEMP(C)	WT (MG)	WT CORRECTED (MG)	FRACTION EVAPORATED
.0	.59	14.48	9.61	9.61	.00
15.0	.90	22.22	8.95	9.26	.04
40.0	1.12	27.55	8.72	9.03	.06
60.0	1.27	31.20	8.64	8.95	.07
120.0	1.80	43.99	7.78	8.09	.16
180.0	1.87	45.65	7.25	7.57	.21
240.0	1.81	44.29	6.70	7.02	.27
300.0	1.85	45.16	6.65	6.97	.27
360.0	1.86	45.53	6.63	6.94	.28
480.0	1.79	43.73	5.76	6.08	.37
540.0	1.87	45.77	5.01	5.32	.45
600.0	1.89	46.16	5.01	5.32	.45
660.0	1.89	46.26	4.82	5.14	.47
720.0	1.89	46.13	4.59	4.90	.49
780.0	1.90	46.35	4.59	4.90	.49
840.0	2.02	49.25	4.59	4.90	.49
900.0	2.01	49.03	4.59	4.90	.49

APPENDIX B2 SODIUM CHLORIDE

EXPERIMENTAL RESULTS

EXPERIMENTAL REFERENCE		D21
SODIUM CHLORIDE		40.0 WT %
AIR TEMP----------(C)	=	54.10
AIR VELOCITY----(M/S)	=	1.00
DROP REYNOLDS NUMBER	=	111.42
FILAMENT REYNOLDS NUMBER	=	10.97

TIME	MV	TEMP(C)	WT (MG)	WT CORRECTED (MG)	FRACTION EVAPORATED
.0	.60	17.28	5.81	5.81	.00
15.0	1.02	27.47	4.25	4.55	.22
30.0	1.04	27.98	3.73	4.03	.31
60.0	1.05	28.20	3.52	3.82	.34
120.0	1.09	29.11	2.69	2.98	.49
180.0	1.08	28.82	1.75	2.05	.65
240.0	2.12	53.95	.91	1.21	.79
300.0	2.13	54.04	.91	1.22	.79
360.0	2.13	53.97	.91	1.21	.79
400.0	2.13	54.09	.91	1.21	.79

EXPERIMENTAL RESULTS

EXPERIMENTAL REFERENCE		D23
SODIUM CHLORIDE		40.0 WT %
AIR TEMP----------(C)	=	66.30
AIR VELOCITY----(M/S)	=	1.00
DROP REYNOLDS NUMBER	=	103.16
FILAMENT REYNOLDS NUMBER	=	10.29

TIME	MV	TEMP(C)	WT (MG)	WT CORRECTED (MG)	FRACTION EVAPORATED
.0	.56	16.39	5.60	5.60	.00
15.0	1.17	30.99	2.69	2.97	.47
30.0	1.18	31.15	2.16	2.46	.56
45.0	1.18	31.37	1.96	2.25	.60
60.0	1.21	31.99	1.75	2.04	.64
90.0	1.36	35.46	1.23	1.52	.73
120.0	1.33	34.83	1.12	1.42	.75
150.0	1.41	36.73	1.12	1.41	.75
180.0	2.51	63.28	1.12	1.42	.75
240.0	2.64	66.33	1.12	1.42	.75
300.0	2.64	66.40	1.12	1.42	.75

EXPERIMENTAL RESULTS
==========

EXPERIMENTAL REFERENCE D25
SODIUM CHLORIDE 40.0 WT %
AIR TEMP----------(C) = 113.00
AIR VELOCITY----(M/S) = 1.00
DROP REYNOLDS NUMBER = 87.57
FILAMENT REYNOLDS NUMBER = 8.18

TIME	MV	TEMP(C)	WT (MG)	WT CORRECTED (MG)	FRACTION EVAPORATED
.0	.55	16.05	6.80	6.80	.00
15.0	1.58	40.82	4.31	4.60	.32
30.0	1.57	40.65	3.48	3.78	.44
60.0	1.53	39.76	1.82	2.12	.69
120.0	4.41	108.84	.00	.31	.96
180.0	4.54	111.99	.00	.31	.95
210.0	4.55	112.26	.00	.30	.96
240.0	4.57	112.64	.00	.30	.96

EXPERIMENTAL RESULTS
==========

EXPERIMENTAL REFERENCE D30
SODIUM CHLORIDE 20.0 WT %
AIR TEMP----------(C) = 22.90
AIR VELOCITY----(M/S) = 1.00
DROP REYNOLDS NUMBER = 102.50
FILAMENT REYNOLDS NUMBER = 13.12

TIME	MV	TEMP(C)	WT (MG)	WT CORRECTED (MG)	FRACTION EVAPORATED
.0	.52	13.81	2.30	2.30	.00
15.0	.38	10.37	1.65	1.90	.17
60.0	.38	10.50	1.37	1.62	.30
90.0	.39	10.62	1.18	1.43	.38
120.0	.39	10.76	1.00	1.25	.46
150.0	.42	11.30	.81	1.06	.54
180.0	.41	11.23	.62	.87	.62
210.0	.40	10.98	.44	.69	.70
240.0	.40	10.86	.34	.59	.74
270.0	.40	10.98	.25	.50	.78
300.0	.41	11.23	.16	.41	.82
375.0	.43	11.71	.00	.25	.89
420.0	.45	12.10	.00	.25	.89
480.0	.46	12.42	.00	.25	.89
540.0	.46	12.37	.00	.25	.89
600.0	.53	14.18	.00	.25	.89
660.0	.77	20.03	.00	.25	.89
720.0	.79	20.29	.00	.25	.89
780.0	.78	20.25	.00	.25	.89
840.0	.78	20.27	.00	.25	.89

EXPERIMENTAL RESULTS
==========

EXPERIMENTAL REFERENCE		D32
SODIUM CHLORIDE		20.0 WT %
AIR TEMP----------(C)	=	30.2
AIR VELOCITY----(M/S)	=	1.00
DROP REYNOLDS NUMBER	=	109.88
FILAMENT REYNOLDS NUMBER	=	12.56

TIME	MV	TEMP(C)	WT (MG)	WT CORRECTED (MG)	FRACTION EVAPORATED
.0	.53	14.05	3.23	3.23	.00
45.0	.48	12.84	1.65	1.92	.41
60.0	.49	12.98	1.37	1.64	.49
75.0	.50	13.23	1.18	1.45	.55
90.0	.50	13.37	1.09	1.36	.58
120.0	.51	13.71	.90	1.17	.64
135.0	.52	13.88	.81	1.08	.67
180.0	.55	14.49	.53	.80	.75
240.0	.58	15.25	.16	.43	.87
360.0	.63	16.49	.00	.27	.92
420.0	.71	18.51	.00	.27	.92
600.0	1.13	28.68	.00	.27	.92
660.0	1.13	28.78	.00	.27	.92
720.0	1.13	28.80	.00	.27	.92

EXPERIMENTAL RESULTS
==========

EXPERIMENTAL REFERENCE		D35
SODIUM CHLORIDE		20.0 WT %
AIR TEMP----------(C)	=	23.00
AIR VELOCITY----(M/S)	=	1.00
DROP REYNOLDS NUMBER	=	108.93
FILAMENT REYNOLDS NUMBER	=	13.08

TIME	MV	TEMP(C)	WT (MG)	WT CORRECTED (MG)	FRACTION EVAPORATED
.0	.70	18.46	3.70	3.70	.00
15.0	.49	12.99	3.34	3.62	.02
45.0	.49	13.09	2.90	3.17	.14
90.0	.50	13.27	2.80	3.06	.17
180.0	.52	13.94	2.35	2.61	.29
240.0	.53	14.25	2.11	2.38	.36
360.0	.54	14.43	1.72	1.98	.47
480.0	.53	14.07	1.34	1.61	.57
540.0	.53	14.10	1.22	1.48	.60
660.0	.54	14.30	.86	1.12	.70
780.0	.56	14.92	.77	1.03	.72
840.0	.60	15.89	.59	.85	.77
960.0	.67	17.79	.59	.85	.77
1020.0	.72	18.92	.59	.85	.77
1080.0	.78	20.54	.59	.85	.77
1200.0	.86	22.59	.59	.85	.77

EXPERIMENTAL RESULTS
==========

EXPERIMENTAL REFERENCE		D39
SODIUM CHLORIDE		20.0 WT %
AIR TEMP----------(C)	=	23.00
AIR VELOCITY----(M/S)	=	0.45
DROP REYNOLDS NUMBER	=	45.37
FILAMENT REYNOLDS NUMBER	=	5.88

TIME	MV	TEMP(C)	WT (MG)	WT CORRECTED (MG)	FRACTION EVAPORATED
.0	.69	18.18	2.90	2.93	.00
15.0	.55	14.71	2.86	2.93	.00
45.0	.56	14.84	2.85	2.93	.00
60.0	.56	15.02	2.81	2.88	.02
90.0	.58	15.33	2.75	2.82	.04
150.0	.60	15.87	2.64	2.71	.08
180.0	.60	15.84	2.60	2.67	.09
240.0	.59	15.58	2.46	2.53	.14
300.0	.60	15.89	2.39	2.46	.16
360.0	.62	16.53	2.29	2.36	.19
480.0	.73	19.15	2.17	2.24	.24
540.0	.79	20.69	2.14	2.21	.25
600.0	.84	22.08	2.09	2.16	.26
660.0	.85	22.44	2.09	2.16	.26
780.0	.87	22.82	2.06	2.13	.28
840.0	.87	22.90	2.06	2.13	.28
900.0	.87	22.95	2.06	2.13	.28

EXPERIMENTAL RESULTS
==========

EXPERIMENTAL REFERENCE		D40
SODIUM CHLORIDE		20.0 WT %
AIR TEMP----------(C)	=	33.30
AIR VELOCITY----(M/S)	=	0.50
DROP REYNOLDS NUMBER	=	56.26
FILAMENT REYNOLDS NUMBER	=	6.19

TIME	MV	TEMP(C)	WT (MG)	WT CORRECTED (MG)	FRACTION EVAPORATED
.0	.68	18.00	4.52	4.53	.00
20.0	.75	19.85	4.43	4.53	.00
45.0	.76	20.13	4.29	4.39	.03
75.0	.77	20.39	4.23	4.33	.04
90.0	.78	20.54	4.14	4.23	.07
120.0	.79	20.77	3.96	4.05	.11
180.0	.79	20.87	3.71	3.81	.16
240.0	.77	20.31	3.36	3.45	.24
390.0	.86	22.64	2.97	3.06	.32
420.0	.89	23.29	2.85	2.94	.35
480.0	1.02	26.73	2.71	2.80	.38
540.0	1.05	27.62	2.55	2.64	.42
600.0	1.10	28.88	2.55	2.64	.42

EXPERIMENTAL RESULTS
==========

EXPERIMENTAL REFERENCE D42
SODIUM CHLORIDE 20.0 WT %
AIR TEMP----------(C) = 31.00
AIR VELOCITY----(M/S) = 0.50
DROP REYNOLDS NUMBER = 54.59
FILAMENT REYNOLDS NUMBER = 6.24

TIME	MV	TEMP(C)	WT (MG)	WT CORRECTED (MG)	FRACTION EVAPORATED
.0	.68	17.95	4.26	4.26	.00
20.0	.71	18.90	4.10	4.20	.01
65.0	.73	19.38	3.92	4.02	.06
100.0	.75	19.85	3.77	3.86	.09
130.0	.77	20.28	3.58	3.68	.14
190.0	.79	20.90	3.20	3.29	.23
220.0	.79	20.92	3.03	3.11	.27
250.0	.79	20.92	2.85	2.94	.31
290.0	.78	20.67	2.77	2.85	.33
320.0	.78	20.49	2.56	2.65	.38
420.0	.76	20.15	2.13	2.21	.48
480.0	.77	20.26	1.89	1.98	.53
540.0	.79	20.72	1.71	1.79	.58
600.0	.85	22.39	1.54	1.62	.62
660.0	1.15	30.14	1.39	1.48	.65
720.0	1.20	31.35	1.39	1.48	.65

EXPERIMENTAL RESULTS
==========

EXPERIMENTAL REFERENCE D46
SODIUM CHLORIDE 5.0 WT %
AIR TEMP----------(C) = 38.80
AIR VELOCITY----(M/S) = 0.60
DROP REYNOLDS NUMBER = 43.43
FILAMENT REYNOLDS NUMBER = 7.21

TIME	MV	TEMP(C)	WT (MG)	WT CORRECTED (MG)	FRACTION EVAPORATED
.0	.52	12.88	5.42	5.80	.00
15.0	.66	16.21	5.66	5.80	.00
60.0	.67	16.50	5.14	5.28	.09
120.0	.67	16.43	4.35	4.49	.23
180.0	.66	16.38	3.78	3.91	.33
240.0	.66	16.31	3.31	3.43	.41
300.0	.66	16.28	2.86	2.98	.49
420.0	.67	16.46	2.13	2.24	.61
480.0	.68	16.75	1.81	1.92	.67
540.0	.73	18.04	1.47	1.57	.73
600.0	.73	17.87	1.29	1.38	.76
660.0	1.14	27.94	1.13	1.22	.79
780.0	1.27	31.22	1.08	1.17	.80
840.0	1.32	32.44	1.08	1.17	.80
900.0	1.38	33.75	1.08	1.17	.80

EXPERIMENTAL RESULTS

EXPERIMENTAL REFERENCE		D47
SODIUM CHLORIDE		5.0 WT %
AIR TEMP----------(C)	=	35.50
AIR VELOCITY----(M/S)	=	0.60
DROP REYNOLDS NUMBER	=	40.61
FILAMENT REYNOLDS NUMBER	=	7.19

TIME	MV	TEMP(C)	WT (MG)	WT CORRECTED (MG)	FRACTION EVAPORATED
.0	.53	13.22	4.64	4.64	.00
15.0	.69	16.89	4.40	4.54	.02
60.0	.69	17.01	4.04	4.17	.10
120.0	.69	17.06	3.54	3.67	.21
300.0	.70	17.23	2.15	2.26	.51
360.0	.71	17.43	1.71	1.81	.61
420.0	.75	18.45	1.37	1.47	.68
480.0	.76	18.74	1.13	1.23	.74
540.0	1.18	28.94	.90	.98	.79
600.0	1.39	34.09	.82	.90	.81
660.0	1.30	31.81	.82	.90	.81
720.0	1.41	34.43	.82	.90	.81
780.0	1.45	35.53	.82	.90	.81

APPENDIX B3 POTASSIUM SULPHATE

EXPERIMENTAL RESULTS

EXPERIMENTAL REFERENCE		D66
POT SULPHATE		15.0 WT %
AIR TEMP----------(C)	=	22.7
AIR VELOCITY----(M/S)	=	0.90
DROP REYNOLDS NUMBER	=	101.97
FILAMENT REYNOLDS NUMBER	=	11.81

TIME	MV	TEMP(C)	WT (MG)	WT CORRECTED (MG)	FRACTION EVAPORATED
.0	.50	12.44	2.76	2.76	.00
15.0	.39	9.64	1.80	2.03	.26
60.0	.40	9.69	1.50	1.73	.37
120.0	.40	9.77	1.35	1.58	.43
180.0	.40	9.80	1.12	1.34	.51
300.0	.40	9.87	.76	.98	.64
420.0	.40	9.67	.28	.51	.82
540.0	.43	10.60	.00	.23	.92
600.0	.84	20.90	.00	.23	.92
660.0	.84	20.90	.00	.23	.92
720.0	.84	20.87	.00	.23	.92

EXPERIMENTAL RESULTS

EXPERIMENTAL REFERENCE		D68
POT SULPHATE		15.0 WT %
AIR TEMP----------(C)	=	22.00
AIR VELOCITY----(M/S)	=	1.30
DROP REYNOLDS NUMBER	=	152.84
FILAMENT REYNOLDS NUMBER	=	17.11

TIME	MV	TEMP(C)	WT (MG)	WT CORRECTED (MG)	FRACTION EVAPORATED
.0	.50	12.42	3.06	3.06	.00
30.0	.40	9.82	1.71	2.14	.30
60.0	.40	9.87	1.30	1.73	.44
120.0	.41	10.10	.97	1.40	.54
190.0	.41	10.15	.70	1.13	.63
300.0	.42	10.20	.31	.74	.76
420.0	.41	10.07	.00	.43	.86
540.0	.47	11.46	.00	.43	.86
660.0	.85	21.20	.00	.43	.86
720.0	.85	21.20	.00	.43	.86

EXPERIMENTAL RESULTS
==========

EXPERIMENTAL REFERENCE D69
POT SULPHATE 15.0 WT %
AIR TEMP----------(C) = 22.00
AIR VELOCITY----(M/S) = 1.20
DROP REYNOLDS NUMBER = 155.28
FILAMENT REYNOLDS NUMBER = 17.11

TIME	MV	TEMP(C)	WT (MG)	WT CORRECTED (MG)	FRACTION EVAPORATED
.0	.51	12.47	3.21	3.21	.00
15.0	.40	9.90	1.74	2.18	.32
60.0	.41	9.97	1.59	2.03	.37
120.0	.41	10.07	1.24	1.67	.48
180.0	.41	10.17	1.00	1.43	.55
240.0	.41	10.17	.76	1.19	.63
300.0	.42	10.20	.40	.83	.74
420.0	.44	10.75	.00	.44	.86
540.0	.49	11.94	.00	.44	.86
600.0	.55	13.50	.00	.44	.86
660.0	.85	21.07	.00	.44	.86
720.0	.85	21.07	.00	.44	.86

EXPERIMENTAL RESULTS
==========

EXPERIMENTAL REFERENCE D72
POT SULPHATE 5.0 WT %
AIR TEMP----------(C) = 36.40
AIR VELOCITY----(M/S) = 1.20
DROP REYNOLDS NUMBER = 104.44
FILAMENT REYNOLDS NUMBER = 14.52

TIME	MV	TEMP(C)	WT (MG)	WT CORRECTED (MG)	FRACTION EVAPORATED
.0	.52	12.77	2.46	2.46	.00
12.0	.65	16.13	1.83	2.17	.12
120.0	.67	16.61	1.15	1.46	.41
180.0	.69	17.11	.85	1.16	.53
240.0	.73	18.17	.55	.86	.65
300.0	.84	20.80	.31	.62	.75
360.0	1.11	27.66	.13	.44	.82
420.0	1.31	32.73	.04	.36	.86
480.0	1.44	36.11	.04	.36	.86
540.0	1.44	36.14	.04	.36	.86

EXPERIMENTAL RESULTS

EXPERIMENTAL REFERENCE		D76
POT SULPHATE		10.0 WT %
AIR TEMP----------(C)	=	36.40
AIR VELOCITY----(M/S)	=	1.20
DROP REYNOLDS NUMBER	=	118.73
FILAMENT REYNOLDS NUMBER	=	14.57

TIME	MV	TEMP(C)	WT (MG)	WT CORRECTED (MG)	FRACTION EVAPORATED
.0	.53	13.18	2.43	2.43	.00
15.0	.66	16.33	1.77	2.12	.13
60.0	.66	16.36	1.50	1.85	.24
120.0	.69	17.11	1.03	1.37	.44
180.0	.82	20.44	.67	1.01	.58
240.0	1.14	28.47	.61	.95	.61
300.0	1.23	30.76	.49	.83	.66
360.0	1.27	31.87	.37	.71	.71
420.0	1.29	32.38	.28	.62	.74
540.0	1.32	32.96	.22	.56	.77
600.0	1.32	33.08	.10	.44	.82
660.0	1.33	33.23	.10	.44	.82

EXPERIMENTAL RESULTS

EXPERIMENTAL REFERENCE		D77
POT SULPHATE		10.0 WT %
AIR TEMP----------(C)	=	36.40
AIR VELOCITY----(M/S)	=	1.20
DROP REYNOLDS NUMBER	=	121.81
FILAMENT REYNOLDS NUMBER	=	14.54

TIME	MV	TEMP(C)	WT (MG)	WT CORRECTED (MG)	FRACTION EVAPORATED
.0	.52	12.85	2.64	2.64	.00
15.0	.64	15.88	2.01	2.36	.11
60.0	.65	16.08	1.74	2.09	.21
120.0	.66	16.28	1.38	1.74	.34
180.0	.66	16.36	1.00	1.35	.49
240.0	.67	16.48	.64	.99	.63
300.0	.70	17.26	.28	.63	.76
420.0	1.39	34.90	.00	.35	.87
480.0	1.39	34.90	.00	.35	.87
540.0	1.39	34.82	.00	.35	.87

EXPERIMENTAL RESULTS
==========

EXPERIMENTAL REFERENCE		D86
POT SULPHATE		15.0 WT %
AIR TEMP----------(C)	=	61.00
AIR VELOCITY----(M/S)	=	1.20
DROP REYNOLDS NUMBER	=	115.68
FILAMENT REYNOLDS NUMBER	=	12.69

TIME	MV	TEMP(C)	WT (MG)	WT CORRECTED (MG)	FRACTION EVAPORATED
.0	.50	12.48	3.25	3.25	.00
30.0	.98	24.70	1.93	2.29	.30
60.0	1.04	26.25	1.53	1.89	.42
120.0	1.70	42.95	.87	1.24	.62
240.0	2.00	50.47	.00	.37	.89
300.0	2.41	60.89	.00	.37	.89
360.0	2.41	60.91	.00	.37	.89
420.0	2.40	60.79	.00	.37	.89

EXPERIMENTAL RESULTS
==========

EXPERIMENTAL REFERENCE		D90
POT SULPHATE		5.0 WT %
AIR TEMP----------(C)	=	91.00
AIR VELOCITY----(M/S)	=	0.80
DROP REYNOLDS NUMBER	=	49.45
FILAMENT REYNOLDS NUMBER	=	7.27

TIME	MV	TEMP(C)	WT (MG)	WT CORRECTED (MG)	FRACTION EVAPORATED
.0	.58	14.39	2.56	2.56	.00
30.0	1.37	34.66	1.41	1.57	.39
60.0	1.45	36.52	.70	.84	.67
120.0	3.52	89.20	.01	.16	.94
180.0	3.58	90.62	.01	.16	.94
240.0	3.59	90.92	.01	.15	.94

EXPERIMENTAL RESULTS
==========

EXPERIMENTAL REFERENCE		D93
POT SULPHATE		10.0 WT %
AIR TEMP----------(C)	=	91.00
AIR VELOCITY----(M/S)	=	0.80
DROP REYNOLDS NUMBER	=	61.51
FILAMENT REYNOLDS NUMBER	=	7.32

TIME	MV	TEMP(C)	WT (MG)	WT CORRECTED (MG)	FRACTION EVAPORATED
.0	.57	14.18	2.68	2.68	.00
30.0	1.35	34.11	1.67	1.84	.31
60.0	1.33	33.57	.93	1.10	.59
120.0	2.03	51.36	.13	.30	.89
180.0	3.34	84.57	.00	.17	.94
240.0	3.33	84.39	.00	.17	.94

EXPERIMENTAL RESULTS
==========

EXPERIMENTAL REFERENCE		D94
POT SULPHATE		10.0 WT %
AIR TEMP----------(C)	=	91.00
AIR VELOCITY----(M/S)	=	0.80
DROP REYNOLDS NUMBER	=	62.61
FILAMENT REYNOLDS NUMBER	=	7.27

TIME	MV	TEMP(C)	WT (MG)	WT CORRECTED (MG)	FRACTION EVAPORATED
.0	.53	13.14	2.88	2.88	.00
30.0	1.28	32.22	1.62	1.79	.38
60.0	1.37	34.54	1.04	1.22	.58
120.0	1.85	46.71	.13	.30	.89
180.0	3.58	90.72	.07	.25	.91
240.0	3.60	91.13	.00	.18	.94
300.0	3.59	90.90	.00	.17	.94

EXPERIMENTAL RESULTS

EXPERIMENTAL REFERENCE		D98
POT SULPHATE		15.0 WT %
AIR TEMP----------(C)	=	91.00
AIR VELOCITY----(M/S)	=	0.80
DROP REYNOLDS NUMBER	=	63.91
FILAMENT REYNOLDS NUMBER	=	7.29

TIME	MV	TEMP(C)	WT (MG)	WT CORRECTED (MG)	FRACTION EVAPORATED
.0	.56	14.11	2.96	2.96	.00
30.0	1.33	33.60	2.07	2.25	.24
60.0	1.36	34.41	1.44	1.62	.45
120.0	1.73	43.61	.33	.51	.83
180.0	3.47	87.98	.13	.31	.90
240.0	3.47	87.98	.13	.31	.90

EXPERIMENTAL RESULTS

EXPERIMENTAL REFERENCE		D99
POT SULPHATE		15.0 WT %
AIR TEMP----------(C)	=	91.00
AIR VELOCITY----(M/S)	=	0.80
DROP REYNOLDS NUMBER	=	63.67
FILAMENT REYNOLDS NUMBER	=	7.28

TIME	MV	TEMP(C)	WT (MG)	WT CORRECTED (MG)	FRACTION EVAPORATED
.0	.56	14.03	2.93	2.93	.00
30.0	1.37	34.49	2.16	2.33	.21
60.0	1.42	35.96	1.33	1.51	.49
120.0	2.96	75.04	.30	.48	.84
180.0	3.51	88.94	.27	.45	.85
240.0	3.50	88.76	.27	.45	.85

APPENDIX B4 COPPER SULPHATE

EXPERIMENTAL RESULTS

EXPERIMENTAL REFERENCE		D104
COPPER SULPHATE		18.0 WT %
AIR TEMP----------(C)	=	36.9
AIR VELOCITY----(M/S)	=	1.00
DROP REYNOLDS NUMBER	=	114.78
FILAMENT REYNOLDS NUMBER	=	12.08

TIME	MV	TEMP(C)	WT (MG)	WT CORRECTED (MG)	FRACTION EVAPORATED
.0	.71	18.12	4.34	4.34	.00
60.0	.70	17.87	3.24	3.52	.19
120.0	.70	17.96	2.54	2.83	.35
240.0	.76	19.17	1.67	1.96	.55
300.0	.82	20.58	1.32	1.61	.63
360.0	1.13	27.79	1.15	1.43	.67
540.0	1.47	35.78	.86	1.14	.74
600.0	1.49	36.11	.86	1.14	.74
660.0	1.49	36.20	.86	1.14	.74

EXPERIMENTAL RESULTS

EXPERIMENTAL REFERENCE		D111
COPPER SULPHATE		18.0 WT %
AIR TEMP----------(C)	=	70.00
AIR VELOCITY----(M/S)	=	1.00
DROP REYNOLDS NUMBER	=	86.72
FILAMENT REYNOLDS NUMBER	=	10.10

TIME	MV	TEMP(C)	WT (MG)	WT CORRECTED (MG)	FRACTION EVAPORATED
.0	.67	16.33	3.20	3.20	.00
35.0	1.28	31.32	1.73	1.98	.38
60.0	1.42	34.69	1.29	1.54	.52
120.0	2.69	65.65	1.00	1.26	.61
180.0	2.29	56.02	.88	1.14	.64
240.0	2.95	72.09	.76	1.01	.68
300.0	2.87	69.97	.76	1.01	.68
360.0	2.80	68.45	.76	1.01	.68

EXPERIMENTAL RESULTS
==========

EXPERIMENTAL REFERENCE D112
COPPER SULPHATE 18.0 WT %
AIR TEMP----------(C) = 22.70
AIR VELOCITY----(M/S) = 1.00
DROP REYNOLDS NUMBER = 124.85
FILAMENT REYNOLDS NUMBER = 13.10

TIME	MV	TEMP(C)	WT (MG)	WT CORRECTED (MG)	FRACTION EVAPORATED
.0	.67	16.55	4.38	4.38	.00
25.0	.46	11.33	3.97	4.26	.03
60.0	.46	11.26	3.77	4.06	.07
120.0	.46	11.38	3.28	3.57	.18
180.0	.47	11.48	2.95	3.25	.26
240.0	.47	11.58	2.59	2.88	.34
300.0	.48	11.75	2.34	2.64	.40
360.0	.49	12.02	2.02	2.31	.47
420.0	.51	12.63	1.78	2.07	.53
480.0	.54	13.26	1.57	1.87	.57
600.0	.67	16.45	1.17	1.46	.67
720.0	.81	19.96	.96	1.26	.71
900.0	.89	21.87	.92	1.22	.72
1020.0	.90	22.18	.76	1.05	.76
1200.0	.92	22.55	.76	1.05	.76

EXPERIMENTAL RESULTS
==========

EXPERIMENTAL REFERENCE D114
COPPER SULPHATE 18.0 WT %
AIR TEMP----------(C) = 20.90
AIR VELOCITY----(M/S) = 1.00
DROP REYNOLDS NUMBER = 114.15
FILAMENT REYNOLDS NUMBER = 13.24

TIME	MV	TEMP(C)	WT (MG)	WT CORRECTED (MG)	FRACTION EVAPORATED
.0	.58	14.19	3.24	3.24	.00
25.0	.41	10.16	2.18	2.45	.24
60.0	.41	10.21	2.02	2.29	.29
120.0	.42	10.31	1.61	1.88	.42
180.0	.42	10.41	1.37	1.64	.49
240.0	.43	10.58	1.00	1.27	.61
300.0	.44	10.87	.76	1.03	.68
360.0	.47	11.55	.47	.74	.77
480.0	.55	13.58	.07	.34	.90
600.0	.65	16.01	.00	.27	.92
780.0	.78	19.13	.00	.27	.92
900.0	.82	20.23	.00	.27	.92
1020.0	.83	20.45	.00	.27	.92

EXPERIMENTAL RESULTS

EXPERIMENTAL REFERENCE		D117
COPPER SULPHATE		25.0 WT %
AIR TEMP----------(C)	=	20.90
AIR VELOCITY----(M/S)	=	1.00
DROP REYNOLDS NUMBER	=	115.04
FILAMENT REYNOLDS NUMBER	=	13.24

TIME	MV	TEMP(C)	WT (MG)	WT CORRECTED (MG)	FRACTION EVAPORATED
.0	.65	13.39	3.57	3.57	.00
30.0	.42	6.06	2.99	3.26	.09
60.0	.44	6.86	2.81	3.08	.14
120.0	.51	8.99	2.55	2.83	.21
180.0	.58	11.38	2.30	2.57	.28
240.0	.66	13.87	2.09	2.37	.34
360.0	.75	16.71	1.90	2.18	.39
480.0	.81	18.52	1.81	2.08	.42
600.0	.85	19.99	1.70	1.97	.45
720.0	.87	20.43	1.66	1.93	.46
780.0	.87	20.53	1.66	1.93	.46

EXPERIMENTAL RESULTS

EXPERIMENTAL REFERENCE		D119
COPPER SULPHATE		5.0 WT %
AIR TEMP----------(C)	=	20.90
AIR VELOCITY----(M/S)	=	1.00
DROP REYNOLDS NUMBER	=	87.89
FILAMENT REYNOLDS NUMBER	=	13.22

TIME	MV	TEMP(C)	WT (MG)	WT CORRECTED (MG)	FRACTION EVAPORATED
.0	.64	13.04	3.38	3.38	.00
90.0	.41	5.71	2.63	2.90	.14
120.0	.41	5.74	2.47	2.74	.19
180.0	.41	5.74	2.16	2.42	.29
240.0	.41	5.74	1.90	2.15	.36
300.0	.41	5.74	1.66	1.90	.44
360.0	.41	5.74	1.40	1.63	.52
480.0	.41	5.90	1.40	1.62	.52
540.0	.46	7.40	.94	1.16	.66
660.0	.73	16.04	.71	.93	.72
720.0	.90	21.58	.68	.91	.73
780.0	.91	21.65	.68	.91	.73

EXPERIMENTAL RESULTS

EXPERIMENTAL REFERENCE D122
COPPER SULPHATE 10.0 WT %
AIR TEMP----------(C) = 20.90
AIR VELOCITY----(M/S) = 1.00
DROP REYNOLDS NUMBER = 103.88
FILAMENT REYNOLDS NUMBER = 13.24

TIME	MV	TEMP(C)	WT (MG)	WT CORRECTED (MG)	FRACTION EVAPORATED
.0	.65	13.36	2.85	2.85	.00
30.0	.41	5.93	2.46	2.72	.05
60.0	.41	5.93	2.31	2.56	.10
180.0	.41	6.00	1.68	1.94	.32
240.0	.42	6.15	1.33	1.58	.44
300.0	.44	6.67	1.10	1.35	.53
360.0	.48	7.97	.75	1.00	.65
420.0	.54	9.85	.57	.82	.71
480.0	.61	12.27	.40	.65	.77
540.0	.68	14.32	.34	.59	.79
660.0	.81	18.68	.34	.59	.79
720.0	.84	19.64	.34	.59	.79
840.0	.90	21.61	.34	.59	.79

EXPERIMENTAL RESULTS

EXPERIMENTAL REFERENCE D124
COPPER SULPHATE 5.0 WT %
AIR TEMP----------(C) = 65.80
AIR VELOCITY----(M/S) = 1.00
DROP REYNOLDS NUMBER = 47.70
FILAMENT REYNOLDS NUMBER = 10.31

TIME	MV	TEMP(C)	WT (MG)	WT CORRECTED (MG)	FRACTION EVAPORATED
.0	.69	17.56	1.89	1.89	.00
25.0	1.30	31.38	1.07	1.28	.32
65.0	1.31	31.65	.50	.69	.64
95.0	1.49	35.67	.22	.39	.79
120.0	1.57	37.70	.01	.17	.91
180.0	2.77	65.06	.00	.17	.91
240.0	2.82	66.02	.00	.17	.91
300.0	2.82	66.06	.00	.17	.91

EXPERIMENTAL RESULTS

EXPERIMENTAL REFERENCE		D126
COPPER SULPHATE		5.0 WT %
AIR TEMP----------(C)	=	65.80
AIR VELOCITY----(M/S)	=	1.00
DROP REYNOLDS NUMBER	=	68.87
FILAMENT REYNOLDS NUMBER	=	10.31

TIME	MV	TEMP(C)	WT (MG)	WT CORRECTED (MG)	FRACTION EVAPORATED
.0	.68	17.34	3.77	3.77	.00
35.0	1.13	27.46	2.49	2.75	.27
60.0	1.14	27.78	1.89	2.13	.44
95.0	1.17	28.53	1.43	1.65	.56
120.0	1.21	29.35	.93	1.14	.70
180.0	2.17	51.31	.40	.61	.84
240.0	2.75	64.56	.22	.43	.89
300.0	2.82	66.02	.22	.43	.89
360.0	2.82	66.13	.11	.32	.91
420.0	2.83	66.22	.11	.32	.91

EXPERIMENTAL RESULTS

EXPERIMENTAL REFERENCE		D127
COPPER SULPHATE		10.0 WT %
AIR TEMP----------(C)	=	65.80
AIR VELOCITY----(M/S)	=	1.00
DROP REYNOLDS NUMBER	=	66.16
FILAMENT REYNOLDS NUMBER	=	10.31

TIME	MV	TEMP(C)	WT (MG)	WT CORRECTED (MG)	FRACTION EVAPORATED
.0	.67	17.02	2.25	2.25	.00
25.0	1.16	28.28	1.32	1.54	.31
60.0	1.20	29.17	.72	.92	.59
120.0	2.00	47.34	.11	.32	.86
180.0	2.78	65.29	.00	.21	.91
240.0	2.84	66.66	.00	.21	.91
300.0	2.82	66.04	.00	.20	.91

EXPERIMENTAL RESULTS
==========

EXPERIMENTAL REFERENCE D129
COPPER SULPHATE 10.0 WT %
AIR TEMP----------(C) = 65.80
AIR VELOCITY----(M/S) = 1.00
DROP REYNOLDS NUMBER = 79.27
FILAMENT REYNOLDS NUMBER = 10.32

TIME	MV	TEMP(C)	WT (MG)	WT CORRECTED (MG)	FRACTION EVAPORATED
.0	.69	17.54	2.10		
20.0	1.24	30.01	1.11	2.10	.00
60.0	1.28	31.08	.65	1.34	.36
120.0	1.94	46.02	.00	.88	.58
180.0	2.75	64.56	.00	.23	.89
240.0	2.81	65.90	.00	.24	.89
				.23	.89

EXPERIMENTAL RESULTS
==========

EXPERIMENTAL REFERENCE D130
COPPER SULPHATE 18.0 WT %
AIR TEMP----------(C) = 65.80
AIR VELOCITY----(M/S) = 1.00
DROP REYNOLDS NUMBER = 107.24
FILAMENT REYNOLDS NUMBER = 10.33

TIME	MV	TEMP(C)	WT (MG)	WT CORRECTED (MG)	FRACTION EVAPORATED
.0	.67	17.15	5.66	5.66	.00
25.0	1.12	27.41	4.41	4.71	.17
60.0	1.15	28.03	3.67	3.97	.30
120.0	1.33	32.02	2.60	2.90	.49
180.0	2.42	56.96	2.25	2.55	.55
240.0	2.59	60.86	1.96	2.27	.60
300.0	2.68	62.96	1.96	2.26	.60
360.0	2.72	63.90	1.96	2.26	.60
420.0	2.74	64.28	1.89	2.19	.61
480.0	2.75	64.44	1.78	2.09	.63
540.0	2.75	64.51	1.78	2.09	.63
600.0	2.75	64.47	1.78		

EXPERIMENTAL RESULTS

EXPERIMENTAL REFERENCE		D131
COPPER SULPHATE		18.0 WT %
AIR TEMP----------(C)	=	65.80
AIR VELOCITY----(M/S)	=	1.00
DROP REYNOLDS NUMBER	=	86.63
FILAMENT REYNOLDS NUMBER	=	10.32

TIME	MV	TEMP(C)	WT (MG)	WT CORRECTED (MG)	FRACTION EVAPORATED
.0	.70	17.81	2.99	2.99	.00
25.0	1.31	31.63	1.89	2.14	.29
60.0	1.62	38.79	1.43	1.68	.44
120.0	2.47	58.10	.90	1.15	.62
180.0	2.70	63.37	.86	1.11	.63
240.0	2.77	64.88	.86	1.11	.63
300.0	2.79	65.40	.86	1.11	.63
360.0	2.80	65.56	.86	1.11	.63

EXPERIMENTAL RESULTS

EXPERIMENTAL REFERENCE		D136
COPPER SULPHATE		5.0 WT %
AIR TEMP----------(C)	=	114.00
AIR VELOCITY----(M/S)	=	1.00
DROP REYNOLDS NUMBER	=	58.65
FILAMENT REYNOLDS NUMBER	=	8.17

TIME	MV	TEMP(C)	WT (MG)	WT CORRECTED (MG)	FRACTION EVAPORATED
.0	.67	17.18	3.42	3.42	.00
25.0	1.53	36.76	1.71	1.94	.43
90.0	2.94	68.87	.00	.21	.94
120.0	4.44	103.02	.00	.21	.94
180.0	4.77	110.57	.00	.21	.94
240.0	4.79	111.01	.00	.21	.94

APPENDIX B5 SODIUM ACETATE

EXPERIMENTAL RESULTS

EXPERIMENTAL REFERENCE		D143
SODIUM ACETATE		10.0 WT %
AIR TEMP----------(C)	=	58.00
AIR VELOCITY----(M/S)	=	1.10
DROP REYNOLDS NUMBER	=	92.86
FILAMENT REYNOLDS NUMBER	=	11.86

TIME	MV	TEMP(C)	WT (MG)	WT CORRECTED (MG)	FRACTION EVAPORATED
.0	.63	17.67	7.35	7.35	.00
15.0	1.02	25.61	6.71	7.10	.03
50.0	1.05	26.18	5.76	6.14	.16
90.0	1.07	26.64	4.40	4.76	.35
120.0	1.10	27.25	3.53	3.86	.48
180.0	1.25	30.37	2.34	2.63	.64
210.0	1.52	35.82	1.94	2.22	.70
270.0	2.35	52.54	1.54	1.82	.75
300.0	2.42	54.09	1.54	1.82	.75
360.0	2.52	56.19	1.54	1.82	.75

EXPERIMENTAL RESULTS

EXPERIMENTAL REFERENCE		D147
SODIUM ACETATE		20.0 WT %
AIR TEMP----------(C)	=	58.00
AIR VELOCITY----(M/S)	=	1.10
DROP REYNOLDS NUMBER	=	118.98
FILAMENT REYNOLDS NUMBER	=	11.85

TIME	MV	TEMP(C)	WT (MG)	WT CORRECTED (MG)	FRACTION EVAPORATED
.0	.69	18.89	7.19	7.19	.00
20.0	1.08	26.81	5.84	6.21	.14
60.0	1.13	27.80	4.88	5.24	.27
120.0	1.37	32.75	3.37	3.71	.48
180.0	1.84	42.31	2.34	2.68	.63
240.0	2.34	52.42	1.86	2.20	.69
300.0	2.49	55.47	1.86	2.20	.69
420.0	2.54	56.51	1.86	2.20	.69

EXPERIMENTAL RESULTS
==========

EXPERIMENTAL REFERENCE		D149
SODIUM ACETATE		30.0 WT %
AIR TEMP----------(C)	=	58.00
AIR VELOCITY----(M/S)	=	1.10
DROP REYNOLDS NUMBER	=	129.19
FILAMENT REYNOLDS NUMBER	=	11.83

TIME	MV	TEMP(C)	WT (MG)	WT CORRECTED (MG)	FRACTION EVAPORATED
.0	.68	18.71	6.31	6.31	.00
20.0	1.07	26.68	5.20	5.57	.12
60.0	1.16	28.52	4.01	4.38	.31
120.0	1.38	32.97	2.97	3.34	.47
180.0	2.09	47.40	2.18	2.55	.60
240.0	2.47	55.19	1.94	2.31	.63
300.0	2.54	56.53	1.94	2.31	.63
360.0	2.56	56.90	1.94	2.31	.63
420.0	2.57	57.08	1.94	2.31	.63
480.0	2.57	57.12	1.94	2.31	.63

EXPERIMENTAL RESULTS
==========

EXPERIMENTAL REFERENCE		D153
SODIUM ACETATE		40.0 WT %
AIR TEMP----------(C)	=	58.00
AIR VELOCITY----(M/S)	=	1.10
DROP REYNOLDS NUMBER	=	139.13
FILAMENT REYNOLDS NUMBER	=	11.85

TIME	MV	TEMP(C)	WT (MG)	WT CORRECTED (MG)	FRACTION EVAPORATED
.0	.77	20.42	8.22	8.22	.00
15.0	1.30	31.38	7.43	7.82	.05
60.0	1.78	41.03	6.71	7.11	.14
120.0	2.01	45.73	5.76	6.16	.25
180.0	2.18	49.15	5.20	5.60	.32
240.0	2.29	51.47	4.96	5.36	.35
360.0	2.39	53.52	4.56	4.96	.40
600.0	2.51	55.82	3.93	4.33	.47
840.0	2.52	56.11	3.93	4.33	.47

EXPERIMENTAL RESULTS
==========

EXPERIMENTAL REFERENCE		D155
SODIUM ACETATE		10.0 WT %
AIR TEMP----------(C)	=	104.40
AIR VELOCITY----(M/S)	=	1.00
DROP REYNOLDS NUMBER	=	69.65
FILAMENT REYNOLDS NUMBER	=	8.59

TIME	MV	TEMP(C)	WT (MG)	WT CORRECTED (MG)	FRACTION EVAPORATED
.0	.64	17.85	7.91	7.91	.00
35.0	1.42	33.68	4.56	4.86	.39
70.0	1.55	36.41	2.57	2.83	.64
90.0	1.85	42.39	1.78	2.01	.75
120.0	2.82	62.13	.90	1.14	.86
180.0	4.41	94.50	.43	.66	.92
240.0	4.55	97.37	.43	.66	.92

APPENDIX B6 WATER

Expt No D157 T_g 17.3° C T_d 6.5° C

Time (s)	Diameter (mm)	Air Vel (m/s)	Re	Nu	Pr	$Re^{0.5}Pr^{0.33}$
0	1.43	1.12	109.6		0.724	9.4
85	1.31		100.5	8.68		9
225	1.11		84.8	8.07		8.27
285	1.02		78.4	6.75		7.95
415	0.76		58.2	8.25		6.85
545	0.51		38.9	5.58		5.60
605	0.37		28.6	4.51		4.80
660	0.23		17.9	3.48		3.79
685	0.11		8.5	3.92		2.60
700	0.06		4.5	1.37		1.90

Expt No D158 T_g 17.3° C T_d 6.5° C

Time (s)	Diameter (mm)	Air Vel (m/s)	Re	Nu	Pr	$Re^{0.5}Pr^{0.33}$
0	1.62	1.12	124.4		0.724	10.02
60	1.56		119.4	7.85		9.81
150	1.46		111.9	7.44		9.49
310	1.23		94.5	8.72		8.73
390	1.11		84.8	8.39		8.27
625	0.71		54.0	7.03		6.59
660	0.63		48.5	6.37		6.25
750	0.42		32.3	5.37		5.10
800	0.27		20.9	5.05		4.11
815	0.19		14.3	3.41		3.65
840	0.03		2.1	2.62		1.30

Expt No D159 T_g 17.3° C T_d 6.5° C

Time (s)	Diameter (mm)	Air Vel (m/s)	Re	Nu	Pr	$Re^{0.5}Pr^{0.33}$
0	1.41	1.12	107.9		0.724	9.33
60	1.34		102.7	7.17		9.09
185	1.18		90.7	7.17		8.55
260	1.08		82.4	7.47		8.15
330	0.95		72.6	8.42		7.65
350	0.91		69.8	7.70		7.50
405	0.82		62.5	6.74		7.09
485	0.68		52.4	5.65		6.49
560	0.51		38.9	6.37		5.60
590	0.41		31.6	6.76		5.05
630	0.29		22.9	4.55		4.29
670	0.09		7.4	4.55		2.44

Expt No D160 T_g 38.8° C T_d 11.3° C

Time (s)	Diameter (mm)	Air Vel (m/s)	Re	Nu	Pr	$Re^{0.5}Pr^{0.33}$
0	1.52	1.2	113.8		0.728	9.61
60	1.34		100.1	7.51		9.00
150	1.00		75.2	7.43		7.80
190	0.86		64.1	5.96		7.20
225	0.69		52.2	6.09		6.49
245	0.59		44.5	5.61		6.00
270	0.46		34.7	4.84		5.29
300	0.26		19.8	4.14		4.00

Expt No D161 T_g 38.8° C T_d 11.3° C

Time (s)	Diameter (mm)	Air Vel (m/s)	Re	Nu	Pr	$Re^{0.5}Pr^{0.33}$
0	1.36	1.2	101.9		0.728	9.09
60	1.16		87.2	7.24		8.4
88	1.06		79.1	6.85		8
120	0.93		69.5	6.99		7.5
150	0.81		60.6	6.02		7
185	0.65		49.0	5.75		6.3
205	0.55		41.6	5.18		5.8
230	0.38		28.5	5.49		4.8
240	0.29		21.8	5.18		4.2

Expt No D162 T_g 74° C T_d 24.4° C

Time (s)	Diameter (mm)	Air Vel (m/s)	Re	Nu	Pr	$Re^{0.5}Pr^{0.33}$
0	1.79	1.2	112.9		0.729	9.6
30	1.67		104.5	6.64		9.2
40	1.63		102.2	5.26		9.1
85	1.42		89.2	6.03		8.5
120	1.23		77.0	6.34		7.9
165	0.96		60.5	5.52		7.0
190	0.81		50.6	4.83		6.4
215	0.59		37.3	5.09		5.5
225	0.49		30.9	4.78		5.0
240	0.29		18.8	4.39		3.9

Expt No D163 T_g 74° C T_d 24.4° C

Time (s)	Diameter (mm)	Air Vel (m/s)	Re	Nu	Pr	$Re^{0.5}Pr^{0.33}$
0	1.73	1.2	108.4		0.729	
30	1.59		99.9	6.49		8.99
65	1.42		89.2	6.31		8.50
120	1.14		71.3	5.71		7.59
135	1.05		65.8	5.52		7.30
155	0.91		57.1	5.86		6.80
180	0.73		45.9	5.04		6.09
190	0.64		40.1	5.43		5.69
215	0.39		24.9	4.31		4.49
230	0.24		15.1	2.88		3.49

Expt No D164 T_g 107° C T_d 32.4° C

Time (s)	Diameter (mm)	Air Vel (m/s)	Re	Nu	Pr	$Re^{0.5}Pr^{0.33}$
0	1.99	1.2	108.7		0.732	9.39
30	1.82		99.7	5.58		8.99
64	1.63		88.9	5.31		8.49
93	1.44		78.8	5.21		8.00
104	1.37		74.9	4.19		7.79
118	1.27		69.3	5.11		7.50
140	1.10		60.3	4.49		6.99
168	0.95		52.0	4.63		6.49
173	0.81		44.3	4.39		5.99
195	0.56		30.8	4.10		5.00

Expt No D165 T_g 107° C T_d 32.4° C

Time (s)	Diameter (mm)	Air Vel (m/s)	Re	Nu	Pr	$Re^{0.5}Pr^{0.33}$
0	2.19	1.2	119.8		0.732	
30	2.03		111.1	5.99		9.5
60	1.86		101.9	5.71		9.1
90	1.70		93.2	5.40		8.7
113	1.55		84.8	5.40		8.3
140	1.37		74.9	5.19		7.8
165	1.19		65.6	4.89		7.3
176	1.10		60.3	4.98		6.9
193	0.95		52.0	4.82		6.5
204	0.84		45.8	4.76		6.1
222	0.66		35.9	3.99		5.4
228	0.57		32.0	4.92		5.1

APPENDIX B7 A COMPARISON OF THE DIFFERENT HEAT TRANSFER TERMS

Experimental Reference	Air Temperature (C)	% Heat Transferred		
		Filament	Radiation	Convection
D61	18.4	7.9	2.8	89.3
D2	20.4	4.0	5.0	91.0
D68	22.0	6.3	3.7	90.0
D3	31.0	6.0	5.4	88.6
D71	36.4	7.4	3.9	88.7
D21	54.1	5.2	5.5	89.3
D143	58.0	5.8	5.2	89.0
D149	58.0	4.6	5.8	89.6
D126	65.8	7.6	4.7	87.7
D23	66.3	5.3	5.8	88.9
D111	70.0	6.9	5.4	87.7
D15	74.0	5.3	6.1	88.6
D90	91.0	5.8	8.8	85.4
D101	100.0	9.3	5.4	85.3

APPENDIX C

COMPUTER PROGRAMS

```
*     ================================================================
*                              EXPT1
*                              -----
*
*     THIS PROGRAM CONVERTS EXPERIMENTAL READINGS OF
*     FILAMENT-THERMOCOUPLE DEFLECTION'S AND MV'S TO
*     DROP WEIGHT'S AND TEMPERATURE'S.
*     THE EFFECT OF BUOYANCY AND HEAT TRANSFER BY
*     CONVECTION,CONDUCTION VIA THE FILAMENT AND
*     RADIATION ARE ALL CALCULATED.
*
*                           NOMENCLATURE
*                           ------------
*     AC          - SURFACE AREA OF COPPER IN CONTACT WITH
*                   THE DROP                                  - M2
*     AG          - SURFACE AREA OF GLASS IN CONTACT WITH
*                   THE DROP                                  - M2
*     AW          - SURFACE AREA OF CONSTANTAN WIRE IN
*                   CONTACT WITH THE DROP                     - M2
*     CC          - HEAT OF CRYSTALLISATION                   - J/KG
*     CD          - DROP DRAG COEFFICIENT
*     CF          - FILAMENT DRAG COEFFICIENT
*     CPS         - SPECIFIC HT CAPACITY OF THE SOLUTION      - J/KG/K
*     DC          - CORE DENSITY                              - KG/M3
*     DCO         - ORIGINAL CORE DENSITY                     - KG/M3
*     DF          - FILAMENT OUTER DIAMETER                   - M
*     DI          - FILAMENT INNER DIAMETER                   - M
*     ES          - EMISSIVITY OF THE DROP
*     EW          - EMISSIVITY OF THE WIRE
*     G           - ACCELERATION DUE TO GRAVITY               - M/S2
*     GR          - GRASHOF NUMBER
*     HF          - FILAMENT HEAT TRANSFER COEFFICIENT        - W/M2/K
*     KA          - THERMAL CONDUCTIVITY OF AIR               - W/M/K
*     KG          - THERMAL CONDUCTIVITY OF THE FILAMENT      - W/M/K
*     KS          - THERMAL CONDUCTIVITY OF THE DROP          - W/M/K
*     KW          - THERMAL CONDUCTIVITY OF THE WIRE          - W/M/K
*     KWAT        - THERMAL CONDUCTIVITY OF WATER             - W/M/K
*     LANDA       - LATENT HEAT OF VAPORISATION               - J/KG
*     LENGTH      - LENGTH OF FILAMENT IN THE WIND TUNNEL     - M
*     MF          - MASS FRACTION OF WATER
*     PA          - AIR DENSITY                               - KG/M3
*     PRS         - PRANDTL NUMBER
*     RED         - DROP REYNOLD NUMBER
*     REF         - FILAMENT REYNOLD NUMBER
*     SIG         - STEFAN BOLTZMANN CONSTANT
*     TEMP(I)     - DROP TEMPERATURE                          - K
*     TG          - AIR TEMPERATURE                           - K
*     UA          - VISCOSITY OF AIR                          - KG/M/S
*     VISCS       - VISCOSITY OF THE SOLUTION                 - KG/M/S
*     VISCW       - VISCOSITY OF WATER                        - KG/M/S
*     W(I)        - WEIGHT OF THE DROP                        - KG
*     ================================================================
      REAL PA,VA,DD,UA,G,KG,DF,SIG,HF,WI,DW,KW,LAT,CC
      REAL DS,CD,RED,REF,CF,FD,DP,LENGTH,ES,TG,EW,W1,LANDA
      REAL MV,TGC,Y,ANS,MVC,DI,TC,KC,R,X
      REAL K,AC,AW,AG,A1,A2,A3,PI,B,C,D1,E
      REAL MF1,MF,RAD,MOISTURE
      REAL KA,CH1,CH2,CH3
      REAL VISCW,VISCS,CPS,P,KS,KWAT,PRS,BETA,GR
      REAL Y1,Y2,DELT,CVOL
      INTEGER DAY,MONTH,YEAR,EXPT
      CHARACTER*8 FILENAME
```

```
      DIMENSION T(50),D(50),MV(50),TEMP(50)
      DIMENSION W(50),DO(50),TSM(50),QF(50)
      DIMENSION QR(50),QW(50),WC(50),WC1(50),WC2(50),FIW(50)
      DIMENSION QG(50),QC(50),QG1(50),QC1(50)
      DIMENSION QR1(50),QF1(50),QW1(50)
      DIMENSION CHART(50),T1(50),MVC(50),EVAP(50),DDW(50)
      DIMENSION FD(50),FF(50),FT(50),DW(50),RD(50),DP(50)
      DIMENSION MOISTURE(50),RATE(50),RAD(50)
      DIMENSION RATE1(50),QWW(50)
      DIMENSION DPM(50),QG2(50),QC2(50),QW2(50),QR2(50)
      DIMENSION QF2(50)
      DIMENSION QCONV(50),PR(50)
      DIMENSION RED(50)
      DIMENSION QCONV2(50)
      G=9.81
      PI=3.1412
      DF=0.2E-3
      DI=.1E-3
      ES=0.955
      EG=0.94
      LENGTH=12E-3
      SIG=5.6697E-8
      EW=0.05
      KW=21.0
      TC=50E-10
      TW=50E-6
      KG=0.6404
      KC=389.34
      CA=1036.2
      OPEN(UNIT=10,FILE=' ')
      PRINT*,'  INPUT NO OF DATA POINTS'
      READ*,J
      PRINT*,'INPUT FILENAME'
      READ*,FILENAME
      OPEN(UNIT=15,FILE=FILENAME,STATUS='OLD')
      REWIND 15
      DO 4 I=1,J
      READ(15,*) T(I),D(I),MV(I)
4     CONTINUE
      PRINT*,'   INPUT THE FOLLOWING DATA'
      PRINT*,' '
      PRINT*,'IS THE MATERIAL'
      PRINT*,'                1-NA2SO4 10H2O'
      PRINT*,'                2-NACL'
      PRINT*,'                3-K2SO4'
      PRINT*,'                4-CUSO4'
      PRINT*,'                5-CH3COONA'
      PRINT*,'                6-H2O'
      READ*,CH1
      PRINT*,'              INPUT EXPT NO'
      READ*,EXPT
      IF(Y.EQ.1)THEN
      GOTO 62
      ENDIF
      PRINT*,'              INPUT MASS FRACTION OF WATER'
      READ*,MF1
      PRINT*,'              INPUT STARTING DEFLECTION'
      READ*,SD
      PRINT*,'              INPUT AIR TEMP'
      READ*,TGC
      TG=TGC+273.15
      PRINT*,'              INPUT AIR VELOCITY'
      READ*,VA
*     TO CONVERT DEFLECTIONS AND MV READINGS TO WEIGHTS AND TEMPS RESPECTIV
```

```
      PRINT*,'INPUT CALIBRATION OF CHOICE'
      PRINT*,' '
      PRINT*,'WEIGHT CALIBRATIONS'
      PRINT*,' '
      PRINT*,' (1) W(I)=0.37288+5.78229*(SD-D(I))*1E-6 DAT 1-9'
      PRINT*,' (2) W(I)=-0.48665+6.91775*(SD-D(I))*1E-6 DAT 10-18'
      PRINT*,' (3) W(I)=(0.0798+10.4226*(SD-D(I)))*1E-6 DAT 19-23'
      PRINT*,' (4) W(I)=(-1.5102+8.3163*(SD-D(I)))*1E-6 DAT 24-28'
      PRINT*,' (5) W(I)=(-.9589+.9308*(D(I)-SD))*1E-6 DAT 29-34'
      PRINT*,' (6) W(I)=(-0.055+0.081*(SD-D(I)))*1E-6 DAT 35-42'
      PRINT*,' (7) W(I)=(0.1411+2.615*(SD-D(I)))*1E-6 DAT 44-57'
      PRINT*,' (8) W(I)=(.0995+2.989*(SD-D(I)))*1E-6 DAT 58-77'
      PRINT*,' (9) W(I)=(-.0463+2.865*(SD-D(I)))*1E-6 DAT 78-101'
      PRINT*,' (10) W(I)=(.1247+3.022*(SD-D(I)))*1E-6 DAT 102-103'
      PRINT*,' (11) W(I)=(.1011+5.8048*(SD-D(I)))*1E-6 DAT 104-108'
      PRINT*,' (12) W(I)=(.1889+4.0675*(SD-D(I)))*1E-6 DAT 109-116'
      PRINT*,' (13) W(I)=(.01502+1.3574*(SD-D(I)))*1E-6 DAT 117-123'
      PRINT*,' (14) W(I)=(.1135+3.5527*(SD-D(I)))*1E-6 DAT 124-138'
      PRINT*,' (15) W(I)=(-.05201+7.9572*(SD-D(I)))*1E-6 DAT 139-156'
      PRINT*,' (16) W(I)=(0.1775+19.466*(SD-D(I))*1E-6  WATER EXPTS'
      PRINT*,'            INPUT CHOICE'
      READ*,CH2
      PRINT*,' '
      PRINT*,'            TEMPERATURE CALIBRATIONS'
      PRINT*,' '
      PRINT*,'(1) TEMP(I)=6.2755+22.3698*MV(I) DAT 1-18'
      PRINT*,'(2) TEMP(I)=2.877+24.0446*MV(I) DAT 19-28'
      PRINT*,'(3) TEMP(I)=1.1612+24.3733*MV(I) DAT 29-34'
      PRINT*,'(4) TEMP(I)=0.542+25.6702*MV(I) DAT 35-42'
      PRINT*,'(5) TEMP(I)=0.2286+24.3277*MV(I) DAT 43-57'
      PRINT*,'(6) TEMP(I)=-0.2961+25.2295*MV(I) DAT 58-77'
      PRINT*,'(7) TEMP(I)=-0.2508+25.4111*MV(I) DAT 78-101'
      PRINT*,'(8) TEMP(I)=-4.4212+29.483*MV(I) DAT 102-103'
      PRINT*,'(9) TEMP(I)=1.575+23.2391*MV(I) DAT 104-108'
      PRINT*,'(10) TEMP(I)=.1189+24.3795*MV(I) DAT 109-116'
      PRINT*,'(11) TEMP(I)=-7.2325+31.875*MV(I) DAT 117-123'
      PRINT*,'(12) TEMP(I)=1.8069+22.80195*MV(I) DAT 124-138'
      PRINT*,'(13) TEMP(I)=4.8321+20.3466*MV(I) DAT 139-156'
      PRINT*,'(14) TEMP(I)=1.085+22.598*MV(I)   WATER EXPTS'
      PRINT*,'            INPUT CHOICE'
      READ*,CH3
      DO 20 I=1,J
      IF(CH2.EQ.1)THEN
      W(I)=(0.37288+5.78229*(SD-D(I)))*1E-6
      ELSEIF(CH2.EQ.2)THEN
      W(I)=(-.48665+6.91775*(SD-D(I)))*1E-6
      ELSEIF(CH2.EQ.3)THEN
      W(I)=(0.0798+10.4226*(SD-D(I)))*1E-6
      ELSEIF(CH2.EQ.4)THEN
      W(I)=(-1.5102+8.3136*(SD-D(I)))*1E-6
      ELSEIF(CH2.EQ.5)THEN
      W(I)=(-0.9589+0.9308*(D(I)-SD))*1E-6
      ELSEIF(CH2.EQ.6)THEN
      W(I)=(-0.055+0.081*(SD-D(I)))*1E-6
      ELSEIF(CH2.EQ.7)THEN
      W(I)=(0.1411+2.615*(SD-D(I)))*1E-6
      ELSEIF(CH2.EQ.8)THEN
      W(I)=(0.0995+2.989*(SD-D(I)))*1E-6
      ELSEIF(CH2.EQ.9)THEN
      W(I)=(-.0463+2.865*(SD-D(I)))*1E-6
      ELSEIF(CH2.EQ.10)THEN
      W(I)=(.1247+3.022*(SD-D(I)))*1E-6
      ELSEIF(CH2.EQ.11)THEN
      W(I)=(.1011+5.8048*(SD-D(I)))*1E-6
```

```
      ELSEIF(CH2.EQ.12)THEN
      W(I)=(.1889+4.0675*(SD-D(I)))*1E-6
      ELSEIF(CH2.EQ.13)THEN
      W(I)=(.01502+1.3574*(SD-D(I)))*1E-6
      ELSEIF(CH2.EQ.14)THEN
      W(I)=(.1135+3.5527*(SD-D(I)))*1E-6
      ELSEIF(CH2.EQ.15)THEN
      W(I)=(-.05201+7.9572*(SD-D(I)))*1E-6
      ELSE
      W(I)=(0.1775+19.466*(SD-D(I)))*1E-6
      ENDIF
      IF(W(I).LE.0)THEN
      W(I)=0
      ENDIF
      IF(CH3.EQ.1)THEN
      TEMP(I)=6.2755+22.3698*MV(I)
      ELSEIF(CH3.EQ.2)THEN
      TEMP(I)=2.877+24.0446*MV(I)
      ELSEIF(CH3.EQ.3)THEN
      TEMP(I)=1.1612+24.3733*MV(I)
      ELSEIF(CH3.EQ.4)THEN
      TEMP(I)=0.542+25.6702*MV(I)
      ELSEIF(CH3.EQ.5)THEN
      TEMP(I)=0.2286+24.3277*MV(I)
      ELSEIF(CH3.EQ.6)THEN
      TEMP(I)=-.29613+25.2295*MV(I)
      ELSEIF(CH3.EQ.7)THEN
      TEMP(I)=-0.2508+25.4111*MV(I)
      ELSEIF(CH3.EQ.8)THEN
      TEMP(I)=-4.4212+29.483*MV(I)
      ELSEIF(CH3.EQ.9)THEN
      TEMP(I)=1.575+23.2391*MV(I)
      ELSEIF(CH3.EQ.10)THEN
      TEMP(I)=.1189+24.3795*MV(I)
      ELSEIF(CH3.EQ.11)THEN
      TEMP(I)=-7.2325+31.875*MV(I)
      ELSEIF(CH3.EQ.12)THEN
      TEMP(I)=1.8069+22.80195*MV(I)
      ELSEIF(CH3.EQ.13)THEN
      TEMP(I)=4.8321+20.3466*MV(I)
      ELSE
      TEMP(I)=1.085+22.598*MV(I)
      ENDIF
      TEMP(I)=TEMP(I)+273.15
20    CONTINUE
      DO 25 I=2,J
      WS=W(1)*(1-MF1)
      IF(W(I).LE.0)THEN
      MF=0
      CONC=1
      ELSE
      MF=(W(I)-WS)/W(I)
      CONC=WS/W(I)
      ENDIF
      TSM(I)=(TEMP(I)+TEMP(I-1))/2
      KWAT=0.1689+1.47006E-3*TSM(I)
      IF(CH1.EQ.1)THEN
      DCO=1000*MF1+1464*(1-MF1)
      DC=1000*MF+1464*(1-MF)
      IF(TSM(I).LE.306.15)THEN
      SOLU=0.292*10**(0.0331*(TSM(I)-273.15))
      ELSE
      SOLU=3.7125*10**(-0.001*(TSM(I)-273.15))
      ENDIF
```

```
      CS=142.04*SOLU/(1000+(142.04*SOLU))
      KS=0.6*(1-MF)+KWAT*MF
      CPS=3300
      CC=152
      ELSEIF(CH1.EQ.2)THEN
      CALL DENS(MF1,TEMP(1),DCO)
      CALL DENS(MF,TSM(I),DC)
      SOLU=35.48+0.024748*(TSM(I)-273.15)+0.0001*((TSM(I)-273.15)
     +**2)+0.00000265555*((TSM(I)-273.15)**3)
      SOLU=SOLU/100
      CPS=3880.061+0.6059*TSM(I)
      P=CONC*W(I)/100
      KS=KWAT*(1-(1E-5*248*P))
      CS=SOLU/(1+SOLU)
      CC=25.8
      ELSEIF(CH1.EQ.3)THEN
      CALL DENS1(MF1,TEMP(1),DCO)
      CALL DENS1(MF,TSM(I),DC)
      SOLU=.4199+.0114*(TSM(I)-273.15)-1.807E-5*((TSM(I)
     +-273.15)**2)
      CS=174.25*SOLU/(1000+(174.25*SOLU))
      CC=116.95
      CPS=4639-201.3182*CONC+11.5909*(CONC**2)
      P=CONC*W(I)/100
      KS=KWAT*(1-(1E-5*70*P))
      ELSEIF(CH1.EQ.4)THEN
      CALL DENS2(MF1,TEMP(1),DCO)
      CALL DENS2(MF,TSM(I),DC)
      SOLU=0.864925+.03085*(TSM(I)-273.15)-.000695672*((TSM(I)
     +-273.15)**2)+1.47825E-5*((TSM(I)-273.15)**3)-7.21281E-8*
     +((TSM(I)-273.15)**4)
      CS=159.61*SOLU/(1000+(159.61*SOLU))
      CC=116
      ELSEIF(CH1.EQ.5)THEN
      CALL DENS3(MF1,TEMP(1),DCO)
      CALL DENS3(MF,TSM(I),DC)
      SOLU=4.584+0.0188*(TSM(I)-273.15)+0.0016*((TSM(I)-273.15)**2)
      CS=82.04*SOLU/(1000+(82.04*SOLU))
      CC=170
      ELSE
      DC=1000
      DCO=1000
      ENDIF
      CUB1=1
      CUB2=3
      CUB=CUB1/CUB2
      DP(1)=2*((3*W(1))/(4*3.1412*DCO))**CUB
      IF(CONC.LT.CS.OR.CH1.EQ.6)THEN
      DP(I)=2*((3*W(I))/(4*3.1412*DC))**CUB
      ELSE
      DP(I)=DP(I-1)
      ENDIF
      DPM(I)=(DP(I)+DP(I-1))/2
      VOL=PI*DPM(I)**3/6
      CVOL=CONC*W(I)/VOL
      VISCW=(2.1482*((TSM(I)-281.435)+((8078.4+((TSM(I)
     +-281.435)**.2))**.5))-120)**(-1)
      IF(CH1.EQ.1)THEN
      VISCS=1+0.015*(CVOL**.5)+0.357*CVOL
      ELSEIF(CH1.EQ.2)THEN
      VISCS=1+0.0067*(CVOL**.5)+0.0762*CVOL+0.01291*CVOL**2
      ELSEIF(CH1.EQ.3)THEN
      VISCS=.9974+.0139*CONC
      ENDIF
```

```
      VISCS=VISCS*VISCW*1E-1
      CALL UPDATE(W(I),DPM(I),TG,TSM(I)
     +,DF,LENGTH,VA,FD(I),FF(I),FT(I),DW(I),REF,RED(I),WC1(I))
      DO(I)=T(I)-T(I-1)
      UA=4.568E-8*(TGC+(TSM(I)-273.15))/2+1.72E-5
      KA=(4.2956E-5*((TGC+(TSM(I)-273.15)/2))+0.014)*1.7307
      PR(I)=CA*UA/KA
      IF(DPM(I).LE.0)THEN
      CH=0
      ELSE
      CH=KA/DPM(I)*(2+0.6*RED(I)**.5*PR(I)**.33)
      ENDIF
      QCONV(I)=CH*3.1412*DPM(I)**2*(TG-TSM(I))
      IF(QCONV(I).LE.0)THEN
      QCONV(I)=0
      ENDIF
      IF(REF.LT.4)THEN
      CR=0.989
      M=0.33
      ELSE IF(REF.GE.4.AND.REF.LT.40)THEN
      CR=0.911
      M=0.385
      ELSE
      CR=0.683
      M=0.466
      ENDIF
      HF=CR*(REF**M)*(PR(I)**0.33)*KG/DF
      QR2(I)=SIG*DO(I)*ES*3.1412*DPM(I)**2*(TG**4-TSM(I)**4)
      QR(I)=SIG*ES*3.1412*DPM(I)**2*(TG**4-TSM(I)**4)
      IF(QR(I).LT.0.OR.QR2(I).LT.0)THEN
      QR(I)=0
      QR2(I)=0
      ENDIF
      AC=PI*TC**2/4
      AG=PI*(DF-DI)**2/4
      AW=PI*TW**2/4
      AT=PI*DF**2/4
      A1=KW*AW
      A2=KC*AC
      A3=KG*AG
      K=(A1+A2+A3)/AT
      TD1=TSM(I)
      B=SIG*EG*(TSM(I)**5-TG**5)/5
      C=SIG*EG*TG**4*(TSM(I)-TG)
      D1=CH*(TSM(I)-TG)**2/2
      E=-(8/K/DF*(B-C+D1))**.5
      PRS=CPS*VISCS/KS
      BETA=1/TSM(I)
      GR=BETA*G*DF**3*DC**2/VISCS**2
      Y1=(PRS*GR)**.25
      Y2=KS*PI*DF
      DELT=(-8.511*K*E/Y1/Y2)**(1.25**-1)
      IF(DELT.GE.0.5)THEN
      TD=DELT+TSM(I)
      TSM(I)=TD
      GOTO 22
      ENDIF
      QWW(I)=KW*PI*TW*(TD-TD1)
      AF=(PI/4*(DF**2-TW**2))+(PI*TW*0.1E-3)
      QF(I)=-K*AF*E
      QF2(I)=QF(I)*DO(I)
      QCONV2(I)=QCONV(I)*DO(I)
      LANDA=2.326*1000*(1075.95-(1.025*TSM(I)))
      QF1(I)=QF(I)/(LANDA-CC)
```

```
      QR1(I)=QR(I)/(LANDA-CC)
      WC2(I)=QF1(I)+QR1(I)
25    CONTINUE
      DO 55 I=1,J
      IF(I.EQ.1)THEN
      WC(I)=W(I)
      ELSE
      WC(I)=WC1(I)+WC2(I-1)
      ENDIF
55    CONTINUE
      IF(WC(1).LT.WC(2))THEN
      WC(1)=WC(2)
      ENDIF
      IF(CH1.EQ.6)THEN
      GOTO 30
      ENDIF
      DO 57 I=1,J
      IF(WC(I).LE.WS.OR.I.EQ.0)THEN
      MOISTURE(I)=0
      RATE(I)=0
      RATE1(I)=0
      ELSE
      MOISTURE(I)=(WC(I)-WS)/WS
      IF(WC(I).LT.WC(I+1))THEN
      RATE(I)=0
      RATE1(I)=0
      ELSE
      RATE(I)=((WC(I)-WC(I+1))*1E6)/(T(I+1)-T(I))
      RATE1(I)=RATE(I)/(3.1412*DP(I)**2)
      RATE1(I)=RATE1(I)*1E-6
      ENDIF
      ENDIF
      FIW(I)=(WC(1)-WC(I))/WC(1)
57    CONTINUE
30    TIME=0.000
      COUN=1
      DO 60 I=1,J
      W(I)=W(I)*1E+6
      WC(I)=WC(I)*1E+6
      TEMP(I)=TEMP(I)-273.15
60    CONTINUE
62    CONTINUE
      WRITE(10,100)
      WRITE(10,110)
      WRITE(10,175) EXPT
      IF(CH1.EQ.1)THEN
      WRITE(10,700) (1-MF1)*100
      ELSEIF(CH1.EQ.2)THEN
      WRITE(10,710) (1-MF1)*100
      ELSEIF(CH1.EQ.3)THEN
      WRITE(10,720) (1-MF1)*100
      ELSEIF(CH1.EQ.4)THEN
      WRITE(10,730) (1-MF1)*100
      ELSEIF(CH1.EQ.5)THEN
      WRITE(10,740) (1-MF1)*100
      ELSE
      WRITE(10,750)
      ENDIF
      WRITE(10,200) TGC
      WRITE(10,210) VA
      WRITE(10,212) RED(J)
      WRITE(10,214) REF
      WRITE(10,220)
      WRITE(10,222)
```

```
      WRITE(10,225)
      DO 1000 I=1,J
      WRITE(10,230) T(I),MV(I),TEMP(I),W(I),WC(I),FIW(I)
1000  CONTINUE
      IF(CH1.EQ.6)THEN
      WRITE(10,500)
      DO 1010 I=1,J
      DP(I)=2*((3*WC(I))/(4*3.1412*1))**CUB
      WRITE(10,510) T(I),WC(I),DP(I)
1010  CONTINUE
      ENDIF
      WRITE(10,280)
      WRITE(10,300)
      DO 1030 I=1,J
      DDW(I)=DW(I)*1E6
      WRITE(10,320) T(I),FD(I),FF(I),FT(I),DDW(I)
1030  CONTINUE
      WRITE(10,415)
      WRITE(10,330)
      DO 1032 I=1,J
      WRITE(10,340) T(I),QF(I),QR(I),QCONV(I)
1032  CONTINUE
      WRITE(10,420)
      WRITE(10,330)
      DO 1035 I=1,J
      WRITE(10,342) T(I),QF2(I),QR2(I),QCONV2(I)
1035  CONTINUE
      WRITE(10,425)
      WRITE(10,332)
      DO 1040 I=1,J
      QF1(I)=QF1(I)*1E6
      QR1(I)=QR1(I)*1E6
      QW1(I)=QW1(I)*1E6
      QC1(I)=QC1(I)*1E6
      QG1(I)=QG1(I)*1E6
      WRITE(10,350) T(I),QF1(I),QR1(I)
1040  CONTINUE
      WRITE(10,175) EXPT
      WRITE(10,400)
      DO 1050 I=1,J-1
      WRITE(10,410) T(I+1),MOISTURE(I),RATE(I),RATE1(I)
1050  CONTINUE
      PRINT 100
      PRINT 110
      PRINT 130
      PRINT 140
      PRINT 150
      PRINT 160
      PRINT 170
      PRINT 172
64    PRINT*,'     CHOOSE OPTION OF INTEREST-------(1-6)'
      READ*,N
      IF(N.EQ.1)THEN
      PRINT 175 ,EXPT
      PRINT 180
      PRINT 200,TGC
      PRINT 210,VA
      PRINT 212,RED(I)
      PRINT 214,REF
      ELSEIF(N.EQ.2)THEN
      PRINT 175 ,EXPT
      PRINT 217
      DO 65 I=1,J
      PRINT 230,T(I),MV(I),TEMP(I)
```

```
65      CONTINUE
        ELSEIF(N.EQ.3)THEN
        PRINT 175 ,EXPT
        PRINT 240
        PRINT 241
        DO 70 I=1,J
        PRINT 250,T(I),W(I),WC(I)
70      CONTINUE
        ELSEIF(N.EQ.4)THEN
        PRINT 175 ,EXPT
        PRINT 260
        PRINT 261
        DO 75 I=1,J
        PRINT 270,T(I),TEMP(I),FIW(I)
75      CONTINUE
        ELSEIF(N.EQ.5)THEN
        PRINT 175,EXPT
        PRINT 280
        PRINT 290
        PRINT 300
        DO 80 I=1,J
        DDW(I)=DW(I)*1E6
        PRINT 320,T(I),FD(I),FF(I),FT(I),DDW(I)
80      CONTINUE
        PRINT 415
        PRINT 330
        DO 83 I=1,J
        PRINT 340,T(I),QF(I),QR(I),QCONV(I)
83      CONTINUE
        PRINT*,' '
        PRINT*,' '
        PRINT*,'        AMOUNT OF HEAT--------J '
        PRINT*,' '
        PRINT 330
        DO 85 I=1,J
        PRINT 342,T(I),QF2(I),QR2(I),QCONV2(I)
85      CONTINUE
        PRINT*,' '
        PRINT*,'        CORRECTION TO WEIGHT----MG'
        PRINT*,' '
        PRINT 332
        DO 87 I=1,J
        PRINT 350,T(I),QF1(I),QR1(I)
87      CONTINUE
        ELSEIF(N.EQ.6)THEN
        PRINT 400
        DO 95 I=1,J-1
        PRINT 410,T(I+1),MOISTURE(I),RATE(I),RATE1(I)
95      CONTINUE
        ELSE
        PRINT*,'  YOU HAVE MADE AN INCORRECT CHOICE'
        ENDIF
        PRINT*,'  DO YOU WISH TO RETURN TO THE MENU'
        PRINT*,'                    YES=KEY 1'
        PRINT*,'                    NO=ANY KEY FROM 2-9'
        READ*,ANS
        IF(ANS.EQ.1)THEN
        GOTO 64
        ELSE
        PRINT*,'THE END'
        ENDIF
700     FORMAT(20X,'SODIUM SUL DECAHYDRATE',3X,F4.1,1X,'WT %',/)
710     FORMAT(20X,'SODIUM CHLORIDE',3X,F4.1,1X,'WT %',/)
720     FORMAT(20X,'POT SULPHATE   ',3X,F4.1,1X,'WT %',/)
```

```
730    FORMAT(20X,'COPPER SULPHATE',3X,F4.1,1X,'WT %',/)
740    FORMAT(20X,'SODIUM ACETATE ',3X,F4.1,1X,'WT %',/)
750    FORMAT(20X,'WATER',/)
100    FORMAT(25X,'EXPERIMENTAL RESULTS')
110    FORMAT(25X,'==================',/)
130    FORMAT(20X,'(1)--------EXPERIMENTAL CONDITIONS',/)
140    FORMAT(20X,'(2)--------MILLIVOLTS/TEMP',/)
150    FORMAT(20X,'(3)--------WEIGHT',/)
160    FORMAT(20X,'(4)--------TEMP/FRAC OF WEIGHT',/)
170    FORMAT(20X,'(5)--------CORRECTION FACTORS',/)
172    FORMAT(20X,'(6)--------MOISTURE/RATE     ',/)
175    FORMAT(20X,'EXPERIMENTAL REFERENCE   D',I4,/)
180    FORMAT(20X,'EXPERIMENTAL CONDITIONS',///)
200    FORMAT(20X,'AIR TEMP----------(C)=',5X,F7.3,/)
210    FORMAT(20X,'AIR VELOCITY----(M/S)=',5X,F6.3,/)
212    FORMAT(20X,'DROP REYNOLDS NUMBER=',5X,F9.3,/)
214    FORMAT(20X,'FILAMENT REYNOLDS NUMBER=',3X,F6.3,//)
217    FORMAT(5X,'TIME',13X,'MV',9X,'TEMP',//)
220    FORMAT(22X,'TIME',6X,'MV',7X,'TEMP(C)',8X,'WEIGHT',10X,'WEIGHT'
      +,5X,'FRACTION')
222    FORMAT(55X,'(MG)',5X,'CORRECTED',2X,'EVAPORATED')
225    FORMAT(67X,'(MG)',/)
230    FORMAT(20X,F6.1,4X,F5.2,4X,F7.2,8X,F5.2,7X,F5.2,4X,F3.2)
240    FORMAT(19X,'TIME',7X,'WEIGHT',5X,'CORRECTED')
241    FORMAT(42X,'WEIGHT',/)
250    FORMAT(15X,F9.1,2(5X,F6.3))
260    FORMAT(20X,'TIME',11X,'TEMP',8X,'FRAC OF ')
261    FORMAT(49X,'WEIGHT',/)
270    FORMAT(15X,F9.1,2(5X,F9.3))
280    FORMAT(//,30X,'CORRECTION FACTORS',//)
290    FORMAT(30X,'==================')
300    FORMAT(8X,'TIME',9X,'SPHERE ',4X,' FILAMENT',
      +3X,'TOTAL FORCE',3X,'WT CORRECTION',/)
310    FORMAT(61X,'(MG)',/)
320    FORMAT(5X,F6.1,3(5X,F9.8),5X,F4.3)
325    FORMAT(15X,'WEIGHT CORRECTION=',F9.8,8X,'MG',/)
330    FORMAT(22X,'TIME',9X,'FILAMENT',5X,'RADIATED',8X,'CONVECTED',//)
332    FORMAT(20X,'TIME',8X,'FILAMENT',8X,'RADIATED',//)
340    FORMAT(20X,F6.1,3(9X,F6.5))
342    FORMAT(20X,F6.1,2(9X,F6.5),9X,F6.4)
350    FORMAT(10X,F6.1,2(9X,F6.5))
400    FORMAT(20X,'TIME',5X,'MOISTURE',5X,'RATE MG/S',
      +5X,'RATE KG/M2/S',/)
410    FORMAT(15X,F6.1,9X,F9.3,5X,F9.7,5X,F9.8)
415    FORMAT(//,20X,'A COMPARISION OF THE DIFFERENT HEAT EFFECTS',/)
420    FORMAT(//,10X,'HEAT CONDUCTED BY THE FILAMENT,BY RADIATION
      +AND CONVECTION IN J',/)
425    FORMAT(//,10X,'WEIGHT CORRECTION          -----MG',/)
500    FORMAT(10X,'TIME',8X,'TEMP',8X,'WEIGHT',8X,'DIAMETER',/)
510    FORMAT(10X,F6.1,9X,F5.2,9X,F12.9)
       END
       SUBROUTINE UPDATE(WT,X1,TG,T,DF,LENGTH,VA,
      +FORCE1,FORCE2,FORCE3,DWT,REF,RED,WC1)
       REAL LENGTH
       G=9.81
       PA=1.2929*(273.15/TG)
       UA=4.568E-8*((TG-273.15)+(T-273.15))/2+1.72E-5
       RED=PA*VA*X1/UA
       IF(X1.LE.0)THEN
       GOTO 5000
       ENDIF
       IF(RED.LT.0.3)THEN
       CD=24/RED
       ELSEIF(RED.GT.0.3.AND.RED.LT.1000)THEN
```

```
      CD=18.5/(RED**0.6)
      ELSE
      CD=0.44
      ENDIF
5000  REF=PA*VA*DF/UA
      CF=0.8
      FORCE1=CD*3.1412*(X1**2)*PA*(VA**2)/8
      FORCE2=CF*DF*LENGTH*PA*(VA**2)/2
      FORCE3=FORCE2+FORCE1
      DWT=FORCE3/G
      WC1=WT+DWT
      RETURN
      END
```

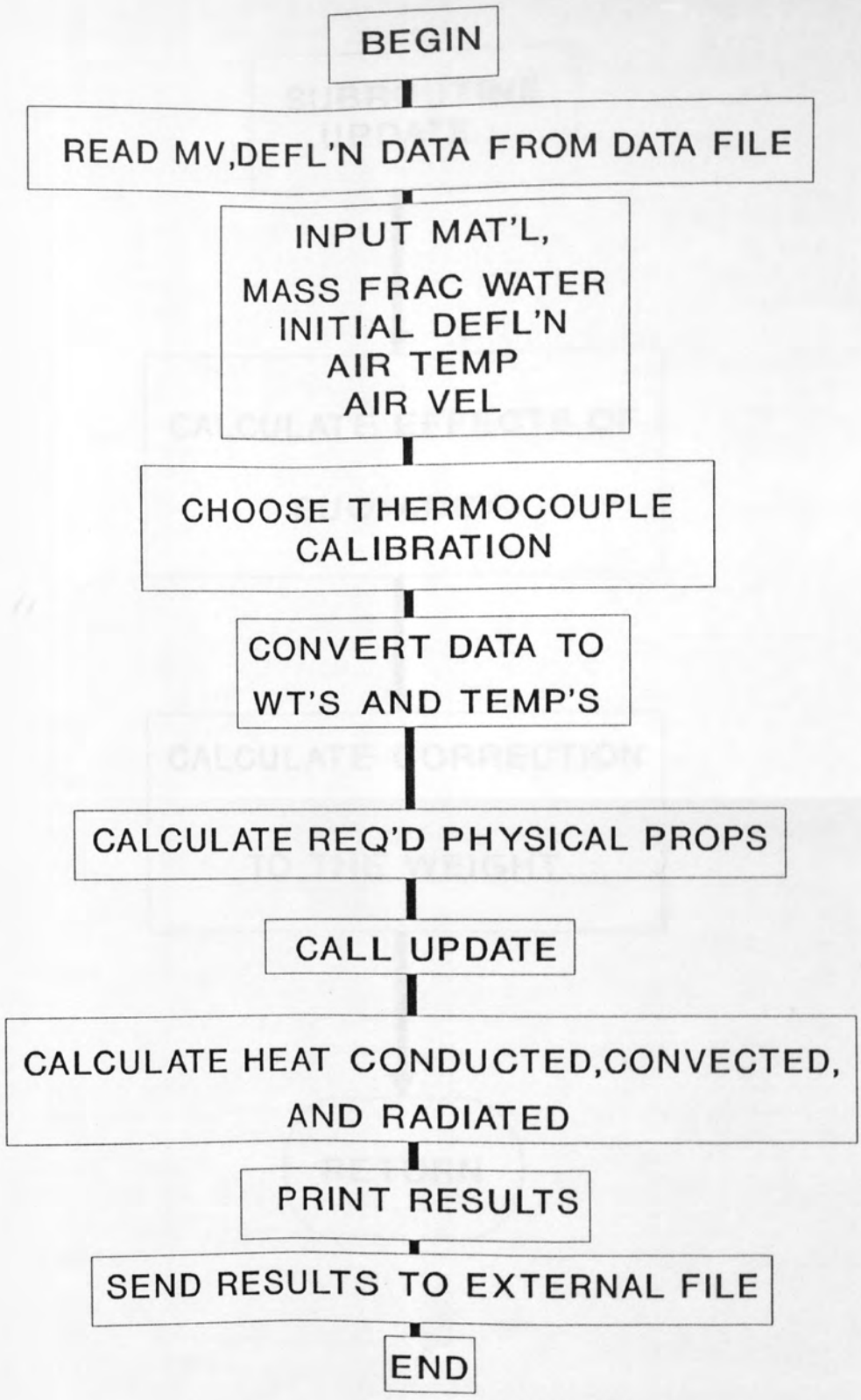
BEGIN
READ MV,DEFL'N DATA FROM DATA FILE
INPUT MAT'L,
MASS FRAC WATER
INITIAL DEFL'N
AIR TEMP
AIR VEL
CHOOSE THERMOCOUPLE CALIBRATION
CONVERT DATA TO WT'S AND TEMP'S
CALCULATE REQ'D PHYSICAL PROPS
CALL UPDATE
CALCULATE HEAT CONDUCTED,CONVECTED, AND RADIATED
PRINT RESULTS
SEND RESULTS TO EXTERNAL FILE
END

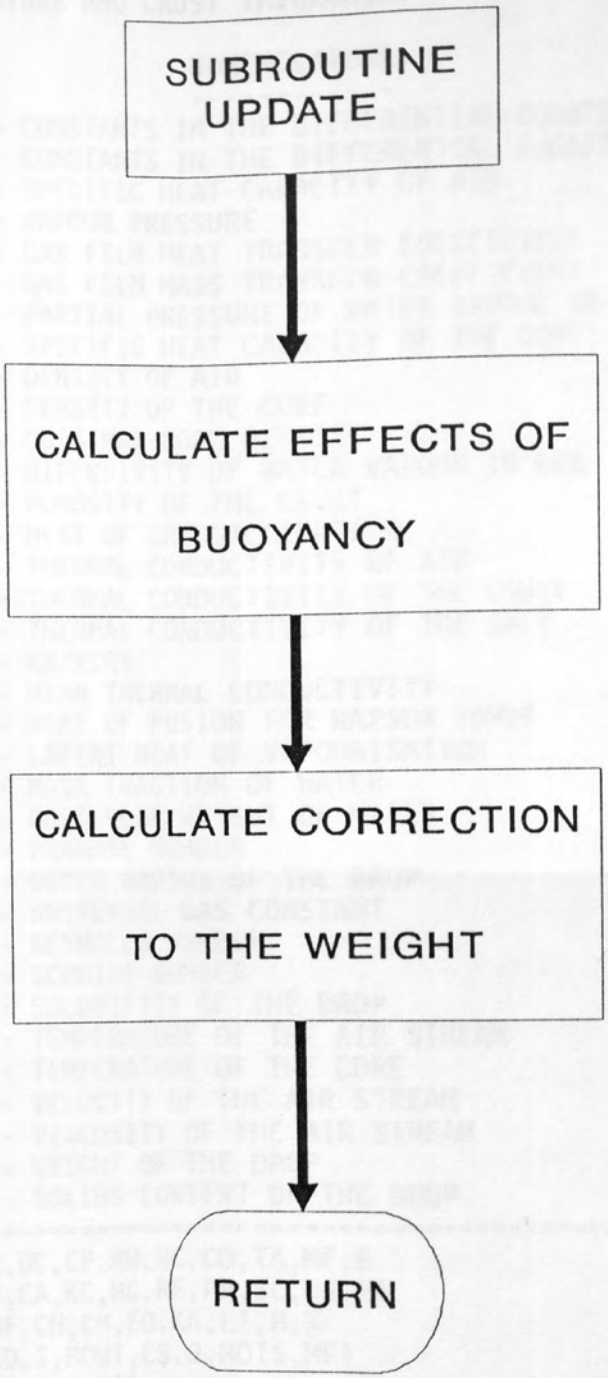
SUBROUTINE
UPDATE
CALCULATE EFFECTS OF
BUOYANCY
CALCULATE CORRECTION
TO THE WEIGHT
RETURN

```
*     ================================================
*                          GSB5
*                          ----
*
*     THIS PROGRAM USES A 4th ORDER RUNGE-KUTTA INTEGRATION
*     METHOD TO CALCULATE THE VARIATION IN DROP WEIGHT,DROP
*     TEMPERATURE AND CRUST THICKNESS.
*
*                       NOMENCLATURE
*                       ------------
*     A1-A4 - CONSTANTS IN THE DIFFERENTIAL EQUATIONS
*     B1-B3 - CONSTANTS IN THE DIFFERENTIAL EQUATIONS
*     CA    - SPECIFIC HEAT CAPACITY OF AIR              - J/KG/K
*     CC    - VAPOUR PRESSURE                            - ATMOSPHERES
*     CH    - GAS FILM HEAT TRANSFER COEFFICIENT         - W/M2/K
*     CM    - GAS FILM MASS TRANSFER COEFFICIENT         - M/S
*     CO    - PARTIAL PRESSURE OF WATER VAPOUR IN AIR    - ATMOSPHERES
*     CP    - SPECIFIC HEAT CAPACITY OF THE CORE         - J/KG/K
*     DA    - DENSITY OF AIR                             - KG/M3
*     DC    - DENSITY OF THE CORE                        - KG/M3
*     DCO   - ORIGINAL CORE DENSITY                      - KG/M3
*     DF    - DIFFUSIVITY OF WATER VAPOUR IN AIR         - M2/S
*     E     - POROSITY OF THE CRUST
*     HC    - HEAT OF CRYSTALLISATION                    - J/KG
*     KA    - THERMAL CONDUCTIVITY OF AIR                - W/M/K
*     KC    - THERMAL CONDUCTIVITY OF THE CRUST          - W/M/K
*     KCRY  - THERMAL CONDUCTIVITY OF THE SALT           - W/M/K
*     KD    - KA/KCRY
*     KM    - MEAN THERMAL CONDUCTIVITY
*     LF    - HEAT OF FUSION FOR NA2SO4 10H2O            - J/KG
*     LT    - LATENT HEAT OF VAPOURISATION               - J/KG
*     MF    - MASS FRACTION OF WATER
*     MW    - MOLECULAR WEIGHT OF WATER
*     PR    - PRANDTL NUMBER
*     R     - OUTER RADIUS OF THE DROP                   - M
*     RC    - UNIVERSAL GAS CONSTANT                     - ATMM3/KGMOLE/K
*     RE    - REYNOLDS NUMBER
*     SC    - SCHMIDT NUMBER
*     SOLU  - SOLUBILITY OF THE DROP
*     TA    - TEMPERATURE OF THE AIR STREAM              - K
*     T1    - TEMPERATURE OF THE CORE                    - K
*     V     - VELOCITY OF THE AIR STREAM                 - M/S
*     VA    - VISCOSITY OF THE AIR STREAM                - KG/M/S
*     W1    - WEIGHT OF THE DROP                         - KG
*     WS    - SOLIDS CONTENT OF THE DROP                 - KG
      ================================================================
      REAL R,DC,CP,MW,RC,CO,TA,MF,E
      REAL V,CA,KC,HC,RE,PR,SC,DA,VA
      REAL DF,CH,CM,ED,KA,LT,H,X
      REAL KO,I,MOUT,CS,J,MOIS,MF1
      REAL RO,DCO,KC1
      REAL KD,KM,CC,KCRY
      REAL VS,CMM,DIFFTM,DIFFPM,TRM
      DOUBLE PRECISION CUB
      INTEGER COUN
      COMMON HTC(0:2000),KO(0:2000),UO(0:2000)
      COMMON FOUT(0:2000)
      COMMON C(0:2000),P(0:2000),D(0:2000)
      COMMON X1(0:2000),TC(0:2000),HGD(0:2000),X2(0:2000)
      COMMON HCRCO(0:2000),HOUT(0:2000),MOUT(0:2000)
      COMMON ACCULN1(0:2000),VAP(0:2000)
      COMMON POR(02000),CCOEFF(0:2000)
      COMMON GASF(0:2000),HEATF(0:2000),CCOEFF(0:2000)
      COMMON TIME(0:2000),MOIS(0:2000),WT(0:2000)
```

```
      COMMON KC1(0:2000),CMM(0:2000),TR(0:2000)
      COMMON CHM(0:2000),X1M(0:2000),TCM(0:2000)
      COMMON CMM(0:2000),DIFFTM(0:2000),DIFFPM(0:2000)
      COMMON TRM(0:2000),DIFFT(0:2000),DIFFP(0:2000)
9000  CT=0
      MW=18.0
      PI=3.14159
      RC=8.20562E-2
      COUN2=1
      COUN3=0
      ======================================
      INPUT THE INITIAL OPERATING CONDITIONS
      ======================================
      PRINT*,'     WHICH MATERIAL ARE YOU USING'
      PRINT*,' '
      PRINT*,'     (1)      - NA2SO4 10H2O'
      PRINT*,'     (2)      - NACL'
      PRINT*,'     (3)      - K2SO4'
      PRINT*,'     (4)      - CUSO4'
      PRINT*,'     (5)      - CH3COONA'
      READ*,CH1
      PRINT*,'INPUT INITIAL TEMP---(C)'
      READ*,T1
      T1=T1+273.15
      PRINT*,'INPUT INITIAL WT  ---(MG)'
      READ*,W1
      W1=W1*1E-6
      PRINT*,'INPUT AIR TEMP    ---(C)'
      READ*,TA
      TA=TA+273.15
      PRINT*,'INPUT AIR VELOCITY---(M/S) '
      READ*,V
      PRINT*,'INPUT STEP SIZE'
      READ*,H
      PRINT*,'INPUT MASS FRACTION OF WATER'
      READ*,MF
      MF1=MF
      PRINT*,'INPUT PARTIAL PRESS OF H2O VAP IN AIR-(ATMOS)'
      READ*,CO
      W=W1
      WS=W1*(1-MF)
      CONC=WS/W1
      IF(CH1.EQ.1)THEN
      IF(T1.LE.306.15)THEN
      SOLU=0.292*10**(0.0331*(T1-273.15))
      ELSE
      SOLU=3.7125*10**(-0.001*(T1-273.15))
      ENDIF
      CS=142.04*SOLU/(1000+(142.04*SOLU))
      DCO=(1000*1464)/(1000*(1-MF)+1464*MF)
      ELSEIF(CH1.EQ.2)THEN
      SOLU=35.48+0.024748*(T1-273.15)+0.0001*((T1-273.15)
     +**2)+0.00000265555*((T1-273.15)**3)
      SOLU=SOLU/100
      CS=SOLU/(1+SOLU)
      CALL DENS(MF,T1,DCO)
      ELSEIF(CH1.EQ.3)THEN
      SOLU=0.4199+0.0114*(T1-273.15)-1.807E-5*((T1-273.15)**2)
      CS=174.25*SOLU/(1000+(174.25*SOLU))
      CALL DENS1(MF,T1,DCO)
      ELSEIF(CH1.EQ.4)THEN
      SOLU=0.864925+.03085*(T1-273.15)-0.00100695672*((T1-273.15)**2)
     ++1.47825E-5*((T1-273.15)**3)-7.21281E-8*((T1-273.15)**4)
      CS=159.61*SOLU/(1000+(159.61*SOLU))
```

```
CALL DENS2(MF,T1,DCO)
ELSE
SOLU=4.584+0.0188*(T1-273.15)+0.0016*((T1-273.15)**2)
CS=82.04*SOLU/(1000+(82.04*SOLU))
CALL DENS3(MF,T1,DCO)
ENDIF
PRINT*,'CONC  SOLU CS',CONC,SOLU,CS
CUB1=1
CUB2=3
CUB=CUB1/CUB2
R=(3*W1/4/PI/DCO)**CUB
X=R
DO 5 I=0,2000,1
IF(CH1.EQ.1.AND.T1.GE.306.15.AND.CT.LT.1)THEN
CALL LATENT(CT,DC,T1,W1,CP,X,QG,MF,MF1)
ENDIF
X1(I)=X
X2(I)=X1(I)*1000
TC(I)=T1
D(I)=(R-X)*1000
T(I)=W1
C(I)=T1-273.15
P(I)=(W-W1)/W
FRAC=P(I)
CALL PROPS(TA,T1,KA,LT,VA,DA,DF,CH1,DC,HC,CC,CP,KC,MF,CA,E)
IF(CONC.LT.CS.AND.CT.NE.1)THEN
IF(COUN3.NE.1)THEN
PRINT*,'INPUT WHETHER YOU WANT '
PRINT*,'       (1) VAP PRESS WATER IN CONSTANT RATE'
PRINT*,'       (2) VAP PRESS SAT SOLN IN CONSTANT RATE'
PRINT*,'       (3) NO CONSTANT RATE
READ*,CH3
COUN3=1
ENDIF
X=(3*W1/4/PI/DC)**CUB
KC1(I)=KC
KC1(0)=0
R=X
X1(I)=X
X2(I)=X1(I)*1000
ENDIF
IF(I.EQ.0)THEN
PRINT*,'DO YOU WISH TO USE A VARIABLE POROSITY'
PRINT*,' '
PRINT*,'OR A FIXED POROSITY'
PRINT*,'VARIABLE=1'
PRINT*,'FIXED=2'
READ*,CH2
IF(CH2.EQ.1)THEN
PRINT*,'INPUT A FINAL DRIED CRUST POROSITY'
READ*,EF
ELSE
PRINT*,'INPUT A FIXED CRUST POROSITY'
READ*,E
ENDIF
ENDIF
IF(CH2.EQ.1)THEN
E=1-2.4*((R-X)/R)
IF(E.LE.EF)THEN
E=EF
ENDIF
ENDIF
IF(CONC.LT.CS.AND.CT.NE.1)THEN
E=1
```

```
ENDIF
ED=(E**1.5)*DF
POR(I)=E
RE=2*R*V*DA/VA
PR=CA*VA/KA
SC=VA/DA/DF
CH=KA/2/R*(2+0.6*(RE**.5)*(PR**.33))
CM=DF/2/R*(2+0.6*(RE**.5)*(SC**.33))
GASF(I)=CM
HEATF(I)=CH
CHM(I)=(HEATF(I)+HEATF(I-1))/2
CMM(I)=(GASF(I)+GASF(I-1))/2
X1M(I)=(X1(I)+X1(I-1))/2
TCM(I)=(TC(I)+TC(I-1))/2
MOIS(I)=(W1-WS)/WS
IF(MOIS(I).LE.0)THEN
MOIS(I)=0
ENDIF
IF(D(I).LE.0)THEN
CCOEFF(I)=0
HTC(I)=0
KO(I)=CM
UO(I)=CH
ELSE
CCOEFF(I)=ED*E**1.5*X/R/D(I)
HTC(I)=KC*X/R/D(I)
CCOEFF(I)=1000*CCOEFF(I)
HTC(I)=HTC(I)*1000
KO(I)=CM*CCOEFF(I)/(CM+CCOEFF(I))
UO(I)=CH*HTC(I)/(CH+HTC(I))
ENDIF
IF(CONC.LT.CS.AND.CT.NE.1.AND.CH3.NE.3)THEN
J=I
IF(I.GT.0)THEN
HGD(I)=(CHM(I)*4*PI*X1M(I)**2*(TA-TCM(I)))
MOUT(I)=(WT(I-1)-WT(I))/H*1E-6
HOUT(I)=MOUT(I)*LT
ACCULN1(I)=HGD(I)-HOUT(I)
VAP(I)=MOUT(I)*1E+6
ENDIF
CALL CONSTANT(TA,V,RE,MF,X,T1,W1,SC,H,CO,CH1,CH3,E)
R=X
CONC=WS/W1
MF=(W1-WS)/W1
IF(CH1.EQ.1)THEN
IF(T1.LE.306.15)THEN
SOLU=0.292*10**(0.0331*(T1-273.15))
ELSE
SOLU=3.7125*10**(-0.001*(T1-273.15))
ENDIF
CS=142.04*SOLU/(1000+(142.04*SOLU))
ELSEIF(CH1.EQ.2)THEN
SOLU=35.48+0.024748*(T1-273.15)+0.0001*((T1-273.15)
+**2)+0.00000265555*((T1-273.15)**3)
SOLU=SOLU/100
CS=SOLU/(1+SOLU)
ELSEIF(CH1.EQ.3)THEN
SOLU=0.4199+0.0114*(T1-273.15)-1.807E-5*((T1-273.15)**2)
CS=174.25*SOLU/(1000+(174.25*SOLU))
ELSEIF(CH1.EQ.4)THEN
SOLU=0.864925+.03085*(T1-273.15)-0.0000695672*((T1-273.15)**2)
++1.47825E-5*((T1-273.15)**3)-7.21281E-8*((T1-273.15)**4)
CS=159.61*SOLU/(1000+(159.61*SOLU))
ELSE
```

```
      SOLU=4.584+0.0188*(T1-273.15)+0.0016*((T1-273.15)**2)
      CS=82.04*SOLU/(1000+(82.04*SOLU))
      ENDIF
      ELSE
      IF(COUN2.EQ.1)THEN
      COUN2=2
      PRINT*,'RADIUS OF THE DROP',R
      ENDIF
      IF(X.LE.0.OR.FRAC.GE.MF1)THEN
      HGD(I)=(CHM(I)*4*PI*R**2*(TA-TCM(I)))
      ACCULN1(I)=4*PI*R**3*CP*DC*(TC(I)-TC(I-1))/3
      GOTO 7
      ENDIF
      AO=R*(R-X)*CH/KC/X
      TR(I)=(AO*TA+T1)/(1+AO)
      BO=CM*R*(R-X)/ED/X
      VS=(MW/(1+BO)/RC)*((BO*CO/TA)+CC/T1)
      IF(R.EQ.X)THEN
      DIFFT(I)=0
      DIFFP(I)=0
      ELSE
      DIFFT(I)=(AO/(1+AO))*(R/X/(R-X))*(TA-T1)
      DIFFP(I)=(R/X/(R-X))*(BO/(1+BO))*(MW/RC)*(CO/TA-CC/T1)
      ENDIF
      IF(I.GT.J)THEN
      IF(TR(I-1).EQ.0)THEN
      TRM(I)=TR(I)
      ELSE
      TRM(I)=(TR(I)+TR(I-1))/2
      ENDIF
      DIFFTM(I)=(DIFFT(I)+DIFFT(I-1))/2
      DIFFPM(I)=(DIFFP(I)+DIFFP(I-1))/2
      HGD(I)=(CHM(I)*4*PI*R**2*(TA-TRM(I)))
      HCRCO(I)=(4*PI*X1M(I)**2*KC*DIFFTM(I))
      MOUT(I)=(WT(I-1)-WT(I))/H*1E-6
      HOUT(I)=MOUT(I)*(LT-HC)
      ACCULN1(I)=HGD(I)-HOUT(I)
      VAP(I)=MOUT(I)*1E6
      ENDIF
7     CALL RUNGE(X,TA,T1,R,MF,MF1,W1,ED,V,MW,RC,FRAC,H,
     +CC,CO,RE,SC,CH1,E)
      ENDIF
      IF(H.EQ.0.001.AND.COUN.EQ.0)THEN
      GOTO 3
      ENDIF
      TIME(I)=I
5     CONTINUE
      PRINT 200
      PRINT 210
      PRINT 220
      PRINT 230
      PRINT 240
      PRINT 250
      PRINT 260
      PRINT 270
      PRINT*,' INPUT CHOICE OF INTEREST---(1-6)'
      READ*,N
400   PRINT*,'INPUT COUNTERS FOR DATA OUTPUT'
      PRINT*,'C1-C2----GIVES DATA POINTS IN STEPS OF C3'
      PRINT*,'C4-C5----GIVES DATA POINTS IN STEPS OF C6'
      READ*,C1,C2,C3,C4,C5,C6
405   CONTINUE
410   IF(N.EQ.1)THEN
      PRINT 280
```

```
      DO 500 I=C1,C2,C3
      PRINT 290,TIME(I),POR(I),KC1(I),X2(I),WT(I)
 500  CONTINUE
      DO 505 I=C4+1,C5,C6
      PRINT 290,TIME(I),POR(I),KC1(I),X2(I),WT(I)
 505  CONTINUE
      IF(N.EQ.2)THEN
      PRINT*,'              MASS TRANSFER COEFFICIENTS'
      PRINT*,'                    (M/S)'
      PRINT*,'              ========================='
      PRINT*,' '
      PRINT*,' '
      PRINT 300
      DO 510 I=C1,C2,C3
      PRINT 310,I,CCOEFF(I),GASF(I),KO(I)
510   CONTINUE
      DO 515 I=C4+1,C5,C6
      PRINT 310,I,CCOEFF(I),GASF(I),KO(I)
515   CONTINUE
      ELSEIF(N.EQ.3)THEN
      PRINT*,'              HEAT TRANSFER COEFFICIENTS'
      PRINT*,'                    (W/M2/K)'
      PRINT*,'              ========================='
      PRINT*,' '
      PRINT*,' '
      PRINT*,' '
      PRINT 300
      DO 520 I=C1,C2,C3
      PRINT 315,I,HTC(I),HEATF(I),UO(I)
520   CONTINUE
      DO 525 I=C4+1,C5,C6
      PRINT 315,I,HTC(I),HEATF(I),UO(I)
525   CONTINUE
      ELSEIF(N.EQ.4)THEN
      PRINT*,'                      HEAT BALANCE---WATTS'
      PRINT 320
      DO 530 I=C1,C2,C3
      PRINT 340,TIME(I),HGD(I),HCRCO(I),HOUT(I),ACCULN1(I)
 530  CONTINUE
      DO 535 I=C4+1,C5,C6
      PRINT 340,TIME(I),HGD(I),HCRCO(I),HOUT(I),ACCULN1(I)
 535  CONTINUE
      ELSEIF(N.EQ.5)THEN
      PRINT*,'              MASS BALANCE----MG/S'
      PRINT 330
      DO 540 I=C1,C2,C3
      PRINT 350,TIME(I),VAP(I),MOIS(I)
 540  CONTINUE
      DO 545 I=C4+1,C5,C6
      PRINT 350,TIME(I),VAP(I),MOIS(I)
 545  CONTINUE
      ELSE
      PRINT 360
      PRINT 363
      PRINT 365
      DO 550 I=C1,C2,C3
      PRINT 370,I,D(I),C(I),P(I)
550   CONTINUE
      DO 555 I=C4+1,C5,C6
      PRINT 370,I,D(I),C(I),P(I)
555   CONTINUE
      ENDIF
100   FORMAT(//////////,25X,'EXPERIMENTAL CONDITIONS')
102   FORMAT(25X,'======================',/)
```

```
104   FORMAT(17X,'NA2SO41OH2O----',F4.1,'WT %',/)
105   FORMAT(17X,'NACL       ----',F4.1,'WT %',/)
106   FORMAT(17X,'K2SO4      ----',F4.1,'WT %',/)
107   FORMAT(17X,'CUSO4      ----',F4.1,'WT %',/)
108   FORMAT(17X,'CH3COONA   ----',F4.1,'WT %',/)
109   FORMAT(17X,'AIR TEMP(C)----',F6.2,/)
110   FORMAT(17X,'AIR VELOCITY  (M/S)',5X,F4.2,/)
112   FORMAT(17X,'INITIAL DROP WEIGHT (MG)',5X,F4.2,/)
120   FORMAT(17X,'EXPERIMENTAL REFERENCE',5X,'D',I3)
200   FORMAT(25X,'EXPERIMENTAL RESULTS')
210   FORMAT(25X,'====================')
220   FORMAT(5X,'(1)------  POROSITY',/)
230   FORMAT(5X,'(2)------  MASS TRANSFER COEFFICIENTS',/)
240   FORMAT(5X,'(3)------  HEAT TRANSFER COEFFICIENTS',/)
250   FORMAT(5X,'(4)------  HEAT BALANCE',/)
260   FORMAT(5X,'(5)------  MASS BALANCE',/)
270   FORMAT(5X,'(6)------  PREDICTED RESULTS',/)
280   FORMAT(7X,'TIME(S)',5X,'POROSITY',7X,'KCRUST',7X,'RADIUS'
     +,9X,'WEIGHT',//)
290    FORMAT(2X,F9.4,4(5X,F9.6))
300    FORMAT(4X,'TIME(S)',10X,'CRUSTCOEFF',10X,'GAS COEFF',10X
     +,'OVERALLCOEFF',//)
310    FORMAT(1X,F9.4,10X,F12.5,10X,F10.5,10X,F10.3)
315    FORMAT(1X,F9.4,10X,F12.3,10X,F10.3,10X,F10.3)
320    FORMAT(2X,'TIME(S)',4X,'HEAT IN GAS',4X,'HEAT IN CRUST',3X,
     +'HEAT OUT',4X,'ACCUMULATION')
330    FORMAT(2X,'TIME(S)',7X,'MASS OUT',7X,'MOISTURE CONTENT')
340    FORMAT(2X,F9.4,4(5X,F9.5))
350    FORMAT(2X,F9.4,5X,F6.5,5X,F9.5)
360    FORMAT(///,22X,'TIME(S)',6X,'CRUST',9X,'DROP ',10X,
     +'FRACTION OF')
363    FORMAT(35X,'THICKNESS',5X,'TEMPERATURE',4X,'INITIAL WEIGHT')
365    FORMAT(37X,'(MM)',8X,'(C)',12X,'EVAPORATED')
370    FORMAT(17X,F9.1,5X,F9.2,5X,F9.2,5X,F9.2)
375    FORMAT(///)
380    FORMAT(25X,'MASS TRANSFER COEFFICIENTS M/S',/)
385    FORMAT(25X,'HEAT TRANSFER COEFFICIENTS W/M2/K',/)
390    FORMAT(25X,'HEAT BALANCE   WATTS',/)
395    FORMAT(25X,'MASS BALANCE   MG/S',/)
397    FORMAT(25X,'PREDICTED RESULTS',/)
       PRINT*,'DO YOU WISH TO SEE ANOTHER TABLE Y=1,N=2-9'
       READ*,ANS
       IF(ANS.EQ.1)THEN
       PRINT*,'INPUT CHOICE OF INTEREST  1-6'
       READ*,N
       PRINT*,'DO YOU WISH TO CHANGE STEP SIZE FOR'
       PRINT*,'         DATA OUTPUT     Y=1,N=2-9'
       READ*,ANS1
       IF(ANS1.EQ.1)THEN
       GOTO 400
       ELSE
       GOTO 405
       ENDIF
       ENDIF
       PRINT*,'DO YOU WISH TO SEND THE RESULTS TO'
       PRINT*,'AN EXTERNAL FILE'
       PRINT*,'YES=1 AND ENTER FILENAME'
       READ*,ANS1
       IF(ANS1.EQ.1)THEN
       OPEN(UNIT=10,FILE=' ')
       PRINT*,'INPUT COUNTERS FOR DATA OUTPUT'
       PRINT*,'C1-C2----GIVES DATA POINTS IN STEPS OF C3'
       PRINT*,'C4-C5----GIVES DATA POINTS IN STEPS OF C6'
       READ*,C1,C2,C3,C4,C5,C6
```

```
      PRINT*,'INPUT EXPERIMENTAL REFERENCE'
      READ*,REF
      WRITE(10,100)
      WRITE(10,102)
      IF(CH1.EQ.1)THEN
      WRITE(10,104) (1-MF1)*100
      ELSEIF(CH1.EQ.2)THEN
      WRITE(10,105) (1-MF1)*100
      ELSEIF(CH1.EQ.3)THEN
      WRITE(10,106) (1-MF1)*100
      ELSEIF(CH1.EQ.4)THEN
      WRITE(10,107) (1-MF1)*100
      ELSE
      WRITE(10,108) (1-MF1)*100
      ENDIF
      WRITE(10,109) TA-273.15
      WRITE(10,110) V
      WRITE(10,112) W*1E6
      WRITE(10,120) REF
      WRITE(10,375)
      WRITE(10,280)
      DO 1000 I=C1,C2,C3
      WRITE(10,290) TIME(I),POR(I),KC1(I),X2(I),WT(I)
1000  CONTINUE
      DO 1600 I=C4,C5,C6
      WRITE(10,290) TIME(I),POR(I),KC1(I),X2(I),WT(I)
1600  CONTINUE
      WRITE(10,375)
      WRITE(10,380)
      WRITE(10,300)
      DO 1100 I=C1,C2,C3
      WRITE(10,310) I,CCOEFF(I),GASF(I),KO(I)
1100  CONTINUE
      DO 1700 I=C4,C5,C6
      WRITE(10,310) I,CCOEFF(I),GASF(I),KO(I)
1700  CONTINUE
      WRITE(10,375)
      WRITE(10,385)
      WRITE(10,300)
      DO 1200 I=C1,C2,C3
      WRITE(10,315) I,HTC(I),HEATF(I),UO(I)
1200  CONTINUE
      DO 1800 I=C4,C5,C6
      WRITE(10,315) I,HTC(I),HEATF(I),UO(I)
1800  CONTINUE
      WRITE(10,375)
      WRITE(10,390)
      WRITE(10,320)
      DO 1300 I=C1,C2,C3
      WRITE(10,340) TIME(I),HGD(I),HCRCO(I),HOUT(I),ACCULN1(I)
1300  CONTINUE
      DO 1900 I=C4,C5,C6
      WRITE(10,340) TIME(I),HGD(I),HCRCO(I),HOUT(I),ACCULN1(I)
1900  CONTINUE
      WRITE(10,375)
      WRITE(10,395)
      WRITE(10,330)
      DO 1400 I=C1,C2,C3
      WRITE(10,350) TIME(I),VAP(I),MOIS(I)
1400  CONTINUE
      DO 2000 I=C4,C5,C6
      WRITE(10,350) TIME(I),VAP(I),MOIS(I)
2000  CONTINUE
      WRITE(10,375)
```

```
      WRITE(10,397)
      WRITE(10,360)
      WRITE(10,363)
      WRITE(10,365)
      DO 1500 I=C1,C2,C3
      WRITE(10,370) I,D(I),C(I),P(I)
1500  CONTINUE
      DO 2100 I=C4,C5,C6
      WRITE(10,370) I,D(I),C(I),P(I)
2100  CONTINUE
      ENDIF
      PRINT*,'DO YOU WISH TO RUN THE PROGRAM AGAIN'
      PRINT*,'YES = 1 NO = 2-9'
      READ*,ANS3
      IF(ANS3.EQ.1)THEN
      GOTO 9000
      ENDIF
      END
      ========================================================
      SUBROUTINE TO CALCULATE THE PHYSICAL PROPERTIES OF THE
      SYSTEM
      ========================================================
      SUBROUTINE PROPS(TA,T1,KA,LT,VA,DA,DF,CH1,DC,HC,CC,CP,KC,MF,CA,E)
      REAL TA,T1,KA,LT,VA,DA,DF,KC,DC,HC,CC,CP,MF,CA
      REAL KCRY,KD,KM
      CA=1036.23
      TM=((TA-273.15)+(T1-273.15))/2
      KA=(4.2956E-5*TM+0.014)*1.7307
      LT=(1075.95-1.0246*(T1-273.15))*2326.0
      VA=4.568E-8*TM+1.7199E-5
      DA=(1.2929*273.15)/(T1+TA)*2
      CONC1=(1-MF)*100
      IF(CH1.EQ.1)THEN
      DC=(1000*1464)/(1000*(1-MF)+1464*MF)
      HC=152
      CC=(EXP(-5104.054/T1+20.207))/760
      CP=3300
      KCRY=0.6
      ELSEIF(CH1.EQ.2)THEN
      CALL DENS(MF,T1,DC)
      CALL PRESS(MF,T1,CC)
      HC=25.8
      CP=3880.061+0.6059*T1
      KCRY=11.2142-0.0157*T1
      ELSEIF(CH1.EQ.3)THEN
      CALL DENS1(MF,T1,DC)
      CALL PRESS1(MF,T1,CC)
      HC=116.95
      CP=4870-327.5*CONC1+33.75*CONC1**2-1.25*CONC1**3
      KCRY=0.104
      ELSEIF(CH1.EQ.4)THEN
      CALL DENS2(MF,T1,DC)
      CC=(EXP(19.4297-4281.1/T1))/760
      HC=116
      CP=4184.22-48.1576*CONC1+0.400408*CONC1**2-0.0147358*CONC1**3
      KCRY=0.4
      ELSE
      CALL DENS3(MF,T1,DC)
      CC=(EXP(20.767-5600/T1))/760
      HC=170
      CP=4188.47-36.2015*CONC1+0.629099*CONC1**2-0.00851489*CONC1**3
      KCRY=0.42
      ENDIF
      KD=KA/KCRY
```

```
      KM=(KD+2-(2*E*(1-KD)))/(KD+2+(E*(1-KD)))
      KC=KM*KCRY
      DF=0.22*(((TA+T1)/2/273.15)**1.75)/1E+4
      RETURN
      END
      ================================
      SUBROUTINE FOR THE CONSTANT RATE
      ================================
      SUBROUTINE CONSTANT(TA,V,RE,MF,X,T1,W1,SC,H,CO,CH1,CH3,E)
      REAL KA,LT,CA,TA,V,DA,UA,PR,RE,MF,T1,W1,MW,KC
      REAL KT1,KT2,KT3,KT4
      REAL KW1,KW2,KW3,KW4
      CUB1=1
      CUB2=3
      CUB=CUB1/CUB2
      PI=3.14159
      MW=18
      CALL PROPS(TA,T1,KA,LT,VA,DA,DF,CH1,DC,HC,CC,CP,KC,MF,CA,E)
      RC=8.20562E-2
      IF(CH3.EQ.1)THEN
      CC=(EXP(18.3036-(3816.44/(T1-46.13))))/760
      ENDIF
      CM=DF/2/X*(2+0.6*(RE**.5)*(SC**.33))
      DW=CM*4*PI*X**2*MW*((CO/TA)-(CC/T1))/RC
      CALL UPTEMP(Z1,Z2,Z3,TA,T1,X,MF,MW,RC,V,CO,CH1,CH3,W1,DC)
      DT=4*PI*X**2*(Z1+Z2)/Z3
      W=W1
      T=T1
      KW1=H*DW
      KT1=H*DT
      W1=W+KW1/2
      T1=T+KT1/2
      DW1=CM*4*PI*X**2*MW*((CO/TA)-(CC/T1))/RC
      CALL UPTEMP(Z1,Z2,Z3,TA,T1,X,MF,MW,RC,V,CO,CH1,CH3,W1,DC)
      DT1=4*PI*X**2*(Z1+Z2)/Z3
      KW2=H*DW1
      KT2=H*DT1
      W1=W+KW2/2
      T1=T+KT2/2
      DW2=CM*4*PI*X**2*MW*((CO/TA)-(CC/T1))/RC
      CALL UPTEMP(Z1,Z2,Z3,TA,T1,X,MF,MW,RC,V,CO,CH1,CH3,W1,DC)
      DT2=4*PI*X**2*(Z1+Z2)/Z3
      KW3=H*DW2
      KT3=H*DT2
      W1=W+KW3
      T1=T+KT3
      DW3=CM*4*PI*X**2*MW*((CO/TA)-(CC/T1))/RC
      CALL UPTEMP(Z1,Z2,Z3,TA,T1,X,MF,MW,RC,V,CO,CH1,CH3,W1,DC)
      DT3=4*PI*X**2*(Z1+Z2)/Z3
      KW4=H*DW3
      KT4=H*DT3
      T1=T
      W1=W
90    T1=T1+(KT1+2*KT2+2*KT3+KT4)/6
      W1=W1+((KW1+2*KW2+2*KW3+KW4)/6)
      RETURN
      END
      ================================
      SUBROUTINE FOR THE FALLING RATE
      ================================
      SUBROUTINE RUNGE(X,TA,T1,R,MF,MF1,W1,ED
     +,V,MW,RC,FRAC,H,CC,CO,RE,SC,CH1,E)
      REAL A1,A2,A3,A4,B1,B2,B3,T1,W1
      REAL KA,LT
```

```
REAL KT1,KT2,KT3,KT4
REAL KW1,KW2,KW3,KW4
REAL KX1,KX2,KX3,KX4
REAL MF1,H,KC,MF,MW
PI=3.14159
DCO=DC
CALL PROPS(TA,T1,KA,LT,VA,DA,DF,CH1,DC,HC,CC,CP,KC,MF,CA,E)
FF=MF1-FRAC
IF(FF.LE.0.05.OR.X.LE.0)THEN
CALL UPT1(CH,TA,T1,R,CP,V,CA,CH1,MF)
DT=3*CH*(TA-T1)/R/DC/CP
T=T1
KT1=H*DT
T1=T+KT1/2
CALL UPT1(CH,TA,T1,R,CP,V,CA,CH1,MF)
DT1=3*CH*(TA-T1)/R/DC/CP
KT2=H*DT1
T1=T+KT2/2
CALL UPT1(CH,TA,T1,R,CP,V,CA,CH1,MF)
DT2=3*CH*(TA-T1)/R/DC/CP
KT3=H*DT2
T1=T+KT3
CALL UPT1(CH,TA,T1,R,CP,V,CA,CH1,MF)
DT3=3*CH*(TA-T1)/R/DC/CP
KT4=H*DT3
T1=T
KX1=0
KX2=0
KX3=0
KX4=0
KW1=0
KW2=0
KW3=0
KW4=0
GOTO 110
ENDIF
CALL UPX(B1,B2,B3,DC,MF,RC,ED,RE,SC,DF,X,R)
DX=(B1/(B2*(X**2)+(B3*X)))*((CO/TA)-(CC/T1))
CALL UPT(A1,A2,A3,A4,T1,TA,R,MW,RC,MF,V,CO,CH1)
DT=(((A1*(TA-T1))/(A2*X**2+A3*X)/A4/X)+(DX/A4/X))
DW=4*PI*DC*MF*DX*X**2
X1=X
W=W1
T=T1
KT1=H*DT
KX1=H*DX
KW1=H*DW
X=X1+KX1/2
W1=W+KW1/2
T1=T+KT1/2
CALL UPX(B1,B2,B3,DC,MF,RC,ED,RE,SC,DF,X,R)
DX1=(B1/(B2*(X**2)+(B3*X)))*((CO/TA)-(CC/T1))
CALL UPT(A1,A2,A3,A4,T1,TA,R,MW,RC,MF,V,CO,CH1)
DT1=(((A1*(TA-T1))/(A2*X**2+A3*X)/A4/X)+(DX1/A4/X))
DW1=4*PI*DC*MF*DX1*X**2
KX2=H*DX1
KW2=H*DW1
KT2=H*DT1
T1=T+KT2/2
X=X1+KX2/2
W1=W+KW2/2
CALL UPX(B1,B2,B3,DC,MF,RC,ED,RE,SC,DF,X,R)
DX2=(B1/(B2*(X**2)+(B3*X)))*((CO/TA)-(CC/T1))
CALL UPT(A1,A2,A3,A4,T1,TA,R,MW,RC,MF,V,CO,CH1)
```

```
      DT2=(((A1*(TA-T1))/(A2*X**2+A3*X)/A4/X)+(DX2/A4/X))
      DW2=4*PI*DC*MF*DX2*X**2
      KX3=H*DX2
      KW3=H*DW2
      KT3=H*DT2
      X=X1+KX3
      W1=W+KW3
      T1=T+KT3
      CALL UPX(B1,B2,B3,DC,MF,RC,ED,RE,SC,DF,X,R)
      DX3=(B1/(B2*(X**2)+(B3*X)))*((CO/TA)-(CC/T1))
      CALL UPT(A1,A2,A3,A4,T1,TA,R,MW,RC,MF,V,CO,CH1)
      DT3=(((A1*(TA-T1))/(A2*X**2+A3*X)/A4/X)+(DX3/A4/X))
      DW3=4*PI*DC*MF*DX3*X**2
      KX4=H*DX3
      KW4=H*DW3
      KT4=H*DT3
      W1=W
      X=X1
      T1=T
      IF(X.LE.0)THEN
      X=0
      ENDIF
110   T1=T1+(KT1+2*KT2+2*KT3+KT4)/6
      W1=W1+(KW1+2*KW2+2*KW3+KW4)/6
      X=X+(KX1+2*KX2+2*KX3+KX4)/6
      RETURN
      END
      SUBROUTINE UPTEMP(Z1,Z2,Z3,TA,T1,X,MF,MW
     +,RC,V,CO,CH1,CH3,W1,DC)
      REAL MF,MW,KA,LT,KC
      CPW=1700+0.572*T1
      CALL PROPS(TA,T1,KA,LT,VA,DA,DF,CH1,DC,HC,CC,CP,KC,MF,CA,E)
      IF(CH3.EQ.1)THEN
      CC=(EXP(18.3036-(3816.44/(T1-46.13))))/760
      CP=CPW
      DC=1000
      ENDIF
      RE=2*X*V*DA/VA
      PR=CA*VA/KA
      SC=VA/DA/DF
      CM=DF/2/X*(2+0.6*(RE**.5)*(SC**.33))
      CH=KA/2/X*(2+0.6*(RE**.5)*(PR**.33))
      Z1=CH*(TA-T1)
      Z2=-CM*MW*((CC/T1)-(CO/TA))*(LT+CPW*TA)/RC
      Z3=W1*CP
      END
      SUBROUTINE UPX(B1,B2,B3,DC,MF,RC,ED,RE,SC,DF,X,R)
      REAL MF,MW
      MW=18
      IF(X.EQ.0)THEN
      GOTO 9
      ENDIF
      CM=DF/2/X*(2+0.6*(RE**.5)*(SC**.33))
      B1=R**2*ED*MW*CM/DC/MF/RC
      B2=ED-R*CM
      B3=R**2*CM
9     RETURN
      END
      SUBROUTINE UPT(A1,A2,A3,A4,T1,TA,R,MW,RC,MF,V
     +,CO,CH1)
      REAL KC,MW,MF,KA,LT,HC
      CPW=1700+0.572*T1
      CALL PROPS(TA,T1,KA,LT,VA,DA,DF,CH1,DC,HC,CC,CP,KC,MF,CA,E)
```

```
      DT2=(((A1*(TA-T1))/(A2*X**2+A3*X)/A4/X)+(DX2/A4/X))
      DW2=4*PI*DC*MF*DX2*X**2
      KX3=H*DX2
      KW3=H*DW2
      KT3=H*DT2
      X=X1+KX3
      W1=W+KW3
      T1=T+KT3
      CALL UPX(B1,B2,B3,DC,MF,RC,ED,RE,SC,DF,X,R)
      DX3=(B1/(B2*(X**2)+(B3*X)))*((CO/TA)-(CC/T1))
      CALL UPT(A1,A2,A3,A4,T1,TA,R,MW,RC,MF,V,CO,CH1)
      DT3=(((A1*(TA-T1))/(A2*X**2+A3*X)/A4/X)+(DX3/A4/X))
      DW3=4*PI*DC*MF*DX3*X**2
      KX4=H*DX3
      KW4=H*DW3
      KT4=H*DT3
      W1=W
      X=X1
      T1=T
      IF(X.LE.0)THEN
      X=0
      ENDIF
110   T1=T1+(KT1+2*KT2+2*KT3+KT4)/6
      W1=W1+(KW1+2*KW2+2*KW3+KW4)/6
      X=X+(KX1+2*KX2+2*KX3+KX4)/6
      RETURN
      END
      SUBROUTINE UPTEMP(Z1,Z2,Z3,TA,T1,X,MF,MW
     +,RC,V,CO,CH1,CH3,W1,DC)
      REAL MF,MW,KA,LT,KC
      CPW= 1700 + 0·572 T1
      CALL PROPS(TA,T1,KA,LT,VA,DA,DF,CH1,DC,HC,CC,CP,KC,MF,CA,E)
      IF(CH3.EQ.1)THEN
      CC=(EXP(18.3036-(3816.44/(T1-46.13))))/760
      CP=CPW
      DC=1000
      ENDIF
      RE=2*X*V*DA/VA
      PR=CA*VA/KA
      SC=VA/DA/DF
      CM=DF/2/X*(2+0.6*(RE**.5)*(SC**.33))
      CH=KA/2/X*(2+0.6*(RE**.5)*(PR**.33))
      Z1=CH*(TA-T1)
      Z2=-CM*MW*((CC/T1)-(CO/TA))*(LT+CPW*TA)/RC
      Z3=W1*CP
      END
      SUBROUTINE UPX(B1,B2,B3,DC,MF,RC,ED,RE,SC,DF,X,R)
      REAL MF,MW
      MW=18
      IF(X.EQ.0)THEN
      GOTO 9
      ENDIF
      CM=DF/2/X*(2+0.6*(RE**.5)*(SC**.33))
      B1=R**2*ED*MW*CM/DC/MF/RC
      B2=ED-R*CM
      B3=R**2*CM
9     RETURN
      END
      SUBROUTINE UPT(A1,A2,A3,A4,T1,TA,R,MW,RC,MF,V
     +,CO,CH1)
      REAL KC,MW,MF,KA,LT,HC
      CPW=1700+0·572 T1
      CALL PROPS(TA,T1,KA,LT,VA,DA,DF,CH1,DC,HC,CC,CP,KC,MF,CA,E)
      RE=2*R*V*DA/VA
```

```
PR=CA*VA/KA
SC=VA/DA/DF
CH=KA/2/R*(2+0.6*(RE**.5)*(PR**.33))
CM=DF/2/R*(2+0.6*(RE**.5)*(SC**.33))
FAC=(CH-(CM*CP*MW*(((CO/TA)-(CC/T1))/RC)))
A1=R**2*KC*FAC/DC/MF/(LT-HC)
A2=KC-R*FAC
A3=R**2*FAC
A4=CP/3/MF/(LT-HC)
RETURN
END
SUBROUTINE UPT1(CH,TA,T1,R,CP,V,CA,CH1,MF)
REAL KA,LT,KC,MF
CALL PROPS(TA,T1,KA,LT,VA,DA,DF,CH1,DC,HC,CC,CP,KC,MF,CA,E)
RE=2*R*V*DA/VA
PR=CA*VA/KA
CH=KA/2/R*(2+0.6*(RE**.5)*(PR**.33))
RETURN
END
SUBROUTINE DENS(CONC,T,DC)
REAL CONC,T
REAL F
REAL A1,A2,A3,A4,A5,A6,A7,A8,B1,B2,B3,B4,B5,B6
REAL C1,C2,C3,C4,DC,CONC1,T1,CC
INTEGER M,N,P,Q
DIMENSION F(0:14,0:10)
DATA((F(I,J),J=0,10),I=0,14)/0,0,10,20,25,30,40,50,60
+,80,100
+,1,1.00747,1.00707,1.00534,1.00409,1.00261,.99908
+,0.99482,.99,.9785,.9651
+,2,1.01509,1.01442,1.01246,1.01112,1.00957,1.00593
+,1.00161,.9967,.9852,.9719
+,4,1.03038,1.0292,1.0268,1.0253,1.02361,1.01977
+,1.01531,1.0103,.9988,.9855
+,6,1.04575,1.04408,1.04127,1.03963,1.03781,1.03378
+,1.02919,1.0241,1.0125,.9994
+,8,1.06121,1.05907,1.05589,1.05412,1.05219,1.04798
+,1.04326,1.0381,1.0264,1.0134
+,10,1.07677,1.07419,1.07068,1.06879,1.06676,1.06238
+,1.05753,1.0523,1.0405,1.0276
+,12,1.09244,1.08946,1.08566,1.08365,1.08153,1.07699
+,1.07202,1.0667,1.0549,1.0420
+,14,1.10824,1.10491,1.10085,1.09872,1.09651,1.09182
+,1.08674,1.0813,1.0694,1.0565
+,16,1.12419,1.12056,1.11621,1.11401,1.11171,1.10688
+,1.1017,1.0962,1.0842,1.0713
+,18,1.14031,1.13643,1.1319,1.12954,1.12715,1.12218
+,1.11691,1.1113,1.0993,1.0864
+,20,1.15663,1.15254,1.14779,1.14533,1.14285,1.13774
+,1.13238,1.1268,1.1146,1.1017
+,22,1.17318,1.16891,1.16395,1.1614,1.15883,1.15358
+,1.14812,1.1425,1.1303,1.1172
+,24,1.18999,1.18557,1.1804,1.17776,1.17511,1.16971
+,1.16414,1.1584,1.1463,1.1331
+,26,1.20709,1.20254,1.19717,1.19443,1.19170,1.18614
+,1.18045,1.1747,1.1626,1.1492/
 T=T-273.15
 T2=T
 IF(T.LT.0)THEN
 T=0
 ENDIF
 CONC=(1-CONC)*100
 CONC2=CONC
 IF(CONC.GE.26)THEN
```

```
      M=13
      GOTO 20
      ENDIF
      Q=0
      DO 10 P=1,14
      CONC1=F(P,Q)
      IF(CONC1.EQ.CONC)THEN
      M=P
      ELSEIF(CONC1.GT.CONC)THEN
      M=P-1
      GOTO 20
      ENDIF
10    CONTINUE
20    P=0
      IF(T.GT.100)THEN
      N=8
      GOTO 40
      ENDIF
      DO 30 Q=1,10
      T1=F(P,Q)
      IF(T1.EQ.T)THEN
      N=Q
      ELSEIF(T1.GT.T)THEN
      N=Q-1
      GOTO 40
      ENDIF
30    CONTINUE
40    CONTINUE
      IF(M.EQ.0.OR.M.EQ.1)THEN
      M=2
      ELSEIF(M.EQ.14)THEN
      M=13
      ENDIF
      IF(N.EQ.0.OR.N.EQ.1)THEN
      N=2
      ELSEIF(N.EQ.9.OR.N.EQ.10)THEN
      N=8
      ENDIF
      A1=(T-F(0,N))*(T-F(0,N+1))*(T-F(0,N+2))
      A2=(F(0,N-1)-F(0,N))*(F(0,N-1)-F(0,N+1))*(F(0,N-1)
     +-F(0,N+2))
      A3=(T-F(0,N-1))*(T-F(0,N+1))*(T-F(0,N+2))
      A4=(F(0,N)-F(0,N-1))*(F(0,N)-F(0,N+1))*(F(0,N)-F(0,N+2))
      A5=(T-F(0,N-1))*(T-F(0,N))*(T-F(0,N+2))
      A6=(F(0,N+1)-F(0,N-1))*(F(0,N+1)-F(0,N))*(F(0,N+1)-F(0,N+2))
      A7=(T-F(0,N-1))*(T-F(0,N))*(T-F(0,N+1))
      A8=(F(0,N+2)-F(0,N-1))*(F(0,N+2)-F(0,N))*(F(0,N+2)-F(0,N+1))
      B1=(CONC-F(M,0))*(CONC-F(M+1,0))
      B2=(F(M-1,0)-F(M,0))*(F(M-1,0)-F(M+1,0))
      B3=(CONC-F(M-1,0))*(CONC-F(M+1,0))
      B4=(F(M,0)-F(M-1,0))*(F(M,0)-F(M+1,0))
      B5=(CONC-F(M-1,0))*(CONC-F(M,0))
      B6=(F(M+1,0)-F(M-1,0))*(F(M+1,0)-F(M,0))
      C1=A1/A2*((B1/B2*F(M-1,N-1))+(B3/B4*F(M,N-1))+(B5/B6
     +*F(M+1,N-1)))
      C2=A3/A4*((B1/B2*F(M-1,N))+(B3/B4*F(M,N))+(B5/B6*F(M+1,N)))
      C3=A5/A6*((B1/B2*F(M-1,N+1))+(B3/B4*F(M,N+1))+(B5/B6
     +*F(M+1,N+1)))
      C4=A7/A8*((B1/B2*F(M-1,N+2))+(B3/B4*F(M,N+2))+(B5/B6
     +*F(M+1,N+2)))
      DC=C1+C2+C3+C4
      DC=DC*1000
      T=T2+273.15
      CONC=1-(CONC2/100)
```

```
      GOTO 520
      ENDIF
      DO 530 Q=1,10
      T1=F(P,Q)
      IF(T1.EQ.T)THEN
      N=Q
      ELSEIF(T1.GT.T)THEN
      N=Q-1
      GOTO 520
      ENDIF
530   CONTINUE
520   CONTINUE
      IF(M.EQ.0.OR.M.EQ.1)THEN
      M=2
      ELSEIF(M.EQ.6)THEN
      M=5
      ENDIF
      IF(N.EQ.0.OR.N.EQ.1)THEN
      N=2
      ELSEIF(N.EQ.9.OR.N.EQ.10)THEN
      N=8
      ENDIF
      A1=(T-F(0,N))*(T-F(0,N+1))*(T-F(0,N+2))
      A2=(F(0,N-1)-F(0,N))*(F(0,N-1)-F(0,N+1))*(F(0,N-1)
     +-F(0,N+2))
      A3=(T-F(0,N-1))*(T-F(0,N+1))*(T-F(0,N+2))
      A4=(F(0,N)-F(0,N-1))*(F(0,N)-F(0,N+1))*(F(0,N)-F(0,N+2))
      A5=(T-F(0,N-1))*(T-F(0,N))*(T-F(0,N+2))
      A6=(F(0,N+1)-F(0,N-1))*(F(0,N+1)-F(0,N))*(F(0,N+1)-F(0,N+2))
      A7=(T-F(0,N-1))*(T-F(0,N))*(T-F(0,N+1))
      A8=(F(0,N+2)-F(0,N-1))*(F(0,N+2)-F(0,N))*(F(0,N+2)-F(0,N+1))
      B1=(CONC-F(M,0))*(CONC-F(M+1,0))
      B2=(F(M-1,0)-F(M,0))*(F(M-1,0)-F(M+1,0))
      B3=(CONC-F(M-1,0))*(CONC-F(M+1,0))
      B4=(F(M,0)-F(M-1,0))*(F(M,0)-F(M+1,0))
      B5=(CONC-F(M-1,0))*(CONC-F(M,0))
      B6=(F(M+1,0)-F(M-1,0))*(F(M+1,0)-F(M,0))
      C1=A1/A2*((B1/B2*F(M-1,N-1))+(B3/B4*F(M,N-1))+(B5/B6
     +*F(M+1,N-1)))
      C2=A3/A4*((B1/B2*F(M-1,N))+(B3/B4*F(M,N))+(B5/B6*F(M+1,N)))
      C3=A5/A6*((B1/B2*F(M-1,N+1))+(B3/B4*F(M,N+1))+(B5/B6
     +*F(M+1,N+1)))
      C4=A7/A8*((B1/B2*F(M-1,N+2))+(B3/B4*F(M,N+2))+(B5/B6
     +*F(M+1,N+2)))
      DC=C1+C2+C3+C4
      DC=DC*1000
      T=T2+273.15
      CONC=1-(CONC2/100)
      RETURN
      END
      SUBROUTINE DENS3(CONC,T,DC)
      REAL CONC,T
      REAL F
      REAL A1,A2,A3,A4,A5,A6,A7,A8,B1,B2,B3,B4,B5,B6
      REAL C1,C2,C3,C4,DC,CONC1,T1,CC
      INTEGER M,N,P,Q
      DIMENSION F(0:15,0:10)
      DATA((F(I,J),J=0,10),I=0,15)/0,10,18,20,25,30,40,50,60,70,80
     +,1,1.0049,1.0037,1.0033,1.0021,1.007,.9971,.993
     +,0.9881,.9826,.9766
     +,2,1.0101,1.0088,1.0084,1.0072,1.0057,1.0021,.9979
     +,.993,.9875,.9815
     +,4,1.0205,1.0191,1.0186,1.0173,1.0157,1.012,1.0077
     +,1.0028,.9972,.9912
```

```
     +,6,1.031,1.0294,1.0289,
     +,1.0126,1.007,1.0009
     +,8,1.0415,1.0397,1.0392
     +,1.0224,1.0168,1.0107
     +,10,1.052,1.05,1.0495,1.
     +,1.0322,1.0266,1.0205
     +,12,1.0626,1.0604,1.059
     +,1.0421,1.0364,1.0303
     +,14,1.0733,1.0709,1.070
     +,1.0521,1.0463,1.0402
     +,16,1.0841,1.0815,1.080
     +,1.0621,1.0562,1.0562
     +,18,1.095,1.0922,1.0913,
     +,1.0722,1.0662,1.0662
     +,20,1.106,1.103,1.1021,1
     +,1.0824,1.0763,1.0763
     +,22,1.1171,1.1139,1.113,
     +,1.0926,1.0862,1.0865
     +,24,1.1282,1.1249,1.124,
     +,1.1029,1.0968,1.0968
     +,26,1.1394,1.136,1.1351,
     +,1.1133,1.1072,1.1072
     +,28,1.1508,1.1472,1.1462
     +,1.1238,1.1176,1.1176/
      T=T-273.15
      T2=T
      IF(T.LT.0)THEN
      T=0
      ENDIF
      CONC=(1-CONC)*100
      CONC2=CONC
      IF(CONC.GE.28)THEN
      M=14
      GOTO 20
      ENDIF
      Q=0
      DO 10 P=1,15
      CONC1=F(P,Q)
      IF(CONC1.EQ.CONC)THEN
      M=P
      ELSEIF(CONC1.GT.CONC)THEN
      M=P-1
      GOTO 20
      ENDIF
10    CONTINUE
20    P=0
      IF(T.GT.80)THEN
      N=8
      GOTO 40
      ENDIF
      DO 30 Q=1,10
      T1=F(P,Q)
      IF(T1.EQ.T)THEN
      N=Q
      ELSEIF(T1.GT.T)THEN
      N=Q-1
      GOTO 40
      ENDIF
30    CONTINUE
40    CONTINUE
      IF(M.EQ.0.OR.M.EQ.1)THEN
```

```
     +,6,1.031,1.0294,1.0289,1.0275,1.0258,1.022,1.0176
     +,1.0126,1.007,1.0009
     +,8,1.0415,1.0397,1.0392,1.0377,1.0359,1.032,1.0275
     +,1.0224,1.0168,1.0107
     +,10,1.052,1.05,1.0495,1.0479,1.0461,1.042,1.0375
     +,1.0322,1.0266,1.0205
     +,12,1.0626,1.0604,1.0598,1.0582,1.0563,1.0521,1.0475
     +,1.0421,1.0364,1.0303
     +,14,1.0733,1.0709,1.0702,1.0686,1.0666,1.0623,1.0575
     +,1.0521,1.0463,1.0402
     +,16,1.0841,1.0815,1.0807,1.079,1.0769,1.0725,1.0676
     +,1.0621,1.0562,1.0562
     +,18,1.095,1.0922,1.0913,1.0895,1.0873,1.0828,1.0778
     +,1.0722,1.0662,1.0662
     +,20,1.106,1.103,1.1021,1.1001,1.0978,1.0931,1.088
     +,1.0824,1.0763,1.0763
     +,22,1.1171,1.1139,1.113,1.1109,1.1085,1.1035,1.0983
     +,1.0926,1.0862,1.0865
     +,24,1.1282,1.1249,1.124,1.1218,1.1193,1.1141,1.1087
     +,1.1029,1.0968,1.0968
     +,26,1.1394,1.136,1.1351,1.1327,1.1302,1.1248,1.1192
     +,1.1133,1.1072,1.1072
     +,28,1.1508,1.1472,1.1462,1.1437,1.1412,1.1355,1.1298
     +,1.1238,1.1176,1.1176/
      T=T-273.15
      T2=T
      IF(T.LT.0)THEN
      T=0
      ENDIF
      CONC=(1-CONC)*100
      CONC2=CONC
      IF(CONC.GE.28)THEN
      M=14
      GOTO 20
      ENDIF
      Q=0
      DO 10 P=1,15
      CONC1=F(P,Q)
      IF(CONC1.EQ.CONC)THEN
      M=P
      ELSEIF(CONC1.GT.CONC)THEN
      M=P-1
      GOTO 20
      ENDIF
10    CONTINUE
20    P=0
      IF(T.GT.80)THEN
      N=8
      GOTO 40
      ENDIF
      DO 30 Q=1,10
      T1=F(P,Q)
      IF(T1.EQ.T)THEN
      N=Q
      ELSEIF(T1.GT.T)THEN
      N=Q-1
      GOTO 40
      ENDIF
30    CONTINUE
40    CONTINUE
      IF(M.EQ.0.OR.M.EQ.1)THEN
      M=2
      ELSEIF(M.EQ.15)THEN
      M=14
```

```
 IF(N.EQ.0.OR.N.EQ.1)THEN
 N=2
 ELSEIF(N.EQ.9.OR.N.EQ.10)THEN
 N=8
 ENDIF
 A1=(T-F(0,N))*(T-F(0,N+1))*(T-F(0,N+2))
 A2=(F(0,N-1)-F(0,N))*(F(0,N-1)-F(0,N+1))*(F(0,N-1)
+-F(0,N+2))
 A3=(T-F(0,N-1))*(T-F(0,N+1))*(T-F(0,N+2))
 A4=(F(0,N)-F(0,N-1))*(F(0,N)-F(0,N+1))*(F(0,N)-F(0,N+2))
 A5=(T-F(0,N-1))*(T-F(0,N))*(T-F(0,N+2))
 A6=(F(0,N+1)-F(0,N-1))*(F(0,N+1)-F(0,N))*(F(0,N+1)-F(0,N+2))
 A7=(T-F(0,N-1))*(T-F(0,N))*(T-F(0,N+1))
 A8=(F(0,N+2)-F(0,N-1))*(F(0,N+2)-F(0,N))*(F(0,N+2)-F(0,N+1))
 B1=(CONC-F(M,0))*(CONC-F(M+1,0))
 B2=(F(M-1,0)-F(M,0))*(F(M-1,0)-F(M+1,0))
 B3=(CONC-F(M-1,0))*(CONC-F(M+1,0))
 B4=(F(M,0)-F(M-1,0))*(F(M,0)-F(M+1,0))
 B5=(CONC-F(M-1,0))*(CONC-F(M,0))
 B6=(F(M+1,0)-F(M-1,0))*(F(M+1,0)-F(M,0))
 C1=A1/A2*((B1/B2*F(M-1,N-1))+(B3/B4*F(M,N-1))+(B5/B6
+*F(M+1,N-1)))
 C2=A3/A4*((B1/B2*F(M-1,N))+(B3/B4*F(M,N))+(B5/B6*F(M+1,N)))
 C3=A5/A6*((B1/B2*F(M-1,N+1))+(B3/B4*F(M,N+1))+(B5/B6
+*F(M+1,N+1)))
 C4=A7/A8*((B1/B2*F(M-1,N+2))+(B3/B4*F(M,N+2))+(B5/B6
+*F(M+1,N+2)))
 DC=C1+C2+C3+C4
 DC=DC*1000
 T=T2+273.15
 CONC=1-(CONC2/100)
 RETURN
 END
 SUBROUTINE DENS2(CONC,T,DC)
 REAL CONC,T
 REAL F
 REAL A1,A2,A3,A4,A5,A6,A7,A8,B1,B2,B3,B4,B5,B6
 REAL C1,C2,C3,C4,DC,CONC1,T1,CC
 INTEGER M,N,P,Q
 DIMENSION F(0:10,0:6)
 DATA((F(I,J),J=0,6),I=0,10)/0,0,10,20,25,30,40
+,1,1.0104,1.01,1.0086,1.0073,1.0058,1.0024
+,2,1.0211,1.0206,1.019,1.0176,1.0161,1.0126
+,4,1.429,1.042,1.0401,1.0387,1.037,1.0332
+,6,1.0654,1.0638,1.0616,1.0602,1.0585,1.0545
+,8,1.0887,1.0866,1.084,1.0825,1.0807,1.0764
+,10,1.1128,1.1101,1.1071,1.1054,1.1035,1.099
+,12,1.1379,1.1345,1.1308,1.1289,1.1267,1.1222
+,14,1.1590,1.1590,1.1544,1.1544,1.1544,1.1544
+,16,1.18,1.183,1.180,1.180,1.180,1.180
+,18,1.208,1.208,1.206,1.206,1.206,1.206/
 T=T-273.15
 T2=T
 IF(T.LT.0)THEN
 T=0
 ENDIF
 CONC=(1-CONC)*100
 CONC2=CONC
 IF(CONC.GE.18)THEN
 M=9
 GOTO 20
 ENDIF
 Q=0
```

```
      DO 10 P=1,10
      CONC1=F(P,Q)
      IF(CONC1.EQ.CONC)THEN
      M=P
      ELSEIF(CONC1.GT.CONC)THEN
      M=P-1
      GOTO 20
      ENDIF
10    CONTINUE
20    P=0
      IF(T.GT.40)THEN
      N=4
      GOTO 40
      ENDIF
      DO 30 Q=1,6
      T1=F(P,Q)
      IF(T1.EQ.T)THEN
      N=Q
      ELSEIF(T1.GT.T)THEN
      N=Q-1
      GOTO 40
      ENDIF
30    CONTINUE
40    CONTINUE
      IF(M.EQ.0.OR.M.EQ.1)THEN
      M=2
      ELSEIF(M.EQ.10)THEN
      M=9
      ENDIF
      IF(N.EQ.0.OR.N.EQ.1)THEN
      N=2
      ELSEIF(N.EQ.5.OR.N.EQ.6)THEN
      N=4
      ENDIF
      A1=(T-F(0,N))*(T-F(0,N+1))*(T-F(0,N+2))
      A2=(F(0,N-1)-F(0,N))*(F(0,N-1)-F(0,N+1))*(F(0,N-1)
     +-F(0,N+2))
      A3=(T-F(0,N-1))*(T-F(0,N+1))*(T-F(0,N+2))
      A4=(F(0,N)-F(0,N-1))*(F(0,N)-F(0,N+1))*(F(0,N)-F(0,N+2))
      A5=(T-F(0,N-1))*(T-F(0,N))*(T-F(0,N+2))
      A6=(F(0,N+1)-F(0,N-1))*(F(0,N+1)-F(0,N))*(F(0,N+1)-F(0,N+2))
      A7=(T-F(0,N-1))*(T-F(0,N))*(T-F(0,N+1))
      A8=(F(0,N+2)-F(0,N-1))*(F(0,N+2)-F(0,N))*(F(0,N+2)-F(0,N+1))
      B1=(CONC-F(M,0))*(CONC-F(M+1,0))
      B2=(F(M-1,0)-F(M,0))*(F(M-1,0)-F(M+1,0))
      B3=(CONC-F(M-1,0))*(CONC-F(M+1,0))
      B4=(F(M,0)-F(M-1,0))*(F(M,0)-F(M+1,0))
      B5=(CONC-F(M-1,0))*(CONC-F(M,0))
      B6=(F(M+1,0)-F(M-1,0))*(F(M+1,0)-F(M,0))
      C1=A1/A2*((B1/B2*F(M-1,N-1))+(B3/B4*F(M,N-1))+(B5/B6
     +*F(M+1,N-1)))
      C2=A3/A4*((B1/B2*F(M-1,N))+(B3/B4*F(M,N))+(B5/B6*F(M+1,N)))
      C3=A5/A6*((B1/B2*F(M-1,N+1))+(B3/B4*F(M,N+1))+(B5/B6
     +*F(M+1,N+1)))
      C4=A7/A8*((B1/B2*F(M-1,N+2))+(B3/B4*F(M,N+2))+(B5/B6
     +*F(M+1,N+2)))
      DC=C1+C2+C3+C4
      DC=DC*1000
      T=T2+273.15
      CONC=1-(CONC2/100)
      RETURN
      END
      SUBROUTINE PRESS(CONC,T,CC)
      REAL A1,A2,A3,A4,A5,A6,A7,A8
```

```
      REAL B1,B2,B3,B4,B5,B6,C1,C2,C3,C4
      INTEGER M,N,P,Q
      REAL CONC,T,T1,CC
      DIMENSION F(0:12,0:11)
      DATA((F(I,J),J=0,11),I=0,12)
     +/0,0,2.5,5,7.5,10,12.5,15,17.5,20,22.5,25
     +,0,4.579,4.5,4.4,4.4,4.3,4.2,4.1,4,3.8,3.7,3.5
     +,10,9.21,9.1,8.9,8.8,8.6,8.4,8.2,8,7.7,7.4,7.1
     +,20,17.54,17.3,17,16.7,16.4,16.1,15.7,15.3,14.8,14.2,13.6
     +,30,31.83,31.4,30.9,30.4,29.8,29.2,28.5,27.7,26.8,25.8,24.7
     +,40,55.34,54.5,53.6,52.7,51.7,50.7,49.5,48.1,46.6,44.9,43
     +,50,92.54,91.2,89.7,88.1,86.4,84.7,82.8,80.5,78.1,75.3,72.2
     +,60,149.46,147.2,144.8,142.3,139.7,136.8,133.7,130,126,121.7
     +,116.8
     +,70,233.79,230.2,226.4,222.4,218.3,213.9,208.9,203.5,197.5
     +,190.7,183.1
     +,80,355.47,350,344,338,332,325,318,309.5,300.5,290.2,278.9
     +,90,526,517,509,500,491,481,470,458,445.1,430,414
     +,100,760,748,736,723,710,695,680,665,643,622,599
     +,110,1074.5,1057,1040,1022,1003,983,961,936,911,881,849/
      T=T-273.15
      T2=T
      IF(T.LT.0)THEN
      T=0
      ENDIF
      CONC=(1-CONC)*100
      CONC2=CONC
      IF(CONC.GE.25)THEN
      CONC=25
      N=9
      GOTO 60
      ENDIF
      P=0
      DO 50 Q=1,11
      CONC1=F(P,Q)
      IF(CONC1.EQ.CONC)THEN
      N=Q
      ELSEIF(CONC1.GT.CONC)THEN
      N=Q-1
      GOTO 60
      ENDIF
50    CONTINUE
60    Q=0
      IF(T.GT.110)THEN
      P=11
      GOTO 80
      ENDIF
      DO 70 P=1,12
      T1=F(P,Q)
      IF(T1.EQ.T)THEN
      M=P
      ELSEIF(T1.GT.T)THEN
      M=P-1
      GOTO 80
      ENDIF
70    CONTINUE
80    CONTINUE
      IF(M.EQ.0.OR.M.EQ.1)THEN
      M=2
      ELSEIF(M.EQ.12)THEN
      M=11
      ENDIF
      IF(N.EQ.0.OR.N.EQ.1)THEN
      N=2
```

```
 ELSEIF(N.EQ.10.OR.N.EQ.11)THEN
 N=9
 ENDIF
 A1=(CONC-F(0,N))*(CONC-F(0,N+1))*(CONC-F(0,N+2))
 A2=(F(0,N-1)-F(0,N))*(F(0,N-1)-F(0,N+1))*(F(0,N-1)
+-F(0,N+2))
 A3=(CONC-F(0,N-1))*(CONC-F(0,N+1))*(CONC-F(0,N+2))
 A4=(F(0,N)-F(0,N-1))*(F(0,N)-F(0,N+1))*(F(0,N)-F(0,N+2))
 A5=(CONC-F(0,N-1))*(CONC-F(0,N))*(CONC-F(0,N+2))
 A6=(F(0,N+1)-F(0,N-1))*(F(0,N+1)-F(0,N))*(F(0,N+1)-F(0,N+2))
 A7=(CONC-F(0,N-1))*(CONC-F(0,N))*(CONC-F(0,N+1))
 A8=(F(0,N+2)-F(0,N-1))*(F(0,N+2)-F(0,N))*(F(0,N+2)-F(0,N+1))
 B1=(T-F(M,0))*(T-F(M+1,0))
 B2=(F(M-1,0)-F(M,0))*(F(M-1,0)-F(M+1,0))
 B3=(T-F(M-1,0))*(T-F(M+1,0))
 B4=(F(M,0)-F(M-1,0))*(F(M,0)-F(M+1,0))
 B5=(T-F(M-1,0))*(T-F(M,0))
 B6=(F(M+1,0)-F(M-1,0))*(F(M+1,0)-F(M,0))
 C1=A1/A2*((B1/B2*F(M-1,N-1))+(B3/B4*F(M,N-1))+(B5/B6
+*F(M+1,N-1)))
 C2=A3/A4*((B1/B2*F(M-1,N))+(B3/B4*F(M,N))+(B5/B6*F(M+1,N)))
 C3=A5/A6*((B1/B2*F(M-1,N+1))+(B3/B4*F(M,N+1))+(B5/B6
+*F(M+1,N+1)))
 C4=A7/A8*((B1/B2*F(M-1,N+2))+(B3/B4*F(M,N+2))+(B5/B6
+*F(M+1,N+2)))
 CC=C1+C2+C3+C4
 CC=CC/760
 CONC=1-(CONC2/100)
 T=T2+273.15
 RETURN
 END
 SUBROUTINE PRESS1(CONC,T,CC)
 REAL A1,A2,A3,A4,A5,A6,A7,A8
 REAL B1,B2,B3,B4,B5,B6,C1,C2,C3,C4
 INTEGER M,N,P,Q
 REAL CONC,T,T1,CC
 DIMENSION F(0:5,0:11)
 DATA((F(I,J),J=0,11),I=0,5)
+/0,0,0.99,1.96,2.91,3.85,4.76,5.66,7.41,9.09,13,16.7
+,0,4.579,4.568,4.557,4.548,4.538,4.529,4.52,4.52,4.52,4.52,4.52
+,30,31.834,31.76,31.68,31.62,31.55,31.49,31.43,31.3,31.18,31.18
+,31.18,60,149.46,149.1,148.8,148.4,148.1,147.8,147.5,147
+,146.4,144.9,144.9,80,355.47,354.6,353.8,353,352.3,351.6,350.9
+,349.6,348.2,344.7,341.2,100,760,758.1,756.4,754.8,753.3,751.8
+,750.3,747.4,744.4,737,729.5/
 T=T-273.15
 T2=T
 IF(T.LT.0)THEN
 T=0
 ENDIF
 CONC=(1-CONC)*100
 CONC2=CONC
 IF(CONC.GE.20)THEN
 CONC=20
 N=9
 GOTO 60
 ENDIF
 P=0
 DO 50 Q=1,11
 CONC1=F(P,Q)
 IF(CONC1.EQ.CONC)THEN
 N=Q
 ELSEIF(CONC1.GT.CONC)THEN
 N=Q-1
```

```
      GOTO 60
      ENDIF
50    CONTINUE
60    Q=0
      IF(T.GT.100)THEN
      P=4
      GOTO 80
      ENDIF
      DO 70 P=1,5
      T1=F(P,Q)
      IF(T1.EQ.T)THEN
      M=P
      ELSEIF(T1.GT.T)THEN
      M=P-1
      GOTO 80
      ENDIF
70    CONTINUE
80    CONTINUE
      IF(M.EQ.0.OR.M.EQ.1)THEN
      M=2
      ELSEIF(M.EQ.5)THEN
      M=4
      ENDIF
      IF(N.EQ.0.OR.N.EQ.1)THEN
      N=2
      ELSEIF(N.EQ.10.OR.N.EQ.11)THEN
      N=9
      ENDIF
      A1=(CONC-F(0,N))*(CONC-F(0,N+1))*(CONC-F(0,N+2))
      A2=(F(0,N-1)-F(0,N))*(F(0,N-1)-F(0,N+1))*(F(0,N-1)
     +-F(0,N+2))
      A3=(CONC-F(0,N-1))*(CONC-F(0,N+1))*(CONC-F(0,N+2))
      A4=(F(0,N)-F(0,N-1))*(F(0,N)-F(0,N+1))*(F(0,N)-F(0,N+2))
      A5=(CONC-F(0,N-1))*(CONC-F(0,N))*(CONC-F(0,N+2))
      A6=(F(0,N+1)-F(0,N-1))*(F(0,N+1)-F(0,N))*(F(0,N+1)-F(0,N+2))
      A7=(CONC-F(0,N-1))*(CONC-F(0,N))*(CONC-F(0,N+1))
      A8=(F(0,N+2)-F(0,N-1))*(F(0,N+2)-F(0,N))*(F(0,N+2)-F(0,N+1))
      B1=(T-F(M,0))*(T-F(M+1,0))
      B2=(F(M-1,0)-F(M,0))*(F(M-1,0)-F(M+1,0))
      B3=(T-F(M-1,0))*(T-F(M+1,0))
      B4=(F(M,0)-F(M-1,0))*(F(M,0)-F(M+1,0))
      B5=(T-F(M-1,0))*(T-F(M,0))
      B6=(F(M+1,0)-F(M-1,0))*(F(M+1,0)-F(M,0))
      C1=A1/A2*((B1/B2*F(M-1,N-1))+(B3/B4*F(M,N-1))+(B5/B6
     +*F(M+1,N-1)))
      C2=A3/A4*((B1/B2*F(M-1,N))+(B3/B4*F(M,N))+(B5/B6*F(M+1,N)))
      C3=A5/A6*((B1/B2*F(M-1,N+1))+(B3/B4*F(M,N+1))+(B5/B6
     +*F(M+1,N+1)))
      C4=A7/A8*((B1/B2*F(M-1,N+2))+(B3/B4*F(M,N+2))+(B5/B6
     +*F(M+1,N+2)))
      CC=C1+C2+C3+C4
      CC=CC/760
      CONC=1-(CONC2/100)
      T=T2+273.15
      RETURN
      END
```

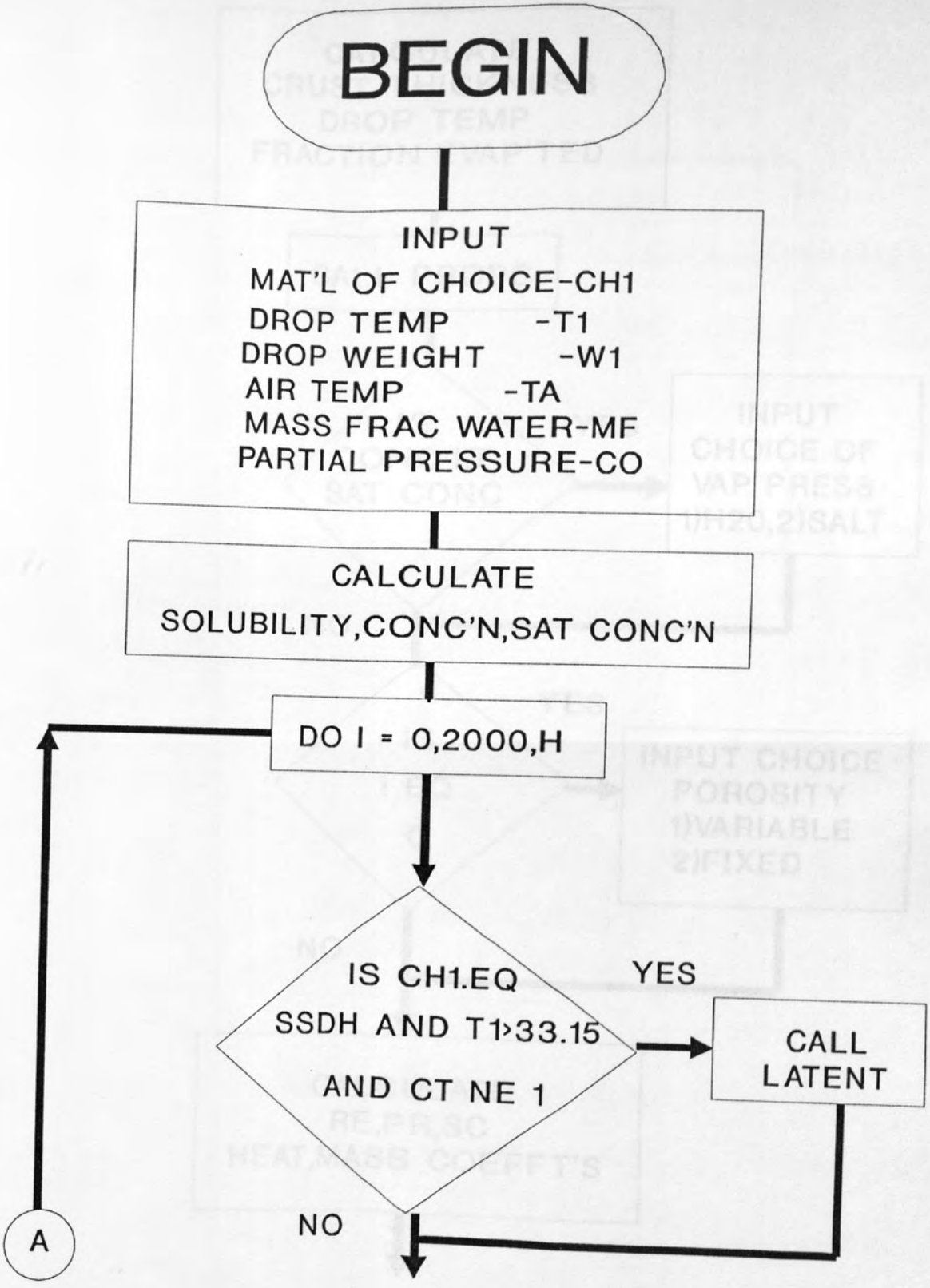
BEGIN
INPUT
MAT'L OF CHOICE-CH1
DROP TEMP -T1
DROP WEIGHT -W1
AIR TEMP -TA
MASS FRAC WATER-MF
PARTIAL PRESSURE-CO
CALCULATE
SOLUBILITY,CONC'N,SAT CONC'N
DO I = 0,2000,H
IS CH1.EQ
SSDH AND T1>33.15
AND CT NE 1
YES
CALL
LATENT
NO
A

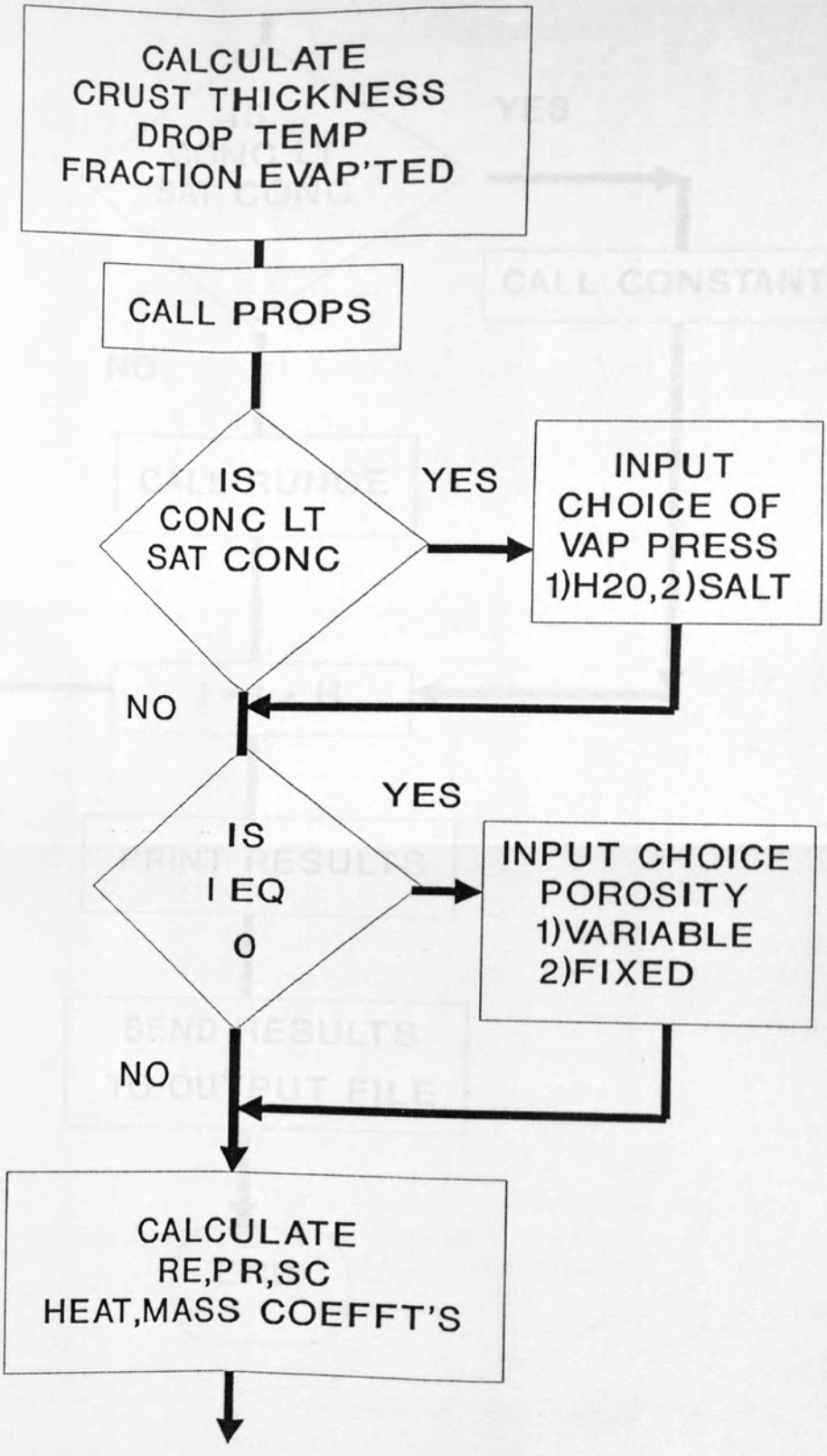
CALCULATE
CRUST THICKNESS
DROP TEMP
FRACTION EVAP'TED
CALL PROPS
IS
CONC LT
SAT CONC
YES
INPUT
CHOICE OF
VAP PRESS
1)H20,2)SALT
NO
IS
I EQ
0
YES
INPUT CHOICE
POROSITY
1)VARIABLE
2)FIXED
NO
CALCULATE
RE,PR,SC
HEAT,MASS COEFFT'S

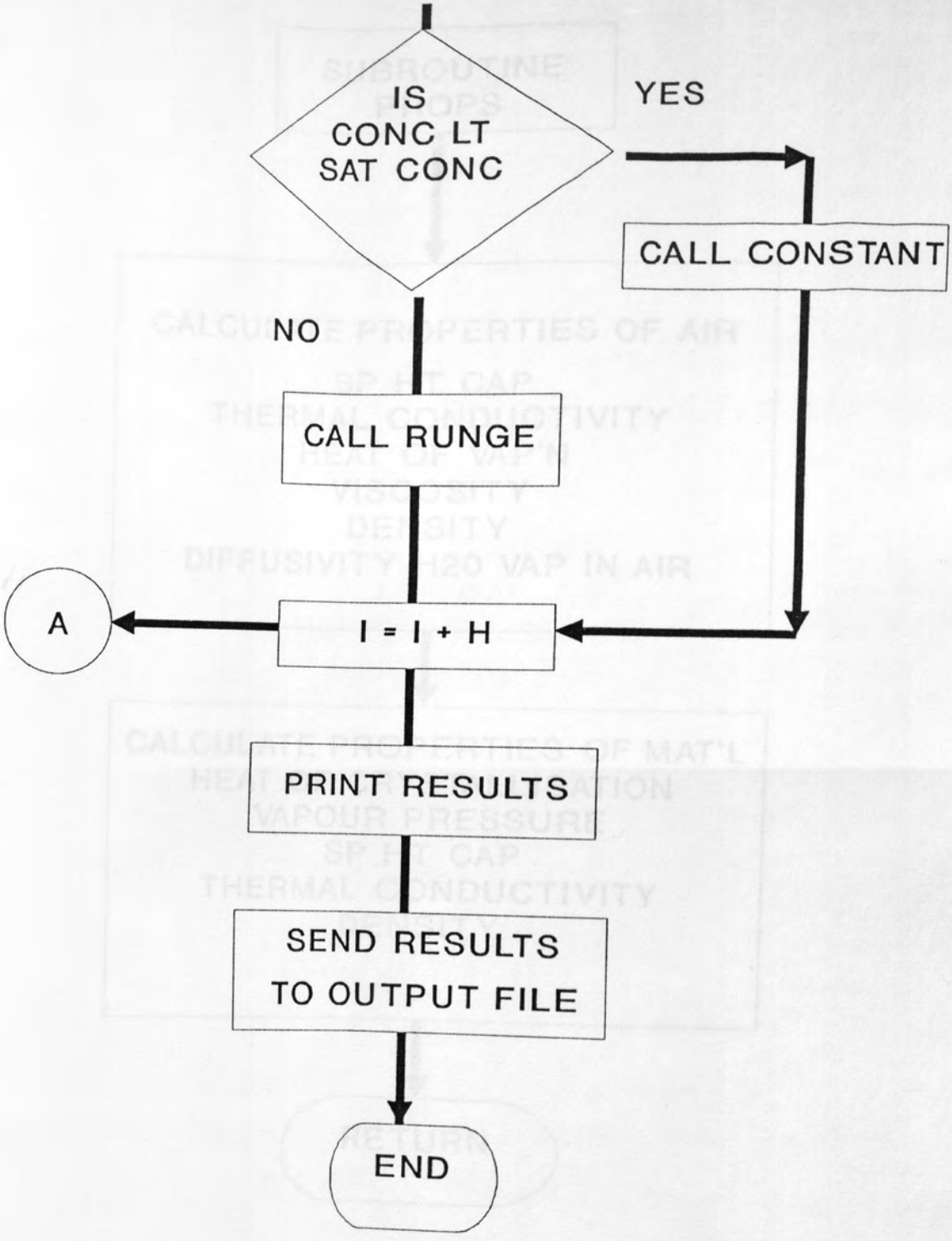
IS
CONC LT
SAT CONC
YES
CALL CONSTANT
NO
CALL RUNGE
A
I = I + H
PRINT RESULTS
SEND RESULTS
TO OUTPUT FILE
END

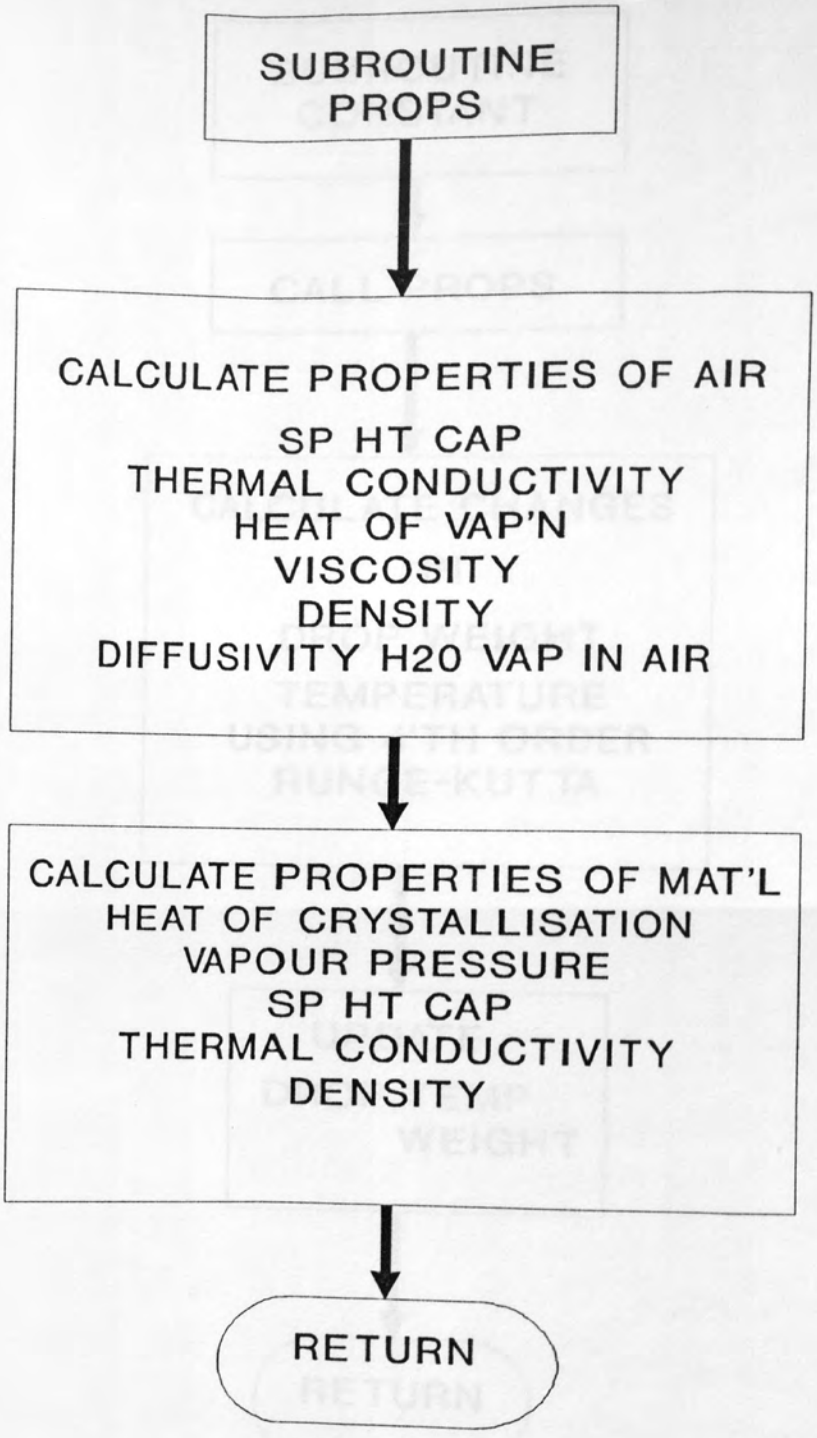
SUBROUTINE
PROPS
CALCULATE PROPERTIES OF AIR
SP HT CAP
THERMAL CONDUCTIVITY
HEAT OF VAP'N
VISCOSITY
DENSITY
DIFFUSIVITY H20 VAP IN AIR
CALCULATE PROPERTIES OF MAT'L
HEAT OF CRYSTALLISATION
VAPOUR PRESSURE
SP HT CAP
THERMAL CONDUCTIVITY
DENSITY
RETURN

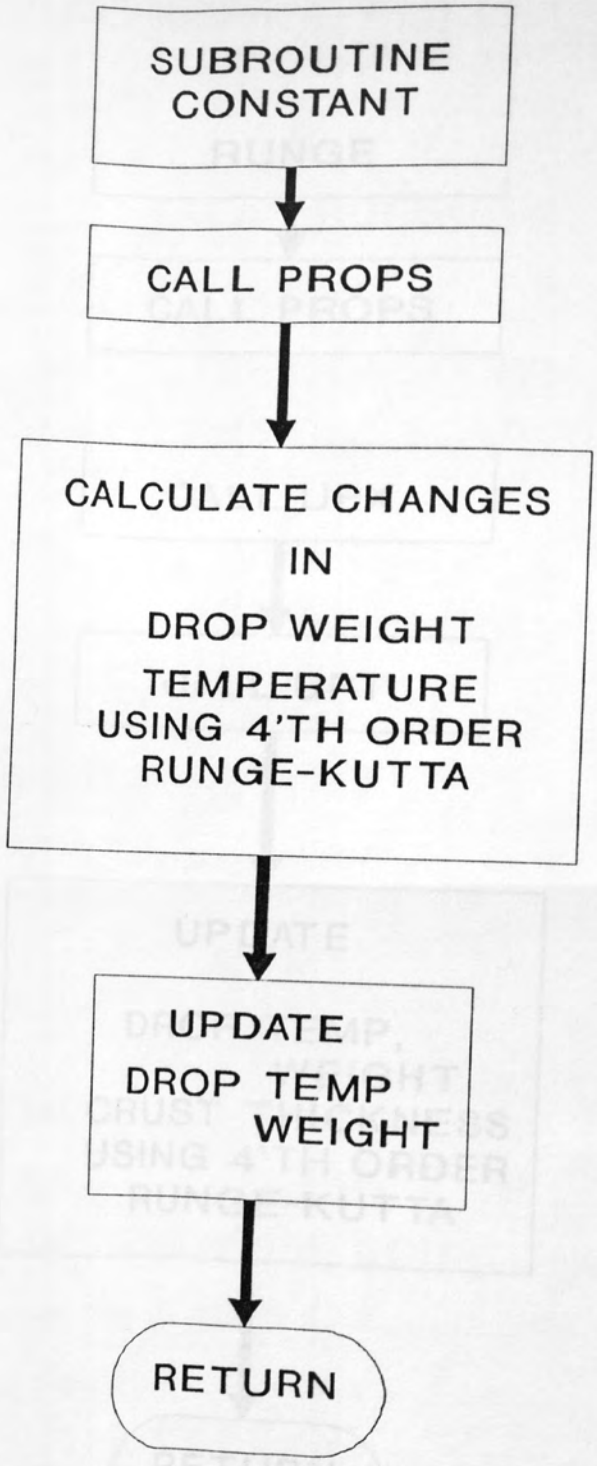
SUBROUTINE
CONSTANT
CALL PROPS
CALCULATE CHANGES
IN
DROP WEIGHT
TEMPERATURE
USING 4'TH ORDER
RUNGE-KUTTA
UPDATE
DROP TEMP
WEIGHT
RETURN

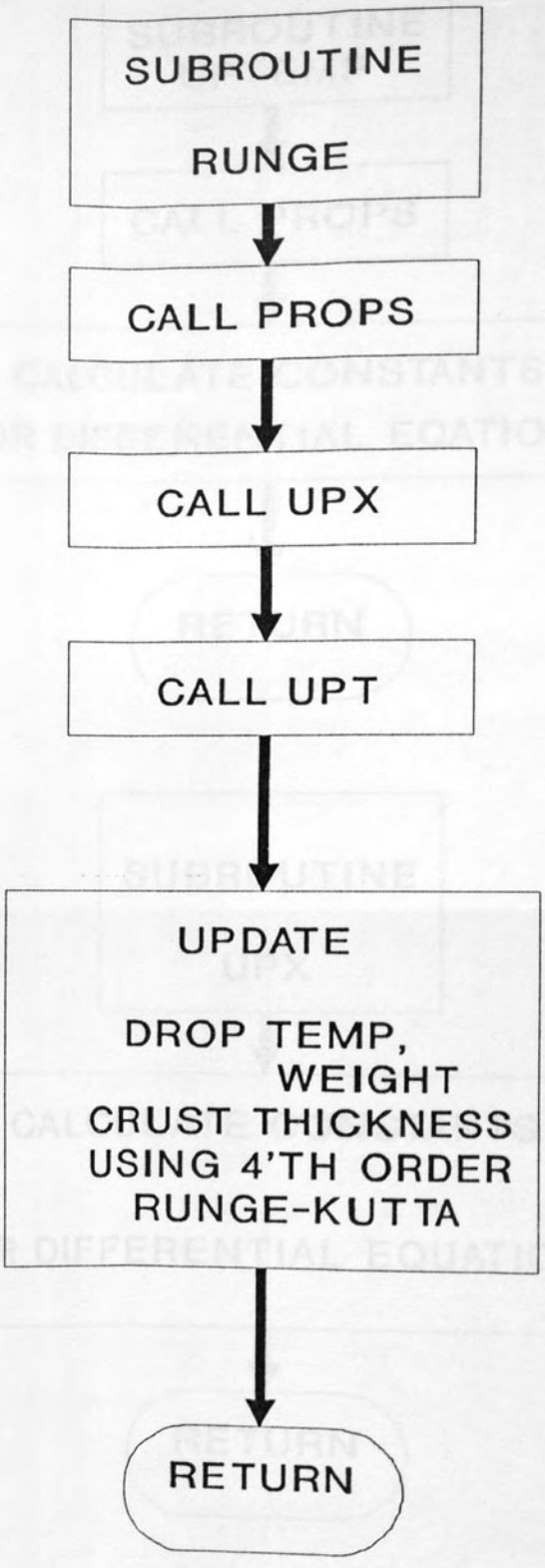
SUBROUTINE
RUNGE
CALL PROPS
CALL UPX
CALL UPT
UPDATE
DROP TEMP,
WEIGHT
CRUST THICKNESS
USING 4'TH ORDER
RUNGE-KUTTA
RETURN

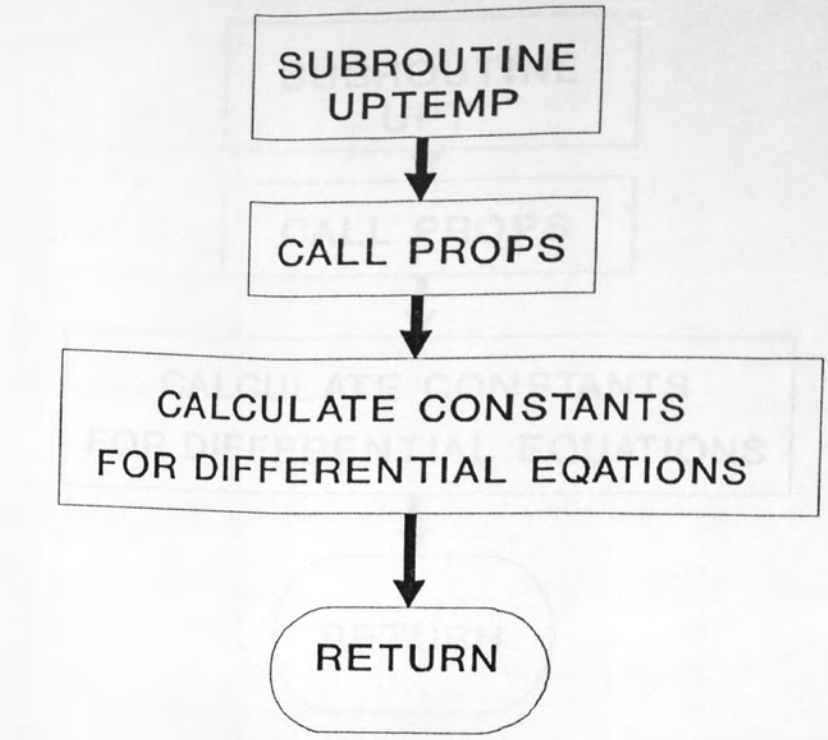
SUBROUTINE
UPTEMP
CALL PROPS
CALCULATE CONSTANTS
FOR DIFFERENTIAL EQATIONS
RETURN

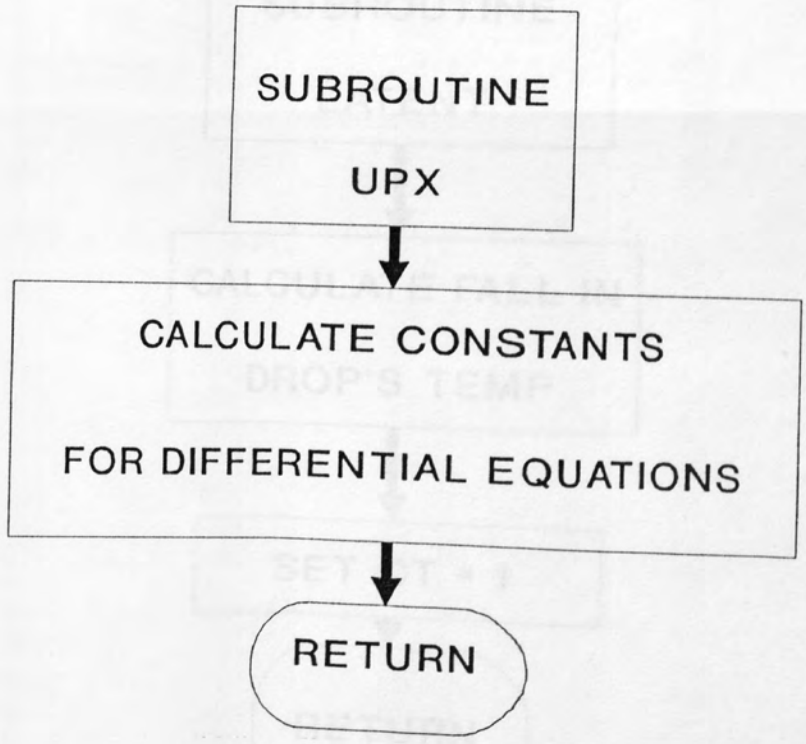
SUBROUTINE
UPX
CALCULATE CONSTANTS
FOR DIFFERENTIAL EQUATIONS
RETURN

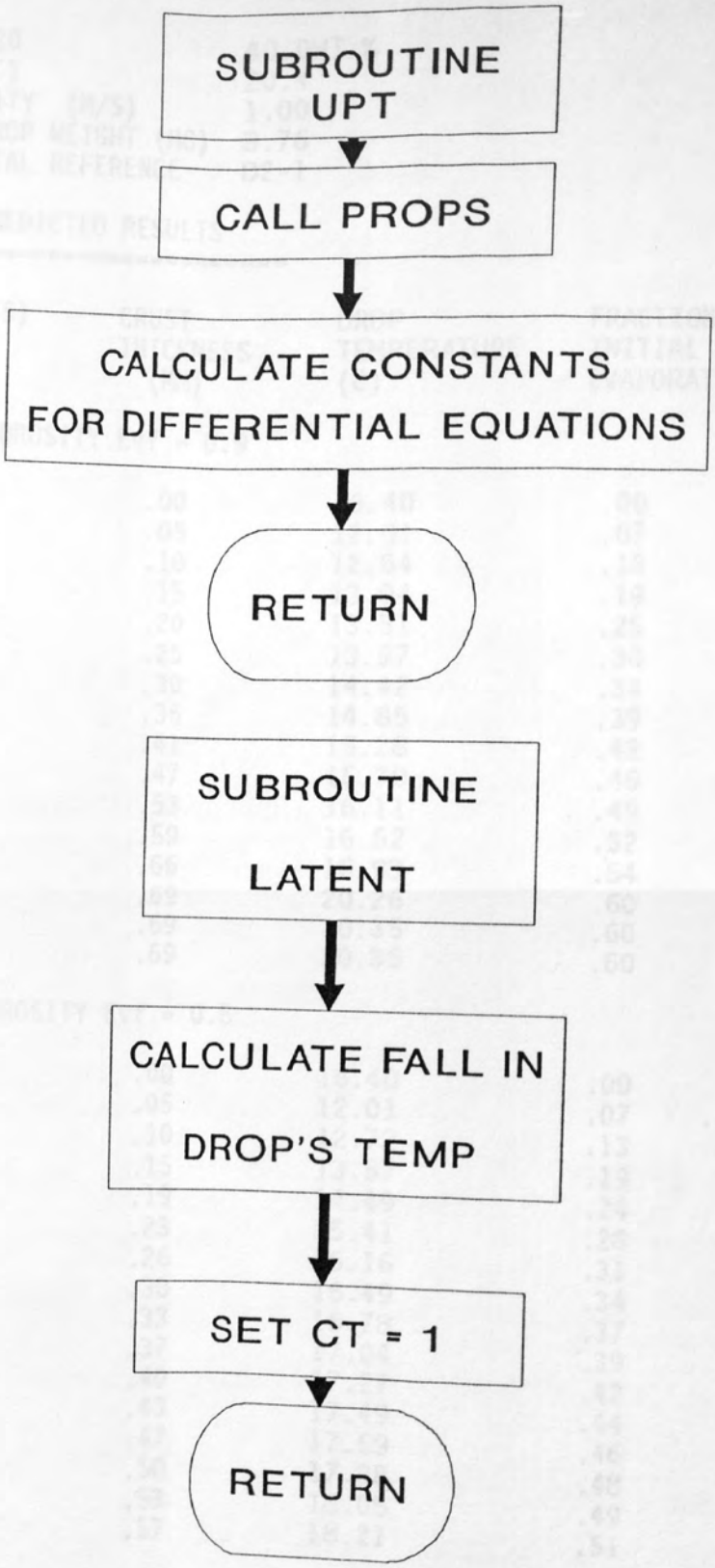
SUBROUTINE
UPT
CALL PROPS
CALCULATE CONSTANTS
FOR DIFFERENTIAL EQUATIONS
RETURN
SUBROUTINE
LATENT
CALCULATE FALL IN
DROP'S TEMP
SET CT = 1
RETURN

APPENDIX C3-SODIUM SULPHATE DECAHYDRATE

EXPERIMENTAL CONDITIONS

NA2SO410H20	40.0WT %
AIR TEMP(C)	20.4
AIR VELOCITY (M/S)	1.00
INITIAL DROP WEIGHT (MG)	8.76
EXPERIMENTAL REFERENCE	D2-1

PREDICTED RESULTS

TIME(S)	CRUST THICKNESS (MM)	DROP TEMPERATURE (C)	FRACTION OF INITIAL WT EVAPORATED
VARIABLE POROSITY Evf = 0.9			
.0	.00	16.40	.00
100.0	.05	12.01	.07
200.0	.10	12.54	.13
300.0	.15	13.04	.19
400.0	.20	13.51	.25
500.0	.25	13.97	.30
600.0	.30	14.42	.34
700.0	.35	14.85	.39
800.0	.41	15.28	.42
900.0	.47	15.70	.46
1000.0	.53	16.11	.49
1100.0	.59	16.52	.52
1200.0	.66	16.93	.54
1300.0	.69	20.26	.60
1400.0	.69	20.35	.60
1500.0	.69	20.35	.60
VARIABLE POROSITY Evf = 0.5			
.0	.00	16.40	.00
100.0	.05	12.01	.07
200.0	.10	12.72	.13
300.0	.15	13.57	.19
400.0	.19	14.49	.24
500.0	.23	15.41	.28
600.0	.26	16.16	.31
700.0	.30	16.49	.34
800.0	.33	16.78	.37
900.0	.37	17.04	.39
1000.0	.40	17.27	.42
1100.0	.43	17.49	.44
1200.0	.47	17.69	.46
1300.0	.50	17.88	.48
1400.0	.53	18.05	.49
1500.0	.57	18.21	.51
FIXED POROSITY Ef = 0.9			
.0	.00	16.40	.00
100.0	.05	12.02	.07
200.0	.10	12.54	.13
300.0	.15	13.03	.19
400.0	.20	13.51	.25

500.0	.25	13.97	.30
600.0	.30	14.42	.34
700.0	.35	14.85	.39
800.0	.41	15.28	.42
900.0	.47	15.69	.46
1000.0	.53	16.11	.49
1100.0	.59	16.52	.52
1200.0	.66	16.93	.54
1300.0	.69	20.26	.60
1400.0	.69	20.35	.60
1500.0	.69	20.35	.60

FIXED POROSITY Ef = 0.5

.0	.00	16.40	.00
100.0	.05	12.76	.07
200.0	.09	13.70	.12
300.0	.13	14.42	.17
400.0	.17	15.00	.21
500.0	.20	15.48	.25
600.0	.24	15.89	.29
700.0	.27	16.25	.32
800.0	.31	16.57	.35
900.0	.34	16.85	.38
1000.0	.37	17.10	.40
1100.0	.41	17.33	.42
1200.0	.44	17.54	.44
1300.0	.47	17.74	.46
1400.0	.51	17.92	.48
1500.0	.54	18.09	.50

EXPERIMENTAL CONDITIONS
==========

NA2SO410H2O	40.0WT %
AIR TEMP(C)	54.70
AIR VELOCITY (M/S)	1.00
INITIAL DROP WEIGHT (MG)	10.49
EXPERIMENTAL REFERENCE	D7-1

PREDICTED RESULTS
==========

TIME(S)	CRUST THICKNESS (MM)	DROP TEMPERATURE (C)	FRACTION OF INITIAL WT EVAPORATED

VARIABLE POROSITY Evf = 0.9

.0	.00	17.30	.00
100.0	.17	25.99	.21
200.0	.37	30.13	.38
300.0	.34	29.53	.53
400.0	.53	33.25	.67
500.0	.64	53.78	.73
262.0	.52	32.96	.47
263.0	.28	14.16	.47
264.0	.28	17.70	.47
265.0	.28	20.49	.47
266.0	.28	22.63	.47
267.0	.28	24.26	.47

EXPERIMENTAL CONDITIONS

NA2SO410H20	15.0WT %
AIR TEMP(C)	74.00
AIR VELOCITY (M/S)	1.00
INITIAL DROP WEIGHT (MG)	6.78
EXPERIMENTAL REFERENCE	D15-1

PREDICTED RESULTS

TIME(S)	CRUST THICKNESS (MM)	DROP TEMPERATURE (C)	FRACTION OF INITIAL WT EVAPORATED
VARIABLE POROSITY Evf = 0.9, VAPOUR PRESSURE WATER			
.0	.00	20.00	.00
25.0	.00	21.34	.08
50.0	.01	25.72	.16
75.0	.06	28.13	.25
100.0	.12	29.81	.35
125.0	.18	31.54	.43
150.0	.15	30.44	.52
175.0	.21	32.44	.60
200.0	.28	34.28	.68
225.0	.35	36.25	.75
250.0	.39	58.93	.84
275.0	.39	72.01	.84
300.0	.39	73.74	.84
145.0	.23	32.98	.50
146.0	.14	28.33	.50
147.0	.14	29.23	.51
148.0	.14	29.81	.51
149.0	.15	30.19	.51
150.0	.15	30.44	.52
VARIABLE POROSITY Evf = 0.9, VAPOUR PRESSURE SALT			
.0	.00	20.00	.00
25.0	.00	22.23	.08
50.0	.00	22.23	.15
75.0	.03	27.03	.24
100.0	.08	28.83	.33
125.0	.14	30.59	.42
150.0	.21	32.42	.50
175.0	.18	31.56	.58
200.0	.24	33.41	.66
225.0	.31	35.39	.74
250.0	.37	53.23	.84
275.0	.37	71.41	.84
300.0	.37	73.68	.84
157.0	.23	32.95	.52
158.0	.14	28.06	.53
159.0	.14	29.06	.53
160.0	.14	29.69	.53
161.0	.14	30.10	.54
162.0	.14	30.36	.54

APPENDIX C4-SODIUM CHLORIDE

EXPERIMENTAL CONDITIONS

NACL	20.0WT %
AIR TEMP(C)	23.00
AIR VELOCITY (M/S)	1.00
INITIAL DROP WEIGHT (MG)	3.70
EXPERIMENTAL REFERENCE	D35-1

PREDICTED RESULTS

VARIABLE POROSITY Evf = 0.9, VAPOUR PRESSURE WATER

TIME(S)	CRUST THICKNESS (MM)	DROP TEMPERATURE (C)	FRACTION OF INITIAL WT EVAPORATED
.0	.00	18.50	.00
100.0	.00	10.71	.11
200.0	.00	10.71	.20
300.0	.03	14.85	.29
400.0	.07	15.51	.38
500.0	.12	16.16	.46
600.0	.18	16.82	.53
800.0	.29	18.17	.65
900.0	.35	18.88	.69
1000.0	.42	19.62	.73
1100.0	.46	22.98	.80
1200.0	.46	23.00	.80

VARIABLE POROSITY Evf = 0.9, VAPOUR PRESSURE SALT

.0	.00	18.50	.00
100.0	.00	12.65	.09
200.0	.00	13.02	.17
300.0	.00	14.26	.25
400.0	.05	15.17	.34
500.0	.10	15.82	.42
600.0	.15	16.48	.49
800.0	.26	17.82	.62
900.0	.32	18.51	.67
1000.0	.39	19.23	.72
1100.0	.46	21.22	.80
1200.0	.46	23.00	.80

VARIABLE POROSITY Evf = 0.9, VAPOUR PRESSURE SAT SOLN

.0	.00	18.50	.00
100.0	.00	14.15	.08
200.0	.00	14.15	.15
300.0	.00	14.14	.22
400.0	.03	15.72	.29
500.0	.07	16.28	.37
600.0	.11	16.81	.44
800.0	.20	17.88	.56
900.0	.25	18.41	.61
1000.0	.31	18.96	.66
1100.0	.36	19.51	.70
1200.0	.42	20.08	.74

EXPERIMENTAL CONDITIONS

NACL	20.0WT %
AIR TEMP(C)	35.00
AIR VELOCITY (M/S)	0.50
INITIAL DROP WEIGHT (MG)	2.80
EXPERIMENTAL REFERENCE	D41-1

PREDICTED RESULTS

VARIABLE POROSITY Evf = 0.9, VAPOUR PRESSURE WATER

TIME(S)	CRUST THICKNESS (MM)	DROP TEMPERATURE (C)	FRACTION OF INITIAL WT EVAPORATED
.0	.00	17.95	.00
50.0	.00	15.12	.08
100.0	.00	15.12	.15
150.0	.00	15.12	.22
200.0	.02	20.24	.29
250.0	.06	20.82	.36
300.0	.10	21.43	.43
400.0	.18	22.90	.56
450.0	.23	23.78	.61
550.0	.35	26.04	.71
600.0	.42	29.99	.75
650.0	.42	34.92	.80
700.0	.42	35.00	.80

VARIABLE POROSITY Evf = 0.9, VAPOUR PRESSURE SALT

.0	.00	17.95	.00
50.0	.00	17.18	.07
100.0	.00	17.51	.13
150.0	.00	17.87	.20
200.0	.00	19.73	.25
250.0	.04	20.55	.33
300.0	.08	21.13	.40
400.0	.16	22.52	.53
450.0	.21	23.35	.59
550.0	.32	25.43	.69
600.0	.39	26.81	.74
650.0	.41	34.51	.80
700.0	.41	34.99	.80

VARIABLE POROSITY Evf = 0.9, VAPOUR PRESSURE SAT SOLN

.0	.00	17.95	.00
50.0	.00	19.15	.06
100.0	.00	19.15	.12
150.0	.00	19.15	.18
200.0	.00	19.15	.23
250.0	.02	21.37	.29
300.0	.06	21.90	.36
350.0	.09	22.46	.43
450.0	.17	23.76	.54
500.0	.21	24.51	.60
600.0	.32	26.34	.69
650.0	.38	27.48	.73
700.0	.42	34.08	.75

APPENDIX C5-POTASSIUM SULPHATE

EXPERIMENTAL CONDITIONS

K2SO4	15.0WT %
AIR TEMP(C)	22.7
AIR VELOCITY (M/S)	0.90
INITIAL DROP WEIGHT (MG)	3.87
EXPERIMENTAL REFERENCE	D64-1

PREDICTED RESULTS

TIME(S)	CRUST THICKNESS (MM)	DROP TEMPERATURE (C)	FRACTION OF INITIAL WT EVAPORATED
VARIABLE POROSITY Evf = 0.9			
.0	.00	12.87	.00
100.0	.05	12.38	.13
200.0	.10	12.89	.24
300.0	.15	13.36	.35
400.0	.21	13.79	.44
500.0	.26	14.20	.52
600.0	.32	14.60	.59
700.0	.37	14.97	.66
800.0	.43	15.34	.71
900.0	.50	15.71	.76
1000.0	.57	16.08	.80
1100.0	.57	22.65	.85
VARIABLE POROSITY Evf = 0.5			
.0	.00	12.87	.00
100.0	.05	12.41	.13
200.0	.10	13.33	.24
300.0	.15	14.47	.33
400.0	.19	15.70	.41
500.0	.23	16.40	.48
600.0	.26	16.77	.53
700.0	.30	17.10	.58
800.0	.34	17.40	.63
900.0	.37	17.67	.67
1000.0	.41	17.91	.71
1100.0	.45	18.14	.74
1200.0	.48	18.35	.77
1300.0	.52	18.55	.79
1400.0	.53	22.64	.85
1500.0	.53	22.65	.85
VARIABLE POROSITY Evf = 0.2			
.0	.00	12.87	.00
100.0	.05	12.41	.13
200.0	.10	13.33	.24
300.0	.15	14.47	.33
400.0	.19	15.70	.41
500.0	.23	16.91	.47
600.0	.26	18.01	.52
700.0	.28	18.95	.56

800.0	.30	19.73	.59
900.0	.32	20.35	.61
1000.0	.33	20.56	.63
1100.0	.35	20.63	.64
1200.0	.36	20.69	.66
1300.0	.37	20.75	.67
1400.0	.39	20.80	.69
1500.0	.40	20.85	.70

FIXED POROSITY Ef = 0.9

.0	.00	12.87	.00
100.0	.05	12.38	.13
200.0	.10	12.89	.24
300.0	.15	13.36	.35
400.0	.21	13.79	.44
500.0	.26	14.20	.52
600.0	.32	14.59	.59
700.0	.37	14.97	.66
800.0	.43	15.34	.71
900.0	.50	15.70	.76
1000.0	.57	16.08	.80
1100.0	.57	22.65	.85
1200.0	.57	22.65	.85

FIXED POROSITY Ef = 0.5

.0	.00	12.87	.00
100.0	.05	13.36	.12
200.0	.09	14.38	.22
300.0	.13	15.12	.31
400.0	.17	15.70	.38
500.0	.21	16.18	.45
600.0	.25	16.59	.51
700.0	.28	16.94	.56
800.0	.32	17.26	.61
900.0	.35	17.54	.65
1000.0	.39	17.79	.69
1100.0	.43	18.03	.73
1200.0	.46	18.25	.76
1300.0	.50	18.45	.79
1400.0	.53	22.54	.85
1500.0	.53	22.65	.85

FIXED POROSITY Ef = 0.2

.0	.00	12.87	.00
100.0	.04	15.65	.10
200.0	.07	17.02	.17
300.0	.09	17.81	.23
400.0	.11	18.34	.28
500.0	.13	18.73	.32
600.0	.15	19.03	.36
700.0	.17	19.28	.40
800.0	.19	19.49	.43
900.0	.21	19.66	.46
1000.0	.22	19.82	.49
1100.0	.24	19.95	.52
1200.0	.25	20.07	.54
1300.0	.27	20.18	.56
1400.0	.28	20.27	.58
1500.0	.30	20.36	.61

EXPERIMENTAL CONDITIONS

K2SO4	5.0WT %
AIR TEMP(C)	36.40
AIR VELOCITY (M/S)	1.20
INITIAL DROP WEIGHT (MG)	2.46
EXPERIMENTAL REFERENCE	D72-1

PREDICTED RESULTS

TIME(S)	CRUST THICKNESS (MM)	DROP TEMPERATURE (C)	FRACTION OF INITIAL WT EVAPORATED
VARIABLE POROSITY Evf = 0.9, VAPOUR PRESSURE WATER			
.0	.00	12.77	.00
50.0	.00	15.46	.12
100.0	.00	15.46	.23
150.0	.00	15.46	.34
200.0	.00	15.46	.44
250.0	.03	21.28	.53
300.0	.08	21.84	.62
350.0	.13	22.40	.70
400.0	.18	22.98	.77
450.0	.24	23.59	.83
500.0	.31	24.24	.88
550.0	.35	36.15	.95
600.0	.35	36.40	.95
VARIABLE POROSITY Evf = 0.9, VAPOUR PRESSURE SALT			
.0	.00	12.77	.00
50.0	.00	19.58	.09
100.0	.00	19.59	.18
150.0	.00	19.61	.27
200.0	.00	19.63	.36
250.0	.00	19.64	.44
300.0	.01	20.97	.51
350.0	.05	21.55	.60
400.0	.10	22.13	.69
450.0	.16	22.73	.76
500.0	.22	23.35	.82
550.0	.28	24.02	.87
600.0	.33	35.35	.95
VARIABLE POROSITY Evf = 0.5, VAPOUR PRESSURE WATER			
.0	.00	12.77	.00
50.0	.00	15.46	.12
100.0	.00	15.46	.23
150.0	.00	15.46	.34
200.0	.00	15.46	.44
250.0	.03	21.29	.53
300.0	.08	22.35	.62
350.0	.12	24.17	.69
400.0	.17	25.56	.75
450.0	.21	26.33	.80
500.0	.26	27.03	.84
550.0	.30	27.68	.87
600.0	.35	33.39	.90

650.0	.35	36.40	.95
700.0	.35	36.40	.95
750.0	.35	36.40	.95
800.0	.35	36.40	.95

VARIABLE POROSITY Evf = 0.5, VAPOUR PRESSURE SALT

.0	.00	12.77	.00
50.0	.00	19.58	.09
100.0	.00	19.59	.18
150.0	.00	19.61	.27
200.0	.00	19.63	.36
250.0	.00	19.64	.44
300.0	.01	20.97	.51
350.0	.05	21.73	.60
400.0	.10	23.26	.68
450.0	.15	25.20	.74
500.0	.19	26.05	.79
550.0	.24	26.81	.84
600.0	.29	27.51	.87
650.0	.33	30.55	.90
700.0	.33	36.40	.95
750.0	.33	36.40	.95
800.0	.33	36.40	.95

EXPERIMENTAL CONDITIONS

K2SO4	10.0WT %
AIR TEMP(C)	45.80
AIR VELOCITY (M/S)	1.20
INITIAL DROP WEIGHT (MG)	5.17
EXPERIMENTAL REFERENCE	D84-3

PREDICTED RESULTS

TIME(S)	CRUST THICKNESS (MM)	DROP TEMPERATURE (C)	FRACTION OF INITIAL WT EVAPORATED

VARIABLE POROSITY Evf = 0.9

.0	.00	11.57	.00
50.0	.06	19.83	.14
100.0	.12	20.75	.27
150.0	.18	21.61	.39
200.0	.24	22.43	.50
250.0	.31	23.23	.59
300.0	.38	24.02	.67
350.0	.46	24.81	.74
400.0	.54	25.62	.80
450.0	.63	29.29	.85
500.0	.63	45.50	.90
550.0	.63	45.79	.90
600.0	.63	45.80	.90

EXPERIMENTAL CONDITIONS
==========

K2SO4	15.0WT %
AIR TEMP(C)	61.00
AIR VELOCITY (M/S)	1.20
INITIAL DROP WEIGHT (MG)	3.08
EXPERIMENTAL REFERENCE	D88-2

PREDICTED RESULTS
==========

TIME(S)	CRUST THICKNESS (MM)	DROP TEMPERATURE (C)	FRACTION OF INITIAL WT EVAPORATED
VARIABLE POROSITY Evf = 0.9			
.0	.00	12.63	.00
20.0	.03	25.69	.09
40.0	.07	26.33	.19
60.0	.10	26.93	.29
100.0	.18	28.14	.46
140.0	.27	29.37	.61
180.0	.36	30.66	.73
220.0	.43	53.32	.80
240.0	.43	60.20	.85
280.0	.43	60.99	.85
300.0	.43	61.00	.85

EXPERIMENTAL CONDITIONS
==========

K2SO4	10.0WT %
AIR TEMP(C)	91.00
AIR VELOCITY (M/S)	0.80
INITIAL DROP WEIGHT (MG)	2.68
EXPERIMENTAL REFERENCE	D93-3

PREDICTED RESULTS
==========

TIME(S)	CRUST THICKNESS (MM)	DROP TEMPERATURE (C)	FRACTION OF INITIAL WT EVAPORATED
VARIABLE POROSITY Evf = 0.9			
.0	.00	14.18	.00
20.0	.05	27.64	.15
30.0	.08	28.25	.23
50.0	.14	29.52	.38
60.0	.17	30.19	.45
70.0	.21	30.90	.51
100.0	.32	33.24	.68
110.0	.36	34.14	.73
130.0	.46	36.21	.82
140.0	.51	37.48	.85
150.0	.52	69.56	.85
170.0	.52	88.31	.90
190.0	.52	90.67	.90
200.0	.52	90.88	.90

EXPERIMENTAL CONDITIONS

K2SO4	15.0WT %
AIR TEMP(C)	91.00
AIR VELOCITY (M/S)	0.80
INITIAL DROP WEIGHT (MG)	2.93
EXPERIMENTAL REFERENCE	D99-3

PREDICTED RESULTS

VARIABLE POROSITY Evf = 0.9

TIME(S)	CRUST THICKNESS (MM)	DROP TEMPERATURE (C)	FRACTION OF INITIAL WT EVAPORATED
.0	.00	14.03	.00
10.0	.02	26.93	.07
20.0	.05	27.57	.15
30.0	.08	28.16	.23
40.0	.11	28.77	.30
50.0	.14	29.40	.37
60.0	.17	30.05	.44
70.0	.20	30.72	.50
80.0	.24	31.42	.56
90.0	.27	32.16	.61
100.0	.31	32.94	.67
110.0	.35	33.76	.71
120.0	.39	34.66	.76
130.0	.44	35.63	.80
140.0	.45	68.94	.80
150.0	.45	83.20	.80
160.0	.45	88.27	.80
170.0	.45	90.05	.80
180.0	.45	90.67	.80
190.0	.45	90.88	.80
200.0	.45	90.96	.80

APPENDIX C6-COPPER SULPHATE

EXPERIMENTAL CONDITIONS

CUSO4	18.0WT %
AIR TEMP(C)	36.9
AIR VELOCITY (M/S)	1.00
INITIAL DROP WEIGHT (MG)	4.34
EXPERIMENTAL REFERENCE	D104-1

PREDICTED RESULTS

VARIABLE POROSITY Evf = 0.9, VAPOUR PRESSURE WATER

TIME(S)	CRUST THICKNESS (MM)	DROP TEMPERATURE (C)	FRACTION OF INITIAL WT EVAPORATED
.0	.00	18.12	.00
50.0	.04	16.81	.11
100.0	.09	17.84	.22
150.0	.14	18.87	.31
200.0	.19	19.91	.41
250.0	.24	20.97	.49
300.0	.30	22.07	.57
350.0	.36	23.23	.63
400.0	.43	24.47	.69
450.0	.51	25.83	.74
500.0	.57	35.06	.82
550.0	.57	36.83	.82
600.0	.57	36.85	.82

VARIABLE POROSITY Evf = 0.9, VAPOUR PRESSURE SALT

.0	.00	18.12	.00
50.0	.04	16.89	.11
100.0	.09	17.91	.22
150.0	.14	18.93	.32
200.0	.19	19.97	.41
250.0	.25	21.03	.49
300.0	.30	22.13	.57
350.0	.37	23.29	.64
400.0	.44	24.52	.70
450.0	.52	25.89	.75
500.0	.57	35.33	.82
550.0	.57	36.83	.82
600.0	.57	36.85	.82

VARIABLE POROSITY EvF = 0.5, VAPOUR PRESSURE WATER

.0	.00	18.12	.00
50.0	.04	16.81	.11
100.0	.09	18.28	.21
150.0	.13	20.28	.31
200.0	.18	22.69	.39
250.0	.22	24.63	.45
300.0	.26	25.63	.51
350.0	.30	26.55	.56
400.0	.34	27.39	.61
450.0	.38	28.19	.65

500.0	.43	28.94	.69
550.0	.47	29.67	.72
600.0	.52	30.39	.75
650.0	.57	33.92	.77
700.0	.57	36.81	.82
750.0	.57	36.85	.82
800.0	.57	36.85	.82

VARIABLE POROSITY Evf = 0.5, VAPOUR PRESSURE SALT

.0	.00	18.12	.00
100.0	.09	18.28	.21
200.0	.18	22.69	.39
300.0	.25	27.74	.50
400.0	.30	31.63	.57
500.0	.34	32.98	.61
600.0	.37	33.35	.64
700.0	.40	33.68	.67
800.0	.44	33.97	.69
900.0	.47	34.24	.72
1000.0	.50	34.48	.74

EXPERIMENTAL CONDITIONS
==========

CUSO4	10.0WT %
AIR TEMP(C)	20.90
AIR VELOCITY (M/S)	1.00
INITIAL DROP WEIGHT (MG)	2.85
EXPERIMENTAL REFERENCE	D122-2

PREDICTED RESULTS
==========

TIME(S)	CRUST THICKNESS (MM)	DROP TEMPERATURE (C)	FRACTION OF INITIAL WT EVAPORATED

VARIABLE POROSITY Evf = 0.2, VAPOUR PRESSURE WATER

.0	.00	13.36	.00
100.0	.00	3.21	.18
200.0	.04	5.22	.35
300.0	.12	9.49	.52
400.0	.19	14.01	.62
500.0	.23	17.05	.68
600.0	.26	18.62	.71
700.0	.28	18.83	.73
800.0	.30	19.01	.76
900.0	.32	19.17	.77
1000.0	.34	19.31	.79
1100.0	.36	19.44	.81
1200.0	.39	19.56	.82

EXPERIMENTAL CONDITIONS

CUSO4	5.0WT %
AIR TEMP(C)	65.80
AIR VELOCITY (M/S)	1.00
INITIAL DROP WEIGHT (MG)	4.23
EXPERIMENTAL REFERENCE	D125-1

PREDICTED RESULTS

VARIABLE POROSITY Evf = 0.5, VAPOUR PRESSURE WATER

TIME(S)	CRUST THICKNESS (MM)	DROP TEMPERATURE (C)	FRACTION OF INITIAL WT EVAPORATED
.0	.00	17.38	.00
25.0	.00	15.67	.10
50.0	.00	15.66	.19
75.0	.00	15.66	.28
100.0	.00	15.66	.37
125.0	.00	15.65	.44
150.0	.00	15.65	.52
175.0	.00	15.64	.59
200.0	.00	15.64	.65
225.0	.00	15.63	.71
250.0	.04	20.76	.77
275.0	.11	28.61	.83
300.0	.18	35.07	.87
325.0	.24	54.65	.90
350.0	.24	65.67	.95

EXPERIMENTAL CONDITIONS

CUSO4	
AIR TEMP(C)	18.0WT %
AIR VELOCITY (M/S)	65.80
INITIAL DROP WEIGHT (MG)	1.00
EXPERIMENTAL REFERENCE	5.66
	D130-1

PREDICTED RESULTS

TIME(S)	CRUST THICKNESS (MM)	DROP TEMPERATURE (C)	FRACTION OF INITIAL WT EVAPORATED
VARIABLE POROSITY Evf = 0.5			
.0	.00	17.15	.00
25.0	.00	21.01	.07
50.0	.01	23.00	.14
75.0	.06	24.69	.23
100.0	.10	26.93	.32
125.0	.15	29.98	.39
150.0	.19	33.76	.46
175.0	.24	36.42	.52
200.0	.28	38.13	.57
225.0	.33	39.76	.62
250.0	.38	41.36	.66
275.0	.44	42.96	.70
300.0	.49	44.60	.73
325.0	.56	46.34	.76
350.0	.57	61.85	.82
375.0	.57	65.30	.82
400.0	.57	65.74	.82
VARIABLE POROSITY Evf = 0.2			
.0	.00	17.15	.00
25.0	.00	21.01	.07
50.0	.01	23.00	.14
75.0	.06	24.69	.23
100.0	.10	26.93	.32
125.0	.15	29.98	.39
150.0	.19	33.76	.46
175.0	.24	38.06	.51
200.0	.27	42.55	.56
225.0	.31	46.90	.59
250.0	.33	50.69	.62
275.0	.36	51.47	.64
300.0	.38	52.12	.66
325.0	.40	52.74	.68
350.0	.43	53.33	.70
375.0	.45	53.90	.71
400.0	.48	54.47	.73
425.0	.51	55.02	.74
450.0	.53	55.57	.75
475.0	.56	56.11	.77
500.0	.57	63.28	.82

APPENDIX C7-SODIUM ACETATE

EXPERIMENTAL CONDITIONS

CH3COONA	10.0WT %
AIR TEMP(C)	58.00
AIR VELOCITY (M/S)	1.00
INITIAL DROP WEIGHT (MG)	6.31
EXPERIMENTAL REFERENCE	D144-1

PREDICTED RESULTS

VARIABLE POROSITY Evf = 0.9, VAPOUR PRESSURE WATER

TIME(S)	CRUST THICKNESS (MM)	DROP TEMPERATURE (C)	FRACTION OF INITIAL WT EVAPORATED
.0	.00	18.40	.00
50.0	.00	19.72	.12
100.0	.00	19.72	.23
150.0	.00	19.72	.34
200.0	.00	19.71	.44
250.0	.00	19.71	.53
300.0	.00	19.71	.61
350.0	.00	31.77	.68
400.0	.07	39.31	.74
450.0	.14	41.05	.78
500.0	.23	42.98	.83
550.0	.29	56.62	.90
600.0	.29	58.00	.90

VARIABLE POROSITY Evf = 0.9, VAPOUR PRESSURE SALT

.0	.00	18.40	.00
100.0	.00	35.13	.13
200.0	.00	35.13	.27
300.0	.00	35.13	.40
400.0	.00	35.12	.51
500.0	.00	35.12	.61
600.0	.00	35.12	.70
700.0	.10	40.07	.79
800.0	.23	57.71	.90
900.0	.23	58.00	.90
1000.0	.23	58.00	.90

EXPERIMENTAL CONDITIONS

CH3COONA	20.0WT %
AIR TEMP(C)	58.00
AIR VELOCITY (M/S)	1.10
INITIAL DROP WEIGHT (MG)	4.48
EXPERIMENTAL REFERENCE	D146-1

PREDICTED RESULTS

TIME(S)	CRUST THICKNESS (MM)	DROP TEMPERATURE (C)	FRACTION OF INITIAL WT EVAPORATED
VARIABLE POROSITY Evf = 0.9, VAPOUR PRESSURE WATER			
.0	.00	18.61	.00
50.0	.00	13.94	.17
100.0	.00	13.93	.32
150.0	.07	34.02	.44
200.0	.16	36.71	.54
250.0	.25	39.39	.63
300.0	.36	42.20	.71
350.0	.46	54.04	.75
400.0	.46	57.98	.80
450.0	.46	58.00	.80
500.0	.46	58.00	.80
VARIABLE POROSITY Evf = 0.9, VAPOUR PRESSURE SALT			
.0	.00	18.61	.00
50.0	.00	27.43	.11
100.0	.00	27.42	.23
150.0	.00	27.42	.33
200.0	.01	31.47	.43
250.0	.10	35.00	.54
300.0	.19	38.02	.63
350.0	.30	41.14	.71
400.0	.40	54.67	.75
450.0	.40	57.99	.80
500.0	.40	58.00	.80
550.0	.40	58.00	.80
600.0	.40	58.00	.80

EXPERIMENTAL CONDITIONS

CH3COONA	40.0WT %
AIR TEMP(C)	58.00
AIR VELOCITY (M/S)	1.10
INITIAL DROP WEIGHT (MG)	8.46
EXPERIMENTAL REFERENCE	D153-1

PREDICTED RESULTS

TIME(S)	CRUST THICKNESS (MM)	DROP TEMPERATURE (C)	FRACTION OF INITIAL WT EVAPORATED
VARIABLE POROSITY Evf = 0.9			
.0	.00	20.42	.00
50.0	.05	38.61	.07
100.0	.10	39.68	.14
200.0	.23	41.75	.28
300.0	.36	43.83	.39
400.0	.52	46.02	.49
450.0	.61	47.21	.52
550.0	.69	57.80	.60
600.0	.69	57.99	.60
VARIABLE POROSITY Evf = 0.5			
.0	.00	20.42	.00
50.0	.05	38.61	.07
100.0	.10	40.07	.14
200.0	.21	44.28	.27
300.0	.31	47.32	.35
400.0	.41	48.95	.43
450.0	.46	49.67	.46
500.0	.51	50.36	.48
600.0	.62	51.63	.53
650.0	.68	52.25	.55
700.0	.69	57.53	.60
VARIABLE POROSITY Evf = 0.2			
.0	.00	20.42	.00
100.0	.10	40.07	.14
300.0	.30	48.97	.35
400.0	.37	52.65	.40
500.0	.41	54.39	.43
700.0	.49	55.01	.47
900.0	.56	55.50	.51
1000.0	.60	55.71	.52
FIXED POROSITY Ef = 0.2			
.0	.00	20.42	.00
100.0	.07	46.29	.10
200.0	.13	49.35	.18
400.0	.23	52.03	.29
600.0	.32	53.40	.36
800.0	.40	54.28	.42
900.0	.44	54.63	.44
1000.0	.48	54.93	.46

EXPERIMENTAL CONDITIONS

CH3COONA	10.0WT %
AIR TEMP(C)	104.40
AIR VELOCITY (M/S)	1.00
INITIAL DROP WEIGHT (MG)	7.91
EXPERIMENTAL REFERENCE	D155-1

PREDICTED RESULTS

TIME(S)	CRUST THICKNESS (MM)	DROP TEMPERATURE (C)	FRACTION OF INITIAL WT EVAPORATED
VARIABLE POROSITY Evf = 0.9, VAPOUR PRESSURE WATER			
.0	.00	17.85	.00
25.0	.00	22.24	.11
50.0	.00	22.24	.21
75.0	.00	22.23	.31
100.0	.00	22.23	.41
125.0	.00	22.22	.49
150.0	.00	22.22	.57
175.0	.00	22.21	.64
200.0	.02	44.45	.70
225.0	.12	49.21	.77
250.0	.24	54.10	.83
275.0	.30	94.96	.88
300.0	.30	103.93	.90
325.0	.30	104.38	.90
350.0	.30	104.40	.90
375.0	.30	104.40	.90
400.0	.30	104.40	.90
VARIABLE POROSITY Evf = 0.9, VAPOUR PRESSURE SALT			
.0	.00	17.85	.00
25.0	.00	38.69	.08
50.0	.00	38.72	.16
75.0	.00	38.72	.25
100.0	.00	38.72	.33
125.0	.00	38.71	.40
150.0	.00	38.71	.47
175.0	.00	38.70	.54
200.0	.00	38.70	.60
225.0	.00	38.70	.66
250.0	.00	38.69	.71
275.0	.03	45.79	.76
300.0	.15	51.00	.82
325.0	.24	92.31	.85
350.0	.24	103.98	.90
375.0	.24	104.38	.90
400.0	.24	104.40	.90

APPENDIX C8-A COMPARIS ON OF MODEL 1 AND MODEL 2

EXPERIMENTAL CONDITIONS

NA2SO410H20	40.0WT %
AIR TEMP(C)	20.4
AIR VELOCITY (M/S)	1.00
INITIAL DROP WEIGHT (MG)	8.76
EXPERIMENTAL REFERENCE	D2-1

PREDICTED RESULTS

MODEL 1

TIME(S)	CRUST THICKNESS (MM)	DROP TEMPERATURE (C)	FRACTION OF INITIAL WT EVAPORATED
.0	.00	16.40	.00
100.0	.05	12.22	.07
200.0	.10	12.72	.13
300.0	.15	13.20	.19
400.0	.20	13.67	.25
500.0	.25	14.11	.30
600.0	.30	14.55	.34
700.0	.35	14.97	.38
800.0	.41	15.38	.42
900.0	.46	15.79	.46
1000.0	.52	16.19	.49
1100.0	.59	16.59	.52
1200.0	.66	16.99	.54
1300.0	.69	20.23	.60
1400.0	.69	20.35	.60
1500.0	.69	20.35	.60

EXPERIMENTAL CONDITIONS

K2SO4
AIR TEMP(C) 15.0WT %
AIR VELOCITY (M/S) 200.00
INITIAL DROP WEIGHT (MG) 0.80
EXPERIMENTAL REFERENCE 2.68
D99-1

PREDICTED RESULTS

TIME(S)	CRUST THICKNESS (MM)	DROP TEMPERATURE (C)	FRACTION OF INITIAL WT EVAPORATED
MODEL 1			
.0	.00	14.18	.00
10.0	.07	42.04	.21
20.0	.16	44.86	.43
30.0	.27	48.25	.62
40.0	.40	52.52	.77
50.0	.45	134.49	.85
60.0	.45	178.57	.85
70.0	.45	192.58	.85
80.0	.45	197.37	.85
90.0	.45	199.06	.85
100.0	.45	199.66	.85
MODEL 2			
.0	.00	14.03	.00
10.0	.06	37.23	.16
20.0	.12	38.90	.33
30.0	.20	40.78	.49
40.0	.28	42.95	.62
50.0	.38	45.56	.74
60.0	.45	89.58	.81
70.0	.45	162.72	.86
80.0	.45	186.72	.86
90.0	.45	195.09	.86
100.0	.45	198.16	.86

APPENDIX D

PAPERS PUBLISHED

A STUDY OF EVAPORATION FROM, AND DRYING OF, SINGLE DROPLETS

H H ALI, C J HUMFORD, G V JEFFREYS & G S BAINS

DEPT OF CHEMICAL ENGINEERING & APPLIED CHEMISTRY
ASTON UNIVERSITY, BIRMINGHAM, UK

ABSTRACT

An investigation was undertaken of the mass transfer and heat transfer rates from single drops suspended from a rotating nozzle, in a specially-designed horizontal wind tunnel. The study covered pure liquid (water), solutions (eg sodium sulphate decahydrate, organic and inorganic products), and slurries of various organic products over a range of air temperatures (20-200°C) and air velocities (0.1-2.1 m/s). Revised correlations were obtained for mass and heat transfer coefficients from pure liquid drops. In the drying of drops of solutions and slurries very good agreement was obtained between experimental and predicted overall mass transfer coefficients.

1. INTRODUCTION

Evaporation of moisture from, and subsequently drying of, atomised droplets in a spray drier involves simultaneous heat, mass and momentum transfer. Heat necessary for evaporation is transferred by convection from the hot gases to the drop surface and thence by conduction into each drop; vapour is transferred from the drop by diffusion and convection back into the gas stream. The mass transfer flux at the interface is therefore a function of the temperature, humidity and transport properties of the gas and the diameter, temperature, and relative velocity of the drop. Initially a free liquid interface exists between the gas stream and the droplet and evaporation proceeds as for a pure liquid. However once the droplet solution is concentrated beyond saturation, or almost instantaneously in the case of slurry drops, the commencement of formation of a solid crust separates the gas and liquid interface. Subsequent drying takes place by heat conduction through the crust and evaporation through the pores. As the crust increases in thickness during drying there is increased resistance to heat and mass transfer.

The mass transfer process is highly complex and difficult to model mathematically. With some materials the constant drying rate period is succeeded by film formation representing an added resistance [9]. Furthermore, following crust formation, the heat and mass transport paths differ and the Colburn analogy no longer applies[6]. This is confirmed by the fracture, shrinkage or inflation observed with many dried particles. These further complicate the modelling of heat and mass transfer and affect the final particulate forms which may be of greater, or lesser, diameter than the initial drops and include hollow spheres, particle fragments and hemispheres.

The majority of research pertaining to heat and mass transfer in spray drying has been carried out with single, relatively large, (1-5mm) stationary drops of pure liquid.

Evaporation of droplets at finite air velocities was treated theoretically and experimentally by Frossling [1]; Ranz and Marshall [2] proposed the following equations for heat and mass transfer coefficients from spheres.

$$Sh = 2 + 0.6\, Re^{0.5}\, Sc^{0.33} \qquad (1)$$

$$Nu = 2 + 0.6\, Re^{0.5}\, Pr^{0.33} \qquad (2)$$

Rates of evaporation for drops of pure liquids in streams of high-temperature air were subsequently correlated by Downing (3) who introduced two empirical correlation factors into equations (1) and (2). The first factor $(1/B)\ln(1+B)$ accounts for the heat taken up by the outwardly diffusing vapour and the second factor T_D/T_A accounts for the film properties being functions of temperature.

$$Nu = MN\left(\frac{1}{B}\right)\ln(1+B)\,(2 + 0.6\, Re^{0.5} Pr^{0.33}) \qquad (3)$$

$$Sh = M(2 + 0.6\, Re^{0.5}\, Sc^{0.33}) \qquad (4)$$

$$\text{where } M = 1 - 0.4\,(1 - T_D/T_A) \qquad (5)$$

$$N = 1 - 0.4\left[1 - \left(\frac{1}{B}\right)\ln(1+B)\right] \qquad (6)$$

Cheong et al (4) developed a model based on a receding interface to predict the simultaneous heat and mass transfer rates in the drying of slurry droplets. Predicted wet core temperatures, and drop weights prior to crust formation, were in good agreement with experimental data for the drying of filament-suspended drops of a slurry of sodium sulphate decahydrate, although under these conditions evaporation is not uniform from the drop surface, i.e. evaporation occurs more rapidly from the drop side facing the direction of air flow than in the wake.

The present investigation comprised a study of the rate of evaporation from water droplets at different temperatures followed by a study of the drying of drops containing different dissolved, and suspended, solids under various conditions.

PAPER PRESENTED AT 6'TH INTERNATIONAL DRYING SYMPOSIUM, IDS'88, VERSAILLES, FRANCE (1988)

2. EXPERIMENTAL APPARATUS AND PROCEDURES

The flow system was designed to supply hot, dry air to the working section at a selected constant humidity and uniform temperature. The experimental apparatus is shown in Figure 1 [after 5,6].

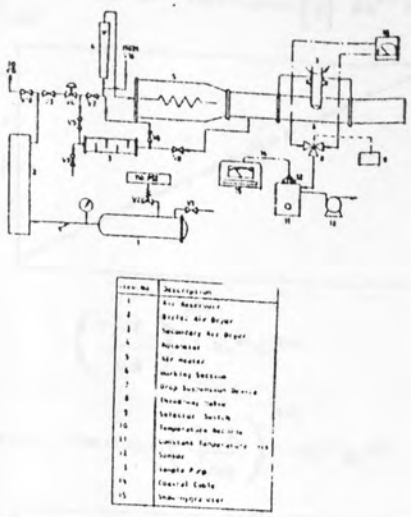

Fig 1 Schematic Diagram of Experimental Apparatus

Compressed air was transferred via a reservoir, to dampen any fluctuations, and then into a Birlec air dryer. The pressure was reduced to 1.5 bar and the air passed to the system via the secondary air dryer. The flowrate was controlled by a gate valve at the inlet to the wind tunnel. The air was heated to any desired temperature in the range 21°C to 300°C using three, 1 kw electric heating elements controlled by a rotary voltage regulator. Stainless steel nozzles, 2.8 mm ID and 4,6 or 8 mm OD, were designed to be easily introduced into, or removed from, the working section. Each nozzle could accommodate a thermocouple for drop temperature measurement.

The air flowrate, temperature and humidities upstream and downstream of the drop, and the drop diameter were recorded at incremental time intervals during each experiment.

To ensure uniform evaporation, the drop was rotated on the suspension device at 15 rpm and its size was measured using both a cathetometer and from photographs taken with a 35 mm Chinon camera. For drops containing solids, the crust formed was gently sliced off onto a filter paper at the end of each run; this absorbed the excess solution in the hollow shell of the crust leaving a rigid, hollow, hemispherical crust.

For crust thickness measurements, or to study the internal and external crust structure, the above procedure was repeated after drying periods of 5,10,15,20,25 and 30 minutes. Each specimen was introduced into the chamber of the Stereoscan microscope and microphotographs were obtained on 35 mm film. A Zetron Optical Microscope with a 35 mm camera attached to it was mainly used for crust thickness measurements.

3. EXPERIMENTAL RESULTS

3.1 Water Droplets

Audu [6] developed the following equation for the gas film mass transfer coefficient,

$$k_g = \frac{\dot{m}_{DA}(Y_o - Y_i)}{A_D(P_{ws} - P_p)} \frac{R T_A}{M_w} \qquad (7)$$

The heat transfer film coefficient, h_g, and the experimental Nusselt number were calculated as follows. The rate of heat transfer to a spherical drop can be expressed as,

$$\frac{dQ}{dt} = h_g A (T_A - T_D) \qquad (8)$$

The mass transfer from the drop is,

$$-\frac{dG}{dt} = \frac{dQ/dt}{\Delta h v} = -\frac{h_g A (T_A - T_D)}{\Delta h v} \qquad (9)$$

and since in this case

$$G = \frac{\pi d_o^3 \rho d}{12} \qquad (10)$$

then,

$$hg = \frac{-\Delta h v \rho_D}{6(T_A - T_D)} \frac{1}{d_D^2} \frac{d(d_D^3)}{dt} \qquad (11)$$

$$Nu = \frac{-\Delta h v \rho_D}{4\lambda_A (T_A - T_D)} \frac{d(d_D^2)}{dt} \qquad (12)$$

where $d(d_D^2)/dt$ can be determined from a plot of d_D^2 versus t.

Experimental results for water droplets within the temperature range 21°C -120°C were correlated according to the conventional equations (1) and (2). A least squares technique was used to correlate the data and the resulting correlations were,

$$Sh = 2 + 0.501 \left[\frac{T_A - T_D}{T_{AMB}}\right]^{-0.03} Re^{0.5} Sc^{0.33} \qquad (13)$$

and $$Nu = 2 + 0.228\left[\frac{1}{B}\right]^{0.2} Re^{0.5} Pr^{0.33} \qquad (14)$$

Figures (2) and (3) are plots of Sh against $\frac{[T_A - T_D]}{T_{AMB}}^{-0.03} Re^{0.5} Sc^{0.33}$ and Nu against $\left[\frac{1}{B}\right]^{0.2} Re^{0.5} Pr^{0.33}$

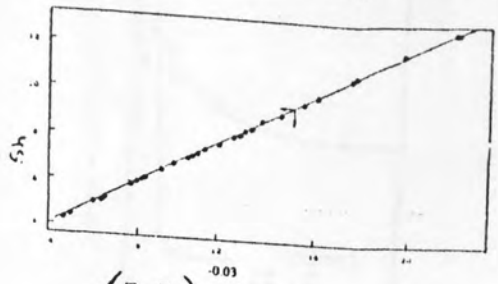

$$\left(\frac{T_A - T_D}{T_{AMB}}\right)^{-0.03} Re^{0.5} Sc^{0.33}$$

Fig 2. Plot of Sh vs $\left(\frac{T_A - T_D}{T_{AMB}}\right)^{-0.03} Re^{0.5} Sc^{0.33}$

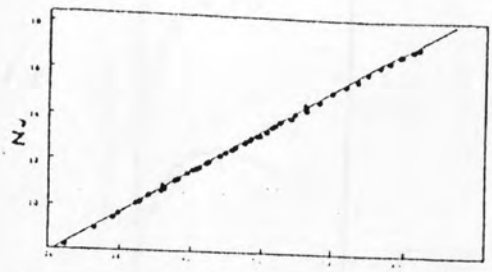

$$\left[\frac{1}{B}\right]^{0.2} Re^{0.5} Pr^{0.33}$$

Fig 3. Plot of Nu vs $\left(\frac{1}{B}\right)^{0.2} Re^{0.5} Pr^{0.33}$

The exponent on the temperature correction term in equation (13) is small so that, over the range of temperatures covered experimentally, this term had only a marginal effect. Equation (13) was subsequently used to predict k_g values for substitution into equation (17) to predict overall mass transfer coefficients in the drying of solution or slurry droplets.

3.2 Drops containing solids in solution or slurry form

The solutions investigated comprised,

i) Sodium sulphate decahydrate solution, up to 60% wt/wt solids, which tended to form smooth crystalline crusts of even thickness which contained few cracks and pores.

ii) Two different, organic dyes (A, B) as paste slurries with solid contents between 12% wt/wt to 18% wt/wt.

iii) Two organic pigment dye solutions.

iv) Solutions of three inorganic chelating agents (C,P,E) containing total solids in the range 25% wt/wt to 70% wt/wt.

Investigations were carried out by varying initial drop diameter, density, air velocity (and hence Reynolds number) air temperature, and nature of solid. The effect of additives was also studied.

Evaporation Rates

Plots of evaporation rate versus time after injection for droplets containing solids tend to exhibit three periods. The first period is characterised by a sharp increase in rate whilst evaporation takes place from the free liquid surface of the drop; the drop temperature also decreases to the wet-bulb temperature. The second stage is characterised by partial crust formation and the drop temperature starts to increase. Behaviour during this stage, which is specific for the material studied, was very short in the case of sodium sulphate decahydrate drops, since once this material reached saturation the crust formed quickly and hence the resistance to mass transfer increased. In the third stage,there is a sharp decrease in evaporation rate because a crust has formed completely. Crust structure, thickness and porosity have a marked effect on the rate during this stage.

Air velocity, air temperature, the initial solids content, the nature of any additive, and the nature of the solid were the experimental variables. These effects were evaluated in terms of the evaporation rate, crust thickness, overall mass transfer coefficient, crust mass transfer coefficient, and crust porosity.

Data for sodium sulphate decahydrate are shown in Figure 4 at air temperatures of 100°C and 120°C, a constant initial concentration of 50% wt/wt solids, and an air velocity of 0.93 ms^{-1}. Evaporation rates from drops of Organic Paste A slurry at high air temperatures (200°C and 300°C) with the addition of 13% additive (sodium chloride solution or Dispersol) are shown in Figure 5. Figures 6-9 illustrate evaporation rates of drops of different solutions.

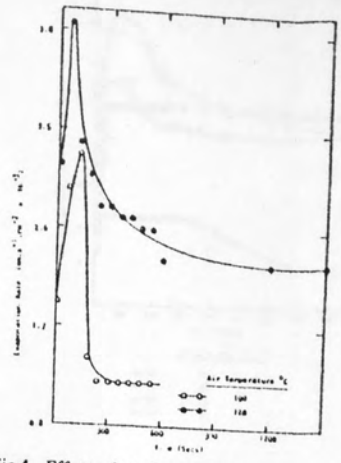

Fig 4 Effects of Air Temperature on the Evaporation Rates of Drops of Sodium Sulphate Decahydrate.

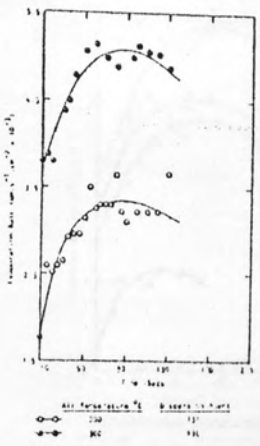

Fig 5 Effects of Air Temperature on the Evaporation Rates of Organic Paste Formulation A Slurry Drops of Initial Solids Content, 12% wt/wt.

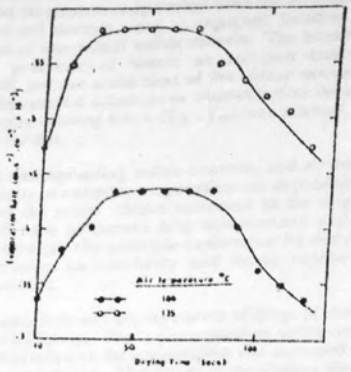

Fig 6 Evaporation Rates from 22% wt/wt solutions of Organic Pigment A at Air Temperatures 100°C and 135°C

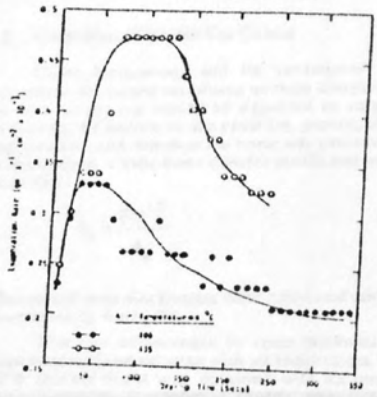

Fig 7 Evaporation Rates from Drops of Organic Pigment B at Air Temperatures 100°C and 135°C

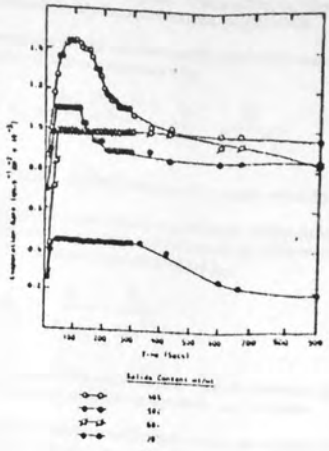

Fig 8 Evaporation Rates from Different Concentration Solutions of Inorganic Powder C at a constant Air Temperature of 130°C

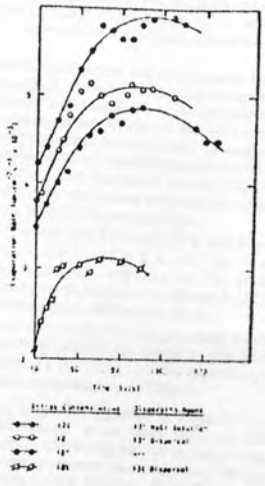

Fig 9 Effect of Additive on the Evaporation Rates of Organic Paste Formulation A Slurry Drops at 300°C

At initial concentration ranges between 12-70 wt% solids the maximum evaporation rates for different drops of solutions and slurries were, as expected, found to be higher for drops of low initial solids content. The lowering of the vapour pressure of water as solution concentration increased, and the attainment of the critical saturation point with concentrated solutions or slurries before the maximum temperature driving force ($T_A - T_w$) was reached, probably account for this.

At corresponding solids contents, and air temperature and velocity, maximum evaporation rate depended upon the nature of the solid. Since reference to the original data shows that the minimum drop temperatures attained were almost identical, the probable explanation for this difference is a variation in solubility and hence vapour-pressure depression (7).

Figure 9 shows drying curves of drops of slurries with different additives. For a corresponding solids content and identical conditions the evaporation rate increased when the additive was present. The nature of the additive also affected the evaporation rate, for example a drop of organic Paste Slurry Formulation A containing sodium chloride solution dried more rapidly, ie 40 seconds quicker, than a similar drop containing Dispersol at corresponding air velocity and temperature.

3.3 Crust Mass Transfer Coefficient

Crust formation, and its subsequent thickening, represents the major resistance to mass transfer. Therefore the rate of drying would be expected to vary with crust thickness, the nature of the crust (ie, porous, crystalline or impervious), and whether the crust was preceded by a skin, or membrane. Crust mass transfer coefficient was predicted from (5).

$$k_c = \frac{D\epsilon^{1.5}}{\delta_c} \qquad (15)$$

Theoretical crust thicknesses were calculated using the model developed by Audu (5).

The rate of increase in crust thickness was found experimentally to increase with air temperature. In general a 32% thicker crust was obtained with an increase in air temperature from 100°C to 120°C. This is in agreement with the predictable increase in temperature driving force for heat transfer. The rate of crust growth also increased by 8% with an increase in air velocity from 0.6 ms^{-1} to 1.2 ms^{-1}. This confirms the relatively small resistance offered by the gas film once a crust is formed since, according to equation (13) k_g would differ by a factor of $\sim(2)^{0.5} \sim 1.4$ between these runs.

As would be expected, crust porosity was affected by the nature of the solid forming the crust. It was found that selected additives increased crust porosity to different degrees. The presence of an additive remarkably changed the crust structure again depending upon the nature of the additive, eg, addition of Dispersol produced a completely different crust structure with the same material compared with sodium chloride addition. Obviously an additive could inhibit the drying rate if it tended to reduce the crust porosity or vice versa. In fact Dispersol apparently migrates to the surface and, being amorphous, increased the porosity, but

segregation of sodium chloride crystals at the surface resulted in the most porous crust. These effects, illustrated in Plate 1 would clearly be concentration-dependent.

Experimental mass transfer coefficients were calculated from a modified form of equation (7);

$$K_E = \frac{m_{DA}(Y_o - Y_i)}{A} \frac{R}{M_w} \frac{\Pi}{P_{vs} - P_p} \qquad (16)$$

where, $A = 2\pi(R^2 - \delta_c)^2)/e$ is the area for mass transfer.

Theoretical overall mass transfer coefficients were estimated from the following equation after substituting from equation (15) for the value of the crust coefficient k_c.

$$\frac{1}{K_T} = \frac{1}{H_1 k_g} + \frac{\delta_c}{De^{1.5}} \qquad (17)$$

Table 1 summarises the experimental and theoretical mass transfer coefficients for different solutions and slurries.

Crust mass transfer coefficients were calculated from equation (15) for specific materials. Eight different materials were used for drying studies but crust mass transfer coefficients were calculated for only three, covering a range of temperatures from 100°C to 200°C and solids content between 12% to 60%, since the other materials formed either a non-hollow, sometimes brittle impervious crust, or a crust containing many cracks and recovery of these types of crust proved very difficult. Table 2 lists values of k_c estimated from equation (15), denoted (*). and values calculated from the overall mass transfer coefficient and the evaporation rates of each specific material, denoted (**). Good agreement was found except for 50% and 60% wt/wt solids content of Inorganic Powder Formulation C, due to the formation of crusts characterised by cracks, fractures and an undulating surface. The first two features would represent additional areas for vapour release and the latter would result in a variation in pore area. The maximum evaporation rate for a 40% wt/wt; solids content of this material was 1.6×10^{-3} gs^{-1} cm^{-2} whilst for 50% and 60% wt/wt solids content it was 1.3×10^{-3} and 1.2×10^{-3} gs^{-1} cm^{-2} respectively. This, and crust structure in the electron microphotographs, suggest that there was indeed a different crust formation compared with 40% wt/wt solids.

Once a crust is completely formed pressure build-up may occur inside the drop which may result in cracking of the crust, or explosion of the drop, or the appearance of blow holes, such as that commencing in Plate 2.

During drying, Organic Pigment B formed a non-porous skin, or 'membrane' at an early state ie after 8 seconds; this acted as an additional barrier to mass transfer so that the interior core remained 'wet' even for a drop left suspended on the nozzle for 1 hour. In such cases the overall mass transfer coefficient should contain a term to include for the resistance to mass transfer due to this primary film [9].

Table 1. Experimental and Theoretical Mass Transfer Coefficients

Wt%	Solids	K_E	K_T
18%	Organic Paste Slurry A	2.3	2.2
15%	Organic Paste Slurry A	2.2	2.6
15%	Organic Paste Slurry A with sodium chloride	2.5	2.7
12%	Organic Paste Slurry A	2.7	3.0
40%	Inorganic Powder C solution at 110°C	4.4	3.9
40%	" 130°C	4.0	4.4
50%	" 130°C	4.1	3.9
60%	" 130°C	4.3	4.5
50%	Sodium Decahydrate solution at 100°C	9.9	9.6
60%	" 100°C	7.9	8.1
50%	" 120°C	9.5	9.5
60%	" 120°C	7.9	7.8

Table 2. Values of Crust Mass Transfer Coefficient

Nature of Solids Forming Crust	% Solids Content wt/wt	T_a °C	k_c (*) cms^{-1}	k (**) cms^{-1}
Organic paste B Formulation	18 – Dispersol	200	4.1	5.9
	15 – Dispersol		5.8	5.8
	15 – Sodium Chloride		7.2	11.1
	12 – Dispersol		10.1	12.5
Inorganic Powder Formulation C	40	110	14.4	12.8
	40	130	16.3	12.7
	50	130	3.9	12.9
	60	130	4.5	13.3
Sodium Sulphate Decahydrate	50	100	6.9	6.2
	60	100	4.6	5.8
	50	120	6.5	4.3
	60	120	4.5	3.4

* = Predicted from Eqn (15) ** = Experimental

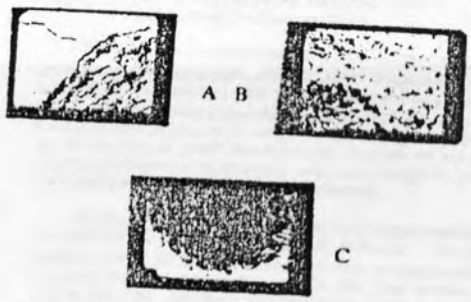

T_A = 200°C t = 900s A - No additive
B - 13% Dispersol Additive C - 13% NaCl Solution

Plate 1. The effect of Additives on Crust Structure of Organic Paste A Slurry Drop containing 12% wt/wt.

3.4 Film Resistance Prior to Crust Formation

At low temperatures transfer of moisture is apparently by diffusion through the film, since the steady hemispherical profile (Plate 3) suggests that intermittent film rupture and reformation was not involved. The material (Organic Pigment B) which exhibited film formation also formed a crust with a smooth outer surface, which would be excepted since the crust initially grows inwards from a smooth film. All other materials produced crusts with a rough, or crystalline, outer surface.

$T_A = 93°C$ $t = 600s$

Plate 2. Crust of Inorganic Powder Formulation E showing initiation of a blow hole prior to 'exploding'.

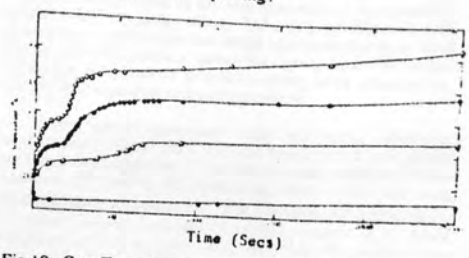

Fig 10 Core Temperature profile of Sodium Sulphate Decahydrate drops

In practical spray drying processes, materials that form films ie a 'skin' during drying (which may be desirable to 'seal-in' trace constituents e.g. flavours) tend to produce particles with an undesirable, transient stickiness which can result in interparticle agglomeration. Conversely particles which impinge on the chamber wall prior to 'dryness' but may not adhere, bounce off. On the other hand materials which do not form a skin during drying form non-sticking products but may adhere to the chamber wall on impingment.

Comparison of Figures 6 and 7, for which both pigments had the same initial solids-content, shows that the evaporation rate of Organic Pigment B prior to crust formation is 30% <Organic Pigment A at an identical air temperature. Hence, the film accounted for 30% of the resistance to mass transfer prior to crust formation.

3.5 Drop Core Temperature Measurements

Core temperature-profile measurements were made on drops of sodium sulphate decahydrate and Inorganic Powder Formulation C solutions. A comparison between drop core temperature behaviour is shown in Figures 10 and 11.

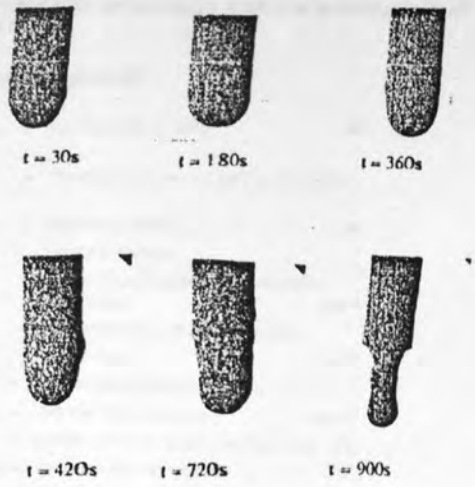

Plate 3. Photographs of Drops of Organic Pigment B. $T_A = 165°C$

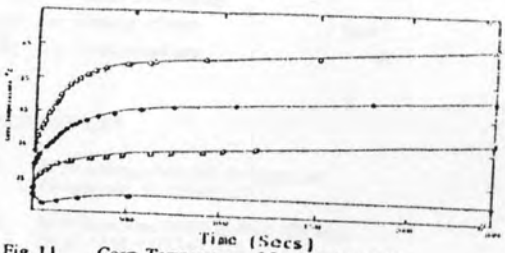

Fig 11 Core Temperature of Inorganic powder formulation C solution drops.

The behaviour of sodium sulphate decahydrate during drying at air temperatures above 33°C is unusual in that it forms different hydrates with incongruent melting points (8). Below the transition temperature of 32.4°C, the monoclinic decahydrate crystals are in equilibrium with the liquid phase. At the transition point, the rhombic crystals of anhydrous sulphate commence to separate and exist in equilibrium with the decahydrate and the saturated solution.

Figure 10 shows the shape of core temperature curves of sodium sulphate decahydrate solution. At an air temperature of 20°C a depression in core temperature occurs initially due to evaporation from the free surface as it approaches the wet-bulb temperature, then starts to rise again. This lowering in temperature was not observed at higher drying temperatures as shown in Figures 10 and 11. The values of the constant core temperatures attained depended on the temperature of the drying media. This behaviour was indicative of a phase change in sodium sulphate decahydrate (4) and dry crust samples were therefore prepared from drops of sodium sulphate decahydrate dried at air temperatures ranging from 22°C to

120°C. Thermogravimetry undertaken in a Linseis Thermobalance L81 showed that the crust of a drop dried at 22°C contained 7 to 9 crystalline hydrated water molecules; one dried at 35°C contained 4 to 6 molecules; one dried at 65°C contained 1 to 3 molecules, and the last sample dried at 120°C contained no hydrated water molecules. This confirmed the phase change which occurs during drying.

The shape of core temperature curve for a drop of Inorganic Powder Formulation C at an air temperature of 20°C showed a similar trend to sodium sulphate decahydrate at the same temperature. The lowering in the drop core temperature, due to evaporation from the free surface before the crust started to form, reached a minimum corresponding to the wet-bulb temperature. Once the crust started to form the temperature gradually increased. Core temperature curves for drops at 40°C, 61°C and 79°C did not exhibit the constant temperature period, confirming that there was no phase change. At these temperatures core temperatures started to increase gradually but remained less than the surrounding temperature even after a residence time of 1 hour.

4. CONCLUSIONS

The experimental data for pure liquid drops were well-correlated by the modified equations (1) and (2). When drops of solution, or slurry, were dried a hollow crust was eventually formed. The crust thickness growth rate increased with increase in air mass flowrate, air temperature and the initial moisture content. The crusts structure varied; some were crystalline porous, rough non-crystalline, or very smooth and less porous. Hence the drying rate after crust formation was, and in practical drying will always be, specific to the product under consideration.

Very good agreement was obtained between experimental overall mass transfer coefficients and those predicted from equation (17) where k_g was predicted from equation (13) and k_c the controlling crust coefficient was predicted from equation (15). For this purpose porosity, ε, was predicted via a modified Kozeny equation [5,6] from crust pressure drop data and the crust thickness was measured using an ESM or optical microscope. With droplets at higher temperatures, crusts tended to deform. Some deformation was characterised by longitudinal expansion or formation of a 'protrusion' from the side; sometimes two protrusions formed, followed either by an explosion of repetitive re-building of the crust resulting in a final product with a rough surface. Some of the crusts cracked to release the internal pressure and formed blow holes.

As previously observed, drying of drops was characterised by two distinct periods; an initial constant rate period and a falling rate period as soon as the crust was formed. After crust formation fractures occurred randomly but were more frequent at higher temperatures. The optimum air temperature for an industrial spray tower has been predicted from that allowing retention of uniform crusts on single droplets.

Core temperature measurements for drops of sodium sulphate decahydrate solution were characterised by a distinct constant temperature period during crust formation, confirmed by thermalgravimetry to be due to a solid phase change.

The presence of selected additives (either Dispersol or sodium chloride) increased the drying rate which was shown by ESM to be due to changes in the structure and porosity of the crust.

NOMENCLATURE

A_D	=	surface area of drop	m^2
B	=	Transfer number = $Cp(T_A-T_D) / \Delta hv$	
d_D	=	diameter of drop	m
H_I	=	Henry's constant	
K_E	=	experimental overall mass transfer coefficient	ms^{-1}
K_T	=	theoretical overall mass transfer coefficient	ms^{-1}
M_w	=	molecular weight	
$\dot{m}_{DA}$	=	dry air mass flowrate	kgs^{-1}
P_p	=	partial pressure water vapour in air	P_a
T_{AMB}	=	ambient air temperature	K
T_D	=	temperature of the drop	K
T_i	=	inlet air temperature	K
Y_i	=	inlet air humidity	
Y_O	=	outlet air humidity	
ρ_D	=	density of drop	kgm^{-3}
δ_C	=	crust thickness	m

REFERENCES

1. N Frossling, Gerlands Beitrage zur Geophysik, 52 (1938) 170
2. W E Ranz and W R Marshall, Ch Eng Prog, 48 (1952) 141, 173
3. C G Downing, AIChEJ, 12 (1966) 760
4. H.W.Cheong, G.V. Jeffreys, and C.J. Mumford, AIChE.Journal, 32, 8, 1986, 1334.
5. T O K Audu, PhD thesis, University of Aston in Birmingham, England (1973)
6. T O K Audu and G V Jeffreys. Trans Inst Ch Eng, 53 (1975) 165
7. H H Ali, PhD Thesis, University of Aston in Birmingham, England (1985)
8. S Glasstone, Text Book of Physical Chemistry, 1st edition, Macmillan Ltd, London (1940)
9. G.S. Bains, Unpublished work, Aston University

MECHANISMS OF DRYING OF PARTICULATE SLURRIES

GS Bains, CJ Mumford, GV Jeffreys†

Introduction

In spray drying discrete dried particles are produced continuously by spraying a feed which may be either a solution, slurry or paste into a hot drying medium, usually air. The feed is atomised; a large surface area is thereby created and moisture is removed by simultaneous heat and mass transfer processes.

A knowledge of the controlling mechanisms within the heat and mass transfer processes is required for the optimum design of a spray drier. Considerable research has been carried out on the evaporation of pure liquid drops [1, 2] but there are limited experimental data on the drying of drops containing solids. This can be attributed, in part, to the complexities in analysing the heat and mass transfer processes after a solid crust has formed. A study is therefore continuing into the mechanisms by which single suspended droplets dry, encompassing both the mass and temperature histories [3].

The drying of drops containing dissolved/suspended solids

The feed will contain either dissolved/suspended solids. Their presence leads to a decrease in the vapour pressure of the liquid at the drop surface. This leads to a reduction in the mass transfer rate. The surface temperature of the evaporating droplet will consequently increase above the thermodynamic wet bulb temperature. The drying characteristics are then related to the formation of a solid phase on the surface of the droplet, providing an additional resistance to moisture transfer into the surrounding media.

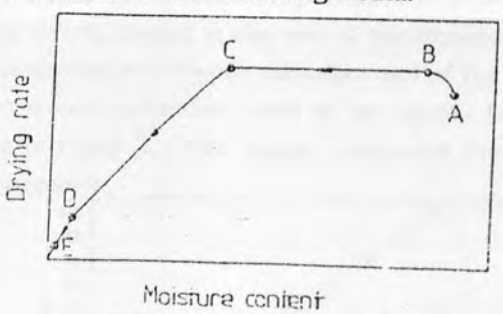

Figure 1 - Drying rate curve

Intially drying commences immediately the droplet contacts the hot gas as represented by period AB [4]. The drying rate initially increases until the heat transfer across the droplet-gas interface reaches equilibrium. Period BC represents conditions of dynamic equilibrium, characterised by evaporation from a free liquid surface, termed the "constant rate" period. The

† Department of Chemical Engineering, Aston University, Birmingham B4 7ET

PAPER PRESENTED AT INST. CHEM. ENGRS. RESEARCH MEETING, NOTTINGHAM UNIVERSITY (1987).

droplet surface is maintained saturated by adequate migration of moisture from within the droplet to the surface. Point C is the "critical point" at which moisture within the droplet can no longer maintain surface saturation. Period CD represents the "falling rate" period which may have a different character, if local areas of wetness remain on the droplet surface. Period CD continues until no areas of wetness remain. The major resistance to mass transfer is then represented by the solid crust. Evaporation continues at a decreasing rate until the droplet acquires a moisture content in equilibrium with the surrounding gas.

Experimental Investigation

Droplets of 1 to 2 mm were suspended in a vertical wind tunnel. The advantage of using a vertical wind tunnel with upward flowing air was that the suspension device resided in the wake of the drop, where it was least likely to disturb the flow. Convection currents also tended to move symmetrically around the drop, simulating more closely a drop in free flight.

Different forms of suspension device include nozzles [5, 6], capillaries and glass filaments [1]. A novel thin film copper/constantan thermocouple (– 2 mm od) based on the original design of Cheong [2] has been developed for the simultaneous measurement of drop weight (by deflection) and drop temperature.

The method of formation of this thermocouple was unique and involved insertion of a 50 micron constantan wire into a 10 cm long soda lime glass tube (– 13 mm od). One end of the tube was heated and the end sealed with the wire encased in it. The tube was then heated – 2 cm from this end until the glass began to flow. The tube was rapidly stretched and the wire was pulled through the filament so formed (filaments as fine as 0.1 mm od were produced). A 25 cm length filament was gently heated at one end to give a smooth 45° bend. A fine tip (– 0.1 mm) was exposed at this end which was subsequently sealed. Copper was finally deposited onto the filament by a vacuum deposition technique.

A junction was thereby created at one end of the filament. A second junction was created by wrapping constantan wire around the other end of the filament and placing this inside an ice bath. A typical calibration chart of mv output from the thermocouple vs temperature is shown in Figure 2. The output compared favourably with a standard copper-constantan thermocouple.

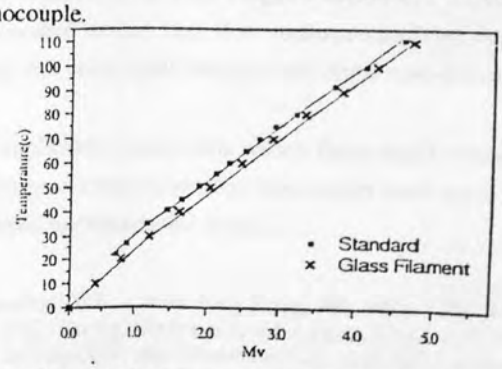

Figure 2 - A comparison of the outputs from a standard copper/constantan thermocouple vs the glass filament.

This arrangement facilitates a simultaneous measurement of droplet weight and temperature during the drying of droplets of 1 to 2 mm irrespective of the drying mechanisms involved.

Receding Evaporation interface Model

A mathematical model developed by Cheong [2] for slurries has been modified, and extended to cover the drying of solutions. The model is based on the following assumptions and predicts changes in drop temperature, drop weight and crust thickness, with time.

i) If the initial concentration is less than the saturated concentration, drying proceeds initially at a constant rate.

ii) A crust begins to form once the concentration reaches the saturated concentration.

ii) Evaporation only occurs at the evaporation interface, which is the interface between the wet core and dry crust.

iv) The evaporation interface recedes into the wet core as evaporation proceeds.

v) The crust once formed does not shrink or inflate and no fractures occur.

vi) The core temperature is uniform throughout the core.

vii) Heat is transferred from the drying air to the crust solely by convection.

viii) Heat is transferred through the crust by conduction.

ix) Moisture is transferred from the evaporation interface by vapour diffusion through the pores, represented by an effective diffusivity.

x) The core density remains constant during the falling rate period.

xi) The energy and vapour storage within the crust are negligible.

The model has been programmed in Fortran 77 and a comparison made with experimental data.

Discussion of Results

The drying characteristics of 1-2 mm drops of sodium sulphate decahydrate were studied over a range of air temperatures (20 - 80 °C) and concentrations (5 - 40% wt solids). Typical results are shown in Figures 2, 3 and 4. Good agreement was obtained between the experimental and predicted results for the weight evaporated. The temperature history of the drop was however obscured by the fact that sodium sulphate decahydrate melts at 33 °C. Studies are continuing with other rigid porous, and rigid non-porous, crust-forming inorganic salts.

The model is applicable to materials which form rigid crusts. Many materials however experience different forms of crust formation noticeably non-rigid and skin forming materials and future work is in hand to characterise these.

References

1 Ranz WE, Marshall WR, Chem Eng Prog, 48, 141, 173 (1952).
2 Cheong HW, PhD Thesis, University of Aston, England (1983).
3 Cheong HW, Jeffreys GV and Mumford CJ, AIChE Journal 32, 8, 1334 (1986).
4 Masters K, Spray Drying, 2nd Edition, John Wiley & Sons, NY (1976).
5 Audu TOK, PhD Thesis, University of Aston, England (1973).
6 Ali HH, PhD Thesis, University of Aston, England (1985).

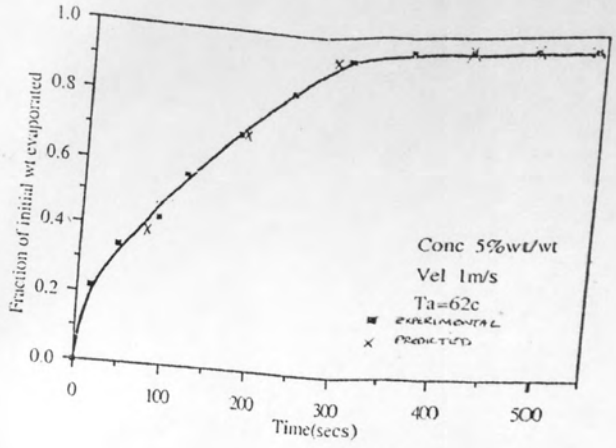

Figure 3 - Fraction of initial weight evaporated vs time (1.5 mm drop)

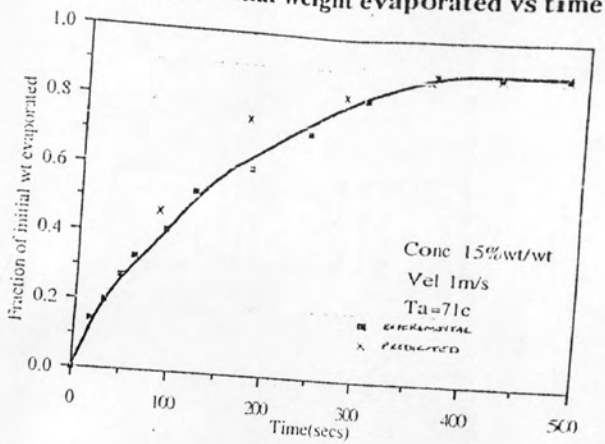

Figure 4 - Fraction of initial weight evaporated vs time (1.5 mm drop)

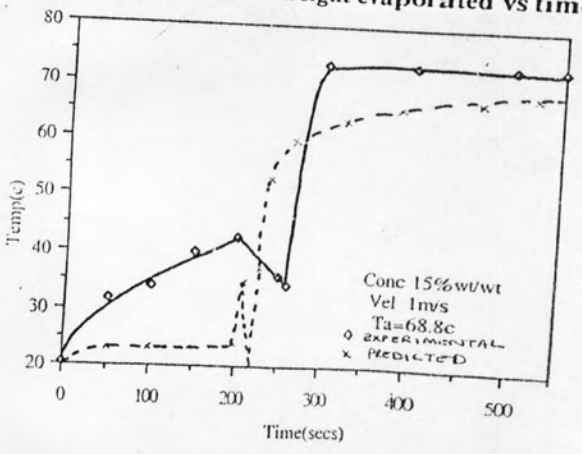

Figure 5 - Drop temperature history vs time (1.5 mm drop)